COMMONWEALTH OF AUSTRALIA

(Patents Act 1990)

IN THE MATTER OF: Australian Patent Application 696764 (73941/94). In the name of: Human Genome Sciences Inc.

- and -

IN THE MATTER OF: Opposition thereto by Ludwig Institute for Cancer Research, under Section 59 of the Patents Act.

STATUTORY DECLARATION

I, **Gary Baxter Cox** of Wray and Associates, 239 Adelaide Terrace, Perth WA 6101, Australia, declare as follows:

1. I am a Registered Patent Attorney, and a member of the firm Wray and Associates, Australian patent attorneys for Human Genome Sciences, Inc., the applicant in this matter.

2.1. Now produced and shown to me marked "**GBC-1**" is a copy of Grimmond *et al.*, 1996, Genome Research 6: 124-131.

2.2. Now produced and shown to me marked "**GBC-2**" is a copy of Townson *et al.*, 1996, Biochemical and Biophysical Research Communications 220: 922-928.

2.3. Now produced and shown to me marked "**GBC-3**" is a copy of Silins *et al.*, 1997, Biochemical and Biophysical Research Communications 230: 413-418.

2.4. Now produced and shown to me marked "**GBC-4**" is a copy of Bellomo *et al.*, 2000, Circulation Research 86: e29-e35.

WRAY & ASSOCIATES
Patent & Trade Mark Attorneys

6th Floor, GHD House
239 Adelaide Terrace, Perth
Western Australia 6000
Australia

Tel: (618) 9325 6122
Fax: (618) 9325 2883
Email: wray@wray.com.au
Our Ref: GBC:NJF 100868

GBC

2.5. Now produced and shown to me marked "**GBC-5**" is a copy of Stratagene Cloning Systems Catalogue 1994, page 45.

2.6. Now produced and shown to me marked "**GBC-6**" is a copy of Pharmacia LKB Biotechnology: Molecular and Cell Biology Catalogue 1992, page 5.

2.7. Now produced and shown to me marked "**GBC-7**" is a copy of Joukov *et al.*, 1996, EMBO Journal 15: 1751.

2.8. Now produced and shown to me marked "**GBC-8**" is a copy of Shibuya *et al.*, 1990, Oncogene 5: 519-524.

2.9. Now produced and shown to me marked "**GBC-9**" is a copy of Cockerill, Gamble, Vadas, 1994, "Angiogenesis: models and model vectors". In: International Reviews of Cytology. A Survey of Cell Biology 159: 113-160

2.10. Now produced and shown to me marked "**GBC-10**" is a copy of Litwin, Gamble, Vadas, 1995, "Role of growth factors in endothelial cell functions." In: Human Growth factors: Their role in Disease and Therapy, BB Aggarwal & RK Puri (Eds), Blackwell Science, Inc. USA Chapter 7 101-129.

2.11. Now produced and shown to me marked "**GBC-11**" is a copy of Gamble J.R. *et al.*, 1993, Journal of Cell Biology 121: 931-934.

2.12. Now produced and shown to me marked "**GBC-12** is a copy of US Patent Number 6,130,071 filed 5 February 1997 by Helsinki University Licensing, Ltd.

2.13. Now produced and shown to me marked "**GBC-13** is a copy of Goldspiel BR, et al (1993) *Clin. Pharm.* 12:488-505.

2.14. Now produced and shown to me marked "**GBC-14** is a copy of Hyde SC et al. (1993) *Nature* 362:250-255.

2.15. Now produced and shown to me marked "**GBC-15** is a copy of Kay M A et al. (1993) *Science* 262:117-119.

2.16. Now produced and shown to me marked "**GBC-16** is a copy of Kolodka TM, et al (1993) *Somat. Cell Mol. Genet.* 19:491-497.

2.17. Now produced and shown to me marked "**GBC-17** is a copy of Passaniti A, et al. (1992) *Lab. Invest.* 67:519-528.

2.18. Now produced and shown to me marked "**GBC-18** is a copy of Splawinski J, et al (1988) *Methods Find Exp. Clin. Pharmacol.* 10:221-226.

2.19. Now produced and shown to me marked "**GBC-19** is a copy of Stewart C, et al (1993) *J. Mol. Endocrinol.* 11:335-341.

2.20. Now produced and shown to me marked "**GBC-20** is a copy of Walsh CE, et al (1993) *Proc. Soc. Exp. Biol. Med.* 204:289-300.

2.21. Now produced and shown to me marked "**GBC-21** is a copy of Witte MH, Witte CL (1987) *Lymphology* 20:257-266.

2.22. Now produced and shown to me marked "**GBC-22** is a copy of Yong LC, Jones BE (1991) *Exp. Pathol.* 42:11-25.

2.23. In this declaration I have only identified those publications that have not already been served by Ludwig Institute for Cancer research in these proceedings. Now produced and shown to me marked "**GBC-23** is a Table identifying where all publications in Applicant's evidence in Answer may be found.

AND I make this solemn declaration by virtue of the Statutory Declarations Act, 1959 and subject to the penalties provided by that Act for the making of false statements in statutory declarations, conscientiously believing the statements contained in this declaration to be true in every particular.

DATED this day Thirteenth day of December 2000.

DECLARED at: Perth, Western Australia

BEFORE me:)

.....

Gary Baxter Cox

.....

Patent Attorney PETTEE IP PTY LTD

COMMONWEALTH OF AUSTRALIA

(Patents Act 1990)

IN THE MATTER OF: Australian Patent Application 696764 (73941/94). In the name of: Human Genome Sciences Inc.

- and -

IN THE MATTER OF: Opposition thereto by Ludwig Institute for Cancer Research, under Section 59 of the Patents Act.

Annexure GBC-1

This is **Annexure GBC-1** referred to in my Statutory Declaration made this Thirteenth day of December 2000.

Gary Baxter Cox

WITNESS: _____

Patent Attorney PEY TEE KHOO

RESEARCH

Cloning and Characterization of a Novel Human Gene Related to Vascular Endothelial Growth Factor

Sean Grimmond,[1,4] Jacob Lagercrantz,[2] Cathy Drinkwater,[3] Ginters Silins,[1] Steven Townson,[1] Pamela Pollock,[1] David Gotley,[1] Emma Carson,[2] Steven Rakar,[3] Magnus Nordenskjöld,[2] Larry Ward,[3] Nicholas Hayward,[1] and Günther Weber[2]

[1]Queensland Cancer Fund Research Unit Joint Experimental Oncology Program, Queensland Institute of Medical Research, Herston, Queensland, 4029, Australia; [2]Department of Molecular Medicine, Karolinska Institute, S-17176, Stockholm, Sweden; [3]AMRAD Burnley, Private Bag 29, Richmond, VIC, 3121, Australia

This paper describes the cloning and characterization of a new member of the vascular endothelial growth factor (VEGF) gene family, which we have designated VRF for VEGF-related-factor. Sequencing of cDNAs from a human fetal brain library and RT-PCR products from normal and tumor tissue cDNA pools indicate two alternatively spliced messages with open reading frames of 621 and 564 bp, respectively. The predicted proteins differ at their carboxyl ends resulting from a shift in the open reading frame. Both isoforms show strong homology to VEGF at their amino termini, but only the shorter isoform maintains homology to VEGF at its carboxyl terminus and conserves all 16 cysteine residues of $VEGF_{165}$. Similarity comparisons of this isoform revealed overall protein identity of 48% and conservative substitution of 69% with $VEGF_{189}$. VRF is predicted to contain a signal peptide, suggesting that it may be a secreted factor. The *VRF* gene maps to the D11S750 locus at chromosome band 11q13, and the protein coding region, spanning ~5 kb, is comprised of 8 exons that range in size from 36 to 431 bp. Exons 6 and 7 are contiguous and the two isoforms of VRF arise through alternate splicing of exon 6. *VRF* appears to be ubiquitously expressed as two transcripts of 2.0 and 5.5 kb; the level of expression is similar among normal and malignant tissues.

Vascular endothelial growth factor (VEGF), also known as vascular permeability factor (VPF), is a secreted, covalently linked homodimeric glycoprotein that specifically activates endothelial tissues (Keck et al. 1989; Leung et al. 1989; Senger et al. 1993). This factor is involved in a variety of physiological processes, including normal angiogenesis, formation of the corpus luteum (Yan et al. 1993), placental development (Sharkey et al. 1993), regulation of vascular permeability (Senger et al. 1993), inflammatory angiogenesis (Sunderkotter et al. 1994), and autotransplantation (Dissen et al. 1994), as well as pathological conditions such as tumor-promoting angiogenesis (Plate et al. 1992; Christofori et al. 1994).

VEGF is a distant relative of the platelet-derived growth factor (PDGF) gene family with many of the cysteine residues involved in dimerization of these proteins conserved in position (Leung et al. 1989; Keck et al. 1989). A more closely related homolog of VEGF is placenta growth factor (PlGF) (Maglione et al. 1991), which shares 39% amino acid identity and 62% conservative substitution. Furthermore, VEGF and PlGF contain 8 cysteine residues in homologous positions, occur as dimeric proteins, and are therefore likely to have similar tertiary structures (Maglione et al. 1991). VEGF and PlGF have been found to occur together as heterodimers in vivo (DiSalvo et al. 1995). No other closely related homologs of the two proteins have yet been reported.

While attempting to identify candidate genes for multiple endocrine neoplasia type 1 (MEN1), which maps to chromosomal region 11q13 (Lars-

[4]Corresponding author.
E-MAIL seanG@qimr.edu.au; FAX 61-7-33620107.

6:124–131 ©1996 by Cold Spring Harbor Laboratory Press ISSN 1054-9803/96 $5.00

son et al. 1988), we isolated a panel of cDNAs using cosmid cCLGW4 (D11S750) known to map to this region (Larsson et al. 1992). This cosmid was found to contain two previously described genes, *PLCB3* (Weber et al. 1994) and *FKBP2* (Grimmond et al. 1995), as well as novel genes (Lagercrantz et al. 1995a,b). Here we describe the cloning and characterization of a differentially spliced gene from the D11S750 locus, encoding a protein that we have designated VRF (VEGF-related factor), that has striking sequence homology with VEGF.

RESULTS

Cloning of *VRF* cDNAs

The original *VRF* cDNA, termed pSOM175, was isolated by screening a human fetal brain library (Stratagene) with the cosmid D11S750 (Larsson et al. 1992). cDNA library screening with pSOM175 recovered several partial but overlapping cDNAs for *VRF*. A composite sequence of the entire coding region was determined and found to consist of a 621-bp open reading frame (ORF), 412 bp of 3′ untranslated region (UTR), and 2 bp of 5′ UTR (Fig. 1, GenBank accession no. U43368). Attempts to isolate cDNAs with longer 5′ UTRs were unsuccessful; therefore, the corresponding region from genomic DNA was sought. An 850-bp *Pst*I restriction fragment from cosmid cCLGW4 (D11S750) (Larsson et al. 1992), which contained exon 1 and an undetermined amount of the 5′ UTR, was cloned and partially sequenced, from which −60 bp of the 5′ UTR immediately upstream of the initiation codon was determined (GenBank accession no. U43370). To confirm that the sequences upstream of the ATG were 5′ UTR, an ExoIII deletion subclone of this region (corresponding approximately to nucleotide positions −250 to −750 with respect to the initiation codon) was used to screen Northern blots. Bands corresponding in size to messages obtained with *VRF* cDNA probes were observed (data not shown).

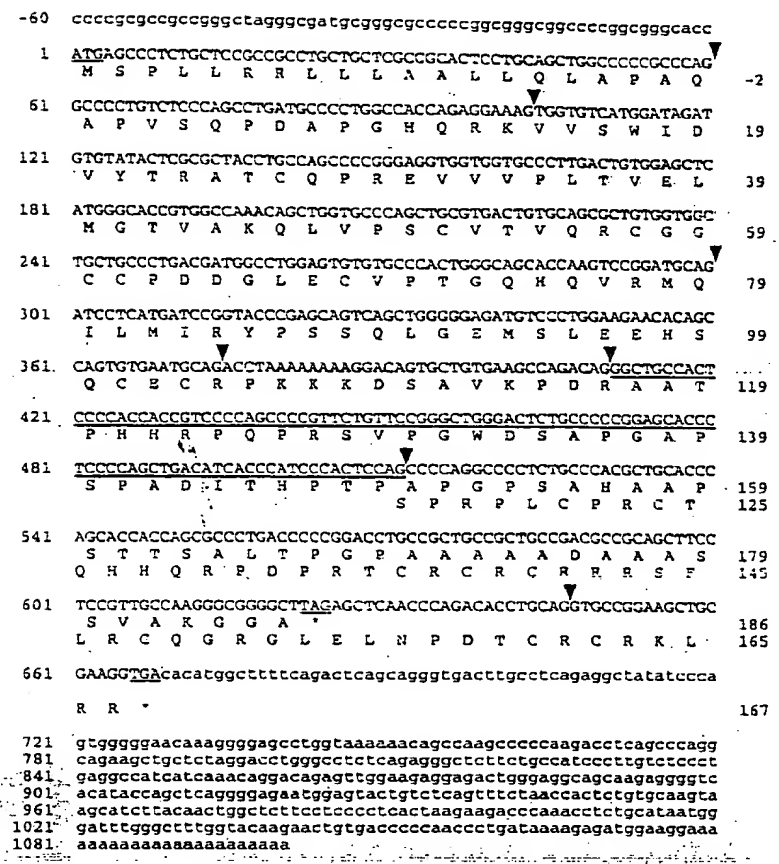

Figure 1 Nucleotide and predicted peptide sequences of VRF derived from the cDNA clone pSOM175 (nucleotides −2 to poly(A) tract) or genomic DNA (nucleotides −60 to −3 inclusive). The numbering of nucleotides is given at *left* starting from the A of the initiation codon. Amino acids are numbered at *right*, starting from the first residue of the predicted mature protein after the putative signal peptide has been removed. The alternately spliced region is double underlined, and the resulting peptide sequence from each mRNA is included. Start and stop codons are underlined. The positions of intron/exon boundaries are indicated by inverted arrowheads.

The putative start codon (Fig. 1) matches the vertebrate consensus sequence [(GCC)GCC[A/G]CCATGG] described by Kozak (1987). Furthermore, based on *VRF*'s homology to *VEGF* (see below), this ATG is likely to represent the genuine translation start site. However, in-phase stop codons were not identified upstream of this site. An out-of-frame ATG is located at position −37 but is not part of a Kozak consensus sequence.

The 3′ end of the cDNA contained a long poly(A) tail that was not preceded by a canonical polyadenylation signal (AATAAA) (Birnstiel et al. 1985); a related sequence, GATAAA, is −18 nucleotides upstream of the poly(A) tail (Fig. 1).

A second isoform of VRF [designated VRF_{167} in keeping with the nomenclature for VEGF (Tischer et al. 1991; Houck et al. 1991) whereby the isoforms are identified by the amino acid lengths of the mature proteins once the signal peptides have been cleaved from the NH_2-termini] was identified after sequencing PCR products generated from human fetal brain cDNA lysates and RT-PCR products from a renal cell carcinoma. VRF_{167} (GenBank accession no. U43369) differs from VRF_{186} as a result of a 101-bp deletion between positions +411–+511 (inclusive) in the cDNA encoding the latter (Fig. 1). This not only deletes ~33 amino acids from within VRF_{186} but also results in a different carboxy-terminal peptide sequence through the introduction of a frameshift within the ORF that terminates at a new site downstream of the stop codon utilized in generating VRF_{186}.

Comparison of VRF Isoforms to the VEGF Family

The nucleotide sequences and predicted translation products of *VRF* cDNAs (Fig. 1) were compared against peptide and nucleotide data bases with BLAST. Four expressed sequenced tags (ESTs) (GenBank accession nos. H28025, H39505, R56770, T08411) were identified as having regions of identity with *VRF*. Significant homology was observed with *VEGF* and other gene family members. Nucleotide alignment of the respective cDNAs revealed regions of sequence identity on the order of 59% (124/212 bp). The amino acid homology between VRF_{186} and $VEGF_{189}$ was 32% identity and 49% similarity over the entire peptide. However, it was notable that no similarity was observed over the carboxy-terminal quarter of the proteins. Sequence alignments of the VRF_{167} isoform showed greater overall similarity to members of the VEGF gene family than VRF_{186}. Peptide homology comparisons revealed 48% identity and 69% similarity between VEGF and VRF_{167}, respectively. This increase in VEGF homology relative to VRF_{186} was attributable to additional conservation of several distinct regions located toward the carboxyl-terminus of the protein (Fig. 2).

The predicted peptide lengths for the two VRF isoforms (Fig. 1) and the four isoforms of VEGF (Houck et al. 1991) are similar, and a region homologous to the signal peptide at the amino terminus of VEGF (von Heijne 1986; see Fig. 2) is also present in both VRF isoforms. The nomenclature of the VRF isoforms has been derived assuming that the signal peptide is cleaved from the preprotein in the same place as VEGF (Keck et al. 1989; Leung et al. 1989), that is, after alanine 21 in VRF or alanine 26 of VEGF (Fig. 2). Cysteine residues were found to be highly conserved between VRF_{167} and other members of the VEGF gene family. Both VRF isoforms contained the 8 cysteines maintained among VEGF, PlGF, and the PDGFs, but an additional 8 cysteine residues were conserved among VRF_{167}, $VEGF_{189}$, and PlGF, all of which were located within the divergent carboxy-terminal end of VRF_{167}. The striking conservation of number and position of these residues suggests that these three proteins are likely to have very similar tertiary structures.

Several peptide regions within VEGF that are believed to be associated with protein dimerization are maintained between VEGF and both VRF isoforms. The strongest areas of homology include regions located in the mature protein after amino acids 49–71 (PSCVxxxRCGGCCxDxGLECVPT) and 101–107 (CECRPKK) of VRF. In addition, VRF_{167} also displays homology to VEGF at the extreme carboxy-terminal end (TCRCxKxRR; amino acids 159–167).

```
VRF167    -21 MSPLLRRLL..LAALLQLAPA...QAPVSQPDAPGHQRKVVSWIDVYTRA 24
VEGF189   -26 MNFLLSWVHWSLALLLYLHHAKWSQAAPMAEGGGQNHHEVVKFMDVYQRS 24
VRF167     25 TCQPREVVVPLTVELMGTVAKQLVPSCVTVQRCGGCCPDDGLECVPTGQH 74
VEGF189    25 YCHPIETLVDIFQEYPDEIEYIFKPSCVPLMRCGGCCNDEGLECVPTEES 74
VRF167     75 QVRMQILMIR.YPSSQLGEMSLEEHSQCECRPKKKDSAVKPDSPRP.... 119
VEGF189    75 NITMQIMRIKPHQGQHIGEMSFLQHNKCECRPKKDRARQEKKSVRGKGKG 124
VRF167    120 .............LCPRCTQHHQR...PDPRTCRCRCRRRSFLRCQGR 151
VEGF189   125 QKRKRKKSRYKSWSVPCGPCSERRKHLFVQDPQTCKCSCKNTDS.RCKAR 173
VRF167    152 GLELNPDTCRCRKLRR 167
VEGF189   174 QLELNERTCRCDKPRR 189
```

Figure 2 Homology comparison between VRF_{167} and $VEGF_{189}$ peptide sequences. The arrow marks the signal peptide cleavage site of VEGF. Identical amino acids are indicated by vertical bars and conservative substitutions by colons. The numbering of amino acids is as described in the legend to Fig. 1.

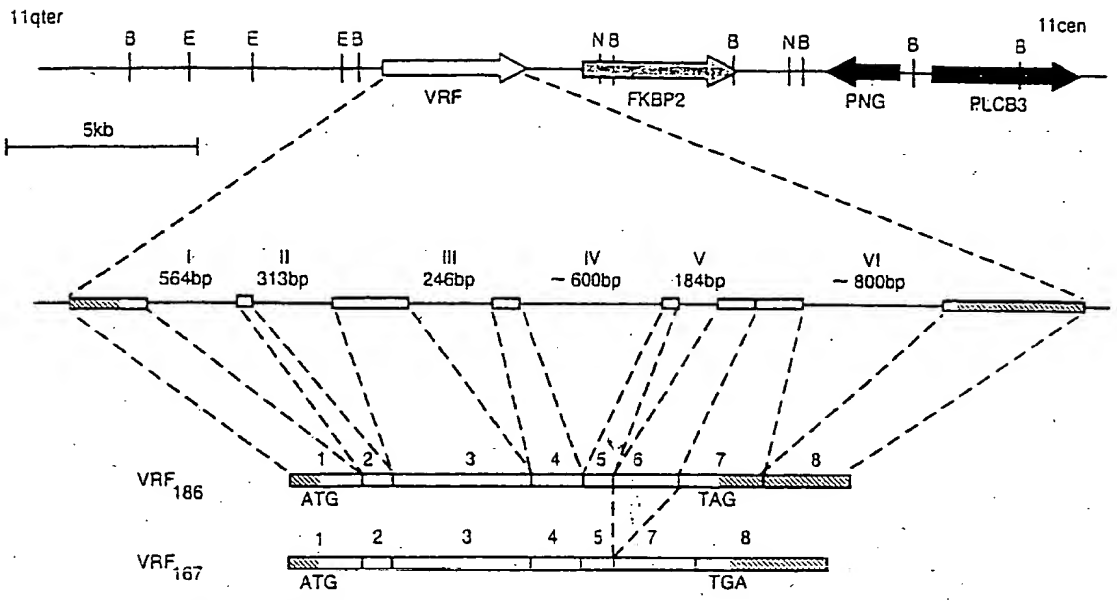

Figure 3 Genomic restriction map (B, E, and N represent restriction sites *Bam*HI, *Eco*RI, and *Not*I, respectively) and intron/exon structure of the *VRF* gene together with its orientation relative to other genes within cosmid cCLGW4 (D11S750). Sizes of introns and alternatively spliced RNAs are indicated.

The putative heparin binding clusters located at positions 121–135 of mature VEGF (Leung et al. 1989) are not conserved within the VRF isoforms. However, a noncontiguous clustering of basic residues located at the far carboxyl terminus of the $VEGF_{121}$ peptide, which is believed to account for its heparin binding ability (Cohen et al. 1995), is present in VRF_{167}.

Characterization of the *VRF* Gene

We have shown above that the *VRF* gene is alternately spliced to yield two major mRNA and protein isoforms. From establishing the intron/exon structure of the protein coding region of this gene (Fig. 3, Table 1) we have found that the VRF_{167} isoform is generated by the removal of exon 6 from pre-mRNA prior to translation (Fig. 3). The hypothesis that VRF_{167} (pSOM175-6) was derived by alternate splicing of *VRF* and not another closely related gene was further confirmed by hybridizing a *VRF* cDNA to Southern blots of human genomic DNA. As the genomic region of the *VRF* gene had been restriction mapped previously (Fig. 3), genomic DNA was digested with restriction enzymes (*Eco*RI, *Bam*HI) that were known not to cut within *VRF*, hybridized with pSOM175-6, and revealed a single band of the expected size. The *VRF* gene was also mapped against a human–hamster hybrid panel, confirming single-gene copy number and localization to 11q13 (data not shown).

The strong conservation of exon/intron organization between members of the VEGF family (Houck et al. 1991; Tis-

Table 1. Intron/Exon Boundaries of the Human *VRF* Gene

5'UTR.....	Exon 1 (Xbp*)	GCCCAG	gtacgtgcgg	Intron I (564bp)
tctcccacag	GCCCCT Exon 2 (43bp)	GGAAAG	gtaatactta	Intron II (313bp)
ctgctcccag	TGGTGT Exon 3 (197bp)	ATGCAG	gtcctgggca	Intron III (246bp)
ctgagcacag	ATCCTC Exon 4 (74bp)	ATGCAG	gtgccagcca	Intron IV (~600bp)
tactttccag	ACCTAA Exon 5 (36bp)	AGACAG	gtgagtcttt	Intron V (184bp)
tcctccctag	GGCTGC Exon 6 (101bp)			(No intron)
CCCACTCCAG	CCCCAG Exon 7 (135bp)	CTGCAG	gtgaggcgtc	Intron VI (~800bp)
ccctcctcag	GTGCCG Exon 8 (431bp)	GGAAGG		

Upper- and lowercase letters denote exonic and intronic sequences, respectively.
*The 5' end of exon 1 has not yet been determined.

cher et al. 1991) was similarly extended to the genomic structure of *VRF*. In nearly every case, the exon/intron boundaries (Table 1) were found to be in the same location as the *VEGF* gene. The exception was exon 6 of *VRF*, which was contiguous with exon 7 (i.e., no intervening sequence but conservation of the exon/intron boundary position). This suggests that exon 6 in the *VRF* gene is derived from a partially retained intron.

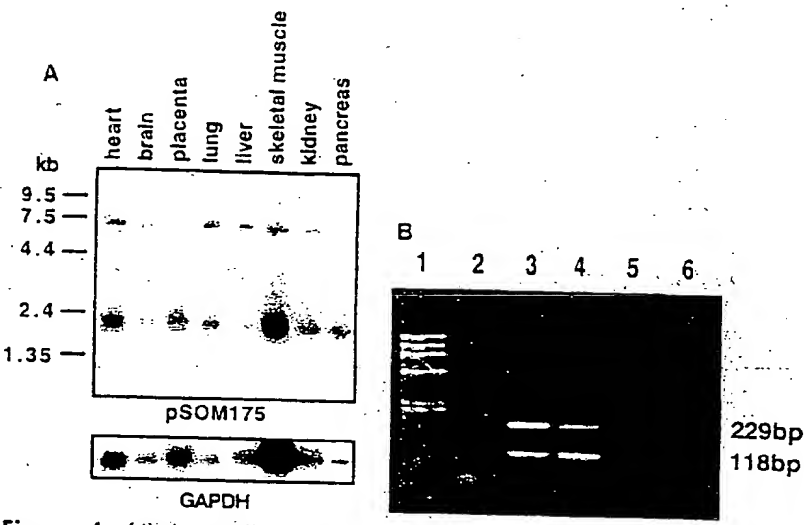

Figure 4 (*A*) Autoradiograph of multiple tissue Northern blot hybridized with the *VRF* cDNA clone pSOM175. Size markers are indicated in kilobases at *left*. Two transcripts of 5.5 and 2.0 kb were detected in all samples. Results of control hybridization of the same blots using GAPDH cDNA are included in the lower panel. (*B*) RT–PCR of alternative splice forms of *VRF* in normal human tissue mRNAs. (Lane *1*) Size markers (ΦX174 DNA cut with *HaeIII*); (lane *2*) negative control; (lane *3*) normal kidney; (lane *4*) normal lung; (lane *5*) normal pancreas; (lane *6*) normal colon.

Orientation of the *VRF* Gene

The location and orientation of the human *VRF* gene (Fig. 3) within cosmid cCLGW4 (the D11S750 locus), which maps to chromosome 11q13 (Larsson et al. 1992), was determined by PCR between primers from either end of the *VRF* cDNA and a primer located within the 5′ end of *FKBP2*. Only an exon 7-specific *VRF* primer and a primer within the 5′ UTR of *FKBP2* gave a specific amplification product using both genomic DNA and cCLGW4 as template. Direct sequencing of the termini confirmed the specificity of this product (data not shown).

Expression Studies of *VRF*

Northern blot analysis of a total of 20 normal human tissues as well as cultured fibroblasts and lymphoblastoid cell lines revealed that *VRF* was expressed in all samples studied, with no obvious predominance in any tissue after normalization with GAPDH (Fig. 4A). Two bands of 5.5 and 2.0 kb were visible in all samples assayed. We assessed *VRF* expression in normal endocrine tissues, an insulinoma, and a medullary thyroid carcinoma. *VRF* was expressed in all samples, although the level in both tumors was reduced by 50% which corresponded to the loss of one chromosome 11 allele (Weber et al. 1994). Because VEGF has been shown previously to be overexpressed in highly malignant tumors (Plate et al. 1992) we assayed levels of *VRF* mRNA in a panel of 11 glioblastomas, 13 metastasizing and 12 nonmetastasizing breast carcinomas, and 34 renal cell carcinomas. Compared with their normal counterparts or nonmalignant cell lines, elevated transcription was not found in any of the tumors.

As it was not possible to differentiate between the alternately spliced VRF_{186} and VRF_{167} mRNAs by Northern analysis owing to the small size difference (101 nucleotides), RT–PCR was performed to confirm further the presence of both messages in normal and tumor tissues. A region corresponding to the carboxy-terminal end of the ORF (nucleotide positions + 362–+ 590; see Fig. 1) was amplified from a panel of matched human normal tissue/tumor mRNAs with two major products being identified (Fig. 4B). Direct sequencing of these products confirmed that they represented the two different VRF isoforms.

DISCUSSION

We have cloned and characterized a new member of the VEGF gene family, which we have designated VRF. The strong homology between VEGF, PlGF, and VRF reflects conservation of structural

motifs important for peptide function (i.e., homo/heterodimerization and heparin binding).

As yet, the various roles of VRF in vivo remain to be elucidated. We have shown here that VRF possesses strong homolgy to several angiogenic factors, and investigations into its effect on endothelial cell function are ongoing. Furthermore, its ubiquitous expression pattern suggests that its role may extend beyond the endothelium. In light of the recent report that VEGF and PIGF form heterodimers in vivo (DiSalvo et al. 1995), it is possible that VRF may also interact with one or both of these factors in a similar fashion. As VRF proteins have divergent carboxy-terminal ends, with the longer isoform lacking some of the motifs involved in VEGF stability and function, it is tempting to speculate that this isoform could act as an antagonist/regulator of the shorter isoform.

Recent studies of VEGF function have reported the importance of heparin binding that is involved in dimerization and transport and assists in binding of the protein to some receptors such as *flt1* (Gengrinovitch et al. 1995). One of the major heparin binding domains (basic cluster of residues at position 121–135; see Fig. 2) of VEGF (Leung et al. 1989; Ferrara et al. 1992) is absent from both VRF isoforms. However, VRF_{167} may still be capable of heparin binding through a region of basic amino acids at its carboxyl terminus, provided the tertiary structure of the protein allows the clustering of these noncontiguous residues.

The strong sequence homology between VEGF, PIGF, and VRF reflect conservation of genomic structure between their genes with a similar number of exons, near identical intron/exon borders, and the existence of alternately spliced mRNA, particularly involving exon 6. One significant difference between *VRF* and the other *VEGF* gene family members is that the alternately spliced messages of *VRF* reported here give rise to proteins with different carboxyl termini. We show that this phenomenon arises through the retention or deletion of exon 6. Retention of intervening sequences in mRNA has been documented as a post-translational regulatory mechanism in several genes including P-transposase in *Drosophila* (for review, see Maniatis 1991) and bovine growth hormone pre-mRNA (Dirksen et al. 1995). The retention of an intron that results in a frameshift and different carboxyl termini is an uncommon phenomenon but has been reported recently for the β1-adrenergic receptor in the turkey (Wang and Ross 1995). In the case of β-adrenergic receptor, intronic retention gives rise to two receptor types and is involved in providing tissue specificity. The mechanisms that control intron retention in pre-mRNAs have been studied for some genes and involve specific splicing repressor factors (for review, see Maniatis 1991). Thus, studies to determine the possible role of such factors in regulation of the *VRF* gene appear warranted.

While the elucidation of all the possible roles of VRF continues, it is tempting to speculate that the two VRF protein isoforms act in an antagonistic or self-regulatory manner, similar to that reported for the turkey β-adrenergic receptor isoforms (Wang and Ross 1995).

The genomic localization of *VRF* at D11S750 places it within a 900-kb region known to contain the *MEN1* gene (Weber et al. 1994). In a large panel of tumors of endocrine and nonendocrine origin, a reduction in expression of *VRF* was only observed in those endocrine tumors known to be hemizygous for chromosome 11q, suggesting this was a gene dosage effect. Although *VRF* has not yet been excluded as a *MEN1* candidate by mutation analysis, its putative role as a growth factor makes it an unlikely candidate for the *MEN1* tumor suppressor gene.

METHODS

cDNA Cloning Sequencing, and Analysis

Screening of a human fetal brain library (Stratagene) with the cosmid D11S750 (Larsson et al. 1992) was performed as described (Viskochil et al. 1992). The 1.1-kb insert of SOM175 was used as a probe to isolate other cDNAs from a human fetal spleen library (Stratagene). The isolated cDNAs were sequenced on both strands using standard manual sequencing and automated sequencing protocols (PRISM, Applied Biosystems, Inc., model 373A). Oligonucleotides, nested deletions (Erase-a-base, Promega), and specific cDNA subclones were generated to complete total cDNA sequences. PCR products generated from the cDNAs were first purified from agarose gels (Qiagex gel purification columns, Qiagen) and then sequenced. Sequences were compared with the current GenBank data base at the National Center for Biotechnology Information (NCBI) using the BLAST algorithm (Altschul et al. 1990). Peptide homology alignments were performed using the program BESTFIT (GCG Wisconsin).

Northern Blot Analysis

Multiple tissue Northern blots (Clontech) containing poly(A)$^+$ RNA from heart, brain, placenta, lung, liver, skel-

etal muscle, kidney, pancreas, spleen, thymus, prostate, testis, ovary, small intestine, colon, and peripheral blood leukocytes were used to determine expression of *VRF* in normal human tissues. Northern filters from renal cell carcinomas and breast carcinomas were kindly provided from Drs. Ulf Bergerheim, Moraima Zelada, and Esther Schmidt. The extraction of poly(A)$^+$ RNA from normal adrenal, pancreas, thyroid, parathyroid, kidney, fibroblasts, lymphoblastoid cell lines, and endocrine tumors, the preparation of blots, and the hybridization conditions with cDNA probes were performed as described (Weber et al. 1994).

RT–PCR

Total RNA was isolated from a panel of human tumors and matching normal tissues (colon, lung, liver, kidney, pancreas), and cDNA synthesis reactions were carried out using 5 μg of RNA, random hexamers, and AMV reverse transcriptase (Promega) following methods recommended by the manufacturer. Five hundred nanograms of reverse-transcribed cDNA mixture (1 μl) was used in a PCR reaction to detect possible alternately spliced messages. Alternatively, 1 μl of high titer (>10^9 PFU/ml) cDNA library lysate was used as a template. The primers were 362F (5′-AGTGTGAATGCAGACCT-3′) and S90R (5′-GCGTCGGCAGCGGCAGCGG-3′). PCR products were visualized after electrophoresis through high percentage (3%) agarose gels stained with ethidium bromide. Alternately spliced products were confirmed by direct sequencing as described above.

Genomic Sequencing and Intron/Exon Mapping of the *VRF* Gene

Cosmid cCLGW4 (Larsson et al. 1992) was used as template and sequenced on both strands using both manual dideoxy sequencing methods and automated fluorescently labeled "dye terminator" (PRISM, Applied Biosystems, Inc.) cycle sequencing as described above, except that 2 μg of cosmid template and 20 pmoles of primer were used in each reaction. PCR products from genomic DNA were also sequenced using dye terminator cycle sequencing after purification of products from agarose gels using Qiagex gel purification columns (Qiagen). An oligonucleotide (19F, 5′-CGCCTGCTGCTCGCCGCACT-3′) was made to a region corresponding to nucleotides 19–38 with respect to the initiation codon, end-labeled with [γ-^{32}P] dATP, and hybridized to a Southern blot of a series of shotgun-cloned *Pst*I restriction fragments from cosmid cCLGW4 subcloned into pBluescript KS– (Stratagene). A single hybridizing clone with an 850 bp insert was sequenced on both strands as described above.

Intervening sequences were located by sequencing of cosmid cCLGW4 (Larsson et al. 1992) using oligonucleotide primers from the *VRF* cDNA sequence determined above. Comparison of cDNA and cosmid sequences revealed the exact location of each exon/intron boundary. The size of each intron was then determined by PCR amplification using flanking exonic primers and cCLGW4 or genomic DNA as template. Amplified products were gel purified and directly sequenced to confirm intron/exon boundaries. The intron sizes were determined either by complete sequencing of the intervening sequence or estimated by electrophoresis through high percentage agarose gels.

ACKNOWLEDGMENTS

This work was supported by the National Health and Medical Research Council of Australia, AMRAD Operations Proprietary Ltd, and the Swedish Cancer Foundation. We thank Dr. Catharina Larsson for technical help and comments on the manuscript, and Drs. Kerstin Sandelin and Jan Zedenius for providing tissue samples.

The publication costs of this article were defrayed in part by payment of page charges. This article must therefore be hereby marked "advertisement" in accordance with 18 USC section 1734 solely to indicate this fact.

REFERENCES

Aiello, L.P., R.L. Avery, P.G. Arrigg, B.A. Keyt, H.D. Jampel, S.T. Shah, L.R. Pasquale, H. Thieme, M.A. Iwamoto, J.E. Park, H.V. Nguyen, L.M. Aiello, N. Ferrara, and G.L. King. 1994. Vascular endothelial growth factor in ocular fluid of patients with diabetic retinopathy. *N. Engl. J. Med.* **331:** 1480–1487.

Altschul, S.F., W. Gish, W. Miller, E.W. Myers, and D.J. Lipman. 1990. Basic local alignment search tool. *J. Mol. Biol.* **215:** 403–410.

Birnstiel, M.L., M. Busslinger, and K. Strub. 1985. Transcription termination and 3′ processing: the end is in site! *Cell* **41:** 349–359.

Christofori, G., P. Naik, and D. Hanahan. 1994. A second signal supplied by insulin-like growth factor II in oncogene induced tumorigenesis. *Nature* **369:** 414–418.

Cohen, T., H. Gitay-Goren, R. Sharon, M. Shibuya, R. Halaban, B.Z. Levi, and G. Neufeld. 1995. VEGF(121), a vascular endothelial growth factor (VEGF) isoform lacking binding ability, requires cell surface heparan sulfates for efficient binding to the VEGF receptors of human melanoma cells. *J. Biol. Chem.* **270:** 11322–11326.

Dirksen, W.P., Q. Sun, and F.M. Rottman. 1995. Multiple splicing signals control alternative intron retention of bovine growth hormone pre-mRNA. *J. Biol. Chem.* **270:** 5346–5352.

DiSalvo, J., M.L. Bayne, G. Conn, P.W. Kwok, P.G. Trivedi, D.D. Soderman, T.M. Palisi, K.A. Sullivan, and K.A. Thomas. 1995. Purification and characterisation of a naturally occurring vascular endothelial growth factor-placenta growth factor heterodimer. *J. Biol. Chem.* **270:** 7717–7723.

Dissen, G.A., H.E. Lara, W.H. Fahrenbach, M.E. Costa, and S.R. Ojeda. 1994. Immature rat ovaries become revascularized rapidly after autotransplantation and show a gonadotropin-dependent increase in angiogenic factor gene expression. *Endocrinology* **134:** 1146–1154.

Ferrara, N., K. Houck, L. Jakeman, and D.W. Leung. 1992. Molecular and biological properties of the vascular endothelial growth factor family of proteins. *Endocr. Rev.* **13:** 18–32.

Gengrinovitch, S., S.M. Greenberg, T. Cohen, H. Gitay-Goren, P. Rochwell, T.E. Maione, B.Z. Levi, and G. Neufeld. 1995. Platelet factor-4 inhibits the mitogenic activity of VEGF121 and VEGF165 using several concurrent mechanisms. *J. Biol. Chem.* **270:** 15059–15065.

Grimmond, S., G. Weber, C. Larsson, M. Walters, B. Teh, J. Shepherd, M. Nordenskjöld, and N. Hayward. 1995. Exclusion of the 13 kD rapamycin binding protein gene (FKBP2) as a candidate for multiple endocrine neoplasia type 1. *Hum. Genet.* **95:** 455–458.

Houck, K.A., N. Ferrara, J. Winer, G. Cachianes, G. Li, and D.W. Leung. 1991. The vascular endothelial growth factor family: Identification of a fourth molecular species and characterization of alternative splicing of RNA. *Mol. Endocrinol.* **5:** 1806–1814.

Keck, P.J., S.D. Hauser, G. Krivi, K. Sanzo, T. Warren, J. Feder, and D.T. Connolly. 1989. Vascular permeability factor, an endothelial cell mitogen related to PDGF. *Science* **246:** 1309–1312.

Kotch, A.E., L.A. Harlow, G.K. Haines, E.P. Amento, E.N. Unemori, W.L. Wong, R.M. Pope, and N. Ferrara. 1994. Vascular endothelial growth factor. A cytokine modulating function in rheumatoid arthritis. *J. Immunol.* **152:** 4149–4156.

Kozak, M. 1987. An analysis of 5′-noncoding sequences from 699 vertebrate messenger RNAs. *Nucleic Acids Res.* **15:** 8125–8148.

Lagercrantz, J., C. Larsson, S. Grimmond, B. Skogseid, A. Gobl, E. Friedman, E. Carson, C. Phelan, K. Öberg, M. Nordenskjöld, N.K. Hayward, and G. Weber. 1995a. Candidate genes for multiple endocrine neoplasia type 1. *J. Intern. Med.* **238:** 245–248.

Lagercrantz, J., E. Carson, C. Larsson, M. Nordenskjöld, and G. Weber. 1995b. Isolation and characterization of a novel gene close to the human phosphatidylinositol-specific phospholipase Cβ3 gene on chromosomal region 11q13. *Genomics* (in press).

Larsson, C., B. Skogseid, K. Öberg, Y. Nakamura, and M. Nordenskjöld. 1988. Multiple endocrine neoplasia type 1 gene maps to chromosome 11 and is lost in insulinoma. *Nature* **332:** 85–87.

Larsson, C., G. Weber, E. Kvanta, C. Lewis, M. Janson, C. Jones, T. Glaser, G. Evans, and M. Nordenskjöld. 1992. Isolation and mapping of polymorphic cosmid clones used for sublocalisation of the multiple endocrine neoplasia type 1 (MEN1) locus. *Hum. Genet.* **89:** 187–193.

Leung, D.W., G. Cachianes, W.J. Kuang, D.V. Goeddel, and N. Ferrara. 1989. Vascular endothelial growth factor is a secreted angiogenic mitogen. *Science* **246:** 1306–1309.

Maglione, D., V. Guerriero, G. Viglietto, P. Delli-Bovi, and M.G. Persico. 1991. Isolation of a human placenta cDNA coding for a protein related to the vascular permeability factor. *Proc. Natl. Acad. Sci.* **88:** 9267–9271.

Maniatis, T. 1991. Mechanisms of alternative pre-mRNA splicing. *Science* **251:** 33–34.

Plate, K.H., G. Greier, H.A. Weich, and W. Risau. 1992. Vascular enothelial growth factor is a potential tumour angiogenesis factor in human gliomas *in vivo*. *Nature* **359:** 845–848.

Senger, D.R., L. Van de Water, L.F. Brown, J.A. Nagy, K.T. Yeo, T.K. Yeo, B. Berse, R.W. Jackman, A.M. Dvorak, and H.F. Dvorak. 1993. Vascular permeability factor (VPF, VEGF) in tumor biology. *Cancer Metastasis Rev.* **12:** 303–324.

Sharkey, A.M., D.S. Charnock-Jones, C.A. Boocock, K.D. Brown, and S.K. Smith. 1993. Expression of mRNA for vascular endothelial growth factor in human placenta. *J. Reprod. Fertil.* **99:** 609–615.

Sunderkotter, C., K. Steinbrink, M. Goebeler, R. Bhardwaj, and C. Sorg. 1994. Macrophages and angiogenesis. *J. Leukocyte Biol.* **55:** 410–422.

Tischer, E., R. Mitchell, T. Hartman, M. Silva, D. Gospodarowicz, J.C. Fiddes, and J.A. Abraham. 1991. The human gene for vascular endothelial growth factor: Multiple protein forms are encoded through alternative exon splicing. *J. Biol. Chem.* **266:** 11947–11954.

Viskochil, D., A.M. Buchberg, G. Xu, R.M. Cawthon, J. Stevens, R.K. Wolff, M. Culver, J.C. Carey, N.G. Copeland, N.A. Jenkins, R. White, and P. O'Connell. 1990. Deletions and a translocation interrupt a cloned gene at the neurofibromatosis type 1 locus. *Cell.* **14:** 187–192.

Von Heijne, G. 1986. A new method for predicting signal cleavage sites. *Nucleic Acids Res.* **14:** 4683–4690.

Wang, J. and E.M. Ross. 1995. The carboxyl-terminal anchorage domain of the turkey β1-adrenergic receptor is encoded by an alternatively spliced exon. *J. Biol. Chem* **270:** 6488–6495.

Weber, G., E. Friedman, S. Grimmond, N. Hayward, C. Phelan, B. Skogseid, A. Gobl, J. Zedenius, K. Sandelin, B.T. Teh, E. Carson, I. White, K. Öberg, J. Shepherd, M. Nordenskjöld, and C. Larsson. 1994. The phospholipase Cβ3 gene located in the MEN1 region shows loss of expression in MEN1 related tumours. *Hum. Mol. Genet.* **3:** 1775–1781.

Yan, Z., H.A. Weich, W. Bernart, M. Breckwoldt, and J. Neulen. 1993. Vascular endothelial growth factor (VEGF) messenger ribonucleic acid (mRNA) expression in luteinized human granulosa cell in vitro. *J. Clin. Endocrinol. Metab.* **77:** 1723–1725.

Received December 7, 1995; accepted in revised form February 5, 1996.

COMMONWEALTH OF AUSTRALIA

(Patents Act 1990)

IN THE MATTER OF: Australian Patent Application 696764 (73941/94). In the name of: Human Genome Sciences Inc.

- and -

IN THE MATTER OF: Opposition thereto by Ludwig Institute for Cancer Research, under Section 59 of the Patents Act.

Annexure GBC-2

This is **Annexure GBC-2** referred to in my Statutory Declaration made this Thirteenth day of December 2000.

Gary Cox

Gary Baxter Cox

WITNESS: Peytee Kho

Patent Attorney PEYTEE KHOO

BIOCHEMICAL AND BIOPHYSICAL RESEARCH COMMUNICATIONS 220, 922–928 (1996)
ARTICLE NO. 0507

Characterization of the Murine VEGF-Related Factor Gene

Steven Townson,* Jacob Lagercrantz,† Sean Grimmond,* Ginters Silins,* Magnus Nordenskjöld,† Günther Weber,† and Nicholas Hayward*,[1]

*Queensland Cancer Fund Research Unit, Joint Experimental Oncology Program, Queensland Institute of Medical Research, Herston, QLD 4029, Australia; and †Department of Molecular Medicine, Clinical Genetics Unit, Karolinska Institute, L6 S-17176 Stockholm, Sweden

Received February 7, 1996

We describe here the molecular cloning and characterization of the murine homolog of the human vascular endothelial growth factor-related factor (*VRF*) gene. cDNAs for two alternatively spliced forms of the murine *vrf* gene have been isolated, the putative translation products of which differ at their carboxyl termini due to a shift in reading frame caused by insertion, or lack thereof, of exon 6, in a similar fashion to human VRF (hVRF). The message lacking exon 6 encodes a protein (mvrf$_{167}$) with 86% identity and 92% conservation of amino acid residues with hVRF. The protein coding region of the gene spans approximately 5kb of genomic DNA and is composed of 8 exons ranging in size from 36 to 398bp. The genomic structure of murine *vrf* is highly conserved with the human homolog in relation to position of splice junctions and the presence of contiguous exons 6 and 7. A short polymorphic AC repeat is present in the 3' untranslated region of murine *vrf*. A major band of approximately 1.3kb was expressed in all adult mouse tissues examined. © 1996 Academic Press, Inc.

Angiogenesis is an important physiological process in embryonic development, somatic growth, wound healing, tissue and organ regeneration and cyclical growth of the corpus luteum and endometrium [reviewed in 1, 2]. The growth and differentiation of capillary vessels is a complex process in which endothelial cells migrate, proliferate and are involved in degradation of the extracellular matrix and tube formation. The formation of capillaries is also associated with a number of pathological conditions which include tumor growth [3–5], diabetes-related retinopathy [6], atherosclerosis and rheumatoid arthritis [7]. Vascular endothelial growth factor (VEGF), is a mitogen that is highly selective for endothelial cells [8, 9], and belongs to a family of growth factors that includes platelet derived growth factor (PDGF) -A and PDGF-B [8, 9], and placenta growth factor (PlGF) [10]. Native VEGF is normally found as a homodimer and is one of the ligands for the *flt/flk* family of receptor tyrosine kinases found on the surface of vascular endothelial cells [reviewed in 11, 12]. Heterodimers of VEGF and PlGF were identified recently *in vivo* and found to be mitogenic [13].

The VEGF transcript is differentially spliced to produce four distinct peptides that have variable biological properties and activities [reviewed in 14, 15]. We recently cloned and characterized a gene from humans that encodes a VEGF-related factor (VRF) [16]. Human VRF (hVRF) transcripts are alternately spliced with two major isoforms (hVRF$_{186}$ and hVRF$_{167}$) being present. The smaller isoform (hVRF$_{167}$) lacks an 101bp exon (exon 6) and maintains strong amino acid sequence homology to VEGF throughout the peptide while the larger message possesses a divergent alanine-rich carboxyl terminus. In this report we describe the isolation of the homologous gene from mouse

Sequences presented in this article have been submitted to the GENBANK database and appear under accession numbers U43836 and U43837.

[1] To whom correspondence should be sent at Queensland Institute of Medical Research, P.O. Royal Brisbane Hospital, Herston 4029, Australia. Fax: (61) 7 3362 0107; E-mail: nickH@qimr.edu.au.

Abbreviations: hVRF - human VEGF-related factor; mVRF - murine VEGF-related factor; PDGF - platelet derived growth factor; PlGF - placenta growth factor; UTR - untranslated region; VEGF - vascular endothelial growth factor; *VRF* - human VEGF-related factor gene; *vrf* - murine VEGF-related factor gene.

0006-291X/96 $18.00

which likewise encodes two m
exon 6.

Isolation of cDNAs. Murine *vrf* clones
Primary phage from high density filters
generated by PCR from an human *VRF* c
of nylon membranes (Hybond-N) were
plaques were picked, purified and excise

Isolation of genomic clones. Genomic
II vector (Stratagene). High density filte
PCR amplification of the nucleotide 233
re-screened with filters containing 400–
kit or by $ZnCl_2$ purification [18].

Nucleotide sequencing and analysis.
primers with Applied Biosystems Inco
specifications. Sequences were analyzed
were performed using the program BES

Identification of intron/exon boundar
PCR with mouse genomic DNA or mu
introns were derived from the human V
annealing temperatures 5–10°C below
phoresis and gel purified using QIAquic
from these products. In addition, some
exon boundaries were identified by con

Northern analysis. Total cellular RN
liver, muscle) using the method of Chor
a nylon membrane (Hybond-N, Amersh
0.1 × SSC (20 × SSC is 3M NaCl/0.3M
at ~70°C for 1–3 days.

Characterization of Murine vrf

Murine *vrf* homologs were i
cDNA clone. Five clones of si
cDNA sequences were compile
open reading frame (621bp or
(379bp), as well as 189bp of th

The predicted initiation codo
other ATG codons (positions –
upstream and out of frame with

The predicted N-terminal sig
identity (17/21 amino acids). P
(Fig. 2). These data suggest that
as a growth factor.

As with hVRF, two open rea
screening. Four of five clones
number U43837) and lacked
predicted peptide sequences of
corresponding human isoforms

The message encoding mvrf
position +622, towards the end
terminates downstream of the +

ted Factor Gene

d,* Ginters Silins,*
olas Hayward*,†

m, Queensland Institute of Medical
re, Clinical Genetics Unit, Karolinska

homolog of the human vascular
vely spliced forms of the murine
at their carboxyl termini due to a
r fashion to human VRF (hVRF).
92% conservation of amino acid
tely 5kb of genomic DNA and is
of murine *vrf* is highly conserved
sence of contiguous exons 6 and
of murine *vrf*. A major band of

development, somatic growth,
wth of the corpus luteum and
capillary vessels is a complex
volved in degradation of the
ries is also associated with a
5], diabetes-related retinopathy
ial growth factor (VEGF), is a
belongs to a family of growth
PDGF-B [8, 9], and placenta
homodimer and is one of the
the surface of vascular endo-
were identified recently *in vivo*

inct peptides that have variable
tly cloned and characterized a
3]. Human VRF (hVRF) tran-
d $hVRF_{167}$) being present. The
ins strong amino acid sequence
possesses a divergent alanine-
homologous gene from mouse

e and appear under accession numbers

search, P.O. Royal Brisbane Hospital,

ated factor; PDGF - platelet derived
scular endothelial growth factor; *VRF*

which likewise encodes two major protein isoforms which arise through alternative splicing of exon 6.

MATERIALS AND METHODS

Isolation of cDNAs. Murine *vrf* clones were selected from a lambda Zap new born whole brain cDNA library (Stratagene). Primary phage from high density filters (5×10^4 pfu/plate) were identified by hybridization with a 682bp ^{32}P-labelled probe generated by PCR from an human *VRF* cDNA (pSOM175) as described previously [16]. Hybridization and stringent washes of nylon membranes (Hybond-N) were carried out at 65°C under conditions described by Church and Gilbert [17]. Positive plaques were picked, purified and excised *in vivo* to produce bacterial colonies containing cDNA clones in pBluescript SK-.

Isolation of genomic clones. Genomic clones were isolated from a mouse strain SV/129 library cloned in the lambda Fix II vector (Strategene). High density filters (5×10^4 pfu/filter) were screened with a 563bp ^{32}P-labelled probe generated by PCR amplification of the nucleotide 233-798 region of the murine *vrf* cDNA (see Fig. 1). Positive clones were plugged and re-screened with filters containing 400–800 pfu. Large scale phage preparations were prepared using the QIAGEN lambda kit or by $ZnCl_2$ purification [18].

Nucleotide sequencing and analysis. cDNAs were sequenced on both strands using a variety of vector-based and internal primers with Applied Biosystems Incorporated (ABI) dye terminator sequencing kits according to the manufacturer's specifications. Sequences were analyzed on an ABI Model 373A automated DNA sequencer. Peptide homology alignments were performed using the program BESTFIT (GCG, Wisconsin).

Identification of intron/exon boundaries. Identification of exon boundaries and flanking regions was carried out using PCR with mouse genomic DNA or murine *vrf* genomic lambda clones as templates. The primers used in PCR to identify introns were derived from the human *VRF* sequence [16] and to allow for potential human-mouse sequence mismatches annealing temperatures 5–10°C below the estimated T_m were used. All PCR products were sized by agarose gel electrophoresis and gel purified using QIAquick spin columns (Qiagen) and the intron/exon boundaries were sequenced directly from these products. In addition, some splice junctions were sequenced from subcloned genomic fragments of *vrf*. Intron/exon boundaries were identified by comparing cDNA and genomic DNA sequences.

Northern analysis. Total cellular RNA was prepared from a panel of fresh normal adult mouse tissues (brain, kidney, liver, muscle) using the method of Chomczynski and Sacchi [19]. 20μg of total RNA were electrophoresed, transferred to a nylon membrane (Hybond N, Amersham) and hybridised under standard conditions [17]. Filters were washed at 65°C in 0.1 × SSC (20 × SSC is 3M NaCl/0.3M trisodium citrate), 0.1% SDS and exposed to X-ray film with intensifying screens at -70°C for 1–3 days.

RESULTS AND DISCUSSION

Characterization of Murine vrf cDNAs

Murine *vrf* homologs were isolated by screening a murine cDNA library with a human *VRF* cDNA clone. Five clones of sizes varying from 0.8–1.5kb were recovered and sequenced. The cDNA sequences were compiled to give a full length 1233bp cDNA sequence covering the entire open reading frame (621bp or 564bp depending on the splice form, see below) and 3′ UTR (379bp), as well as 189bp of the 5′ UTR (Fig. 1, GENBANK accession number U43836).

The predicted initiation codon matched the position of the start codon in human *VRF* [16]. Two other ATG codons (positions −34 and −80) and a termination codon (position −41) were observed upstream and out of frame with the putative initiation codon.

The predicted N-terminal signal peptide of hVRF [16] appears to be present in mvrf with 81% identity (17/21 amino acids). Peptide cleavage within mvrf is expected to occur after residue 21 (Fig. 2). These data suggest that mature mvrf is secreted and could therefore conceivably function as a growth factor.

As with hVRF, two open reading frames (ORFs) were detected in cDNAs isolated by library screening. Four of five clones were found to be alternatively spliced (GENBANK accession number U43837) and lacked an 101bp fragment homologous to exon 6 of hVRF [16]. The predicted peptide sequences of the two isoforms of mvrf were determined and aligned with the corresponding human isoforms (Fig. 2).

The message encoding $mvrf_{186}$ contains a 621bp ORF with coding sequences terminating at position +622, towards the end of exon 7 (Fig. 1). The smaller message encoding $mvrf_{167}$ actually terminates downstream of the +622 TAG site due to a frame shift resulting from splicing out of the

```
-189  ctcaggccgtcgctgcggcgctgcgttgcgctgcctgcgcccagggctcgggaggggggcc
-129  gcggaggagccgccccctgcgccccgccccgggtccccgggtccgcgccatggggctctg
 -69  gctgccgccgcccccacgccgccgggctagggccatgcgggcgctcccgcctcgcccc
  -9  cgcggcaccATGAGCCCCCTGCTCCGTCGCCTGCTGCTTGTTGCACTGCTGCAGCTGGCT
                M  S  P  L  L  R  R  L  L  L  V  A  L  L  Q  L  A   -5

  52  CGCACCCAGGCCCCTGTGTCCCAGTTTGATGGCCCCAGCCACCAGAAGAAAGTGGTGCCA
       R  T  Q  A  P  V  S  Q  F  D  G  P  S  H  Q  K  K  V  V  P   16

 112  TGGATAGACGTTTATGCACGTGCCACATGCCAGCCCAGGGAGGTGGTGGTGCCTCTGAGC
       W  I  D  V  Y  A  R  A  T  C  Q  P  R  E  V  V  V  P  L  S   36

 172  ATGGAACTCATGGGCAATGTGGTCAAACAACTAGTGCCCAGCTGTGTGACTGTGCAGCGC
       M  E  L  M  G  N  V  V  K  Q  L  V  P  S  C  V  T  V  Q  R   56

 232  TGTGGTGGCTGCTGCCCTGACGATGGCCTGGAATGTGTGCCCACTGGGCAACACCAAGTC
       C  G  G  C  C  P  D  D  G  L  E  C  V  P  T  G  Q  H  Q  V   76

 292  CGAATGCAGATCCTCATGATCCAGTACCCGAGCAGTCAGCTGGGGGAGATGTCCCTGGAA
       R  M  Q  I  L  M  I  Q  Y  P  S  S  Q  L  G  E  M  S  L  E   96

 352  GAACACAGCCAATGTGAATGCAGACCAAAAAAAAAAGGAGAGTGCTGTGAAGCCAGACAGG
       E  H  S  Q  C  E  C  R  P  K  K  K  E  S  A  V  K  P  D  R  116

 412  GTTGCCATACCCCACCACCGTCCCCAGCCCCGCTCTGTTCCGGGCTGGGACTCTACCCCG
       V  A  I  P  H  H  R  P  Q  P  R  S  V  P  G  W  D  S  T  P  136

 472  GGAGCATCCTCCCCAGCTGACATCATCCATCCCACTCCAGCCCCAGGATCCTCTGCCCGC
       G  A  S  S  P  A  D  I  I  H  P  T  P  A  P  G  S  S  A  R  156
                                                S  P  R  I  L  C  P  122

 532  CTTGCACCCAGCGCCGTCAACGCCCTGACCCCCGGACCTGCCGCTGCCGCTGCAGACGCC
       L  A  P  S  A  V  N  A  L  T  P  G  P  A  A  A  A  A  D  A  176
       P  C  T  Q  R  R  Q  R  P  D  P  R  T  C  R  C  R  C  R  R  142

 592  GCCGCTTCCTCCATTGCCAAGGGCGGGGCTTAGAGCTCAACCCAGACACCTGTAGGTGCC
       A  A  S  S  I  A  K  G  G  A  *                              186
       R  R  F  L  H  C  Q  G  R  G  L  E  L  N  P  D  T  C  R  C   162

 652  GGAAGCCGCGAAAGTGAcaagctgctttccagactccacgggcccggctgcttttatggc

       R  K  P  R  K  *  ....                                       167

 712  cctgcttcacagggagaagagtggagcacaggcgaacctcctcagtctgggaggtcactg
 772  ccccaggacctggacctttagagagctctctcgccatcttttatctcccagagctgcca
 832  tctaacaattgtcaaggaacctcatgtctcacctcaggggccagggtactctctcactta
 892  accaccctggtcaagtgagcatctttctggctggctgtctcccctcactatgaaaacccca
 952  aacttctaccaataacgggatttgggttctgttatgataactgtgacacacacacacact
1012  cacactctgataaaagagatggaagacactaacaaaaaaaaaaaaaaaaaaaaaaaaa
```

FIG. 1. Nucleotide and predicted peptide sequences derived from murine *vrf* cDNA clones. Numbering of nucleotides is given on the left, starting from the A of the initiation codon. Amino acids are numbered on the right, starting from the first residue of the predicted mature protein after the putative signal peptide has been removed. The alternately spliced region is double underlined and the resulting peptide sequence from each mRNA is included. A potential polyadenylation signal is indicated in boldface. Start and stop codons of $mvrf_{167}$ and $mvrf_{186}$ are underlined and a polymorphic AC repeat in the 3' UTR is indicated by a stippled box. The positions of intron/exon boundaries are indicated by arrowheads.

101bp exon 6 and the introduction of a stop codon (TGA) at position +666, near the beginning of exon 8 (Fig. 1).

The $mvrf_{186}$ protein has strong homology to the amino and central portions of VEGF while the carboxyl end is completely divergent and is alanine rich. The $mvrf_{167}$ possesses these similarities

A

```
hVRF167   -21 MSPLLRRL
mvrf167   -21 MSPLLRRL
hVRF167    30 EVVVPLTV
mvrf167    30 EVVVPLSM
hVRF167    80 ILMIRYPS
mvrf167    80 ILMIQYPS
hVRF167   130 RPDPRTCR
mvrf167   130 RPDPRTCR
```

B

```
hVRF186   116 RAATPHHF
mvrf186   116 RVAIPHHF
hVRF186   166 TPGPAAAA
mvrf186   166 TPGPAAAA
```

FIG. 2. BESTFIT alignments of hum $hVRF_{186}$ from the point where the sequ are marked with vertical bars and conser site of human and murine VRF.

```
mvrf167    -21 MSPLLRI
mvegf188   -26 MNFLLSI
mvrf167     25 TCQPRE
mvegf188    24 YCRPIE
mvrf167     75 QVRMQI
mvegf188    74 NITMQII
mvrf167    119 ......
mvegf188   124 QKRKRK
mvrf167    152 GLELNP
mvegf188   173 QLELNE
```

FIG. 3. BESTFIT alignment of mv cleavage site of mvegf. Identical amir Numbering of amino acids is as descril

```
agggctcgggaggggggcc
ccgcgccatggggctctg
gctcccggcctcgcccc
GCACTGCTGCAGCTGGCT
 A  L  L  Q  L  A   -5
CAGAAGAAAGTGGTGCCA
 Q  K  K  V  V  P   16
GTGGTGGTGCCTCTGAGC
 V  V  V  P  L  S   36
TGTGTGACTGTGCAGCGC
 C  V  T  V  Q  R   56
ACTGGGCAACACCAAGTC
 T  G  Q  H  Q  V   76
GGGGAGATGTCCCTGGAA
 G  E  M  S  L  E   96
GCTGTGAAGCCAGACAGG
 A  V  K  P  D  R   115
GGCTGGGACTCTACCCCG
 G  W  D  S  T  P   136
CCAGGATCCTCTGCCCGC
 P  G  S  S  A  R   156
    R  I  L  C  P   122
GCTGCCGCTGCAGACGCC
 A  A  A  A  D  A   176
    C  R  C  R  R   142
AGACACCTGTAGGTGCC
                    186
 P  D  T  C  R  C   162
ccggctgcttttatggc
                    167
agtctgggaggtcactg
tatctcccagagctgcca
agggtactctctcactta
tcactatgaaaacccca
tgacacacacacacact
aaaaaaaaaaaaaa
```

NA clones. Numbering of nucleotides
mbered on the right, starting from the
een removed. The alternately spliced
included. A potential polyadenylation
derlined and a polymorphic AC repeat
es are indicated by arrowheads.

on +666, near the beginning of

l portions of VEGF while the
167 possesses these similarities

A

```
hVRF167   -21 MSPLLRRLLLAALLQLAPAQAPVSQPDAPGHQRKVVSWIDVYTRATCQPR 29
mvrf167   -21 MSPLLRRLLLVALLQLARTQAPVSQFDGPSHQKKVVPWIDVYARATCQPR 29

hVRF167    30 EVVVPLTVELMGTVAKQLVPSCVTVQRCGGCCPDDGLECVPTGQHQVRMQ 79
mvrf167    30 EVVVPLSMELMGNVVKQLVPSCVTVQRCGGCCPDDGLECVPTGQHQVRMQ 79

hVRF167    80 ILMIRYPSSQLGEMSLEEHSQCECRPKKKDSAVKPDSPRPLCPRCTQHHQ 129
mvrf167    80 ILMIQYPSSQLGEMSLEEHSQCECRPKKKESAVKPDSPRILCPPCTQRRQ 129

hVRF167   130 RPDPRTCRCRCRRRSFLRCQGRGLELNPDTCRCRKLRR* 167
mvrf167   130 RPDPRTCRCRCRRRRFLHCQGRGLELNPDTCRCRKPRK* 167
```

B

```
hVRF186   116 RAATPHHRPQPRSVPGWDSAPGAPSPADITHPTPAPGPSAHAAPSTTSAL  165
mvrf186   116 RVAIPHHRPQPRSVPGWDSTPGASSPADIIHPTPAPGSSARLAPSAVNAL  165

hVRF186   166 TPGPAAAAADAAASSVAKGGA* 186
mvrf186   166 TPGPAAAAADAAASSIAKGGA* 186
```

FIG. 2. BESTFIT alignments of human and murine VRF protein isoforms. (A) $mvrf_{167}$ and $hVRF_{167}$. (B) $mvrf_{186}$ and $hVRF_{186}$ from the point where the sequences diverge from the respective 167 amino acid isoforms. Amino acid identities are marked with vertical bars and conserved amino acids with colons. An arrow marks the predicted signal peptide cleavage site of human and murine VRF.

```
mvrf167    -21 MSPLLRRL..LLVALLQL..AR.TQAPVSQFDGPSHQKKVVPWIDVYARA 24
mvegf188   -26 MNFLLSWVHWTLALLLYLHHAKWSQAAPTT.EGEQKSHEVIKFMDVYQRS 23

mvrf167    25 TCQPREVVVPLSMELMGNVVKQLVPSCVTVQRCGGCCPDDGLECVPTGQH 74
mvegf188   24 YCRPIETLVDIFQEYPDEIEYIFKPSCVPLMRCAGCCNDEALECVPTSES 73

mvrf167    75 QVRMQILMIQYPSSQ.LGEMSLEEHSQCECRPKKKESAVKPDSPR..... 118
mvegf188   74 NITMQIMRIKPHQSQHIGEMSFLQHSRCECRPKKDRTKPEKKSVRGKGKG 123

mvrf167   119 .............ILCPPCTQRRQR...PDPRTCRCRCRRRRFLHCQGR 151
mvegf188  124 QKRKRKKSRFKSWSVHCEPCSERRKHLFVQDPQTCKCSCKNTDS.RCKAR 172

mvrf167   152 GLELNPDTCRCRKPRK                                   167
mvegf188  173 QLELNERTCRCDKPRR                                   188
```

FIG. 3. BESTFIT alignment of $mvrf_{167}$ and $mvegf_{188}$ [20] protein sequences. An arrow marks the signal peptide cleavage site of mvegf. Identical amino acids are indicated by vertical bars and conservative substitutions by colons. Numbering of amino acids is as described in the legend to Figure 1.

TABLE I
Splice Junctions of the Murine *vrf* Gene

5′ UTR*.....	Exon 1 >249bp	CCCAGgtacgtgcgt	Intron I	395bp
tttccacagGCCCC	Exon 2 43bp	GAAAGgtaataatag	Intron II	288bp
ctgcccacagTGGTG	Exon 3 197bp	TGCAGgtaccagggc	Intron III	196bp
ctgagcacagATCCT	Exon 4 74bp	TGCAGgtgccagcca	Intron IV	182bp
ctcttttcagACCAA	Exon 5 36bp	GACAGgtgagtttt	Intron V	191bp
ctcctcctagGGTTG	Exon 6 101bp		(no intron)	
CCCACTCCAGCCCCA	Exon 7 135bp	TGTAGgtaaggagtc	Intron VI	~220bp
cactccccagGTGCC	Exon 8 398bp	ATGGAAGACACTAAC		

Uppercase and lowercase letters denote exonic and intronic sequences, respectively. *Indicates that the 5′ end of exon 1 has not yet been determined.

and also maintains homology to mvegf right through to the C-terminus (Fig. 3). The overall homology of $mvrf_{167}$ to $hVRF_{167}$ was 86% identity and 92% similarity respectively (Fig. 2). Likewise, homology between $mvrf_{167}$ and mvegf [20] was 49% identity and 71% conservative amino acid substitution respectively (Fig. 3).

A canonical vertebrate polyadenylation signal (AATAAA) [21] was not present in the *vrf* cDNA, however, the closely matching sequence GATAAA is present at similar positions in both mouse and human *VRF* cDNAs (Fig. 1). In contrast to human *VRF*, murine *vrf* was found to contain an AC dinucleotide repeat at the extreme 3′ end of the 3′ UTR (nucleotide positions 997 to 1010, Fig. 1). Polymorphism of this repeat region was observed between some of the *vrf* cDNAs, with the number of dinucleotides varying from 7 to 11 (results not shown).

Genomic Characterisation of Murine vrf

Intron/exon boundaries (Table I) were mapped using primers which flanked sequences homologous to the corresponding human *VRF* boundaries [16]. Introns I, III, IV and VI of murine *vrf* (Table I, Fig. 4) were smaller than the hVRF intervening sequences [16]. There was complete concordance between the human *VRF* and murine *vrf* genes with respect to lengths of each of the exons. The complete genomic sequence was compiled from the 5′ UTR of *vrf* through to intron VI, the largest intervening region (2.2kb), by sequencing amplified introns and cloned genomic portions of *vrf* (data not shown).

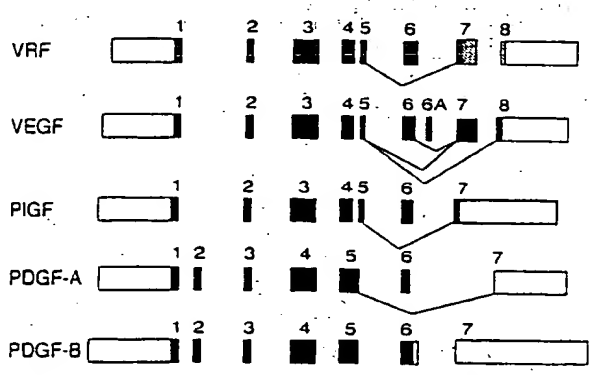

FIG. 4. Comparison of gene structure between VRF (a generic VRF gene is shown since the intron/exon organization of the mouse and human homologs is identical) and other members of the human VEGF/PIGF/PDGF gene family. Exons are represented by boxes. Protein coding regions and untranslated regions are shown by filled and open sections, respectively. The hatched region in VRF indicates the additional 3′ UTR sequence formed by alternate splicing of the VRF_{206} isoform. Potential alternate splice products of each gene are shown.

FIG. 5. Autoradiogram of a Northe
a murine *vrf* cDNA clone. A major tr

Exons 6 and 7 are contiguou
strong sequence homology at th
in the first half of Fig. 2B) sugg
encodes a functional part of th

General intron/exon structur
of the VEGF gene family and t
the murine *vrf* gene is very sin

Previous comparative mapp
multiple endocrine neoplasia ty
the proximal segment of mouse
to within 1Mb of the human *M.*
the centromere of chromosome

Expression Studies of vrf

Northern analysis of RNA fr
expression appears to be ubiqu
in size (Fig. 5). This is somew
major bands of 2.0 and 5.5kb t
message presumably correspor
thereof is most likely due to a

This work was supported by the Nat
Ltd., and the Swedish Cancer Foundat

1. Sharkey, A. M., Charnock-Jones, I
609–615.
2. Yan, Z., Weich, H. A., Bernart, W
3. Plate, K. H., Greier, G., Weich, H
4. Kim, K. J., Lane, B. L., Winer, J.,
5. Christofori, G., Naik, P., and Han
6. Aiello, L. P., Avery, R. L., Arrigg,
M. A., Park, J. E., Nguyen, H. V.,
7. Koch, A. E., Harlow, L. A., Haine
(1994) *J. Immunol.* 152, 4149–41
8. Leung, D. W., Cachianes, G., Kuc

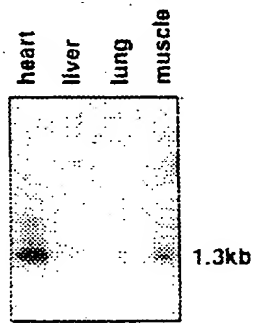

FIG. 5. Autoradiogram of a Northern blot of total RNA from various adult mouse tissues (as indicated) hybridized with a murine *vrf* cDNA clone. A major transcript of 1.3kb was detected in all samples.

Exons 6 and 7 are contiguous in *vrf*, as has been found to occur in the human homolog [16]. The strong sequence homology at the amino acid level between exon 6 of *vrf* and human *VRF* (depicted in the first half of Fig. 2B) suggests that this sequence is not a retained intronic sequence but rather encodes a functional part of the vrf$_{186}$ isoform.

General intron/exon structure is conserved between the various members (VEGF, PlGF, VRF) of the VEGF gene family and therefore it is not surprising that the overall genomic organisation of the murine *vrf* gene is very similar to these genes (Fig. 4).

Previous comparative mapping studies have shown that the region surrounding the human multiple endocrine neoplasia type I (*MEN1*) disease locus on chromosome 11q13 is syntenic with the proximal segment of mouse chromosome 19 [22]. Since we have mapped the human *VRF* gene to within 1Mb of the human *MEN1* locus [16], it is most likely that the murine *vrf* gene maps near the centromere of chromosome 19.

Expression Studies of vrf

Northern analysis of RNA from adult mouse tissues (muscle, heart, lung, and liver) showed that expression appears to be ubiquitous and occurs primarily as a major band of approximately 1.3kb in size (Fig. 5). This is somewhat different to the pattern observed for human *VRF* in which two major bands of 2.0 and 5.5kb have been identified in all tissues examined [16]. The 1.3kb murine message presumably corresponds to the shorter of the human transcripts and the size variation thereof is most likely due to a difference in the length of the respective 5′ UTRs.

ACKNOWLEDGMENTS

This work was supported by the National Health and Medical Research Council of Australia, AMRAD Operations Pty. Ltd., and the Swedish Cancer Foundation.

REFERENCES

1. Sharkey, A. M., Charnock-Jones, D. S., Boocock, C. A., Brown, K. D., and Smith, S. K. (1993) *J. Reprod. Fertil.* 99, 609–615.
2. Yan, Z., Weich, H. A., Bernart, W., Breckwoldt, M., and Neulen, J. (1993) *J. Clin. Endocrinol. Metab.* 77, 1723–1725.
3. Plate, K. H., Greier, G., Weich, H. A., and Risau, W. (1992) *Nature* 359, 845–848.
4. Kim, K. J., Lane, B. L., Winer, J., Armanini, Gillett N., Phillips, H. S., and Ferrara, N. (1993) *Nature* 362, 841–846.
5. Chrisofori, G., Naik, P., and Hanahan, D. (1994) *Nature* 369, 414–418.
6. Aiello, L. P., Avery, R. L., Arrigg, P. G., Keyt, B. A., Jampel, H. D., Shah, S. T., Pasquale, L. R., Thieme, H., Iwamoto, M. A., Park, J. E., Nguyen, H. V., Aiello, L. M., Ferrara, N., and King, G. L. (1994) *N. Engl. J. Med.* 331, 1480–1487.
7. Kochs, A. E., Harlow, L. A., Haines, G. K., Amento, E. P., Unemori, E. N., Wong, W. L., Pope, R. M., and Ferrara, N. (1994) *J. Immunol.* 152, 4149–4156.
8. Leung, D. W., Cachianes, G., Kuang, W. J., Goeddel, D. V., and Ferrara, N. (1989) *Science* 246, 1306–1309.

9. Keck, P. J., Hauser, S. D., Krivi, G., Sanzo, K., Warren, T., Feder, J., and Connolly, D. T. (1989) *Science* 246, 1309–1312.
10. Maglione, D., Guerriero, V., Viglietto, G., Delli-Bovi, P., and Persico, M. G. (1991) *Proc. Natl. Acad. Sci. USA* 88, 9267–9271.
11. Ferrara, N., Houck, K., Jakeman, L., and Leung, D. W. (1992) *Endocrine Rev.* 13, 18–32.
12. Senger, D. R., Van de Water, L., Brown, L. F., Nagy, J. A., Yeo, K. T., Yeo, T. K., Berse, B., Jackman, R. W., Dvorak, A. M., and Dvorak, H. F. (1993) *Cancer Metastasis Rev.* 12, 303–324.
13. DiSalvo, J., Bayne, M. L., Conn, G., Kwok, P. W., Trivedi, P. G., Soderman, D. D., Palisi, T. M., Sullivan, K. A., and Thomas, K. A. (1995) *J. Biol. Chem.* 270, 7717–7723.
14. Houck, K. A., Ferrara, N., Winer, J., Cachianes, G., Li, G., and Leung, D. W. (1991) *Mol. Endocrinol.* 5, 1806–1814.
15. Tischer, E., Mitchell, R., Hartman, T., Silva, M., Gospodarowicz, D., Fiddes, J. C., and Abraham, J. A. (1991) *J. Biol. Chem.* 266, 11947–11954.
16. Grimmond, S., Lagercrantz, J., Drinkwater, C., Silins, G., Townson, S., Pollock, P., Gotley, D., Carson, E., Raker, S., Nordenskjöld, M., Ward, L., Hayward, N., and Weber, G. (1995) *Genome Res.* in press.
17. Church, G., and Gilbert, W. (1984) *Proc. Natl. Acad. Sci. USA.* 18, 1991–1995.
18. Santos, M. A. (1991) *Nucleic Acids Res.* 19, 5442.
19. Chomczynski, P., and Sacchi, N. (1987) *Analyt. Biochem.* 162, 156–159.
20. Breier, G., Albrecht, U., Sterrer, S., and Risau, W. (1992) *Development* 114, 521–532.
21. Birnstiel, M. L., Busslinger, M., and Strub, K. (1985) *Cell* 41, 349–359.
22. Rochelle, J. M., Watson, M. L., Oakey, R. J., and Seldin, M. F. (1992) *Genomics* 14, 26–31.

BIOCHEMICAL AND BIOPHYSICAL RESEARCH
ARTICLE NO. 0508

A Novel Use for Cooma Procedure and As

A

Department of Pharmacolo

The present study provides an separated using sodium dodecyl su with coomassie brilliant blue (R-2 membranes. This method exhibitec shrinkage of gel). 2) it allowed as time of gel-drying procedure by a proteins with the same efficiency method is simple, economical and

Coomassie brilliant blue (R-: (1–7), thin layer chromatograph protein concentrations (11–13). storage. However, gels shrink a gel-drying procedure is laboriou replace the conventional methoc age problems. In this study, usi gel drying process can be elimir Also, the described procedure h

Materials. Nitrocellulose membranes glycine leupeptin, aprotonin, soybean purchased from Sigma Chemical Co. (S rats were purchased from Harlan Sprag

Preparation of rat brain protein extra 0.5 mM EGTA, 1 mM EDTA, 2 mM dit soybean trypsin inhibitor). The total hor resulting supernatant was solubilized wi 0.05% (v/v) 2-β-mercaptoethanol, and electrophoresis as described below.

Gel electrophoresis and electroblottin 7.5% acrylamide. Gels were stained with acetic acid and 20% methanol) for 1/2 for 10–15 minutes. Stained gels were e methanol) for 15 minutes and electrobl lulose membranes were washed briefly i photographed using a Nikon camera.

Amidoblack staining of membranes. 10% acetic acid and 45% methanol and

[1] To whom correspondence should b Department of Pharmacology, 3500 Ca

COMMONWEALTH OF AUSTRALIA

(Patents Act 1990)

IN THE MATTER OF: Australian Patent Application 696764 (73941/94). In the name of: Human Genome Sciences Inc.

- and -

IN THE MATTER OF: Opposition thereto by Ludwig Institute for Cancer Research, under Section 59 of the Patents Act.

Annexure GBC-3

This is **Annexure GBC-3** referred to in my Statutory Declaration made this Thirteenth day of December 2000.

Gary Baxter Cox

WITNESS: Peyti Kuo

Patent Attorney PEYTEE KUO

BIOCHEMICAL AND BIOPHYSICAL RESEARCH COMMUNICATIONS 230, 413–418 (1997)
ARTICLE NO. RC965979

Analysis of the Promoter Region of the Human VEGF-Related Factor Gene[1]

Ginters Silins,*[,2] Sean Grimmond,* Mark Egerton,† and Nicholas Hayward*
*Queensland Cancer Fund Research Unit, Joint Experimental Oncology Program and †Transplantation Biology Unit, Queensland Institute of Medical Research, Herston, Queensland 4029, Australia

Received December 9, 1996

We have characterised the promoters of the human and murine *VRF* (vascular endothelial growth factor (VEGF) related factor) gene. A series of deletions were made of a 553-bp region 5′ of the *VRF* initiation codon and were used in a luciferase reporter gene assay to determine the minimal promoter of the *VRF* gene. The region between base pairs −443 and −195 was sufficient to mediate transcription in lymphocytes and the region between −550 and −443 enhanced this promoter activity. Primer extension studies identified two regions of transcription initiation, both of which are preceded by Sp1, AP-2 and Egr-1 transcription factor binding sites. The *VRF* promoter is similar to *VEGF* in that it is associated with a CpG island, contains sites for Sp1 and AP-2, and lacks a TATA box. However, it has marked differences in that the promoter contains Egr-1 sites and lacks both hypoxia-inducible factor-1 and AP-1 sites. These data may indicate that expression of these two growth factors is regulated by different physiological stimuli. © 1997 Academic Press

We recently described the characterisation of a new member of the vascular endothelial cell growth factor (VEGF) gene family which we called *VRF* for VEGF-related growth factor [1, 2], but which is also known as *VEGFB* [3]. To date, this family of growth factors consists of VEGFA/VEGF/VPF [4, 5], VEGFB/VRF [1-3], VEGFC/VRP [6, 7], placenta growth factor [8], as well as the more distantly related platelet-derived growth factor (PDGFs) A and B [9].

The intron-exon architecture of human *VRF* and murine *Vrf* [1, 2] are similar to that of *VEGFA*, and although only two alternately spliced forms of *VRF* have been identified (that give rise to proteins with different carboxyl tails), more isoforms are expected based on the gene's similarity to *VEGFA*. VRF has a wide tissue distribution in adults [1-3] and expression during mouse fetal development has been shown to be most abundant in heart, spinal cord, cerebral cortex and brown fat [10]. *VEGFA*, in comparison, is chiefly expressed in brain, kidney, liver, lung, spleen, as well as heart [11-13]. The expression pattern of these genes appears to be quite distinct, although specific roles for VEGFA and VRF/VEGFB in vasculogenic and angiogenic events have yet to be distinguished.

As a first step to understanding the regulation of *VRF* gene expression, we have characterised the promoters of the human (*VRF*) and murine (*Vrf*) genes. Reporter gene assays and primer extension studies were employed in identifying the minimal promoter region of *VRF*, and analysis of transcription factor binding motifs revealed that although the *VRF* and *VEGFA* promoters share common elements, there are also marked differences between the two promoters.

MATERIALS AND METHODS

Cloning, nucleotide sequencing and analysis. The cloning of genomic fragments containing the human *VRF* [1] and murine *Vrf* genes [2] have been reported previously. A *Pst*I-restriction fragment containing part of the first coding exon of *VRF* plus the 5′ flanking region (that included the 3′ end of a novel gene (manuscript in preparation)) was subcloned from cosmid cCLGW4 [1]. Both nested deletions (Erase-a-base, Promega) and cloned restriction fragments of the region were sequenced on both strands as described previously [1, 2].

The cloning of a phage genomic clone (λ121) containing the mouse *Vrf* gene has been reported previously [2]. Two *Nco*I-restriction fragments from λ121 that collectively spanned exon 3 to the 5′ flanking region were blunt-ended and cloned into the *Eco*RV site of pBluescript II KS (Stratagene) and sequenced as described for *VRF*. The sequence data were compiled using MacVector 4.2.1 software (IBI-Kodak). ClustalW [14], CpGPlot (GCG, Wisconsin), Sigscan [15] and BLAST [16] analyses were conducted using the Australian National

[1] Sequences presented in this article have been submitted to the GENBANK database and appear under accession numbers U80601 and U80602.

[2] To whom correspondence should be sent at Queensland Institute of Medical Research, P.O. Royal Brisbane Hospital, Herston 4029, Australia. Fax: (61) 7 3362 0107; E-mail: gintS@qimr.edu.au.

Abbreviations: HIF-1 - hypoxia-inducible factor-1; PDGF - platelet derived growth factor; UTR - untranslated region; VEGF - vascular endothelial growth factor; *VRF* - human VEGF-related factor gene; *Vrf* - murine VEGF-related factor gene.

0006-291X/97 $25.00

Genome Information Service computer faculty at the University of Sydney, Australia.

Primer extension analysis. The oligonucleotide 5' - TCC CGA GCC CTG GGT GCA G-3' was radiolabelled with [γ-^{32}P]ATP (6000Ci mmol^{-1}, Amersham) and T4 polynucleotide kinase (New England Biolabs). 5ng of labelled primer (1μl) were annealed to 60μg of total RNA in 10μl of annealing buffer consisting of 250mM KCl and 10mM Tris-HCl, pH 8.3. Total RNA was isolated from a lymphoblastoid cell line using an RNeasy Total RNA Kit (Qiagen). Annealing proceeded at 80°C for 5 min and then at 58°C for 45 min. First strand synthesis was allowed to proceed at 52°C for 45 min after the addition of 22.4μl of a reverse-transcription mix consisting of 3mM $MgCl_2$, 47mM Tris-HCl, pH 8.3, 10mM dithiothreitol, 0.5mM dNTP mix and 200U of Superscript II RNaseH- reverse transcriptase (GIBCO, BRL). The RNA component was hydrolysed, the cDNA was precipitated, resuspended, resolved on an 8M urea/6% polyacrylamide gel and visualised by autoradiography. The primer extension product sizes were estimated by comparison to a sequencing ladder generated from pGEM-3zf(+) (Promega) with the pUC/M13 forward primer (fmol DNA Sequencing System, Promega).

Human VRF *promoter constructs.* The most proximal 45bp of the first coding exon ending at a *PstI* site (GENBANK accession number U43370) plus varying lengths of 5' flanking region derived from the human *PstI* genomic clone were inserted into the polylinker of the pGL2-basic luciferase vector (Promega). Restriction sites within this genomic *PstI* fragment were utilised in generating directional deletions of the region. These included, (in addition to the full-length *PstI* fragment shown in Fig. 1), the *SacI* site (position −550), the *BstXI* site (position −443), the *EagI* site (position −195) and the *NcoI* site (position −85).

Transfections and measurements of luciferase activity. 4×10^6 EL4 T cells were suspended in 400μl RPMI 1640 tissue culture medium supplemented with 2mM glutamine and 20mM Hepes pH 7.2, and electroporated with 5μg of each luciferase reporter construct, or with 5μg empty pGL2-basic vector as a background control. Pulse conditions were 290V, 960μF. Electroporated cells were transferred to 10ml DMEM supplemented with 8% fetal calf serum, 2mM glutamine and 50μM β-mercaptoethanol, and grown for 24hr at 37°C in 5% CO_2 prior to harvesting. Harvested cells were washed in phosphate-buffered saline, and lysates prepared and assayed for luciferase activity using a Luciferase Assay Kit (Promega), according to the manufacturer's instructions. Luciferase activity was measured using a Packard Microplate Scintillation Counter. The protein content of each sample was measured by Bradford Assay (BioRad, Hercules CA), and values ranged from 42-68μg per sample. All data have been normalised to 50μg protein.

RESULTS AND DISCUSSION

Sequence Analysis of VRF

Sequence data for the open reading frame of *VRF* plus an adjacent 60bp of the 5' UTR have been reported previously [1]. We have extended the sequence of the 5' flanking region up to the transcribed region of a novel neighbouring gene as shown in Fig. 1. The program BLASTN identified nucleotide positions −629 to −553 as matching the 3' UTR of several cDNA entries from the expressed sequence tag database, complete with a polyadenylation signal (AATAAA) beginning at position −570 (manuscript in preparation). The promoter of *VRF* was therefore expected to reside downstream of this region.

The cloning and partial characterisation of *Vrf* has been published by Townson et al. [2]. The previously reported 5' UTR of 189bp was extended an additional ~440bp up to the 3' UTR of the neighbouring gene (Fig. 1). (Note that 3 nucleotide discrepancies with respect to our previously described 5' UTR sequence have been corrected in the updated GENBANK entry U43836). Nucleotide sequences for the 5' flanking regions of the *VRF* and *Vrf* genes are aligned in Fig. 1 and show ~70% identity over this region. The sequences are G+C rich (~85% human, ~79% mouse) downstream of the 3' UTR of the neighbouring gene and contain a high frequency of CpG dinucleotides. Fig. 2 shows that the promoter of *VRF* coincides with a CpG island that spans the entire length of the region upstream of the initiation codon (Fig. 1). *VEGFA*, *PDGF A* and *B*, as well as numerous other growth factor genes (as discussed in [17]) also have G+C rich 5' UTRs.

Human *VRF* has three additional, apparently non-utilised ATG codons (positions −37, −83, −296) upstream of the reported translation start site (position +1). This start site was identified on the basis of sequence homology to *VEGFA* as well as matching the Kozak consensus sequence for vertebrate translation initiation sites [1]. The three non-utilised ATG codons are also conserved in *Vrf* (positions −37, −83, −306) and the latter two are not in-frame with the translation initiation site in either organism. The ATG codon at position −296 in *VRF* is also out of frame, but translation from the equivalent ATG codon from *Vrf* (position −306) would extend the reported murine protein by an additional 102 amino acids [2]. However, primer extension studies with *VRF* (discussed below) predict that this ATG codon overlaps one region of transcription initiation and is therefore unlikely to be present in a large proportion of *VRF* transcripts.

The possible function of these upstream ATG codons is unknown, however, they may play a role in translational control as has been suggested in the case of the genes encoding the A- and B- chains of PDGF which have also been reported to each have three additional ATG codons [18]. Similarly, a second conserved ATG codon appears within the 5' UTR of human [17], mouse [19] and rat [20] *VEGFA*.

Reporter Gene Assays

In order to define the proximal promoter of *VRF*, restriction sites within the 5' flanking region (shown in Fig. 1) were used to generate successive deletions from within the 3' UTR of the neighbouring gene towards the transcription start site of *VRF*. These restriction fragments were directionally cloned into the promoterless vector pGL2, transiently transfected into lymphocytes, and assayed for luciferase activity. The results from each of three experiments showed a similar trend (Fig. 3), with the *PstI* construct (Fig. 3, A: *PstI*) that spans the coding region of *VRF* exon 1 to the

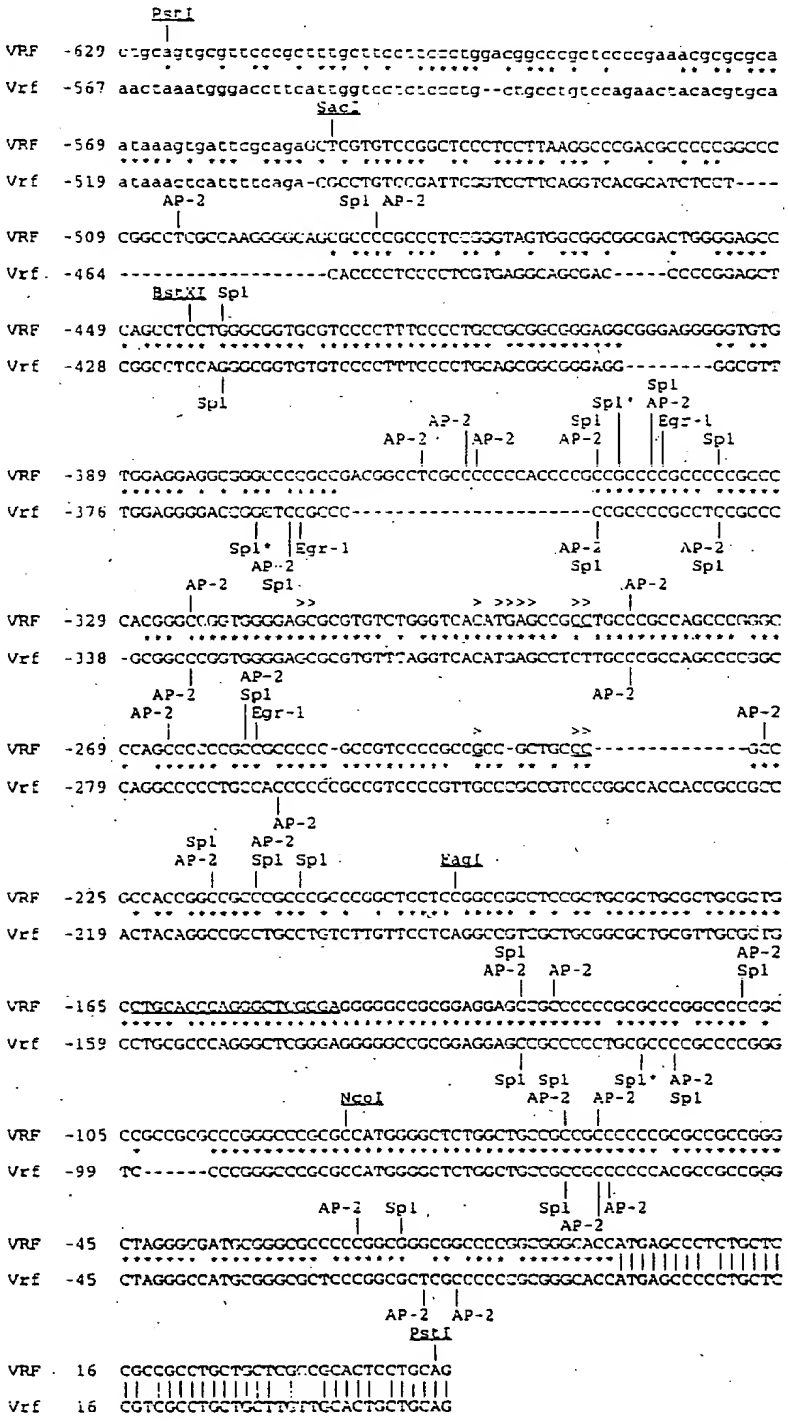

FIG. 1. Nucleotide sequence alignment of human (*VRF*) and murine (*Vrf*) *VRF* 5′ flanking regions using the program ClustalW, where an asterisk denotes a conserved nucleotide position and a vertical line indicates conservation within the open reading frame. The *VRF* start codon is designated position +1. The 3′ UTR of the neighbouring gene is represented in lower case lettering. Restriction sites used in generating the promoter constructs are labelled. Positions of the transcription start sites as determined by primer extension studies are shown by the symbol ">" and the major sites are underlined. The position of the oligonucleotide used for primer extension is underlined. Starting positions of the consensus binding sites for the transcription factors Sp1, "strong" Sp1 (*), AP-2 and Egr-1 are labelled and described in the text.

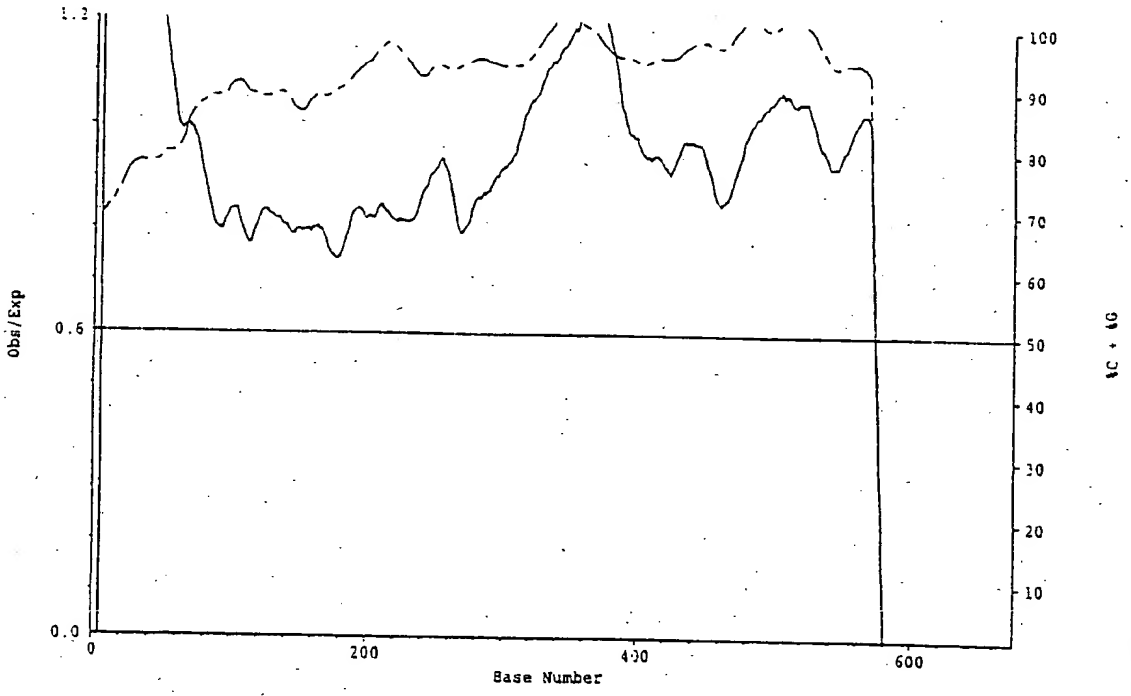

FIG. 2. CpGPlot of the *VRF* promoter region (based on the sequence of Fig. 1). Plot of Obs/Exp CpG dinucleotide (solid line) and %(G+C) (broken line) against the position in the nucleotide sequence. The CpG island of the *VRF* gene meets the criteria described by Larsen et al. [25] (>200bp region; moving average %(G+C) > 50; moving Obs/Exp CpG > 0.6).

3′ UTR of the neighbouring gene, producing a 1.6 to 9.6-fold increase in luciferase activity over background levels. The *Sac*I deletion construct (Fig. 3, B-*Sac*I) produced the highest promoter activity (3.8 to 12.9-fold increase), presumably because the polyadenylation signal (and possibly other *cis*-acting elements involved in transcription termination) from the neighbouring gene had been removed. The *Bst*XI deletion construct (Fig. 3, C-*Bst*XI) produced a lower (28-47%) promoter activity compared to the *Sac*I construct, but roughly equivalent to the activity observed for the *Pst*I construct. The *Eag*I and *Nco*I deletion constructs (Fig. 3, D-*Eag*I, E-*Nco*I) had luciferase activities at background levels. We therefore conclude that the 248bp region between *Bst*XI (position −443) and *Eag*I (position −195) is sufficient to promote basal transcription of the *VRF* gene in lymphocytes, and that the 108-bp region upstream of this (up to the *Sac*I site at position −50) is necessary for maximal basal activity.

Primer Extension Analysis, Structural Analyses of the Promoter Region

Primer extension analysis, using an antisense oligonucleotide designed to anneal downstream (positions −146 to −164) of the minimal promoter region was employed to identify the 5′ end of the human *VRF* transcript. These assays consistently demonstrated the *VRF* gene to have two major regions of transcription initiation, although additional start sites were observed on longer exposure of the autoradiographs (Fig. 4). The first region of transcription initiation consisted of a cluster of sites between positions −229 and −238 (Fig. 1). A second and more frequently used cluster of transcription initiation sites appeared between positions −313 to −287, suggesting a maximum 5′ UTR length of 313bp that is highly conserved (~84%) in the murine gene. The *VRF* 5′ UTR is therefore much shorter in length than that of the *VEGFA* gene [17].

The mouse and human *VRF* promoter regions were scanned for consensus transcription factor binding sites using the program Sigscan. Sites that potentially play a role in the regulation of *VRF* gene expression, or that have been reported for *VEGFA* [18, 19, 20], are shown in Fig. 1. The region of transcription initiation between positions −313 and −287 is preceded by multiple consensus sites for Sp1 (5′-CCGCCC-3′ or its complement [21, 22]) and AP-2 (5′-T/CCC/GCCA/CNC/GC/GC/G-3′ or its complement [23]), as well as a single site for Egr-1 (5′-GCGGGGGCG-3′ or its complement [24]). Sites for Sp1, AP-2 and Egr-1 are also found clustered in a similar position in the mouse gene. The same combination of sites (in the human but not in the mouse gene) precede the downstream region of transcription initia-

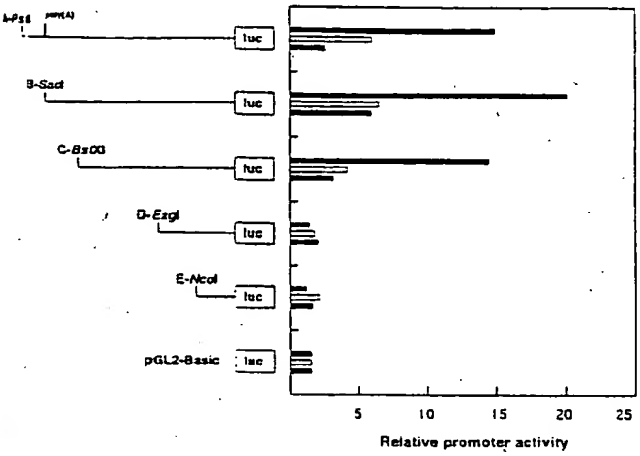

FIG. 3. Determination of the *VRF* minimal promoter region. Sections of the *VRF* 5′ flanking region were cloned into the pGL2 luciferase vector and assayed for their ability to induce luciferase activity in EL4 T cells. The position of the poly(A) tail for the neighbouring gene is shown in construct A and the exact locations of the restriction sites are shown in Fig. 1. Relative promoter activities for the constructs based on triplicate experiments are represented by different shadings.

tion (positions −265 to −209). Examination of the highly conserved *Bst*XI to *Eag*I region of *VRF* and *Vrf* revealed additional Sp1 and AP-2 sites. The Sp1 site at position −344 in the human gene (position −364 in mouse) is also a perfect match to the "strong" Sp1 consensus 5′-G/AC/TC/TCCGCCCC/A-3′ that has been reported for some of the Sp1 sites within the *VEGFA* promoter [17]. Indeed, the promoters of *VEGFA* and *VRF* appear to be organised similarly with respect to Sp1 and AP-2 sites, and both promoters are associated with a CpG island (data not shown for *VEGFA*), which typically encompass the transcription start sites of housekeeping and widely expressed genes [25]. The presence of AP-2 sites is consistent with the observed expression patterns of these genes in tissues of neural origin [10, 26]. As with *VEGFA* [17, 19, 20], a consensus TATA box is absent from the *VRF* proximal promoter.

The promoter of *VRF* also shows potentially important differences to the promoter of *VEGFA*, for example, more than one region of transcription initiation appears to be utilised by *VRF*, and the human and mouse *VEGFA* promoter regions also contain CCAAT boxes upstream of their transcription start sites [17, 19]. Although multiple AP-1-like binding sites were reported for human *VEGFA*, only one consensus AP-1 site, located near to the hypoxia element, is conserved between human, mouse and rat sequences [17, 19, 20]. There is an absence of consensus AP-1 sites (5′-TGANTC/AA-3′ [27]) and sequences resembling the hypoxia-inducible factor (HIF-1: 5′-G/C/TACGTGCG/T-3′ [28]; *VEGFA* HIF-1 match: 5′-TACGTGGG-3′ [20]) in the *VRF* promoter region. However, it is possible that other hypoxia-responsive sequence elements, not related to HIF-1, influence transcription, potentially also from other regions of the gene (such as the 3′ end) as has been reported for *VEGFA* [29].

The human *VRF* promoter has two occurrences of overlapping Egr-1 and Sp1 sites, upstream of the two major regions of transcription initiation. The replacement of Sp1 by Egr-1 at an overlapping site can lead to inducible gene expression, as observed for the *PDGF A* and *B* genes [30, 31]. Overlapping Sp1 and Egr-1 sites, however, are not present in the promoter region of *VEGFA* [17, 19, 20]. Studies of the *PDGF A* and *B* promoter regions infer that *VRF* may utilise novel transcription factor binding sites as well as perhaps

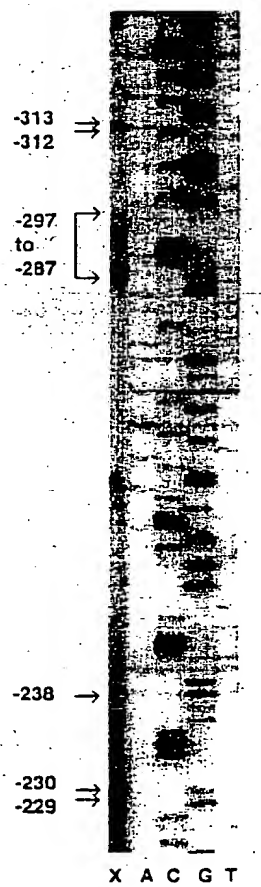

FIG. 4. Mapping of the *VRF* transcription start site using primer extension analysis. Primer extension products (lane labelled X) were generated from lymphoblastoid cell line total RNA using the oligonucleotide shown in Fig. 1 and the sites of transcription initiation are labelled with arrows. The size standard was generated from pGEM−3zf(+) using the pUC/M13 forward primer (lanes G, A, T and C).

non-consensus sites [32, 33]. A candidate region likely to contain these sites is positioned between −404 and −455 of *VRF*, as the region is highly conserved in mouse and precedes the upstream region of transcription initiation.

The findings reported in this paper provide the first insight into the organisation of the *VRF* proximal promoter and address possible differences with respect to the promoter of *VEGFA*. Further studies will be aimed at elucidating the sequence elements important for inducible gene expression, in an effort to understand the role of *VRF* in vasculogenic and angiogenic events.

ACKNOWLEDGMENTS

This work was supported by the National Health and Medical Research Council of Australia, and AMRAD Operations Pty. Ltd. The authors would like to thank Drs G. Weber and C. Larsson for providing cosmid cCLGW4.

REFERENCES

1. Grimmond, S., Lagercrantz, J., Drinkwater, C., Silins, G., Townson, S., Pollock, P., Gotley, D., Carson, E., Rakar, S., Nordenskjöld, M., Ward, L., Hayward, N., and Weber, G. (1996) *Genome Res.* **6**, 124–131.
2. Townson, S., Lagercrantz, J., Grimmond, S., Silins, G., Nordenskjöld, M., Weber, G., and Hayward, N. (1996) *Biochem. Biophys. Res. Commun.* **220**, 922–928.
3. Olofsson, B., Pajusola, K., Kaipainen, A., Von Euler, G., Joukov, V., Saksela, O., Orpana, A., Pettersson, R. F., Alitalo, K., and Eriksson, U. (1996) *Proc. Natl. Acad. Sci. USA* **93**, 2576–2581.
4. Leung, D. W., Cachianes, G., Kuang, W.-J., Goeddel, D. V., and Ferrara, N. (1989) *Science* **246**, 1306–1309.
5. Keck, P. J., Hauser, S. D., Krivi, G., Sanzo, K., Warren, T., Feder, J., and Connolly, D. T. (1989) *Science* **246**, 1309–1312.
6. Joukov, V., Pajusola, K., Kaipainen, A., Chilov, D., Lahtinen, I., Kukk, E., Saksela, O., Kalkkinen, N., and Alitalo, K. (1996) *EMBO J.* **15**, 290–298.
7. Lee, J., Gray, A., Yuan, J., Luoh, S-M., Avraham, H., and Wood, W. I. (1996) *Proc. Natl. Acad. Sci. USA* **93**, 1988–1992.
8. Maglione, D., Guerriero, V., Viglietto, G., Delli-Bovi, P., and Persico, M. G. (1991) *Proc. Natl. Acad. Sci. USA* **88**, 9267–9271.
9. Betsholtz, C., Johnsson, A., Heldin, C.-H., Westermark, B., Lind, P., Urdea, M. S., Eddy, R., Shows, T. B., Philpott, K., Mellor, A. L., Knott, T. J., and Scott, J. (1986) *Nature* **320**, 695–699.
10. Lagercrantz, J., Larsson, C., Grimmond, S., Fredriksson, M., Weber, G., and Piehl, F. (1996) *Biochem. Biophys. Res. Commun.* **220**, 147–152.
11. Breier, G., Albrecht, U., Sterrer, S., and Risau, W. (1992) *Development* **114**, 521–532.
12. Jakeman, L. B., Armanini, M., Phillips, H. S., and Ferrara, N. (1993) *Endocrinology* **133**, 848–859.
13. Monacci, W. T., Merrill, M. J., and Oldfield, E. H. (1993) *Am. J. Physiol.* **264**, C995–1002.
14. Thompson, J. D., Higgins, D. G., and Gibson, T. J. (1994) *Nucleic Acids Res.* **22**, 4673–4680.
15. Prestridge, D. S. (1996) *Comput. Appl. Biosci.* **12**, 157–160.
16. Altschul, S. F., Gish, W., Miller, W., Myers, E. W., and Lipman, D. J. (1990) *J. Mol. Biol.* **215**, 403–410.
17. Tischer, E., Mitchell, R., Hartman, T., Silva, M., Gospodarowicz, D., Fiddes, J. C., Abraham, J. A. (1991) *J. Biol. Chem.* **266**, 11947–11954.
18. Bonthron, D. T., Morton, C. C., Orkin, S. H., and Collins, T. (1988) *Proc. Natl. Acad. Sci. USA* **85**, 1492–1496.
19. Shima, D. T., Kuroki, M., Deutsch, U., Ng, Y.-S., Adamis, A. P., and D'Amore, P. A. (1996) *J. Biol. Chem.* **271**, 3877–3883.
20. Levy, A. P., Levy, N. S., Wegner, S., and Goldberg, M. A. (1995) *J. Biol. Chem.* **270**, 13333–13340.
21. Gidoni, D., Dynan, W. S., and Tjian, R. (1984) *Nature* **312**, 409–413.
22. Kadonaga, J. T., Jones, K. A., and Tjian, R. (1986) *Trends Biochem. Sci.* **11**, 20–23.
23. Imagawa, M., Chiu, R., and Karin, M. (1987) *Cell* **51**, 251–260.
24. Faisst, S., and Meyer, S. (1992) *Nucleic Acids Res.* **20**, 3–26.
25. Larsen, F., Gundersen, G., Lopez, R., and Prydz, H. (1992) *Genomics* **13**, 1095–1107.
26. Mitchell, P. J., Timmons, P. M., Hébert, J. M., Rigby, P. W. J., and Tjian, R. (1991) *Genes Dev.* **5**, 105–119.
27. Lee, W., Mitchell, P., and Tjian, R. (1987) *Cell* **49**, 741–752.
28. Semenza, G. L., Roth, P. H., Fang, H.-M., and Wang, G. L. (1994) *J. Biol. Chem.* **269**, 23757–23763.
29. Minchenko, A., Salceda, S., Bauer, T., and Caro, J. (1994) *Cell. Mol. Biol. Res.* **40**, 35–39.
30. Khachigian, L. M., Lindner, V., Williams, A. J., and Collins, T. (1996) *Science* **271**, 1427–1431.
31. Khachigian, L. M., Williams, A. J., and Collins, T. (1995) *J. Biol. Chem.* **270**, 27679–27686.
32. Khachigian, L. M., Fries, J. W. U., Benz, M. W., Bonthron, D. T., and Collins, T. (1994) *J. Biol. Chem.* **269**, 22647–22656.
33. Bhandari, B., Wenzel, U. O., Marra, F., and Abboud, H. E. (1995) *J. Biol. Chem.* **270**, 5541–5548.

COMMONWEALTH OF AUSTRALIA

(Patents Act 1990)

IN THE MATTER OF: Australian Patent Application 696764 (73941/94). In the name of: Human Genome Sciences Inc.

- and -

IN THE MATTER OF: Opposition thereto by Ludwig Institute for Cancer Research, under Section 59 of the Patents Act.

Annexure GBC-4

This is **Annexure GBC-4** referred to in my Statutory Declaration made this Thirteenth day of December 2000.

Gary Cox

Gary Baxter Cox

WITNESS: Peytee Kitoo

Patent Attorney PEYTEE KITOO

Circulation Research: Journal of the American Heart Association

Volume 86(2) 4 February 2000 pp e29-e35

Mice Lacking the Vascular Endothelial Growth Factor-B Gene (*Vegfb*) Have Smaller Hearts, Dysfunctional Coronary Vasculature, and Impaired Recovery From Cardiac Ischemia

[Ultrarapid Communications]

Bellomo, Daniela; Headrick, John P.; Silins, Ginters U.; Paterson, Carol A.; Thomas, Penny S.; Gartside, Michael; Mould, Arne; Cahill, Marian M.; Tonks, Ian D.; Grimmond, Sean M.; Townson, Steve; Wells, Christine; Little, Melissa; Cummings, Margaret C.; Hayward, Nicholas K.; Kay, Graham F.

From the QCF Transgenic Laboratory and Human Genetics Laboratory, Joint Experimental Oncology Program, the Queensland Institute of Medical Research (D.B., G.U.S., C.A.P., M.G., A.M., M.M.C., I.D.T., S.M.G., S.T., N.K.H., G.F.K.), and the Department of Pathology, University of Queensland (M.C.C.), Brisbane, Australia; Griffith University (J.P.H.), Gold Coast Campus, Southport, Australia; Department of Cardiothoracic Surgery (P.S.T.), Imperial College School of Medicine, National Heart and Lung Institute, London, UK; and Centre for Molecular and Cellular Biology (C.W., M.L.), University of Queensland, Brisbane, Australia.

Received December 29, 1999; accepted December 29, 1999.

Correspondence to Graham Kay, Queensland Institute of Medical Research, Post Office Royal Brisbane Hospital, Queensland 4029, Australia. E-mail grahamK@qimr.edu.au

Outline

Graphics

Abstract

Abstract: Vascular endothelial growth factor-B (VEGF-B) is closely related to VEGF-A, an effector of blood vessel growth during development and disease and a strong candidate for angiogenic therapies. To further study the in vivo function of VEGF-B, we have generated *Vegfb* knockout mice (*Vegfb*$^{-/-}$). Unlike *Vegfa* knockout mice, which die during embryogenesis, *Vegfb*$^{-/-}$ mice are healthy and fertile. Despite appearing overtly normal, *Vegfb*$^{-/-}$ hearts are reduced in size and display vascular dysfunction after coronary occlusion and impaired recovery from experimentally induced myocardial ischemia. These findings reveal a role for VEGF-B in the development or function of coronary vasculature and suggest potential clinical use in therapeutic angiogenesis. The full text of this article is available at http://www.circresaha.org.

Vascular endothelial growth factor-B (VEGF-B) [1,3] is a secreted growth factor that has strong sequence homology with VEGF-A, a primary regulator of angiogenesis in development, corpus luteum formation, wound healing, and cancer. [4] VEGF-B can form stable heterodimers with VEGF-A [3] and is generally coexpressed with VEGF-A. [5,6] VEGF-B can bind to two of the VEGF-A receptors, VEGFR-1 [7] and neuropilin-1, [8] suggesting that it may regulate the bioavailability and/or action of VEGF-A. [5] Although VEGF-B has been reported to behave as an endothelial cell mitogen, [2] part of the mitogenic activity reported may be due to VEGF-B/VEGF-A heterodimers. [5]

Several mouse models have been generated by gene knockout technology where the genes encoding Vegf-A or its receptors have been mutated. Both *Vegfa*$^{-/-}$ and *Vegfa*$^{+/-}$ mice are unable to survive to term due to a general impairment of blood vessel formation in the early embryo. [9,10] *Vegfa*$^{120/120}$ mice, where only two of the three major Vegf-A isoforms have been knocked out, die postnatally after cardiac failure due to widespread myocardial ischemia. [11] *Vegfr1*$^{-/-}$ mice die as embryos due to defects in angiogenesis, [12] but partial knockout mice, where only the tyrosine kinase–encoding portion of the *Vegfr1* gene is deleted, develop normal vasculature. [13]

To study the in vivo role of Vegf-B, we have generated a knockout mouse line and found that, unlike the Vegf-A–related knockouts, *Vegfb*$^{-/-}$ mice appear outwardly normal and fertile. Because *Vegfb* transcripts are expressed predominantly in the heart during murine embryogenesis and adult life, [1,14–16] suggesting a specific role for Vegf-B during cardiac development, we have concentrated on studying the cardiac phenotype in these mice. *Vegfb*$^{-/-}$ hearts are reduced in size compared with hearts of *Vegfb*$^{+/+}$ littermates and display clinical symptoms of impaired recovery from experimentally induced ischemia. The results suggest an essential role for Vegf-B in establishment of a fully functional coronary vasculature and highlight the potential of this cytokine for application in the emerging field of therapeutic angiogenesis.

Materials and Methods

Generation of *Vegfb*$^{+/-}$ Mice

All mice used for the present study were supplied by the Animal Resources Centre (Western Australia), and their treatment was in accordance with the National Health and Medical Research Council (NH&MRC) guidelines for the care of experimental animals.

Targeted inactivation of the *Vegfb* gene was achieved by replacing exons 3 to 7 (Figure 1a) with a promoter-less *[beta]-geo* cassette. The *[beta]-geo* gene was preceded by an internal ribosomal entry site to give cap-independent translation of [beta]-geo. [17] Targeted 129/SvJ ES cells (C1368) were injected into C57BL/6J blastocysts to produce chimeras. Progeny of germline-transmitting chimeras were genotyped by polymerase chain reaction (PCR) amplification of tail-tip DNA using PCR1, 5'-TTT GAT GGC CCC AGC CAC-3'; PCR2, 5'-CCC CCA GCT GAC TGC TCG-3'; and PCR3, 5'-CTA GTG GAT CCC CCG GGC-

3' (Figure 1b).

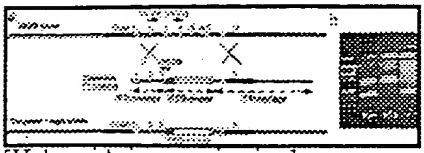

[Help with image viewing]

Figure 1. a, Diagram of the murine *Vegfb* gene (top), the targeting construct used to generate a *Vegfb*$^{+/-}$ mouse (middle), and the final targeted locus (bottom). The exons of the *Vegfb* gene are shown as numbered boxes with the open reading frame as open boxes. The location and orientation of the PCR primers used to genotype mice are shown as PCR1, PCR2, and PCR3. b, Genotyping PCR on *Vegfb*$^{+/+}$, *Vegfb*$^{+/-}$, and *Vegfb*$^{-/-}$ DNA, using the primers shown in panel a.

[beta]-Gal Staining and Immunohistochemistry

Frozen sections and whole embryos were stained for [beta]-Gal as described. [18] For quantitation of capillary density, transverse sections of the left ventricle (LV) were cut at comparable levels in *Vegfb*$^{+/+}$ and *Vegfb*$^{-/-}$ P30 hearts (30 days postpartum) (4 hearts each), immunostained with anti–PECAM-1 (clone M13, Pharmingen), and the capillaries counted using ImagePlus software on 7 randomly chosen fields (×40 magnification, [almost equal to] 0.06 mm 2 per field) in the epicardial, endocardial, and midmyocardial portion of the LV. Because no difference between genotypes was found within each portion, capillary density data were averaged for each heart. Coronary vessels were counted as anti–smooth muscle [alpha]-actin (FITC conjugated, clone 1A4, Sigma)–stained vessels in whole sections.

Heart Weight and LV Thickness

Vegfb$^{+/+}$, *Vegfb*$^{+/-}$, and *Vegfb*$^{-/-}$ mice of either 129/SvJ or C57BL/6J×129/SvJ background were weighed. After dissection, the hearts were trimmed of surrounding tissue and weighed. A subset of the P25 hearts was fixed in formalin and microdissected to obtain a similar angle of section. LV thickness was measured on sections with a stage micrometer (n=10 *Vegfb*$^{+/+}$ hearts; n=16 *Vegfb*$^{+/-}$ hearts; n=14 *Vegfb*$^{-/-}$ hearts).

Langendorff Perfusion

Hearts were isolated from mice anesthetized with 60 mg/kg sodium pentobarbital. *Vegfb*$^{+/+}$ (161±7 mg wet heart weight [WHW], n=15), *Vegfb*$^{+/-}$ (152±6 mg WHW, n=14), and *Vegfb*$^{-/-}$ mice (155±7 mg WHW, n=16) hearts were perfused in the Langendorff mode as described. [19]

For ischemia, baseline measurements were recorded from *Vegfb*$^{+/+}$ (n=8), *Vegfb*$^{+/-}$ (n=8), and *Vegfb*$^{-/-}$ hearts (n=8) after 30 minutes of stabilization. Global normothermic ischemia was initiated for 20 minutes before 30 minutes of aerobic reperfusion. To examine reactive hyperemia, a subset of hearts (n=7 for *Vegfb*$^{+/+}$, n=6 for *Vegfb*$^{+/-}$, and n=8 for *Vegfb*$^{-/-}$) was perfused as described above and after stabilization was subjected to a single 20-second period of zero flow followed by reperfusion at 90 mm Hg perfusion pressure. The coronary flow response was recorded, peak hyperemic flows were measured in individual experiments, and percentage of flow-debt repayment over the initial 60 seconds of reperfusion was calculated as follows: MATH where total coronary flows were measured in mL/g and were calculated by digital integration of coronary flow for the 60 seconds before and 60 seconds after occlusion using the Chart V3.5.6 program (AD Instruments, Castle Hill, Australia), and flow-debt was calculated as basal coronary flow (mL/60 seconds/g)×20 seconds of occlusion.

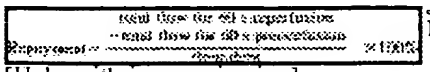

[Help with image viewing]

Equation 1.

Statistical Analyses

Body/heart weight, LV thickness, and capillary density data were analyzed using unpaired Student's *t* tests. Body/heart weight data were also analyzed using the generalized estimation equation. [20] Hyperemia data were analyzed via one-way ANOVA and functional parameters by two-way ANOVA for repeated measures. Where significant effects were detected, the

Tukey's HSD post hoc test was used. In all tests, significance was accepted at $P < 0.05$.

An expanded Materials and Methods section is available online at http://www.circresaha.org.

Results

Generation of the *Vegfb*$^{-/-}$ Mouse

The *Vegfb* knockout mice generated with the modified *Vegfb* locus shown in Figure 1a were produced in normal mendelian ratios, were healthy and fertile, and did not display any overt phenotype. The genotype of mice was determined by PCR amplification of tail-tip DNA from P10 pups (Figure 1b). Rather than producing Vegf-B, this modified locus results in [beta]-Gal expression under the control of the endogenous *Vegfb* promoter (herein referred to as Vegf-B/[beta]-Gal). Because the *Vegfb*$^{+/-}$ mice generated in this manner had no obvious developmental defects, we assumed that Vegf-B/[beta]-Gal expression in these mice accurately reflects the endogenous *Vegfb* expression pattern.

Cardiac Vegf-B/[beta]-Gal Expression Pattern in the *Vegfb*$^{+/-}$ Mouse

Using [beta]-Gal staining, Vegf-B/[beta]-Gal expression was first detected in the heart at E10.5 (embryonic day 10.5), it became prominent at E12.5 (Figure 2a) and further increased thereafter (Figure 2b). Throughout development, Vegf-B/[beta]-Gal expression appeared to be restricted to the myocardium (Figures 2c through 2g) and subepicardium (Figures 2g and 2h) and remained undetectable in endothelial cells, including those of the endocardium and coronary endothelium. Endocardial derivatives, such as the valve leaflets were always devoid of Vegf-B/[beta]-Gal expression. During development, the highest concentration of Vegf-B/[beta]-Gal–expressing cells was seen in the right ventricular myocardium and right aspect of the interventricular septum (Figures 2a through 2c). Lower Vegf-B/[beta]-Gal expression was detectable in the LV (Figures 2a and 2c) and the right atrial appendage (Figure 2d). The lowest expression was found in the atrial wall (Figures 2c, 2d, and 2f), where coronary angiogenesis is less conspicuous (Figures 2e and 2f). Within the right ventricle (RV), Vegf-B/[beta]-Gal staining was prevalent in the trabeculations (Figure 2d). The intensity of Vegf-B/[beta]-Gal expression increased further in the neonate heart (Figures 2i and 2j) in correlation with the massive early postnatal coronary capillary and vessel growth. [11] The prevalence of Vegf-B/[beta]-Gal expression switches from the RV to the LV in the early neonatal period (Figures 2i and 2j) reflects the predominant early postnatal capillarization of this chamber. [21] In the juvenile heart, the ventricular prevalence of expression is lost, and the density of Vegf-B/[beta]-Gal–expressing cells is similar in the ventricles and the atria (data not shown).

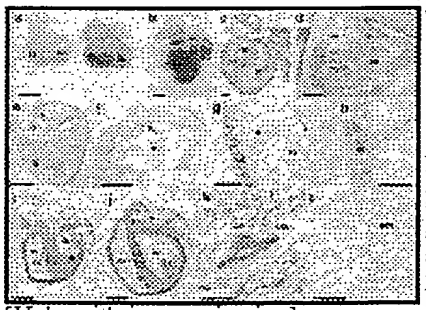

[Help with image viewing]

Figure 2. Vegf-B/[beta]-Gal localization in the heart during development and after birth. a, Whole-mount E12.5 Vegf-B/[beta]-Gal–stained *Vegfb*$^{+/-}$ (right) and *Vegfb*$^{+/-}$ (left) hearts showing higher expression in the RV. b through d, Whole mount and sections of Vegf-B/[beta]-Gal–stained E15.5 hearts. b, *Vegfb*$^{+/-}$ whole mount. Vegf-B/[beta]-Gal levels are very low in the aorta and pulmonary trunk. c, Longitudinal section of the *Vegfb*$^{+/-}$ heart shown in panel b. Note higher levels of Vegf-B/[beta]-Gal expression (staining blue) in the RV and right side of the interventricular septum (*) than the LV. d, Sagittal section through the RV. Note expression in the trabeculations of the ventricle and absence in the atria. e through h, E17.5 hearts. e, Longitudinal heart section stained for PECAM-1 (staining brown). The rectangles represent the regions in panels f and g. f and g, Vegf-B/[beta]-Gal and anti–PECAM-1 double labeling. f, Atrial region. The endocardium (arrows) is stained with anti–PECAM-1, but no capillaries have formed in this region. g, RV. Anti–PECAM-1 stains the endocardium (arrow) and the endothelium of numerous capillaries (arrowhead) surrounded by Vegf-B/[beta]-Gal–expressing cardiomyocytes in the myocardium and subepicardium. h, Higher magnification of the subepicardial region stained for Vegf-B/[beta]-Gal expression showing several Vegf-B/[beta]-Gal–positive cells. i through k, P3 *Vegfb*$^{+/-}$ mouse hearts. i and j, Vegf-B/[beta]-Gal staining of transverse heart sections. j, Section through the atrioventricular transition. Note prominent staining in the LV. j, Section through the ventricular region. Note the absence of staining around the coronary vessels (arrowheads). k and l, Contiguous sections through a coronary arteriole stained for PECAM-1 (j) and Vegf-B/[beta]-Gal (k). Vegf-B/[beta]-Gal–expressing cardiomyocytes surround the capillaries, but Vegf-B/[beta]-Gal is undetectable in the endothelium and smooth muscle layers surrounding the artery. rv indicates right ventricle; lv, left ventricle; *, interventricular septum; ra, right atrium; aa, atrial appendage; m, myocardium; se, subepicardium; and p, pulmonary trunk. Bar=500 μm (a, b, d, e, i, and j) and 100 μm (c, f, g, h, k, and l).

The great arteries in the heart expressed low levels of Vegf-B/[beta]-Gal at all stages of development (eg, Figure 2b) and in juvenile mice (data not shown). Vegf-B/[beta]-Gal was undetectable in the tunica intima and media of coronary vessels (Figures 2i, arrowheads, and 2k and 2l), although we found Vegf-B/[beta]-Gal expression in other vessels in the body (eg, the intralobar component of the pulmonary arteries) (data not shown).

Postnatal Heart Growth in *Vegfb*$^{-/-}$ Mice

Although histological examination of all organs revealed no differences between genotypes, *Vegfb*$^{-/-}$ hearts frequently appeared marginally smaller than their *Vegfb*$^{+/+}$ and *Vegfb*$^{+/-}$ littermates (Figure 3a). We recorded the total body and heart weight of 122 animals including male and female *Vegfb*$^{+/+}$, *Vegfb*$^{+/-}$, and *Vegfb*$^{-/-}$ mice at several ages between P3 and P91. These mice were grouped as P3 to P9 mice (*Vegfb*$^{+/+}$, n=15; *Vegfb*$^{+/-}$, n=20; and *Vegfb*$^{-/-}$, n=13) and P25 or older (*Vegfb*$^{+/+}$, n=20; *Vegfb*$^{+/-}$, n=28; and *Vegfb*$^{-/-}$, n=27). We found no consistent genotype-dependent decrease in body weigh; however, heart weight was always reduced in *Vegfb*$^{-/-}$ mice. To account for the inherent interlitter and intralitter variability in body weight, due to sex, age, and genetic background, we used heart/body ratios to display the results. Although we found no significant difference in heart/body ratio in relation to sex or genetic background, statistical analysis revealed a dramatic increase in heart/body ratio from P3-9 to P25 (or older) in all animals regardless of genotype (Figure 3b). There were no differences in percentage of heart/body weight ratios among genotypes in P3-9 mice (*Vegfb*$^{+/+}$, 0.64±0.02; *Vegfb*$^{+/-}$, 0.59±0.03; and *Vegfb*$^{-/-}$, 0.66±0.03), but we found a significant (P <0.05) decrease in percentage of heart/body weight ratio in P25 (or older) *Vegfb*$^{-/-}$ (0.78±0.02) mice compared with *Vegfb*$^{+/+}$ (0.87±0.04) and *Vegfb*$^{+/-}$ (0.89±0.02) mice (Figure 3b). When familial (litter/parents) correlation among mice was taken into account, this significant difference remained (data not shown). No significant difference was found between *Vegfb*$^{+/+}$ and *Vegfb*$^{+/-}$ mice at any stage.

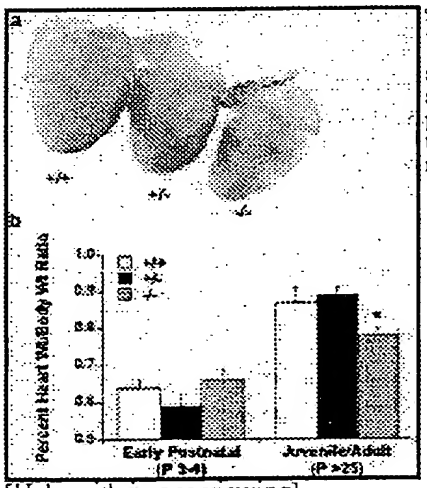

[Help with image viewing]

Figure 3. Reduced postnatal heart size in *Vegfb*$^{-/-}$ hearts. a, Appearance of P25 *Vegfb*$^{-/-}$, *Vegfb*$^{+/-}$, and *Vegfb*$^{+/+}$ hearts from same-sex littermates, illustrating a slightly reduced *Vegfb*$^{-/-}$ heart size. b, Percentage of body/weight ratio is significantly reduced in the juvenile (>P25) *Vegfb*$^{-/-}$ mice but not in early postnatal mice (P3-9), indicating the impaired growth of the *Vegfb*$^{-/-}$ hearts in the first few weeks after birth. Values are mean±SEM. *P <0.05 vs *Vegfb*$^{+/+}$ mice; P <0.01 vs *Vegfb*$^{+/-}$ mice.

The dramatic increase in heart weight during the first few weeks after birth is well documented and appears to be mainly due to massive growth of the coronary capillaries and vessels, but cardiomyocyte proliferation and hypertrophy also contribute.[22] No difference in the size of myocardial cells was found in histological sections in *Vegfb*$^{+/+}$, *Vegfb*$^{+/-}$, or *Vegfb*$^{-/-}$ hearts (data not shown). LV thickness was significantly decreased in P25 *Vegfb*$^{-/-}$ (0.80±0.03 mm,* n=14) compared with *Vegfb*$^{+/+}$ (0.89±0.03 mm, n=10) and *Vegfb*$^{+/-}$ (0.91±0.02 mm, n=16) hearts (*P =0.059 versus *Vegfb*$^{+/+}$ and P <0.05 versus *Vegfb*$^{+/-}$). Analysis of capillary density using standard morphometric measures found no significant differences between P30 *Vegfb*$^{+/+}$ (2321±255 capillaries/mm^2) and *Vegfb*$^{-/-}$ (2334±253 capillaries/mm^2) hearts. Vessel density measures in adjacent heart sections also showed no differences between *Vegfb*$^{+/+}$ (270±10 vessels/section) and *Vegfb*$^{-/-}$ (275±14 vessels/section) hearts.

Reactive Hyperemic Responses in *Vegfb*$^{+/+}$, *Vegfb*$^{+/-}$, and *Vegfb*$^{-/-}$ Hearts

Baseline contractile function and coronary flow were equivalent in Langendorff-perfused hearts from all three groups under normoxic conditions (see Table online, http://www.circresaha.org). To test whether alterations in vascular function would be more evident during active responses to modified myocardial O_2 delivery, we exposed hearts to transient (20 seconds) coronary occlusion and studied the hyperemic response on reperfusion. The reactive hyperemic responses differed subtly between groups (Figure 4). Although peak hyperemic flow was comparable in all three groups of hearts (32 to 36 mL · min^{-1} · g^{-1}) (Figure 4a), overall flow-debt repayment during the initial 60 seconds of reperfusion (during which flow recovered to preocclusion levels) was significantly lower in *Vegfb*$^{-/-}$ mice ([almost equal to]60%) versus the other two groups ([almost equal to]100%) (Figure 4b). There were no differences in repayment between *Vegfb*$^{+/+}$ and *Vegfb*$^{+/-}$ hearts. These findings indicate that the functional status of the coronary vasculature is impaired in *Vegfb*$^{-/-}$ mice.

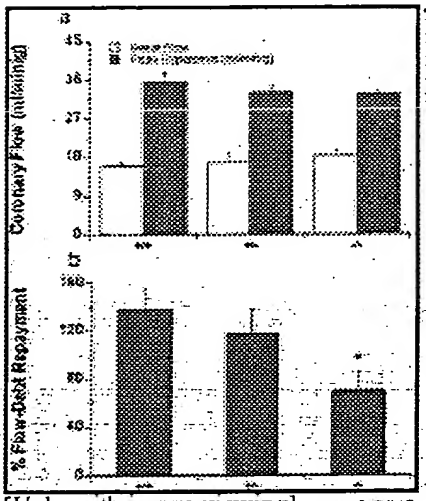

[Help with image viewing]

Figure 4. Reactive hyperemic responses to 20-second coronary occlusion in Langendorff-perfused *Vegfb*$^{+/+}$, *Vegfb*$^{+/-}$, and *Vegfb*$^{-/-}$ hearts. a, Baseline and peak hyperemic flows. b, Flow-debt repayments over the initial 60 seconds of reperfusion. Values are mean±SEM. *P <0.05 vs *Vegfb*$^{+/+}$ hearts.

Responses to Ischemia-Reperfusion in *Vegfb*$^{+/+}$, *Vegfb*$^{+/-}$, and *Vegfb*$^{-/-}$ Hearts

As noted, baseline functional parameters were comparable in hearts from *Vegfb*$^{+/+}$, *Vegfb*$^{+/-}$, and *Vegfb*$^{-/-}$ mice (see Table online, http://www.circresaha.org). Global normothermic ischemia completely abolished contractile function in all hearts within 2 to 3 minutes and caused a rapid rise in diastolic pressure. Time to onset of contracture and peak-developed contracture are indicators of the severity of ischemic injury. Although no difference was found in the rate of contracture development, peak contracture during ischemia was greater in *Vegfb*$^{-/-}$ compared with *Vegfb*$^{+/+}$ and *Vegfb*$^{+/-}$ hearts (Figure 5a). Diastolic pressure was significantly elevated in *Vegfb*$^{-/-}$ hearts compared with *Vegfb*$^{+/+}$ and *Vegfb*$^{+/-}$ hearts during reperfusion and recovered minimally ([almost equal to]73 mm Hg) relative to the other two groups ([almost equal to]35 mm Hg) (Figure 5a). Recovery of contractile function was slightly depressed throughout reperfusion in *Vegfb*$^{-/-}$ hearts, with the rate-pressure product being significantly lower at 30 minutes compared with *Vegfb*$^{+/+}$ and *Vegfb*$^{+/-}$ hearts (Figure 5b). Coronary flow responses did not differ between the three groups at any time point (Figure 5c).

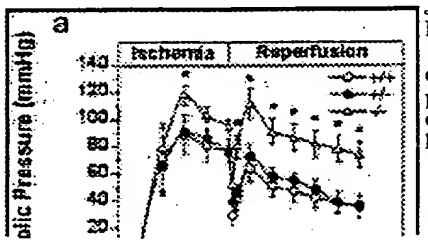

Figure 5. Functional responses of Langendorff-perfused *Vegfb*$^{+/+}$, *Vegfb*$^{+/-}$, and *Vegfb*$^{-/-}$ hearts to 20 minutes of global normothermic ischemia and 30 minutes of reperfusion. a, Responses for left ventricular diastolic pressure. Rate-pressure product (heart rate×left ventricular developed pressure) (b) and coronary flow (c) are shown. Values are mean±SEM. *P<0.05 vs *Vegfb*$^{+/+}$ hearts.

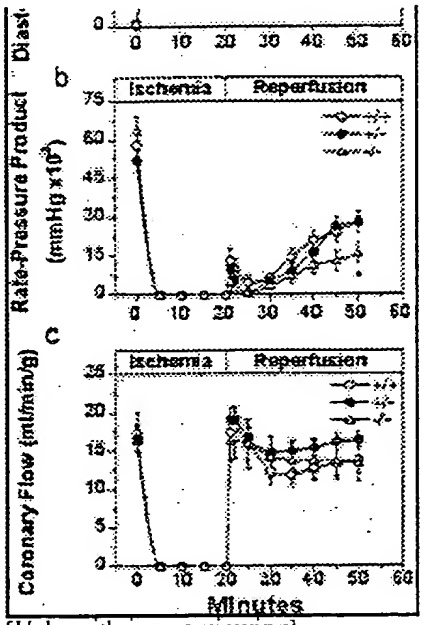

[Help with image viewing]

Discussion

In the present study, we have used promoter trap *LacZ* expression in the *Vegfb*$^{+/-}$ mouse to correlate Vegf-B/[beta]-Gal expression to processes of vascularization in the heart, the major site of Vegf-B expression. The general developmental pattern of Vegf-B expression has previously been interpreted to reflect a paracrine action of Vegf-B on the developing vasculature, although no attempts were made to correlate expression patterns with developmental processes of vascularization in any individual organ. 16 Although *Vegfb* transcripts are produced in the heart from E8.5, Vegf-B protein expression is not detected until E10.5. 16 We can first detect Vegf-B/[beta]-Gal at E10.5 in the interventricular septum and propose that Vegf-B/[beta]-Gal (and therefore Vegf-B) production increases substantially at this time point, in spatial and temporal correlation with the commencement of coronary endothelial growth in the heart. 23 Indeed, Vegf-B/[beta]-Gal levels increase both throughout development and after birth, closely correlating with the progression of cardiac angiogenesis. Vegf-B/[beta]-Gal is conspicuous in the subepicardium where heart angiogenesis has been shown to commence. 24 It is more densely expressed in the ventricles than the atria and correlates with the degree of coronary angiogenesis that is more advanced in the ventricles than in the atria at fetal stages. After birth, Vegf-B/[beta]-Gal expression increases further in the LV, at a time when substantial capillary growth occurs predominantly in this chamber. 21,22 The disparity between LV and RV capillary growth rates decreases several days after birth. 21 Accordingly, by P25, Vegf-B/[beta]-Gal expression becomes even throughout the heart with levels of expression similar in RV, LV, and the atria. Despite the correlation between capillarization and Vegf-B/[beta]-Gal expression, such expression was not found in the smooth muscle cells of the differentiated coronary vessels. It is therefore likely that Vegf-B may exert its paracrine action on the microvasculature surrounding the expressing myocardium, rather than on the endothelium of the coronary vessels.

We find that *Vegfb*$^{-/-}$ hearts appear morphologically and functionally normal in the unstressed animal but do not undergo the same extent of postnatal growth as those of *Vegfb*$^{+/+}$ and *Vegfb*$^{+/-}$ animals. Postnatal heart growth appears to be mainly due to the substantial increase in the coronary microvasculature and vessels. 11,22 This increase has been attributed to the action of Vegf-A_{164} and Vegf-A_{188}, 11 because mice lacking these Vegf-A isoforms die as a consequence of severe heart ischemia due to an almost total absence of postnatal capillary and coronary vessel growth. Postnatal ablation of Vegf-A (and possibly Vegf-B) function by administering a soluble Flt-1 receptor (mFlt(1–3)-IgG) 25 is also lethal. In the heart, this treatment leads to cardiomyocyte necrosis and massive capillary and vessel density reduction. 25 Because Vegf-B is coexpressed with Vegf-A in the myocardium of the ventricles, 6 can form biologically active heterodimers with Vegf-A, and also binds Flt-1, 7 it is likely that the abnormal coronary angiogenesis described above is a result of interference

with the normal function of both Vegf-A and Vegf-B. We tested whether the observed *Vegfb*$^{-/-}$ reduction in heart weight was a consequence of impaired growth of the vascular network by measures of coronary capillary and vessel density. We found no significant differences between *Vegfb*$^{-/-}$ and *Vegfb*$^{+/+}$ hearts, although additional studies measuring lumen size, patency, and permeability of capillaries and vessels in the heart will reveal whether any structural abnormalities in the vascular network of *Vegfb*$^{-/-}$ hearts may be responsible for reduced volume of this organ. Alternatively, the observed microcardia could be attributed to an effect of Vegf-B on cardiomyocyte growth. Vegf-B effect on heart muscle could be mediated by the Vegf-B_{167} (and Vegf-A_{165}) receptor, neuropilin-1, which is expressed in the developing cardiac muscle. However, this is unlikely, because cardiomyocytes do not appear affected in size or function in the *Vegfb*$^{-/-}$ heart, and we cannot rule out a direct effect of Vegf-B ablation on myocytes. It is worth noting, nevertheless, that cardiomyocytes are normal in the *Vegfa*$^{120/120}$ mouse, where neuropilin-1 ligand Vegf-A_{165} has been ablated. 11 A slight decrease in left ventricular thickness in the *Vegfb*$^{-/-}$ heart may indicate that some developmental hypoplasia, resulting from suboptimal vascularization, could be responsible for the observed microcardia.

Ablating *Vegfb* expression reduced the ability to repay coronary flow after a transient coronary occlusion. This occurred despite baseline coronary flow in the *Vegfb*$^{-/-}$ heart appearing normal, which was not unexpected given that moderate impairment of vascularization or vascular function that might result from deletion of the *Vegfb* gene could be compensated by enhanced intrinsic vasodilatation. Impairment of flow-debt repayment, despite similar peak flows, suggests inhibition of flow-mediated dilatation, which occurs subsequent to the immediate hyperemic response, indicating that the functional status of the coronary vasculature is impaired in some way in *Vegfb*$^{-/-}$ hearts. Reactive hyperemia is thought to be mediated by the combined actions of nitric oxide (NO) and adenosine, 26 with potential involvement of K_{ATP} channels. 27 The prolongation of the hyperemic response is thought to be at least partially NO dependent. 28 Thus, one possible mechanism contributing to this change is an impaired NO production. However, deletion of the endothelial NO synthase gene fails to alter peak hyperemic flow, flow repayment, and adenosine responses in murine hearts. 29

Heart rate was almost identical in hearts of all genotypes before and after ischemia, and no significant differences existed for heart rate between any groups at any time. Interestingly, deletion of *Vegfb* reduced functional recovery from ischemia-reperfusion and appeared to worsen contracture during ischemia. The mechanism of contracture is not well understood but may involve rigor-bond formation as a result of impaired glycolytic ATP formation. 30 During reperfusion, diastolic dysfunction was significantly greater in knockout mice; the difference was wholly due to a change in contractile force and not rate. Recovery of the rate-pressure product was slightly reduced whereas coronary flow was similar in all three groups. Although a reduced reflow or perfusion could have explained the dysfunction, this was not supported by the measures of total myocardial perfusion. However, this does not exclude a more subtle change in flow distribution that is not reflected in the total flow response. The postischemic elevation in diastolic pressure is likely to reflect altered Ca^{2+} handling in reperfused tissue, resulting in enhanced diastolic Ca^{2+} levels. 31 Ca^{2+} handling is energy dependent, particularly at the level of the sarcoplasmic reticulum. Knockout of the *Vegfb* gene could conceivably lead to impaired postischemic recovery of energy metabolism, owing to maldistribution of coronary flow, such that myocardial handling of Ca^{2+} is impaired. Further experiments addressing patency, permeability, and responses to vasodilatory stimuli in the ventricular microvasculature of *Vegfb*$^{-/-}$ hearts will reveal whether this is indeed the case. The increased diastolic dysfunction during ischemia is largely independent of the coronary vasculature and may reflect a developmental effect of *Vegfb* deletion on heart growth or function, as suggested by the smaller hearts and reduced left ventricular thickness in *Vegfb*$^{-/-}$ mice.

In the present study, we have shown that, despite heart morphology and function being normal in *Vegfb*$^{-/-}$ mice, the response to coronary occlusion and myocardial recovery from ischemia are compromised. Thus, although Vegf-B may play a redundant role in establishing the coronary vasculature, our results define a unique role in the development and maintenance of function in response to ischemic insult.

Acknowledgments

This work was supported by the Queensland Cancer Fund and AMRAD Corporation Ltd. Nicholas K. Hayward is a recipient of a NH&MRC Senior Research Fellowship, and Sean M. Grimmond holds a NH&MRC C.J. Martin Traveling Fellowship. Graham F. Kay and Melissa Little are Fellows of the Sylvia and Charles Viertel Charitable Foundation. We would like to thank Michael Walsh for histological services and Dr Patrick Ward for advanced statistical analysis.

References

1. Grimmond S, Lagercrantz J, Drinkwater C, Silins G, Townson S, Pollock P, Gotley D, Carson E, Rakar S, Nordenskjold M, Ward L, Hayward N, Weber G. Cloning and characterization of a novel human gene related to vascular endothelial growth factor. Genome Res. 1996; 6:124–131. [Context Link]

2. Olofsson B, Pajusola K, Kaipainen A, von Euler G, Joukov V, Saksela O, Orpana A, Pettersson RF, Alitalo K, Eriksson U. Vascular endothelial growth factor B, a novel growth factor for endothelial cells. Proc Natl Acad Sci U S A. 1996; 93:2576–2581. [Context Link]

3. Olofsson B, Pajusola K, von Euler G, Chilov D, Alitalo K, Eriksson U. Genomic organization of the mouse and human genes for vascular endothelial growth factor B (VEGF-B) and characterization of a second splice isoform. J Biol Chem. 1996; 271:19310–19317. [Context Link]

4. Ferrara N. Vascular endothelial growth factor: molecular and biological aspects. Curr Top Microbiol Immunol. 1999; 237:1–30. [Context Link]

5. Eriksson U, Alitalo K. Structure, expression and receptor-binding properties of novel vascular endothelial growth factors. Curr Top Microbiol Immunol. 1999; 237:41–57. [Context Link]

6. Miquerol L, Gertsenstein M, Harpal K, Rossant J, Nagy A. Multiple developmental roles of VEGF suggested by a LacZ-tagged allele. Dev Biol. 1999; 212:307–322. [Context Link]

7. Olofsson B, Korpelainen E, Pepper MS, Mandriota SJ, Aase K, Kumar V, Gunji Y, Jeltsch MM, Shibuya M, Alitalo K, Eriksson U. Vascular endothelial growth factor B (VEGF-B) binds to VEGF receptor-1 and regulates plasminogen activator activity in endothelial cells. Proc Natl Acad Sci U S A. 1998; 95:11709–11714. [Context Link]

8. Makinen T, Olofsson B, Karpanen T, Hellman U, Soker S, Klagsbrun M, Eriksson U, Alitalo K. Differential binding of vascular endothelial growth factor B splice and proteolytic isoforms to neuropilin-1. J Biol Chem. 1999; 274:21217–21222. [Context Link]

9. Ferrara N, Carver-Moore K, Chen H, Dowd M, Lu L, O'Shea KS, Powell-Braxton L, Hillan KJ, Moore MW. Heterozygous embryonic lethality induced by targeted inactivation of the VEGF gene. Nature. 1996; 380:439–442. [Fulltext Link] [Context Link]

10. Carmeliet P, Ferreira V, Breier G, Pollefeyt S, Kieckens L, Gertsenstein M, Fahrig M, Vandenhoeck A, Harpal K, Eberhardt C, Declercq C, Pawling J, Moons L, Collen D, Risau W, Nagy A. Abnormal blood vessel development and lethality in embryos lacking a single VEGF allele. Nature. 1996; 380:435–439. [Fulltext Link] [Context Link]

11. Carmeliet P, Ng YS, Nuyens D, Theilmeier G, Brusselmans K, Cornelissen I, Ehler E, Kakkar VV, Stalmans I, Mattot V, Perriard JC, Dewerchin M, Flameng W, Nagy A, Lupu F, Moons L, Collen D, D'Amore PA, Shima DT. Impaired myocardial angiogenesis and ischemic cardiomyopathy in mice lacking the vascular endothelial growth factor isoforms VEGF164 and VEGF188. Nat Med. 1999; 5:495–502. [Context Link]

12. Fong GH, Rossant J, Gertsenstein M, Breitman ML. Role of the Flt-1 receptor tyrosine kinase in regulating the assembly of vascular endothelium. Nature. 1995; 376:66–70. [Fulltext Link] [Context Link]

13. Hiratsuka S, Minowa O, Kuno J, Noda T, Shibuya M. Flt-1 lacking the tyrosine kinase domain is sufficient for normal development and angiogenesis in mice. Proc Natl Acad Sci U S A. 1998; 95:9349–9354. [Context Link]

14. Lagercrantz J, Larsson C, Grimmond S, Fredriksson M, Weber G, Piehl F. Expression of the VEGF-related factor gene in pre- and postnatal mouse. Biochem Biophys Res Commun. 1996; 220:147–152. [Context Link]

15. Lagercrantz J, Farnebo F, Larsson C, Tvrdik T, Weber G, Piehl F. A comparative study of the expression patterns for vegf, vegf-b/vrf and vegf-c in the developing and adult mouse. Biochim Biophys Acta. 1998; 1398:157–163.

ssaki A, Kaipainen A, Olofsson B, Alitalo K, Eriksson U. Localization of VEGF-B in the sts a paracrine role of the growth factor in the developing vasculature. Dev Dyn. 1999; 215:12–

mik B, Duwel A, Nichols J, Li M, Dani C, Robertson M, Chambers I, Smith A. Dicistronic reporters and modifiers of mammalian gene expression. Proc Natl Acad Sci U S A. 1994; xt Link]

ace JD, Lewin A, Smeyne RJ. Transgenic expression to monitor dynamic organization of it: use of the Escherichia coli lacZ gene product, B-galactosidase. Neuroprotocols. 1994; 5:54–

Kirdy JC, Willis RJ. Functional and metabolic effects of extracellular magnesium in normoxic dium. Am J Physiol. 1998; 275:H917–H929. [Context Link]

Liard NM, Rotnitzky AG. Regression models for discrete and longitudinal responses. Stat Sci. ntext Link]

sa P, Loud AV. Morphometric study of early postnatal development in the left and right um of the rat, II: tissue composition, capillary growth, and sarcoplasmic alterations. Circ Res. Context Link]

vn MD. Postnatal growth of the heart and its blood vessels. J Vasc Res. 1996; 33:266–287.

e CE. The origin of the epicardium and the embryonic myocardial circulation in the mouse. 157–168. [Context Link]

lie RG. Pericardial mesoderm generates a population of coronary smooth muscle cells migrating ith ingrowth of the epicardial organ. Dev Biol. 1996; 174:221–232. [Context Link]

KJ, Ryan AM, Kowalski J, Keller GA, Rangell L, Wright BD, Radtke F, Aguet M, Ferrara N. growth and survival in neonatal mice. Development. 1999; 126:1149–1159. [Context Link]

hlopicki S, Niezabitowski P. Endothelial control of coronary flow in perfused guinea pig heart. 995; 90:119–124. [Context Link]

iguchi N, Sato K, Akai K, Wang Y, Komaru T, Ashikawa K, Takishima T. Microvascular sites onsible for reactive hyperemia in the coronary circulation of the beating canine heart. Circ Res. Context Link]

aro P, Linden RJ, Merletti A, Losano G. The role of nitric oxide in the initiation and in the odilator responses in the coronary circulation. Pflugers Arch. 1995; 430:96–104. [Context Link]

ing UK, Ding Z, Hirchenhain J, Bidmon HJ, Godecke S, Schrader J. Coronary hemodynamics nthase knockout mice. Circ Res. 1998; 82:186–194. [Fulltext Link] [Context Link]

o EY, Yang MQ, Zimmer SD, Ugurbil K, Foker JE, From AH. Ischemic contracture begins olysis stops: a 31P-NMR study of isolated rat hearts. Am J Physiol. 1991; 261:H469–H478.

gan JP. Contractile dysfunction and abnormal Ca^{2+} modulation during postischemic reperfusion ysiol. 1995; 268:H100–H111. [Context Link]

ngiogenesis; cardiac ischemia; coronary vasculature

COMMONWEALTH OF AUSTRALIA

(Patents Act 1990)

IN THE MATTER OF: Australian Patent Application 696764 (73941/94). In the name of: Human Genome Sciences Inc.

- and -

IN THE MATTER OF: Opposition thereto by Ludwig Institute for Cancer Research, under Section 59 of the Patents Act.

Annexure GBC-5

This is **Annexure GBC-5** referred to in my Statutory Declaration made this Thirteenth day of December 2000.

Gary Baxter Cox

WITNESS: Peyte Kho

Patent Attorney PEY TEE KHOO

STRATAGENE

CLONING SYSTEMS

1994

10 Years of Innovation

Creating the tools for the creative mind

STRATAGENE

DESCRIPTION

- Direct secretion of recombinant proteins into insect cell supernatant
- Simplifies purification and characterization of expressed proteins
- Ease of purification further enhanced by serum-free medium
- Choice of 2 different signal sequences
- Fusion genes transcribed under strong polyhedrin promoter
- Compatible with all *Ac*NPV expression systems

UNIQUE SECRETORY SIGNAL SEQUENCES

pMbac and pPbac contain secretory signal sequences that direct the nascent polypeptide chain toward the secretory pathway of the cell, thereby leading to secretion into the cell supernatant. The sequences to be expressed are inserted 3′ to the signal sequences to generate a fusion gene that is transcribed under the strong polyhedrin promoter. The signal sequence is cleaved off by signal-sequence peptidase as the nascent polypeptide is channeled toward the secretory pathway of the host insect cell, leading to the secretion of mature recombinant protein. Proper processing of signal peptidase at the expected cleavage site has been verified by protein sequencing of secreted material.

EASY PURIFICATION OF RECOMBINANT PROTEINS

With no need for cell lysis, purification of the secreted recombinant proteins is extremely easy. The process starts with simple separation of the insect cells from the supernatant. Downstream processing of the protein is made even more efficient when the pMbac and pPbac transfer vectors are used with Stratagene's Cell/Perfect™ Bac serum-free insect cell culture medium.

PROTOCOL FOR USE WITH BACULOVIRUS EXPRESSION SYSTEMS

The pMbac and pPbac baculovirus transfer vectors are compatible with systems based on the baculovirus species most commonly used for expression work, *Autographica californica* nuclear polyhedrosis virus (*Ac*NPV). Once in the nucleus of infected cells, the baculovirus expresses the protein polyhedrin late in the infectious cycle under a very strong promoter. The polyhedrin gene is not essential for viral propagation in tissue culture, so it can be replaced by cDNA whose expression will then be driven by the strong polyhedrin promoter.

To replace the polyhedrin gene in the baculovirus genome:

1. Insert the cDNA fragment into the pMbac or pPbac transfer vector, each of which contains recombination sequences.
2. Cotransfect the baculovirus DNA and transfer vector into the insect cell line SF9. The resulting double recombination event replaces the polyhedrin gene with the vector fragment containing the gene to be expressed.
3. Identify recombinant virus based on the presence of the *lacZ* gene in the recombination fragment.

CONTENTS

20 µg of pMbac and/or pPbac transfer vector
2.5 µg each of forward and reverse sequencing primers

REFERENCES

1. Lernhardt, W., et al. (1993) *Strategies* 6: 20-21.

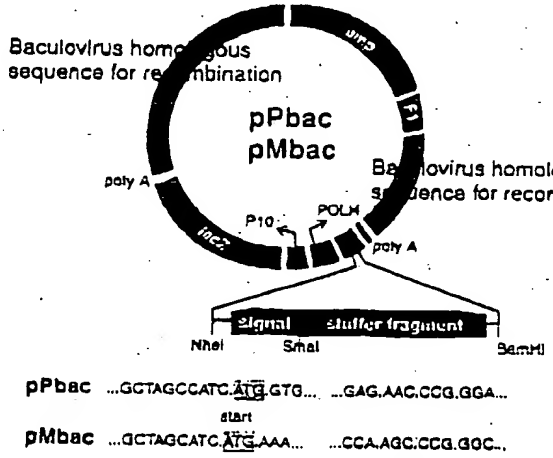

Map of Baculovirus Transfer Vectors

To create the pMbac and pPbac vectors, the melittin and human placental alkaline phosphatase secretory signal sequences were introduced into the *Nhe* I and *BamH* I sites, respectively, of the transfer vector pJVP10Z. Therefore, genes to be expressed can be introduced unidirectionally into the *Sma I/BamH* I sites of the vectors

Baculovirus Transfer Vectors

pMbac and pPbac

Catalog # 211502

$225

pMbac

Catalog # 211503

$125

pPbac

Catalog # 211504

$125

Baculovirus Sequencing Primers

Forward primer

2.5 µg

Catalog # 300313

$105

Reverse primer

2.5 µg

Catalog # 300314

$105

Cell/Perfect™ Bac Serum-Free Insect Cell Culture Medium

1 liter

Catalog # 205120

$35

COMMONWEALTH OF AUSTRALIA

(Patents Act 1990)

IN THE MATTER OF: Australian Patent Application 696764 (73941/94). In the name of: Human Genome Sciences Inc.

- and -

IN THE MATTER OF: Opposition thereto by Ludwig Institute for Cancer Research, under Section 59 of the Patents Act.

Annexure GBC-6

This is **Annexure GBC-6** referred to in my Statutory Declaration made this Thirteenth day of December 2000.

Gary Baxter Cox

WITNESS: _____

Patent Attorney PEY TEE Ltd

Molecular and Cell Biology Catalog 1992

Pharmacia

Pharmacia LKB Biotechnology

Vector Applications Guide (cont.)

Promoter	Induction	ATG	RBS	Translation termination	Enzymatic cleavage	Prokaryotic Gene Fusion Vectors
pGEX-1λT						• Induction: *tac* promoter inducible with 1–5 mM IPTG. • Expression: Proteins are expressed as fusion proteins with the 26-kDa glutathione S-transferase (GST). The GST gene contains an ATG and ribosome-binding site, and is under control of the *tac* promoter. Translation terminators are provided in all three reading frames. The resulting fusion protein may be purified on Glutathione Sepharose (17-0756-01) or on prepacked Glutathione Sepharose columns (17-0757-01). • Enzymatic cleavage: For pGEX-1λT: The GST carrier protein may be separated from the fusion protein using the site-specific protease thrombin. For pGEX-2T: The GST carrier protein may be separated from the fusion protein using the site-specific protease thrombin. For pGEX-3X: The GST carrier protein may be separated from the fusion protein using the site-specific protease factor Xa. • Reading frame: For pGEX-1λT: The reading frame at the *Eco*R I site is GAA TTC ATC. This is compatible with the *Eco*R I site in λ gt11. For pGEX-2T: The reading frame at the *Eco*R I site is GGA ATT CAT. For pGEX-3X: The reading frame at the *Eco*R I site is GGG AAT TCA. • Host(s): *E. coli*. The plasmid provides *lac* I^q repressor. • Selectable marker(s): Plasmid confers resistance to 50 μg/ml ampicillin. • Amplification: Recommended.
tac	X	X	X	X	X	
pGEX-2T						
tac	X	X	X	X	X	
pGEX-3X						
tac	X	X	X	X	X	
pRIT2T						• Induction: The lambda P_R promoter is induced by shifting the growth temperature from 30°C to 42°C for 90 minutes. • Expression: Proteins are expressed as fusion proteins with *Staphylococcal* protein A. The lambda *cro* gene supplies an ATG. No signal sequence is provided; therefore the protein remains intracellular. Transcription and translation termination signals are provided. Fusion protein may be purified on IgG Sepharose (17-0969-01). The size of the protein A carrier protein is about 24 kDa. • Host(s): N4830-1/NC99I*. N4830-1 must be used for expression, as it contains the temperature-sensitive *cI857* repressor. • Selectable marker(s): Plasmid confers resistance to 100 μg/ml ampicillin.
λP_R	X	X	X	X		
pEZZ 18						• Expression: Expression is controlled by both the *lacUV5* and protein A promoters and is not inducible. Proteins are expressed as fusions with the synthetic ZZ peptide which is based on an IgG binding domain of protein A. The protein A signal sequence is provided so expression in *E. coli* leads to secretion of fusion proteins into the culture medium. Elements of the protein A gene provide both the ATG and ribosome-binding site. Stop codons must be provided by the insert. Fusion protein may be purified on IgG Sepharose (17-0969-01). The size of the ZZ carrier is about 14 kDa. • Sequencing: M13 Universal Sequencing Primer and M13 -40 Sequencing Primer can be used for both double-stranded and single-stranded sequencing. A protocol for production of single-stranded DNA is provided with the vector. • Cloning: Inserts containing a stop codon will yield white colonies when grown on media containing X-gal. • Host(s): *E. coli*. • Selectable marker(s): Plasmid confers resistance to 70 μg/ml ampicillin. • Amplification: Recommended.
spaI UV5		X	X			
pMC1871						• Expression: The *lac* gene is promoterless and missing the first eight non-essential amino acids. Inserts cloned into the *Sma* I site give fusion proteins with β-gal. Insert must contain a promoter, ATG, and ribosome-binding site. • Host(s): *E. coli* strains carrying a *lac* deletion. • Selectable marker(s): Plasmid confers resistance to 15 μg/ml tetracycline.
			X			

Note: For high-level transformation of host cells (*E. coli*), we recommend the "Hanahan" protocol [Hanahan, D., *J. Mol. Biol.* 166, 557 (1983)].

COMMONWEALTH OF AUSTRALIA

(Patents Act 1990)

IN THE MATTER OF: Australian Patent Application 696764 (73941/94). In the name of: Human Genome Sciences Inc.

- and -

IN THE MATTER OF: Opposition thereto by Ludwig Institute for Cancer Research, under Section 59 of the Patents Act.

Annexure GBC-7

This is **Annexure GBC-7** referred to in my Statutory Declaration made this Thirteenth day of December 2000.

gary cox

Gary Baxter Cox

WITNESS: Peyton Lee

Patent Attorney PEYTEE LEE

The EMBO Journal vol.15 no.7 p.1751, 1996

Corrigendum/Erratum

A novel vascular endothelial growth factor, VEGF-C, is a ligand for the Flt4 (VEGFR-3) and KDR (VEGFR-2) receptor tyrosine kinases

Vladimir Joukov, Katri Pajusola, Arja Kaipainen, Dmitri Chilov, Isto Lahtinen, Eola Kukk, Olli Saksela, Nisse Kalkkinen and Kari Alitalo

The EMBO Journal, 15, 290–298, 1996

Our recent results on the nascent VEGF-C polypeptide immunoprecipitated from metabolically labelled cells suggest that the intracellular precursor protein is larger than the secreted protein, for which we predicted the open reading frame given in our paper in *EMBO J.*, 15 (2), 290–298 (1996). This would suggest that an upstream ATG codon at position 352 in the same reading frame of the VEGF-C cDNA sequence (accession number X94216) is used for initiation of translation, resulting in an additional N-terminal 'prepro-VEGF-C' peptide: MHLLGFFSVACSLLAAALLPGPREAPAAAAAFESGLDLSDAEPDAGEATAYASKDLEEQLRSVSSVDEL. This sequence is identical to the N-terminus of the peptide sequence of Lee *et al.* (U43142), submitted to the database on December 12, 1995. The numbering of amino acid residues of VEGF-C presented in Figure 3B would then be 70–419 and in Figure 3C 275–365 (starting from the first methionine residue of the 'prepro-VEGF-C'). The sequence underlined in Figure 3B thus represents the C-terminal part of the 'prepro-VEGF-C' peptide rather than the signal peptide. However, the alignment of the homologous sequences in Figure 3B and C remains unchanged. The predicted molecular mass of the entire VEGF-C precursor is 46 883 and the length is 419 amino acid residues. Our EMBL, GenBank and DDBJ entry X94216 includes these features.

The sentence on the title page 290: 'B.Olofsson and K.Pajusola contributed equally to this work, as did K.Alitalo and U.Eriksson' was erroneously copied by Oxford University Press from the given title page of the reference: Olofsson,B. *et al.* (1996) *Proc. Natl Acad. Sci. USA*, in press.

COMMONWEALTH OF AUSTRALIA

(Patents Act 1990)

IN THE MATTER OF: Australian Patent Application 696764 (73941/94). In the name of: Human Genome Sciences Inc.

- and -

IN THE MATTER OF: Opposition thereto by Ludwig Institute for Cancer Research, under Section 59 of the Patents Act.

Annexure GBC-8

This is **Annexure GBC-8** referred to in my Statutory Declaration made this Thirteenth day of December 2000.

Gary Baxter Cox

Gary Baxter Cox

WITNESS: Peyton Kwo

Patent Attorney PEYTEE KWOO

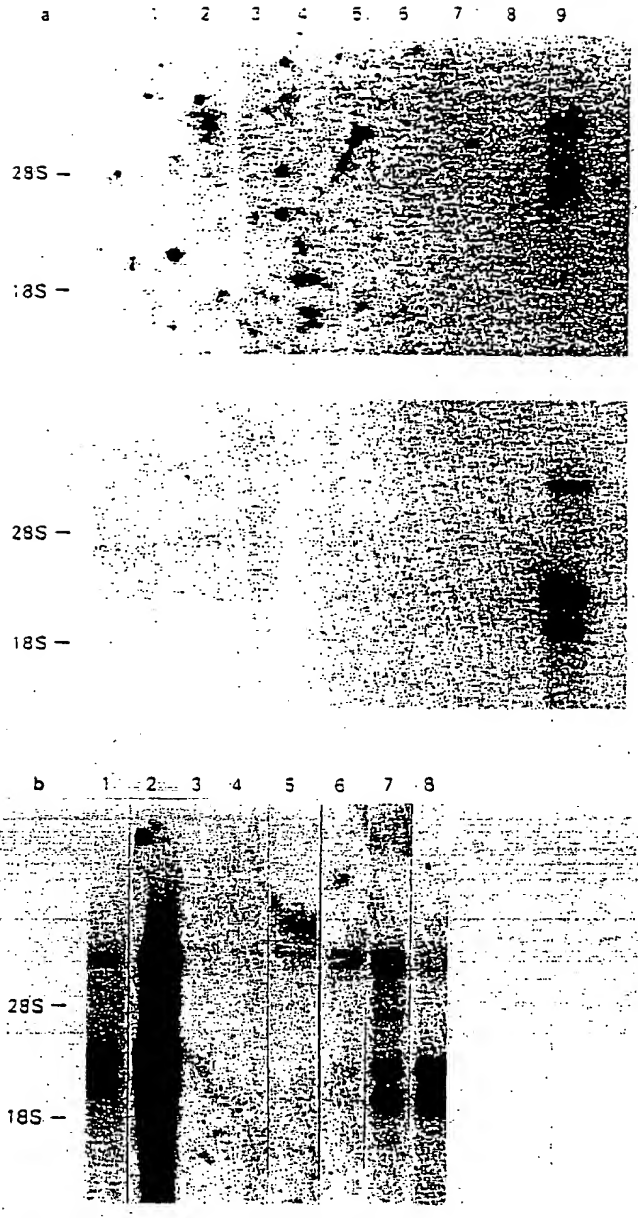

Figure 1 Northern blot analysis of the human *flt* gene. Poly (A)$^+$ RNA was prepared from various tissues and cell lines (see Materials and methods), and 2 μg of these RNAs were separated on a gel, transferred to a nitrocellulose filter and hybridized with EcoRI-BamHI 0.8 kb fragment of human genomic *flt* DNA (Matsushime *et al.*, 1987) (upper panel in a) or with #3–7 *flt* cDNA (lower panel in a, and b) as a probe. RNA samples in (a): lane 1, KB cell; lane 2, 293 cell (a cell line derived from human embryo kidney); lane 3, Daudi (B-lymphoma); lane 4, Namalwa (B-lymphoma); lane 5, Kato-III (human gastric adenocarcinoma cell line); lane 6, Ito-II (human testicular tumor cell line); lane 7, Molt-4 (T-lymphoma); lane 8, B16 (mouse melanoma cell line); lane 9, human placenta. RNA samples in (b): lane 1, human placenta (low amount of RNA, 0.2 μg); lane 2, human placenta; lane 3, human liver; lane 4, human muscle; lane 5, human kidney; lane 6, 293 cell line; lane 7, 293E1 cell line; lane 8, BeWo (human choriocarcinoma cell line)

upstream from this ATG codon, we consider that this ATG is the initiation codon of *flt* gene product for the following reasons: (1) the nucleotide residue 1 to 249 are extremely GC-rich (approximately 80%) and this characteristic is similar to that of the upstream noncoding region of several other receptor-type tyrosine kinase genes, i.e. EGF receptor and insulin receptor genes (Ullrich *et al.*, 1984; Ebina *et al.*, 1985; Ullrich *et al.*, 1985), (2) a short stretch including the 250–252 ATG codon, TCACCATGG, is well matched with Kozak's criteria CC(A/G)CCATGG for the initiation codon in mammalian species (Kozak, 1984); (3) this ATG is followed by 21 codons which are mostly for hydrophobic amino acids, and therefore the features of this region are consistent with these of a signal peptide of membrane proteins; (4) the position of this ATG codon is identical to the position of the initiation codons in the *fms* gene family when the cysteine residues in the *flt* extracellular domain are aligned to those of the *fms* gene product. Calculating from this ATG codon as the amino acid residue 1, the predicted *flt* gene product consists of 1338 amino acid residues and the molecular weight was expected to be 150 565 daltons.

Possible domain structure of the flt *gene product*

The *flt* product can be subdivided into three regions: a 758-amino-acid extracellular domain; a 22-amino-acid transmembrane domain which is followed by a cluster of basic amino acids (Arg-Lys-Met-Lys-Arg); a 558-amino-acid cytoplasmic region containing a tyrosine kinase domain. This kinase domain has a Gly-x-Gly-x-x-Gly stretch at the residues 834–839, a conserved lysine at the ATP binding site (residue 861) and a tyrosine residue (#1053) as the putative autophosphorylation site which corresponds to tyrosine-#416 in the *src* gene product. One of the most remarkable features of the *flt* tyrosine kinase domain is a very long peptide (66 amino acids) insertion at the middle of the kinase domain. The position and the length of this insert are essentially the same as those in the *fms* gene family (Figure 3). Furthermore, a striking similarity between *flt* gene product and the c-*fms* gene family was also detected in the distribution of cysteine residues within the extracellular domain, as shown in Figures 3 and 4. Thus, the *flt* gene appears to belong to the *fms* family, and also to the 'Immunoglobulin superfamily' in which cysteine residues form intramolecular disulfide bonds for appropriate folding of ligand binding domain (Williams, 1989).

However, a clear structural difference exists between the *flt* gene product and the *fms* family: the length of the extracellular domain in the *flt* gene product is about 220 amino acids longer than those in the *fms*, *kit* and PDGF receptor gene products. Although there are several possible explanations for the origin of this *flt*-specific region (Stretch b in Figure 4), a partial gene duplication in the extracellular domain seems most likely, because a weak but significant amino acid homology was observed between the *flt*-specific sequence (residues 550–745) and the 230-amino-acid region just upstream of the transmembrane domain in the *fms* family (Figure 4). Recently we have confirmed the presence of this *flt*-specific region in murine *flt* cDNA (Yamane & Shibuya, unpublished results).

Homology between flt *and other tyrosine kinase genes*

Since the *flt* gene was originally isolated on the basis of a weak nucleotide homology with v-*ros* DNA, the overall homologies of the *flt* tyrosine kinase domain except for the insert region at the amino acid level were

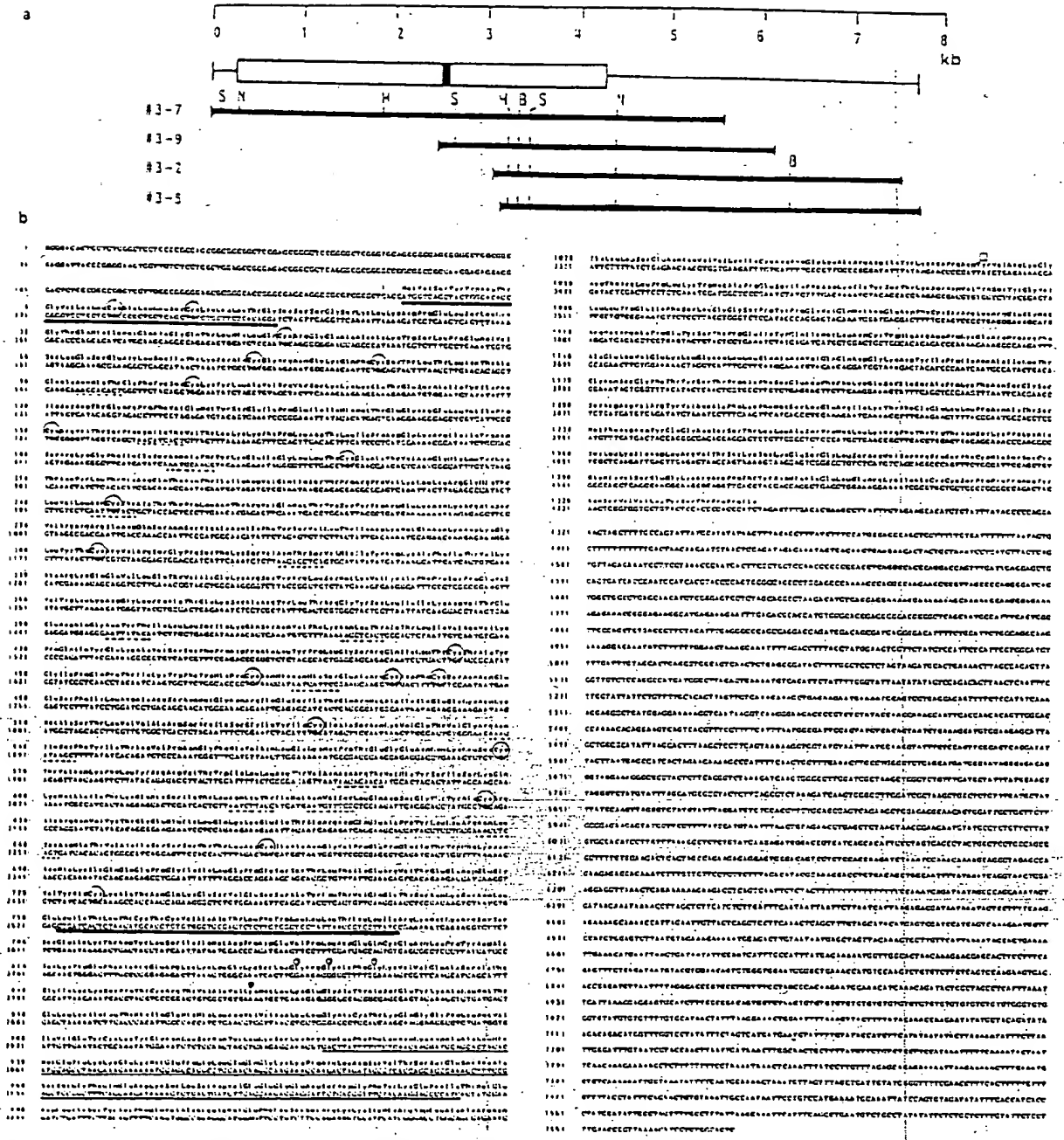

Figure 2 Nucleotide sequence and predicted amino acid sequence of the *flt* cDNA. (a) Representative cDNA clones, restriction sites and the open reading frame are indicated. (b) Nucleotide and amino acid sequences in the *flt* gene. The number of amino acid residues is started from the putative initiation codon at nucleotide residue 250–252. A heavy underline at the amino terminal region indicates a possible signal peptide. Another heavy underline in the middle of the sequence shows putative transmembrane domain. Cysteine residues within the extracellular domain (1–19) are encircled. Potential N-glycosylation sites in the same domain are shown by broken lines. Small open circles indicate glysine residues at G-X-G-X-X-G region in the tyrosine kinase domain, and closed circle represents putative ATP binding site. Thin underline in the middle of the cytoplasmic domain indicates the long insert within the kinase domain, and the open square shows the tyrosine residue for a possible autophosphorylation. B, BglII; H, HindIII; N, NcoI; S, SmaI

compared among various other protein kinase genes. As shown in Table 1, the homology was higher with the *fms* family (54–60%), whereas those with other receptor-type (including c-*ros* gene) or non-receptor-type tyrosine kinase genes were lower (35–38%). Thus the homology score further supports the hypothesis that the *flt* gene is closely related to the *fms* family (Figure 5).

Although the amino acid homology in the tyrosine kinase domain is remarkable between the *flt* and *fms* families, the long peptide insert in the middle of the *flt* tyrosine kinase domain has little or no significant homology with the insert of any member of the *fms* family. Thus, this region might have a role in specific function(s) of each gene product of the c-*fms*/*flt* family. Recently, Escobedo & Williams (1988) have reported that a mutant of PDGF receptor carrying a deletion within the insert region in the kinase domain cannot stimulate mitogenic response in spite of exhibiting tyrosine kinase activity and other biological functions in response to PDGF.

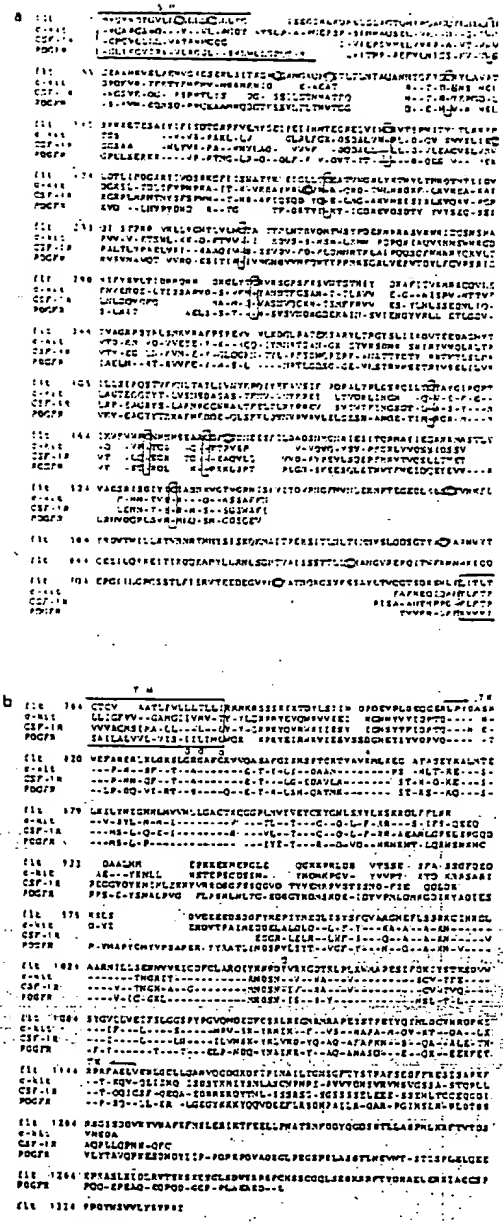

Figure 3 Comparison of the amino acid sequences between *flt* gene and other members of *fms* family (*fms*, *kit*, and PDGF receptor). The amino acid sequences were aligned and gaps (empty space) were introduced for optimal homology. Amino acids in the *fms* family identical to those in the *flt* gene product are indicated by a dash. The sequence of PDGF receptor is that reported by Yarden *et al.* (1986). (a) Similarity of the extracellular domain. The regions from signal peptides (SP) to the middle of transmembrane domains are indicated. All cysteine residues are circled or boxed. Amino acid residues #550 to #745 are *flt*-specific. (b) Similarity of the intracellular domain. The regions from the middle of transmembrane domain (TM) to the carboxyl ends are indicated. Three conserved glysine residues, the lysine for the potential ATP binding site and the potential tyrosine autophosphorylation site are indicated by open circles, by a closed circle and by a open square, respectively. The region of tyrosine kinase domain is shown by arrows

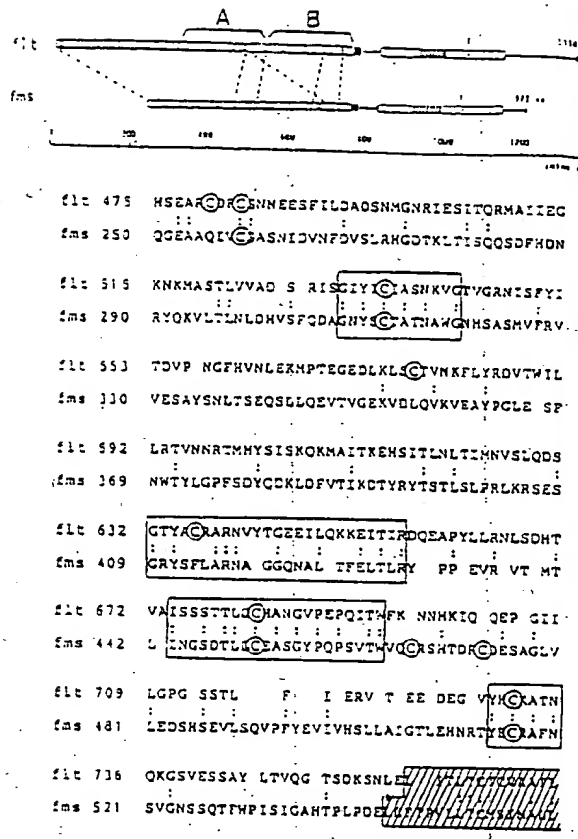

Figure 4 A possible partial gene duplication of extracellular domain in the *flt* sequence. About 280 amino acid residues upstream from the transmembrane domain (shadowed box) in the *flt* and the *fms* genes are compared. Highly conserved regions are boxed and all cysteine residues are circled. Sequences in (a) and in (b) are considered to be partially duplicated in the *flt* genome

Expression of the flt *gene in cell lines and normal tissues*

In order to study the physiological significance of the *flt* gene, its expression was examined by Northern blot analysis using molecularly cloned *flt* cDNA. Poly(A)$^+$ RNAs obtained from a variety of normal tissues and cell lines were hybridized with #3–7 5.6 kb human *flt* cDNA. As shown in Figure 1b, a higher expression was detected in human placenta tissue, and weakly hybridized bands were observed in human embryo kidney-derived cell lines, 293 and 293E1, and a choriocarcinoma cell line, BeWo (Graham *et al.*, 1977; Chinnadurai *et al.*, 1978; Pattillo *et al.*, 1968). In addition, faint bands were also detected in liver, muscle and kidney of human.

To examine further the tissue-specific expression of the *flt* gene in animals, we molecularly cloned the entire

Table 1 Amino acid homology in tyrosine kinase domain between *flt* gene and other genes of *src* family

Gene	*Amino-half** %	*Insert*** %	*Carboxyl-half*† %
v-*fms*	57	5	53
PDGF-R*α*††	59	13	58
PDGF-R*β*‡	57	13	53
v-*kit*	62	11	58
v-*erbB*	26	—	42
v-*ros*	32	—	43
v-*src*	30	—	38
v-*fps*	32	—	41

* *flt* residue #813–#929
** #930–#994
† #995–#1152
†† PDGF-R*α*: Matsui *et al.*, 1989
‡ PDGF-R*β*: Yarden *et al.*, 1986

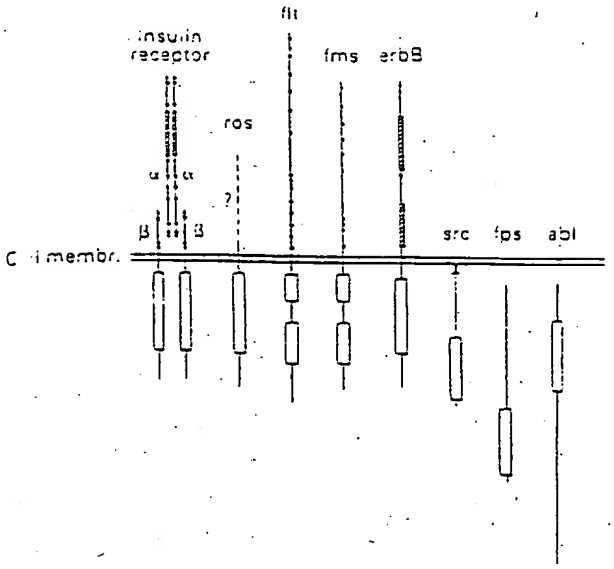

Figure 5 Schematic comparison of the *flt* gene product with those of other representative tyrosine kinase genes

coding region of *flt* cDNA of rat, and both human and rat *flt* cDNAs were used as probes. The nucleotide sequence of rat *flt* cDNA will be described elsewhere (Yamane & Shibuya, unpublished). In adult tissues of rat, *flt* mRNA was detected in many tissues such as lung, placenta, liver, kidney, heart and brain the highest expression was observed in the lung (Figure 6, Table 2).

In contrast to these findings, the *flt* mRNA was not detectable or extremely low, if any, in most of the 20 human tumor cell lines examined. These malignant cell lines include epithelial and adenomatous carcinomas, T- and B-lymphomas, and leukemias of erythroid, granulocytic and monocytic lineages (Figure 1, Table 2). These results might suggest that the *flt* gene is not directly

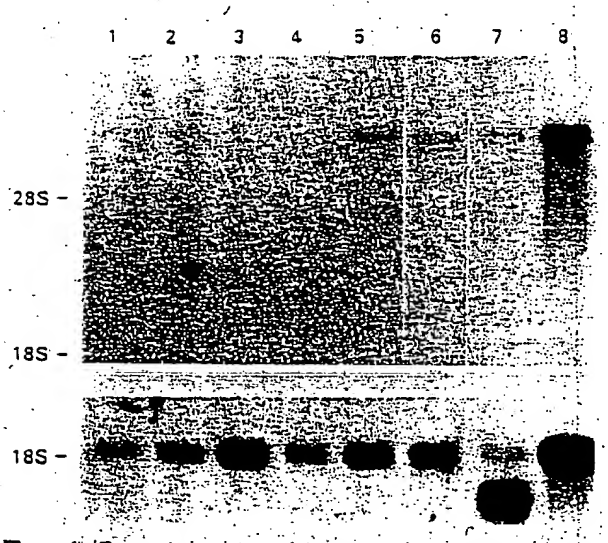

Figure 6 Expression of *flt* gene in various normal tissues of rat. About 2 μg of poly (A)$^+$ RNA was separated on an agarose gel, transferred to a nitrocellulose filter and hybridized with 0.9 kb rat *flt* cDNA corresponding to tyrosine kinase domain (upper panel) or chicken beta-actin cDNA (lower panel) as probes. Lane 1, liver; lane 2, kidney; lane 3, thymus; lane 4, testis; lane 5, placenta; lane 6, brain; lane 7, heart; lane 8, lung

Table 2 Expression of *flt* gene in normal tissues and cell lines

Normal tissues		*Cell line*	
Human		Human	
placenta	+ +	BeWo (choriocarcinoma)	+
muscle	+	T3M3 (choriocarcinoma)	–
liver	+	293 (embryo kidney)	+
kidney	+	293E1 (embryo kidney)	+
Rat		Daudi (B-lymphoma)	–
placenta	+	Namalwa (B-lymphoma)	–
lung	+	Raji (B-lymphoma)	–
heart	+	Molt-4 (T-lymphoma)	–
brain	+	HL60 (promyelocytic leukemia)	–
testis	–	K562 (chronic myelogenous leukemia)	+/–
thymus	–	Hela (cervical cancer)	–
kidney	+	A431 (epitheloid cancer)	–
liver	+	Kato-III (gastric cancer)	–
		GK-T3 (small cell lung ca.)	–
		Ito-II (testicular tumor)	–
		FL (amnion tissue)	–
		A549	–
		143B	+/–
		Mouse	
		B16 melanoma	–

involved in the process of cell proliferation, but in differentiation or maintenance of normal tissues in physiological conditions.

Subgenomic fragments of the flt *mRNA*

A genomic *flt* DNA corresponding to the middle portion of the kinase domain detected only 7.5–8.0 kb species of mRNA (Figure 1a), whereas, #3–7 cDNA probe, which bear the entire coding region of *flt* gene, detected other species of mRNA (2.2 and 3.0 kb) as well as 7.5–8.0 kb mRNA (Figure 1). As an explanation for these small-sized mRNAs, cross-hybridization of this cDNA probe with other tyrosine kinase genes seems unlikely, because most of the cells expressing 7.5–8.0 kb *flt* mRNA also showed 2.2 and 3.0 kb mRNAs when hybridized with #3–7 cDNA probe. Our preliminary results (Ikeda & Shibuya, unpublished results) indicate that these short mRNAs appear to be due to premature termination of the transcripts within the extracellular domain of the *flt* gene. Since these small *flt* mRNAs could encode for about amino-terminal half of the extracellular domain of this gene product, these molecules might have a regulatory role in physiological condition, through binding and absorbing the yet unidentified *flt* ligand.

Is the flt *gene involved in carcinogenesis of animals?*

A relationship between the *flt* gene and tumorigenicity in higher organisms was examined by Southern blot analysis. Approximately 100 human tumor cells (about 30 gastric cancers, 25 brain tumors, 10 colon cancers and other types) did not carry gene amplification or rearranged fragments of *flt* DNA at a detectable level (data not shown). Thus, we have no direct evidence to support the involvement of *flt* gene in carcinogenesis of animals. However, Walker *et al.* (1987) have recently reported overexpression of an 8.5 kb mRNA in experimental rat tracheal carcinoma which was detected by cross-hybridization with v-*fms* probe. It would be interesting to clarify whether this 8.5 kb *fms*-like gene in rats is a cognate cellular gene of the human *flt*.

Materials and methods

Construction of the cDNA library

Poly (A)$^+$ RNA was prepared from fresh tissue of normal human placenta and used for making a cDNA library. The library was constructed by the method described by LaPolla *et al.* (1984). Briefly, 5 μg of poly (A)$^+$ RNA was used for synthesis of the first strand cDNA with AMV reverse transcriptase and oligo(dT) primer. The second strand was then synthesized with *E. coli* DNA polymerase I and RNAase H for RNA primers. The cDNAs were treated with T4 DNA polymerase to make the ends flush, and the internal EcoRI sites were methylated. Both ends of cDNAs were ligated with EcoRI linkers and digested with EcoRI restriction endonuclease. Since the size of *flt* mRNA detected in Northern analysis was 7.5–8.0 kb, cDNAs were size-fractionated on a Bio-Rad A5m Sepharose column, and the fraction containing larger cDNA molecules were collected and ligated to λgt10 or λgt11 arms. The DNAs were packaged into phage particles with a Gigapack plus kit and approximately 5×10^5 independent phase clones were obtained. The size of inserts in these clones was about 2 kb on average. This cDNA library was screened with *flt* genomic DNA probe using a method described by Benton & Davis (1977).

DNA sequencing

Two overlapping cDNA clones, #3–7 and #3–5 were sequenced by the dideoxynucleotide method (Sanger *et al.*, 1977). To sequence both strands, these *flt* cDNAs were subcloned in pUC plasmid vectors in both orientations and various deletions from the 5'- or 3'-end were introduced into the cDNA molecules by using a DNA deletion kit (Takara Shuzo, Kyoto). For DNA sequencing these deletion-containing plasmid DNAs were prepared and denatured to single-stranded form by an alkali method. The coding regions of the *flt* DNA were sequenced at least three times, including both directions.

Northern blotting analysis

Total cellular RNA was prepared from various cell lines and tissues by a guanidine/cesium chloride centrifugation method (Chirgwin *et al.*, 1979). Poly (A)$^+$ RNA was obtained using oligo(dT) column chromatography and separated on a formaldehyde-containing agarose gel (Lehrach *et al.*, 1977). RNA was transferred to a nitrocellulose filter, baked for fixation and hybridized with *flt* genomic or complementary DNA sequences. Hybridization condition was 3 × SSC (1 × SSC: 0.15 M NaCl, 0.015 M Na citrate), 50% formamide at 37°C.

Acknowledgements

We thank Dr Takeshi Odaka for helpful discussions. We are also grateful to Japanese Cancer Research Resources Bank for supplying cell lines, Kato-III, Ito-II and Molt-4.

This work was supported by a Grant-in-aid (01614505) for Special Project Research on Cancer-Bioscience from the Ministry of Education, Science and Culture of Japan, a Research Grant from the Princess Takamatsu Cancer Research Fund, and a Research Grant from the Foundation for Promotion of Cancer Research in Japan. A.T. acknowledges a fellowship from the Japan Society for the Promotion of Science.

References

Benton, W.D. & Davis, R.W. (1977). *Science*, 196, 180–182.

Besmer, P., Murphy, J.E., George, P.C., Qiu, F., Bergold, P.J., Lederman, L., Snyder, H.W., Jr, Brodeur, D., Zuckerman, E.E. & Hardy, W.D. (1986). *Nature*, 320, 415–421.

Bishop, J.M. (1985). *Cell*, 42, 23–38.

Chabot, B., Stephenson, D.A., Chapman, V.M., Besmer, P. & Bernstein, A. (1988). *Nature*, 335, 88–89.

Chinnadurai, G., Chinnadurai, S. & Green, M. (1978). *J. Virol.*, 26, 195–199.

Chirgwin, J.M., Przybyla, A.E., Macdonald, J.R. & Rutter, W.J. (1979). *Biochemistry*, 18, 5294–5299.

Das, S.K. & Stanley, E.R. (1982). *J. Biol. Chem.*, 257, 13679–13684.

Ebina, Y., Ellis, L., Jarnagin, K., Edery, M., Graf, L., Clauser, E., Ou, J.-H., Masiarz, F., Kan, Y.W., Goldfine, I.D., Roth, R.A. & Rutter, W.J. (1985). *Cell*, 40, 747–758.

Escobedo, J.A. & Williams, L.T. (1988). *Nature*, 335, 85–87.

Geissler, E.N., Ryan, M.A. & Housman, D.E. (1988). *Cell*, 55, 185–192.

Graham, F.L., Smiley, J., Russell, W.C. & Nairn, R. (1977). *J. Gen. Virol.*, 36, 59–72.

Hampe, A., Gobet, M., Sherr, C.J. & Galibert, F. (1984). *Proc. Natl. Acad. Sci. USA*, 81, 85–89.

Johnsson, A., Heldin, C.-H., Wasteson, A., Westermark, B., Deuel, T.F., Huang, J.S., Seeburg, P.H., Gray, A., Ullrich, A., Scrace, G., Strobant, P. & Waterfield, M.D. (1984). *EMBO J.*, 3, 921–928.

Kozak, M. (1984). *Nucleic Acids Res.*, 12, 857–872.

LaPolla, R.J., Mayne, K.M. & Davidson, N. (1984). *Proc. Natl. Acad. Sci. USA*, 81, 7970–7974.

Lehrach, H., Diamond, D., Wozney, J.M. & Boedtker, H. (1977). *Biochemistry*, 16, 4743–4751.

Matsui, T., Heidaran, M., Miki, T., Popescu, N., La Rochelle, W., Kraus, M., Pierce, J. & Aaronson, S. (1989). *Science*, 243, 800–805.

Matsushime, H., Yoshida, M.C., Sasaki, M. & Shibuya, M. (1987). *Jpn. J. Cancer Res. (Gann)*, 78, 655–661.

Pattillo, R.A., Gey, G.O., Delfs, E. & Mattingly, R.F. (1968). *Science*, 159, 1467–1469.

Qiu, F., Ray, P., Brown, K., Barker, P.E., Jhanwar, S., Ruddle, F.H. & Besmer, P. (1988). *EMBO J.*, 7, 1003–1011.

Sanger, F., Nicklen, S. & Coulson, A.R. (1977). *Proc. Natl. Acad. Sci. USA*, 74, 5463–5467.

Satoh, H., Yoshida, M.C., Matsushime, H., Shibuya, M. & Sasaki, M. (1987). *Jpn. J. Cancer Res. (Gann)*, 78, 772–775.

Sherr, C.J., Rettenmier, C.W., Sacca, R., Roussel, M.F., Look, A.T. & Stanley, E.R. (1985). *Cell*, 41, 665–676.

Stanley, E.R. & Heard, P.M. (1977). *J. Biol. Chem.*, 252, 4305–4312.

Ullrich, A., Bell, J.R., Chen, E.Y., Herrera, R., Petruzzelli, L.M., Dull, T.J., Gray, A., Coussens, L., Liao, Y.-C., Tsubokawa, M., Mason, A., Seeburg, P.H., Grunfeld, C., Rosen, O.M. & Ramachandran, J. (1985). *Nature*, 313, 756–761.

Ullrich, A., Coussens, L., Hayflick, J.S., Dull, T.J., Gray, A., Tam, A.W., Lee, J., Yarden, Y., Libermann, T.A., Schlessinger, J., Downward, J., Mayes, E.L.V., Whittle, N., Waterfield, M.D. & Seeburg, P.H. (1984). 309, 418–425.

Walker, C., Nettesheim, P., Barrett, J.C. & Gilmer, T.M. (1987). *Proc. Natl. Acad. Sci. USA*, 84, 1804–1808.

Waterfield, M.D., Scarce, G.T., Whittle, N., Strooabant, P., Johnsson, A., Wasteson, A., Westermark, B., Heldin, C.-H., Huang, J.S. & Deuel, T.F. (1983). *Nature*, 304, 35–39.

Williams, L.T. (1989). *Science*, 243, 1564–1570.

Yarden, Y., Escobedo, J.A., Kuang, W-J., Yang-Feng, T.L., Daniel, T.O., Tremble, P.M., Chen, E.Y., Ando, M.E., Harkins, R.N., Francke, U., Freied, V.A., Ullrich, A. & Williams, L.T. (1986). *Nature*, 323, 226–232.

Yarden, Y., Kuang, W-J., Yang-Feng, T., Coussens, L., Munemitsu, S., Dull, T.J., Chen, E., Schlessinger, J., Francke, U. & Ullrich, A. (1987). *EMBO J.*, 6, 3341–3351.

These sequence data will appear in the EMBL/GenBank/DDBJ Nucleotide Sequence Databases under the accession numbers X51602.

COMMONWEALTH OF AUSTRALIA

(Patents Act 1990)

IN THE MATTER OF: Australian Patent Application 696764 (73941/94). In the name of: Human Genome Sciences Inc.

- and -

IN THE MATTER OF: Opposition thereto by Ludwig Institute for Cancer Research, under Section 59 of the Patents Act.

Annexure GBC-9

This is **Annexure GBC-9** referred to in my Statutory Declaration made this Thirteenth day of December 2000.

Gary Baxter Cox

Gary Baxter Cox

WITNESS: _____

Patent Attorney PEYTEE KEMP

Angiogenesis: Models and Modulators

Gillian W. Cockerill, Jennifer R. Gamble, and Mathew A. Vadas
Hanson Center for Cancer Research, Institute of Medical and Veterinary Research, Adelaide 5000, South Australia, Australia

Angiogenesis *in vivo* is distinguished by four stages: subsequent to the transduction of signals to differentiate, stage 1 is defined as an altered proteolytic balance of the cell allowing it to digest through the surrounding matrix. These committed cells then proliferate (stage 2), and migrate (stage 3) to form aligned cords of cells. The final stage is the development of vessel patency (stage 4), generated by a coalescing of intracellular vacuoles. Subsequently, these structures anastamose and the initial flow of blood through the new vessel completes the process. We present and discuss how the available models most closely represent phases of *in vivo* angiogenesis. The enhancement of angiogenesis by hyaluronic acid fragments, transforming growth factor β, tumor necrosis factor α, angiogenin, okadaic acid, fibroblast growth factor, interleukin 8, vascular endothelial growth factor, haptoglobin, and gangliosides; and the inhibition of the process by hyaluronic acid, estrogen metabolites, genestein, heparin, cyclosporin A, placental RNase inhibitor, steroids, collagen synthesis inhibitors, thrombospondin, fumagellin, and protamine are also discussed.

KEY WORDS: Angiogenesis, Cell proliferation, Cell migration, Proteolytic balance, Collagen synthesis inhibitors.

I. Introduction

Endothelial cells are derived from pluripotent mesodermal precursors during the process of vasculogenesis, which occurs in the extraembryonic

mesoderm of the yolk sac in both avian and mammalian embryos, and in selected organ systems (Risau and Lemmon, 1988; Pardanaud *et al.*, 1989). Angiogenesis is the development of the complex network of blood vessels that occurs following vasculogenesis, when endothelial cells proliferate and migrate throughout the embryo. The process of angiogenesis is important not only during embryological development, but during a variety of normal and pathological conditions in the adult, including ovulation, implantation, during mammary gland changes associated with lactation, bone formation, inflammation wound repair (Jakob *et al.*, 1977; Gospodarowicz and Thakral, 1978; Nomura *et al.*, 1989; Brannström *et al.*, 1988; Knighton *et al.*, 1990), and tumor growth (Folkman, 1985; Furcht, 1986).

Light and electron microscopy studies, combined with *in situ* hybridization, of both the normal genesis of vessels during embryological development and during tumor angiogenesis have demonstrated a number of discrete events that occur during antiogenesis (Schoefl, 1963; Yamagami, 1970). Following a stimulus for neovascularization endothelial cells change their morphology and begin to degrade their surrounding basement membrane (Ausprunk and Folkman, 1977; Moscatelli *et al.*, 1980; Gross *et al.*, 1983). These "leading" cells must modulate the expression of their proteases to allow degradation of existing extracellular matrix (ECM) components, and the migrating cells following this front must be supported by the appropriate ECM to allow for their proliferation, migration, and differentiation into vascular tubes. This initial migration and proliferation is in a fibronectin-rich ECM, and during the later stages of angiogenesis, when cords of endothelial cells align, the cells express laminin, a matrix component associated with vascular maturation (Risau and Lemmon, 1988). Finally, the generation of vessel patency is achieved by the coalescing of intra- and intercellular vacuoles (Sabin, 1920; Lewis, 1925; Clark and Clark, 1937).

The dependence of tumor growth on angiogenesis is well documented (Folkman, 1990). This relationship has been demonstrated for many types of tumor, invasive breast cancer (Weidner *et al.*, 1991), non-small cell lung cancer (Macchiarini *et al.*, 1992), and prostate carcinoma (Weidner *et al.*, 1993). Studies using the pancreatic β cells of animals transgenic for a hybrid oncogene (RIP1–Tag2) (Brinster *et al.*, 1993) would indicate that angiogenesis is an important step in carcinogenesis in this system (Folkman *et al.*, 1989a).

To investigate factors that influence angiogenesis and to gain a more fundamental understanding of the cellular processes involved in the generation of capillaries, it has been necessary to develop a number of models of angiogenesis.

II. Models of Angiogenesis

A. Chicken Chorioallantoic Membrane Assay

The chicken chorioallantoic membrane assay is a technique traditionally used by embryologists that involves analysis of the developmental potential of grafts transplanted onto the chorioallantoic membrane (CAM). Because the early chicken embryo lacks a complete immune system xenografts from mammalian species become established and grow. Vascularization of these grafts is rapid.

Sorgente and colleagues (1975) first described the inhibitory effects of cartilage grafts on vascular development using this model. Subsequently, Folkman and co-workers (1979) used the model to study tumor angiogenesis directly. Fertile eggs were incubated for 72 hr and prepared for grafting by removal of enough albumin to facilitate the placement of a graft without causing subsequent cramping and sticking to the shell membrane. A rectangular window was cut in the shell to place and access the graft or test substance on the CAM. Angiogenesis was scored 3–4 days after grafting. Angiogenesis was considered to have been induced if a spoke–wheel arrangement of vessels was generated, directed toward the graft. Substances were lyophilized onto coverslips, then applied to the CAM to examine the effects on angiogenesis (Folkman *et al.*, 1979).

Quantitation of angiogenesis using the CAM assay was initially done on a graded score of 0–4, by observation. Computer analysis was subsequently applied to score the total number of vessels and obtain a directional vector value (Voss *et al.*, 1984; Jakob and Voss, 1984). The use of labeled sulfate to follow the angiogenic process has also made quantitation more accurate (Spisni *et al.*, 1992). Apart from problems associated with quantitation, the most common problem is the result of false positives due to wounding or irritants generated during the initial setting up of the assay. Because an angiogenic response may be consequent to wound healing or inflammation (Mahaderan *et al.*, 1989), this problem is not surprising. The CAM assay is sensitive to modification by many factors, including gas content and pH. The most pronounced variation observed is of keratinization, which in turn has significant effects on the CAM response to stimulation (Ausprunk *et al.*, 1991). This method has been applied to a wide range of both inhibitors and inducers of angiogenesis, as discussed in subsequent sections of this article (Folkman and Klagsbrun, 1987).

A further development of this model has been the *in vitro* method of maintaining the chick embryo in culture (Auerbach *et al.*, 1974). Although this is an *in vitro* assay, it is closest to a whole animal assay because the

entire embryo and its membranes remain intact. In this assay, the egg content is transferred to a petri dish, where development continues to take place. This model has the advantage that multiple grafts can be placed on one embryo, and the effects can be photographed over time. Quantitation is simplified by the fact that the *in vitro* CAM presents a two-dimensional monolayer, not subject to the distortion of the *in ovo* CAM assay. The advantage is that multiple grafts may then be placed on the one embryo, and they can more easily be photographed over time. A further modification of the *in vitro* CAM assay, in which the embryo is supported on Gladwrap stretched across the mouth of a beaker (Dunn *et al.*, 1981), has improved embryo survival. The advantages of increased viability are offset by the difficulty in photographing the results. This model is technically easier that the *in ovo* assay and is better suited to large-scale experiments. The addition of sterile silicon rings on the yolk sac membrane creates discrete observation windows and assists in quantitation (Takigawa *et al.*, 1990).

B. Corneal Neovascularization Model

As the cornea is normally avascular, induction of an angiogenic reaction is a true demonstration of neovascularization (Hendkin, 1978). The earliest studies of corneal neovascularization were in the rabbit (Gimbrone *et al.*, 1974), in which insertion of tumor cells or extracts placed within 2 mm of the cornea–scleral junction generated vascular sprouts within 36 hr. However, because of the absence of genetically similar strains, expense, and difficulty in handling, other species have been used for angiogenesis studies in the cornea, including guinea pigs, rats, and mice (Fournier *et al.*, 1981; Muthukkaruppan and Auerbach, 1979; Muthukkaruppan *et al.*, 1982). Although the use of mice overcame the strain variation problem their small size makes the introduction of slow-release polymer into the eye a procedure requiring microsurgical skill. Quantitation of corneal neovascularization is difficult owing to the variability arising from an inability to achieve uniform placement of the test substance. Consequently, reagents under test have been incorporated into ethylene–vinyl acetate pellets (Elvax) prior to implantation into the cornea (Gimbrone *et al.*, 1974; Risau, 1986). The implantation of tumor cells also requires the incorporation of those cells into an inert medium that allows for accurate placement (Ausprunk and Folkman, 1977). The expression of corneal-derived cytokines such as interleukin 8 (IL-8), which has been shown to be angiogenic, may also lead to some variability in assays of angiogenic factors (Strieter *et al.*, 1992).

Advances in image analysis (Proia *et al.*, 1988; Haynes *et al.*, 1989) have improved the capacity to quantitate using the corneal model. Often a computerized digitalyzer, for example the Optomax Image analysis system (Optomax, Hollis, NY) or similar, is used. This system consists of a high-sensitivity closed circuit television (CCTV) camera mounted on a Nikon Optiphot-2 microscope. The image is displayed on a color video monitor that is interfaced with a microprocessor. Histological slides stained with von Willebrand factor antibodies may be used to locate blood vessel formation. Sequential monitoring of neovascularization in individual animals makes it possible to evaluate progressive changes in the process (Folkval, 1991). Indeed, development of computer-assisted image analysis has made many models of angiogenesis more quantitative (Parke *et al.*, 1988).

C. Pouch Assays

The hamster cheek pouch is considered to be an "immune privileged" site because allogeneic or xenogeneic grafts may grow without eliciting an immune response. The anterior eye chamber is another "immune privileged" site that has been used to study neovascularization of preneoplastic mammary tumor cells (Folkman *et al.*, 1989b). Quantitation of this model is by morphometric analysis of histologically prepared sections following angiogenesis. Tumor implants have also been used (Auerbach *et al.*, 1976) in this model, as have slow-release vectors to assess the effects of transforming growth factor (TGF-α) (Schreiber *et al.*, 1986).

The dorsal air sac method was developed by Selye (1953), to monitor vascularization of tumor grafts. Dorsal air sacs are created by injecting 10–15 ml of air into the backs of rats, and the model modified by the insertion of a transparent window in the skin, through which the process may be monitored. Using this model, angiogenesis mediated by the injection of tumor cells (Sakamoto *et al.*, 1991) or endothelial cells (Schweigerer *et al.*, 1992) has been assayed in response to various reagents.

The method of subcutaneous implantation of polyvinyl acetate (PVA) sponge disks impregnated with angiogenic factors is in common use (Fajardo *et al.*, 1988). Flat sponges of PVA foam are cut into 11-mm disks and their flat sides are sealed with Millipore (Bedford, MA) filters. Prior to sealing, a core is cut where the test material is to be inserted. This core is sealed with a slow-release polymer, ethylene–vinyl acetate copolymer (Elvax) (Langer *et al.*, 1980), then reinserted into the sponge. The sponges are recovered 1–3 weeks after subcutaneous implantation. Xenon clear-

ance has been shown to be a useful means of quantifying new blood vessel formation (Andrade *et al.*, 1987).

Several *in vivo*, or *in ovo*, angiogenesis assays rely on being able to deliver a discrete amount of effector substance or cells to a precise location. Currently reagents are imbedded in Elvax; and the rate of release of components is dependent on the thickness of the coating of Elvax, making it difficult to reproduce these inserts. Alginate, a glycuron extracted from brown seaweed algae, gels in the presence of calcium ions or other multivalent counterions by anisocooperatively forming junctions between contiguous blocks of α1,4-L-glucuronan residues present in the polysaccharide. Growth of avian and mammalian chondrocytes in ionotrophically gelled alginate beads demonstrates the potential of using this model for an alternative delivery system in angiogenesis models (Guo *et al.*, 1989), or it may provide an alternative method for the slow release of effectors of angiogenesis (Downs *et al.*, 1982). Matrigel can also be injected subcutaneously in mice, and used as a vehicle to assess angiogenic activity of different compounds (Passanti *et al.*, 1992; Kibbey *et al.*, 1992). Although the subcutaneous injection of Matrigel alone is insufficient to induce focal angiogenesis when fibroblast growth factor (FGF)–heparin is mixed with the Matrigel, in-growth of vessels is observed within days. The Matrigel plug can be removed, and processed for vessel quantitation (Passanti *et al.*, 1992; Kibbey *et al.*, 1992).

D. Mesenteric Window Assay

The mesenteric window assay examines the effect of reagents on normally vascularized mammalian tissues. Angiogenesis in this model is mediated by autologous mast cells, and probably occurs frequently because mast cells are activated in tissue trauma, wound healing, inflammation, as well as in many clinical and experimental tumors (Enerback and Norrby, 1989). Although the mechanism of the mast cell-mediated angiogenic reaction is not completely understood it is known that preformed mast cell products such as heparin and histamine can be angiogenic (Norrby *et al.*, 1986, 1990; Garrison, 1990; Norrby and Sorbo, 1992; Sorbo and Norrby; 1992). Mast cell-mediated angiogenesis has also been reported using the CAM assay (Clinton *et al.*, 1988; Duncan *et al.*, 1992).

The mesenteric window assay is well suited to quantitative analysis. In addition to the number of vessels per unit length of tissue and the vascularized area, it permits quantitation of vascular density and total vascular quantity, as well as measurement of the branching pattern (Norrby *et al.*, 1990; Jakobsson and Norrby, 1991).

COMMONWEALTH OF AUSTRALIA

(Patents Act 1990)

IN THE MATTER OF: Australian Patent Application 696764 (73941/94). In the name of: Human Genome Sciences Inc.

- and -

IN THE MATTER OF: Opposition thereto by Ludwig Institute for Cancer Research, under Section 59 of the Patents Act.

Annexure GBC-10

This is **Annexure GBC-10** referred to in my Statutory Declaration made this Thirteenth day of December 2000.

Gary Cox

Gary Baxter Cox

WITNESS: Peytee Kmoo

Patent Attorney PEYTEE KMOO

CHAPTER 7

ROLE OF CYTOKINES IN ENDOTHELIAL CELL FUNCTIONS

Marek S. Litwin, Jennifer R. Gamble, and Mathew A. Vadas

Vascular endothelium, consisting of the cells and the extracellular matrices (ECM) that line the blood vessels, displays two characteristic properties: (a) endothelial renewal and angiogenesis, and (b) interactions with blood molecules and leukocytes. The turnover of endothelial cells (ECs) in most adult tissues is exceedingly slow, varying from just under 100 days in lung, liver, and mesentery to 1,000 days in brain, but replication periods may shorten 20 to 2,000 times during wound healing, inflammation, and malignancy, and are even faster in uteroplacental tissue and embryogenesis (1,2). Established endothelium regulates the blood coagulation system (3), the lumenal diameter of its vessel (4), attachment of leukocytes to its surface and their migration into interstitium (5), and antigen presentation to lymphocytes (6).

Each of the endothelial functions described is coordinated by cytokines. These soluble, small molecular weight proteins are directed at ECs and their neighbors from adjoining mast cells, T cells, and macrophages, from other ECs, and from distant sites upstream in the circulation. Many cytokines possess binding sites on the ECM or endothelial surface, which prevent them from being washed away in the axial blood stream, potentially creating an important periendothelial cytokine reservoir (7,8). We discuss the cytokines involved in EC proliferation and interactions with the blood, with an emphasis on their contribution to pathophysiological mechanisms.

RENEWAL AND ANGIOGENESIS

Endothelial renewal entails EC multiplication and migration (9,10). However, in addition to local EC division, there may be a role in vivo for a circulating pool of EC precursors, the existence of which has been implied by the finding of ECs in the bloodstream (11).

Angiogenesis, in contrast, summarizes a myriad of activities leading to the formation of an entire new blood vessel. It may be divided into component stages, using models such as cultured ECs on a three-dimensional (3D) gel or the growth of vessels on cornea or chorioallantoic membrane. New capillaries begin the process by sprouting from venules as ECs move in response to a migratory stimulus through basement membrane that has been locally degraded. The motile ECs elongate and align to create a solid sprout, which lengthens, canalizes, and joins other sprouts to form a loop. Pericytes adjoin the ECs, and the mature, stable capillary is formed (12). The place of cytokines in each stage may be studied.

Fibroblast growth factor

BACKGROUND: Fibroblast growth factor (FGF) comprises a family of at least seven heparin binding growth factors sharing 35 to 55% amino acid identity.

FGF-1 and FGF-2 (acidic and basic FGF) are the best characterized isoforms and are the subject of this review, in which they are generally viewed synonomously. Each is a 154 amino acid polypeptide and together they are produced by most cell types, including ECs (13).

FGF is thought by some to be the principal cytokine involved in the in vivo induction of angiogenesis (9,14). It is expressed ubiquitously in normal adult tissues, but a paradox is raised in that endothelial proliferation in these tissues is generally quiescent, except in the female reproductive organs and at sites of pathology. This inactivity is not accounted for by FGF's lack of a classic signal sequence for secretion, because it is found extracellularly, possibly due to a truncated receptor, which serves as a secretory carrier (15). A more likely explanation is that the cellular responses to FGF are mediated by a receptor complex comprising heparin sulfate moieties, rather than by a single protein, which is subject to considerable polymorphism (16).

EFFECTS ON ECS IN VITRO: FGF stimulates proliferation and migration of cultured ECs (9,14,17), but, in addition to promitotic actions, it has several other effects that are likely to be important. One of the phenotypic hallmarks of migrating ECs is expression of plasminogen activator (PA), a central mediator of extracellular proteolysis. FGF up-regulates the synthesis of PA and collagenase (17–19). Wounding of an EC monolayer triggers a marked, rapid, and sustained increase in expression of a specific high-affinity receptor for the urokinase-type PA (u-PA) on the surface of migrating cells, the postulated role of which is to mediate efficient and spatially restricted extracellular proteolytic activity by migrating ECs (20,21). Increases in u-PA and u-PA receptor are both dependent on endogenous FGF.

EC invasiveness and formation of patent capillaries in fibrin and collagen gels is stimulated by FGF (22). It increases expression of the $\alpha v\beta 3$ integrin, which correlates with an increased ability of microvascular ECs to bind to vitronectin, but not to fibronectin-coated surfaces (23). There is up-regulated biosynthesis of the collagen/laminin receptor, the $\alpha 2\beta 1$ integrin and the $\alpha 5$-chain, which conjugates with $\beta 1$ to form a fibronectin receptor. These effects of FGF may provide ECs with an enhanced capacity to attach to, or migrate through, both their underlying basement membrane and the interstitial matrix (24).

FGF INTRACELLULAR SIGNALING: The signaling pathway of FGF appears to involve both a membrane receptor and a direct nuclear site of action. There are two FGF receptors, one of high affinity, which possesses an intracellular tyrosine kinase domain (25), and the other of low affinity, a heparan sulfate proteoglycan (HSPG) (26,27). It appears that binding to cell surface HSPG is a prerequisite for high-affinity binding and mitogenic activity (16). Studies employing peptide mutants of FGF and anti-FGF antibodies to regulate the FGF-receptor interaction suggest that the mitogenic and PA-inducing activities of FGF depend on different domains of the FGF high-affinity receptor and different intracellular transduction pathways (28). Mitogenic activity involves triggering of protein kinase C (PKC), whereas plasminogen activation is independent of PKC, but requires a calcium flux (29).

FGF translocates to and accumulates in the nucleolus of ECs, independent of its high affinity receptor binding (30). It appears to stimulate the transcription of ribosomal genes during the transition from G_0 to G_1 phases of the cell cycle, a step closely linked to ribosome assembly and cell proliferation (31). Confluent ECs, in contrast to growing cells, contain no nuclear FGF (32). A mutant FGF lacking a nuclear translocation sequence fails to induce DNA synthesis and EC proliferation at concentrations sufficient to give rise to receptor-mediated tyrosine phosphorylation and c-fos expression (33).

A long-lasting interaction between FGF and cultured ECs with prolonged activation of PKC has been thought by others to be required to induce cell proliferation (34). Because high-affinity receptors lead to rapid internalization of FGF, and the low affinity sites mediate a slow internalization of FGF (35), the HSPG binding sites may be essential for FGF's growth factor activity.

FGF-HEPARAN SULFATE PROTEOGLYCAN INTERACTIONS: Heparan sulfate proteoglycans (HSPGs) are ubiquitous constituents of mammalian cell surfaces and most extracellular matrices. EC surface heparan sulfates facilitate the interaction of FGF with its receptor by concentrating FGF at the cell surface, possibly through phosphorylation of FGF at its receptor-binding domain because this process is associated with increased receptor affinity (16,36,37). FGF binding to HSPGs offers protection against proteolytic degradation and creates a reservoir of growth factor in tissues (8,38). Degradative enzymes may not be needed to release FGF from the heparan sulfates in instances where receptors and heparan sulfate–bound FGF are in close proximity because dissociation from heparan sulfates occurs rapidly enough to allow FGF to bind to unoccupied receptors by laws of mass action (36).

In a model of neuroepithelial embryogenesis that may hold clues for the endothelial scenario, Nurcombe and colleagues (39) showed that by sequentially binding different forms of FGF, differentially glycosylated HSPG species regulate development. This regulatory mechanism does not rely on changes in cell surface receptor expression or cessation of growth factor production and allows for rapid changes in cell signaling during development (39).

FGF INHIBITORS: The activities of FGF are limited by transforming growth factor-β (TGF-β), interferon-γ (IFN-γ), and platelet factor-4 (PF-4). TGF-β can be activated from its latent, secreted form by plasmin, which is activated by FGF. TGF-β then limits the PA-inducing activity of FGF through increased synthesis of PA inhibitor-1 (PAI-1) and decreased transcription of the u-PA gene (18). IFN-γ inhibits EC growth possibly by decreasing FGF receptor expression (40). PF-4 blocks the binding of FGF to its receptor and therefore inhibits the migration and tube formation of bovine capillary ECs in culture (41).

A bacterially derived sulfated polysaccharide inhibits the growth and chemotaxis of ECs stimulated by FGF possibly by preventing the binding of FGF at both its low and high affinity binding sites (42). Chloroquine, a drug used to treat malaria and inflammatory diseases, inhibits FGF-stimulated EC growth in a dose-dependent fashion (43).

EFFECTS IN VIVO: Antisense oligonucleotides complementary to FGF messenger RNA (mRNA) illustrate the significant role of FGF as an endothelial growth promoter in an in vitro environment (44). In vivo experiments confirm that FGF has a critical part in the formation of new blood vessels.

Nanogram amounts of FGF induce angiogenesis in the chick embryo chorioallantoic membrane and in the cornea (45). Nabel and colleagues (46) used a eukaryotic expression vector encoding a secreted form of FGF-1 and introduced it by direct gene transfer into porcine arteries. In this somatic transgenic model, FGF-1 expression induced intimal thickening and angiogenesis within 21 days, in comparison with control arteries transfected with an *Escherichia coli* β-galactosidase gene. The neointimal ECs appeared to originate from adjacent arterial luminal ECs because both were negative for von Willebrand factor (46).

Using rabbit ear excision wounds and introducing various cytokines, Pierce and associates (47) showed that FGF induces an angiogenic response with a marked increase in ECs and neovessels. This effect appears to delay wound maturation. In contrast, platelet-derived growth factor (PDGF) augments early glycosaminoglycan and fibronectin deposition and induces greater amounts of collagen, whereas TFG-β1 rapidly enhances collagen synthesis and maturation. Each agent appears to have complementary actions (47).

Villaschi and Nicosia (48) found that addition of purified FGF increases both the number and the length of microvessels sprouting from the explants in a rat aortic injury model and prevents microvessel regression. Neutralizing anti-FGF antibodies cause a 40% reduction of angiogenesis (48).

Vascular endothelial growth factor/vascular permeability factor

BACKGROUND AND EC EFFECTS: Vascular endothelial growth factor (VEGF) and vascular permeability factor (VPF) are two terms for an identical 46-kd protein related to PDGF and produced by several tumor cells, luteal cells, renal glomerular visceral epithelial cells, and vascular smooth muscle cells (VSMCs) (49–51). It is a selective and potent EC mitogen both in vitro and in vivo (50,52); it has no proliferative activity on VSMCs, fibroblasts, and epithelial cells (49). VEGF is angiogenic in vitro, and it causes microvascular ECs grown on 3D collagen gels to invade the underlying matrix and to form capillary-like tubules (52).

VEGF promotes vascular leakage, causes von Willebrand factor release, and synergizes with tumor necrosis factor-α (TNF-α) to promote procoagulant activity on ECs (49). In addition, it induces expression of the only metalloproteinase that can initiate the degradation of interstitial collagen types I to III under normal physiological conditions (53).

VEGF SIGNALING: Several tyrosine kinase receptors have been described for VEGF, including flt and flk-1 (2,54). These receptors are detected only on ECs. Flk-1 in particular is found on ECs during embryogenesis; it is especially abundant in blood islands of the yolk sac, where EC progenitors originate, and on vascular sprouts and branching vessels of developing brain. In contrast, flk-1 transcripts are drastically reduced in adult brain, in which vascular proliferation has ended (2). These findings contrast with the lack of detectable FGF receptors on ECs during embryogenesis (55).

VEGF binds heparin via a nonreceptor binding domain, which strongly potentiates its binding to flt, whereas α2-macroglobulin, a major serum protein, inactivates the receptor binding ability of VEGF (50). Akin to FGF, VEGF induces an angiogenic response via a direct effect on endothelial cells, and, when acting in concert, these two cytokines have a potent synergistic effect on the induction of angiogenesis in vitro (52).

VEGF IN ANGIOGENESIS, MALIGNANCY, AND WOUND HEALING: VEGF mRNA is expressed in cells surrounding an expanding vasculature in embryonic implantation sites, ovarian follicles, corpus luteum, and at sites of repair of endometrial vessels. It predominates in tissues that acquire a new capillary network, but its binding activity is found on both quiescent and proliferating ECs. VEGF expression may be hormonally regulated because it increases with the acquisition of cellular steroidogenic activity and varies with the ovarian cycle in the endometrium. During the early proliferative phase, it

is found in the estrogen-responsive, secretory columnar epithelium. Under the influence of progesterone in the secretory phase, when new blood vessel development is maximal, VEGF expression shifts to cells of the underlying stroma comprising the functional endometrium (56).

A particular role for VEGF in tumor angiogenesis is apparent. Expression of VEGF on Chinese hamster ovary (CHO) cells confers on them the ability to form tumors in nude mice (57). Monoclonal antibodies to VEGF inhibit the growth of rhabdomyosarcoma, glioblastoma multiforme, and leiomyosarcoma cell lines in nude mice, but they have no effect on the growth rate of these tumor cells in vitro, implying a direct effect on reducing the vascular density in antibody-treated tumors (57).

In situ analysis of glioblastoma multiforme brain tumor specimens shows that VEGF production is specifically induced in a subset of glioblastoma cells distinguished by their proximity to necrotic foci. Capillaries appear to cluster alongside these VEGF-producing tumor cells. VEGF mRNA levels are dramatically responsive to their O_2 milieu, suggesting a mechanism for these findings. Within a few hours of exposing glioma and muscle cell cultures to hypoxia, VEGF mRNA levels increase and return to background when a normal O_2 supply is restored (58). Comparison of astrocytomas with the more malignant glioblastoma, which is characterized by necrosis and vascular proliferation, reveals that more VEGF is expressed in the latter. Flt is not expressed in normal brain ECs, but it is found in these tumor ECs (59).

The other activity of VEGF on ECs—increased permeability—is a characteristic feature of normal wound healing. Persistent microvascular permeability to plasma proteins, even after cessation of injury, results in extravasation of fibrinogen, and the resultant fibrin serves as a provisional matrix that promotes angiogenesis and scar formation. VEGF mRNA levels in keratinocytes at wound edges are greatly increased, and they correlate with the permeability of wound tissue vessels (60).

Hepatocyte growth factor/scatter factor

Hepatocyte growth factor (HGF) and scatter factor (SF) are identical, basic, heparin-binding glycoproteins that share 38% amino acid identity with plasminogen (61,62). They are produced by fibroblasts and VSMCs. HGF induces renal epithelial cells to form branching networks of tubules in a collagen matrix (63), whereas SF disperses cohesive epithelial colonies and stimulates cell motility (64,65). The receptor for HGF/SF is c-met, a transmembrane tyrosine kinase (66), which is expressed and stimulated by HGF on ECs (67).

HGF stimulates EC growth and motility in vitro and promotes wound repair in EC monolayers. ECs assume a dendritic phenotype. HGF does not induce procoagulant activity or platelet-activating factor (67), but EC secretion of plasminogen activators and urokinase, which are required during the early stages of angiogenesis when ECs degrade ECM, are induced by SF (68). In a corneal model, HGF produced angiogenesis (67). Immunoreactive SF is present in a perivascular distribution surrounding sites of blood vessel formation in the skin of psoriatic plaques, but not in normal skin, in which angiogenesis is not a feature (68).

Transforming growth factor-β

TGF-β is unlike other cytokines with proangiogenic effects. Some investigators have found that TGF-β induces tube formation by ECs in 3D collagen gels without affecting cell proliferation (69,70), but in other in vitro systems, it is a potent inhibitor of EC proliferation, migration, tube formation, and protease synthesis (71–75). Dramatic increases in collagen and fibronectin synthesis and inhibition of matrix-degrading enzyme production (76,77), brought about by TGF-β, may modulate its effects on endothelial phenotype and explain differences between various in vitro models (69). In vivo TGF-β is angiogenic, although it has been suspected that this action is not directly on ECs but rather on other cells (e.g., fibroblasts and macrophages, whose many products may potentiate the angiogenic response) (78,79).

TGF-β may signal resolution of the angiogenic process begun by factors that are principally initiating stimuli, such as FGF and VEGF. Wound studies in vivo show that FGF produces marked increases in new vessels and persistence of the provisional ECM, whereas TGF-β accelerates maturation of the provisional ECM through rapidly enhanced collagen synthesis, leading to coverage of wound defects with fibrous tissue (47,80). In chorioallantoic membranes, FGF induces primarily small blood vessels, whereas the vessels formed in response to TGF-β are large and bear intercellular junctional complexes (70,79). TGF-β1 also promotes the differentiation of ECs into VSMCs in vitro (81) and stimulates intimal VSMCs to synthesize increased amounts of lipoprotein-binding proteoglycans (82).

TGF-β is secreted constitutively by ECs as a high molecular weight inactive complex, with a latency-associated peptide and a latent TGF-β binding protein. Activation of latent TGF-β occurs in cocultures of ECs with VSMCs or pericytes and is thought to be at least in part mediated by plasmin cleavage of the aminoterminal propeptide. This process is facilitated by FGF, which increases plasminogen activator activity (18,72). Thus, the presence and effectiveness of TGF-β are determined by proximal cell types and the ability to activate the latent form.

Hematopoietic colony-stimulating factors

The colony-stimulating factors (CSFs) are characterized by their profound effects on the proliferation of blood cell precursors. ECs and hematopoietic cells share surface markers such as PECAM-1 (83,84), CD34 (85,86), CD36 (87), and CD45 (88), and they closely interact in the bone marrow, suggesting the common ancestry of their lineages and the possible effectiveness of the CSFs upon the former.

Granulocyte and granulocyte-macrophage CSFs (G-CSF, GM-CSF) have been shown to induce human ECs to migrate and proliferate, without altering their hemostatic or inflammatory phenotypes. In comparison to FGF, induction of migration was of a similar order of magnitude, although the extent of proliferation was less (89,90). In the corneal model, G-CSF induced neovascularization. An inability to repeat these results, however (91), and in particular the lack of demonstrable receptors for GM-CSF on human umbilical vein ECs (HUVECs) by binding analysis, surface expression, and receptor mRNA analysis (92,93), leave the significance of the original observations unclear.

In the last year, it has emerged that resting HUVECs express mRNA for the α- and β-chains of the interleukin-3 (IL-3) receptor (90,91,94). This receptor is functional in mediating IL-3 stimulation of HUVEC DNA synthesis and proliferation (92). Furthermore, use of recombinant human IL-3 and GM-CSF after high-dose cancer chemotherapy is associated with expansion of the vascular network of the bone marrow and an increase in the proportion of CD34-expressing ECs (95). Erythropoietin is also reported to possess mitogenic and chemotactic activity on ECs (96).

Other cytokines affecting EC renewal and angiogenesis

ONCOSTATIN M: Oncostatin M is a glycoprotein of 196 amino acids produced by activated T cells that inhibits the growth of several human tumor cell lines. It also inhibits the growth of normal bovine aortic ECs, while stimulating the growth of a number of fibroblast cell lines (97).

INTERLEUKIN-4: IL-4 is a potent EC mitogen (98), and it also stimulates the expression of u-PA (99), suggesting that it has a role in angiogenesis. Both these effects of IL-4 occur preferentially in microvascular, rather than in macrovascular, endothelium.

INTERLEUKIN-8: IL-8 has been reported to stimulate the chemotaxis of HUVECs with effects comparable to FGF. TNF-α or IL-8 antibodies reduce the chemotactic response for HUVECs to conditioned media from lipopolysaccharide-stimulated peripheral blood monocytes or synovial tissue macrophages. Antisense RNA oligonucleotide to IL-8 blocks the production of angiogenic activity by monocytes. IL-8 binds to heparin, as do the well characterized angiogenic factors, such as FGF and VEGF (100).

EPIDERMAL GROWTH FACTOR: Epidermal growth factor (EGF) is a mitogenic polypeptide that accelerates angiogenesis (101). EGF and EGF receptor immunoreactivity is present at the cytoplasmic interdigitations between ECs and pericytes in the angiogenic immature capillaries of human granulation tissue, but it is absent in mature capillaries (102).

PLATELET-DERIVED GROWTH FACTOR: PDGF is a mitogen and a chemotaxin for VSMCs and fibroblasts (103), and it has roles in wound healing and angiogenesis (47,104,105). It stimulates fibroblasts to synthesize collagen and collagenase, which leads to modification of the ECM; it is also a potent vasoconstrictor (101). PDGF is stored in platelet α-granules, ECs, VSMCs, and macrophages, in particular those in newly formed atherosclerotic plaques (101,106). Two receptors, α and β, are ligand-activated tyrosine kinases (107). IL-1, TNF-α, lipopolysaccharide, and blood flow induce accumulation of PDGF mRNA in ECs, whereas IFN-γ and nitric oxide have the opposite effect (108,109).

INSULIN-LIKE GROWTH FACTOR: Insulin-like growth factor-1 is secreted by ECs from their basal abluminal surface. It supports VSMC and fibroblast growth in vitro (110,111).

INTERLEUKIN-1: IL-1 inhibits the proliferation of ECs in vitro, particularly when combined with FGF (112). It promotes growth of VSMCs and fibroblasts, possibly via increased PDGF release (106).

ENDOTHELIN-1: Endothelin-1 (ET-1) is a 21 amino acid peptide released from the endothelium. It elicits a variety of biological effects that include VSMC contraction and proliferation (113). ET-1 production by ECs is augmented by thrombin, G-CSF, TGF-β, and IL-1 (114–116). Fluid shear stress induces rapid and significant down-regulation of ET-1 mRNA and peptide release (117).

Summary of the pathophysiological effects of endothelial mitogens

Knowledge of the actions, structures, and encoding genes of the endothelial mitogenic factors has been applied to pathophysiology, and examples of the in vivo relevance of each cytokine have been given. A range of studies, includ-

ing those of cytokine or cytokine-induced mediator expression in pathological specimens and those of direct addition of a cytokine (e.g., by gene transfection) or its withdrawal (e.g., by antisense oligonucleotide), permit increasing levels of confidence with regard to conclusions of causality.

The descriptive method, which is more suited to human samples, is exemplified by work on VEGF expression in the uterus (56) and the role of angiogenic factors in rheumatoid arthritis. Synovial pannus tissue in rheumatoid arthritic joints is invasive and destructive of adjacent cartilage and bone. Its formation is accompanied by ingrowth of new vascular networks, and the level of angiogenic activity correlates with infiltration of inflammatory cells, synovial hyperplasia, and clinical score (118,119). FGF expression has been shown in ECs of the rheumatoid pannus and in streptococcal-induced arthritis in rats (120,121). EGF and PDGF localization is also associated with areas of new vessel growth (122). Agents effective in the therapy of rheumatoid arthritis inhibit EC proliferation (123,124).

A study of injured rat aorta implicates FGF more conclusively in endothelial cell responses, but its application in human disease has not been established. Immunohistochemical staining of rat aorta shows FGF in the cytoplasm of endothelial and smooth muscle cells. Endogenous FGF is demonstrable by Western blot analysis in aorta-conditioned medium after ring dissection. Neutralizing anti-FGF antibodies inhibit the increased numbers and length of sprouting microvessels provoked by injury, suggesting that the FGF present is functional. Purified FGF increases both the number and the length of microvessels sprouting from the explants, particularly late after the injury, when release of endogenous FGF is minimal. FGF release by vascular cells thus appears to have a role in the autoregulation of angiogenesis after vascular injury (48).

Surgical interventions, such as bypass grafting, atherectomy, or endarterectomy, involve similar vascular injury, but they are also often complicated by intimal hyperplasia of VSMCs. The increased rate of migration and turnover of VSMCs in response to injury is dependent on the presence of dividing ECs. VSMC proliferation is maximal when the ECs are proliferating. When the ECs stabilize and cover the lumenal surface, VSMC proliferation slows. The relationship of this phenomenon to EC-derived FGF or PDGF is not clear (125), although the failure of confluent ECs to localize FGF to their nuclei is interesting (32). TGF-β also decreases VSMC proliferation (72). This effect may explain why VSMC proliferation slows when ECs cover an injury.

A recent innovation of in vitro assays—coculturing ECs with their supporting stromal cells to parallel the in vivo situation—provides another demonstration of interactions between ECs with their neighboring pericytes or VSMCs. Pericytes grown in coculture with ECs inhibit EC proliferation (126), on the basis of the ability of cocultures but not homocellular cultures to produce activated TGF-β (72). Angiogenesis in the fetal retina ceases as mural pericytes appear, and pathological neovascularization in diabetic retinopathy is associated with loss of pericytes (127).

EC cocultures with keratinocytes shed light on the common dermatological disease psoriasis, which is characterized by hyperproliferation of keratinocytes and abnormally extensive dermal capillary networks. Keratinocytes produce TGF-α, which in an autocrine manner leads to their hyperproliferation. TGF-α also stimulates human omental microvascular ECs in type I collagen gels to form tubular-like structures. When keratinocytes are cocultured with omental ECs, tubular-like EC structures appear in collagen gels, which are inhibitable by anti-TGF-α antibodies (128). It thus appears that TGF-α acts in an autocrine fashion on keratinocytes and in a paracrine manner on ECs, therefore appearing to facilitate the neovascularization required to allow for the increased surface keratinocyte population.

Angiogenesis appears to be closely related to malignancy (129). Angiogenic agents have been isolated from tumors, and neovascularization is present in most malignancies at the time of their detection, thus appearing to be directly related to malignant grade and prognosis. The malignant progression of melanoma from normal skin to dysplastic melanocytic nevus, to cutaneous malignant melanoma, and finally to metastatic malignant melanoma is associated with increasing vascularity (130). Horak and associates (131) showed that the number of microvessels in primary breast cancers is directly correlated with pathological indicators of an increasingly poor prognosis. The association of VEGF with rhabdomyosarcoma, glioblastoma multiforme, and leiomyosarcoma is an example of the role of cytokine-induced angiogenesis in malignancy (57). Tumor-cell hypoxia is believed to stimulate production of VEGF. In acquired immunodeficiency syndrome–related Kaposi's sarcoma, the malignant cells also express cytokines with autocrine and paracrine growth effects, which foster growth of this vascular tumor (132–134). Coculture of ECs with human glioblastoma cells demonstrates how angiogenic cytokines may be working. In contact with glioma cells, ECs form tubes, an in vitro surrogate for capillaries. Only glioma-cell lines that possess high levels of FGF mRNA induce such tube formation, and this process can be blocked by coadministration of anti-FGF antibody (135).

Because EC renewal and angiogenesis are key events in important pathological processes such as wound healing, inflammation, and malignancy, but are not a feature of normal tissues except in the female reproductive system, attempts to define angiogenic inhibitors have been in progress. Physiological inhibitors of angiogenesis are present in blood and urine, and they include cortisol me-

tabolites that lack glucocorticoid and mineralocorticoid activities (136). These metabolites may act by increasing the synthesis of PAI-1 (137). Heparin potentiates their action, and it is believed to function by virtue of its high affinity for angiogenic factors, such as FGF and VEGF (138).

IFN-α has been used successfully in pulmonary hemangiomatosis with an associated decrease in the density of abnormal vessels (139). Derivatives of *Aspergillus fumigatus* products are effective inhibitors of angiogenesis in vitro, as well as in tumors and collagen-induced arthritis in rats, with minimal toxicity (140,141). A number of other compounds inhibit angiogenesis in vitro, including antiestrogens (142), cyclosporine (143), ribonuclease inhibitors (144), protein kinase inhibitors (145), and calcium channel blockers (146). In vitro experimentation has shown that changes in the constitution of ECM or monoclonal antibodies directed to β1 and β3 integrins, which mediate EC-matrix interactions, can alter the type and number of capillary tubes formed (147,148). This finding offers prospects for the development of targeted inhibitors of angiogenesis.

ENDOTHELIAL CELL INTERACTIONS WITH BLOOD MOLECULES AND LEUKOCYTES

In this section, the roles of cytokines acting on or produced by endothelia, which affect its relationship with the elements of blood, are considered. It appears that specific, separate mechanisms exist that deal with the arrest of mobile leukocytes, their secure attachment to the endothelial surface, and finally their passage between surface ECs into the interstitium. These inflammatory processes and others leading to thrombosis or immune recognition are controlled by specific cytokines with both facilitatory and inhibitory actions.

Tumor necrosis factor-α and interleukin-1

TNF-α and IL-1 are proinflammatory cytokines with effects on multiple biological systems. Both act on ECs, most often with a similar outcome; thus, they are considered together, but mention will be made of each individually when their effects differ.

IL-1 is a 17-kd peptide with two biologically active forms, IL-1α and IL-1β (149). TNF-α is a trimer of three 17-kd subunits. Its main source is the monocyte-macrophage when it is stimulated by lipopolysaccharide (LPS), IL-1, IFN-α, IFN-γ, OR GM-CSF (150). The mast cell may be another important source of TNF-α in vivo (151). Peripheral blood lymphocytes, natural killer (NK) cells, and polymorphs produce a relatively small amount of TNF-α (150). VSMCs adjacent to the endothelium express TNF-α mRNA and protein on exposure to inflammatory signals, and this process is superinduced by protein synthesis inhibitors (152). Sources of IL-1 are extensive and include blood monocytes, neutrophils, T and B lymphocytes, tissue macrophages, VSMCs, and ECs. The most common stimulus for IL-1 transcription is endotoxin (149).

In general, TNF-α promotes selective cytotoxicity and catabolism. There are changes in ECM through induction of collagenases, which lead to bone resorption, and of plasminogen activator, which leads to angiogenesis (153). On blood cells, TNF-α and IL-1 have a proinflammatory effect. Neutrophils and monocytes gain an increased capacity for phagocytosis, antibody-dependent cellular cytotoxicity, degranulation, and production of reactive oxygen species. T cells express more IL-2 receptor and major histocompatibility complex (MHC) class II antigens. They achieve a greater proliferative potential in synergy with IL-2, and they produce more IFN-γ. B cells also augment their proliferation, differentiation, and production of antibodies (149,150). The general proinflammatory effects of these cytokines, however, also depend on their endothelial functions, as well as on these leukocyte changes.

COAGULATION: TNF-α and IL-1 regulate the coagulation system through actions on the endothelium. Procoagulant activity of ECs is induced (3,154). The production of thrombomodulin, a surface glycoprotein on ECs that controls intravascular coagulation cascades through interactions with proteins C and S, is suppressed (154,155). Arachidonate metabolism is activated; in particular, prostacyclin synthesis in cultured vascular ECs is induced (156). TNF-α induces expression of an EC plasminogen activator inhibitor (157–159). Effects on plasminogen activator are recognized, but both increases and decreases have been reported (153,157). In patients treated with recombinant human TNF-α in a Phase I cancer trial, induction of endothelial-derived tissue-type plasminogen activator, recognized by the presence of fibrin degradation products in plasma, occurred within one hour of the initiation of TNF-α (160).

The surface of TNF-α-activated ECs elicits a hemostatic response when exposed to flowing nonanticoagulated blood. Tissue factor is expressed, and deposition of fibrin, platelet aggregates, and leukocytes follows; in an experimental model, 63% of the EC surface became covered. Resting ECs, in contrast, show no or little fibrin, platelet, and leukocyte deposition. The addition of antibodies against tissue factor to TNF-α-activated ECs abrogates fibrin and platelet deposition, but it allows leukocyte adherence to occur to the same extent. Thus, the endothelial effects of TNF-α on hemostasis and leukocyte

capture involve related but dissociated mechanisms (161).

ADHESION: TNF-α and IL-1 increase the adhesiveness of endothelium for bloodstream leukocytes by an EC-specific mechanism (162). They also modulate the interactions between adjoining ECs. This process involves induction, up-regulated expression, or activation of molecules on the endothelial surface, which interact with ligands on leukocytes and ECs. The main groups of such regulated adhesins are the selectins, the L-selectin ligands, the immunoglobulin superfamily, and the integrins.

SELECTINS: E-selectin (ES; ELAM-1) and P-selectin (PS; GMP-140; CD62) are endothelial, lectin-bearing glycoproteins that mediate the initial contacts between leukocyte and endothelium as leukocytes move away from the axial bloodstream and roll over the endothelial surface, prior to their firm attachment (163–165). Their leukocyte ligands are sialylated, fucosylated oligosaccharides (166).

ES is found in low to undetectable quantities on resting ECs in vitro and in vivo. Both IL-1 and TNF-α induce ES mRNA and protein synthesis. Surface expression in vitro reaches a maximal level at 4 hours, after which it declines to background by 24 hours, despite the continued presence of the agonists (167–170). Mast-cell degranulation leads to the display of ES on adjacent ECs in vivo. Antiserum to TNF-α abrogates this potentially important pathway of induction (151). Surface ES is lost by internalization and external release, processes not known to be controlled by cytokines (171). The rate of internalization of ES is comparatively higher than that of intercellular adhesion molecule (ICAM)-1; therefore, its pro-adhesive effects may be relatively acute (1.7% of membrane-bound ES/min vs < 0.1% of membrane-bound ICAM-1/minute) (172,173).

PS is expressed in varying levels on resting ECs, which maintain a large stock of PS in cytoplasmic granules (Weibel-Palade bodies). This store is rapidly transferred to the EC membrane in response to histamine and thrombin, but expression is brief, and its functional aspect is lost within 30 minutes (174,175). PS is inducible by TNF in mouse and bovine ECs at both mRNA and cell surface protein levels. The PS protein increase is 2- to 4-fold, and it is maximal at 3 to 4 hours (176).

L-SELECTIN LIGANDS: CD34 is a highly glycosylated, negatively charged, sialomucin-like transmembrane molecule better known for its presence on hematopoietic progenitor cells, which has recently been recognized as an endothelial ligand for L-selectin (LS; LAM-1; LECAM-1), the leukocyte adhesion molecule (177,178). It has a broad EC distribution, including high endothelial venules, but it is absent from most large vessels and placental sinuses (178). The function of CD34 is likely to be controlled by differential vessel-specific glycosylation, as well as translocation to and oligomerization at the EC surface. Vessel-specific glycosylation may explain why leukocytes only adhere to postcapillary venules, even though CD34 appears to be expressed on capillaries and venules (162). TNF-α, IL-1β, and IFN-γ have been reported to decrease the expression of CD34 on cultured ECs (179).

Glycam-1 (or Sgp50) is a 50-kd, mucin-like glycoprotein that also serves as an LS ligand. It is restricted, however, to lymph node high endothelial venules, and it is not known to be influenced by cytokines (180). Both CD34 and Glycam-1 were characterized by precipitation with a chimeric molecule containing the extracellular domain of mouse LS and human immunoglobulin.

A third endothelial ligand for LS must be proposed on the basis of older evidence describing an antigen on HUVECs that is optimally induced by TNF-α and IL-1β, but also to a lesser extent by IFN-γ and IL-4 (181). This ligand is a neuraminidase-sensitive molecule, which implies that it bears sialic acid, as do CD34 and Glycam-1. It is expressed between 2 and 4 hours after HUVEC stimulation, and it persists for at least 24 hours (181). Its induction by cytokines is thus unlike CD34, and its distribution is wider than that known for Glycam-1.

Soluble LS is shed from the surface of leukocytes after their stimulation by cytokines such as TNF-α. Soluble LS inhibits LS-specific attachment of lymphocytes to TNF-α–activated ECs (182). Fluid-phase PS also inhibits adhesion of TNF-α–activated neutrophils to resting ECs, through inhibition of a CD18-dependent process. The control of soluble PS production is not currently understood (183).

IMMUNOGLOBULIN SUPERFAMILY ENDOTHELIAL ADHESINS: Intercellular adhesion molecule-1 and -2 (ICAM-1, 2), vascular cell adhesion molecule-1 (VCAM-1), and platelet endothelial cell adhesion molecule-1 (PECAM-1; CD31) are members of the immunoglobulin superfamily. ICAM-1, and ICAM-2 and VCAM-1 interact with leukocyte β2 and β1 integrins respectively, to serve a shear-resistant adhesion between ECs and leukocytes, which follows and stabilizes the rolling attachment initiated by the selectins (148). ICAM-1, the ligand for CD11a-CD11b/CD18, is constitutively expressed on ECs. TNF-α or IL-1 increase its expression, with a plateau at 24 to 72 hours (169). ICAM-2 is also constitutively expressed on ECs, but it is not subject to regulation (184).

VCAM-1 expression is absent on resting ECs. TNF-α or IL-1 induce it within 2 hours (peak, 12–24 hours), and levels substantially higher than baseline persist for at least 72 hours (185,186). There are two isoforms of VCAM-1 with 6 and 7 Ig-like domains and subtlely different binding characteristics (187). The former is expressed earlier than the latter, which then becomes the main EC isoform. VSMCs are normally devoid of adhesion proteins in vivo, and they express only small amounts of VCAM-1 in cul-

ture. TNF-α and IL-1 induce human saphenous vein SMCs to express VCAM-1 (Gamble JR, et al., unpublished observations).

PECAM-1 is constitutively expressed in a homogeneous pattern on EC membranes in vivo, but it concentrates predominately at points of cell-to-cell contact on cultured ECs (188,189). It appears to have a role in EC-to-EC contacts and in leukocyte transmigration through the intercellular junctions of ECs (190). Using tissue specimens from breast, skin, stomach, colon, uterine cervix, endometrium, myometrium, and bronchus incubated with TNF-α for up to 6 hours, as well as a dermal ragweed antigen injection model, Ioffreda and colleagues (191) showed that TNF-α leads to a redistribution of PECAM-1 from its original uniform pattern on EC surfaces to one localized to areas of contact between adjacent ECs (191). Thus, TNF-α–stimulated molecules, ES and PECAM-1, may sequentially enhance leukocyte-EC binding in postcapillary venules, direct adherent cells to sites most conducive to transvascular diapedesis, and lead to transmigration.

INTEGRINS: ECs express a number of integrins believed to function as interendothelial adhesins or as ECM receptors. TNF-α and IFN-γ decrease EC β3 integrins, and they induce α1β1. The α1β1 integrin is normally absent from HUVECs, but is present on capillary ECs. The laminin receptor α6β1 is strongly decreased by TNF-α or IL-1β, whereas α2β1, α3β1, and α5β1 are not altered. Laminin adhesion by ECs is consequently decreased (192).

MAJOR HISTOCOMPATIBILITY COMPLEX GENES: Class I MHC is expressed on ECs, but at a level relatively lower than that on macrophages or lymphocytes. This expression is increased 2- to 4-fold over 24 hours by TNF-α (but not by IL-1) through an increase in transcription. There is a synergistic elevation in class I antigen with IFN-γ or IFN-β, without any alteration in TNF receptor number due to a multiplicative increase in transcriptional rate (193,194). Synthesis and expression of transporter in antigen processing-1 (TAP-1), an MHC-encoded gene product that is required for efficient association of intracellular peptide antigen with nascent human leukocyte antigen (HLA) class I H-chain and β2-microglobulin, are increased in human ECs by TNF-α, IFN-β, or IFN-γ (195). TNF-α does not induce class II expression de novo in human ECs (193), and neither TNF-α nor IL-1 alters MHC on VSMCs (196). TNF-α thus allows ECs to present class I–restricted antigens to T cells, which may propagate the inflammatory response.

ENDOTHELIAL PERMEABILITY TO MACROMOLECULES: The permeability of endothelial surfaces to macromolecules such as albumin is an important feature of edematous processes. TNF-α, IL-1, and IFN-γ increase EC monolayer permeability to albumin in vitro, and this effect is augmented by combining these cytokines (197,198). The ECs undergo parallel changes in morphology, from cobblestone to elongated cells, with formation of prominent intercellular gaps and actin stress fibers. There is an accompanying loss of fibronectin and remodeling of the ECM (199). ECs from different sites show varying susceptibility to this change: HUVECs require prolonged exposures of 72 hours, whereas bovine ECs demonstrate a change within 1 to 3 hours after exposure (198,200).

Endothelial glycosaminoglycans (GAGs) are important in regulating vascular permeability as well as cell interactions with soluble factors and resistance to thrombosis. IL-1 and TNF-α alter GAG metabolism in cultured HUVECs, causing a marked increase in culture supernatant GAGs and a decrease in cell-associated GAGs that is detectable after 12 to 48 hours of coincubation. There is a concomitant increase in GAG synthesis. Histochemically, these changes are associated with marked reduction and redistribution of endothelial surface anionic sites. Such changes may contribute to the disturbances of vascular endothelial homeostasis associated with inflammatory states (201).

LEUKOCYTE TRANSMIGRATION: HUVECs incubated with TNF-α or IL-1 for 4 hours do not display morphological changes or increased albumin permeability, but they do show an increase in leukocyte transmigration (202). Migration occurs across EC junctions, and it is dependent on the ECs being biosynthetically active. Neutrophils are polarized but not degranulated, and there are no signs of ECM lysis. Because the number of traversing neutrophils is no greater when cytokine stimulation is joined by a chemotactic gradient in some systems, it is suggested that both operate through this mechanism (203–205).

Conditioned media of TNF-α- or IL-1–stimulated ECs induce transmigration of neutrophils when added to the basal EC compartment. IFN-γ, IL-2, PDGF, and platelet-activating factor (PAF) are unable to mimic this effect. Antisera to IL-6, G-CSF, and GM-CSF, all products of stimulated ECs, do not diminish the chemotactic activity of the conditioned medium. IL-8, a member of the chemokine family, is present in this conditioned medium (206), and it acts as a chemoattractant for granulocytes. Other products of activated ECs, such as macrophage inflammatory protein-1 (MIP-1) and monocyte chemotactic protein-1 (MCP-1), are selective for lymphocyte and monocyte chemotaxis. Adhesion to ECs and transmigration through EC monolayers by leukocytes are thus both facilitated by TNF-α or IL-1 in separate, sequential processes (204).

EFFECTS ON CYTOKINE PRODUCTION: TNF-α and IL-1 foster EC production of a number of cytokines that often have proinflammatory actions (e.g., IL-1 itself)

(106,207), the chemokines (207), and G-CSF and GM-CSF (208,209). They mediate the release of PDGF from cultured ECs, and they augment IL-6 secretion (106, 210–212). IL-1 increases EC production of ET-1 (116).

Synthesis and release of the signaling phospholipid PAF is stimulated by TNF-α or IL-1α treatment of ECs (213). Such ECs support adhesion of neutrophils that are unactivated and do not adhere to plastic, suggesting that PAF may be a proadhesion signal from ECs to neutrophils. Although PAF antagonists inhibit adhesion, the time course for adhesion and PAF production are not strictly concordant. Acetyl coenzyme A raises PAF levels, but it has no effect on adhesion, and although both IL-1α and IL-1β stimulate adhesion, only the former results in PAF production (214).

TNF-α also decreases expression of endothelial antigens. Westphal and associates (215) reported a monoclonal antibody recognizing a 180-kd molecule expressed on the EC luminal surface, which is down-regulated by TNF-α and is possibly endoglin, a TGF-β–binding cell surface protein.

EFFECTS ON LIPOPROTEIN METABOLISM: TNF-α or IL-1 increase low density lipoprotein (LDL) receptor expression on microvascular ECs in culture. There is a parallel increase in internalization and degradation of LDL (216). Because ECs oxidize LDLs, and because LDLs are atherogenic, cytokines produced by adherent monocytes found in early atherosclerosis may facilitate this pathological process.

INTRACELLULAR SIGNALING

TNF-α RECEPTORS: TNF-α acts on cells via two receptors, p55 and p75, which are partially homologous in their extracellular domains, but lack any intracytoplasmic similarity. The role of these two moieties is still controversial, and it varies with the analytical method (217). ECs possess both receptors (218). Using TNF-α mutants with preferential binding to either p55 or p75, Barbara and colleagues (219) showed that the p55 receptor is necessary for induction of ES, neutrophil transmigration across EC monolayers, and EC IL-8 secretion. The p75 receptor only facilitates an increase in the potency of TNF (219,220). N-terminal amino acids of TNF-α are also critical for both receptor binding and biological activity on ECs (221).

POSTRECEPTOR PATHWAYS: TNF-α increases EC monolayer permeability via a G-protein intermediary (200), but activators of the stimulatory or inhibitory guanine nucleotide–dependent binding proteins do not affect TNF-α–induced surface expression of ES or VCAM-1 (222).

There is partial evidence of protein kinase C and A (PKC, PKA) involvement in the induction of ES expression and IL-6 production. PMA and forskolin, both agonists of these respective protein kinases, can mediate these effects, and appropriate kinase inhibitors impede them. These kinase inhibitors, however, do not block the effects of TNF-α, and other cyclic adenosine monophosphate agonists are not effective (193,222).

Absence of PKC translocation from cytosol to the plasma or nuclear membrane particulate fractions of HUVECs after TNF-α exposure, has argued against a significant PKC-mediated pathway for the actions of TNF-α. The β-I PKC isozyme, however, becomes activated without translocation, and it is sufficient for expression of ES and VCAM-1. This evidence from Harlan's group (223) suggests that PKC may mediate some effects of TNF-α. PKC is also strongly implicated in TNF-α induction of tissue plasminogen activator, because this substance is interdicted by the PKC inhibitors, H7 and staurosporine, and it is stimulated by 4β phorbol, 12 myristate, 13 acetate (PMAs) (153).

IL-1β–mediated endothelial cell phospholipase A2 activity and prostacyclin synthesis occur via a novel transducing pathway that does not involve early activation of phospholipase C, phospholipase D, or adenylate cyclase (224).

ACTIVATION OF TRANSCRIPTION FACTORS: TNF-α and IL-1 signaling on ECs involves activation of the transcription factors AP-1, NF-kappa B (NF-kB), interferon regulatory factor 1, cAMP response element (CRE), and TRE (PMA response element) (193,225). This level of the signaling pathway offers some explanation for the selective endothelial induction of ES. Two proximal ES promoter elements, in addition to NF-kB, are essential for cytokine induction of ES transcription. One of these elements, however, is not endothelial-specific, because it can function as a T-cell enhancer, as well as cooperate with NF-kB to yield cytokine induction of ES gene transcription in ECs (226). DNA methylation of the ES promoter represses NF-kB transactivation in nonendothelial cells, and, in comparison, the ES promoter in ECs is undermethylated, suggesting that methylation could have a role in cell-type–specific expression of this gene (227).

The cytokine-responsive regions of the VCAM-1 promoter are functional NF-kB and GATA elements (228). A comparison of the transcriptional control of VCAM-1 in muscle and ECs is enlightening. Muscle cells display high basal VCAM-1 expression that is not cytokine-inducible; a position-specific enhancer overrides other promoter elements. ECs have octamer binding sites that act as silencers, thus dampening VCAM-1 expression in unstimulated cells. TNF-α overcomes this inhibition through two adjacent NF-kB sites (229).

NF-kB induction by IL-1α, TNF-α, and LPS is inhibited by I-kappa Bα (IKBα or MAD-3), which sequesters NF-kB to the cytoplasm. Cell stimuli, such as TNF-α or

PMA, cause rapid degradation of IKBα, thus relieving this inhibition and allowing NF-kB to translocate to the nucleus and transactivate its target genes. Following this process, there is a dramatic increase in IKBα mRNA and protein synthesis. Expression of IKBα is also inversely regulated by NF-kB in a negative-feedback mechanism: NF-kB down-regulates its own activity after transient activation of target genes has been achieved (230,231).

DISEASE ASSOCIATIONS

ENDOTHELIAL DAMAGE: Several diseases are associated with elevated serum or tissue levels of TNF-α or IL-1, such as idiopathic pulmonary fibrosis (232), systemic vasculitis (233,234), rheumatoid arthritis (235), psoriasis (236), cerebral malaria (237), and sepsis (238). All these disorders have some form of vascular pathology.

There is ex vivo evidence that supports the role of TNF-α and IL-1 in EC injury in Kawasaki's disease (KS). KS histopathology shows panvasculitis with endothelial necrosis and Ig deposition. Sudden death stemming from coronary arteritis is well recognized in this condition. Circulating antibodies in patients with KS display complement-dependent cytotoxic activity against IL-1 or TNF-α–inducible EC antigens, but not against resting ECs (239).

In vitro models of endothelial injury also suggest that these cytokines may bring about EC damage. After IL-1 activation, for instance, EC monolayers coincubated with unstimulated neutrophils show extensive EC detachment and loss of monolayer integrity. This process is mimicked by neutrophil elastase exposure, and it is prevented by serine protease inhibitors or avoidance of direct EC-neutrophil contact (240).

ADHESION MOLECULE EXPRESSION IN TISSUES: Examination of the tissue expression of adhesion molecules confirms their association with inflammatory diseases, and it indirectly implies that TNF-α and IL-1 exhibit widespread endothelial activity.

Normal peripheral lymph node and mucosa-associated lymphoid endothelium show no VCAM-1, but they do exhibit ICAM-1. VCAM-1 is present in follicular centers and interfollicular zones. ECs in most other normal tissues express little or no VCAM-1, but focal reactivity is seen in arterial vasa vasorum, hepatic Kupffer's cells, and some renal tubular epithelial cells (241). ES is absent from normal capillaries, but it is found on large vessel and umbilical vein endothelium (242).

In acute appendicitis or diverticulitis, strong VCAM-1 and ES staining is seen in ECs of dilated serosal venules. Lymphadenitis (sarcoid or toxoplasmal) shows focal venular VCAM-1, but there is little or no ES. VCAM-1 staining is stronger and more widespread in cat-scratch lymphadenitis, and ES is also present. In most dermatoses, VCAM-1 and ES show venular endothelial expression. Vascular pericytes in inflamed skin may also stain for VCAM-1; ECs in the same vessel sometimes stain negative. This finding is consistent with our in vitro observations of the induction of VCAM-1 staining on VSMCs by TNF-α or IL-1.

VCAM-1 is abundant in the synovitis of rheumatoid arthritis. It is present in venules associated with chronic inflammatory cell infiltrates and also on hyperplastic synovial lining cells. ES is also present; it varies in intensity according to disease activity, and it is localized to ECs. The level of expression of both adhesins is far less in the synovium of osteoarthritis, a condition with fewer inflammatory features (241,243). Psoriatic arthritis, usually indistinguishable from rheumatoid disease with regard to the degree of clinical inflammatory joint findings, also shows less EC ES (244).

VCAM-1 is expressed on venular ECs in cardiac and renal allografts, and its presence correlates with T cell infiltrates (245,246). During rejection of human liver transplants, there is increased expression of ICAM-1 on target structures, such as bile ducts and venous endothelium, as well as on lymphocytes infiltrating the graft (247).

Human coronary arteries and abdominal aortas affected by diffuse intimal thickening and atheromatous plaques show a marked increase in expression of ICAM-1, ES, and, to a lesser extent, HLA-DR/DP on ECs adjacent to subendothelial infiltrates of T lymphocytes and macrophages. This effect contrasts with lower or absent expression of these markers at sites without prominent inflammatory cell infiltrates, and it suggests that cytokines produced by these subintimal infiltrates may activate the endothelium in a manner similar to that observed in the microvasculature at sites of immune inflammation (248).

IN VIVO ACTIONS: Subcutaneous injections of TNF-α in baboon skin attempt to stimulate the natural release of this cytokine in vivo. These experiments show that ES, ICAM-1, and VCAM-1 expression are induced at postcapillary sites, which concurs with results seen in cultured ECs. Expression of ES at such sites is evident 2 hours after injection, and it correlates highly with neutrophilic exudates. ICAM-1 and VCAM-1 are seen 24 to 48 hours after TNF-α exposure, and they correlate with mononuclear infiltration. Such results support the hypothesis that selective adhesion molecule expression contributes to selective leukocyte extravasation (249,250).

The tissue injury that accompanies hypoxemia and reoxygenation has features of the host response in inflammation, suggesting that cytokines such as IL-1 may act as mediators in this setting. Human ECs subjected t hypoxia elaborate IL-1 activity. There is an increase in the level of IL-1α mRNA, followed by induction of ES and enhanced expression of ICAM-1 during reoxygenation.

Adherence of leukocytes is increased 3- to 5-fold, and it is partly blocked by antibodies to ES and ICAM-1. Suppression of endothelial-derived IL-1, using antibodies to IL-1α, specific, antisense oligonucleotides, or the IL-1 receptor antagonist, decreases leukocyte adherence to reoxygenated ECs, thus emphasizing the integral role of IL-1 in the adherence phenomenon.

Mice subjected to hypoxia display increased plasma levels of IL-1α, induction of IL-1α mRNA in lung, and enhanced expression of ICAM-1 in pulmonary tissue compared with normoxemic control mice. Thus, hypoxia is a stimulus that induces EC synthesis and release of IL-1α, and it may result in an autocrine enhancement of adhesion molecule expression (251,252).

Plasmodium falciparum–infected erythrocytes isolated from a patient with severe complicated malaria bound to TNF-α–treated human vascular ECs via ES, ICAM-1, and VCAM-1. Attachment of infected erythrocytes to blood vessel walls is understood to be the primary step in the vascular occlusion underlying this disease, in which serum TNF-α levels are characteristically high. ES and VCAM-1 are expressed on brain microvascular endothelium of postmortem brain tissue from patients dying of cerebral malaria (253).

A role for IL-1 and ECs in the neuronal mechanisms related to β-amyloid protein deposition in senile plaques in patients with Alzheimer's disease is suspected. The protein precursor of β-amyloid is expressed on ECs in senile plaques. Its mRNA in human endothelial, neuronal, and brain-derived murine ECs increases when these cells are exposed to IL-1β (254).

Pancreatic carcinoma cells are among a group of neoplastic cells that express the ES ligand, sialyl Lewis (a). Their attachment to activated ECs is thus regulated by cytokines such as IL-1β and TNF-α, which induce endothelial ES (255).

Finally, EC activation by cytokines can also be beneficial. Congenital toxoplasmosis involves infection of umbilical cord vessels as a major route of transmission. IL-1β and TNF-α, in cooperation, inhibit EC replication of *T. gondii*, an obligate intracellular parasite. IFN-γ has a similar retardive effect (256).

Chemokines

Chemokines are a group of 8- to 11-kd proteins produced by ECs as well as leukocytes, fibroblasts, and keratinocytes (206,257). Their primary function is chemoattraction, but stimulation of leukocyte microbicidal activity and respiratory burst become evident at higher concentrations. They are divided into two families on the basis of their leukocyte predilection and structure. The α-subfamily, exemplified by IL-8 (neutrophil-activating protein-1), has an amino acid intervening between the first two cysteines of its amino terminus (i.e., C-X-C), whereas the β-subfamily, exemplified by MCP-1, does not (i.e., C-C) (258,259).

Each chemokine shows some selectivity for a leukocyte species both in vitro and in vivo. IL-8 acts on neutrophils, although there is also some evidence for T cell and eosinophil activity (259–261). MCP-1 is a chemoattractant for human monocytes (262). MIP-1 attracts activated T cells, whereas RANTES (regulated on activation, normal T expressed and secreted) acts on unstimulated T cells, monocytes, and eosinophils (263–265). Furthermore, MIP-1α acts preferentially on CD8+ lymphocytes, whereas MIP-1β attracts CD4+ cells (263). This chemotactic discrimination, plus that offered by the adhesion molecules, provides the means to selectively control extravasation of each leukocyte subset.

IL-8 AND NEUTROPHIL TRANSMIGRATION:

Endothelia treated with IL-1 or TNF-α bring about neutrophil transmigration. This effect appears to be at least partly due to stimulation of the endothelium's endogenous production of IL-8, which acts as a chemoattractant if added to the basal EC compartment in an in vitro model of the vessel wall (205,206). Antisera to IL-8 markedly inhibit neutrophil transmigration across activated EC monolayers, and washing the basilar compartment of the vessel wall, which depletes IL-8 from the subendothelial matrix, also prevents neutrophil invasion unless IL-8 is readded (205). IL-8 is less effective in a chemokinetic role (i.e., when placed on both sides of the endothelium) (202).

Given that neutrophils must contact the endothelium for transmigration to occur, it is suggested that IL-8 creates not only a chemotactic gradient, but also a haptotactic gradient of IL-8 molecules over the EC surface, along which neutrophils may move (7,204). Consistent with this proposal, IL-8 binding sites exist on ECs of postcapillary and collective venules and small veins, but they are not found on arteries or capillaries (266). Immunohistochemical analysis of IL-1β–stimulated ECs in vivo reveals IL-8 in association with both the EC monolayer and the underlying interstitium (205). IL-8 may reach these sites by diffusion from perivascular tissues or through local production by endothelium. A soluble chemotactic mechanism alone would be an unlikely method for neutrophil transmigration, because soluble IL-8 inhibits neutrophil-endothelial interactions, it leads neutrophils to shed L-selectin (a molecule involved in their primary rolling attachment to ECs), and it would be continually eroded by virtue of flow dilution (7,267).

Desensitization of neutrophils to IL-8 confirms the existence of another factor involved in the control of transendothelial migration. The procedure decreases neutrophil transmigration through cytokine-stimulated ECs totally. Desensitization to another chemotactic agent, N-

formyl-methionyl-leucyl-phenylalanine (FMLP), creates neutrophils that still respond to an IL-8 gradient, suggesting that the desensitization process does not prevent neutrophil migration. They are, however, inhibited from transmigrating across cytokine-stimulated ECs by 74%, through a putative second, IL-8–independent pathway (268). TNF-α and IL-8 have additive effects on transmigration, which further suggests the existence of an IL-8–independent mechanism (202).

Chemotactic desensitization also demonstrates the dichotomy between adhesion and transmigration. Neutrophils desensitized to IL-8 adhere avidly to ECs due to activation of their CDIIb/CD18, but they do not migrate (269). Furthermore, lymphocytes will adhere to TNF-α–treated EC monolayers, but they do not migrate through them (204).

IL-8 AND NEUTROPHIL ADHESION: Neutrophils that have established adhesive contact on the endothelium display activation of their β_2-integrins, and they lack L-selectin (7). Soluble IL-8 also causes nonadherent neutrophils to shed L-selectin, and as a result of further, as yet uncertain means, it decreases neutrophil-endothelial interactions (267). Intravenous IL-8 administration to nonhuman primates results in granulocytosis and neutrophil margination in lung, liver, and spleen, but no tissue infiltration (270). Thus, depending on whether more IL-8 is bound or free, neutrophils are either stimulated to or are inhibited from adhering.

Because neutrophil contact with cytokine-activated endothelium may lead to EC damage, IL-8 steers the interactions of these two cells through three possible courses: (a) diapedesis and transmigration, (b) expulsion of granule contents and EC damage, or (c) detachment via soluble IL-8 to reenter the circulating pool (240). The levels of soluble, intravascular IL-8 at a site of inflammation are controlled by the availability of free binding sites, blood flow washing away soluble factors, circulating antibodies to IL-8 (271), and red blood cells, which bind IL-8, rendering it incapable of stimulating neutrophils (272).

MONOKINES: MCP-1, MIP-1, and RANTES are the mononuclear cell chemoattractant equivalents of IL-8. Their synthesis is induced in ECs by IL-1, TNF-α, LPS, and thrombin (273,274). IFN-γ also induces MCP-1 mRNA, but to a lesser extent (274). MCP-1 protein steadily accumulates from ECs exposed to IL-1β over 48 hours. It has chemoattractant properties for monocytes, and it can activate monocyte β_2-integrins (274,275).

Akin to IL-8, MIP-1β is also present on lymph node endothelium in an immobilized form, and thus it is resistant to loss in the flow of the bloodstream. In vitro immobilization of MIP-1β on proteoglycans assists the binding of T cells to VCAM-1 (276). MIP-1β may therefore control not only the chemotaxis of T cells, but also their adhesion to endothelial VCAM-1. This process is similar to IL-8 activation of neutrophil β_2-integrin, although the mechanism of this effect of MIP-1β is unresolved.

DISEASE ASSOCIATIONS: The chemokines are associated with both acute and chronic disease processes. IL-8 appears in the circulation in patients with septic shock, endotoxemia, and after IL-1 administration (277). Bronchioloalveolar lavage IL-8 levels are higher in patients with acute respiratory illnesses in whom the adult respiratory distress syndrome subsequently develops (278), than in those in whom it does not develop. Acute asbestos-induced pleurisy is characterized by an influx of neutrophils. Introduction of crocidolite asbestos or TNF-α into the pleural space leads to the appearance of chemotactic activity for neutrophils, which is inhibited by anti-IL-8 and is accompanied by rapid induction of IL-8 mRNA in mesothelial cells (279).

Extracts of synovium from joints afflicted by rheumatoid arthritis possess diverse chemotactic activities to monocytes, T cells, and neutrophils. mRNA for IL-8, MCP, RANTES, and GRO is expressed in synovial fluid cells and synovial macrophages and fibroblasts. The chemotactic activity can be adsorbed by anti-IL-8 and anti-MCP-1 antibodies. MCP-1 levels are significantly higher in synovial fluid from patients with rheumatoid arthritis than those with osteoarthritis, which is consistent with the relative components of inflammation in the two disorders. The concentration of IL-8 and RANTES mRNA in blood is also less than in synovial fluid cells, which is consistent with the central site of inflammatory activity (280–285).

Circulating antibodies to IL-8 have been demonstrated in patients with rheumatoid arthritis; they correlated strongly with C-reactive protein, number of arthritic joints, and disease activity (271). IL-8 immunostaining is also noted on ECs in the minor salivary glands of patients with Sjögren's syndrome (286).

Minimally modified low density lipoprotein (LDL) induces MCP-1 in human endothelial and smooth muscle cells, and a role in atherosclerosis is further suggested by expression of MCP-1 mRNA and protein in atherosclerotic lesions of rabbits, but not from the intima or the media of normal animals. MCP-1 can be extracted and hybridized from lesional foam cells, but not from alveolar macrophages, sublesional VSMCs, or normal arteries (287,288).

Interferon-γ

IFN-γ is a T-cell product that steers ECs toward a phenotype consistent with chronic inflammation; they express class I and II MHC antigens, and they resemble a high endothelial venule (289). Its intracellular signaling in-

volves phospholipase D–dependent triphasic activation of PKC (290).

EFFECTS ON ADHESION MOLECULES: The effects of IFN-γ on the EC adhesion molecule profile differ from those of IL-1 and TNF-α. IFN-γ stabilizes the surface expression of ES, but it does not induce or prolong its period of synthesis (291). It does not increase PS expression, but ICAM-1 is up-regulated (169,292). IFN-γ has a minor part in the induction of the L-selectin ligand compared with TNF-α and IL-1β (181), but it decreases EC expression of CD34, another L-selectin ligand (179).

IFN-γ has not been found to induce VCAM-1 on cultured ECs (185), but it does lead to a marked up-regulation of endothelial and dermal dendritic cell VCAM-1 after intradermal injection. In comparison to normal skin, in which VCAM-1 is present on perivascular dendritic cells and some follicular keratinocytes only, VCAM-1 is variably up-regulated on dermal endothelial and dendritic cells in allergic contact dermatitis, atopic dermatitis, lichen planus, and psoriasis, all conditions with increased local IFN-γ (293).

EFFECTS ON MHC EXPRESSION: Class I MHC appears on ECs exposed to IFN-γ (169); the ECs then become antigen-presenting cells for lymphocytes (294). IFN-γ increases TAP-1 expression, thus permitting assembly and normal surface expression of the class I MHC molecules. Both class I MHC and TAP-1 are synergistically increased by combinations of TNF-α with IFN-γ (196).

Class II HLA-DR antigens are uniquely induced on ECs by IFN-γ; they selectively increase the adhesion of CD4+ lymphocytes to ECs over other leukocyte populations (289,295,296). Serially passaged EC cultures will stimulate highly purified peripheral blood CD4+ T cells to proliferate if the EC cultures are pretreated with IFN-γ to induce de novo expression of MHC class II molecules (297). T-cell production of IFN-γ correlated with the intensity of EC expression of MHC antigen in a rat model of insulitis (298).

OTHER ENDOTHELIAL EFFECTS: Human recombinant IFN-γ increases HUVEC monolayer permeability to [^{125}I]-labeled bovine serum albumin in a time- and dose-dependent manner. IFN-γ and TNF-α or IL-1 produce an increase in permeability greater than that seen with each cytokine alone (299). Migration of lymphocytes through endothelial cell monolayers is also augmented by an endothelial-specific effect of IFN-γ. This augmentation affects even prebound lymphocytes; therefore affects migration and not just adhesion (300). The mechanism is not resolved, although IFN-γ increases MCP-1 production.

IFN-γ decreases EC αvβ3-integrin (the vitronectin receptor), and it induces α1β1 (192,301). It decreases EC mRNA and protein levels of PDGF and GM-CSF, it increases IL-1 mRNA, and it weakly induces IL-6 production (106,154,302).

Hematopoietic CSFs

IL-3 acts directly on hematopoietic and endothelial cells, and it favors their proliferation, as discussed. Proinflammatory effects of excess levels of CSFs have been evident in clinical practice and in animal models (303,304), but they have been ascribed to actions on mature leukocytes, such as those favoring their adhesion to endothelium (305,306) and activation (307–310). ECs have been seen as a source of G-CSF, GM-CSF, and M-CSF when activated by other cytokines (e.g., IL-1, TNF-α, oncostatin-M) (311–313). Modified LDLs produce a similar effect, and because M-CSF binds preferentially to type V collagen (a collagen reported in atherosclerosis), this effect has led to suggestions that CSFs thus produced and acting on leukocytes may have a role in atherosclerosis (314,315).

We and others have observed that resting HUVECs express mRNA for the α- and β-chains of the IL-3 receptor, and that this is a functional mediator of endothelial interactions with leukocytes (90–92). Previous reports had generally concluded that CSFs do not influence these endothelial properties (e.g., procoagulant activity; production of PAF; expression of ES, PA, or PAI-1) (88,89). Positive reports (e.g., G-CSF augmenting ET-1 production (316), and GM-CSF and M-CSF weakly increasing endothelial ICAM-1 expression) (292,317) are controversial in light of the absence of demonstrable receptors for these cytokines on ECs.

IL-3, however, induces ES surface expression on resting HUVECs, as well as those treated with TNF-α. It supports neutrophil and CD4+ lymphocyte adhesion (90,92). IL-8 production and neutrophil transmigration across TNF-α–activated HUVEC monolayers are also increased by IL-3 (90). Thus, at least one CSF clearly alters endothelial interactions with leukocytes in vitro.

Transforming growth factor-β

TGF-β is a 25-kd dimer that appears to be a vital anti-inflammatory factor. Three isoforms are known in humans, but consideration is given in this discussion only to TGF-β1. At the cellular level, TGF-β has pleiotropic effects on morphogenesis, proliferation, and differentiation (318,319). Lin and Lodish (320) categorize its effects as (a) interruption of cell cycle in mid-to-late G1-phase, thus preventing induction of DNA synthesis and progression into S-phase; (b) induction of ECM and decreased synthesis of matrix-degrading proteinases; and (c) modu-

lation of the secretion of other growth factors and their receptors (320).

Endothelium secretes latent TGF-β which undergoes activation in heterotypic co-cultures with other cell types such as pericytes or VSMCs (18,72). Its production in addition appears to be under positive autocrine control and is increased by TNF-α and IL-1 in a synergistic manner (321,322).

ENDOTHELIAL EFFECTS OF TGF-β1: TGF-β is recognized as a fundamental protein given the multifocal inflammatory disease seen in mice with targeted deletion of the TGF-β1 gene. At birth, these animals show no gross developmental abnormalities, but approximately 20 days later, they succumb to a wasting syndrome accompanied by a mixed inflammatory infiltrate, leading to organ failure in heart, stomach, liver, lung, pancreas, salivary gland, and striated muscle. There are increased numbers of neutrophils and monocytes in peripheral blood, and analysis of cytokine mRNAs from spleen, liver, and lung show increased IFN-γ, MIP-1α, TNF-α, and IL-1β levels (323,324).

Although the mechanisms behind this pathology are not entirely certain and may not be directly applicable to humans, experimental data demonstrate that TGF-β negatively modulates the interactions between human ECs and leukocytes therefore contribute to the inflammatory homeostasis of the organism. The basal and TNF-α/IL-1–induced adhesiveness of ECs for neutrophils (325), T lymphocytes (326), monocytes (Litwin MS, et al., unpublished observations), and tumor cells (327) are decreased by TGF-β. This decrease is accompanied by a reduction in the EC surface expression of ES; there is no change in VCAM-1 or ICAM-1 (328). Neutrophil transmigration across basal and cytokine-stimulated EC monolayers is also inhibited by TGF-β, with an accompanying reduction in EC IL-8 secretion (Smith WC, et al., unpublished observations).

Expression of VCAM-1 on VSMCs in their basal state or after TNF-α stimulation is also inhibited by TGF-β. Because active TGF-β is produced as a result of coculture of VSMCs and ECs, this close cellular association may be responsible for the lack of VCAM-1 expression on in situ normal VSMCs. Interruption of this contact in atheroma and loss of active TGF-β may be important pathogenic events (Gamble JR, et al., unpublished observations).

TGF-β RECEPTORS AND SIGNALING: There are three cell surface TGF-β binding proteins, each reported to be expressed on ECs (74,329). Type I and III receptors are thought to capture TGF-β and present it to type II receptors, which are functional transmembrane serine/threonine kinases (320,330). In addition, there are a number of other binding proteins that exist as soluble forms or in the ECM. α_2-Macroglobulin and β-glycan are believed to deliver TGF-β to its signal transduction receptors, whereas decorin neutralizes TGF-β (8). The effects of TGF-β on ECs, however, may relate more to expression of downstream components of the signaling pathway than to the type of receptor expressed, because these receptors are found even on TGF-β–unresponsive ECs. On other cell types, divergent responses are produced despite expression of the same receptors (331,332).

DISEASE ASSOCIATIONS: In several experimental animal diseases modeling human illnesses marked by a significant inflammatory component, administration of TGF-β leads to amelioration of both disease and tissue infiltration. In experimental allergic encephalomyelitis TGF-β appears to protect against disease relapses. Anti-TGF-β antibody increases the incidence and severity of relapses, whereas anti-TNF-α antibody decreases them. TGF-β treatment does not influence the appearance of sensitized cells in peripheral blood and lymph nodes, but it does prevent accumulation of T cells in brain and spinal cord (333). Similar benefits from TGF-β are claimed in myocardial ischemia/reperfusion injury (334,335), as well as acute and chronic streptococcal-induced arthritis. Histopathological examination of the latter shows reduced inflammatory cell infiltration, pannus formation, and joint erosion (336).

Lipoprotein(a) (Lp[a]) is an LDL-like particle that contains apolipoprotein(a), a molecule with homology to plasminogen. Epidemiological studies have shown significant correlation between blood levels of Lp(a) and coronary/cerebral vascular disease. Lp(a) inhibits generation of TGF-β in cocultures of ECs with VSMCs by competing with plasminogen for EC surface binding, thus decreasing the EC plasmin-generating activity. This process may lead to down-regulation of TGF-β activation, and, because TGF-β is an inhibitor of EC proliferation, adhesiveness for leukocytes, VSMC migration, and VCAM-1 expression, Lp(a) may use this mechanism in the generation of atheromatous lesions (337).

ECs from skin affected by psoriasis show specific unresponsiveness to the inhibitory effects of TGF-β on baseline, IL-1-, and TNF-α–induced increases in lymphocyte adhesion, compared with cultured normal dermal microvascular ECs (338). If this finding reflects only swamping of the relatively weak negative signal of TGF-β by other more powerful proinflammatory influences, it is still a demonstration of the finely balanced forces in inflammation.

Interleukin-4

IL-4 is a product of T cells, mast cells, and bone marrow stroma cells. It has a dominant role in the development of undifferentiated T helper (Th) cells into Th1 and Th2 cells, favoring the Th2 phenotype (339). It also inhibits

several monocyte functions in vitro, including the respiratory burst; adhesion to endothelium and IL-1, TNF-α, IL-6, and IL-8 (340–343).

IL-4 assists endothelial induction of VCAM-1 by IL-1, TNF-α, or IFN-γ. Expression of basal and cytokine-induced ES and, to some extent, ICAM-1, is decreased, however, and together with TGF-β there is additive inhibition of ES (328,344,345). Through these changes, IL-4 increases EC adhesiveness for T cells, eosinophils, and basophils, but not for neutrophils, because the former express very-late antigen (VLA-4); a ligand for VCAM-1, but neutrophils do not (346,347). Furthermore, eosinophils (but not neutrophils) from individuals with atopic dermatitis migrate through IL-4–pretreated EC monolayers (348).

Both IL-4 and TNF-α increase intracellular cyclic AMP in ECs, but only IL-4 uses this pathway to mediate lymphocyte adhesion. Elevation of cAMP in ECs does not induce VCAM-1, the only identified adhesion molecule induced by IL-4, indicating that an increase in cAMP in EC promotes an as yet unidentified adhesion pathway (349).

IL-4 increases resting endothelial MCP-1 production. It does not further increase IL-1 or TNF-induced MCP-1 mRNA, but there is an increase in secreted MCP-1 with these factors in combination; therefore, monocytes that adhere to the vascular wall by IL-4–induced VCAM-1 may be uniquely positioned to respond to EC-produced MCP-1 (350–352). IL-4 decreases IL-8 production by endothelium (Smith WB, et al., unpublished observations), which further suggests its activity favors mononuclear rather than neutrophil transmigration.

IL-4 may alone be insufficient to mediate leukocyte extravasation in vivo. Studies of monocyte morphology after adhesion to IL-4–treated, VCAM-1–bearing endothelium show that although there are more adherent monocytes, they do not stretch over the surface of ECs, which is thought to be a precursor of their transmigration. In contrast, stimulation of ECs with IL-1α for 24 hours increases surface expression of both ICAM-1 and VCAM-1, enhances binding of monocytes to ECs, and increases the percentage of EC-bound monocytes with a stretched morphology (353).

IL-4 induces IL-6 production by ECs in synergy with IFN-γ, IL-1, and TNF-α (354,355).

Interleukin-6

IL-6 is a T-cell cytokine that acts as a B-cell differentiator, a plasmacytoma growth factor, and a stimulator of hepatic acute-phase reactants. It increases endothelial ICAM-1 expression (292). IL-6 is produced by ECs stimulated with a variety of proinflammatory cytokines, such as IL-1, IL-4, TNF, and IFN-γ (221,352,356). Exposure of ECs to mouse hepatitis virus leads to their production of IL-6 (357).

Endothelial monocyte-activating polypeptide II

Endothelial monocyte-activating polypeptide II (EMAP-II) is a 22-kd polypeptide purified to homogeneity from the conditioned medium of murine fibrosarcoma cells based on its ability to induce tissue factor activity in ECs. In addition to procoagulant activity, it induces monocyte migration, and it is chemotactic for granulocytes. Injection into foot pads of mice leads to tissue swelling, with neutrophil infiltration (358).

SUMMARY

The major functions of the endothelium (i.e., renewal, angiogenesis, and interactions with blood components) are subject to the influence of many cytokines (Table 7–1) that often have overlapping, generally redundant effects, but nevertheless a wide spectrum of different actions.

Redundancy and pleiotropism among cytokines

Redundancy among these cytokines is well exemplified by the control of surface adhesion molecules by TNF-α, IL-1, IFN-γ, IL-3, and IL-4, or of EC proliferation by FGF, VEGF, SF, IL-3, and TGF-β. For instance, TNF-α, IL-1, and IL-4 each encourage interaction of ECs with mononuclear cells by increasing endothelial expression of VCAM-1. TNF-α and IL-1 have the additional capacity to induce the display of ES by ECs and, consequently, their attachment of neutrophils. In direct contrast, IL-4 decreases ES expression by the endothelium, and it restricts its interactions to mononuclear cells and eosinophils.

Stimulation of angiogenesis by FGF and TGF-β is another example. Both enhance angiogenesis, but, as described, they appear to have opposite effects on EC division and deposition of ECM. They appear to act in a complementary manner as respective initiators and completors of this process. Therefore, what appears to be redundancy is in fact also specificity and complementary activity created through the varying actions of diverse agents.

Pleiotropism among the cytokines acting on endothelium is also evident. TNF-α and TGF-β provide a clear example. Amid their many actions on endothelium is, however, a consistent pattern. TNF-α is the proinflammatory agent that encourages coagulation, adhesion, and chemokine production, whereas TGF-β prevents these changes or acts to restore the status quo. A clear aid in defining the understanding of pleiotropic agents, such as TGF-β, has been the study of animals with cytokine gene deletions. The multiinflammatory disease of TGF-β–deficient mice now awaits further work to determine to what

TABLE 7–1 CYTOKINE ACTIONS ON ENDOTHELIUM

EC Actions	TNF-α, IL-1	IFN-γ	TGF-β	IL-4	FGF	VEGF	CSF
Mitosis	↓	↔	↓	↑	↑	↑	↑
Migration	↔	↔	↓	↔	↑	↑	↑
Plasminogen activation	↑	ND	↓	ND	↑	ND	ND
Integrin expression	↑	↑	↔	↔	↑	ND	ND
Angiogenesis	↓	↔	↑	ND	↑	↑	↑
Coagulation	↑	↔	↔	ND	↔	ND	ND
Adhesion molecules	↑	↑	↓	↑↓	↔	↔	↑
Permeability to molecules	↑	↑	ND	↔	↔	↑	↔
Permeability to leukocytes	↑	↑	↓	↔	↔	↔	↑
Cytokine production	↑	↑↓	↓	↑	↔	ND	↔
MHC expression	↑	↑	↔	↔	↔	ND	↔

TNF = tumor necrosis factor; IFN = interferon; TGF-β = transforming growth factor-β; IL = interleukin; FGF = fibroblast growth factor; VEGF = vascular endothelial growth factor; CSF = colony-stimulating factor; MHC = major histocompatibility complex; ND = not done.

extent the endothelial effects of TGF-β contribute to its overall phenotype. Transgenic methods have not yet been applied to endothelial biology due to the lack of endothelial-specific promoters. Study of the control of ES transcription, which is uniquely expressed on endothelium, offers hope in this direction.

Local availability of cytokines acting on endothelium

The local availability and source of cytokines are key factors in their relative importance to endothelium. Activated monocytes or lymphocytes, which produce many of the cytokines discussed, are generally features of established, chronic inflammation; thus, their cytokine production would not be expected to begin the first endothelial changes. Mast cells, by virtue of their ubiquity, secretory granule storage (i.e., holding TNF-α), and responsiveness to neural stimuli, are suspected of being the key initiating cell. In delayed-type hypersensitivity reactions in human skin, degranulation of mast cells situated about superficial vessels is the first ultrastructural change seen; it precedes inflammatory cell accumulation by 16 hours (151).

Cytokine availability is influenced by the ECM, which may provide binding sites that function as reservoirs or aids to receptor interaction (8). The presence of binding sites is clearly important for the chemokines; as bound surface molecules, they favor leukocyte haptotaxis, but as free molecules, they inhibit leukocyte adhesion to ECs. ECM–EC interactions can also trigger the same intracellular signals evoked by cytokines, and the ECM is another area in which endothelial cell biologists will find fertile ground.

Signaling

Although cytokines are important signals for ECs, other means of communication are increasingly being understood. Molecules assigned one particular function have been discovered to have a second signaling function. For example, CD31 (PECAM-1) was viewed only as an intercellular junction molecule with a role in leukocyte transmigration, but its ligation selectively assists interaction between the α4β1-integrin found on leukocytes and VCAM-1 (359). Mechanical displacements from the bloodstream lead to changes in cell biochemistry. Flow or shear stress is transduced by ECs into the induction of c-fos, PDGF, and activated factor X expression. Circumferential tensile stress due to blood pressure leads to thickening of the vascular wall (360–362).

The signaling pathways of cytokines, as well as the signals that follow ligation of surface molecules or perceptible displacement of cell membranes, are likely to assume increasing importance. The cyclosporine revolution in clinical medicine has clearly shown that the pathways for intracellular communication are central to an understanding of cytokine actions, and that they are likely to be promising sites for clinically oriented interventions. TNF receptor-binding mutants with decreased endothelial proinflammatory actions that retain antitumor properties offer the promise of isolating the actions of other pleiotropic cytokines and potentially applying these findings selectively to clinical practice (219).

REFERENCES

1. Denekamp J. Vasculature as a target for tumour therapy. Prog Appl Microcirc 1984;4:28–38.
2. Millauer B, Wizigmann-Voos S, Schnurch H, et al. High affinity VEGF binding and developmental expression suggest FLK-1 as a major regulator of vasculogenesis and angiogenesis. Cell 1993;72:835–846.
3. Bevilacqua MP, Pober JS, Majeau GR, Fiers W, Cotran RS, Gimbrone MA Jr. Recombinant tumor necrosis factor induces procoagulant activity in cultured human vascular endothelium: characterisation and comparison with the actions of interleukin 1. Proc Natl Acad Sci USA 1986; 83:4533–4537.
4. Palmer RMJ, Ferrige AG, Moncada S. Nitric oxide release accounts for the biological activity of endothelium-derived relaxing factor. Nature 1987;327:524–526.
5. Moser R, Schleiffenbaum B, Groscurth P, Fehr J. Interleukin 1 and tumor necrosis factor stimulate human vascular endothelial cells to promote transendothelial neutrophil passage. J Clin Invest 1989;83:444–455.
6. Pober JS, Collins T, Gimbrone MA, et al. Lymphocytes recognise human vascular endothelial and dermal fibroblast la antigens induced by recombinant immune interferon. Nature 1983;305:726–729.
7. Rot A. Endothelial cell binding of NAP-1/IL-8: role in neutrophil emigration. Immunol Today 1992;13:291–294.
8. Ruoslahti E. Yamaguchi Y. Proteoglycans as modulators of growth factor activities. Cell 1991;64:867–869.
9. Schweigerer L, Neufeld G, Friedman J, Abraham JA, Fiddes JC, Gospodarowicz D. Capillary endothelial cells express basic fibroblast growth factor, a mitogen that promotes their own growth. Nature 1987;325:257–295.
10. Itoh H, Mukoyama M, Pratt RE, Dzau VJ. Specific blockade of basic fibroblast growth factor gene expression in endothelial cells by antisense oligonucleotide. Biochem Biophys Res Commun 1992;188:1205–1213.
11. George F, Sampol J. Circulating endothelial cells: a marker of vascular lesion. Nouv Rev Fr Hematol 1993;35:259–261.
12. Folkman J, Haudenschild C. Angiogenesis in vitro. Nature 1980;288:551–556.
13. Folkman J, Klagsbrun M. Angiogenic factors. Science 1987;235:442–447.
14. Shing Y, Folkman J, Haudenschild C, Lund D, Crum R, Klagsbrun M. Angiogenesis is stimulated by a tumor-derived endothelial cell growth factor. J Cell Biochem 1985; 29:275–287.
15. Eisemann A, Ahn JA, Graziani G, Tronick SR, Ron D. Alternative splicing generates at least five different isoforms of the human basic-FGF receptor. Oncogene 1991;6:1195–1202.
16. Klagsbrun M, Baird A. A dual receptor system is required for basic fibroblast growth factor activity. Cell 1991:67–229–231.
17. Sato Y, Rifkin DB. Autocrine activities of basic fibroblast growth factor: regulation of endothelial cell movement, plasminogen activator synthesis and DNA synthesis. J Cell Biol 1988;107:1199–1205.
18. Flaumenhaft R, Abe M, Mignatti P, Rifkin DB. Basic fibroblast growth factor-induced activation of latent transforming growth factor β in endothelial cells: regulation of plasminogen activator activity. J Cell Biol 1992;118:901–909.
19. Mostacelli D, Presta M, Rifkin DB. Purification of a factor from human placenta that stimulates capillary endothelial cell protease production, DNA synthesis and migration. Proc Natl Acad Sci USA 1986;83:2091–2095.
20. Mignatti P, Mazzieri R, Rifkin DB. Expression of the urokinase receptor in vascular endothelial cells is stimulated by basic fibroblast growth factor. J Cell Biol 1991;113:1193–1201.
21. Pepper MS, Sappino AP, Stocklin R, Montesano R, Orci L, Vassalli JD. Upregulation of urokinase receptor expression on migrating endothelial cells. J Cell Biol 1993;122:673–684.
22. Montesano R, Vassalli JD, Baird A, Guillemin R, Orci L. Basic fibroblast growth factor induces angiogenesis in vitro. Proc Natl Acad Sci USA 1986;83:7297–7301.
23. Swerlick RA, Brown EJ, Xu Y, Lee KH, Manos S, Lawley TJ. Expression and modulation of the vitronectin receptor on human dermal microvascular endothelial cells. J Invest Dermatol 1992;99:715–722.
24. Enenstein J, Waleh NS, Kramer RH. Basic FGF and TGF-beta differentially modulate integrin expression of human microvascular endothelial cells. Exp Cell Res 1992; 203:499–503.
25. Lee PL, Johnson DE, Cousens LS, Fried VA, Williams LT. Purification and complementary DNA cloning of a receptor for basic fibroblast growth factor. Science 1989;245:57–60.
26. Moscatelli D. High and low affinity binding sites for basic fibroblast growth factor on cultured cells: absence of a role for low affinity binding in the stimulation of plasminogen activator production by bovine capillary endothelial cells. J Cell Physiol 1987;131:123–130.
27. Roghani M, Moscatelli D. Basic fibroblast growth factor is internalized through both receptor-mediated and heparan sulfate-mediated mechanisms. J Biol Chem 1992; 267:22156–22162.
28. Isacchi A, Statuto M, Chiesa R, et al. A six-amino deletion in basic fibroblast growth factor dissociates its mitogenic activity from its plasminogen activator-inducing capacity. Proc Natl Acad Sci USA 1991;88:2628–2632.
29. Presta M, Maier JAM, Ragnotti G. The mitogenic signalling pathway but not the plasminogen activator-inducing pathway of basic fibroblast growth factor is mediated through protein kinase C in fetal bovine aortic endothelial cells. J Cell Biol 1989;109:1877–1884.
30. Dell'Era P, Presta M, Ragnotti G. Nuclear localisation of endogenous fibroblast growth factor in cultured endothelial cells. Exp Cell Res 1991;192:505–510.
31. Bouche G, Gas N, Baldin V, et al. Basic fibroblast growth factor enters the nucleolus and stimulates the transcription of ribosomal genes in ABAE cells undergoing G_0–G_1 transition. Proc Natl Acad Sci USA 1987;84:6770–6774.
32. Baldin V, Roman AM, Bosc-Bierne I, Amalric F, Bouche G. Translocation of bFGF to the nucleus is G_1 phase cell cycle specific in bovine aortic endothelial cells. EMBO J 1990; 9:1511–1517.
33. Imamura T, Engelka K, Zhan X, et al. Recovery of mitogenic activity of a growth factor mutant with a nuclear translocation sequence. Science 1990;249:1567–1570.

34. Presta M, Tiberio L, Rusnati M, Dell'Era P, Ragnotti G. Basic fibroblast growth factor requires a long lasting activation of protein kinase C to induce cell proliferation in transformed fetal bovine aortic endothelial cells. Cell Reg 1991;2:719–726.

35. Rusnati M, Urbinati C, Presta M. Internalization of basic fibroblast growth factor (bFGF) in cultured endothelial cells: role of the low affinity heparin-like bFGF receptors. J Cell Physiol 1993;154:152–161.

36. Mostacelli D. Basic fibroblast growth factor (bFGF) dissociates rapidly from heparan sulfates but slowly from receptors. Implications for mechanisms of bFGF release from pericellular matrix. J Biol Chem 1992;267:25803–25809.

37. Feige JJ, Bradley JD, Fryburg K, et al. Differential effects of heparin, fibronectin and laminin on the phosphorylation of basic fibroblast growth factor by protein kinase C and the catalytic subunit of protein kinase A. J Cell Biol 1989; 109:3105–3114.

38. Schubert D. Collaborative interactions between growth factors and the extracellular matrix. Trends Cell Biol 1992; 2:63–66.

39. Nurcombe V, Ford MD, Wildschut JA, Bartlett PF. Developmental regulation of neural response to FGF-1 and FGF-2 by heparan sulfate proteoglycan. Science 1993;260:103–106.

40. Friesel R, Komoriya A, Maciag T. Inhibition of endothelial proliferation by gamma-interferon. J Cell Biol 1987; 104:689–696.

41. Sato Y, Waki M, Ohno M, Kuwano M, Sakata T. Carboxyl-terminal heparin-binding fragments of platelet factor 4 retain the blocking effect on the receptor binding of basic fibroblast growth factor. Jpn J Cancer Res 1993;84:485–488.

42. Nakayama Y, Iwahana M, Sakamoto N, Tanaka NG, Osada Y. Inhibitory effects of a bacteria-derived sulfated polysaccharide against basic fibroblast growth factor-induced endothelial cell growth and chemotaxis. J Cell Physiol 1993; 154:1–6.

43. Healy AM, Herman IM. Preparation of fluorescent basic fibroblast growth factor: localization in living retinal microvascular endothelial cells. Exp Eye Res 1992;55:663–669.

44. Itoh H, Mukoyama M, Pratt RE, Dzau VJ. Specific blockade of basic fibroblast growth factor gene expression in endothelial cells by antisense oligonucleotide. Biochem Biophys Res Commun 1992;188:1205–1213.

45. Lobb RR, Alderman EM, Fett JW. Induction of angiogenesis by bovine brain derived class 1 heparin-binding growth factor. Biochemistry 1985;24:4969–4973.

46. Nabel EG, Yang ZY, Plautz G, et al. Recombinant fibroblast growth factor-1 promotes intimal hyperplasia and angiogenesis in arteries in vivo. Nature 1993;362:844–846.

47. Pierce GF, Tarpley JE, Yanagihara D, Mustoe TA, Fox GM, Thomason A. Platelet-derived growth factor (BB homodimer), transforming growth factor-β1 and basic fibroblast growth factor in dermal wound healing. Neovessel and matrix formation and cessation of repair. Am J Pathol 1992; 140:1375–1388.

48. Villaschi S, Nicosia RF. Angiogenic role of endogenous basic fibroblast growth factor released by rat aorta after injury. Am J Pathol 1993;143:181–190.

49. Dvorak HF, Nagy JA, Dvorak AM. Structure of solid tumours and their vasculature: implications for therapy with monoclonal antibodies. Cancer Cells 1991;3:77–85.

50. Soker S, Svahn CM, Neufeld G. Vascular endothelial growth factor is inactivated by binding to α2-macroglobulin and the binding is inhibited by heparin. J Biol Chem 1993;268:7685–7691.

51. Brown LF, Berse B, Tognazzi K, et al. Vascular permeability factor mRNA and protein expression in human kidney. Kidney Int 1992;42:1457–1461.

52. Pepper MS, Ferrara N, Orci L, Montesano R. Potent synergism between vascular endothelial growth factor and basic fibroblast growth factor in the induction of angiogenesis in vitro. Biochem Biophys Res Commun 1992;189:824–831.

53. Unemori EN, Ferrara N, Bauer EA, Amento EP. Vascular endothelial growth factor induces interstitial collagenase expression in human endothelial cells. J Cell Physiol 1992; 153:557–562.

54. De Vries C, Escobedo JA, Ueno H, Houck K, Ferrara N, Williams LT. The fms-like tyrosine kinase, a receptor for vascular endothelial growth factor. Science 1992;255:989–991.

55. Peters KG, Werner S, Chen G, Williams LT. Two FGF receptor genes are differentially expressed in epithelial and mesenchymal tissues during limb formation and organogenesis in the mouse. Development 1992;114:233–243.

56. Shweiki D, Itin A, Neufeld G, Gitay-Goren H, Keshet E. Patterns of expression of vascular endothelial growth factor (VEGF) and VEGF receptors in mice suggest a role in hormonally regulated angiogenesis. J Clin Invest 1993;91: 2235–2243.

57. Kim KJ, Li B, Winer J, et al. Inhibition of vascular endothelial growth factor-induced angiogenesis suppresses tumour growth in vivo. Nature 1993;362:841–844.

58. Shweiki D, Itin A, Soffer D, Keshet E. Vascular endothelial growth factor induced by hypoxia may mediate hypoxia-initiated angiogenesis. Nature 1992;359:843–845.

59. Plate KH, Breier G, Weich HA, Risau W. Vascular endothelial growth factor is a potential tumour angiogenesis factor in human gliomas in vivo. Nature 1992;359:845–848.

60. Brown LF, Yeo KT, Berse B, et al. Expression of vascular permeability factor (vascular endothelial growth factor) by epidermal keratinocytes during wound healing. J Exp Med 1992;176:1375–1379.

61. Weidner KM, Arakaki N, Vandekerckhove J, et al. Evidence for the identity of human scatter factor and human hepatocyte growth factor. Proc Natl Acad Sci USA 1991; 88:7001–7005.

62. Nakamura T, Nishizawa T, Hagiya M, et al. Molecular cloning and expression of human hepatocyte growth factor. Nature 1989;342:440–443.

63. Monteasano R, Matsumoto K, Nakamura T, Orci L. Identification of a fibroblast-derived epithelial morphogen as hepatocyte growth factor. Cell 1991;67:901–908.

64. Rosen EM, Goldberg ID, Kacinski DM, Buckholz T, Vinter DW. Smooth muscle releases an epithelial cell scatter factor which binds to heparin. In Vitro Cell Dev Biol 1989; 25:163–173.

65. Stoker M, Gherardi E, Perryman M, Gray J. Scatter factor is a fibroblast-derived modulator of epithelial cell mobility. Nature 1987;327:238–242.

66. Weidner KM, Sachs M, Birchmeier W. The met receptor tyrosine kinase transduces motility, proliferation and morphogenic signals of scatter factor/hepatocyte growth factor in epithelial cells. J Cell Biol 1993;121:145–154.

67. Bussolino F, Di Renzo MF, Ziche M, et al. Hepatocyte growth factor is a potent angiogenic factor which stimulates endothelial cell motility and growth. J Cell Biol 1992; 119:629–641.

68. Grant DS, Kleiman HK, Goldberg ID, et al. Scatter factor induces blood vessel formation in vivo. Proc Natl Acad Sci USA 1993;90:1937–1941.

69. Madri JA, Pratt BM, Tucker AM. Phenotypic modulation of endothelial cells by transforming growth factor-beta depends upon composition and organisation of the extracellular matrix. J Cell Biol 1988;106:1375–1384.

70. Merwin JR, Anderson JM, Kocher O, van Itallie CM, Madri JA. Transforming growth factor β1 modulates extracellular matrix organisation and cell-cell junctional complex formation during angiogenesis. J Cell Physiol 1990;142:117–128.

71. Frater-Schroder M, Muller G, Birchmeier W, Bohlen P. Transforming growth factor-beta inhibits endothelial cell proliferation. Biochem Biophys Res Commun 1986;137: 295–302.

72. Antonelli-Orlidge A, Saunders K, Smith S, D'Amore PA. An activated form of transforming growth factor-β is produced by co-cultures of endothelial cells and pericytes. Proc Natl Acad Sci USA 1989;86:4544–4548.

73. Heimark RL, Twardzik DR, Schwart SM. Inhibition of endothelial regeneration by type-β transforming growth factor from platelets. Science 1986;223:1078–1080.

74. Muller G, Behrens J, Nussbaumer U, Bohlen P, Birchmeier W. Inhibitory action of transforming growth factor β on endothelial cells. Proc Natl Acad Sci USA 1987;84:5600–5604.

75. Saksela O, Moscatelli D, Rifkin DB. The opposing effects of basic fibroblast growth factor and transforming growth factor beta on the regulation of plasminogen activator activity in capillary endothelial cells. J Cell Biol 1987;105:767–775.

76. Ignotz RA, Massague J. Transforming growth factor-β stimulates the expression of fibronectin and collagen and their incorporation into the extracellular matrix. J Biol Chem 1986;261:4337–4345.

77. Edwards DR, Murphy G, Reynolds JJ, et al. Transforming growth factor beta modulates the expression of collagenase and metalloproteinase inhibitor. EMBO J 1987;6:1899–1904.

78. Roberts AB, Sporn MB, Assoian RK, et al. Transforming growth factor type β: rapid induction of fibrosis and angiogenesis in vivo and stimulation of collagen formation in vitro. Proc Natl Acad Sci USA 1986;83:4167–4171.

79. Yang EY, Moses HL. Transforming growth factor β1-induced changes in cell migration, proliferation and angiogenesis in the chick chorioallantoic membrane. J Cell Biol 1990:111:731–741.

80. Gonzlez T, Gutirrez R, Diaz-Flores L. Transforming growth factor β1 and basic fibroblast growth factor in articular cartilage defects. Rev Esp Reumatol 1993;20:S1.

81. Arciniegas E, Sutton AB, Allen TD, Schor AM. Transforming growth factor beta 1 promotes the differentiation of endothelial cells into smooth muscle-like cells in vitro. J Cell Sci 1992;103:521–529.

82. Merrilees MJ, Sodek J. Synthesis of TGF-beta 1 by vascular endothelial cells is correlated with cell spreading. J Vasc Res 1992;29:376–384.

83. Muller WA, Ratti CM, McDonnell SL, Cohn ZA. A human endothelial cell-restricted, externally disposed plasmalemmal protein enriched in intercellular junctions. J Exp Med 1989;170:399–414.

84. Ohto H, Maed H, Shibata Y, et al. A novel leukocyte differentiation antigen: two monoclonal antibodies TM2 and TM3 define a 120-kd molecule present on neutrophils, monocytes, platelets and activated lymphoblasts. Blood 1985;66:873–881.

85. Fina L, Molgaard HV, Robertson D, et al. Expression of the CD34 gene in vascular endothelial cells. Blood 1990;75: 2417–2426.

86. Baumhueter S, Singer MS, Henzel W, et al. Binding of L-selectin to the vascular sialomucin CD34. Science 1993; 262:436–438.

87. Kudo E, Hirose T, Sano T, Hizawa K. Epitopic heterogeneity of the CD36 antigen expressed by normal and neoplastic endothelial cells. An immunohistochemical study with a novel monoclonal antibody 8C9. Acta Pathol Jpn 1992; 42:807–817.

88. Forsyth KD, Chua KY, Talbot V, Thomas WR. Expression of the leukocyte common antigen CD45 by endothelium. J Immunol 1993;150:3471–3477.

89. Bussolino F, Wang JM, Defilippi F, et al. Granulocyte- and granulocyte-macrophage colony stimulating factor induce human endothelial cells to migrate and proliferate. Nature 1988;337:471–473.

90. Bussolino F, Ziche M, Wang JM, et al. In vitro and in vivo activation of endothelial cells by colony stimulating factors. J Clin Invest 1991;87:986–995.

91. Yong K, Cohen A, Khwaja A, Jones HM, Linch DC. Lack of effect of granulocyte-macrophage and granulocyte colony-stimulating factors on cultured human endothelial cells. Blood 1991;77:1675–1680.

92. Korpelainen EI, Gamble JR, Smith WB, et al. The receptor for interleukin 3 is selectively induced in human endothelial cells by tumor necrosis factor-α and potentiates interleukin 8 secretion and neutrophil transmigration. Proc Natl Acad Sci USA 1993;90:11137–11141.

93. Colotta F, Bussolino F, Polentarutti N, et al. Differential expression of the common β and specific α chains of the receptors for GM-CSF, IL-3, and IL-5 in endothelial cells. Exp Cell Res 1993;206:311–317.

94. Brizzi MF, Garbarino G, Rossi PR, et al. Interleukin 3 stimulates proliferation and triggers endothelial-leukocyte adhesion molecule 1 gene activation of human endothelial cells. J Clin Invest 1993;91:2887–2892.

95. Orazi A, Cattoretti G, Sciro R, et al. Recombinant human interleukin 3 and recombinant human granulocyte-macrophage colony stimulating factor administered in vivo after high dose cyclophosphamide cancer chemotherapy: effect on hematopoiesis and microenvironment in human bone marrow. Blood 1992;79:2610–2619.

96. Anagnostou A, Lee ES, Kessiman N, Levinson R, Steiner M. Erythropoietin has a mitogenic and positive chemotactic

activity on endothelial cells. Proc Natl Acad Sci USA 1990; 87:5978–5982.

97. Bruce AG, Hoggatt IH, Rose TM. Oncostatin M is a differentiation factor for myeloid leukemia cells. J Immunol 1992;149:1271–1275.
98. Toi M, Harris AL, Bicknell R. Interleukin-4 is a potent mitogen for capillary endothelium. Biochem Biophys Res Commun 1991;174:1287–1293.
99. Wojta J, Gallicchio M, Zoellner H, Filonzi EL, Hamilton JA, McGrath K. Interleukin-4 stimulates expression of urokinase-type-plasminogen activator in cultured human foreskin microvascular endothelial cells. Blood 1993; 81:3285–3292.
100. Koch AE, Polverini PJ, Kunkel SL, et al. Interleukin-8 as a macrophage-derived mediator of angiogenesis. Science 1992;258:1798–1801.
101. Buckley A, Davidson JM, Kamerath CD, Wolt TB, Woodward SC. Sustained release of epidermal growth factor accelerates wound repair. Proc Natl Acad Sci USA 1985; 82:7340–7344.
102. Wakui S. Epidermal growth factor receptor at endothelial cell and pericyte interdigitation in human granulation tissue. Microvasc Res 1992;44:255–262.
103. Ross R, Raines EW, Bowen-Pope DF. The biology of platelet-derived growth factor. Cell 1986;46:155–169.
104. Risau W, Drexler H, Mironov V, et al. Platelet-derived growth factor is angiogenic in vivo. Growth Factors 1992; 7:261–266.
105. Nabel EG, Yang Z, Liptay S, et al. Recombinant PDGF-B gene expression in porcine arteries induces intimal hyperplasia in vivo. J Clin Invest 1993;91:1822–1829.
106. Ross R, Masuda J, Raines EW, et al. Localisation of PDGF-B protein in macrophages in all phases of atherogenesis. Science 1990;248:1009–1012.
107. Hart CE, Forstrom JW, Kelly JD, et al. Two classes of PDGF receptor recognise different isoforms of PDGF. Science 1988;240:1529–1531.
108. Suzuki H, Shibano K, Okane M, et al. Interferon-γ modulates mRNA levels of c-sis (PDGF-B chain), PDGF-A chain and IL-1β genes in human vascular endothelial cells. Am J Pathol 1989;134:35–43.
109. Kourembanas S, McQuillan LP, Leung GK, Faller DV. Nitric oxide regulates the expression of vasoconstrictors and growth factors by vascular endothelium under both normoxia and hypoxia. J Clin Invest 1993;92:99–104.
110. Gajdusek CM, Luo Z, Mayberg MR. Sequestration and secretion of insulin-like growth factor-1 by bovine aortic endothelial cells. J Cell Physiol 1993;154:192–198.
111. Taylor WR, Nerem RM, Alexander RW. Polarized secretion of IGF-I and IGF-I binding protein activity by cultured aortic endothelial cells. J Cell Physiol 1993;154:139–142.
112. Cozzolino F, Torcia M, Aldinucci D, et al. Interleukin-1 is an autocrine regulator of human endothelial cell growth. Proc Natl Acad Sci USA 1990;87:6487–6491.
113. Janakidevi K, Fisher MA, Del-Vecchio PJ, Tiruppathi C, Figge J, Malik AB. Endothelin-1 stimulates DNA synthesis and proliferation of pulmonary artery smooth muscle cells. Am J Physiol 1992;263:C1295–1301.
114. Namiki A, Hata Y, Fukazawa M, et al. Granulocyte-colony stimulating factor stimulates immunoreactive endothelin-1 release from cultured bovine endothelial cells. Eur J Pharmacol 1992;227:339–341.
115. Emori T, Hirata Y, Imai T, et al. Cellular mechanism of thrombin on endothelin-1 biosynthesis and release in bovine endothelial cell. Biochem Pharmacol 1992;44:2409–2411.
116. Maemura K, Kurihara H, Morita T, Oh-hashi Y, Yazaki Y. Production of endothelin-1 in vascular endothelial cells is regulated by factors associated with vascular injury. Gerontology 1992;38(suppl 1):29–35.
117. Malek AM, Greene AL, Izumo S. Regulation of endothelin 1 gene by fluid shear stress is transcriptionally mediated and independent of protein kinase C and cAMP. Proc Natl Acad Sci USA 1993;90:5999–6003.
118. Fassbender HG, Simmling-Annefield A. The potential aggressiveness of synovial tissue in rheumatoid arthritis. J Pathol 1983;139:399–406.
119. Rooney M, Condell D, Quinlan W, et al. Analysis of the histologic variation in rheumatoid arthritis. Arthritis Rheum 1988;31:956–963.
120. Sano H, Forough R, Maier JAM, et al. Detection of high levels of heparin binding growth factor 1 (acidic fibroblast growth factor) in inflammatory arthritic joints. J Cell Biol 1990;110:1417–1426.
121. Ou Z, Planck R, Hart CE, Rosenbaum JT. Distribution pattern of basic fibroblast growth factor in synovial tissue from patients with rheumatoid arthritis. Arthritis Rheum 1990;33(suppl):75.
122. Shiozawa S, Shiozawa K, Tanaka Y, et al. Human epidermal growth factor for the stratification of synovial lining layer and neovascularisation in rheumatoid arthritis. Ann Rheum Dis 1989;48:820–828.
123. Hirata S, Matsubara T, Saura R, Tateishi H, Hirohata K. Inhibition of in vitro vascular endothelial cell proliferation and in vivo neovascularisation by low dose methotrexate. Arthritis Rheum 1989;32:1065–1073.
124. Matsubara T, Ziff M. Inhibition of endothelial cell proliferation by gold compounds. J Clin Invest 1987;79:1440–1446.
125. Williams SK. Regulation of intimal hyperplasia: do endothelial cells participate? Lab Invest 1991;64:721–723.
126. Orlidge A, D'Amore PA. Inhibition of capillary endothelial cell growth by pericytes and smooth muscle cells. J Cell Biol 1987;105:1455–1462.
127. Kuwubara T, Cogan DG. Retinal vascular patterns. Arch Ophthalmol 1963;69:114–124.
128. Ono M, Okamura K, Nakayama Y, et al. Induction of human microvascular endothelial tubular morphogenesis by human keratinocytes: involvement of transforming growth factor-alpha. Biochem Biophys Res Commun 1992; 189:601–609.
129. Folkman J, Shing Y. Angiogenesis. J Biol Chem 1992;267: 10931–10934.
130. Barnhill RL, Fandrey K, Levy MA, Mihm MC, Hyman B. Angiogenesis and tumor progression of melanoma. Quantification of vascularity in melanocytic nevi and cutaneous malignant melanoma. Lab Invest 1992;67:331–337.
131. Horak ER, Leek R, Klenk N, et al. Angiogenesis, assessed

by platelet/endothelial cell adhesion molecule antibodies, as indicator of node metastases and survival in breast cancer. Lancet 1992;340:1120–1124.

132. Ensoli B, Nakamura S, Salahuddin S, et al. AIDS-Kaposi's sarcoma-derived cells express cytokines with autocrine and paracrine growth effects. Science 1989;243:223–226.
133. Miles SA, Rezai AR, Salazar-Gonzalez JF, et al. AIDS Kaposi sarcoma-derived cells produce and respond to interleukin-6. Proc Natl Acad Sci USA 1990;87:4068–4072.
134. Corbeil J, Evans LA, Vasak E, Cooper DA, Penny R. Culture and properties of cells derived from Kaposi sarcoma. J Immunol 1991;146:2972–2976.
135. Abe T, Okamura K, Ono M, et al. Induction of vascular endothelial tubular morphogenesis by human glioma cells. A model system for tumor angiogenesis. J Clin Invest 1993; 92:54–61.
136. Folkman J. Successful treatment of an angiogenic disease. N Engl J Med 1989;320:1211–1212.
137. Blei F, Wilson EL, Mignatti P, Rifkin DB. Mechanism of action of angiostatic steroids: suppression of plasminogen activator activity via stimulation of plasminogen activator inhibitor synthesis. J Cell Physiol 1993;155:566–578.
138. Folkman J, Shing Y. Control of angiogenesis by heparin and other sulfated polysaccharides. Adv Exp Med Biol 1992;313:355–364.
139. White CW, Sondheimer HM, Crouch EC, Wilson H, Fan LL. Treatment of pulmonary hemangiomatosis with recombinant interferon alpha-2a. N Engl J Med 1989;320: 1197–1200.
140. Ingber D, Fujita T, Kishimoto S, et al. Synthetic analogues of fumagillin that inhibit angiogenesis and suppress tumour growth. Nature 1990;348:555–557.
141. Peacock DJ, Banquerigo ML, Brahn E. Angiogenesis inhibition suppresses collagen arthritis. J Exp Med 1992;175: 1135–1138.
142. Gagliardi A, Collins DC. Inhibition of angiogenesis by antiestrogens. Cancer Res 1993;53:533–535.
143. Norrby K. Cyclosporine is angiostatic. Experientia 1992; 48:1135–1138.
144. Polakowski IJ, Lewis MK, Muthukkaruppan VR, Erdman B, Kubai L, Auerbach R. A ribonuclease inhibitor expresses anti-angiogenic properties and leads to reduced tumor growth in mice. Am J Pathol 1993;143:507–517.
145. Fotsis T, Pepper M, Adlercreutz H, et al. Genistein, a dietary-derived inhibitor of in vivo angiogenesis. Proc Natl Acad Sci USA 1993;90:2690–2694.
146. Kaneko T, Nagata I, Miyamoto S, et al. Effects of nicardipine on tube formation of bovine vascular endothelial cells in vitro. Stroke 1992;23:1637–1642.
147. Ingber DE, Folkman J. Mechanochemical switching between growth and differentiation during fibroblast growth factor-stimulated angiogenesis in vitro: role of extracellular matrix. J Cell Biol 1989;109:317–330.
148. Gamble JR, Matthias L, Meyer G, et al. Regulation of in vitro capillary tube formation by anti-integrin antibodies. J Cell Biol 1993;121:931–943.
149. Dinarello CA. Interleukin-1 and interleukin-1 antagonism. Blood 1991;77:1627–1652.
150. Jaattela M. Biologic activities and mechanisms of action of tumor necrosis factor-α/cachectin. Lab Invest 1991;64: 724–742.
151. Klein LM, Lavker RM, Matis WL, Murphy GF. Degranulation of human mast cells induces an endothelial antigen central to leukocyte adhesion. Proc Natl Acad Sci USA 1989;86:8972–8976.
152. Warner SJC, Libby P. Human vascular smooth muscle cells: target for and source of tumour necrosis factor. J Immunol 1989;142:100–109.
153. Niedbala MJ, Stein-Picarella M. Role of protein kinase C in TNF induction of endothelial cell urokinase-type plasminogen activiator. Blood 1993;81:2608–2617.
154. Hashimoto Y, Hirohata S, Kashiwado T, Itoh K, Ishii H. Cytokine regulation of hemostatic property and IL-6 production of human endothelial cells. Inflammation 1992; 16:613–621.
155. Miyake S, Ohdama S, Tazawa R, Aoki N. Retinoic acid prevents cytokine-induced suppression of thrombomodulin expression on surface of human umbilical vein vascular endothelial cells in vitro. Thromb Res 1992;68:483–487.
156. Kawakami M, Ishibashi S, Ogawa H, Murase T, Takahu F, Shibata S. Cachectin/TNF as well as interleukin-1 induces prostacyclin synthesis in cultured vascular endothelial cells. Biochem Biophys Res Commun 1986;141:482–487.
157. Schleef RR, Bevilacqua MP, Sawdey M, Gimbrone MA Jr. Cytokine activation of vascular endothelium. Effects on tissue-type plasminogen activator and type 1 plasminogen activator inhibitor. J Biol Chem 1988;263:5797–5809.
158. Dosne AM, Dubor F, Lutcher F, Parant M, Chedid L. Tumor necrosis factor (TNF) stimulates plasminogen activator inhibitor (PAI) production by endothelial cells and decreases blood fibrinolytic activity in the rat. Thromb Res 1988;51:115–122.
159. Van Hinsbergh VWM, Kooistra T, Vanderberg EA, Princer HMG, Fiers W, Emeis JJ. Tumor necrosis factor increases the production of plasminogen activator inhibitor in human endothelial cells in vitro and in rats in vivo. Blood 1988;72:1467–1473.
160. Logan TF, Virji MA, Gooding WE, Bontempo FA, Ernstoff MS, Kirkwood JM. Plasminogen activator and its inhibitor in cancer patients treated with tumor necrosis factor. J Natl Cancer Inst 1992;84:1802–1810.
161. Kirchhofer D, Sakariassen KS, Clozel M, et al. Relationship between tissue factor expression and deposition of fibrin, platelets and leukocytes on cultured endothelial cells under venous blood flow conditions. Blood 1993;81:2050–2058.
162. Gamble JR, Harlan JM, Klebanoff SJ, Vadas MA. Stimulation of the adherence of neutrophils to umbilical vein endothelium by recombinant tumor necrosis factor. Proc Natl Acad Sci USA 1985;82:8667–8671.
163. Lawrence MB, Springer TA. Leukocytes roll on a selectin at physiological flow rates: distinct from and prerequisite for adhesion through integrins. Cell 1991;65:859–873.
164. von Adrian UH, Chambers JD, McEvoy LM, Bargatze RF, Arfors KE, Butcher EC. Two-step model of leukocyte-endothelial cell interaction in inflammation: distinct roles for LECAM-1 and the leukocyte β2 integrins in vivo. Proc Natl Acad Sci USA 1991;88:7538–7542.
165. Mayadas TN, Johnson RC, Rayburn H, Hynes RO, Wagner DD. Leukocyte rolling and extravasation are severely com-

promised in P selectin-deficient mice. Cell 1993;74:541–554.

166. Picker LJ, Warnock RA, Burns AR, Doerschuk CM, Berg EL, Butcher EC. The neutrophil selectin LECAM-1 presents carbohydrate ligands to the vascular selectins ELAM-1 and GMP-140. Cell 1991;66:921–933.

167. Pober JS, Bevilacqua MP, Mendrick DL, Lapierre LA, Fiers W, Gimbrone MA. Two distinct monokines, interleukin-1 and tumor necrosis factor, each independently induce biosynthesis and transient expression of the same antigen on the surface of cultured human endothelial cells. J Immunol 1986;136:1680–1687.

168. Bevilacqua MP, Stengelin S, Gimbrone MA, Seed B. ELAM-1. An inducible receptor for neutrophils related to complement regulatory proteins and lectins. Science 1989;243: 1160–1165.

169. Pober JS, Gimbrone MA, Lapierre LA, et al. Overlapping patterns of activation of human endothelial cells by interleukin 1, tumor necrosis factor and immune interferon. J Immunol 1986;137:1893–1896.

170. Messadi DV, Pober JS, Fiers W, Gimbrone MA, Murphy GF. Induction of an activation antigen on post-capillary venular endothelium in human skin organ culture. J Immunol 1987;139:1557–1562.

171. Leeuwenberg JFM, Smeets EF, Neefjes JJ, et al. E-selectin and intercellular adhesion molecule-1 are released by activated human endothelial cells in vitro. Immunology 1992; 77:543–549.

172. Smeets EF, de Vries T, Leeuwenberg JFM, van den Eijnden, Buurman WA, Neefjes JJ. Phosphorylation of surface E-selectin and the effect of soluble ligand (Sialyl Lewis^x) on the half-life of E-selectin. Eur J Immunol 1993;23:147–151.

173. von Asmuth EJU, Smeets EF, Ginsel LA, Onderwater JJM, Leeuwenberg JFM, Buurman WA. Evidence for endocytosis of E-selectin in human endothelial cells. Eur J Immunol 1992;22:2519–2526.

174. Geng J-G, Bevilacqua MP, Moore KL, et al. Rapid neutrophil adhesion to activated endothelium mediated by GMP-140. Nature 1990;343:757–760.

175. Sugama Y, Tiruppathi C, Janakidevi K, Andersen TT, Fenton JW II, Malik AB. Thrombin-induced expression of endothelial P-selectin and intercellular adhesion molecule-1: a mechanism for stabilising neutrophil adhesion. J Cell Biol 1992;119:935–944.

176. Weller A, Isenmann S, Vestweber D. Cloning of the mouse endothelial selectins. Expression of both E- and P-selectin is inducible by tumor necrosis factor α. J Biol Chem 1992; 267:15176–15183.

177. Fina L, Molgaard HV, Robertson D, et al. Expression of the CD34 gene in vascular endothelial cells. Blood 1990; 75:2417–2426.

178. Baumhueter S, Singer MS, Henzel W, et al. Binding of L-selectin to the vascular sialomucin CD34. Science 1993; 262:436–438.

179. Delia D, Lampugnani MG, Resnati M, et al. CD34 expression is regulated reciprocally with adhesion molecules in vascular endothelial cells in vitro. Blood 1993;81:1001–1008.

180. Lasky LA, Singer MS, Dowbenko D, et al. An endothelial ligand for L-selectin is a novel mucin-like molecule. Cell 1992;69:927–938.

181. Spertini O, Luscinskas FW, Kansas GS, et al. Leukocyte adhesion molecule-1 (LAM-1, L-selectin) interacts with an inducible endothelial cell ligand to support leukocyte adhesion. J Immunol 1991;147:2565–2573.

182. Schleiffenbaum B, Spertini O, Tedder TF. Soluble L-selectin is present in human plasma at high levels and retains functional activity. J Cell Biol 1992;119:229–238.

183. Gamble JR, Skinner MP, Berndt MC, Vadas MA. Prevention of activated neutrophil adhesion to endothelium by soluble adhesion protein GMP-140. Science 1990;249: 414–417.

184. Nortamo P, Li R, Renkonen R, et al. The expression of human intercellular adhesion molecule-2 is refractory to inflammatory cytokines. Eur J Immunol 1991;21:2629–2632.

185. Osborn L, Hession C, Tizard R, et al. Direct expression cloning of vascular cell adhesion molecule 1, a cytokine-induced endothelial protein that binds to lymphocytes. Cell 1989;59:1203–1211.

186. Wellicome SM, Thornhill MH, Pitzalis C, et al. A monoclonal antibody that detects a novel antigen on endothelial cells that is induced by TNF, IL-1 or lipopolysaccharide. J Immunol 1990;144:2558–2565.

187. Vonderheide RH, Springer TA. Lymphocyte adhesion through very late antigen 4: evidence for a novel binding site in the alternatively spliced domain of vascular cell adhesion molecule 1 and an additional α4 integrin counter-receptor on stimulated endothelium. J Exp Med 1992; 175:1433–1442.

188. Lampugnani MG, Renati M, Raiteri M, et al. A novel endothelial-specific membrane protein is a marker of cell-cell contacts. J Cell Biol 1992;118:1511–1522.

189. Muller WA, Ratti CM, McDonnell SL, Cohn ZA. A human endothelial cell-restricted, externally disposed plasmalemmal protein enriched in intercellular junctions. J Exp Med 1989;170:399–414.

190. Muller WA, Weigl SA, Deng X, Phillips DM. PECAM-1 is required for transendothelial migration of leukocytes. J Exp Med 1993;178:449–460.

191. Ioffreda MD, Albelda SM, Elder DE, et al. TNF-α induces E-selectin expression and PECAM-1 (CD31) redistribution in extracutaneous tissues. Endothelium 1993;1:47–54.

192. Defilippi P, Silengo L, Tarone G. α6β1 integrin (laminin receptor) is down-regulated by tumor necrosis factor-α and interleukin-1β in human endothelial cells. J Biol Chem 1992;267:18303–18307.

193. Johnson DR, Pober JS. Tumor necrosis factor regulation of major histocompatibility complex gene expression. Immunol Res 1991;10:141–155.

194. Johnson DR, Pober JS. TNF and immune interferon synergistically increase transcription of HLA class I heavy- and light-chain genes in vascular endothelium. Proc Natl Acad Sci USA 1990;87:5183–5187.

195. Epperson DE, Arnold D, Spies T, Cresswell P, Pober JS, Johnson DR. Cytokines increase transporter in antigen processing-1 expression more rapidly than HLA class I expression in endothelial cells. J Immunol 1992:149:3297–3301.

196. Warner SJ, Friedman GB, Libby P. Regulation of major histocompatibility gene expression in human vascular smooth muscle cells. Arteriosclerosis 1989;9:279–288.

197. Burke-Gaffney A, Keenan AK. Modulation of human endothelial cell permeability by combinations of the cytokines interleukin-1 alpha/beta, tumor necrosis factor-alpha and interferon-gamma. Immunopharmacology 1993;25:1–9.

198. Stolpen AH, Guinan EC, Fiers W, Pober JS. Recombinant tumor necrosis factor and immune interferon act singly and in combination to reorganise human vascular endothelial cell monolayers. Am J Physiol 1986;123:16–24.

199. Partridge CA, Horvath CJ, Del-Vecchio PJ, Phillips PG, Malik AB. Influence of extracellular matrix in tumor necrosis factor-induced increase in endothelial permeability. Am J Physiol 1992;263:L627–633.

200. Brett J, Gerlach H, Nawroth P, Steinberg S, Godman G, Stern D. Tumor necrosis factor/cachectin increases permeability of endothelial cell monolayers by a mechanism involving regulatory G proteins. J Exp Med 1989;169:1977–1991.

201. Klein NJ, Shennan GI, Heyderman RS, Levin M. Alteration in glycosaminoglycan metabolism and surface charge on human umbilical vein endothelial cells induced by cytokines, endotoxin and neutrophils. J Cell Sci 1992;102: 821–832.

202. Smith WB, Gamble JR, Clark-Lewis I, Vadas MA. Interleukin-8 induces neutrophil transendothelial migration. Immunology 1991;72:65–72.

203. Furie MB, McHugh DD. Migration of neutrophils across endothelial monolayers is stimulated by treatment of the monolayers with interleukin-1 or tumor necrosis factor-α. J Immunol 1989;143:3309–3317.

204. Moser R, Scheiffenbaum B, Groscurth P, Fehr J. Interleukin 1 and tumor necrosis factor stimulate human vascular endothelial cells to promote transendothelial neutrophil passage. J Clin Invest 1989;83:444–455.

205. Huber AR, Kunkel SL, Todd RF, Weiss SJ. Regulation of transendothelial neutrophil migration by endogenous interleukin-8. Science 1991;254:99–102.

206. Strieter RM, Kunkel SL, Showell HJ, Marks RM. Monokine-induced gene expression of a human endothelial cell-derived neutrophil chemotactic factor. Biochem Biophys Res Commun 1988;156:1340–1345.

207. Warner SJC, Auger KR, Libby P. Interleukin 1 induces interleukin 1. II. Recombinant human interleukin 1 induces interleukin 1 production by adult human vascular endothelial cells. J Immunol 1987;139:1911–1917.

208. Broundy VC, Kaushansky K, Segal GM, Harlan JM, Adamson JW. Tumor necrosis factor α stimulates human endothelial cells to produce granulocyte/macrophage colony-stimulating factor. Proc Natl Acad Sci USA 1986;83: 7467–7471.

209. Broundy VC, Kaushansky K, Harlan JM, Adamson JW. Interleukin 1 stimulates human endothelial cells to produce granulocyte-macrophage colony-stimulating factor. J Immunol 1988;139:464–468.

210. Hajjar KA, Hajjar DP, Silverstein RL, Nachman RL. Tumor necrosis factor-mediated release of platelet-derived growth factor from cultured endothelial cells. J. Exp. Med. 1987; 166:235–245.

211. Jirik FR, Podor TJ, Hirano T, et al. Bacterial lipopolysaccharide and inflammatory mediators augment IL-6 secretion by human endothelial cells. J Immunol 1989;142:144–147.

212. Sironi M, Breviario F, Proserpio P, et al. IL-1 stimulates IL-6 production in endothelial cells. J Immunol 1989;142: 549–553.

213. Bussolino F, Camussi G, Baglioni C. Synthesis and release of platelet-activating factor by human vascular endothelial cells treated with tumor necrosis factor or interleukin-1α. J Biol Chem 1988;263:11856–11861.

214. Breviario F, Bertocchi F, Dejana E, Bussolino F. Interleukin-1 induced adhesion of polymorphonuclear leukocytes to cultured human endothelial cells. J Immunol 1988;141: 3391–3397.

215. Westphal JR, Willems HW, Schalkwijk CJ, Ruiter DJ, de-Waal RM. A new 180-kd dermal endothelial cell activation antigen: in vitro and in situ characteristics. J Invest Dermatol 1993;100:27–34.

216. Hamanaka R, Kimitoshi K, Seguchi T, et al. Induction of low density lipoprotein receptor and a transcription factor SP-1 by tumor necrosis factor in human microvascular endothelial cells. J Biol Chem 1992;267:13160–13165.

217. Tartaglia LA, Goeddel DV. Two TNF receptors. Immunol Today 1992;13:151–153.

218. Shalaby MR, Sundan A, Loetscher H, Brockhaus M, Lesslauer W, Espevik T. Binding and regulation of cellular functions by monoclonal antibodies against human TNF receptors. J Exp Med 1990;172:1517–1520.

219. Barbara AJ, Smith WB, Gamble JR, et al. Dissociation of TNF-α cytotoxic and proinflammatory activities by p55 receptor- and p75 receptor-selective TNF-α mutants. Embo J 1994;13:843–850.

220. Van Ostade X, Vandenabeele P, Everaerdt B, et al. Human TNF mutants with selective activity on the p55 receptor. Nature 1993;361:266–269.

221. Tchorzewski H, Zeman K, Paleolog E, et al. The effects of tumor necrosis factor (TNF) derivatives on TNF receptors. Cytokine 1993;5:125–132.

222. Deisher TA, Garcia I, Harlan JM. Cytokine-induced adhesion molecule expression on human umbilical vein endothelial cells is not regulated by cyclic adenosine monophosphate accumulation. Life Sci 1993;53:365–370.

223. Deisher TA, Sato TT, Pohlman TH, Harlan JM. A protein kinase C agonist, selective for the beta I isozyme, induces E-selectin and VCAM-1 expression on HUVECs but does not translocate PKC. Biochem Biophys Res Commun 1993;193:1283–1290.

224. Garcia JG, Stasek JE, Bahler C, Natarajan V. Interleukin 1-stimulated prostacyclin synthesis in endothelium: lack of phospholipase C, phospholipase D, or protein kinase C involvement in early signal transduction. J Lab Clin Med 1992;120:929–940.

225. Schutze S, Potthoff K, Machleidt T, et al. TNF activates NF-kB by phosphatidylcholine-specific phospholipase c-induced "acidic" sphingomyelin breakdown. Cell 1992;71: 765–776.

226. Hooft van Huijsduijnen R, Whelan J, Pescini R, Becker-Andre M, Schenk AM, DeLamarter JF. A T cell enhancer cooperates with NF-kB to yield cytokine induction of E-selectin gene transcription in endothelial cells. J Biol Chem 1992;267:22385–22391.

227. Smith GM, Whelan J, Pescini R, Ghersa P, DeLamarter JF, Hooft van Huijsduijnen R. DNA-methylation of the

E-selectin promoter represses NF-kappa B transactivation. Biochem Biophys Res Commun 1993;194:215–221.

228. Neish AS, Williams AJ, Palmer HJ, Whitley MZ, Collins T. Functional analysis of the human vascular cell adhesion molecule 1 promoter. J Exp Med 1992;176:1583–1593.

229. Iademarco MF, McQuillan JJ, Dean DC. VCAM-1: contrasting transcriptional control mechanisms in muscle and endothelium. Proc Natl Acad Sci USA 1993;90:3943–3947.

230. de-Martin R, Vanhove B, Cheng Q, Hofer E, Csizmadia V. Cytokine-inducible expression in endothelial cells of an I kappa B alpha-like gene is regulated by NF kappa B. EMBO J 1993;12:2773–2779.

231. Brown K, Park S, Kanno T, Franzoso G, Siebenlist U. Mutual regulation of the transcriptional activator NF-kB and its inhibitor, IkB-α. Proc Natl Acad Sci USA 1993;90:2532–2536.

232. Nash JRG, McLaughlin PJ, Butcher D, Corrin B. Expression of tumour necrosis factor-α in cryptogenic fibrosing alveolitis. Histopathology 1993;22:343–347.

233. Deguchi Y, Shibata N, Kishimoto S. Enhanced transcription of TNF in systemic vasculitis. Lancet 1989;2:745–746.

234. Grau GE, Roux-Lombard P, Gysler C, et al. Serum cytokine changes in systemic vasculitis. Immunology 1989;68:196–198.

235. Arend WP, Dayer JM. Cytokines and cytokine inhibitors or antagonists in rheumatoid arthritis. Arthritis Rheum 1990;33:305–315.

236. Nickoloff BJ, Karabin GD, Barker JNWN, et al. Cellular localisation of interleukin-8 and its inducer tumor necrosis factor-alpha in psoriasis. Am J Pathol 1991;138:129–140.

237. de Kossodo S, Grau GE. Role of cytokines and adhesion molecules in malaria immunopathology. Stem Cells 1993;11:41–48.

238. Casey LC, Balk RA, Bone RC. Plasma cytokine and endotoxin levels correlate with survival in patients with the sepsis syndrome. Ann Intern Med 1993;119:771–778.

239. Leung DYM, Geha RS, Newburger JW, et al. Two monokines, interleukin 1 and tumor necrosis factor, render cultured vascular endothelial cells susceptible to lysis by antibodies circulating Kawasakisyndrome. J Exp Med 1986;164:1958–1972.

240. Westlin WF, Gimbrone MA. Neutrophil-mediated damage to human vascular endothelium. Role of cytokine activation. Am J Pathol 1993;142:117–128.

241. Rice GE, Munro JM, Corless C, Bevilacqua MP. Vascular and nonvascular expression of INCAM-110. A target for mononuclear leukocyte adhesion in normal and inflamed human tissues. Am J Pathol 1991;138:385–393.

242. Page C, Rose M, Yacoub M, Pigott R. Antigenic heterogeneity of vascular endothelium. Am J Pathol 1992;141:673–683.

243. Koch AE, Burrows JC, Haines GK, Carlos TM, Harlan JM, Leibovich SJ. Immunolocalisations of endothelial and leukocyte adhesion molecules in human rheumatoid and osteoarthritic synovial tissues. Lab Invest 1991;64:313–320.

244. Veale D, Yanni G, Rogers S, Barnes L, Bresnihan B, Fitzgerald O. Reduced synovial membrane macrophage numbers, ELAM-1 expression, and lining layer hyperplasia in psoriatic arthritis as compared with rheumatoid arthritis. Arthritis Rheum 1993;36:893–900.

245. Briscoe DM, Schoen FJ, Rice GE, Bevilacqua MP, Ganz P, Pober JS. Induced expression of endothelial leukocyte adhesion molecules in cardiac allografts. Transplantation 1991;51:537–539.

246. Briscoe DM, Pober JS, Harmon WE, Cotran RS. Expression of vascular cell adhesion molecule-1 in human renal allografts. J Am Soc Nephrol 1992;3:1180–1185.

247. Adams DH, Mainolfi E, Elias E, Neuberger JM, Rothlein R. Detection of circulating intercellular adhesion molecule-1 after liver transplantation; evidence of local release within the liver during graft rejection. Transplantation 1993;55:83–87.

248. van der Wal AC, Das PK, Tigges AJ, Becker AE. Adhesion molecules on the endothelium and mononuclear cells in human atherosclerotic lesions. Am J Pathol 1992;141:1427–1433.

249. Briscoe DM, Cotran RS, Pober JS. Effects of tumor necrosis factor, lipopolysaccharide and IL-4 on the expression of vascular cell adhesion molecule-1 in vivo. Correlation with CD3+ T cell infiltration. J Immunol 1992;149:2954–2960.

250. Munro JM, Pober JS, Cotran RS. Tumor necrosis factor and interferon-γ induce distinct patterns of endothelial activation and associated leukocyte accumulation in skin of Papio Anubis. Am J Pathol 1989;135:121–133.

251. Shreeniwas R, Koga S, Karakurum M, et al. Hypoxia-mediated induction of endothelial cell interleukin-1 alpha. An autocrine mechanism promoting expression of leukocyte adhesion molecules on the vessel surface. J Clin Invest 1992;90:2333–2339.

252. Ala Y, Palluy O, Favero J, Bonne C, Modat G, Dornand J. Hypoxia/reoxygenation stimulates endothelial cells to promote interleukin-1 and interleukin-6 production. Effects of free radical scavengers. Agents Actions 1992;37:134–139.

253. Ockenhouse CF, Tegoshi T, Maeno Y, et al. Human vascular endothelial cell adhesion receptors for plasmodium falciparum-infected erythrocytes: roles for endothelial leukocyte adhesion molecule 1 and vascular cell adhesion molecule 1. J Exp Med 1992;176:1183–1189.

254. Forloni G, Demicheli F, Giorgi S, Bendotti C, Angeretti N. Expression of amyloid precursor protein mRNAs in endothelial, neuronal and glial cells: modulation by interleukin-1. Brain Res Mol Brain Res 1992;16:128–134.

255. Iwai K, Ishikura H, Kaji M, et al. Importance of E-selectin (ELAM-1) and sialyl Lewis(a) in the adhesion of pancreatic carcinoma cells to activated endothelium. Int J Cancer 1993;54:972–977.

256. Dimier IH, Bout DT. Il-1β and TNF-α activation of HUVECs co-operatively inhibits Toxoplasma gondii replication. Immunology 1993;79:336–338.

257. Larsen CG, Anderson AO, Oppenheim JJ, Matsushima K. Production of interleukin-8 by human dermal fibroblasts and keratinocytes in response to interleukin-1 or tumor necrosis factor. Immunology 1989;68:31–36.

258. Bischoff SC, Krieger M, Brunner T, et al. RANTES and related chemokines activate human basophil granulocytes through different G protein-coupled receptors. Eur J Immunol 1993;23:761–767.

259. Bagglioni M, Walz A, Kunkel SL. Neutrophil-activating

peptide-1/interleukin 8, a novel cytokine that activates neutrophils. J Clin Invest 1989;84:1045–1049.

260. Collins PD, Web VB, Faccioli LH, Watson ML, Moqbel R, Williams TJ. Eosinophil accumulation induced by human interleukin-8 in the guinea pig in vivo. Immunology 1993; 79:312–318.

261. Larsen CG, Anderson AO, Appella E, Oppenheim JJ, Matsushima K. The neutrophil-activating protein (NAP-1) is also chemotactic for T lymphocytes. Science 1989;243: 1464–1466.

262. Leonard EL, Yoshimura T. Human monocyte chemoattractant protein-1 (MCP-1). Immunol Today 1990;11: 97–101.

263. Taub DD, Conlon K, Lloyd AR, Oppenheim JJ, Kelvin DJ. Preferential migration of activated CD4+ and CD8+ T cells in response to MIP-1α and MIP-1β. Science 1993;260:355–358.

264. Schall T, Bacon K, Toy K, Goedell D. Selective attraction of monocytes and T lymphocytes of the memory phenotype by cytokine RANTES. Nature 1990;347:669–671.

265. Rot A, Krieger M, Brunner T, Bischoff SC, Schall TJ, Dahinden CA. RANTES and macrophage inflammatory protein 1α induce the migration and activation of normal human eosinophil granulocytes. J Exp Med 1992;176: 1489–1495.

266. Rot A. Binding of neutrophil attractant/activation protein-1 (interleukin 8) to resident dermal cells. Cytokine 1992;4: 347–352.

267. Luscinskas FW, Kiely JM, Ding H, et al. In vitro inhibitory effect of IL-8 and other chemoattractants on neutrophil-endothelial adhesive interactions. J Immunol 1992;149: 2163–2171.

268. Smith WB, Gamble JR, Clark-Lewis I, Vadas MA. Chemotactic desensitisation of neutrophils demonstrates interleukin-8 (IL-8)-dependent and IL-8-independent mechanisms of transmigration through cytokine-activated endothelium. Immunology 1993;78:491–497.

269. Detmers PA, Lo SK, Olsen-Egbert E, et al. Neutrophil activating protein 1/IL 8 stimulates the binding activity of the leukocyte adhesion receptor CD11b/CD18 on human neutrophils. J Exp Med 1990;171:1155–1162.

270. Van Zee KJ, Fischer E, Hawes AS, et al. Effects of intravenous IL-8 administration in nonhuman primates. J Immunol 1992;148:1746–1752.

271. Peichl P, Ceska M, Broell H, Effenberger F, Lindley IJD. Human neutrophil activating peptide/interleukin 8 acts as an autoantigen in rheumatoid arthritis. Ann Rheum Dis 1992;51:19–22.

272. Darbonne WC, Rice GC, Mohler MA, et al. Red blood cells are a sink for interleukin 8, a leukocyte chemotaxin. J Clin Invest 1991;88:1362–1369.

273. Strieter RM, Wiggins R, Phan SH, et al. Monocyte chemotactic protein gene expression by cytokine-treated human fibroblasts and endothelial cells. Biochem Biophys Res Commun 1989;162:694–700.

274. Rollins BJ, Yoshimura T, Leonard EJ, Pober JS. Cytokine-activated human endothelial cells synthesize and secrete a monocyte chemoattractant, MCP-1/JE. Am J Pathol 1990; 136:1229–1233.

275. Jiang Y, Beller DI, Frendl G, Graves DT. Monocyte chemoattractant protein-1 regulates adhesion molecule expression and cytokine production in human monocytes. J Immunol 1992;148:2423–2428.

276. Tanaka Y, Adams DH, Hubscher S, Hirano H, Siebenlist U, Shaw S. T-cell adhesion induced by proteoglycan-immobilized cytokine MIP-1 beta. Nature 1993;361:79–82.

277. Van Zee KJ, DeForge LE, Fischer E, et al. IL-8 in septic shock, endotoxemia and after IL-1 administration. J Immunol 1991;146:3478–3482.

278. Donnelly SC, Strieter RM, Kunkel SL, et al. Interleukin-8 and development of adult respiratory distress syndrome in at-risk patient groups. Lancet 1993;341:643–647.

279. Boylan AM, Ruegg C, Jin Kim K, et al. Evidence of a role for mesothelial cell-derived interleukin 8 in the pathogenesis of asbestos-induced pleurisy in rabbits. J Clin Invest 1992; 89:1257–1267.

280. Koch AE, Kunkel SL, Harlow LA, et al. Enhanced production of monocyte chemoattractant protein-1 in rheumatoid arthritis. J Clin Invest 1992;90:772–779.

281. Seitz M, Dewald B, Gerber N, Bagglioni M. Enhanced production of neutrophil-activating peptide-1/interleukin-8 in rheumatoid arthritis. J Clin Invest 1991;87:463–469.

282. Koch AE, Kunkel SL, Burrows JC, et al. Synovial tissue macrophage as a source of the chemotactic cytokine IL-8. J Immunol 1991;147:2187–2195.

283. Hachicha M, Rathanaswami P, Schall TJ, McColl SR. Production of monocyte chemotactic protein-1 in human type b synoviocytes. Synergistic effect of tumor necrosis factor-α and interferon-γ. Arthritis Rheum 1993;36:26–34.

284. Akahoshi T, Kondo H. PCR analysis of intercrine superfamily gene expression in rheumatoid arthritis. Rev Esp Reumatol 1993;20(suppl 1):210.

285. Nishiura H, Matsubara S, Tanaka J, et al. Role of chemotactic cytokines in the leukocyte recruitment into the synovium of rheumatoid arthritis. Rev Esp Reumatol 1993; 20(suppl 1):M06.

286. Cauli A, Yanni G, Challacombe S, Panayi G. Patterns of cytokine expression and mononuclear cell infiltration in the minor salivary glands of patients with Sjögren's syndrome. Br J Rheumatol 1993;32(suppl 1):331.

287. Cushing SD, Berliner JA, Valente AJ, et al. Minimally modified low density lipoprotein induces monocyte chemotactic protein (MCP-1) in human endothelial and smooth muscle cells. Proc Natl Acad Sci USA 1990;87:5134–5138.

288. Yla-Herttuala S, Lipton BA, Rosenfeld ME, et al. Expression of monocyte chemoattractant protein 1 in macrophage-rich areas of human and rabbit atherosclerotic lesions. Proc Natl Acad Sci USA 1991;88:5252–5256.

289. Duijvestijn A, Hamann A. Mechanisms and regulation of lymphocyte migration. Immunol Today 1989;10:23–28.

290. Mattila P, Renkonen R. IFN-gamma induces a phospholipase D dependent triphasic activation of protein kinase C in endothelial cells. Biochem Biophys Res Commun 1992;189:1732–1738.

291. Doukas J, Pober JS. IFN-γ enhances endothelial activation induced by tumor necrosis factor but not IL-1. J Immunol 1990;145:1727–1733.

292. Buchsbaum ME, Kupper TJ, Murphy GF. Differential induction of intercellular adhesion molecule-1 in human

skin by recombinant cytokines. J Cutan Pathol 1993; 20:21–27.

293. Groves RW, Ross EL, Barker JN, MacDonald DM. Vascular cell adhesion molecule-1: expression in normal and diseased skin and regulation in vivo by interferon gamma. J Am Acad Dermatol 1993;29:67–72.

294. Pober JS, Collins T, Gimbrone MA, et al. Lymphocytes recognise human vascular endothelial and dermal fibroblast Ia antigens induced by recombinant immune interferon. Nature 1983;305:726–729.

295. Masuyama J, Minato N, Kano S. Mechanisms of lymphocyte adhesion to human vascular endothelial cells in culture. T lymphocyte adhesion to endothelial cells through endothelial HLA-DR antigens induced by γ-interferon. J Clin Invest 1986;77:1596–1605.

296. Hughes CCW, Male DK, Lantos PL. Adhesion of lymphocytes to cerebral microvascular cells: effects of interferon-γ, tumour necrosis factor and interleukin-1. Immunology 1988;64:677–681.

297. Savage CO, Hughes C, McIntyre BW, Picard JK, Pober JS. Human CD4+ T cells proliferate to HLA-DR+ allogeneic vascular endothelium. Identification of accessory interactions. Transplantation 1993;56:128–134.

298. Doukas J, Mordes JP. T lymphocytes capable of activating endothelial cells in vitro are present in rats with autoimmune diabetes. J Immunol 1993;150:1036–1046.

299. Burke-Gaffney A, Keenan AK. Modulation of human endothelial cell permeability by combinations of the cytokines interleukin-1 alpha/beta, tumor necrosis factor-alpha and interferon-gamma. Immunopharmacology 1993;25:1–9.

300. Oppenheimer-Marks N, Ziff M. Migration of lymphocytes through endothelial cell monolayers; augmentation by interferon-γ. Cell Immunol 1988;114:307–323.

301. Defilippi P, Truffa G, Stefanuto G, Altruda F, Silengo L, Tarone G. Tumor necrosis factor α and interferon γ modulate the expression of the vitronectin receptor (integrin β3) in human endothelial cells. J Biol Chem 1991;266:7638–7645.

302. Akahane K, Pluznik DH. Interferon-gamma destabilizes interleukin-1-induced granulocyte-macrophage colony-stimulating factor mRNA in murine vascular endothelial cells. Exp Hematol 1993;21:878–884.

303. Brandt SJ, Peters WP, Atwater SK, et al. Effect of recombinant granulocyte-macrophage colony stimulating factor on hematopoietic reconstitution after high-dose chemotherapy and autologous bone marrow transplantation. N Engl J Med 1988;318:869–873.

304. Metcalf D. The consequences of excess levels of haemopoietic growth factors. Br J Haematol 1990;75:1–3.

305. Elliott MJ, Vadas MA, Cleland LG, Gamble JR, Lopez AF. IL-3 and granulocyte-macrophage colony stimulating factor stimulate two distinct phases of adhesion in human monocytes. J Immunol 1990;145:167–176.

306. Yong KW, Rowles PM, Patterson KG, Linch DC. Granulocyte-macrophage colony-stimulating factor induces neutrophil adhesion to pulmonary vascular endothelium in vivo: role of β2 integrins. Blood 1992;80:1565–1575.

307. English D, Graves V. Simultaneous mobilisation of Mac-1 (CDIIb/CD18) and formyl peptide chemoattractant receptors in human neutrophils. Blood 1992;80:776–787.

308 Yong KL, Linch DC. Differential effects of granulocyte- and granulocyte-macrophage colony-stimulating factors (G- and GM-CSF) on neutrophil adhesion in vitro and in vivo. Eur J Haematol 1992;49:251–259.

309. Vadas MA, Nicola NA, Metcalf D. Activation of antibody-dependent cell-mediated cytotoxicity of human neutrophils and eosinophils by separate colony-stimulating factors. J Immunol 1983;130:795–799.

310. DeNicholo MO, Stewart AG, Vadas MA, Lopez AF. Granulocyte-macrophage colony-stimulating factor is a stimulant of platelet-activating factor and superoxide anion generation by human neutrophils. J Biol Chem 1991;266:4896–4902.

311. Broudy VC, Kaushansky K, Harland JM, Adamson JW. Interleukin-1 stimulates human endothelial cells to produce granulocyte-macrophage colony-stimulating factor and granulocyte colony-stimulating factor. J Immunol 1987;139:464–468.

312. Broudy VC, Kaushansky K, Segal GM, Harlan JM, Adamson JW. Tumor necrosis factor type alpha stimulates human endothelial cells to produce granulocyte-macrophage colony-stimulating factor. Proc Natl Acad Sci USA 1986;83:7467–7471.

313. Brown TJ, Liu J, Brashem-Stein C, Shoyab M. Regulation of granulocyte colony-stimulating factor and granulocyte-macrophage colony-stimulating factor expression by oncostatin M. Blood 1993;82:33–37.

314. Rajavashisth TB, Andalibi A, Territo MC, et al. Induction of endothelial cell expression of granulocyte and macrophage colony-stimulating factors by modified low-density lipoproteins. Nature 1990;344:254–257.

315. Suzu S, Ohtsuki T, Makishima M, et al. Biological activity of a proteoglycan form of macrophage colony-stimulating factor and its binding to type V collagen. J Biol Chem 1992; 267:16812–16815.

316. Namiki A, Hirata Y, Fukazawa M, et al. Granulocyte-colony stimulating factor stimulates immunoreactive endothelin-1 release from cultured bovine endothelial cells. Eur J Pharmacol 1992;227:339–341.

317. Chin YH, Cai JP, Johnson K. Lymphocyte adhesion to cultured Peyer's patch HEV cells is mediated by organ-specific homing receptors and can be regulated by cytokines. J Immunol 1990;145:3669–3677.

318. Massague J. The TGF-β family of growth and differentiation factors. Cell 1987;49:437–438.

319. Sporn MB, Roberts AB. Transforming growth factor-β: recent progress and new challenges. J Cell Biol 1992;119: 1017–1021.

320. Lin HY, Lodish HF. Receptors for the TGF-β superfamily: multiple polypeptides and serine/threonine kinases. Trends Cell Biol 1993;3:14–19.

321. Das SK, White AC, Fanburg BL. Modulation of transforming growth factor-β1 antiproliferative effects on endothelial cells by cysteine, cystine and n-acetylcysteine. J Clin Invest 1992;90:1649–1656.

322. Phan SH, Gharakee-Kermani M, McGarry B, Kunkel SL, Wolber FW. Regulation of rat pulmonary endothelial cell transforming growth factor-β production by IL-1β and tumor necrosis factor-α. J Immunol 1992;149:103–106.

323. Shull MM, Ormsby I, Kier AB, et al. Targeted disruption of

the mouse transforming growth factor-β1 gene results in multi-focal inflammatory disease. Nature 1992;359:693–699.

324. Kulkarni AB, Huh CG, Becker D, et al. Transforming growth factor-β1 null mutation in mice causes excessive inflammatory response and early death. Proc Natl Acad Sci USA 1993;90:770–774.
325. Gamble JR, Vadas MA. Endothelial adhesiveness for blood neutrophils is inhibited by transforming growth factor-β. Science 1988;242:97–99.
326. Gamble JR, Vadas MA. Endothelial cell adhesiveness for human T lymphocytes is inhibited by transforming growth factor-β. J Immunol 1991;146:1149–1154.
327. Bereta J, Bereta M, Coffman F, Cohen S, Cohen MC. Inhibition of basal and tumor necrosis factor-enhanced binding of murine tumor cells to murine endothelium by transforming growth factor-β. J Immunol 1992;148:2932–2940.
328. Gamble JR, Khew-Goodall Y, Vadas MA. TGF-β inhibits E-selectin expression on human endothelial cells. J Immunol 1993;150:4494–4503.
329. Fafeur V, Terman BJ, Blum J, Bohlen P. Basic FGF treatment of endothelial cells down-regulates the 85-kDa TGF-β receptor subtype and decreases the growth inhibitory response to TGF-β1. Growth Factors 1990;3:237–245.
330. Lin HY, Wang XF, Ng-Eaton E, Weinberg RA, Lodish HF. Expression cloning of the TGF-β type II receptor, a functional transmembrane serine/threonine kinase. Cell 1992; 68:775–785.
331. Fafeur V, O'Hara B, Bohlen P. A glycosylation-deficient endothelial cell mutant with modified responses to transforming growth factor-β and other growth inhibitory cytokines: evidence for multiple growth inhibitory signal transduction pathways. Mol Cell Biol 1993;4:135–144.
332. Kataoka R, Sherlock J, Lanier SM. Signaling events initiated by transforming growth factor-β1 that require $G_{i\alpha1}$. J Biol Chem 1993;268:19851–19857.
333. Santambrogio L, Hochwald GM, Saxena B. Studies on the mechanisms by which transforming growth factor-beta (TGF-beta) protects against allergic encephalomyelitis. Antagonism between TGF-beta and tumor necrosis factor. J Immunol 1993;151:1116–1127.
334. Lefer AM, Tsao P, Aoki N, Pallidino MA Jr. Mediation of cardioprotection by TGF-β. Science 1990;249:61–63.
335. Lefer AM, Ma XL, Weyrich AS, Scalia R. Mechanism of the cardioprotective effect of transforming growth factor-β1 in feline myocardial ischemia and reperfusion. Proc Natl Acad Sci USA 1993;90:1018–1022.
336. Brandes ME, Allen JB, Ogawa Y, Wahl SM. Transforming growth factor β1 suppresses acute and chronic arthritis in experimental animals. J Clin Invest 1991;87:1108–1113.
337. Kojima S, Harpel PC, Rifkin DB. Lipoprotein (a) inhibits the generation of transforming growth factor B: an endogenous inhibitor of smooth muscle migration. J Cell Biol 1991;113:1439–1445.
338. Cai JP, Falanga V, Taylor JR, Chin YH. Transforming gr th factor-beta differently regulates the adhesiveness of normal and psoriatic dermal microvascular endothelial cells for peripheral blood mononuclear cells. J Invest Dermatol 1992;98:405–409.
339. Abehsira-Amar O, Gibert M, Joliy M, Theze J, Jankovic DJ. IL-4 plays a dominant role in the differential development of Th0 and Th1 and Th2 cells. J Immunol 1992;148:3820–3829.
340. Abramson SL, Gallin JL. IL-4 inhibits superoxide production by human mononuclear phagocytes. J Immunol 1990; 144:625–630.
341. Hart PH, Vitti GF, Burgess DR, Whitty GA, Piccoli DS, Hamilton JA. Potential antiinflammatory effects of interleukin 4: suppression of human monocyte tumor necrosis factor alpha, interleukin 1 and prostaglandin E_2. Proc Natl Acad Sci USA 1989;86:3803–3807.
342. te Velde AA, Huijbens RJF, Heije K, de Vries JE, Figdor CG. Interleukin-4 inhibits secretion of IL-1β, tumor necrosis factor α and IL-6 by human monocytes. Blood 1990; 76:1392–1397.
343. Standiford TJ, Strieter RM, Chensue SW, Westwick J, Kasahara K, Kunkel SL. IL-4 inhibits the expression of IL-8 from stimulated human monocytes. J Immunol 1990; 145:1435–1439.
344. Thornhill HM, Haskard DO. IL-4 regulates endothelial cell activation by IL-1, tumor necrosis factor or IFN-γ. J Immunol 1990;145:865–872.
345. Thornhill MH, Wellicome SM, Mahiouz DL, Lanchbury JSS, Kyan-Aung U, Haskard DO. Tumour necrosis factor combines with IL-4 or IFN-γ to selectively enhance endothelial cell adhesiveness for T cells. The contribution of vascular cell adhesion molecule-1-dependent and -independent binding mechanisms. J Immunol 1991;146:592–598.
346. Thornhill MH, Kyan-Aung U, Haskard DO. IL-4 increases human endothelial cell adhesiveness for T cells but not for neutrophils. J Immunol 1990;144:3060–3065.
347. Schleimer RP, Sterbinsky SA, Kaiser J, et al. IL-4 induces adherence of human eosinophils and basophils but not neutrophils to endothelium. J Immunol 1992;148:1086–1092.
348. Moser R, Fehr J, Bruijnzeel PLB. IL-4 controls the selective endothelium-driven transmigration of eosinophils from allergic individuals. J Immunol 1992;149:1432–1438.
349. Galea P, Thibault G, Lacord M, Bardos P, Lebranchu Y. IL-4, but not tumor necrosis factor-alpha, increases endothelial cell adhesiveness for lymphocytes by activating a cAMP-dependent pathway. J Immunol 1993;151:588–596.
350. Rollins BJ, Pober JS. Interleukin-4 induces the synthesis and secretion of MCP-1/JE by human endothelial cells. Am J Pathol 1991;138:1315–1319.
351. Rollins BJ, Yoshimura T, Leonard EJ, Pober JS. Cytokine-activated human endothelial cells synthesize and secrete a monocyte chemoattractant, MCP-1/JE. Am J Pathol 1990; 136:1229–1233.
352. Colotta F, Sironi M, Borre A, Luini W, Maddalena F, Mantovani A. Interleukin-4 amplifies monocyte chemotactic protein and interleukin-6 production by endothelial cells. Cytokine 1992;4:24–28.
353. Beekhuizen H, Verdegaal EM, Blokland I, van-Furth R. Contribution of ICAM-1 and VCAM-1 to the morphological changes in monocytes bound to human venous endothelial cells stimulated with recombinant interleukin-4 or rIL-1 alpha. Immunology 1992;77:469–472.
354. Howell G, Pham P, Taylor D, Foxwell B, Feldmann M. Interleukin-4 induces interleukin-6 production by endo-

thelial cells: synergy with interferon-γ. Eur J Immunol 1991;21:97–101.

355. Paleolog EM, Aluri G, Feldmann M. Interleukin-4 (IL-4) modulates the response of human vascular endothelial cells to other cytokines. J Cell Biochem 1992;16A:18.

356. Sironi M, Breviario F, Proserpio P, et al. IL-1 stimulates IL-6 production in endothelial cells. J Immunol 1989;142: 549–553.

357. Joseph J, Grun JL, Lublin FD, Knobler RL. Interleukin-6 induction in vitro in mouse brain endothelial cells and astrocytes by exposure to mouse hepatitis virus (MHV-4, JHM). J Neuroimmunol 1993;42:47–52.

358. Kao J, Ryan J, Brett G, et al. Endothelial monocyte-activating polypeptide II. A novel tumor-derived polypeptide that activates host-response mechanisms. J Biol Chem 1992; 267:20239–20247.

359. Tanaka Y, Albelda SM, Horgan, et al. CD31 expressed on distinctive T cell subsets is a preferential amplifier of β1 integrin-mediated adhesion. J Exp Med 1992;176:245–253.

360. Hsieh HJ, Li NQ, Frangos JA. Pulsatile and steady flow induces c-fos expression in human endothelial cells. J Cell Physiol 1993;154:143–151.

361. Grabowski EF, Zuckerman DB, Nemerson Y. The functional expression of tissue factor by fibroblasts and endothelial cells under flow conditions. Blood 1993;81:3265–3270.

362. Akira K, Ando J. Vascular endothelial cell functions and biomechanics. Endothelium 1993;1:127–130.

COMMONWEALTH OF AUSTRALIA

(Patents Act 1990)

IN THE MATTER OF: Australian Patent Application 696764 (73941/94). In the name of: Human Genome Sciences Inc.

- and -

IN THE MATTER OF: Opposition thereto by Ludwig Institute for Cancer Research, under Section 59 of the Patents Act.

Annexure GBC-11

This is **Annexure GBC-11** referred to in my Statutory Declaration made this Thirteenth day of December 2000.

Gary Baxter Cox

WITNESS: _____

Patent Attorney PETTEE KMC

Regulation of In Vitro Capillary Tube Formation by Anti-Integrin Antibodies

Jennifer R. Gamble,* Lisa J. Matthias,* Geoffrey Meyer,‡ Pritinder Kaur,* Graeme Russ,§ Randall Faull,§ Michael C. Berndt,‖ and Mathew A. Vadas*

*Hanson Centre for Cancer Research, Division of Human Immunology, Institute of Medical and Veterinary Science, Adelaide, 5000, South Australia; ‡Department of Anatomy and Human Biology, University of Western Australia, Nedlands, Perth, 6009, Western Australia; and §Transplantation Immunology Laboratory, The Queen Elizabeth Hospital, Adelaide and ‖Vascular Biology Laboratory, Baker Medical Research Institute, Prahran, Victoria, Australia 3181

Abstract. Human endothelial cells are induced to form an anastomosing network of capillary tubes on a gel of collagen I in the presence of PMA. We show here that the addition of mAbs, AK7, or RMAC11 directed to the α chain of the major collagen receptor on endothelial cells, the integrin $\alpha_2\beta_1$, enhance the number, length, and width of capillary tubes formed by endothelial cells derived from umbilical vein or neonatal foreskins. The anti-$\alpha_2\beta_1$ antibodies maintained the endothelial cells in a rounded morphology and inhibited both their attachment to and proliferation on collagen but not on fibronectin, laminin, or gelatin matrices. Furthermore, RMAC11 promoted tube formation in collagen gels of increased density which in the absence of RMAC11 did not allow tube formation. Neither RMAC11 or AK7 enhanced capillary formation in the absence of PMA. Lumen structure and size were also altered by antibody RMAC11. In the absence of antibody the majority of lumina were formed intracellularly from single cells, but in the presence of RMAC11, multiple cells were involved and the lumen size was correspondingly increased. Endothelial cells were also induced to undergo capillary formation in fibrin gels after PMA stimulation. The addition of anti-$\alpha_v\beta_3$ antibodies promoted tube formation in fibrin gels and inhibited EC adhesion to and proliferation on a fibrinogen matrix. The enhancement of capillary formation by the anti-integrin antibodies was matrix specific; that is, anti-$\alpha_v\beta_3$ antibodies only enhanced tube formation on fibrin gels and not on collagen gels while anti-$\alpha_2\beta_1$ antibodies only enhanced tubes on collagen and not on fibrin gels. Thus we postulate that changes in the adhesive nature of endothelial cells for their extracellular matrix can profoundly effect their function. Anti-integrin antibodies which inhibit cell–matrix interactions convert endothelial cells from a proliferative phenotype towards differentiation which results in enhanced capillary tube formation.

New blood vessel formation is an essential event in embryogenesis and wound healing. However, little is known about the steps which induce flat, static endothelial cells (EC)[1] to undergo differentiation leading to a new capillary bed. Recently, a number of in vitro assays have been established which are thought to mimic angiogenesis and these have provided insight into possible mechanisms. EC initially undergo a spatial reorientation towards the angiogenic stimulus, invade and disrupt the extracellular matrix (ECM) by production of matrix degrading enzymes such as plasminogen activator and collagenase and undergo tube formation and extension via EC proliferation (for review see Folkman and Handenschild, 1980; Folkman, 1986). Thus, measurement of EC realignment, enzyme secretion, and cell proliferation are taken as indicators of EC differentiation and tube formation. Using such assays, it is clear that a number of factors including basic fibroblast growth factor, TGF-β, and tumor necrosis factor (Folkman and Klagsbrun, 1987) (termed angiogenic factors), can stimulate angiogenesis. In addition to the requirement for an angiogenic factor, in vitro capillary formation is also dependent on the correct matrix. Endothelial cells, plated on a two-dimensional matrix of ECM proteins or on plastic, form capillary tubes slowly (2–3 wk) (Kubota et al., 1988; Iruela-Arispe et al., 1991). However, when plated onto a gel of the ECM proteins, tubes form within 24 h (Kubota et al., 1988). Isolated components of the ECM, such as collagen or fibrinogen, when gelled are also able to induce the formation of capillary tubes (Monte-

Please address all correspondence to J. R. Gamble, Hanson Center for Cancer Research, Institute of Medical and Veterinary Science, Frome Road, Adelaide, 5000, South Australia.

1. *Abbreviations used in this paper*: EC, endothelial cells; ECGS, endothelial cell growth supplement; ECM, extracellular matrix; HUVEC, human umbilical vein endothelial cell; MVEC, microvessel EC; uPA, urokinase plasminogen activator.

sano et al., 1985). In collagen and fibrin gels the process of capillary formation is enhanced by the activation of the EC with the tumor promoter, PMA (Montesano and Orci, 1985; Montesano et al., 1987). Thus, even in the presence of an angiogenic factor, and a permissive milieu, an additional signal is required and this can be provided by PMA.

Cell surface molecules mediating adhesion to either neighboring cells or to substrates are likely to play a key role in angiogenesis. The integrins are a family of cell surface molecules which mediate the attachment of cells to the ECM and to other cells. At least 19 different cell-surface $\alpha\beta$ heterodimers have been identified, some of which mediate adhesion to ECM proteins such as laminin, collagen, fibrinogen, and fibronectin (Ruoslahti and Pierschbacher, 1987; Hynes, 1987; Albelda and Buck, 1990). EC express five of the six β_1 integrins ($\alpha_1\beta_1$, $\alpha_2\beta_1$, $\alpha_3\beta_1$, $\alpha_5\beta_1$, and $\alpha_6\beta_1$) although there is some heterogeneity in the level of expression depending on the source of the EC (Defilippi et al., 1991*a*). The major collagen receptor on EC is $\alpha_2\beta_1$ (Albelda et al., 1989; Languino et al., 1989) which can also mediate binding to laminin (Kramer et al., 1990). EC also express $\alpha_v\beta_3$ which mediates adhesion to fibrinogen (Albelda et al., 1989; Cheresh and Spiro, 1987) as well as laminin (Kramer et al., 1990) and vitronectin (Cheresh and Spiro, 1987).

We describe here for the first time that anti-integrin antibodies directed to the receptors mediating attachment to the tube-permissive matrices of collagen I and fibrin enhance capillary formation as measured by tube number, length, and thickness. Anti-integrin antibodies enhance tube thickness by increasing the number of cells involved in lumen formation. These results suggest that capillary tube formation is dependent on the interaction of EC with the ECM and that restriction of specific cell-matrix interactions can enhance the extent of capillary formation.

Materials and Methods

Endothelial Cells

Human umbilical vein endothelial cells (Huvec) were isolated by collagenase treatment as described (Wall et al., 1978). The cells were cultured in 25 cm^2 gelatin (Eastman Kodak Co., Rochester, NY)-coated flasks (Costar Corp., Cambridge, MA) in M199 with Earles Salts, 20 mM Hepes, 20% FCS (Cytosystems, Sydney), sodium bicarbonate, 2 mM glutamine, nonessential amino acids, sodium pyruvate, fungizone, penicillin, and gentamycin (HUVEC medium). Cells were grown at 37°C, 5% CO_2. Within 2–4 d the HUVEC formed a confluent monolayer and were then harvested by trypsin-EDTA treatment and transferred to a 75-cm^2 gelatin-coated flask. 50 μg/ml of endothelial cell growth supplement (ECGS, Collaborative Research, Bedford, MA) and 50 μg/ml of heparin (Sigma Chem. Co., St. Louis, MO) were added. Cells were passaged (1:2 split) every 3–4 d, and were used between passage 2 and 6. Microvessel EC (MVEC) were prepared from neonatal foreskins according to the method of Marks et al. (1985). Cells were frozen in liquid nitrogen at 1–2 × 10^6/vial at passage 2–6 and thawed as required. Cells were grown to confluence before use. Medium for growth and maintenance of these EC was M199 with Earles Salts, 25 mM Hepes, 50% human serum, sodium bicarbonate, 2 mM glutamine, fungizone, penicillin, streptomycin, 3.3 × 10^{-4} M cAMP, ECGS (50 μg/ml), and heparin (50 μg/ml).

Collagen Gel Capillary Assay

Bovine Type I collagen (Celtrix Laboratories, Palo Alto, CA) gel was prepared by simultaneously raising the pH and the ionic strength of a collagen solution, using a modification (Greenburg and Hay, 1982) of the original method described by Elsdale and Bard (1972). Seven volumes of ice cold collagen solution (3 mg/ml) was mixed with 1 vol of 10× concentrated PBS, pH 7.4, and 2 vol of sodium bicarbonate (11.76 mg/ml) on ice. One hundred μl of the mixture was aliquoted into 96 well flat-bottomed microtiter trays (Nunc, Roskilde, Denmark) and allowed to gel for 10–20 min at 37°C. For more rigid collagen gels, the mixture was allowed to gel for at least 1 h at 37°C. After gel formation, EC, which were removed from confluent monolayers by trypsin treatment, were plated down onto the gel at a concentration of 6.4 × 10^4 cells/160 μl in HUVEC or MVEC medium with ECGS and heparin. As indicated 20 ng/ml PMA (Sigma Chem. Co.) was added to some wells. In some assays, as indicated, cells together with PMA were resuspended in the collagen before gelling (modification of method by Madri et al., 1988).

Fibrin Gel Capillary Assay

Three dimensional fibrin gels were prepared as previously described by Montesano et al. (1985). One hundred μl of plasminogen free fibrinogen, 3 mg/ml in PBS (Sigma Chem. Co.) was placed into 96 well flat-bottomed microtiter wells (Nunc) and clotted by the addition of 2 μl of 1 U/ml thrombin (Parke Davis Pty Ltd., Adelaide, Australia) in PBS. The mixture was allowed to gel for ~2 min at 37°C before addition of EC. Cell numbers and conditions were the same as that described for the collagen gel assay.

Quantification of Capillary Formation

Tube formation was assessed at several different focal plains through the gel. The extent of capillary tube formation was judged in relation to the amount of EC monolayer and to the number, width, and length of the tubes formed. Based on these criteria values from + to ++++ were assigned. Tube formation was also quantified from high power photographs. At least two photographs from random fields from each microtiter well (duplicate wells were set up for each group) were taken. Areas of the well were avoided where the meniscus gave a distortion of the optics. We defined tubes as straight cellular extensions joining two cell masses or branch points. The minimum width of tubes was measured and is given as the width. From the photographs, counts were made of the number, length, and width of tubes.

Proliferation Assay

The mitogenic response of EC to different stimuli was measured using a spectrophotometric assay (Oliver et al., 1989). Cells (5 × 10^4) were plated onto matrix-coated flat-bottomed microtiter trays (Nunc), 150 μl/well in HUVEC medium either with or without ECGS, and heparin. After 3 d, medium was removed and the cells fixed in 10% formal saline for 30 min. One hundred μl of methylene blue (1% wt/vol, in 0.01 M borate buffer, pH 8.5) was then added to each well, incubated for 30 min, the stain flicked off, and the cells washed 3–4 times in borate buffer. The dye was released by addition of ethanol, 0.1 M HCl solution (1:1) with a brief shaking. The optical density at 630 nm (OD630 nm) was then determined. The percentage proliferation was calculated based on the OD630 of the no antibody control group normalized to 100%. Experiments showed that there was a linear relationship between the OD630 nm and the increase in cell number and that as low as 10^3 cells/well could be detected. Similar results were obtained using the methylene blue assay and the uptake of [^{3}H]thymidine (data not shown).

Cell Attachment Assays

Microtiter plates were coated with either collagen I (50 μg/ml), gelatin (1%), or fibronectin (100 μg/ml) for 30 min at room temperature. Fibrin-coated microtiter wells were formed by thrombin treatment (1 U/ml) of fibrinogen which had been previously added to wells. Wells were washed twice with PBS and 5 × 10^3 cells were added per well in 50 μl of HUVE medium without FCS. Plates were incubated at 37°C for the indicated times and cell attachment quantitated using the methylene blue assay (as outline above).

Collagenase Assay

Measurement of active collagenase was performed according to the method of Nethery et al. (1986). Microtiter wells were coated with 0.7 mg/ml collagen I solution (Collaborative Research Inc.), rinsed in water, and air dried. Cell supernatants were treated with 0.5 mg/ml trypsin at 37°C followed by treatment with soybean trypsin inhibitor (Sigma Chem. Co.) at 5 mg/ml.

Collagenase samples (CLS-1 Worthington Biochem. Corp., Freehold, NJ) were prepared at concentrations from 1 to 1,000 μg/ml in assay buffer (50 mM tris-HCl, 100 mM NaCl 10 mM $CaCl_2$, pH 7.5) and were used to generate a standard curve. One hundred μl of samples and standards were then added to the collagen-coated microtiter wells and incubated for 16 h at 37°C. The wells were washed and stained using 0.25% Coomassie blue R-250 (Biorad Labs., NSW, Australia) for 25 min at room temperature. The stain was removed, wells washed in water, dried, and the absorbance at 590 nm determined. The level of collagenase present in the sample was inversely proportional to the optical density reading at 590 nm. The level of detection was 10 ng/ml.

Monoclonal Antibodies

RMAC11 binds the α chain of the $\alpha_2\beta_1$ integrin complex on endothelial cells and fibroblasts and QE2E5 binds the β_1 chain (O'Connel et al., 1991). Preclearing and immunoprecipitation experiments show that AK7 also recognizes the α chain of the $\alpha_2\beta_1$ complex (Mazurov et al., 1991). RMAC11 (IgG2a), QE2.E5 (IgG2b), and AK7 (IgG1) were purified from ascites fluid using a mAb Trap G Sepharose column (Pharmacia LKB, NSW, Australia). Fab_2 fragments of RMAC11 were prepared by pepsin digestion and Fab fragments by papain digestion of the IgG according to the method of Harlow and Lane (1988). P4C10, an IgG_1 antibody directed to the β_1 integrin chain (Carter et al., 1990) was kindly provided by Dr. W. G. Carter, Fred Hutchinson Cancer Research Center, Seattle, WA. Another antibody, 61.2C4, has been shown to be directed to the β_1 chain (Gamble, J. R., and M. A. Vadas, unpublished observations). LM609 and 13C2, both anti-$\alpha_v\beta_3$ antibodies, were kindly provided by Dr. David Cheresh, Scripps, La Jolla, CA and Dr. Michael Horton, Department of Haematology, St. Bartholomew's Hospital, London, respectively.

Analysis by Flow Cytometry

EC were plated on collagen gels either in the presence or absence of PMA. 24 h later, cells either as tubes or as a monolayer were extracted by treatment of the gels for 30 min in 2 mg/ml collagenase at 37°C. Cells were then trypsin-treated for 5 min to obtain single cell suspensions. Cells were stained with the appropriate antibodies for 30 min at 37°C followed by a rabbit anti-mouse-FITC antibody for 30 min at 4°C. Cells were washed three times in PBS and diluted in fixative (2% glucose, 5 mM sodium azide, 1% formaldehyde) before analysis on an Epics Profile Analyzer. Ten thousand cells were analyzed.

Microscopy

At 24 h after stimulation with PMA or PMA and RMAC11, culture medium was removed from the culture wells and replaced with 2% paraformaldehyde, 2.5% glutaraldehyde in sterile PBS (pH 7.4). Cultures were fixed in this solution for 12 h at room temperature (20°C). After 12 h, fixative was washed out with PBS, at least 10 changes every 10 min, and the cultures postfixed for an additional 12 h in 1% osmium tetroxide in PBS. The osmium tetroxide was washed from the cultures, at least 10 changes every 10 min. Cultures were then dehydrated for three 20-min periods in each of a graded series of alcohol (70, 80, 95, and 100% ethanol in twice distilled water), and then for 60 min in each of two 100% ethanol washes. Cultures were transferred to vials containing 100% acetone. After three changes of acetone, each over 1 h, cultures were infiltrated overnight with a 1:1 mixture of acetone and epon-araldite. The next day the acetone was allowed to evaporate off in a fume hood, cultures were placed in fresh epon-araldite for ~6 h, and finally transferred to a mould in a 70°C oven to polymerize overnight. All procedures were carried out at room temperature.

For light microscopic examination, sections were cut 1 μm thick with a dry glass knife using an LKB ultratome. The sections were mounted on glass slides and stained with 1% toluidine blue in 1% borax. Sections were examined with a Leitz Orthoplan microscope. When endothelial cells containing lumens were seen the block was trimmed for thin sectioning (EM). For EM, thin sections of silver interference color were cut with a Swiss diamond knife (Diatome Ltd., Fort Washington, PA), and picked up on clean uncoated 200-mesh copper grids. Sections were stained for 5 min with 2% uranyl acetate in 50% ethanol, and for 5 min with lead citrate. Micrographs were taken on a Philips 410 electron microscope at 80 Kv. Magnifications were determined by means of a carbon grating replica. At both the light microscope level and the electron microscope level, serial sections up to 30 each (1 μm thick or silver interference color) were taken to establish that the lumens were continuous through the endothelial cell.

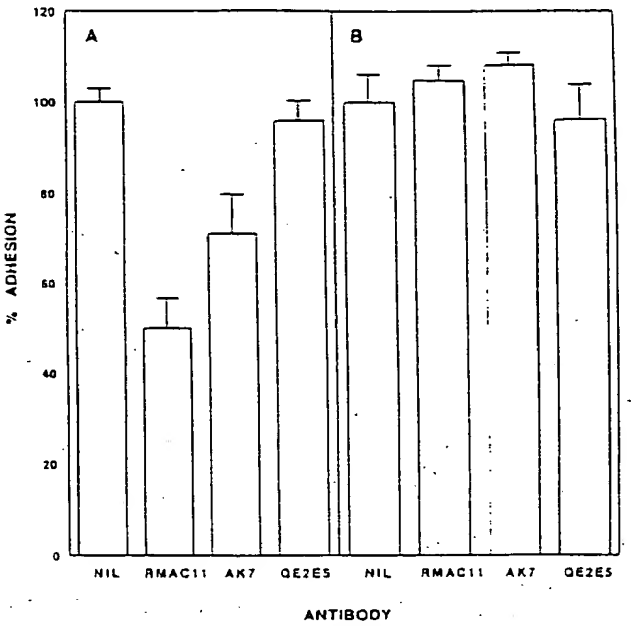

Figure 1. Anti-$\alpha_2\beta_1$ antibodies partially inhibit EC adhesion to collagen I and not to fibronectin. 5×10^3 EC in 50 μl of serum-free medium were added to microtiter wells which had previously been coated with either collagen I (*A*) or fibronectin (*B*). The antibodies, as indicated, were added at a final concentration of 30 μg/ml. The plates were incubated at 37°C for 2 h, washed, and the number of attached cells assessed by the methylene blue assay (as outlined under Proliferation Assay in Materials and Methods). The results were normalized where 100% adhesion is taken as the OD630 nm in wells without antibody. The results show the mean of triplicate wells for each group in one experiment representative of five similar experiments. $p < 0.001$ for groups with RMAC11 and AK7 compared to no antibody group on the collagen I matrix.

Statistics

Significance was determined by the ANOVA test for analysis of variance or by the unpaired *t* test.

Results

Inhibition of Endothelial Cell Adhesion by Anti-Integrin Antibodies

Adhesion of HUVEC to a collagen I matrix was inhibited, although only partially, by RMAC11 and AK7 (Fig. 1 *A*) but the antibodies had no effect on HUVEC attachment to fibronectin (Fig. 1 *B*) or gelatin (data not shown). Cells did not attach to laminin in the absence of FCS. The antibody QE2E5 which binds to the β_1 chain had no effect on the attachment of cells to any of the matrices tested. However, two other β_1 specific antibodies, P4C10 and 612C4, almost totally inhibited HUVEC adhesion to collagen (and fibronectin) (data not shown).

HUVEC Plated onto Collagen Gels Are Induced to Form Capillary Tubes

EC, when plated onto a gel of collagen are induced to form a capillary network within the collagen gel in the presence of PMA (Fig. 2, *B* and *C*) (Montesano et al., 1983; Mon-

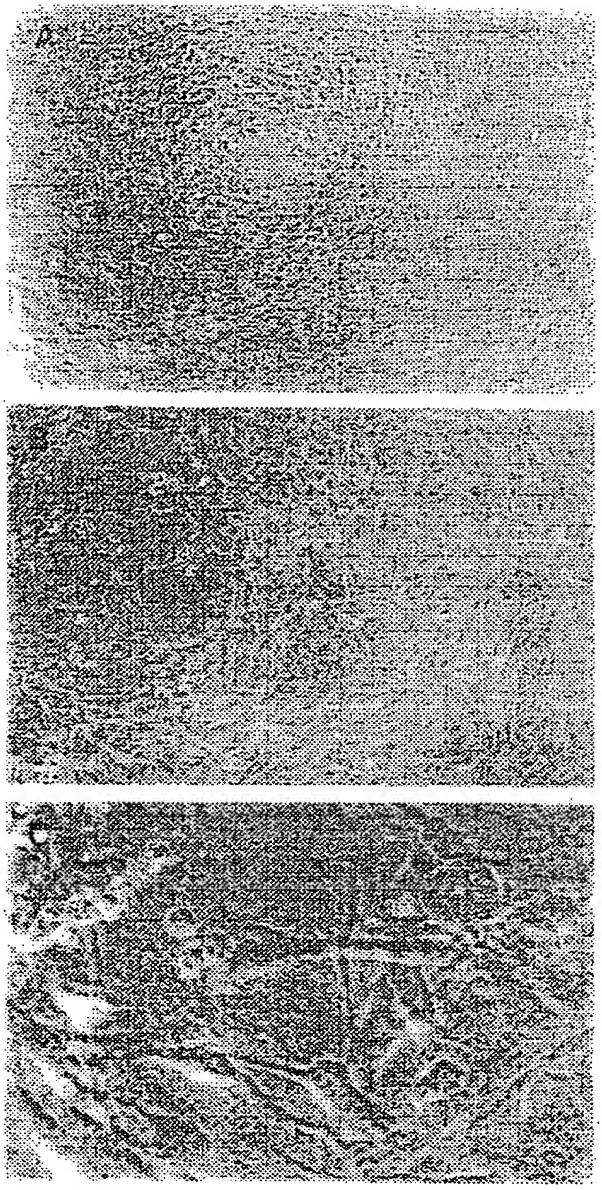

Figure 2. EC plated on collagen I gel in the presence of PMA are induced to form capillary tubes. 6.4×10^4 EC/well in 160 μl of HUVEC medium either in the absence (*A*) or presence (*B*) of 20 ng/ml PMA were plated onto a gel of collagen I formed in microtiter wells. The results were visualized 24 h after cell plating. *C* is a high power photograph of group *B*. Photographs show representative fields of one well of duplicate wells set up for each group. Magnification (*A*) ×60, (*B*) ×60, and (*C*) ×240.

Iesano and Orci, 1985). Realignment of the EC, cell invasion into the gel, and the beginning of cell elongation are evident ~8 h after plating of the cells onto the gel, and tube formation was clearly visible by 12 h. Very little, if any, tube formation occurs in collagen gels in the absence of PMA or with addition of dimethylsulphonic acid, used as a carrier for PMA; the cells are maintained as a monolayer on top of the gel and little invasion into the gel is seen (Fig. 2 *A*). Tube formation was highly dependent on the concentration of cells plated onto the collagen gel, no tubes being observed with less than $1\text{–}2 \times 10^5$ cells/well suggesting that cell–cell contact is important.

Analysis by EM of EC, 24 h after plating on collagen gels with the addition of PMA showed the presence of vacuole-like structures similar to those described by Folkman and Haudenschild (1980) (Fig. 3 *A*). A continuous membrane surrounded each vacuole which was either empty or filled with amorphous material. Fusion of these vacuoles with the plasma membrane was occasionally observed. Serial sectioning to >30 μm and visualization at the light microscopy level showed a continuous vacuole-like structure confirming that these were indeed lumina. At least 70% of all cells visualized showed vacuolization. Only the occasional lumen was formed from multiple cells.

Effect of Anti-Collagen Receptor Antibodies on Capillary Formation

EC were plated onto collagen gels in the presence of PMA with increasing concentrations of antibodies RMAC11, AK7, and QE2.E5. Capillary formation was assessed 24 h later. Fig. 4 *A* shows the capillary tube formation taking place with PMA alone. No change in the extent of tube formation was seen with the addition of QE2E5 (Fig. 4 *B*). However, a more extensive capillary network was seen in wells containing RMAC11. The tubes appeared longer and wider, and less monolayer was evident (Fig. 4 *C*). Similar results were obtained with AK7, P4C10, and 6I2C4 and with EC derived from neonatal foreskins (data not shown). The enhancement of tube formation with RMAC11 over PMA alone was clearly evident in the high power photographs (Fig. 5, *A–F*). Tube number, length, and width were quantified from high power photographs and results from four separate experiments were analyzed and pooled and are shown in Fig. 6. The anti-$\alpha_2\beta_1$ antibody RMAC11 clearly enhanced the length (*A*), width (*B*), and number (*C*) of tubes.

EM showed that in the presence of RMAC11, cells were seen in larger aggregates suggesting cell–cell adhesion was promoted (not shown). Furthermore, larger lumina were evident compared to PMA group only, the majority of which appeared to be formed from multiple cells as shown in Fig. 3 *B*. Intercellular junctions are clearly visible at the EM level and by analysis of these junctions the lumen shown in Fig. 3 *B* is formed from five EC. Analysis of thin sections (silver interface color) taken through gels showed that with PMA 73 ± 5.7% (mean ± SEM) of lumina were formed from single cells (i.e., intracellular lumen, Fig. 3 *A*). The remaining lumina were formed from two or three cells. In contrast, in the presence of RMAC11, 83 ± 7.4% of lumina were formed from three or more cells (values were obtained from four separate experiments with 50 lumen examined in each group in each experiment). Thus the increase in capillary thickness appears to be due to the conversion from intracellular to multicellular lumina.

Maximum levels of tube formation were seen with 30 μg/ml RMAC11 (Table I) but some enhancement over the level seen with PMA alone was normally observed with 3 μg/ml RMAC11. Tube length, width, and number were assessed visually through different focal plains of the gel and assigned values from + to +++++. Tube length, width, and number were also measured from high power photographs.

Figure 3. Formation of lumen-containing capillaries in collagen gels. EC in the presence of 20 ng/ml PMA (*A*) or PMA and 30 μg/ml RMAC11 (*B*) were plated onto a collagen gel. 24 h later the cells were fixed, embedded in epon-araldite, and sectioned for EM. Magnification (*A*) ×7490 and (*B*) ×4000. *C*, collagen; *L*, lumen. Numbers *1–5* relate to cell junctions.

As is seen in Table I, the two assessments for capillary formation showed a good correlation. Analysis of EC by flow cytometry showed that 30 μg/ml of RMAC11 fully saturated the $\alpha_2\beta_1$ receptor binding sites (data not shown). With AK7, an enhancement of tube formation was also seen over the concentration range of 3–30 μg/ml. However, the extent of enhancement was never as great as that seen with RMAC11.

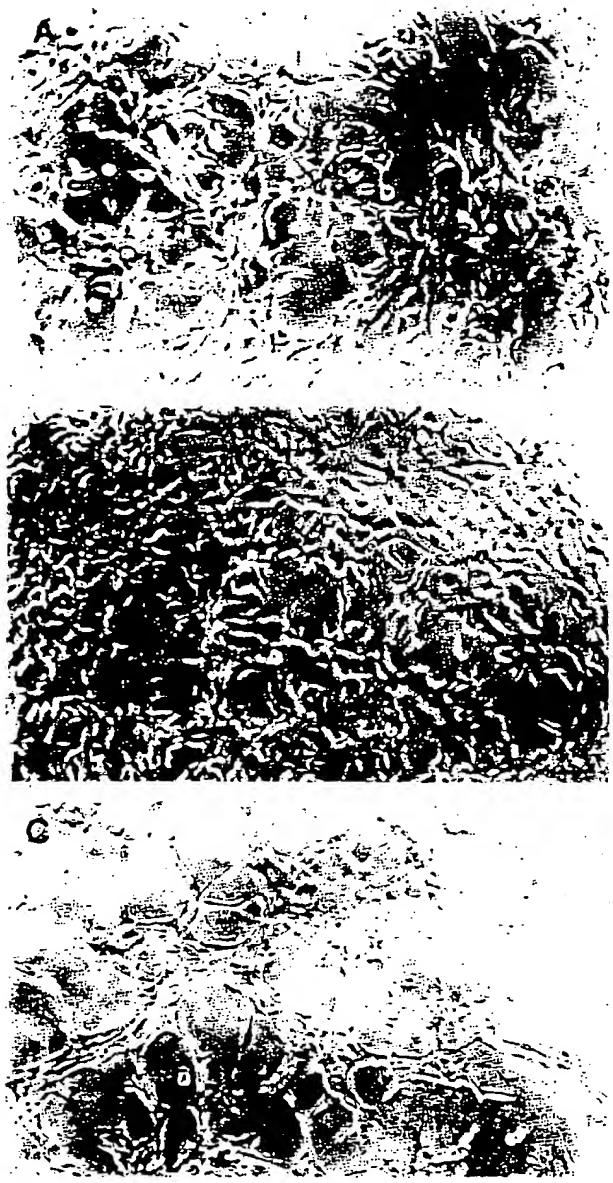

Figure 4: Anti-$\alpha_2\beta_1$ antibodies enhance capillary tube formation in collagen gels. EC were plated onto collagen gel in the presence of 20 ng/ml PMA. To group *B*, QE2E5 was added at plating and to group *C*, RMAC11 both at a final concentration of 30 μg/ml. Groups were assessed for tube formation 24 h later. Each photograph shows a representative field taken from one well of duplicate wells set up for each group. Similar results have been obtained more than 20 times using different EC lines. Magnification ×60.

The effect observed by RMAC11 and AK7 is unlikely to be due to nonspecific effects via Fc receptor mediated events since Fab_2 fragments of RMAC11 exhibit a similar enhancement of tube formation as the whole Ig (data not shown). Furthermore, since Fab' fragments of RMAC11 were also able to enhance tube formation (data not shown), cross-linking of the antigen is also not likely to be responsible for the enhancement.

Pretreatment of the HUVEC with RMAC11 or AK7 for 15 min either at room temperature or 37°C followed by washing to remove unbound antibody, did not result in enhanced tube formation (data not shown).

The enhancement of tube formation was dependent on the addition of RMAC11 or AK7 within the first 2 h of cell plating. If the antibodies were added after this, no enhancement of tube formation was evident (data not shown).

Angiogenesis can also be induced in collagen gels in the presence of PMA by resuspending the cells within the gels rather than layering them on top of the gel (Madri et al., 1988). Pretreatment of EC with PMA and RMAC11 before resuspension within the gel led to enhancement of tube formation over that seen with PMA alone (data not shown). Thus, the anti-$\alpha_2\beta_1$ antibodies were able to enhance tube formation whether the EC contact collagen in a polarized fashion or whether the cells are totally surrounded by the collagen matrix.

Anti-$\alpha_2\beta_1$ Antibodies Induce Capillary Tube Formation in Rigid Gels

The ability of RMAC11 and AK7 to enhance capillary tube formation was most strikingly evident when EC were plated onto rigid collagen gels formed after the collagen was gelled for 1 h at 37°C. Even in the presence of PMA, very little, if any, tube formation is seen with these rigid gels and the cells maintain a flat cobblestone appearance on top of the gel. However, the addition of RMAC11 (or AK7) with PMA overcomes the inhibitory effect caused by the rigidity of the gel; the cells invade into the gel and capillary tubes and an anastomosing network are visible (Fig. 7, *A–D*) although not to the same extent as is normally seen on less rigid gels. Measurements of tube numbers from random high power fields from five separate experiments on rigid gels each using a different HUVEC line were made. The mean tube number with PMA alone was 1.0 ± 0.4 (mean ±SEM) and with RMAC11 was 39.2 ± 4.08 ($p < 0.0005$) clearly demonstrating the promotional activity of RMAC11. One possibility for the antibodies enhancing the ability of the EC to breakdown and invade the gel is by an increase in the synthesis of matrix-degrading enzymes such as collagenase. However, no change in the total level of active collagenase was observed either in normal gels or in rigid gels. The level of detection of collagenase by the assay used (see Materials and Methods) was 10 ng/ml. In a representative experiment, the level of collagenase induced on collagen gels in the presence of 20 ng/ml PMA was 112 ± 5.9 and with PMA and RMAC11 120 ± 2.0 (mean ± SEM, $n = 3$).

Effect of Anti-$\alpha_2\beta_1$ Antibodies on EC Morphology

As was shown in Fig. 1, the addition of RMAC11 and AK7 to HUVEC cultured on 2-D substrates of collagen, but not on gelatin or fibronectin, resulted in a decrease in the number of cells attached when measured 2 h after plating. No differences were seen in the number of cells attached when measured at 4, 6, or 24 h after plating. On collagen gels, in the presence of QE2E5, the cells had become flattened and were beginning to adopt their characteristic cobblestone morphology (Fig. 8 *A*) when viewed 2 h after plating. In the presence of RMAC11 (or AK7), cells remained rounded (Fig. 8 *B*) for ~2–3 h after which time they flattened and no differences from control wells were seen.

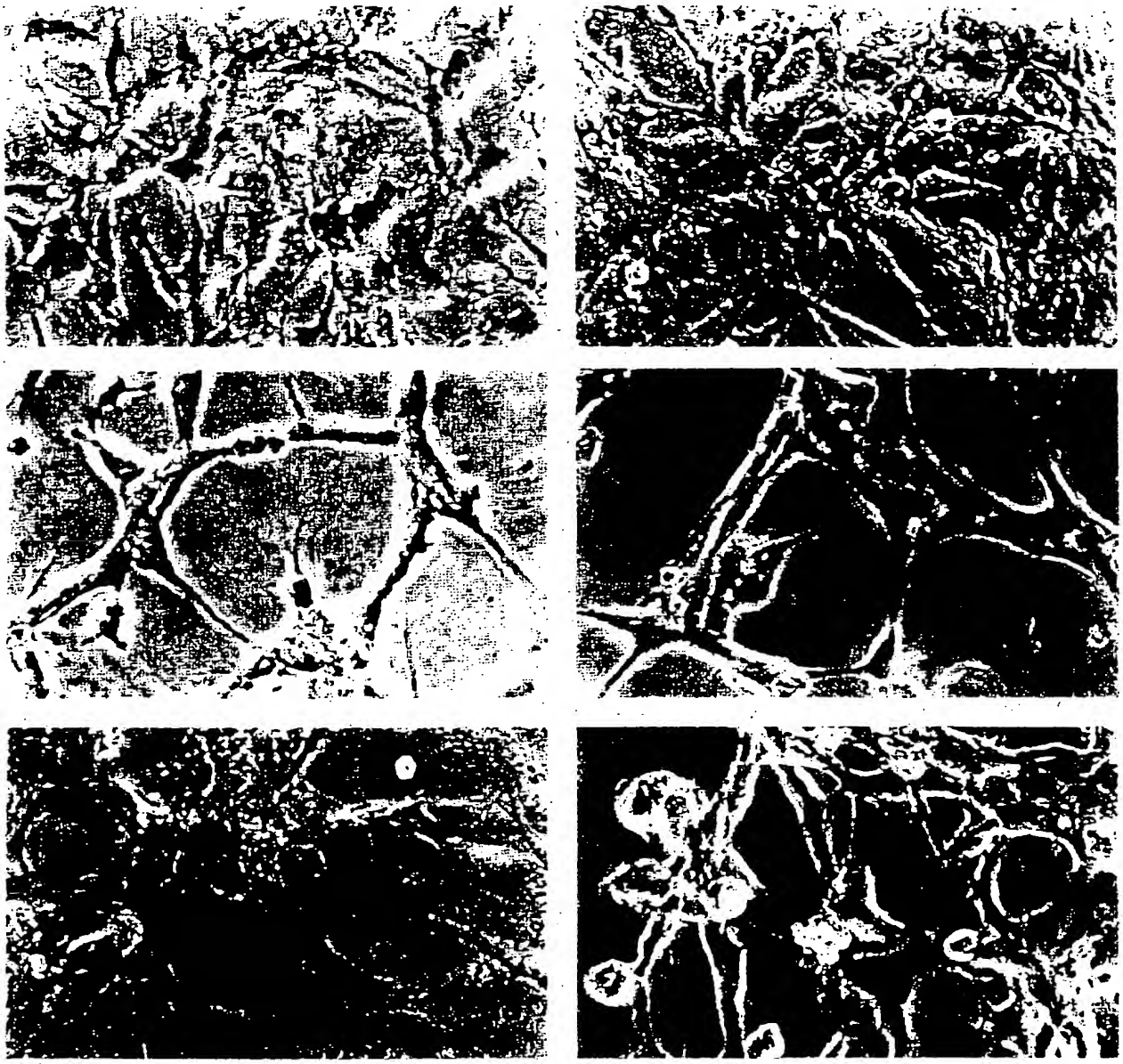

Figure 5. High power photographs of capillary tubes formed on collagen gels in the presence of anti-integrin antibodies. EC were plated onto collagen gel in microtiter wells with 20 ng/ml PMA. *A* and *B* show one EC line, *C* and *D* another line, and *E* and *F* a third line. To one group (*A*, *C*, and *E*), 30 μg/ml of QE2E5 was added and to the other group (*B*, *D*, and *F*), 30 μg/ml RMAC11. All wells were incubated for 24 h. Each photograph shows a representative field taken from one well of duplicate wells set up for each group. Magnification ×264.

Anti-$\alpha_1\beta_1$ Antibodies Inhibit Endothelial Cell Proliferation

Alterations in cell shape can have profound effects on proliferation, and EC proliferation is essential for tube extension although not required for initial sprouting (Sholley et al., 1984; Folkman, 1982). The proliferative response of HUVEC in the presence of RMAC11 and AK7 was therefore measured. A decrease in EC proliferation in the presence of RMAC11 or AK7 was seen when the cells were plated on a 2-D matrix of collagen. This was clearly seen with RMAC11 when the assay was performed in the presence of either 20 (data not shown) or 2% FCS (Fig. 9). AK7, induced a significant level of inhibition only when 2% FCS was used in the assays and this level of inhibition was less than that induced by RMAC11. The results in Fig. 9 have been normalized to the no antibody control. When the actual cell numbers were counted in wells containing 30 μg/ml QE2E5, AK7, or RMAC11 the increase in cell numbers was 2.6, 2.0, and 1.4-fold, respectively. These results clearly show that the ability of antibodies to inhibit proliferation appears to correlate with enhancement of capillary formation. No inhibition

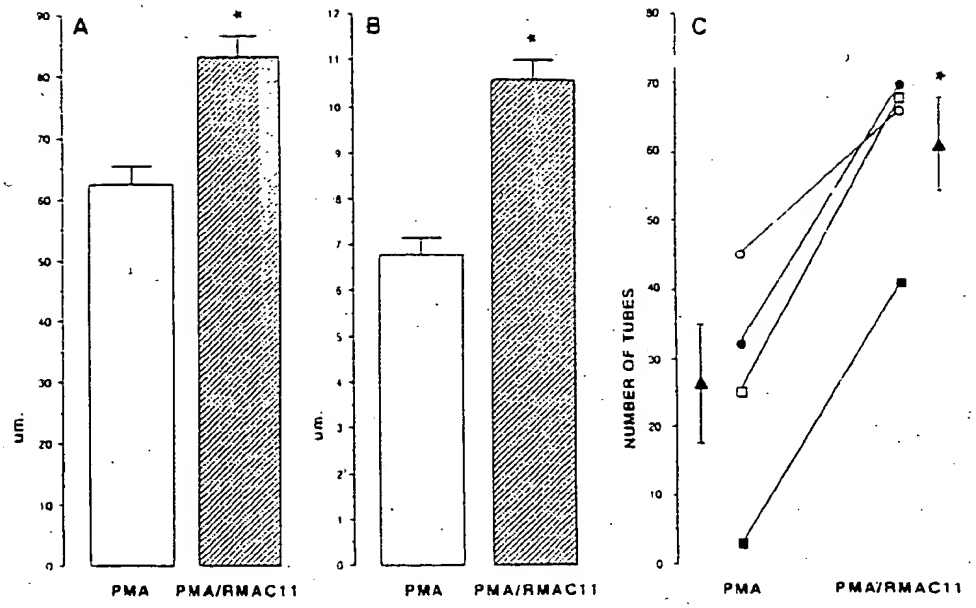

Figure 6. Effect of RMAC11 on tube length (μm *A*), width (μm *B*), and number (*C*) per high power field. EC were plated onto collagen gels in the presence of 20 ng/ml PMA. 30 μg/ml of RMAC11 was added to half the wells. Each group contained duplicate wells. 24 h later the wells were photographed (magnification ×264), random fields being taken for each well. From these photographs, the number, length, and width of tubes were calculated. The pooled results from four separate experiments using four different EC lines are shown for tube length and width (mean ± SEM). Each experiment showed a similar and significant increase with RMAC11. In *C*, the tube numbers for each experiment are shown together with the mean ± SEM (Δ) for the four experiments. * $p < 0.005$ compared to PMA alone.

of proliferation was seen with either antibody when the cells were plated onto fibronectin or gelatin (data not shown).

PMA Does Not Alter Expression of $\alpha_2\beta_1$ on Endothelial Cells

One possibility for the effect of anti-$\alpha_2\beta_1$ antibodies on capillary tube formation in collagen gels is that PMA may alter the surface expression of the $\alpha_2\beta_1$ molecule. To investigate this, HUVEC were plated onto collagen-coated microtiter wells at numbers to give either a confluent monolayer (that is nonproliferating) or a semiconfluent monolayer (that is to give a proliferating population) either in the presence or absence of 20 ng/ml PMA. Huvec were also plated onto collagen gels in the presence or absence of PMA. 24 h later, the cells were detached from the microtiter wells with trypsin or extracted from the gels with collagenase. The cells were stained with saturating concentrations of RMAC11 followed by a fluorescein-conjugated sheep anti-mouse Fab_2 antibody. There was no difference in the mean channel fluorescence between confluent and semiconfluent cells either in the presence or absence of PMA, or between tube forming or nonforming cells suggesting that PMA within this time period did not alter the level of surface expression of $\alpha_2\beta_1$ on HUVEC.

Table I. Antibody RMAC11 Enhances Capillary Tube Formation in a Dose-dependent Manner

Concentration of RMAC11 (μg/ml)	Measurement of capillary tubes			Capillary tube formation
	Number/field	*Length (μm)*	*Width (μm)*	(+ to + + + +)
0	7	43.9 ± 2.4	6.1 ± 0.5	+
0.3	13	46.5 ± 3.7	7.6 ± 0.9	+ +
3	33	52.6 ± 5.4	11.0 ± 1.6	+ + +
10	50	81.8 ± 8.0	12.5 ± 0.8	+ + +
20	87	70.0 ± 4.5	11.7 ± 0.9	+ + + +
30	91	75.4 ± 7.5	11.0 ± 0.7	+ + + +

EC were plated onto a collagen gel in the presence of 20 ng/ml PMA together with varying concentrations of RMAC11. Measurement of the number, length, and width of tubes was made from high power photographs taken at random from each well, the measurements for length and width are given as mean ±SEM. The extent of capillary tube formation was also assessed and is given as + to + + + + based on the length, width, and number of capillary tubes. The results are shown for one experiment which was similar to three performed, each with a different EC line.

Anti-VnR Antibodies Enhance Capillary Formation in Fibrin Gels

Capillary tube formation also takes place in fibrin gels in the presence of PMA (Montesano et al., 1987). Adhesion of EC to fibrinogen is mediated through another integrin complex, the $\alpha_v\beta_3$ (or vitronectin receptor, VnR). To determine whether tube formation in fibrin gels is enhanced in the presence of antibodies which limit cell–matrix interactions, we used two antibodies (LM609 or 13C2) which are directed to the $\alpha_v\beta_3$ complex and known to inhibit EC-fibrinogen adhesion (Cheresh and Spiro, 1987 and unpublished data). Fig. 10 shows that $\alpha_v\beta_3$ is also involved in the adhesion of HUVEC to fibrin, since anti-$\alpha_v\beta_3$ antibody (LM609) partially inhibits attachment of HUVEC to fibrin-coated plastic (*A*) but not to collagen (*B*). Similar results were obtained with 13C2 (data not shown). As seen in Fig. 11, tube formation is enhanced in the presence of LM609 and similarly for 13C2 (data not shown) although the level of tube formation was never as large as that seen in collagen with either RMAC11 or AK7. Functional effects with LM609 were observed with concentrations as low as 3 μg/ml. In the initial 1–2 h on fibrin gels, cells incubated with anti-$\alpha_v\beta_3$ antibody remained rounded and failed to flatten compared to cells

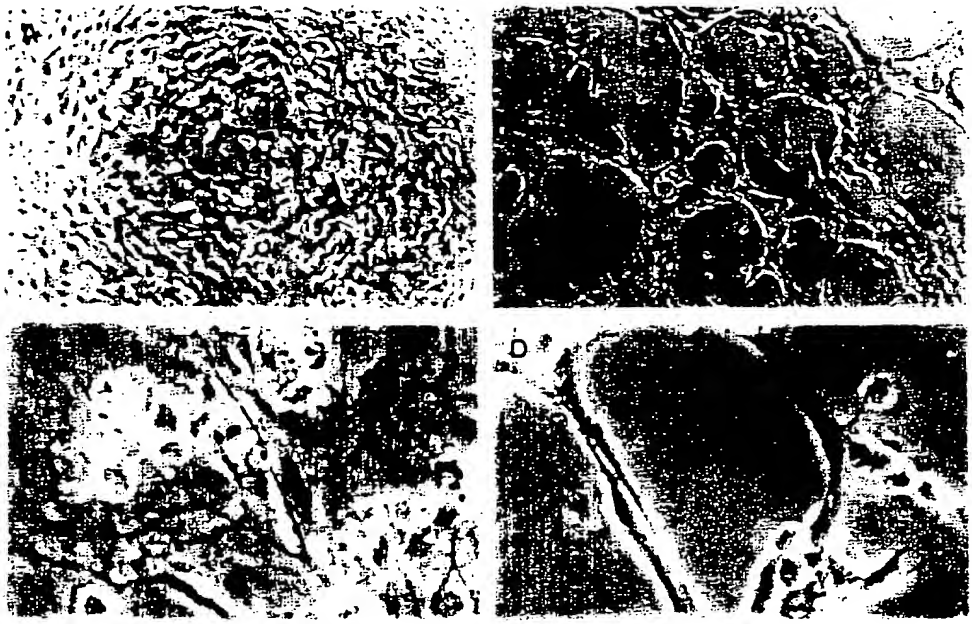

Figure 7. Anti-integrin antibodies promote tube formation in rigid collagen gels. EC were plated onto collagen which had been allowed to gel for 1 h at 37°C giving a more rigid gel than that obtained after our normal gelling time of 10–20 min. *C* and *D* are high powered views of *A* and *B*, respectively. 20 ng/ml of PMA was added to both groups, 30 μg/ml of RMAC11 was added to *B*. Tube formation was assessed after 24 h. *A* and *B* magnification ×80; *C* and *D* magnification ×310. Each is a representative field of one well of duplicate wells set up for each group. The experiment has been performed at least six times using different EC lines and using either RMAC11 or AK7 with similar results being obtained.

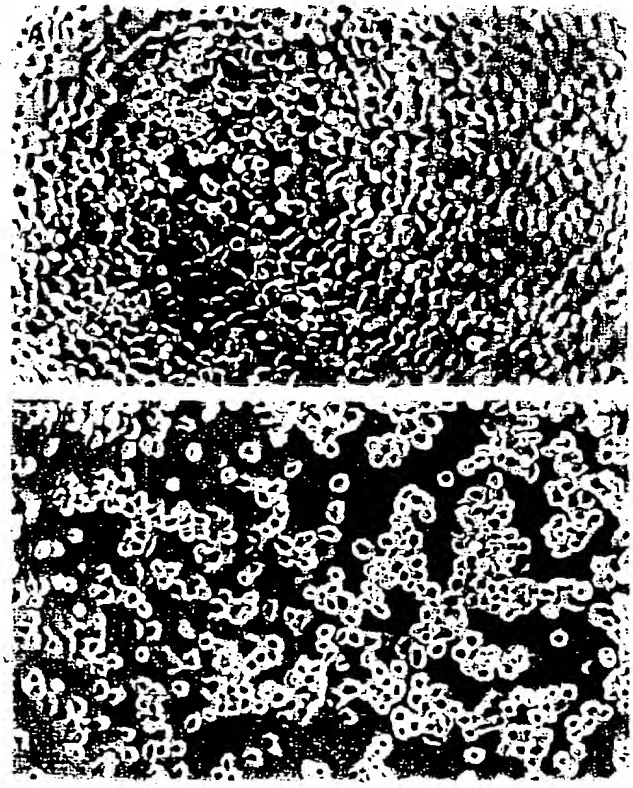

Figure 8. Anti-integrin antibodies maintain EC in a rounded morphology and prevent cell spreading. EC were plated onto collagen I gels with 20 ng/ml PMA either in the presence of 30 μg/ml QE2E5 (*A*) or 30 μg/ml RMAC11 (*B*). The cells were viewed at 1, 2, 3, 4, and 6 h after plating. These photographs were taken at 2 h after plating (magnification ×110). Each shows a representative field of one well from duplicate wells set up for each group. The experiment has been performed on at least four separate EC lines with similar results.

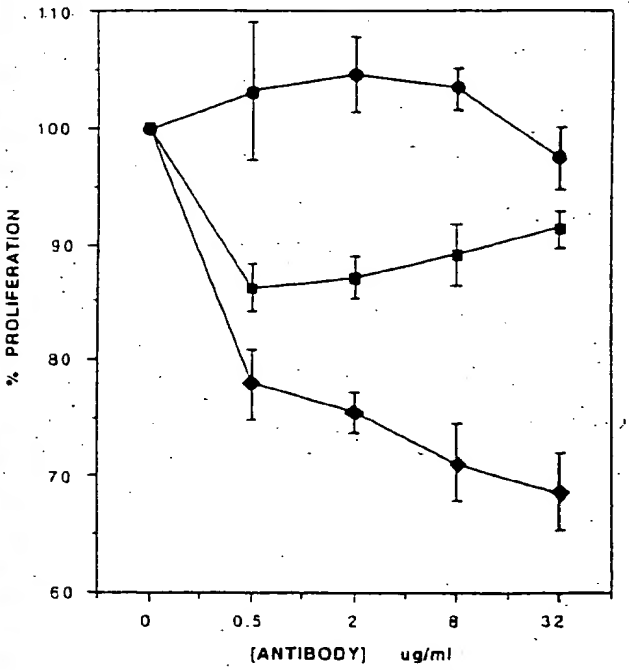

Figure 9. Anti-$\alpha_1\beta_1$ antibodies inhibit EC proliferation. EC were plated onto collagen I–coated microtitre wells at 5×10^3 cells/well in HUVEC medium containing 2% FCS either with QE2E5 (●), RMAC11 (♦), or AK7 (■) at various concentrations. The cells were incubated for 3 d at 37°C, washed, fixed, stained with methylene blue, and the dye solubilized with ethanol. Absorbance was read at 630 nm. The OD630 of wells with no antibody was taken to give 100% proliferation. All other groups were normalized to this. The results show the mean ± SEM of four experiments where each point in each experiment was performed with six replicates. Groups containing RMAC11 and AK7 were significantly different ($p < 0.0001$) from groups containing QE2E5 (ANOVA test for significance).

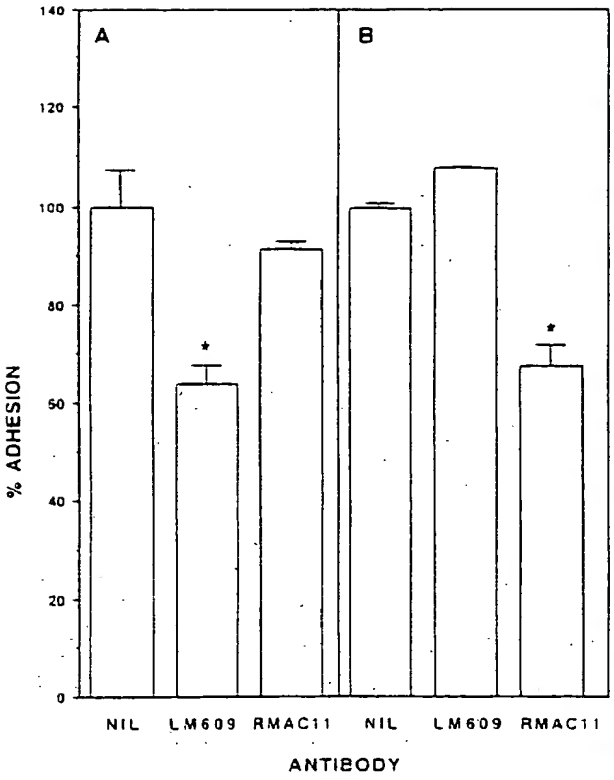

Figure 10. Anti-$\alpha_v\beta_3$ antibody partially inhibits EC adhesion to fibrin (*A*) but not to collagen (*B*). Fibrin-coated microtiter wells were formed by thrombin cleavage of fibrinogen followed by two washes in medium containing FCS. Antibodies as indicated were added at a final concentration of 30 μg/ml to either fibrin (*A*) or collagen (*B*)-coated wells. The plates were incubated at 37°C for 1 h, washed, and the number of attached cells assayed as given for Fig. 1. The results show the mean of triplicate wells for each group of one experiment representative of three experiments. $p < 0.01$ compared to no antibody group on either matrix.

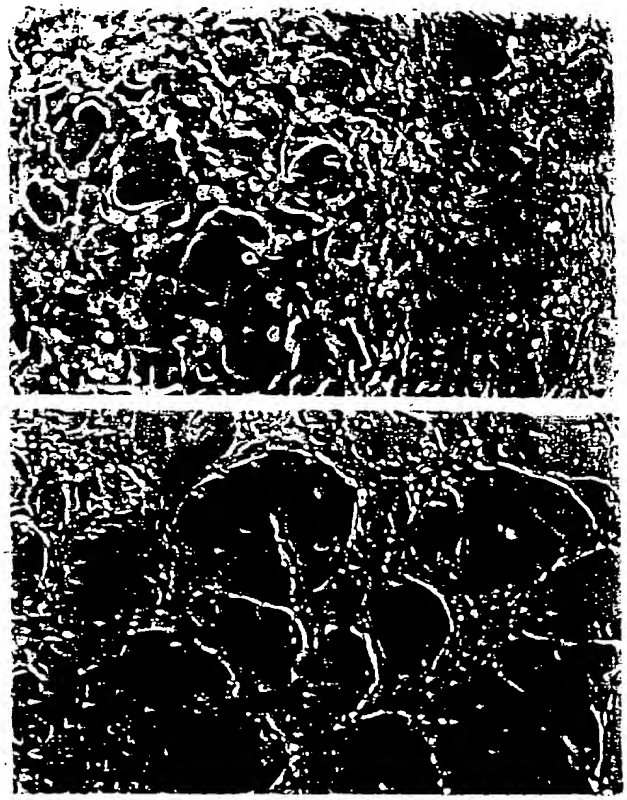

Figure 11. Anti-$\alpha_v\beta_3$ antibody promotes capillary formation in fibrin gels. 6.4×10^4 EC/well were plated onto fibrin gels in the presence of 20 ng/ml PMA. The anti-$\alpha_v\beta_3$ antibody LM609 at a final concentration of 30 μg/ml was added to group *B*. Cells were incubated overnight. A representative field of one well of duplicate wells in each group is shown (magnification ×110). The experiment has been performed at least five times using a different EC line for each experiment, all giving similar results.

without antibody. Sections analyzed by light microscopy showed details similar to that observed in collagen gels. With PMA alone, small lumen formed by intracellular vacuolization were seen. In the presence of LM609 or 13C2 there was extensive cell-cell interactions and lumina were formed between cells. Fig. 12 shows that in the presence of anti-$\alpha_v\beta_3$ antibody, the length, width, and the number of tubes were increased over that seen with PMA alone. Analysis of thin sections showed that with PMA alone, the majority of lumen were formed from single intracellular lumen although lumina formed from two cells were occasionally seen. In the presence of anti-$\alpha_v\beta_3$ antibody, the majority of lumina (>70%) were formed from three cells with some lumina formed from four or five cells. The enhancement of tube formation seen with $\alpha_2\beta_1$ antibodies and with anti-$\alpha_v\beta_3$ antibodies was specific for the matrix used; $\alpha_2\beta_1$ antibodies had no effect in fibrin gels and $\alpha_v\beta_3$ antibody had no effect in collagen gels (data not shown).

Discussion

The central finding of this study is that anti-integrin antibodies are able to enhance the formation of capillary tubes in vitro. Functional monoclonal antibodies directed to the major integrin receptors for the tube-permissive matrices of collagen and fibrin enhanced capillary tube formation increasing the number, length, as well as width. Ingber and Folkman (Ingber and Folkman, 1989*a*,*b*; Ingber, 1990, 1991*a*,*b*) propose that changes in adhesivity (e.g., by altering the density of ECM molecules), and therefore in the ability of the matrix to resist cell tension, may result in alteration in cell function such as proliferation and differentiation. Thus the mechanical forces between cells and their environment will govern their behavior. Our results showing that anti-integrin antibodies, which block adhesion, enhance tube formation suggest that angiogenesis may also be regulated by the adhesivity of EC for the matrix. The balance between cell and matrix adhesivity will clearly be important in determining the function of endothelial cells.

In the presence of antibody (anti-$\alpha_2\beta_1$ and anti-$\alpha_v\beta_3$), the first change observed was that the EC remained rounded, became less adhesive, and failed to spread when plated onto gels or 2-D matrices rather than adopting their normal cobblestone, flattened morphology. It is known that alteration in cell shape can have profound effects on the function of many

Glowacki, J., E. Trepman, and J. Folkman. 1983. Cell shape and phenotypic expression in chondrocytes. *Proc. Soc. Exp. Biol. Med.* 172:93–98.

Gospodarowicz, D., G. Greenburg, and C. R. Birdwell. 1978. Determination of cellular shape by the extracellular matrix and its correlation with the control of cellular growth. *Cancer Res.* 38:4155–4171.

Greenburg, G., and E. Hay. 1982. Epithelia suspended in collagen gels can lose polarity and characteristics of migrating mesenchymal cells. *J. Cell Biol.* 95:333–339.

Harlow, E., and D. Lane. 1988. Antibodies: A Laboratory Manual. Cold Spring Harbor Laboratory, Cold Spring Harbor, NY. 726 pp.

Hemler, M. E., M. J. Elices, B. M. C. Chan, B. Zeuer, N. Matsuura, and Y. Takada. 1990. Multiple ligand binding functions for VLA-2 ($\alpha^2\beta_1$) and VLA-3 ($\alpha^3\beta_1$) in the integrin family. *Cell Differ. Dev.* 32:229–238.

Hynes, R. O. 1987. Integrins: a family of cell surface receptors. *Cell.* 48:549–554.

Ingber, D. E. 1990. Fibronectin controls capillary endothelial cell growth by modulating cell shape. *Proc. Natl. Acad. Sci. USA.* 87:3579–3583.

Ingber, D. 1991*a*. Extracellular matrix and cell shape: potential control points for inhibition of angiogenesis. *J. Biol. Chem.* 47:236–241.

Ingber, D. E. 1991*b*. Integrins as mechanochemical transducers. *Curr. Opin. Cell Biol.* 3:841–848.

Ingber, D., and J. Folkman. 1988. Inhibition of angiogenesis through modulation of collagen metabolism. *Lab. Invest.* 59:44–51.

Ingber, D. E., and J. Folkman. 1989*a*. Mechanochemical switching between growth and differentiation during fibroblast growth factor-stimulated angiogenesis in vitro: role of extracellular matrix. *J. Cell Biol.* 109:317–330.

Ingber, D. E., and J. Folkman. 1989*b*. How does extracellular matrix control capillary morphogenesis. *Cell.* 58:803–805.

Ingber, D. E., J. A. Madri, and J. Folkman. 1987. Endothelial growth factors and extracellular matrix regulate DNA synthesis through modulation of cell and nuclear expansion. *In Vitro Cell. & Dev. Biol.* 23:387–394.

Iruela-Arispe, M. L., P. Hasselaar, H. Sage. 1991*c*. Differential expression of extracellular proteins is correlated with angiogenesis *in vitro*. *Lab. Invest.* 64:174–186.

Kornberg, L. J., H. S. Earp, C. E. Turner, C. Prockop, and R. L. Juliano. 1991. Signal transduction by integrins: increased protein tyrosine phosphorylation caused by clustering of β_1 integrins. *Proc. Natl. Acad. Sci. USA.* 88:8392–8396.

Kramer, R. H., Y.-F. Cheng, and R. Clyman. 1990. Human microvascular endothelial cells use β_1 and β_3 integrin receptor complexes to attach to laminin. *J. Cell Biol.* 111:1233–1243.

Kubota, Y., H. K. Kleinman, G. R. Martin, and T. J. Lawley. 1988. Role of laminin and basement membrane in the morphological differentiation of human endothelial cells into capillary-like structures. *J. Cell Biol.* 107:1589–1598.

Languino, L. R., K. R. Gehlsen, W. G. Carter, E. Engvall, and E. Ruoslahti. 1989. Endothelial cells use alpha2/beta1 integrins as laminin receptors. *J. Cell Biol.* 109:2455–2462.

Madri, J., B. Pratt, and A. Tucker. 1988. Phenotypic modulation of endothelial cells by transforming growth factor-β depends upon the composition and organization of the extracellular matrix. *J. Cell Biol.* 106:1375–1384.

Mallein-Gerin, F., R. Garrone, and M. van der Rest. 1991. Proteoglycan and collagen synthesis are correlated with actin organization in differentiating chondrocytes. *Eur. J. Cell. Biol.* 56:364–373.

Marks, R. M., M. Czerniecki, and R. Penny. 1985. Human dermal microvascular endothelial cells: an improved method for tissue culture and a description of some singular properties in culture. *In Vitro Cell. & Dev. Biol.* 21: 627–635.

Mazurov, A. V., D. V. Vinogradou, N. V. Kabaeva, A. N. Antonova, Y. A. Romanov, T. N. Vasik, A. S. Antonov, and V. N. Smirnow. 1991. A monoclonal antibody VM64, reacts with a 130KDa glycoprotein common to platelets and endothelial cells. Heterogeneity in antibody binding to human aortic endothelial cells. *Thromb. Haemostasis.* 66:494–499.

Mignatti, P., R Mazzieri, and D. B. Rifkin. 1991. Expression of the urokinase receptor in vascular endothelial cells is stimulated by basic fibroblast growth factor. *J. Cell Biol.* 113:1193–1201.

Montesano, R., P. Mouron, and L. Orci. 1985. Vascular outgrowth from tissue explants embedded in fibrin or collagen gels: a simple in vitro model of angiogenesis. *Cell Biol. Int. Rep.* 9:869–875.

Montesano, R., and L. Orci. 1985. Tumor-promoting phorbol esters induce angiogenesis in vitro. *Cell.* 42:469–477.

Montesano, R., L. Orci, and P. Vassalli. 1983. In vitro rapid organization of endothelial cells into capillary-like networks is promoted by collagen matrices. *J. Cell Biol.* 97:1648–1652.

Montesano, R., M. S. Pepper, J.-D. Vassalli, and L. Orci. 1987. Phorbol ester induces cultured endothelial cells to invade a fibrin matrix in the presence of fibrinolytic inhibitors. *J. Cell. Physiol.* 132:509–516.

Nethery, A., J. G. Lyons, and R. L. O'Grady. 1986. A spectrophotometric collagenase assay. *Anal. Biochem.* 159:390–395.

O'Connel, P. J., R. Faull, G. R. Russ, and A. J. D'Apice. 1991. VLA-2 is a collagen receptor on endothelial cells. *Immunol. Cell Biol.* 69:103–110.

Oliver, M. H., N. K. Harrison, J. E. Bishop, P. J. Cole, and G. J. Laurent. 1989. A rapid and convenient assay for counting cells cultured in microwell plates: application for assessment of growth factors. *J. Cell. Sci.* 92: 513–518.

Ruoslahti, E., and M. D. Pierschbacher. 1987. New perspectives in cell adhesion: RGD and integrins. *Science (Wash. DC).* 238:491–497.

Sholley, M. M., G. P. Ferguson, H. R. Seibel, J. L. Montour, and J. D. Wilson. 1984. Mechanisms of neovascularization. Vascular sprouting can occur without proliferation of endothelial cells. *Lab. Invest.* 51:624–634.

Sołowska, J., J.-L. Guan, E. E. Marcantonio, J. E. Trevithick, C. A. Buck, and R. O. Hynes. 1989. Expression of a normal and mutant avian integrin subunits in rodent cells. *J. Cell. Biol.* 109:853–861.

Unemori, E. N., and Z. Werb. 1986. Reorganization of polymerized actin: a possible trigger for induction of procollagenase in fibroblasts cultured in and on collagen gels. *J. Cell Biol.* 103:1021–1031.

Wall, R. T., L. A. Harker, L. J. Quadracci, and G. E. Striker. 1978. Factors influencing endothelial cell proliferation in vitro. *J. Cell. Physiol.* 96:203–213.

Watson, P. A. 1991. Function follows form: generation of intracellular signals by cell deformation. *FASEB (Fed. Am. Soc. Exp. Biol.) J.* 5:2013–2019.

Werb, Z., R. M. Hembry, G. Murphy, and J. Aggeler. 1986. Commitment to expression of the metalloendopeptidases, collagenase, and stromelysin: relationship of inducing events to changes in cytoskeletal architecture. *J. Cell Biol.* 102:697–702.

Werb, Z., P. H. Tremble, O. Behrendtsen, E. Crowley, and C. H. Damsky. 1989. Signal transduction through the fibronectin receptor induces collagenase and stromelysin gene expression. *J. Cell Biol.* 109:877–889.

No capillary tube formation is induced on collagen gels that are too rigid even in the presence of PMA. The cells form a confluent monolayer and little or no invasion into the matrix takes place suggesting that EC differentiation was inhibited by the rigid ECM. However, anti-$\alpha_2\beta_1$ antibody on rigid gels in the presence of PMA did induce EC invasion into the gel and subsequent tube formation. The cells in the presence of RMAC11 were more rounded than with control antibody and failed to spread and flatten. A consequence of changes in cell shape, adhesion, and signaling may be an alteration in the level of matrix degrading enzymes such as collagenase. However, we observed no change in the total collagenase produced by the EC in the presence of RMAC11. One possibility to explain these results is that there is an alteration in the site of collagenase release rather than an alteration in the overall level of production. Enzyme redistribution has been demonstrated for urokinase plasminogen activator (uPA) after anti-fibronectin antibody binding to rabbit fibroblasts (Werb et al., 1989). Thus, as a consequence of antibody-integrin binding (and perhaps integrin redistribution and change in cell shape) collagenase may be redirected to specific localized areas resulting in enhanced cell motility and gel invasion. In addition, since activation of collagenase can occur via cleavage by uPA measurement of uPA or its receptor may indicate altered enzyme activity (Mignatti et al., 1991).

Another possibility to explain the enhancement of tube formation by the antibodies is that the binding of the anti-integrin antibodies to their antigen may simply limit the number of receptors available for cell–matrix interactions thereby resulting in enhanced motility of the cell within the matrix. Indeed, an alteration in the adhesivity of EC for different matrices via changes in the level of expression of the integrins, $\alpha_1\beta_1$ and $\alpha_2\beta_1$, can be achieved by cytokines such as tumor necrosis factor and interferon-γ (Defilippi et al., 1991*a*,*b*). The anti-integrin antibodies may also limit the number of focal contacts which can form an important function mediated through the β subunit (Solowska et al., 1989), reducing adhesion, and enhancing the lateral mobility of the integrins within the cell membrane. This lateral mobility of integrins is known to be important for cell movement (Duband et al., 1988). Alternately, the limitation in the available number of functional $\alpha_2\beta_1$ or $\alpha_v\beta_3$ molecules may redirect the cell to use other integrin molecules. It is interesting to note that RMAC11 or AK7 cannot totally inhibit HUVEC binding to collagen. Anti-β_1 antibodies further inhibit this adhesion suggesting that other β_1 integrins are involved. $\alpha_1\beta_1$ and $\alpha_2\beta_1$ are able to mediate adhesion to collagen at least in some cells (Defilippi et al., 1991*a*; Hemler et al., 1990). Whether these integrins can participate in angiogenesis remains to be determined. The use of alternate matrix receptors may induce a different set of signals which in our system is manifested in enhanced capillary formation. Using chimeric constructs transfected into RD cells, Chan et al. (Chan et al., 1992) have shown that the cytoplasmic domains of the integrin receptors can mediate different signals irrespective of the ligand-binding event.

Angiogenesis is clearly a complex event that can be regulated at multiple levels. In this paper we have demonstrated that the extent of capillary tube formation can be enhanced by the use of anti-integrin antibodies specific for a given receptor-ligand system which inhibit cell–matrix adhesion. These antibodies have profound effects on cell shape, adhesion, proliferation, and subsequent cell differentiation. A corollary of the work presented here suggests that anti-integrin antibodies which promote cell adhesion to the ECM will actually inhibit in vitro angiogenesis. Thus regulation of angiogenesis may be mediated through alteration in the matrix (as has been shown previously), or as our results suggest, by alteration in the function of matrix-adhesion receptors on the EC.

We thank Dr. Gillian Cockerill for helpful discussions, Ms. Leanne Noack, and Mrs. Fiona Bilogrevic for expert technical assistance, Mrs. Mari Walker for preparation of the manuscript, and the staff at the Delivery Ward, Queen Victoria Hospital for collection of umbilical cords.

This work was supported by grants from the Anti-Cancer Foundation of the Universities of South Australia, the National Health and Medical Research Council of Australia, and the National Heart Foundation of Australia. P. Kaur is a recipient of a Florey Fellowship from the Royal Adelaide Hospital.

Received for publication 18 May 1992 and in revised form 8 February 1993.

References

Aggeler, J., S. M. Frisch, and Z. Werb. 1984. Changes in cell shape correlate with collagenase gene expression in rabbit synovial fibroblasts. *J. Cell. Biol.* 98:1662–1671.

Albelda, S. M., and C. A. Buck. 1990. Integrins and other cell adhesion molecules. *FASEB (Fed. Am. Soc. Exp. Biol.) J.* 4:2868–2880.

Albelda, S. M., M. Daise, E. M. Levine, and C. A. Buck. 1989. Identification and characterization of cell-substratum adhesion receptors on cultured human endothelial cells. *J. Clin. Invest.* 83:1992–2002.

Ben-Ze'ev, A. 1980. Protein synthesis requires cell-surface contact while nuclear events respond to cell shape in anchorage-dependent fibroblasts. *Cell.* 21:365–371.

Ben-Zeley, A., G. S. Robinson, N. L. R. Bucher, and S. R. Farmer. 1988. Cell-cell and cell-matrix interactions differentially regulate the expression of hepatocytes and cytoskeletal genes in primary cultures of rat hepatocytes. *Proc. Natl. Acad. Sci. USA.* 85:2162–2165.

Carter, W. G., E. A. Wayner, T. S. Bouchard, and P. Kaur. 1990. The role of integrins $\alpha_2\beta_1$ and $\alpha_3\beta_1$ in cell–cell and cell–substrate adhesion of human epidermal cells. *J. Cell Biol.* 110:1387–1404.

Chan, B. M. C., P. D. Kassner, J. A. Shiro, H. R. Byers, T. S. Kupper, and M. E. Hemler. 1992. Distinct cellular functions mediated by different VLA integrin α subunit cytoplasmic domains. *Cell.* 68:1051–1060.

Cheresh, D. A., and R. C. Spiro. 1987. Biosynthetic and functional properties of Arg-Gly-Asp-directed receptor involved in human melanoma cell attached to vitronectin, fibrinogen and von Willebrand factor. *J. Biol. Chem.* 262:17703–17711.

Defilippi, P., V. van Hinsbergh, A. Bertolotto, P. Rossino, L. Silengo, and G. Tarone. 1991*a*. Differential distribution and modulation of expression of alpha1/beta1 integrin on human endothelial cells. *J. Cell Biol.* 114:855–863.

Defilippi, P., G. Truffa, G. Stefanuto, F. Altruda, L. Silengo, and G. Tarone. 1991*b*. Tumor necrosis factor α and interferon γ modulate the expression of the vitronectin receptor (integrin β_3) in human endothelial cells. *J. Biol. Chem.* 266:7638–7645.

DePersio, C. M., D. A. Jackson, and K. S. Zaret. 1991. The extracellular matrix coordinately modulates liver transcription factors and hepatocyte morphology. *Mol. Cell. Biol.* 11:4405–4414.

Doctrow, S. R., and J. Folkman. 1987. Protein kinase C activators suppress stimulation of capillary endothelial cell growth by angiogenic endothelial mitogens. *J. Cell Biol.* 104:679–687.

Duband, J. L., S. Dufour, K. M. Yamada, and J. P. Thiery. 1988. The migratory behaviour of avian embryonic cells does not require phosphorylation of the fibronectin-receptor complex. *FEBS (Fed. Eur. Biochem. Soc.) Lett.* 230:181–185.

Elsdale, T., and J. Bard. 1972. Collagen: substrata for studies on cell behavior. *J. Cell Biol.* 54:626–637.

Folkman, J. 1982. Angiogenesis: initiation and control. *Ann. NY Acad. Sci.* 401:212–227.

Folkman, J. 1986. How is blood vessel growth regulated in normal and neoplastic tissue? *Cancer Res.* 46:467–473.

Folkman, J., and C. Haudenschild. 1980. Angiogenesis *in vitro*. *Nature (Lond.).* 288:551–556.

Folkman, J., and M. Klagsbrun. 1987. Angiogenic factors. *Science (Wash. DC).* 235:442–447.

Folkman, J., and A. Moscona. 1978. Role of cell shape in growth control. *Nature (Lond.).* 271:345–349.

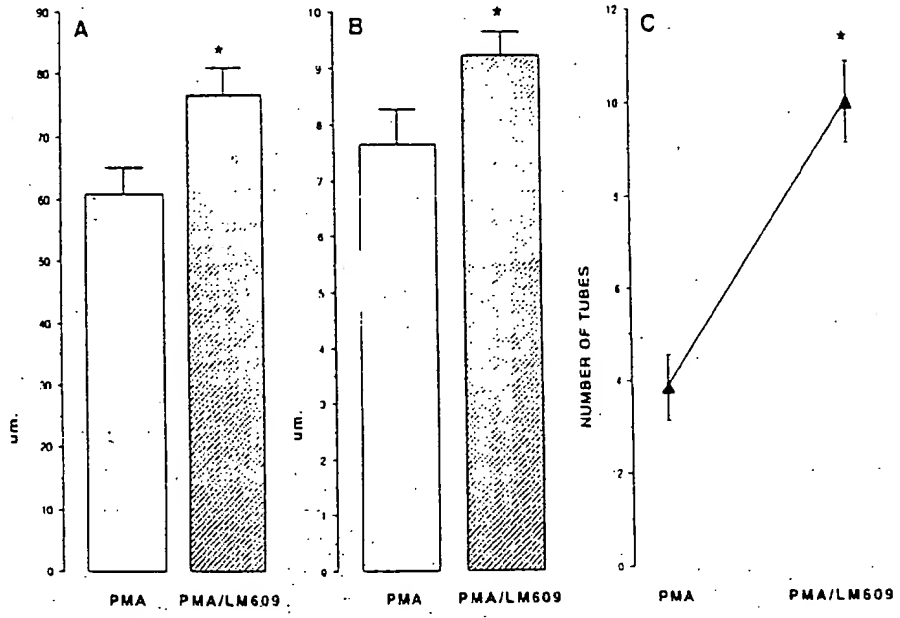

Figure 12. Effect of LM609 on tube length (μm, *A*), width (μm, *B*), and number (*C*) per high power field. EC were plated onto fibrin gels in the presence of 20 ng/ml PMA, and 30 μg/ml LM609 was added to half the wells. 24 h later the wells were photographed (magnification ×264), random fields being taken for each well. The number, length, and width of tubes were measured from these photographs. The pooled results from two separate experiments are given for the length, width, and number. * $p < 0.05$ compared to PMA alone.

cells resulting in changes to cell proliferation and differentiation (Folkman and Moscona, 1978). Gospodarowitz has reported that EC must become attached and flattened in order to proliferate and that those kept rounded in suspension fail to divide (Gospodarowitz et al., 1978). Furthermore, there is a direct correlation between growth inhibition and decreases in cell extension (Ingber et al., 1987). DNA, RNA, and protein synthesis in anchorage dependent fibroblasts is also inhibited if these cells are maintained in suspension (Ben-Ze'ev, 1980). Differentiation and expression of genes which reflect a more differentiated state of hepatocytes, chondrocytes, fibroblasts, and endothelial cells are linked to cell shape and actin reorganization (Aggeler et al., 1984; DiPersio et al., 1991; Mallein-Gerin et al., 1991; Ingber and Folkman, 1989*a*,*b*; Ben-Ze'ev et al., 1988; Glowacki et al., 1983; Unemori and Werb, 1986; Werb et al., 1986). All these studies suggest that the mechanical interaction of cells with the ECM can regulate cell function. Since integrins interconnect the ECM with the cyto-skeleton, they are likely to be involved in the transmission of signals between the cell and its ECM. The biochemical signals (termed mechanotransducers) which are generated as a result of mechanical forces or integrin activation are unknown at present but phosphorylation (Kornberg et al., 1991), activation of the Na^+/H^+ exchanger (Ingber, 1990), Ca^{++} mobilization, and adenylate cyclase (for review see Watson, 1991; Ingber, 1991*b*) have been implicated.

In the studies reported here, the decrease in the adhesion and change in cell shape of EC with anti-integrin antibodies, resulted in an inhibition in proliferation and in a promotion of differentiation as measured by capillary tube formation. These alterations in cell function were matrix specific, that is anti-$\alpha_2\beta_1$ antibodies inhibited EC proliferation and enhanced cell differentiation only on a collagen but not on a fibrin gel, while anti-$\alpha_v\beta_3$ showed effects on fibrin but not on collagen gels. Thus, the effect of anti-integrin antibodies on angiogenesis is ligand dependent. Furthermore, the antibody mediated effects are time dependent. No enhancement of capillary formation was observed when the antibodies were added more than 2 h after cell plating, paralleling the time dependency seen with the antibodies on EC adhesion and cell shape.

EM revealed striking qualitative changes in tubes with anti-integrin antibodies. In the absence of RMAC11, the majority of lumina were formed within single cells in a manner reported by Folkman and Haudenschild (1980). However, with RMAC11, the majority of lumina were formed from multiple cells with clear cellular borders between cells making up the vessel (Fig. 3 *B*). Using fibrin gels and anti-$\alpha_v\beta_3$ antibodies, lumina were also formed from multiple cells. Thus anti-integrin antibodies not only alter the degree of tube formation taking place but also influence the phenotype of tubes. The relationship between intracellular and intercellular lumina is not known at present but one possibility is that intercellular lumen form from coalescence of intracellular vacuole-like structures with the plasma membrane and that these structures define stages in tube formation. Clearly, our in vitro model of angiogenesis may allow a more detailed examination of the stages involved in capillary formation.

The enhancement of capillary tube formation with anti-integrin antibodies was dependent on the presence of PMA since the antibodies alone had no effect. Thus, one signal for tube formation is likely to be protein kinase C–dependent. Indeed activators of protein kinase C inhibit the proliferation of EC in response to mitogens (Doctrow and Folkman, 1987). One possibility for our results is that the antibodies enhance PMA-mediated signals. This, however, is unlikely since the antibodies do not enhance tube formation on an inappropriate matrix. That is, anti-$\alpha_2\beta_1$ antibody had no effect on fibrin gels, and anti-$\alpha_v\beta_3$ antibody had no effect on collagen gels even though tube formation can take place on these matrices. This data therefore suggests that the antibodies do not directly signal the cell to undergo tube formation. This is further supported by the fact that pretreatment of HUVEC with the antibodies and removal by washing does not result in enhanced tube formation.

COMMONWEALTH OF AUSTRALIA

(Patents Act 1990)

IN THE MATTER OF: Australian Patent Application 696764 (73941/94). In the name of: Human Genome Sciences Inc.

- and -

IN THE MATTER OF: Opposition thereto by Ludwig Institute for Cancer Research, under Section 59 of the Patents Act.

Annexure GBC-13

This is **Annexure GBC-13** referred to in my Statutory Declaration made this Thirteenth day of December 2000.

Gary Baxter Cox

WITNESS: _____

Patent Attorney PEYTEE KHO

Clinical Frontiers

Human gene therapy

BARRY R. GOLDSPIEL, LAURENCE GREEN, AND KARIM ANTON CALIS

Abstract: Current concepts in gene transfer and its application to the treatment of human genetic disorders, cancer, and other diseases are discussed.

Gene therapy is a technique in which a functioning gene is inserted into a human cell to correct a genetic error or to introduce a new function to the cell. Many methods, including retroviral vectors, have been developed for ex vivo and in vivo gene insertion into cells. Some pharmacists have likened gene therapy to a sophisticated form of drug delivery and have envisioned an active role for the pharmacy profession. There are several safety and ethical issues related to manipulating the human genome that need to be understood. Current gene therapy efforts focus on gene insertion into somatic (non-germinal) cells only.

Gene therapy has the potential to revolutionize the treatment of genetic disorders, diseases associated with a genetic component (e.g., cystic fibrosis), cancer, AIDS, and many other diseases. Gene transfer may also be used to better understand the biology of disease processes, such as the source of relapse in bone marrow transplant patients. The human genome project will undoubtedly lead to the identification, characterization, and understanding of genes that are responsible for many human diseases, and gene therapy trials are sure to expand accordingly.

To date, over 40 clinical trials have been approved and more than 110 patients have been entered in gene therapy studies. There are still many technical obstacles to overcome before gene therapy can have widespread application. Injectable vectors need to be developed to simplify foreign gene administration. Perhaps the biggest problem to overcome will be engineering the target cells to be able to regulate gene expression according to physiologic needs.

Pharmacists should become knowledgeable about gene transfer techniques and possible clinical applications of gene therapy to keep abreast of the newest trends in medicine.

Index terms: Gene therapy; Genetic engineering; Neoplasms; Research; Transfection

Clin Pharm. 1993; 12:488-505

Recent advances in molecular biology and related disciplines have contributed to major developments in the diagnosis and treatment of human disease. Numerous diagnostic products and biological therapies have been produced by recombinant DNA technology. Identification and cloning of genes involved in various human diseases have heralded the era of human gene therapy, a technique in which a functioning gene is inserted into a human cell to correct a genetic error or to introduce a new function to the cell.[1] Viruses such as murine retroviruses, adenoviruses, herpes viruses, and parvoviruses are gaining wide use for introducing foreign genes into human cells.[1,2] The ultimate success and utility of human gene therapy depend in large part on the ability of scientists to elucidate the structure, function, and regulation of human genes.[3] The human genome project, an international effort to map and sequence the entire genomes of man and several model organisms, will undoubtedly lead to the identification, characterization, and understanding of genes that are responsible for many human diseases.[4]

Gene therapy has the potential to revolutionize the treatment of genetic disorders, diseases associated with a genetic component (e.g., cystic fibrosis), cancer, AIDS, and many other diseases. Gene transfer may also be used to better understand the biology of disease processes. Some pharmacists have likened gene therapy to a sophisticated form of drug delivery and

BARRY R. GOLDSPIEL, PHARM.D., is Oncology Clinical Pharmacy Specialist, Pharmacy Department, Warren G. Magnuson Clinical Center (WGMCC), National Institutes of Health (NIH), Bethesda, MD. LAURENCE GREEN, PHARM.D., is Deputy Chief, Pharmacy Department, WGMCC. KARIM ANTON CALIS, PHARM.D., BCPS, BCNSP, is Coordinator, Drug Information Service, and Endocrinology Clinical Pharmacy Specialist, Pharmacy Department, WGMCC, and Clinical Assistant Professor, School of Pharmacy, University of Maryland, Baltimore.

Address reprint requests to Dr. Green at the NIH Clinical Center, Pharmacy Department, Building 10, Room 1N-257, Bethesda, MD 20892.

Kenneth Culver, M.D., Cellular Immunology Section, Metabolism Branch, National Cancer Institute, is acknowledged for his expert manuscript review.

This is article 680-204-93-025 in the ASHP Continuing Education System: it qualifies for 1.0 hour of continuing-education credit. See page 542 for learning objectives and test questions.

Reviews in the Clinical Frontiers *section summarize recent research advances, such as those that contribute to an understanding of a disease process or the mechanism of drug action, describe new technologies or medical procedures that are likely to affect drug therapy, or describe likely new modes of drug therapy. Preference is given to articles that assess directions of ongoing research and critically evaluate therapeutic implications in new or rapidly changing areas.*

have envisioned an active role for the pharmacy profession.[3] Pharmacists, however, must understand the fundamentals of molecular biology if they are to keep pace with the rapid advances in gene therapy. This knowledge, integrated with expertise in pharmacotherapy, will allow pharmacists to contribute to the development of gene therapy trials and the care of patients undergoing this form of treatment. This article will review basic mechanics of gene transfer and gene therapy, describe the potential applications of gene transfer and gene therapy to better understanding of disease biology, and summarize the ongoing clinical trials employing gene transfer and gene therapy techniques.

Gene Structure, Function, and Regulation

A gene is a segment of DNA with a unique order of purine and pyrimidine bases that encode a specific protein (Figure 1). It is estimated that the human genome contains 3 billion DNA base pairs or the equivalent of 50,000–100,000 genes divided among the chromosomes and the mitochondria.[4] Most genes from eukaryotic cells contain coding sequences (exons) that are interrupted by one or more noncoding regions (introns).[5] The regions adjacent to the introns and exons contain the initiation and termination sequences necessary to regulate messenger RNA (mRNA) transcription. Several similar sequences are found in the 5' regions of many different genes, possibly indicating that these sequences play an important role in gene regulation.[5]

The flow of information from gene to protein product involves many complicated, highly coordinated processes (Figure 2). The template for protein synthesis, mRNA, is formed in the nucleus as a complementary copy of a single-strand portion of DNA through a process called transcription. The mRNA base sequence is then decoded to form a protein through a process known as translation. Ribosomal RNA is responsible for protein synthesis under the direction of transfer RNA, which provides the molecular link between the coded sequence of RNA and that of the protein.[6]

The genetic code is composed of 64 codons, which are sequences of three adjacent bases that specify a particular amino acid. Although up to three different codons can specify the same amino acid, the genetic code is considered universal because all organisms use the same codons. This fact explains why a simple bacterium can translate a human gene into a polypeptide. Moreover, the DNA or RNA base sequence determines the amino acid sequence, and knowledge of the amino acid sequence can be used to deduce the possible DNA sequence that codes for the protein.[7]

The complex regulation of end-product protein production (gene expression) is controlled by many factors, including gene structure, transcription, translation, gene product amount (gene dosage), and protein processing.[6] For many genes, small fluctuations in the amount of the gene product can turn gene expression on or off through feedback mechanisms. For other genes, even large fluctuations do not alter gene expression. The clinical manifestations of altered gene expression can vary greatly as well. Some disorders can arise from small fluctuations in gene product expression, whereas no clinical consequences may be apparent from large fluctuations in some gene products.

Determining where genes are located on the chromosome (mapping) and characterization of DNA requires generation of a sufficient quantity of DNA fragments. Portions of DNA containing a specific gene are removed from the chromosome by using enzymes that recognize specific base-pair sequences (restriction enzymes). The number of DNA fragments is then amplified (increased) and cloned (duplicated) in prokaryotic cells (e.g., bacteria), in eukaryotic cells (e.g., yeast), or by using the polymerase chain reaction (PCR). PCR is an efficient and highly sensitive method that allows the in vitro synthesis of large amounts of a desired DNA sequence. In addition, many other powerful molecular biology techniques have been developed to help researchers and clinicians identify the genetic link to human diseases. To learn more about molecular biology, the reader is referred to several recent review articles.[8–10]

Figure 1. Basic gene structure. A gene is a sequence of chromosomal DNA required to produce a functional RNA or polypeptide product. The basic gene structure consists of both the actual coding sequences (exons) and sequences necessary for proper gene expression. The promoter region (P), located at the 5' terminus, includes the start codon and the sequences that initiate messenger RNA (mRNA) transcription. Very few genes exist as continuous coding sequences; most are interrupted by noncoding sequences (introns). Transcription of the exon regions determines the resultant amino acid sequence. Introns are transcribed in the nucleus to RNA but are not part of the cytoplasmic mRNA and therefore not part of the final protein product. Beyond the stop codon, an untranslated region at the 3' terminus is responsible for adding multiple polyadenosine residues to the mRNA.

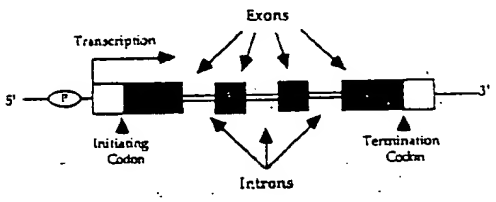

Figure 2. Production of proteins from genes. The production of a protein product is a highly regulated, complex process that starts with the gene. At step 1, transcription of DNA into RNA starts upstream from the coding sequences and continues along the chromosome including both exon and intron sequences. At step 2, the primary RNA transcript is then modified to remove the areas transcribed from intron. At step 3, the resultant messenger RNA is then transported from the nucleus into the cytoplasm where, at step 4, it is translated into the amino acid sequence for the desired protein. Step 5 shows assembly of the completed protein. (From Thompson MW, McInnes RR, Willard HF. Thompson and Thompson genetics in medicine. 5th ed. Philadelphia: Saunders; 1991. Adapted by permission.)

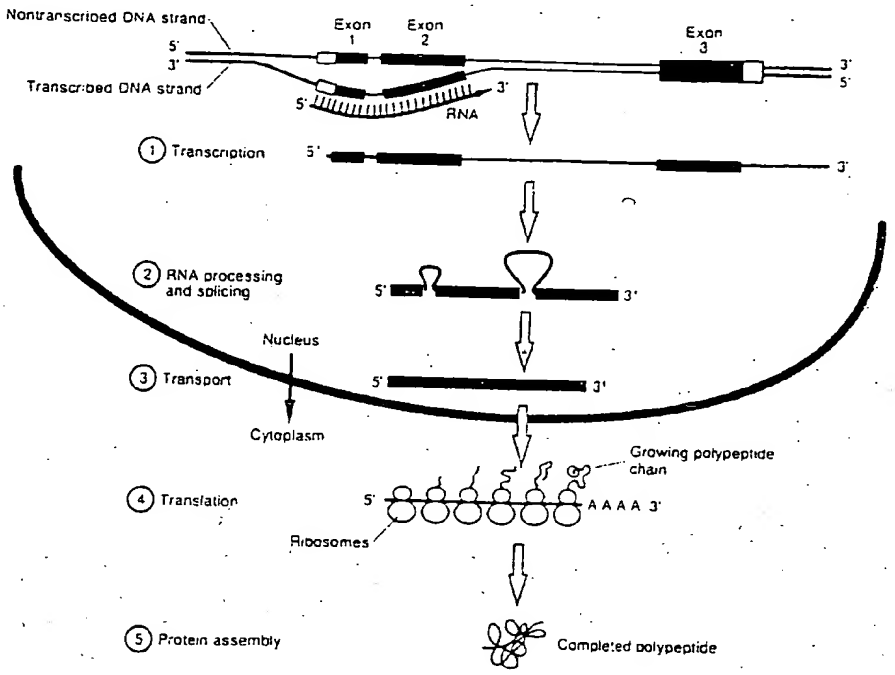

Gene Delivery into Cells

Gene therapy requires introduction of foreign DNA sequences with stable integration, gene expression, and appropriate regulation in target tissues. The introduced gene can replace a missing gene or augment a defective one. For a gene to be expressed, it must first be delivered into the target cell. Once the gene is incorporated into the cell nucleus, the cell can then produce the new or missing gene product. Theoretically, genes can be transferred into many different cell types. Experimental techniques for delivering genes into hepatocytes, keratinocytes, fibroblasts, endothelial cells, epithelial cells, myocytes, and hematopoietic cells are available.[11-17] Most gene transfer experience has been with hematopoietic cells, since bone marrow or blood is easy to obtain and handle.[13,18] In particular, lymphocytes were used in the initial gene therapy experiments for adenosine deaminase (ADA) deficiency and cancer.[19] Unfortunately, while bone marrow stem cells are self-renewing, lymphocytes have a finite life cycle. Therefore, if lymphocytes are used as a cellular target for gene therapy, genes are expressed only as long as the lymphocyte lives. Thus, repeated infusions of gene-altered lymphocytes are required.

The currently available techniques for transferring genes into cells include both physical and viral methods.[20-22] Physical transfection methods include microinjection of DNA directly into cells, electrophoretic transfer across cell membranes (electroporation), coprecipitation with calcium phosphate, and fusion to liposomes or spheroplasts. Microinjection, although 10–100% efficient, is limited in clinical practice by the number of cells that can be injected. With microinjection, each individual cell would need to be treated separately and since 10^8 to 10^9 cells usually need to be treated, this method would not easily apply to many clinical situations, including bone marrow transplantation.[20,23] Other physical methods have limitations that make them less than optimal for current attempts at human gene therapy. Transfection and electroporation are inefficient; less than 1% of cells will have stable DNA integration into their chromosomes with this method. Fusion methods, using spheroplasts developed from bacteria after cell wall lysis or liposomes, involve attachment to the target cell membrane and then intracellular DNA delivery. DNA has been directly transferred to tumor cells via liposomes.[21,24] Although stable integration of DNA in the tumor cells may not be possible using liposomes, it may not be required since transient expression may be sufficient to exert a biological effect.

Viral vectors, primarily retroviruses, improve the efficiency of delivering genes into cells (Table 1).[20,22,25]

A vector is any material containing DNA or RNA that is used to carry a gene into a cell. A viral vector provides a means of inserting genetic information into the genome of host cells. The Moloney murine leukemia virus is the most commonly used retrovirus (Figure 3). To provide the necessary safety factors, the retroviral vector is made replication-deficient (also referred to as replication-defective) by removing the encapsidation (ψ, *psi*) gene sequences necessary for viral replication. The vector can still infect the cell, integrate into the target cell, and deliver genetic information to the nucleus, but it cannot replicate. Viral proteins can then be made by the use of retrovirus "packaging" cell lines (Figure 4).[26] To accomplish this, the vectors are first modified to include the new gene(s) as well as the mechanism to control gene expression.

These genetically modified retroviruses have been used safely in humans for ex vivo gene therapy (Figure 5).[2,19,27,28] Scientists can transduce large numbers of cells by using this method.[20,25] Retroviral vectors provide an advantage over other vector systems because they can stably insert a foreign gene into the host genome. This modification would then be passed on as the cell divides. Retroviral vectors provide a highly efficient means of gene transfer (up to 90%) into replicating cells and precisely integrate transferred genes into cellular DNA.[20,25] Other methods of gene transfer are not as efficient as retroviral transduction and usually do not cause stable DNA integration into target cells, especially primary somatic (nongerminal) cells.[29] However, retroviral vectors do not integrate in nondividing cells.[30]

Adenoviruses provide another viral vector for gene therapy.[20,22,31] Although not studied as extensively as retroviruses, they may play an important role in future gene therapy studies. After the genetic information controlling viral replication is removed from the adenovirus, it can be suitable for gene therapy in a manner similar to the retrovirus. However, adenoviral DNA functions in an extrachromosomal manner, rather than by insertion into the genome. Because of this, the adenovirus should not cause malignant transformation (insertional mutagenesis or insertional oncogenesis). Unfortunately, the gene cannot be passed on to the progeny of the modified cell. Adenoviral vectors may cause transient high-level expression of genes in many cell types and could be useful in short-term gene therapy. The major advantages for using adenoviral vectors are that they are suitable for infecting tissues in situ, especially the lung, and they can be made at high titers (10^{11}–10^{12} plaque-forming units/mL), thereby allowing for high-efficiency transduction. Cells in the lung proliferate slowly and many are terminally differentiated, making them less susceptible to retroviral vector transduction. One example of the current use of an adenoviral vector is to deliver a human cystic fibrosis transmembrane conductance regulator gene by intratracheal instillation to airway epithelial cells.[32,33]

The herpes simplex virus (HSV) is another viral vector with a natural affinity (tropism) for nondividing tissue. This virus is neurotropic and may be suitable

Table 1.
Viral Vectors and Target Tissues

Viral Vector	Target Tissues
Retrovirus	Hematopoietic cells Hematopoietic stem cells Fibroblasts Endothelial cells Myoblasts Smooth muscle cells Hepatocytes
Adenovirus	Airway epithelial cells Hepatocytes Hematopoietic cells (lymphoid, myeloid)
Adeno-associated virus	Hematopoietic cells Fibroblasts Epithelial cells
Herpesvirus	Lymphoid cells Nondividing cells (e.g., differentiated neurons and hepatocytes)
Parvovirus Simian virus 40	Central nervous system Smooth muscle cells

Figure 3. Retroviral gene structure. The Moloney murine leukemia virus is an attractive starting point to produce retroviral vectors with substituted gene sequences of interest because the *gag*, *pol*, and *env* regions can be deleted and the virus can still enter a cell and integrate its genetic material without being able to reproduce. Dual-gene (or multiply-substituted) vectors can be produced by inserting the appropriate promoter sequence before each additional gene. The LNL6 NeoR retroviral vector is a highly modified version of previous NeoR vectors to enhance safety: a stop codon (TAG) replaces the start codon, and murine sarcoma virus sequences (hatched regions) replace some Moloney virus sequences. LTR = long-terminal repeat, ψ (*psi*) = encapsidation sequence, *gag* = viral structural-protein sequences, *pol* = viral enzymes (including reverse transcriptase) sequence, *env* = viral envelope-protein region, P = gene promoter, TAG = thymidine–adenine–guanine stop codon triplet, NeoR = gene that confers resistance to the neomycin analogue G418. (From Cornetta K. Safety aspects of gene therapy. *Br J Haematol*. 1992; 80:421-6. Adapted with permission of Blackwell Scientific Publications Ltd.)

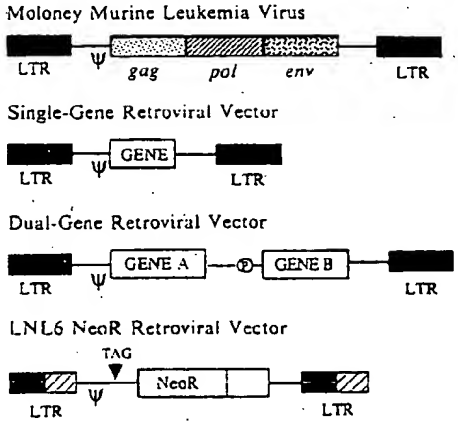

Figure 4. Gene insertion using retroviral vectors and packaging cell lines. A packaging cell line is used to produce replication-deficient retroviral vectors. Lacking the ψ (*psi*) viral encapsidation sequence, the packaging cell line cannot incorporate the viral genome into the virion and produces an empty viral particle. If this cell line is then transfected with a ψ-positive gene (cDNA sequence), the viral genome is preferentially packaged into the particles. (From Cornetta K. Safety aspects of gene therapy. *Br J Haematol.* 1992; 80:421-6. Adapted with permission of Blackwell Scientific Publications Ltd.)

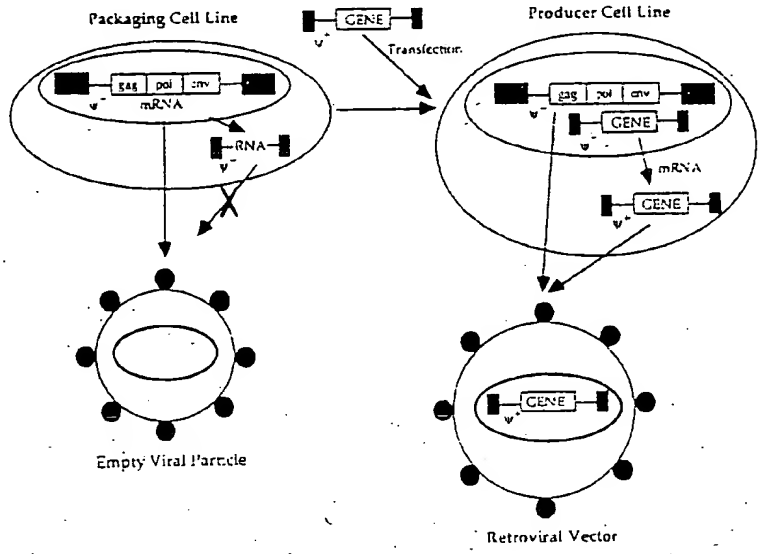

Figure 5. Ex vivo gene therapy in humans. (From Valle D. Treatment of genetic disease: current status and prospects for the future. *Semin Perinatol.* 1991; 15[Suppl 1]:52-6. Adapted with permission.)

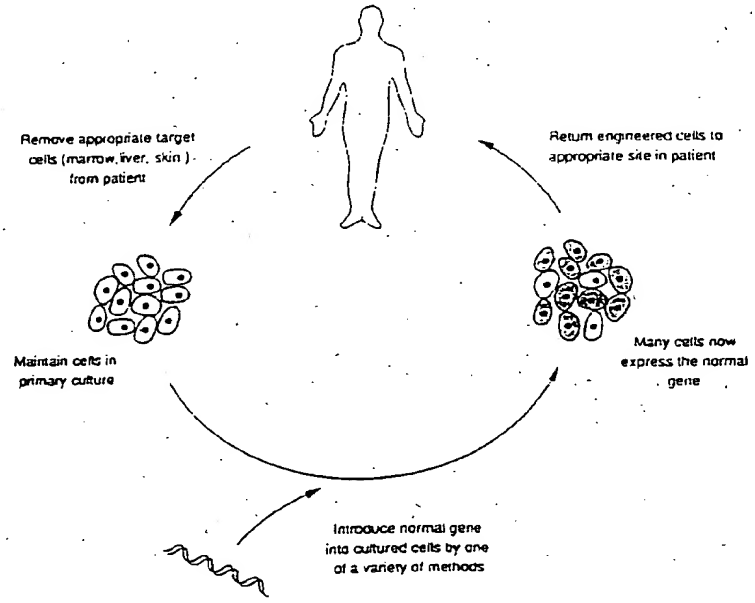

for diseases of the central nervous system.[34] A unique characteristic of HSV that may offer advantages for future gene therapy applications is that there is space available to accommodate larger and more complex gene arrangements than adenoviral and retroviral vectors.[32] HSV has not been used as a vector system in human studies yet.

The parvovirus, an adeno-associated virus (AAV) that is nonpathogenic and replication-defective, is being studied as a gene vector.[32] It has a broad range of possible hosts and can integrate into a specific site in its host's DNA, thus minimizing the risk of insertional mutagenesis. If necessary, introduced sequences may be removed by using a helper virus. The ability of the

AAV to enter latency is attractive for AAV vector development.

Potential Target Tissues

Although many types of tissue would theoretically be appropriate targets for correction of genetic defects, placing a normal gene into diseased tissues depends on several factors, including the proliferative state of the tissue, its accessibility to gene manipulation, the normal site of gene expression, the presence of cofactors, and the reversibility of tissue damage. Hematopoietic cells are favored since there are well-developed procedures for bone marrow transplantation (BMT), several hematopoietic cell types, wide distribution of hematopoietic cells, and a variety of severe diseases affecting hematopoietic cells.[20,22]

For many genetic therapies, the long-term, repopulating pluripotent hematopoietic stem cell is the ideal target for gene transfer.[18,35,36] Because of its extensive self-renewing capacity, a lasting genetic modification of the hematopoietic system can be accomplished by gene transfer.[18,35] Unfortunately, the hematopoietic stem cell is present in low concentrations, so many current gene therapy efforts target more differentiated hematopoietic cells, such as lymphocytes.[15] However, recent advances have made gene transfer into hematopoietic stems cells possible, and current research efforts are under way to make this approach more feasible.[18,35,36]

The liver is also an attractive target to correct the many genetic disorders associated with inborn errors of metabolism.[21,37,38] The liver has a blood supply that can be isolated for gene delivery and then used to distribute the gene product. While the hepatocyte does not proliferate to the extent that other target tissues for gene therapy (e.g., lymphocytes) do, it undergoes sufficient divisions to allow a 3–30% transduction rate.[21,37,38] Furthermore, hepatocytes can be removed by partial liver resection, grown in tissue culture, and then returned via the hepatic artery. While in culture, they can be transduced with recombinant retroviral vectors where, as has been demonstrated, a functional defect can be repaired.[35] Moreover, there are a number of diseases that result from hepatic deficiency states. It may be possible to cure a genetic disorder by supplementing the liver with a gene that is deficient in specific disease states. There is interest in the potential application of gene therapy in antitrypsin deficiency, a common hepatic deficiency state that leads to early-onset lung disease.[2,33]

Many metabolic, exocrine, autocrine, and nutritional disorders may be treated in the future by gene therapy targeting the intestines. Preliminary evidence suggests that intestinal tissue can be transduced by exposure to adenoviral vectors. Other potential targets for gene therapy in the gastrointestinal tract include the bile duct, pancreatic cells, and other secretory cells.[33]

Investigators have transferred the gene encoding tissue plasminogen activator (TPA) into endothelial cells via retroviral vectors. The genetically modified endothelial cells will then express TPA. Although a systemic anticoagulant effect would not be expected from this production, local concentrations of TPA could produce a thrombolytic environment and reduce thrombosis.[39]

Most investigators agree that protocols modifying somatic tissues, as described above, are an ethical therapeutic option. However, controversy still exists as to the ethics of using germ cells (e.g., sperm or eggs) for gene therapy. Future generations could be damaged if the germ line is manipulated. Much is still not known about this type of therapy. Long-term adverse effects may occur if genetic information in patients' germinal cells is altered. Therefore, before gene therapy in human germ cells is considered, more experience is necessary in animal models.[40]

Although preliminary research indicates promise in many of the previously described tissues, formidable obstacles need to be overcome before we see routine use of gene therapy in human disease. In the future, it may be possible to use gene therapy in a variety of cell types as a means of creating customized, localized, drug delivery systems in patients by producing drugs targeted at specific disease processes.

Disease Candidates for Gene Therapy

As scientists make progress in gene transfer techniques and uncover more details of the human genome, the list of potential applications of gene therapy will grow (Table 2). Ethical and scientific considerations are important when choosing initial candidates for gene therapy. At first, clinicians considered severe genetic diseases with a predictable phenotype and

Table 2.
Potential Disease Candidates for Gene Therapy

Genetic diseases or disorders with associated genetic component
SCID[a] with adenosine deaminase deficiency
Familial hypercholesterolemia
Hemophilia
Cystic fibrosis
Antitrypsin deficiency
Chronic granulomatous disease
Gaucher's disease type I
Mucopolysaccharidosis
Emphysema
Phenylketonuria
Ammoniemia
Muscular dystrophy
Thalassemia
Sickle cell anemia
Argininosuccinicaciduria
Citrullinemia
Purine-nucleoside phosphorylase deficiency
Cancer
Nongenetic, nonmalignant diseases
Acquired immunodeficiency syndrome
Cardiovascular disease

[a]SCID = severe combined immunodeficiency.

limitations in current therapy that justified experimental approaches. The basic categories of disorders in which gene therapy will be used are (1) diseases caused by a missing or defective gene, (2) cancer, and (3) nongenetic, nonmalignant diseases such as AIDS.

To correct genetic disorders using the current gene transfer systems, several biological criteria should be met: (1) the disease is genetically recessive, (2) the defective gene has been identified and cloned, (3) precise regulation of gene product is not required, and (4) target cells can be manipulated after removal from the body and safely returned to the patient.[1,2] Furthermore, cells containing the corrected gene(s) should have a selective survival advantage over uncorrected cells. Without the survival advantage, remaining untreated cells would dilute the beneficial effects of the genetically corrected cells. Recent advances in recombinant DNA technology, which make isolation of many genes possible, and new insights into gene regulation mechanisms make meeting these biological requirements feasible.

At present, the most suitable genetic disorders meeting these criteria are those affecting the hematopoietic system. This is because a suitable method for reintroducing genetically altered cells already exists through BMT. In general, BMT is successful in diseases in which (1) the defect causes a complete or partial lack of functioning cells in a particular cell line, (2) there is defective enzyme synthesis, or (3) there is a defective transport molecule. These situations could be corrected by replacing the defective gene with its cloned functional equivalent. This approach is successful in treating hematopoietic disorders like severe combined immunodeficiency due to ADA deficiency.[41,42] Gene therapy may prove more difficult in disorders that involve complex gene regulation (e.g., diabetes mellitus) or where the disease is manifested in relatively inaccessible body tissues, such as the bone matrix or the central nervous system (CNS). With current technology, genes cannot be supplied through hematopoietic pathways to many other tissues, such as muscle, visceral organs, or neurons; and alternative gene delivery pathways are necessary. CNS disease may prove to be particularly difficult to treat. In the CNS, only a relatively small number of diseases may be correctable with currently anticipated technologies. When a gene deficit results in a toxic product, early developmental failure caused by accumulation of toxic metabolites in the CNS may be irreversible. Damage to neurons may also result from physical damage induced by gene insertion (i.e., an immune response to a herpes vector). For these reasons, gene therapy of many CNS diseases may need to take place in the fetus or newborn before irreversible damage occurs and where the blood–brain barrier may be more permeable to treated cells.

Gene therapy is usually thought of as a technique for inserting a functioning gene into cells of a patient to correct an inborn genetic defect.[1] Gene therapy for malignant disease, for the most part, consists of inserting a gene into a cell to provide a new function for the cell. Newer approaches are targeting the genetic basis for many malignancies by introducing missing tumor suppressor genes or inactivating oncogenes.[43] Current approaches to gene therapy for cancer involve gene transfer into immune cells to modify and enhance immune cell functions, modifying tumor cells to stimulate the immune response, inserting genes to make cancer cells sensitive to certain drugs (e.g., ganciclovir sodium), and using gene transfer for marking or enhancing transplanted bone marrow for treatment of lymphoid tumors.[44] Also, genetic marking of autologous bone marrow cells used for transplantation provides a way to determine if the transplanted (reinfused) cells are the cause of posttransplant relapse. Consequently, new ways of reducing residual disease before removal of bone marrow or more rigorous marrow purging could be evaluated.

The gene encoding bacterial neomycin phosphotransferase (usually referred to as the NeoR gene) has been successfully used in gene-marking studies.[45] Cells that produce neomycin phosphotransferase are resistant to the neomycin analogue G418 and can be distinguished from cells that do not express this enzyme. Insertion of the gene NeoR into tumor-infiltrating lymphocytes (TIL) demonstrated that the gene could be inserted and expressed in human TIL and that the marked cells could be detected in blood and tumor samples.[45] Studies done in a limited number of patients have now shown that these gene-modified cells can be detected for up to six months in blood and two months in tumor after cell infusion.[45] The NeoR gene is also being inserted into bone marrow cells used in BMT gene-marking studies.

Gene therapy has been proposed as a treatment for AIDS. Better understanding of modes of transmission and molecular mechanisms of human immunodeficiency virus (HIV) replication has yielded creative approaches to therapy. Gene transfer protocols have been designed to protect modified cells by blocking viral infection or by interfering with HIV gene expression. Investigators are searching for ways to protect T lymphocytes, the primary target of HIV, from infection. Protection of even a small proportion of T cells may salvage immune function in affected individuals and allow normal immune mechanisms to prevent further viral spread.[46]

Ultimately, investigators will have to look at practical issues to determine which current gene therapy strategies will address realistic clinical goals. Further research with viral vectors is needed to achieve both efficient gene transfer into target cell populations and stable expression of foreign gene products in clinically useful concentrations.

Safety of Gene Manipulation

Importance of Assessment. Safety assessment is important with any new technology, but it is especially important for gene therapy studies, where, in some cases, retroviruses are intentionally introduced. All

clinical studies involving gene transfer in human subjects are assessed by local institutional and national review committees. The local institutional review board evaluates the scientific and ethical merit of the study, and the institutional biosafety committee reviews the recombinant DNA aspects. In addition, all gene therapy protocols supported by U.S. government funds were initially reviewed by both the Human Gene Therapy Subcommittee (HGTS) of the Recombinant DNA Advisory Committee (RAC) and then separately by the RAC itself. Once gene therapy trials began and experience was gained, the need for this dual review by the HGTS and the RAC was questioned and the HGTS was subsequently dissolved; now, only the RAC review is required. The RAC acts in an advisory capacity to the director of the National Institutes of Health (NIH; Bethesda, MD), who ultimately grants final approval. For example, the first gene transfer study underwent 15 separate reviews before final approval was granted in January 1989. Most recently, the RAC has adopted a procedure for the compassionate use of gene therapy.[47-49]

During its existence, the HGTS produced a "Points To Consider" document to guide researchers in seeking approval for gene therapy studies.[50] Several points contained in this document deal directly with safety issues. These concern the need for special precautions to prevent the spread of the recombinant DNA, to reduce any potential hazards to persons other than the person being treated, and to explain and provide laboratory evidence regarding the potential harmful effects of the gene transfer (i.e., development of neoplasms, harmful mutations, regeneration of infectious particles, or an immune response). In considering retroviral-mediated gene transfer, the first safety point deals with the construction of a safe viral vector system. Often, this point forms the basis for most of the questions posed during the RAC review to investigators who want to perform gene transfer studies in humans. The investigators must demonstrate that they have considered all potential consequences of their study. The investigators must consider the potential for gene insertion into reproductive cells (e.g., sperm or eggs) and address the concern for retroviral infection of people other than the patient, including health care workers and family members.[51] FDA has produced a similar "Points To Consider" document that establishes the guidelines by which the Center for Biologics Evaluation and Research evaluates gene therapy studies.[52,53]

In the safety assessment of any gene therapy protocol using retroviral vectors, concern about potential harm to the patient, family, health care providers, and the general public needs to be addressed. Potential patient harm can include an increased risk of cancer and exposure to replication-competent retroviruses through recombination. Risks to those who come in close contact with the patient, such as family or health care providers, can include infection from infectious viral particles. The potential harm to the general population includes the possible production of a new and infectious virus and the possible evolutionary effects of inadvertent retroviral infection of the germ line.[54]

Retroviral-Mediated Gene Transfer. Since most concern focuses on the most commonly used gene transfer system—retroviral vectors—it is important to understand the potential safety issues surrounding retroviral-mediated gene transfer.[55-57] These include (1) contamination with replication-competent virus, (2) contamination with pathogens or toxins, (3) potential problems associated with gene insertion into the host genome, and (4) specific problems related to the method by which the gene-altered cells are administered (e.g., hepatectomy) or the intended gene product (e.g., interleukin-2).

The most critical issue in the development of retroviral-mediated gene transfer was the assurance that replication-competent viruses would not be produced. The retroviral vectors are constructed lacking the *gag*, *pol*, and *env* gene sequences necessary for replication. Virion packaging is accomplished by using "packaging cell lines" rather than potentially infectious helper viruses.[56] Initially, these packaging cell lines were produced with a *psi* gene sequence deletion. It was soon learned that these cell lines can develop replication-competent virus through recombination of the *psi* sequence from the vector with the *psi*-negative helper virus. Newer packaging cell lines have been developed that lack both the *psi* gene sequence and parts of the long-terminal repeats at the 5' and 3' termini, thus necessitating two recombination events to produce a replication-competent virus. In addition, vectors have been produced that replace the codon for starting *gag* gene transcription with a codon for stopping transcription. Researchers have also used vectors with substituted sequences from viruses that are not structurally homologous to the helper virus to minimize the frequency of recombination. Further modifications of the retroviral vector and the packaging cell line have produced systems that require three separate recombination events, thereby greatly reducing the chance of producing a replication-competent virus.[55-57] More importantly though, no problems associated with replication-competent virus have been reported in the more than 110 patients treated in gene therapy trials to date.

Original observations suggested that murine retroviruses capable of replicating in the cells of other species in addition to the original host (amphotropic retroviruses) proliferate poorly in primates, suggesting that if replication-competent helper virus infection did occur, the clinical consequences would be minimal or nonexistent. Recently, however, Donahue et al.[58] reported the rapid occurrence of T-cell lymphoma in three profoundly immunosuppressed monkeys intentionally exposed to replication-competent helper virus used in the supernatant for a gene transfer experiment. The monkeys were given fluorouracil and their bone marrow was harvested, then they were irradiated and the bone marrow transplanted. PCR analysis clearly

showed that the malignant cells contained sequences homologous with the helper virus and did not contain sequences from the retroviral vector. This observation stresses the importance of using supernatant that is free from replication-competent helper virus for human gene therapy studies. Given the unique circumstances surrounding this report, the current packaging systems and assay methods still appear to be safe for human use, although improvements in both would be beneficial.[59]

Although precautions are taken to use the safest retroviral vectors and packaging cell lines available, there is still the chance that replication-competent virus can be transferred to the human genome. Researchers have developed sensitive tests to detect virus contamination. These tests include viral amplification in receptive (permissive) cells, which is 10–1000 times more sensitive than currently used S^+/L^- biologic or reverse-transcriptase assays, and the most sensitive test, PCR, which can detect one infected helper virus out of 100,000 transduced cells.[54-56] Before introduction of the transduced cells into the patient, standard FDA tests for contamination are performed on the producer cell line, the viral supernatant, and the transduced cells themselves. This minimizes the potential for infecting the patient with other pathogens or toxins.[52,53]

There are several additional concerns relating to foreign gene integration into the host genome. Retroviruses and retroviral vectors insert randomly into the chromosomes with a possible preference for transcriptionally active regions.[55,56] The potential problems that may result from this insertion are related to the insertion position and normal function of the original cellular gene. If the retrovirus integrates into a control or coding sequence, or possibly even into untranslated, untranscribed, or intervening sequences of an essential gene, it may cause inactivation or disruption of that gene's normal regulation. These alterations may result in no effect, individual cell death, or malignant transformation.[56,57]

The most important concern is that retrovirus insertion may activate a proto-oncogene or inactivate a tumor suppressor gene, resulting in malignant transformation. The probability of malignant transformation is related to the number of cells infected, the number of integrations per cell, the presence of proto-oncogenes, the role of suppressor genes, the number of cellular changes required to cause malignancy, the virus's natural tropism for host cells, environmental factors, and the efficiency by which these insertions operate. It is estimated that as many as 10 separate factors may be involved in the development of certain malignancies.[56,60] Thus, retroviral-mediated gene transfer, which in some cases is designed to insert only one vector per cell, will have a very low probability of causing all of the cellular changes needed to induce malignant transformation.[56,57,60]

It is known, however, that certain human retroviruses can produce malignancies such as T-cell lymphoma or AIDS. The absolute risk of cancer development with murine retroviruses or murine-derived retroviral gene transfer to humans is very low, but it cannot be accurately determined until more experience is gathered by using these techniques. Also, there is a risk for secondary malignancy development when radiation therapy or many chemotherapeutic agents (e.g., alkylating agents) are used for treating cancer. Whether the risk for secondary malignancy is any higher (if it exists at all) with retroviral-mediated gene transfer is yet to be determined. No evidence of malignant transformation has been seen in any of the humans treated since gene transfer trials began in 1989.[40]

Toxicities of Concurrent Therapies. The potential toxicities associated with other biological agents given to support the growth of the gene-altered cells should also be considered. For instance, if the transduced cells need to be given in the presence of aldesleukin (recombinant human interleukin-2), then consideration must be given to the potential combined toxicities related to aldesleukin and the gene product. Likewise, if the gene-altered cells are to be returned to the patient through BMT, then the adverse effects associated with the high-dose antineoplastic preparative regimen given before BMT should also be addressed. Consideration must also be given to the potential toxicities of the intended gene product. For example, if the gene for tumor necrosis factor (TNF) is being introduced into a lymphocyte, consideration must be given to potential systemic TNF toxicities, even if the therapy is intended to be localized.[51,56]

In the first government-approved trial in humans, the NeoR gene, which has no intrinsic therapeutic properties, was used as a marker to identify transduced cells to demonstrate the safety and feasibility of ex vivo retroviral-mediated gene transfer. In this study, 10 patients with malignant melanoma were treated with NeoR-transduced TIL. As in prior TIL studies, aldesleukin was given to patients concurrently with the TIL to support their in vivo growth.[34,45] Therapy-related adverse effects were no different from those normally seen with TIL plus aldesleukin therapy. Rigorous testing showed that the viral supernatant used for gene transduction and TIL was sterile and contained no helper virus. PCR analysis and reverse transcriptase assays demonstrated no amphotropic helper virus in the infused TIL. Results of Western blot analysis for viral *gag* protein and S^+/L^- assay for virus, performed on the patients' serum multiple times throughout the study up to 180 days after cell infusion, were negative. Thus, it was demonstrated for the first time that ex vivo retroviral-mediated gene transfer into T lymphocytes, under the proper conditions, did not produce evidence of disease after infusion in humans. Similar safety assessments with adenoviral vectors are currently in progress.

Safety Record. The accumulated experience with retroviral-mediated gene transfer from the equivalent of 106 monkey-years and 23 patient-years has demonstrated no adverse effects, no pathologic effects, and

no malignancy development related to gene transfer.[49] However, as with any new experimental therapy, the potential risks associated with human gene therapy, including the risk of cancer development, must be judged against the potential toxicities associated with alternative treatments and disease severity.

Clinical Applications of Gene Transfer and Gene Therapy

The possible applications of human gene therapy to treat human diseases are virtually limitless.[1,2,20,61,62] Initial studies were directed at correcting inherited disorders and were subsequently expanded to better understand and possibly treat malignant diseases. Clinical studies for nongenetic, nonmalignant diseases have recently begun. In some trials (gene-marking studies), cells are genetically marked so that they can be tracked throughout the body to enhance understanding of disease biology (Table 3). In other studies, a gene is transferred as a means of treating a human disease; these studies are referred to as gene therapy studies (Table 4). Gene-marking and gene therapy studies are beginning to span the globe, with ongoing trials in Italy, France, Netherlands, China, England, and Germany.

Genetic Disorders or Disorders with Associated Genetic Component. For only a few of more than 4000 known human genetic disorders have the responsible genes been cloned to allow possible correction with gene therapy.[27,63-66] Clinical gene therapy trials have already been initiated in severe combined immunodeficiency syndrome (SCID) associated with ADA deficiency, hemophilia B, familial hypercholesterolemia associated with a defect in the low-density-lipoprotein (LDL) receptor gene, and cystic fibrosis.

ADA-Deficient SCID. Researchers considered ADA-deficient SCID to most closely fit the criteria for an ideal candidate for genetic therapy.[19,41,42] The first human gene therapy attempt took place on September 14, 1990, in the pediatric intensive care unit at the Warren G. Magnuson Clinical Center of NIH. A four-year-old girl with ADA-deficient SCID and persistent immunodeficiency despite pegademase bovine therapy for more than two years was given a transfusion of her own peripheral-blood T lymphocytes that had been transduced ex vivo using retroviral-mediated gene transfer with the gene encoding normal human ADA.[19,40] It was hoped that restoration of ADA enzyme activity would restore cellular immunity and allow this child to return to a more normal life.

She received 11 infusions over the next two years, resulting in her regaining and maintaining some normal immune functions. Her intracellular ADA concen-

Table 3.
Gene-Marking Studies with the Neomycin Resistance (NeoR) Gene

Month First Patient Started	Institution[a]	Condition	Cells Marked[b]
5/89	NIH	Malignant melanoma	TIL
9/91	St. Jude	Pediatric acute myelogenous leukemia	Bone marrow
12/91	Centre Leon Berard	Malignant melanoma	TIL
1/92	St. Jude	Neuroblastoma	Bone marrow
3/92	Pittsburgh	Malignant melanoma	TIL
5/92	Indiana	Adult acute leukemias	Bone marrow and autologous peripheral blood
7/92	M. D. Anderson	Chronic myelogenous leukemia	Bone marrow and PBSC[c]
9/92	NIH	Multiple myeloma or chronic myelogencus leukemia	Bone marrow and PBSC[c]
12/92	NIH	Breast cancer	Bone marrow and PBSC[c]
2/93	UCLA	Malignant melanoma or renal cell cancer	PBL and TIL ($CD4^+$ and $CD8^+$ subsets)
Pending	Baylor	Liver failure	Hepatocytes
Pending	NIH	HIV[d] infection	Syngeneic $CD4^+$ and $CD8^+$ T lymphocytes[c]
Pending	M. D. Anderson	Chronic lymphocytic leukemia	Bone marrow and PBSC[c]
Pending	Fred Hutchinson	Nonmyeloid malignancies	IL-3 or G-CSF-stimulated PBSC
Pending	St. Jude	Neuroblastoma	Purged and unpurged bone marrow
Pending	St. Jude	Pediatric acute myelogenous leukemia	Bone marrow purged by two different methods[c]
Pending	St. Jude	Bone marrow transplant	EBV-specific cytotoxic T lymphocytes

[a]Full names and locations are National Institutes of Health (NIH), Bethesda, MD; St. Jude Children's Research Hospital, Memphis, TN; Centre Leon Berard, Lyon, France; University of Pittsburgh, PA; Indiana University, Indianapolis; The University of Texas M. D. Anderson Cancer Center, Houston; Baylor University, Waco, TX; University of California–Los Angeles (UCLA); Fred Hutchinson Cancer Center, Seattle, WA.
[b]TIL = tumor-infiltrating lymphocytes, PBSC = peripheral-blood stem cells, PBL = peripheral-blood leukocytes, IL-3 = interleukin-3, G-CSF = granulocyte colony-stimulating factor, EBV = Epstein-Barr virus.
[c]Marked with G1Na and LNL6 NeoR vectors.
[d]HIV = human immunodeficiency virus.

Table 4.
Gene Therapy Studies[a]

Month First Patient Started	Institution[b]	Disease	Transferred Genes	Target or Delivery Cells
9/90	NIH	ADA-deficient SCID	ADA	PBTC or PBSC
1/91	NIH	Malignant melanoma	TNF	TIL
10/91	NIH	Advanced cancer	TNF	Tumor
12/91	Fudan–Changhai	Hemophilia B	Factor IX	Autologous skin fibroblasts
2/92	Leiden	ADA-deficient SCID	ADA	Bone marrow and PBL
3/92	San Raffaele	ADA-deficient SCID	ADA	PBTC and progenitor-enriched bone marrow
3/92	NIH	Advanced cancer	IL-2	Tumor
6/92	Michigan	Malignant melanoma	HLA-B7	Melanoma in vivo via liposomes
6/92	Michigan	Familial hypercholesterolemia	LDL receptor	Hepatocytes
12/92	St. Jude	Relapsed or refractory neuroblastoma	IL-2	Tumor
12/92	NIH	Primary or metastatic brain tumor	HSV-TK	Tumor in vivo
2/93	MSKCC	HLA-A2-positive malignant melanoma or renal cell cancer	IL-2	Allogeneic tumor
2/93	Washington	AIDS-related lymphoma	HSV-TK and HPH	$CD8^+$ HIV-specific cytotoxic T lymphocytes
3/93	Netherlands	ADA-deficient SCID	ADA	Bone marrow
4/93	NIH	Cystic fibrosis	CFTR[c]	Respiratory epithelial cells via direct inhalation
Pending	Rochester	Ovarian cancer	HSV-TK	Ovarian cancer
Pending	Viagene	AIDS	HIV *env*	Fibroblasts
Pending	M. D. Anderson	Lung cancer	Antisense K-*ras* or p53	Tumor
Pending	Pittsburgh	Advanced cancer	IL-4	Autologous fibroblasts and Autologous tumor
Pending	Iowa	Cystic fibrosis	CFTR[c]	Nasal epithelial cells via direct inhalation
Pending	Michigan	Cystic fibrosis	CFTR[c]	Lung segment
Pending	Iowa	Primary or metastatic brain tumor	HSV-TK	Tumor in vivo
Pending	Cincinnati	Cystic fibrosis	CFTR[c]	Respiratory epithelial cells
Pending	Johns Hopkins	Renal cell cancer	GM-CSF	Tumor
Pending	North Carolina	Cystic fibrosis	CFTR[c]	Nasal epithelial cells

[a]ADA = adenosine deaminase deficiency, SCID = severe combined immunodeficiency, PBTC = peripheral-blood T cells, PBSC = peripheral-blood stem cells, TNF = tumor necrosis factor, TIL = tumor-infiltrating lymphocytes, PBL-peripheral-blood lymphocytes, IL-2 = interleukin-2, HLA = human lymphocyte antigen, LDL = low-density lipoprotein, HSV-TK = herpes simplex virus thymidine kinase, HPH = hygromycin phosphotransferase, HIV = human immunodeficiency virus, IL-4 = interleukin-4, CFTR = cystic fibrosis transmembrane conductance regulator, GM-CSF = granulocyte–macrophage colony-stimulating factor.

[b]Full names and locations are National Institutes of Health (NIH), Bethesda, MD; Fudan University and Changhai Hospital (Fudan–Changhai), Shanghai, China; University Hospital, Leiden, Netherlands; San Raffaele Scientific Institute, Milan, Italy; University of Michigan, Ann Arbor; St. Jude Children's Research Hospital, Memphis, TN; University of Rochester, NY; Viagene (a for-profit research company), San Diego, CA; The University of Texas M. D. Anderson Cancer Center, Houston; Memorial Sloan–Kettering Cancer Center, New York, NY; University of Washington, Seattle; University of Pittsburgh, PA; University of Iowa, Iowa City; University of Cincinnati, OH; The Johns Hopkins University, Baltimore, MD; University of North Carolina, Chapel Hill.

[c]Disabled adenovirus construct.

tration rose from undetectable to 20–30% of the normal value. Her T lymphocyte count rose to normal value. Some other indicators of immune status also improved, including antibody response to blood group antigens (isohemagglutinin titers), response to some skin test antigens, and in vitro T lymphocyte responses to influenza and allogeneic cells. She is now doing well, is able to play outdoors and swim in the community pool, suffers fewer infections, and has entered public school. A second patient started treatment in January 1991 and is showing similar laboratory and clinical improvement.[67]

Since T lymphocytes are fully differentiated and therefore have a limited life span, it was thought that the beneficial effects of the transduced cells (if any) would be short-lived and that there would be gaps in the patient's immune repertoire. In the first patient treated, the infusions of transduced T lymphocytes were not given during a six-month period to determine the half-life of the infused cells. The number of peripheral-blood T lymphocytes gradually fell toward baseline over the six months, suggesting that the half-life was at least three months. Intracellular ADA concentrations did not decline during this period. These findings suggested that there is a selective survival advantage for the genetically corrected cells in vivo.

As a possible method of conferring lifelong gene correction, the NIH study has since been amended to transduce monoclonal-antibody-separated $CD34^+$ peripheral-blood stem cells harvested under the influence of filgrastim.[68] The transduced peripheral-blood stem cells will be marked with a different ADA vector, enabling the researchers to determine which cell type, peripheral-blood stem cell or peripheral-blood T lymphocyte, is providing the greatest benefit. A trial using this technique has already begun in Italy, with the first patient enrolled in March 1992.[40,69] It is hoped that stem cell transduction will produce lifelong correction

of the enzyme defect and possibly become a one-shot cure for ADA deficiency and other genetic disorders. Other investigators are pursuing gene transfer into hematopoietic stem cells as well.[18,35,36]

Hemophilia, Thalassemia, and Sickle Cell Anemia. While the work with ADA deficiency has provided invaluable insight into the possibilities for gene therapy, ADA deficiency is exceedingly rare compared with other genetic orders. A group of much more common genetic blood disorders, such as hemophilia, thalassemia, and sickle cell anemia, have been targeted for gene therapy.[70-73] A gene therapy trial for hemophilia B began in December 1991 in Shanghai, China.

Gene therapy approaches to the hemophilias are different from the approaches to ADA deficiency.[70-73] Hemophilias A and B are caused by a variety of mutations occurring in the genes encoding clotting factor VIII or IX, respectively, resulting in clotting factor deficiency. Ideally, the mutant gene would be repaired by splicing it with normal DNA. Although preliminary work has shown that this is possible in vitro, it is highly unlikely that this process will be available for in vivo use given the diversity of mutations encountered. As an alternative, researchers are investigating gene insertion techniques that allow cells to produce the missing factor(s). Although the liver might be the ideal target for correcting these hemophilias, much of the work thus far has been done by using transduced fibroblasts.

Preliminary evidence suggests that adequate factor IX production can be achieved in vivo by using these techniques; however, persistent gene expression is a problem that still needs to be solved. Studies initially done in mice have demonstrated that an immune response can be mounted against the newly produced human protein, indicating that gene replacement efforts may be more beneficial in patients who produce insufficient amounts of protein product, rather than no protein at all.[61] Clinical studies using gene therapy to correct the other genetic blood disorders have not started yet; these diseases present difficult obstacles to overcome because the missing or abnormal protein product comes from a series of complex, tightly regulated, gene-containing clusters and the optimal gene delivery system has not yet been determined.[71,72]

Familial Hypercholesterolemia. A gene therapy trial for the treatment of familial hypercholesterolemia, which affects young children, has recently begun. Familial hypercholesterolemia results from a defect in the LDL-receptor gene. Deficient LDL-receptor production results in a lack of LDL catabolism, causing high plasma concentrations of LDL and total cholesterol. This results in premature development of coronary artery disease. In this study, hepatocytes are removed from the patient and transduced with a retroviral vector containing a human LDL-receptor gene. Studies have demonstrated that this technique is feasible, with a transduction efficiency rate approaching 30%.[21,37,74] The transformed hepatocytes are then able to express sufficient quantities of recombinant LDL-receptor protein on the cell surface. It is hoped that this will serve as an adjunct therapy.[37,58,74] According to a preliminary report on the first patient treated, the transferred gene was functioning in the patient's liver, her plasma cholesterol concentration has fluctuated from 20% to 40% below her baseline values, she has experienced no untoward effects as a result of the therapy, and she was recently started on cholesterol-lowering agents (now that she has LDL receptors).[75]

Cystic Fibrosis and Antitrypsin Deficiency. Cystic fibrosis and antitrypsin deficiency are the two most common genetic pulmonary disorders in the United States.[33,76] Gene therapy may offer a promising approach for long-term treatment for both diseases.[32,33,76] Five cystic fibrosis gene therapy trials have recently been approved.

Cystic fibrosis is a disorder caused by a defect in the gene for the cystic fibrosis transmembrane conductance regulator (CFTR) protein, resulting in altered electrolyte transport in the epithelial cells of the pancreas, gastrointestinal tract, and tracheobronchial tree.[33,76] Alpha-1-antitrypsin is a neutrophil elastase inhibitor, and deficiency results from inadequate α-1-antitrypsin production by the liver.[33] Neutrophil elastase is a protease that can destroy the connective tissue backbone of alveolar walls; thus, antitrypsin deficiency can result in progressive lung tissue destruction and emphysema. Infantile hepatic cirrhosis can also occur with antitrypsin deficiency.[2,33] A possible gene therapy approach to correct these disorders would be to deliver the CFTR or α-1-antitrypsin gene directly into the epithelial cells lining the airways.[32,33] Alternatively, the α-1-antitrypsin gene can be directed toward hepatocytes in a more classic gene replacement attempt.[2]

However, unlike other tissues targeted for gene therapy, lung tissue proliferates very slowly, making it less than suitable for using retroviral vectors. Investigators have developed a technique to directly administer the CFTR or α-1-antitrypsin gene to airway epithelial cells by using an adenoviral vector.[31,33] As mentioned previously, an adenovirus-based vector was chosen because adenoviruses can efficiently infect nondividing lung epithelial cells. When adenovirus-based vectors carrying the normal CFTR gene were tested in cells from patients with cystic fibrosis, the infected cells demonstrated restoration of functional chloride channels.[33] A similar positive finding was demonstrated with vectors carrying the α-1-antitrypsin gene. However, it should be noted that these localized strategies would correct only the pulmonary complications for these disorders and would not affect the hepatic complications associated with antitrypsin deficiency or gastrointestinal complications associated with cystic fibrosis.

Although this technique may pave the way for more direct in vivo gene transfer studies, whether it will work in human lung is yet to be demonstrated. Problems may arise in patients who have been previously exposed to adenovirus infection. If immunity devel-

ops, gene transfer efficiency may be compromised. If repeated inoculations are necessary to provide adequate viral episomes, mild immunosuppression may be necessary, which would be less than ideal in a patient already prone to infections.

Hepatic Disease. A soon-to-begin study will use retroviral-mediated gene transfer to mark hepatocytes as part of a hepatocellular transplant protocol.[77] It is thought that engrafting as little as 5% of normal hepatocytes into a diseased liver may restore enough function to provide time to find a suitable liver donor. Marking the donated hepatocytes with a retroviral vector, such as the NeoR gene, will allow researchers to track the progress of the hepatocytes and possibly optimize surgical techniques.

Other Diseases. Gene therapy is being explored for other diseases. It is closest to clinical trials for certain forms of chronic granulomatous disease (CGD) and Gaucher's disease, a hereditary lack of the enzyme used by lysosomes to break down glucocerebroside.[69,78,79] For patients with CGD, researchers are working to insert the gene responsible for superoxide production into bone marrow or peripheral-blood stem cells.[79] Two approaches are being explored for Gaucher's disease.[69,78] One investigator is working on transducing bone marrow stem cells to produce the deficient enzyme. Another is working on maintaining lowered plasma lipid concentrations by using bioengineered fibroblasts or endothelial cells.[69,78]

Much research is under way to examine the potential applications of gene therapy in treating many other genetic disorders. With the expanding possibility of transducing target tissues in vivo, increasing the efficiency of gene transfer, and specifically directing in vivo delivery of the genes, a dramatic increase in the application of gene therapy to correct genetic disorders should occur within the next 10 years.

Cancer. The discovery and application of biological therapy to treat human cancers has provided insight into the many possible approaches for using gene therapy to diagnose and treat cancer and to monitor cancer therapy.[43,44,80-84] In fact, if cancer is a disorder of somatic-cell genetics resulting in uncontrolled growth, it is clear that gene therapy will have a definite impact on cancer therapy in the future. Perhaps there is no area in which gene-marking studies are more relevant for understanding disease biology.

Gene-Marking Studies. The first human gene-marking study attempted to better define the in vivo distribution and survival of TIL through retroviral-mediated gene transfer.[45] In the first reported cases, it was demonstrated that the marked cells can persist in the circulation for at least 21 days and, in one patient, for up to 189 days. Gene-marked TIL was recovered from tumor deposits up to 64 days after administration. Five additional patients have subsequently been treated, with similar results.[28,44]

The persistence of the gene-marked TIL has prompted the use of gene-marked or "reporter" cells to better understand other aspects of cancer biology (Table 3). Several institutions, including one in France, are using NeoR-transduced TIL in patients with melanoma or renal-cell cancer. While these studies demonstrate an institution's ability to perform gene transfer experiments, some investigators have expanded on the original concept. For example, Lotze et al.[85] at the University of Pittsburgh are using a combination of both interleukin-2 (IL-2) and interleukin-4 (IL-4) to cultivate TIL. They will then determine if this combination alters the transduction efficiency and tumor infiltration. Investigators at the University of California at Los Angeles (UCLA) are marking peripheral- blood leukocytes with one NeoR vector (G1Na) and TIL with a slightly different NeoR vector (LNL6) to quantify tumor infiltration by these two cell types.

Autologous BMT is a possible curative modality for several malignancies. Despite bone marrow removal during remission, marrow purging, and marrow purification, many patients relapse after the transplant. To unravel the complexities of transplantation and to determine the source of relapse in patients treated with autologous BMT for hematological malignancies, such as acute or chronic myelogenous leukemia, or for solid tumors, such as neuroblastoma, investigators will use the NeoR-carrying vector to mark bone marrow cells.[80,82] With increased transduction efficiency and very sensitive detection techniques such as PCR, it is estimated that as few as 100 tumor cells need to be marked in order to detect them in the circulation following transplant.[82] Demonstration that marrow can be the source of relapse in these patients might lead to more efficient purging of the marrow before it is infused, whereas demonstration that the relapse comes from circulating peripheral cells might lead to more rigorous ablative therapy. Data are available from two patients with acute myelogenous leukemia treated at St. Jude Children's Research Hospital (Memphis, TN) who have relapsed after BMT and the NeoR gene marker has been identified in the resurgent blast cells, suggesting that bone marrow obtained during remission can contribute to disease relapse.[87] As a result, a new gene-marking study to compare two different marrow purging techniques was developed and has recently been approved.

Peripheral-blood stem cells are used alone or in conjunction with bone marrow to hasten hematological recovery following bone-marrow ablative chemotherapy. While the clinical effects of using peripheral-blood stem cells are well documented, no studies have definitively determined that these cells are an extra source of marrow reconstitution. Studies suggest that peripheral-blood stem cells can be transduced with the NeoR gene vector.[88] In a series of studies conducted at NIH, patients with chronic myelogenous leukemia, multiple myeloma, or breast cancer will have both their peripheral-blood stem cells and their bone marrow removed and transduced with the NeoR gene before receiving high-dose antineoplastic therapy. Similar to the NeoR marking studies at UCLA, the peripheral-blood stem cells will be marked with a

slightly different NeoR vector than the bone marrow. This will enable the investigators to determine the relative contributions of each of the cell types. They will also be able to determine the source of relapse, should that occur, in each of these studies.

Additional studies at NIH are planned using the multidrug resistance gene-1 (MDR1) to mark peripheral-blood stem cells and bone marrow cells from patients receiving BMT for breast cancer. Murine studies have demonstrated that transduction of the MDR1 gene into bone marrow can confer resistance to paclitaxel and provide in vivo enrichment of transduced cells.[89] If the clinical study is successful, it may be possible to use a dominant selectable marker, whereby researchers can amplify cell clones in vivo that have been cotransduced with the MDR1 gene and an additional therapeutic gene.

Gene Therapy Studies. Many studies are under way involving gene therapy for treatment of malignancies. Novel approaches to treating cancer with gene transfer techniques are summarized in Table 5.[90,82]

Adding new genes to cells to give them new functions can have many applications in cancer therapy. Early work toward developing adoptive immunotherapy with lymphokine-activated killer (LAK) cells and then TIL has provided the foundation for several ongoing human gene therapy trials.[28,44,45] Like a sophisticated drug-delivery system, TIL are being used to deliver foreign therapeutic genes directly to tumors. In the first trial, the gene for tumor necrosis factor (TNF) is inserted into TIL (TNF–TIL). In previous clinical studies, TNF was an ineffective antitumor agent, perhaps because dose-limiting hypotension prevented attainment of sufficient cytotoxic concentrations in vivo. However, animal studies using TNF–TIL have demonstrated that localized TNF concentrations of up to 1000 μg/g of tissue can be achieved (concentrations above 400 μg/g of tissue can result in tumor necrosis). Initially, the RAC allowed administration of TNF–TIL alone; when safety was demonstrated, the investigators were allowed to add systemic aldesleukin in increasing dosages.

Data reported from five patients treated with TNF–TIL alone and TNF–TIL plus aldesleukin revealed that both therapies were safe to give to patients and neither produced TNF-related hypotension as seen with TNF alone. When a tumor-site biopsy obtained from a responding patient was examined, the tumor regression seen was consistent with classic TNF-induced coagulative necrosis and not the lymphocyte infiltration seen with TIL therapy.[28,44] This suggests that a local TNF effect was responsible for tumor regression. However, the merits of this trial have recently been questioned, as it appears that the transduced TIL are unable to uniformly express TNF at the projected amounts necessary for tumor regression and the TNF transduced TIL may have a different distribution pattern compared with that previously demonstrated for untransduced TIL.[90]

Other possible genetic modifications of TIL to improve antitumor activity include the introduction of (1) other immunomodulatory cytokines or proteins, such as α-interferon or γ-interferon, interleukin-1_α, interleukin-6 (IL-6), or interleukin-7; (2) Fc receptor, which mediates antibody-dependent cellular cytotoxicity; (3) chimeric T-cell receptors, which have altered T-cell specificity; and (4) the IL-2 receptor, which makes TIL more sensitive to IL-2.[28,44,84]

Because of the difficulties with gene transfer into T lymphocytes, researchers have been investigating cytokine expression in tumor cells.[83,84] Cytokine genes inserted into tumor cells can make the tumor cells more immunogenic by increasing their recognition by host defenses.[28,44,83,84] These observations, made in murine models using genes for interleukin-1_β, IL-2, IL-4, IL-6, TNF, γ-interferon, or granulocyte–macrophage colony-stimulating factor (GM-CSF), led to several clinical trials in which patients were immunized with their own tumor cells after those cells were modified by ex vivo retroviral-mediated gene transfer.

In Rosenberg's first trial, tumor cells were modified by insertion of the TNF or IL-2 gene.[28,44] Small quantities (less than 2% of the estimated total tumor burden) of these gene-modified tumor cells were then injected subcutaneously into the thigh and intradermally into nearby sites. Three weeks later, the draining lymph nodes were removed and grown in IL-2. The resulting TIL were then given back to the patient with systemic aldesleukin doses, just as in previous TIL protocols.[28,44] Preliminary observations reported from five patients who had completed the first part of the study, in which TNF gene was inserted into tumor cells, suggest that a marked immunologic response can be mounted.

Table 5.
Possible Genetic Therapies for Cancer[a]

- Gene addition
  - To lymphocytes to produce active cytokine within tumor (e.g., TNF or IL-2 gene added to TIL)
  - To tumor cells to make them more immunogenic (e.g., TNF, IL-2, or HLA-B7)
  - To produce new cytotoxic or cytostatic product within tumor (e.g., VDEPT or sensitivity genes)
  - To produce protein product with new function (e.g., bone marrow protection by CSF or MDR1 expression)
  - To introduce tumor suppressor genes (e.g., p53)
- Down-regulation of specific gene expression using informational drugs
  - Antisense oligonucleotides targeted at mRNA
  - Specific ribozymes targeted at mRNA
  - Oligonucleotide-triplex DNA formation targeted at DNA
  - Oligonucleotides targeted at RNA polymerase or transcription factors
  - Proteases targeted at proteins
- Gene replacement for mutant oncogenes or tumor suppressor genes
  - Homologous recombination
  - Excision
  - Gene-function blocker

[a]TNF = tumor necrosis factor, IL-2 = interleukin-2, TIL = tumor-infiltrating lymphocytes, HLA = human lymphocyte antigen, VDEPT = virally directed enzyme prodrug therapy, CSF = colony-stimulating factor, MDR1 = multidrug resistance gene-1, mRNA = messenger RNA. (Adapted from reference 78, with permission.)

against these modified tumor cells.[26,44]

Taking a different approach for increasing tumor immunogenicity, investigators at the University of Michigan will introduce the gene for human lymphocyte antigen (HLA)-B7 directly into tumors in vivo by using DNA–liposome complexes.[24] It has been demonstrated in mice that when a cytotoxic T-cell response is induced, the gene product stimulates immunity to other antigens present on unmodified tumor cells and tumor regression occurs. The University of Michigan trial is one of the first gene therapy studies in which the gene transfection occurs directly in vivo rather than by processing the cells ex vivo and returning them to the patient.

Immunizing patients with their own gene-modified tumor cells can also be considered the first step toward developing a tumor vaccine. While the ongoing studies might provide a method for individualized vaccination, it is envisioned that one day the genes coding for tumor-associated antigens could be inserted into a virus, such as vaccinia, that might serve as a primary or secondary cancer prevention method. Studies are ongoing to identify these tumor-associated antigens and to determine if several tumor types share common antigens.[26,44]

Virally directed enzyme prodrug therapy, sometimes referred to as suicide or sensitivity gene therapy, is a manipulation that takes advantage of proliferative, transcriptional, or enzymatic differences between tumor and normal cells to cause preferential tumor cell death.[80,82,91,92] For one technique, a gene for a drug-activating enzyme (e.g., herpes simplex virus thymidine kinase [HSV-TK]) is inserted into a tumor cell either in vivo or ex vivo.[80,82,91,93,94] The actively dividing tumor cell then expresses the protein product of that gene (e.g., thymidine kinase). Upon uptake of a drug that is activated by this enzyme (e.g., acyclovir or ganciclovir sodium), the tumor cell dies. To restrict gene expression of the drug-activating enzyme to tumor cells, a gene can be constructed that is composed of a tissue-specific transcriptional regulatory sequence (e.g., promoter sequence) adjacent to the sequence coding for the drug-activating enzyme.[91] Thus, if the promoter sequence for α-fetoprotein (hepatoma), prostate-specific antigen (prostate cancer), or carcinoembryonic antigen (colorectal or lung cancer) is adjacent to the gene encoding for a drug-activating enzyme, then normal tumor synthesis of the protein or antigen will result in synthesis of an enzyme that will activate the subsequently administered cytotoxic agent.

A trial recently initiated at NIH in patients with either primary brain tumors or brain metastases secondary to lung cancer, breast cancer, malignant melanoma, or renal cell carcinoma is introducing the gene for HSV-TK directly in situ by using retroviral-mediated gene transfer.[93] It has been demonstrated that only actively dividing cells integrate retroviral vectors and express HSV-TK. In animals, normal neural cells, which have lost their capacity to divide, are spared.[92,94] A trial using the HSV-TK suicide-virus gene concept has also been proposed for patients with ovarian cancer.

Gene addition can also be used to provide an indirect therapeutic advantage by manipulating normal cells to make them more resistant to cytotoxic chemotherapy. As already described, peripheral-blood stem cell and bone marrow-marking studies using the MDR1 gene are planned.[89] Preliminary evidence suggests that cell clones expressing MDR1 are resistant to the effects of cytotoxic drugs and can grow after treatment with these drugs. Patients in these studies will receive either paclitaxel or vinblastine sulfate if they have progressive disease following the bone marrow transplant. If the transplanted cells continue to express MDR1 and the population expands, the investigators expect to see progressively shorter and shorter nadir leukocyte counts with subsequent paclitaxel or vinblastine sulfate treatments. Similarly, it is possible that hematopoietic protective effects can be achieved by transducing hematopoietic stem cells with genes coding for protective cytokines such as GM-CSF, granulocyte colony-stimulating factor, interleukin-3, or stem cell factor.[80] Also, as many tumors result in part from inactive or missing tumor suppressor genes, gene addition therapy might be able to provide these missing protective genes.[95-97]

It is also possible to inhibit specific tumor growth functions at the genetic level by down-regulating the expression of oncogenes by introducing "informational" drugs or compounds with antisense relationships to specific nucleotide sequences. These compounds include oligonucleotides (which can block mRNA, DNA, RNA polymerase, or transcription factor activity), ribozymes (which can cut RNA at a specific target site), or proteases (which can inactivate several essential tumor proteins).[80,92]

Human tumors can result from overexpression of oncogenes, failure to express certain tumor suppressor genes, or point mutations that activate transforming functions.[95,96,98] Another strategy for gene therapy manipulation would be to replace mutant genes with a normal copy of the gene by homologous recombination or by molecularly excising the mutant gene and replacing it with a normal copy.[80,82] Homologous recombination has been shown to work well in vitro, but it is currently too inefficient to use in clinical trials.[80]

In the first attempt to target the genetic basis for cancer, researchers at The University of Texas M. D. Anderson Cancer Center (Houston) will focus on two mutations associated with lung cancer: the K-*ras* oncogene, which is present in 30–40% of lung adenocarcinomas, and the p53 tumor suppressor gene, which is deleted in 50–70% of all lung cancers.[95,97,99] For patients with K-*ras*, the investigators will directly inject a retroviral vector supernatant containing a construct with the mirror image of the K-*ras* mRNA into the tumor. This antisense K-*ras* should prevent the decoding of the K-*ras* message and should stop uncontrolled tumor proliferation. For patients with either a p53 gene mutation or deletion, a correct copy of the p53 gene will be

transfected directly into the tumor. In both cases a murine retrovirus will be used to insert the gene, and animal studies have demonstrated that approximately 50% of tumor cells will integrate this new gene. This is the first attempt to individualize gene therapy based on a patient's specific gene mutation.

While many of the clinical trials using gene transfer techniques to better understand cancer biology or to treat cancer are still in very primitive stages, many more studies will soon be initiated. As we gain more insight into the processes behind the interactions of DNA, RNA, and proteins during transcription and as more oncogenes, tumor suppressor genes, and tumor-associated proteins are discovered, it is likely that we will be able to target cancer treatment directly at the genetic level.

Nongenetic, Nonmalignant Diseases. Many nongenetic, nonmalignant diseases are targeted for gene therapy approaches. Among the most actively pursued areas are HIV infection and cardiovascular conditions. Gene therapy for other diseases are sure to be explored shortly.

Perhaps more is known about the molecular biology surrounding HIV infection and perpetuation than any other infectious disease. Gene therapy strategies will take advantage of this knowledge by either modifying cells to protect them from infection or by targeting transcriptional or translational inhibitors of viral protein production.[46,100-102] In the first approved HIV-related gene therapy trial, researchers at the Fred Hutchinson Cancer Center (Seattle, WA) are using $CD8^+$, HIV-specific, cytolytic T cells transduced with both a marker gene and a suicide gene for patients with HIV-related lymphoma undergoing allogeneic BMT. It is hoped that the high-dose antineoplastic therapy, total body irradiation, and these cytolytic T cells will eradicate all HIV-infected cells in the patient and prevent infection of the healthy marrow, and that the transplanted marrow will repopulate the hematologic lines with HIV-free cells. The gene encoding hygromycin phosphotransferase is being used to mark the cytolytic T cells to follow cell survival. Since these cytotoxic T lymphocytes are known to produce central nervous system toxicity and lymphocytic alveolitis, transduction of the gene for HSV-TK will allow the investigators to ablate the transduced cells with acyclovir or ganciclovir sodium should untoward toxicity occur. In another trial, researchers will genetically alter fibroblasts to manufacture gp160, a protein that is part of the HIV protective envelope.[102]

Investigators have also described techniques to construct retroviral vectors capable of expressing soluble CD4, the cell-surface receptor for HIV binding, thus opening the possibility for the patient's own cells to manufacture this protein to block HIV infection of surrounding cells.[46,100] Researchers are also actively constructing decoy molecules directed at the major HIV-genomic elements, such as reverse transcriptase, transactivating factor (TAT), the TAT-binding area (TAR), or REV (a viral protein required for viral mRNA translation).[100,102] Some researchers have proposed to use the HIV-1 virus itself as a retroviral vector delivery vehicle for transducing anti-HIV genes into target cells, as it has been demonstrated that this vector can enter cells in the same manner that HIV can.[102]

Faraji-Shadan et al.[101] have described a novel technique for intracellular immunization against HIV infection by using antibodies created by immunizing naive B cells with reverse transcriptase or TAT. These selected antibodies, when introduced into the cytoplasm and nucleus, would interfere with viral replication. This technique may be applicable to other retroviral diseases such as adult T-cell lymphoma associated with human T-cell lymphotropic virus type I.[101]

Despite what is known about HIV infection and the overwhelming enthusiasm to use gene therapy to prevent or treat this devastating disease, there are still many unanswered questions and hurdles to overcome. For instance, the critical level of T-cell protection that is needed to confer overall patient protection from the clinical consequences of HIV infection is not known. Nonetheless, HIV infection will continue to be actively pursued for gene therapy.

More people die from cardiovascular disorders than any other disease, making it a natural target area for gene therapy. Vascular grafting is commonly used to alleviate the symptoms associated with vascular blockages due to coronary artery or peripheral vascular disease. In other cases, vascular stents are used to maintain vein patency. While these procedures are initially effective, more than 30% fail because the grafts clot. Researchers are currently investigating methods to engineer endothelial cells to secrete anticlotting compounds, such as TPA.[11,17,39,103-105] Preliminary data suggest that these genes can function in vivo.[104,105] These genetically altered endothelial cells can then be implanted in the graft or stent to prevent clotting. This represents yet another application of gene therapy, that is, to prevent a complication associated with a surgical procedure.

Obstacles To Overcome. Will we be able to cure or treat all diseases with gene therapy? There are still many obstacles to overcome. For instance, progress is slow in developing injectable vectors to simplify foreign gene administration. Perhaps the biggest problem to overcome will be engineering the target cells to be able to regulate the gene expression according to physiologic needs. With diabetes mellitus, for example, it might be possible to engineer cells to secrete a constant amount of insulin and prevent the effects of absolute insulin deficiency.[106] But getting these cells to secrete insulin in response to the individual's diet just as the normal pancreas does is not close to being achieved yet.

Conclusion

The initiation of clinical gene therapy trials has heralded a new age in medicine. From the time the first

human received foreign genes just over four years ago, nearly 40 additional clinical trials have been approved and more than 110 patients have been entered in gene therapy studies. As the human genome is deciphered and more pathologic genes are identified, gene therapy trials will surely expand at a logarithmic rate. Pharmacists should become knowledgeable about gene transfer techniques and possible clinical applications of gene therapy to keep abreast of the newest trends in medicine.

References

1. Blaese RM, Culver KW. Prospects for gene therapy of human disease. *Allergol Immunopathol*. 1991; 19:25-8.
2. Kay MA, Ponder KP, Woo SLC. Human gene therapy: present and future. *Breast Cancer Res Treat*. 1992; 21:83-93.
3. Kelly WN. Gene therapy in humans: a new era begins. *Ann Intern Med*. 1991; 114:697-8. Editorial.
4. Green ED, Waterston RH. The human genome project: prospects and implications for clinical medicine. *JAMA*. 1991; 266:1966-75.
5. Check WA. Impact of gene therapy on the future of pharmacy practice. *Am Pharm*. 1991; NS31(Dec):58-60,63.
6. Thompson MW, McInnes RR, Willard HF. Thompson and Thompson genetics in medicine. 5th ed. Philadelphia: Saunders; 1991.
7. Passaro E, Hurwitz M, Samara G et al. Molecular biology: an overview. *Am J Surg*. 1992; 164:146-52.
8. Chirguin JM. Molecular biology for nonmolecular biologists. *Diabetes Care*. 1990; 13:188-97.
9. Cohen PS, Israel MA. Basic molecular biology for the pediatric hematologist/oncologist. *Am J Pediatr Hematol Oncol*. 1989; 11:467-80.
10. Rodgers JR, Rich RR. Molecular biology and immunology: an introduction. *J Allergy Clin Immunol*. 1991; 88:535-51.
11. Nabel EG, Plautz G, Boyce FM. Recombinant gene expression in vivo within endothelial cells of the arterial wall. *Science*. 1989; 244:1342-4.
12. Gage FH, Rosenberg MB, Tuszynski MH et al. Gene therapy in the CNS: intracerebral grafting of genetically modified cells. *Prog Brain Res*. 1990; 86:205-17.
13. Stockschlaeder MA, Storb R, Osborne WR et al. L-Histidinol provides effective selection of retrovirus-vector-transduced keratinocytes without impairing their proliferative potential. *Hum Gene Ther*. 1991; 2:33-9.
14. Salminen A, Elson HF, Mickley LA et al. Implantation of recombinant rat myocytes into adult skeletal muscle: a potential gene therapy. *Hum Gene Ther*. 1991; 2:15-26.
15. Culver K, Cornetta K, Morgan R et al. Lymphocytes as cellular vehicles for gene therapy in mouse and man. *Proc Natl Acad Sci U S A*. 1991; 88:3155-9.
16. Dichek DA, Bratthauer GL, Beg ZH et al. A genetic therapy for familial hypercholesterolemia. *Trans Assoc Am Physicians*. 1990; 103:73-9.
17. Nabel EG, Plautz G, Nabel GJ. Gene transfer into vascular cells. *J Am Coll Cardiol*. 1991; 17(Suppl B):189B-94B.
18. Einerhand MP, Valerio D. Gene transfer into hematopoietic stem cells: prospects for human gene therapy. *Curr Top Microbiol Immunol*. 1992; 177:217-35.
19. Culver KW, Osborne WRA, Miller AD et al. Correction of ADA deficiency in human T-lymphocytes using retroviral-mediated gene transfer. *Transplant Proceed*. 1991; 23:170-1.
20. Fleischman RA. Southwestern internal medicine conference: human gene therapy. *Am J Med Sci*. 1991; 301:353-63.
21. Versland MR, Wu CH, Wu GY. Strategies for gene therapy in the liver. *Semin Liver Dis*. 1992; 12:332-9.
22. Friedmann T. Progress toward human gene therapy. *Science*. 1989; 244:1275-81.
23. Roemer K, Friedmann T. Concepts and strategies for human gene therapy. *Eur J Biochem*. 1992; 208:211-25.
24. Stewart MJ, Plautz GE, Del Buono L et al. Gene transfer in vivo with DNA-liposome complexes: safety and acute toxicity in mice. *Hum Gene Ther*. 1992; 3:267-75.
25. Ledley FD. Somatic gene therapy in gastroenterology: approaches and applications. *J Pediatr Gastroenterol Nutr*. 1992; 14:328-37.
26. Miller AD. Retrovirus packaging cells. *Hum Gene Ther*. 1990; 1:5-14.
27. Valle D. Treatment of genetic disease: current status and prospects for the future. *Semin Perinatol*. 1991; 15(Suppl 1):52-6.
28. Rosenberg SA. Gene therapy for cancer. *JAMA*. 1992; 268:2416-9.
29. Miller AD. Human gene therapy comes of age. *Nature*. 1992; 357:455-60.
30. Miller DG, Adam MA, Miller AD. Gene transfer by retrovirus vectors occurs only in cells actively replicating at the time of infection. *Mol Cell Biol*. 1990; 10:4239-42.
31. Rosenfeld MA, Yoshimura K, Trapnell BC et al. In vivo transfer of the human cystic fibrosis transmembrane conductance regulator gene to airway epithelium. *Cell*. 1992; 68:143-55.
32. Engelhardt JF, Wilson JM. Gene therapy of cystic fibrosis lung disease. *J Pharm Pharmacol*. 1992; 44(Suppl 1):165-7.
33. Crystal RG. Gene therapy strategies for pulmonary disease. *Am J Med*. 1992; 92(Suppl 6A):44S-52S.
34. Geller AI, Keyomarsi K, Bryan J et al. An efficient deletion mutant packaging system for defective herpes simplex virus vectors: potential applications to human gene therapy and neuronal physiology. *Proc Natl Acad Sci U S A*. 1990; 87:8950-4.
35. Schuening FG. Gene transfer into hematopoietic stem cells. *Curr Top Microbiol Immunol*. 1992; 177:237-45.
36. Nienhuis AW, McDonagh KT, Bodine DM. Gene transfer into hematopoietic stem cells. *Cancer*. 1991; 67(Suppl): 2700-4.
37. Grossman M, Raper SE, Wilson JM. Towards liver-directed gene therapy: retrovirus-mediated gene transfer into human hepatocytes. *Somat Cell Mol Genet*. 1991; 17:601-7.
38. Ledley FD. Clinical application of somatic gene therapy in inborn errors of metabolism. *J Inher Metab Dis*. 1990; 13:597-616.
39. Dichek DA, Neville RF, Zwiebel et al. Seeding of intravascular stents with genetically engineered endothelial cells. *Circulation*. 1989; 80:1347-53.
40. Anderson WF. Human gene therapy. *Science*. 1992; 256:808-13.
41. Hirschhorn R. Adenosine deaminase deficiency. *Immunodefic Rev*. 1990; 2:175-98.
42. Parkman R, Gelfand E. Severe combined immunodeficiency disease, adenosine deaminase deficiency and gene therapy. *Curr Opin Immunol*. 1991; 3:547-51.
43. Freidmann T. Gene therapy of cancer through restoration of tumor-suppressor functions? *Cancer*. 1992; 70(Suppl 6): 1810-7.
44. Rosenberg SA. The immunotherapy and gene therapy of cancer. *J Clin Oncol*. 1992; 10:180-99.
45. Rosenberg SA, Aebersold PA, Cornetta K et al. Gene transfer into humans—immunotherapy of patients with advanced melanoma, using tumor-infiltrating lymphocytes modified by retroviral gene transduction. *N Engl J Med*. 1990; 323:570-8.
46. Morgan RA, Looney DJ, Muenchal DD et al. Retroviral vectors expressing soluble CD4: a potential gene therapy for AIDS. *AIDS Res Hum Retroviruses*. 1990; 6:183-91.
47. Gershon D. RAC defers to NIH director on some gene therapy cases. *Nature*. 1993; 361:196. News.
48. Marwick C. 'Desperate use' gene therapy guidelines ready. *JAMA*. 1993; 269:843. News.
49. Jenks S. RAC approves policy for single-patient use of gene therapy. *J Natl Cancer Inst*. 1993; 85:266-7. News.
50. Subcommittee on Human Gene Therapy. Recombinant DNA Advisory Committee, National Institutes of Health.

Points to consider in the design and submission of protocols for the transfer of recombinant DNA into the genome of human subjects. *Hum Gene Ther.* 1990; 1:93-102.

51. Juengst ET. The NIH "Points To Consider" and the limits of human gene therapy. *Hum Gene Ther.* 1990; 1:425-33.
52. Anon. Points to consider in human somatic cell therapy and gene therapy (1991). *Hum Gene Ther.* 1991; 2:251-6.
53. Epstein SL. Regulatory concerns in human gene therapy. *Hum Gene Ther.* 1991; 2:243-9.
54. Temin HM. Safety considerations in somatic gene therapy of human disease with retrovirus vectors. *Hum Gene Ther.* 1990; 1:111-23.
55. Cornetta K. Safety aspects of gene therapy. *Br J Haematol.* 1992; 80:421-6.
56. Cornetta K. Safety issues related to retroviral-mediated gene transfer in humans. *Hum Gene Ther.* 1991; 2:5-14.
57. Tolstoshev P. Retroviral-mediated gene therapy—safety considerations and preclinical studies. *Bone Marrow Transplant.* 1992; 9(Suppl 1):148-50.
58. Donahue RE, Kessler SW, Bodine D et al. Helper virus induced T cell lymphoma in nonhuman primates after retroviral mediated gene transfer. *J Exp Med.* 1992; 176:1125-35.
59. Anderson WF. What about those monkeys that got T-cell lymphoma? *Hum Gene Ther.* 1993; 4:1-2. Editorial.
60. Moolten FL, Cupples A. A model for predicting the risk of cancer consequent to retroviral gene therapy. *Hum Gene Ther.* 1992; 3:479-86.
61. Verma IM. Gene therapy. *Sci Am.* 1990; 263(5):68-84.
62. Moen RC. Directions in gene therapy. *Blood Cells.* 1991; 17:407-16.
63. Kohn DB, Anderson WF, Blaese RM. Gene therapy for genetic diseases. *Cancer Invest.* 1989; 7:179-92.
64. Cournoyer D, Scarpa M, Jones SN et al. Gene therapy: a new approach for the treatment of genetic disorders. *Clin Pharmacol Ther.* 1990; 47:1-11.
65. Johnson MP, Drugan A, Miller OJ et al. Genetic correction of hereditary disease. *Fetal Ther.* 1989; 4(Suppl 1):28-39.
66. Blaese RM, Culver KW. Gene therapy for primary immunodeficiency disease. *Immunodefic Rev.* 1992; 3:329-49.
67. Blaese RM. Development of gene therapy for immunodeficiency: adenosine deaminase deficiency. *Pediatr Res.* 1993; 33(Suppl):S49-55.
68. Cournoyer D, Scarpa M, Mitani K et al. Gene transfer of adenosine deaminase into primitive hematopoietic progenitor cells. *Hum Gene Ther.* 1991; 2:203-13.
69. Abbott A. Italians first to use stem cells. *Nature.* 1992; 356:465. News.
70. Thompson AR. Status of gene transfer for hemophilia A and B. *Thromb Haemost.* 1991; 66:119-22.
71. Steinberg MH. Prospects of gene therapy for hemoglobinopathies. *Am J Med Sci.* 1991; 302:298-303.
72. Brinkhous KM. Gene transfer in the hemophilias: retrospect and prospect. *Thromb Res.* 1992; 67:329-38.
73. Hoeben RC, Valerio D, van der Eb AJ et al. Gene therapy for human inherited disorders; techniques and status. *Crit Rev Oncol Hematol.* 1992; 13:33-54.
74. Grossman M, Wilson JM. Frontiers in gene therapy: LDL receptor replacement for hypercholesterolemia. *J Lab Clin Med.* 1992; 119:457-60.
75. Randall T. First gene therapy for inherited hypercholesterolemia a partial success. *JAMA.* 1993; 269:837-8. News.
76. Collins FS. Cystic fibrosis: molecular biology and therapeutic implications. *Science.* 1992; 256:774-9.
77. *Fed Regist.* 1991; 56:33183.
78. Watson T. Gene therapy research is spread across many disciplines and institutes at NIH. *Nature.* 1992; 359:188-9.
79. Gallin JI, Malech HL. Update on chronic granulomatous diseases of childhood. *JAMA.* 1990; 263:1533-7.
80. Sikora K. Gene therapy for cancer. *Eur J Cancer.* 1991; 27:1069-70.
81. Merrouche Y, Favrot MC. Retroviral gene therapy and its application in oncohematology. *Hum Gene Ther.* 1992; 3:285-91.
82. Guttierrez AA, Lemoine NR, Sikora K. Gene therapy for cancer. *Lancet.* 1992; 339:715-21.
83. Kinnon C, Levinsky RJ. Gene therapy for cancer. *Eur J Cancer.* 1990; 26:638-40.
84. Russell SJ. Lymphokine gene therapy for cancer. *Immunol Today.* 1990; 11:196-200.
85. *Fed Regist.* 1992; 57:3212.
86. *Fed Regist.* 1992; 57:14775.
87. Brenner MK, Rill DR, Moen RC et al. Gene-marking to trace origin of relapse after autologous bone-marrow transplantation. *Lancet.* 1993; 341:85-6.
88. Bregni M, Magni M, Siena S et al. Human peripheral blood hematopoietic progenitors are optimal targets of retroviral-mediated gene transfer. *Blood.* 1992; 80:1418-22.
89. Surrentino BP, Brandt SJ, Bodine D et al. Selection of drug-resistant bone marrow cells in vivo after retroviral transfer of human MDR1. *Science.* 1992; 257:99-103.
90. Anderson C. Gene therapy researcher under fire over controversial cancer trials. *Nature.* 1992; 360:399-400. News.
91. Huber BE, Richards CA, Krentitsky TA. Retroviral-mediated gene therapy for the treatment of hepatocellular carcinoma: an innovative approach for cancer therapy. *Proc Natl Acad Sci U S A.* 1991; 88:8039-43.
92. Ram Z, Culver KW, Walbridge S et al. In situ retroviral-mediated gene transfer for the treatment of brain tumors in rats. *Cancer Res.* 1993; 53:83-8.
93. Culver KW, Ram Z, Wallbridge S et al. In vivo gene transfer with retroviral vector-producer cells for treatment of experimental brain tumors. *Science.* 1992; 256:1550-2.
94. Moolten FL, Wells JM, Heyman RA et al. Lymphoma regression induced by ganciclovir in mice bearing a herpes thymidine kinase transgene. *Hum Gene Ther.* 1990; 1:125-34.
95. Benz EJ. The molecular genetics of cancer. *Cancer.* 1990; 65:731-41.
96. Bishop JM. Molecular themes in oncogenesis. *Cell.* 1992; 64:235-48.
97. Ozturk M, Ponchel F, Puisieux A. p53 as a potential target in cancer therapy. *Bone Marrow Transplant.* 1992; 9(Suppl 1):164-70.
98. Weinberg RA. Tumor suppressor genes. *Science.* 1991; 254:1138-46.
99. Cherfas J. Gene therapy for lung cancer. *Br Med J.* 1992; 305:792. News.
100. Gilboa E. Retroviral gene transfer: applications to human therapy. *Prog Clin Biol Res.* 1990; 352:301-11.
101. Faraji-Shadan F, Stubbs JD, Bowman PD. A putative approach for gene therapy against human immunodeficiency virus (HIV). *Med Hypotheses.* 1990; 32:81-4.
102. Thompson L. At age 2, gene therapy enters a growth phase. *Science.* 1992; 258:744-6. News.
103. Swain JL. Gene therapy: a new approach to the treatment of cardiovascular disease. *Circulation.* 1989; 80:1495-6. Editorial.
104. Dichek DA, Neville RF, Zwiebel JA et al. Seeding of intravascular stents with genetically engineered endothelial cells. *Circulation.* 1989; 80:1347-53.
105. Wilson JM, Birinyi LK, Salomon RN et al. Implantation of vascular grafts lined with genetically modified endothelial cells. *Science.* 1989; 244:1344-6.
106. Friedmann T. Approaches to gene therapy of complex multigenic diseases: cancer as a model and implications for cardiovascular disease and diabetes. *Ann Med.* 1992; 24:411-7.

COMMONWEALTH OF AUSTRALIA

(Patents Act 1990)

IN THE MATTER OF: Australian Patent Application 696764 (73941/94). In the name of: Human Genome Sciences Inc.

- and -

IN THE MATTER OF: Opposition thereto by Ludwig Institute for Cancer Research, under Section 59 of the Patents Act.

Annexure GBC-14

This is **Annexure GBC-14** referred to in my Statutory Declaration made this Thirteenth day of December 2000.

Gary Baxter Cox

WITNESS: _____

Patent Attorney

secreted by transfected COS or Chinese hamster ovary cells begins at a glycine residue at position 21; the non-glycosylated form has a molecular mass of 12,397 by electrospray mass spectrometry, close to the predicted M_r of 12,399, although it migrates as a 9K protein on SDS–PAGE (Fig. 1*C*).

The production by monocytes of inflammatory cytokines such as IL-1, IL-6 and tumour necrosis factor-α (TNF-α) is a crucial initiating event in a number of infectious and inflammatory pathologies. We have found that IL-13 strongly inhibits IL-6 secretion induced by bacterial lipopolysaccharide (LPS) in peripheral blood mononuclear cells (PBMC) (Fig. 3*a*). IL-13 would appear to be acting directly on monocytes because an inhibition of IL-6 mRNA accumulation is observed rapidly (within 4 hours) in cultures of PBMC enriched in monocytes by adherence to tissue culture dishes (Fig. 3*b*). A marked inhibition is also seen for other inflammatory monokine mRNAs (IL-1β, TNF-α, IL-8, gro-β) in LPS-treated monocytes in the presence of IL-13 (Fig. 3*b*, and other data not shown). The action of IL-13 would thus seem to be a generalized block on inflammatory monokine synthesis, a property shared with the other Th2 lymphokines IL-4 and IL-10 (ref. 13). IL-13 and IL-4 show similar levels of inhibition of IL-6 synthesis (Fig. 3*a*). IL-13 also inhibits production of human immunodeficiency virus (HIV) by tissue-culture differentiated macrophages[14], contrasting with the stimulatory effects of macrophage-activating cytokines such as IL-3 and GM-CSF on HIV production that have been reported in comparable conditions[15].

The production of IFN-γ by large granular lymphocytes (LGL) may direct subsequent immune responses, leading to macrophage activation and to a 'Th1-type' cellular immune response[16]. The major cytokine influencing this production of IFN-γ is IL-2 (ref. 17). We have found that IL-13 has a small, direct effect on IFN-γ synthesis by LGL, and synergizes with both suboptimal and optimal doses of IL-2 (Fig. 3*c*). In this respect it resembles IL-12 (ref. 17), rather than IL-4, which strongly inhibits IFN-γ synthesis by these cells (Fig. 3*c*).

IL-13 also affects B lymphocytes, increasing their proliferation and the expression of the CD23 surface antigen (P. Carayon and T. Defrance, personal communication). IL-13 is thus a highly pleiotropic cytokine. In its anti-inflammatory effects on monocytes and its stimulation of the humoral response through B lymphocytes, IL-13 contributes to the 'Th2-type' response together with IL-4 and IL-10 (refs 18, 19). In, however, its effects on IFN-γ synthesis, it might be expected to promote a 'Th1-type' cellular immune response[16,20]. A full understanding of the cytokine network in different pathological situations now needs to take into account the activities of IL-13.

The anti-inflammatory function of IL-13 may be crucial in clinical inflammation, for example in septic shock[21] or rheumatoid arthritis[22]. Its activity on LGL may be clinically interesting in that, unlike IL-4, it does not decrease and can even increase the IL-2-induced lymphokine-activated killer activity of these cells (our unpublished results). As IL-13 also inhibits HIV replication *in vitro*[14], and systemic immunity to parental tumour cells can be induced by IL-13-secreting tumour cells *in vivo* (D. Fradelizi, personal communication), IL-13 would appear to represent a potentially important new member of the therapeutic cytokine arsenal. □

Received 15 December 1992; accepted 25 February 1993.

1. Lindley, P. S., Clark, E. A. & Ledbetter, J. A. *Proc. natn. Acad. Sci. U.S.A.* **87**, 5031–5035 (1990).
2. Gimmi, C. D. *et al. Proc. natn. Acad. Sci. U.S.A.* **88**, 6575–6579 (1991).
3. Thompson, C. B. *et al. Proc. natn. Acad. Sci. U.S.A.* **86**, 1333–1337 (1989).
4. Morgan, J. G., Dorfanov, G. M., Robbins, S. E., Hinton, L. M. & Lovett, M. *Nucleic Acids Res.* **20**, 5173–5179 (1992).
5. Kozak, M. *Nucleic Acids Res.* **12**, 857–872 (1984).
6. van Heijne, G. *Nucleic Acids Res.* **14**, 4683–4690 (1986).
7. Caput, D. *et al. Proc. natn. Acad. Sci. U.S.A.* **83**, 1670–1674 (1986).
8. Shaw, G. & Kamen, R. *Cell* **46**, 659–667 (1986).
9. Powers, R. *et al. Science* **256**, 1673–1677 (1992).
10. Morrison, B. W. & Leder, P. *J. biol. Chem.* **267**, 11967–11963 (1992).
11. Brown, K. D., Zurawski, S. M., Mosmann, T. R. & Zurawski, G. *J. Immun.* **142**, 679–687 (1989).
12. Chernajovski, H. M., Schumacher, J. H., Brown, K. D. & Mosmann, T. R. *J. exp. Med.* **166**, 1229–1244 (1987).
13. de Waal Malefyt, R., Abrams, J., Bennett, B., Figdor, C. G. & de Vries, J. E. *J. exp. Med.* **174**, 1209–1220 (1991).
14. Montaner, L. J. *et al. J. Cell. Biochem. Abstr. suppl.* **17B**, 94 (1993).
15. Koyanagi, Y. *et al. Science* **241**, 1673–1675 (1988).
16. Scott, P. *J. Immun.* **147**, 3149–3155 (1991).
17. Kobayashi, M. *et al. J. exp. Med.* **170**, 827–845 (1989).
18. Boom, W. H., Liano, D. & Abbas, A. K. *J. exp. Med.* **167**, 1350–1363 (1988).
19. Zlotnik, A. & Moore, K. *Cytokine* **3**, 366–371 (1991).
20. Cher, D. J. & Mosmann, T. R. *J. Immun.* **138**, 3688–3694 (1987).
21. Ohlsson, K., Bjork, P., Bergenfeldt, M., Hageman, R. & Thompson, R. C. *Nature* **348**, 550–552 (1990).
22. Williams, R. O., Feldmann, M. & Maini, R. N. *Proc. natn. Acad. Sci. U.S.A.* **89**, 9784–9788 (1992).
23. Seed, B. & Aruffo, A. *Proc. natn. Acad. Sci. U.S.A.* **84**, 3365–3369 (1987).
24. Dorner, A. J., Bole, D. G. & Kaufman, R. J. *J. cell. Biol.* **105**, 2665–2674 (1987).
25. Devereux, J., Haeberli, P. & Smithies, O. *Nucleic Acids Res.* **12**, 387–395 (1984).
26. Aarden, L. A., DeGroot, E. R., Schaap, O. L. & Lansdorp, P. M. *Eur. J. Immun.* **17**, 1411–1416 (1987).
27. Brake, A. *J. Meth. Enzym.* **185**, 408–421 (1990).
28. Timonen, T., Reynolds, C. W., Ortaldo, J. R. & Herberman, R. B. *J. Immun. Meth.* **51**, 269–277 (1982).

ACKNOWLEDGEMENTS. We thank B. and M. Delpech, M. Goncalves and M. F. Jamme for technical assistance, P. Carayon, M. Magazin, B. Pessegue, and N. Vita for discussion, and P. Ramond for help and advice on DNA sequence comparison.

Correction of the ion transport defect in cystic fibrosis transgenic mice by gene therapy

Stephen C. Hyde, Deborah R. Gill, Christopher F. Higgins* & Ann E. O. Trezise

Imperial Cancer Research Fund Laboratories, Institute of Molecular Medicine, University of Oxford, John Radcliffe Hospital, Oxford OX3 9DU, UK

Lesley J. MacVinish & Alan W. Cuthbert

Department of Pharmacology, University of Cambridge, Tennis Court Road, Cambridge CB2 1QJ, UK

Rosemary Ratcliff, Martin J. Evans & William H. Colledge

Wellcome/CRC Institute of Cancer and Developmental Biology and Department of Genetics, University of Cambridge, Tennis Court Road, Cambridge CB2 1QR, UK

CYSTIC fibrosis (CF) is a lethal inherited disorder affecting about 1 in 2,000 Caucasians. The major cause of morbidity is permanent lung damage resulting from ion transport abnormalities in airway epithelia that lead to mucus accumulation and bacterial colonization. CF is caused by mutations in the cystic fibrosis transmembrane conductance regulator (CFTR) gene[1] that encodes a cyclic-AMP-regulated chloride channel[2,3]. Cyclic-AMP-regulated chloride conductances are altered in airway epithelia from CF patients[4–6], suggesting that the functional expression of *CFTR* in the airways of CF patients may be a strategy for treatment. Transgenic mice[7–9] with a disrupted *cftr* gene are appropriate for testing gene therapy protocols. Here we report the use of liposomes to deliver a *CFTR* expression plasmid to epithelia of the airway and to alveoli deep in the lung, leading to the correction of the ion conductance defects found in the trachea of transgenic (*cf/cf*) mice. These studies illustrate the feasibility of gene therapy for the pulmonary aspects of CF in humans.

Plasmid DNA complexed with cationic liposomes can be successfully delivered and expressed in airway epithelia of rodents[10,11]. A suitable plasmid for expressing CFTR protein was constructed in the vector pREP8 (see legend to Fig. 1). In this plasmid, pREP8-CFTR, the human *CFTR* complementary DNA is under transcriptional control of the constitutive Rous sarcoma virus (RSV) 3′ long terminal repeat (LTR) promoter, known to be active in nonproliferating airway epithelial cells[12]. To show that pREP8-CFTR expresses CFTR protein after

* To whom correspondence should be addressed.

transfection, plasmid DNA complexed with cationic liposomes was introduced into HeLa cells and CFTR protein detected by western blotting (Fig. 1*a*). To ascertain whether the expressed CFTR protein was functional, cAMP-stimulated iodide efflux was measured in transfected cells (Fig. 1*b*). In HeLa cells transfected with pREP8-CFTR, iodide efflux was stimulated by a cAMP-agonist cocktail. The cocktail did not stimulate efflux from cells transfected with the vector pREP8. The characteristics of this cAMP-stimulated anion efflux were similar to those reported previously for CFTR-expressing cells[12,13]. Thus, cells transfected with pREP8-CFTR express functional CFTR protein.

RNA *in situ* hybridization was used to demonstrate that the CFTR expression plasmid can be delivered to airway epithelial cells by liposome-mediated transfection *in vivo*. Because *CFTR* messenger RNA is expressed at high levels in human and rodent intestinal crypts[14–16], mouse intestinal sections were used as controls to demonstrate probe specificity. No hybridization to mouse intestine was detected with either of two human *CFTR* probes whereas, in consecutive sections, the mouse antisense *cftr* probe (but not the sense probe) detected abundant *cftr* mRNA in the crypts (data not shown). Additionally, neither the antisense nor the sense *hisD* vector control probes hybridized with mouse intestinal mRNA, as expected (data not shown). This demonstrates that the human *CFTR* and vector *hisD* probes do not cross-hybridize with mouse *cftr* mRNA.

After transfection of pREP8-CFTR DNA into the airways of mice of 20–28 days old, sequences corresponding to human *CFTR* were detected by *in situ* hybridization (Fig. 2). Strong hybridization signals were observed in isolated groups of airway cells using both the human *CFTR* probe (Fig. 2*a–c*) and the *hisD* vector-specific probe (*d–f*). In a series of consecutive sections the hybridization signals observed with the human *CFTR* and *hisD* probes colocalized to the same airways and airspaces (Fig. 2*a–f*). No hybridization was detected with the mouse *cftr* probe. This provides strong evidence that the hybridization signals obtained are highly specific and due to the transfected plasmid. Hybridization of these same probes to lung sections from untransfected animals served as a negative control against nonspecific hybridization; neither the human *CFTR* probe (*g–i*) nor the *hisD* probe (*j–l*) hybridized to any mRNAs in the lungs of untransfected mice. Hybridization signals were obtained with both the sense and antisense probes (Fig. 2*a–f*). Normally the antisense probe is used to detect mRNA whereas the sense probe serves as a negative control. Following transfection, however, both the sense and antisense probes would be expected to recognize vector DNA. The stronger signal observed with the antisense probe indicates transcription. This was seen for the *hisD* gene which is transcribed from a vector promoter. In most hybridizing cells, the signal obtained with the antisense human *CFTR* probe (Fig. 2*b*) was also greater than that obtained with the sense probe (*c*), implying that human *CFTR* mRNA is expressed following transfection.

The data in Fig. 3 show hybridization to sections through different regions of the lungs of a mouse which had been transfected with pREP8-CFTR. No expression of endogenous mouse *cftr* mRNA was detected in any region of the lung (data not shown), consistent with previous studies showing low-level *cftr* expression in rodent lung[14], and with detailed studies of these transgenic animals (A.E.O.T. *et al.*, manuscript in preparation). This shows that the transfection protocol does not induce expression of endogenous mouse *cftr* mRNA. Human *CFTR*

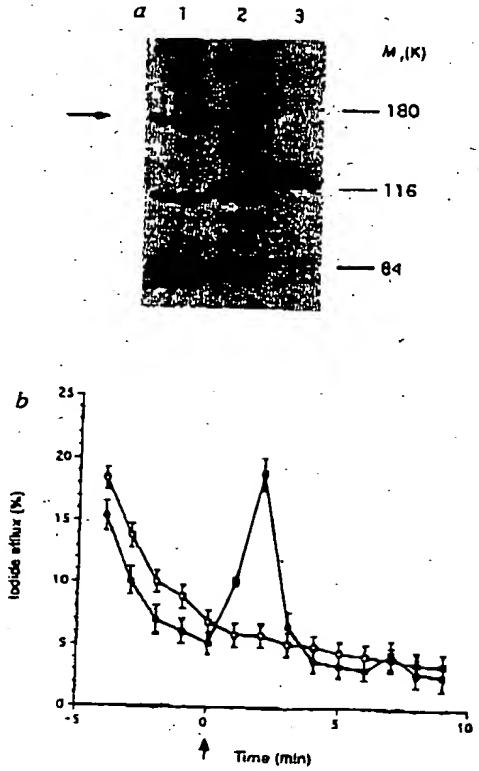

FIG. 1 Expression of functional CFTR protein from plasmid pREP8-CFTR in HeLa cells. *a*, Western blot confirming expression of *CFTR* after transfection of HeLa cells using Lipofectin. Lanes 1, HT29 cells; 2, HeLa cells transfected with pREP8-CFTR; 3, HeLa cells transfected with the vector pREP8. The HT29 cells served as a positive control for *CFTR* expression and migration[25,26], indicated by the arrow. The ~115 and 85K bands are due to nonspecific cross reactions of the antibody[25]. $M_r \times 1{,}000$ of markers is indicated. *b*, Time course of iodide efflux from HeLa cells. Cells were transfected with plasmid pREP8-CFTR (■) or the vector pREP8 (□). The arrow indicates the point at which a cAMP-agonist cocktail was added. The data are displayed as the mean of three individual experiments (±s.e.m.), expressed as a percentage of the total efflux.

METHODS. Human *CFTR* cDNA encoding the entire *CFTR* coding sequence[1] (nucleotides 133–4,620) was inserted into the plasmid pREP8 (Invitrogen), under transcriptional control of the RSV 3′ LTR promoter, to create plasmid pREP8-CFTR. The cDNA incorporated three minor changes from the published sequence (C to G at nucleotide 1368[13]; T to C at nucleotide 936[27]; A to C at nucleotide 1990[28]), and included a Kozak translation initiation sequence[29] (CCACCATG) immediately 5′ to the translation initiation codon. For plasmid transfection, 1×10^6 HeLa cells were seeded into each well of 35-mm, 6-well tissue culture dishes in Dulbecco's modified Eagles medium supplemented with 10% fetal calf serum, and incubated at 37 °C. After 24 h growth, cells in each well were transfected with 8 μg plasmid DNA mixed with 13 μg Lipofectin (Gibco BRL) and diluted to 3 ml in Optimem 1 (Gibco BRL). After a further 24–48-h incubation at 37 °C, cells were either collected for protein extraction or used for anion efflux measurements. For protein extraction, cells were washed five times with ice-cold PBS and collected into a buffer containing 10 mM Tris–Cl pH 8.0, 10 mM KCl, 1.5 mM $MgCl_2$, and the protease inhibitors antipain (50 μg ml^{-1}), aprotinin (10 μg ml^{-1}), benzamidine (310 μg ml^{-1}), leupeptin (5 μg ml^{-1}), pepstatin A (5 μg ml^{-1}) and phenylmethylsulphonyl fluoride (175 μg ml^{-1}). Cells were lysed by repeated passage through a 19-gauge needle. Cellular and nuclear debris were removed from the lysate by a 5-min centrifugation at 300*g* and membranes pelleted by a 30-min centrifugation at 100,000*g*. The membrane pellet was dissolved in 2.5% Triton X-100 and separated by electrophoresis on a 6% SDS-polyacrylamide gel. CFTR was detected by western blotting after transfer to a Hybond C-super membrane (Amersham) using the well characterized anti-CFTR antisera 181[25]. Immunodetection was by enhanced chemiluminescence (ECL; Amersham). To measure cAMP-stimulated efflux, the transfected cells were preloaded with iodide by incubation for 40 min at room temperature in 3 ml loading buffer (136 mM NaI, 3 mM KNO_3, 2 mM $Ca(NO_3)_2$, 11 mM glucose, 20 mM HEPES, pH 7.4). Extracellular NaI was removed by 6 × 1 ml rinses in efflux buffer (loading buffer with 136 mM $NaNO_3$ replacing the NaI). Cells were then washed with 1 ml efflux buffer for 1 min using a sample-replace procedure. After the fifth 1-min sample (designated time 0), cAMP-agonists (1 mM 3-isobutyl-1-methylxanthine (IBMX), 200 μM dibutyryl-cAMP, 10 μM forskolin, dissolved in DMSO) were included in the efflux buffer. The concentration of iodide in each 1-ml aliquot was determined using an iodide-specific electrode (HNU systems).

expression was seen in the airways of three out of four animals transfected with pREP8-CFTR and, in at least one transfected animal, human *CFTR* sequences were detected in all five lobes of the lung. Positive cells were detected in large and small airways (Fig. 2*a–d*), and in cells lining the air spaces of the more distal regions of the lung (*e–j*). It appeared to be the surface epithelial cells of the airways that had been transfected. Colocalization of the *CFTR* signal with the *hisD* probe (Fig. 2), confirmed that the signal was a consequence of transfection. Thus, transfection is effective and expression of human *CFTR* throughout the airway was achieved.

To determine whether delivery of *CFTR* cDNA to the airways could correct the ion transport defects apparent in CF, we used a recently developed mouse model[9,17]. These transgenic (*cf/cf*) mice are homozygous for a null mutation in *cftr* and express little or no detectable endogenous *cftr* mRNA (A.E.O.T. *et al.*, manuscript in preparation). CFTR-dependent, cAMP-stimulated chloride conductances are greatly reduced in the airways

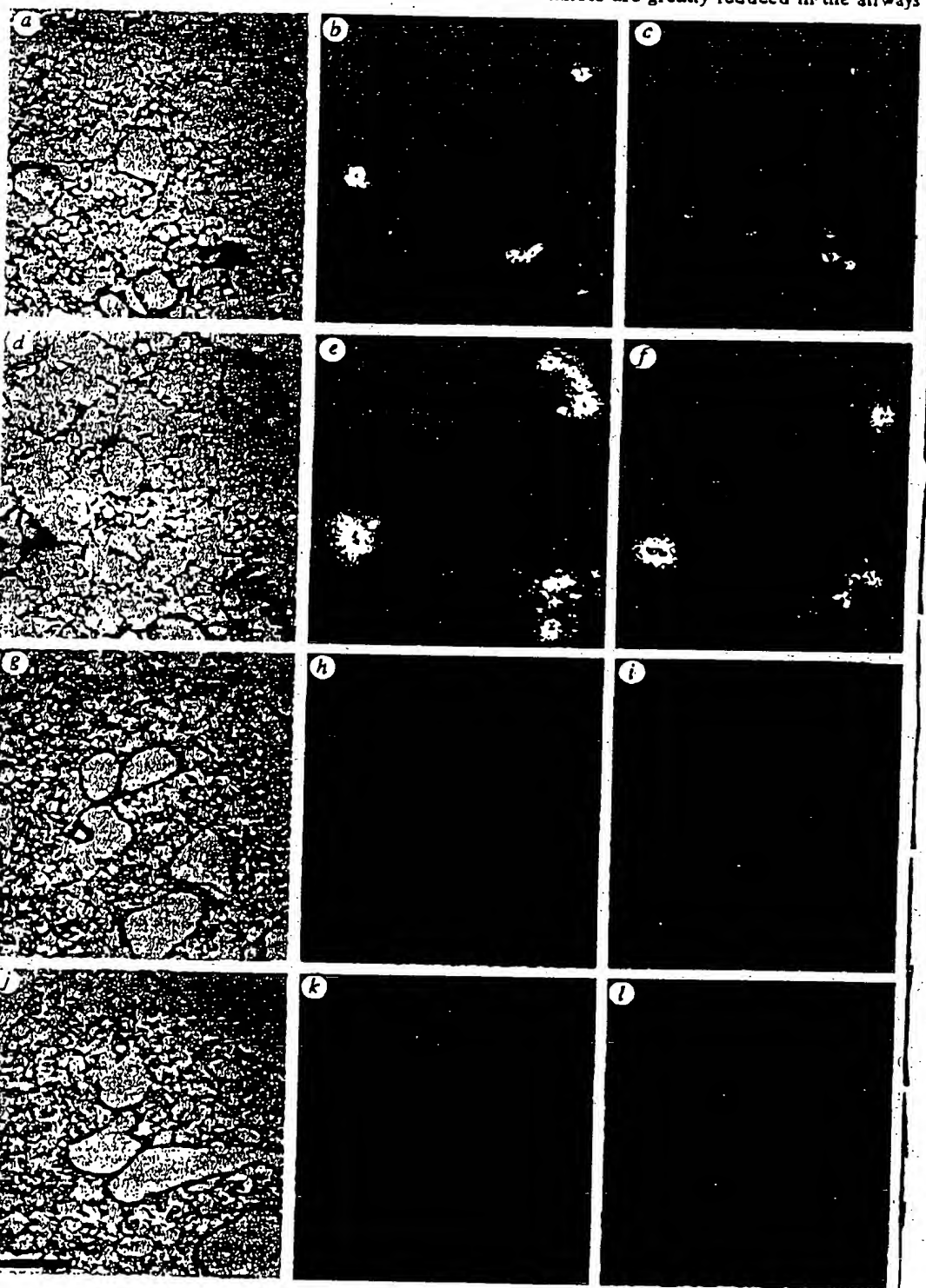

FIG. 2 Detection of human CFTR by *in situ* hybridization in mouse airways following *in vivo* transfection. *a–l*, Data obtained for a mouse transfected with pREP8-CFTR; *G–l*, controls for an untransfected mouse. The probes used were against human *CFTR* exons 1–6 (*a–c* and *g–i*) or the *hisD* vector sequences (*d–f* and *j–l*). For each example, three panels are shown: (1) a brightfield view of a section hybridized with the antisense probe, to illustrate tissue morphology (*a, d, g, j*); (2) a darkfield view of the same section (*b, e, h, k*); (3) a darkfield view of an adjacent section probed with the control sense probe (*c, f, i, l*). Scale bar, 200 μm. Similar results were obtained with several animals.

METHODS. Mice were given enough avertin by intraperitoneal injection to induce very light anaesthesia. For transfection, ~100 μg plasmid DNA was mixed with 25 μg Lipofectin in a total volume of 50 μl and administered to mice by tracheal instillation in two loads by insertion of a metal applicator, adapted from a 25-gauge blunted syringe needle, through the mouth and into the trachea to the point where the main bronchi branch off. The animals used weighed between 5 g and 12 g. Four days after transfection, *in situ* hybridization was performed on perfusion-fixed tissue by a modification of the method described by Simmons *et al.*[30], as described previously[15]. ^{35}S-labelled RNA probes were synthesized *in vitro* by run-off transcription from plasmid DNA, incorporating [^{35}S]UTP. The antisense and sense (control) probes were derived from opposite strands of the same plasmid. The plasmids used for probe generation were as follows. The two human *CFTR* probes, corresponding to nucleotides 62–645 (exons 1–8) and nucleotides 1,977–2,461 (exon 13) (numbering according to ref. 1), have been described previously[16]. The mouse cftr probes were derived by reverse transcriptase PCR from mouse testis mRNA and corresponded to nucleotides 305–691 of exons 3–5. The *hisD* vector probe was subcloned from pREP8 and corresponded to nucleotides 3,167–3,851. All probes were cloned into Bluescript vectors (Stratagene). After developing, sections were counterstained with haematoxylin and eosin and photographed using an Microphot FX microscope.

and caeca of these mice, compared with normal (+/+) animals, mimicking features of the human disorder[17]. The mice frequently die shortly after birth as a consequence of intestinal blockages[8]. Ion transport in the trachea was measured by voltage clamping at zero potential, using pharmacological agents to eliminate or stimulate various processes (Fig. 4). Measurements were also made with the caecum of the same animal as an internal control. Figure 4*A* shows a set of typical results, and Fig. 4*B* a compilation of the data. For each tracheal preparation, three measurements were made: amiloride-sensitive sodium absorption (labelled Na^+), cAMP-stimulated chloride secretion (labelled Cl^- cAMP), and Ca^{2+}-stimulated chloride secretion (labelled Cl^- Ca^{2+}). As expected, CFTR-dependent, cAMP-stimulated chloride secretion was significantly reduced ($P < 0.01$) in both the tracheas and caeca of the *cf/cf* mice compared with the normal (+/+) mice. There was no significant difference in the cAMP-stimulated chloride secretion between untreated and pREP8-transfected normal mice, indicating that transfection itself has no effect on ion transport. Most importantly, transfection of *cf/cf* mice with pREP8-CFTR restored the cAMP-stimulated chloride secretion in the trachea to a level comparable with that of normal (+/+) animals. In sharp contrast, transfection of the *cf/cf* mice with the vector pREP8 had no significant effect on the cAMP-stimulated chloride secretion in the trachea. The caecum of *cf/cf* mice transfected with pREP8-CFTR showed no appreciable cAMP-stimulated chloride secretion

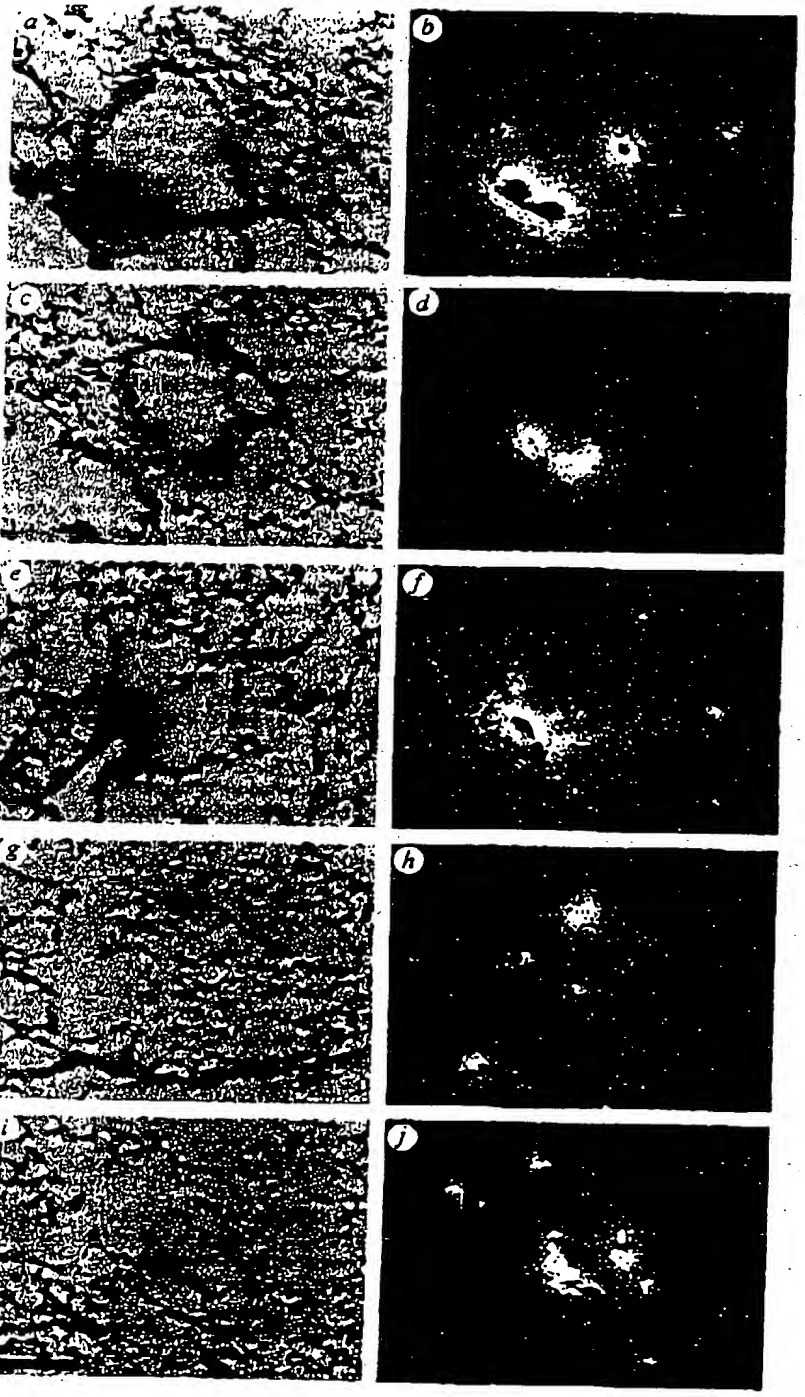

FIG. 3 Detection of human CFTR in different regions of the mouse airway following transfection. Sections from different regions of the airway of a mouse transfected with pREP8–CFTR were hybridized with human antisense *CFTR* probes corresponding to either exons 1–6 (*a–f, i, j*) or exon 13 (*g* and *h*). *a–d* Expression of human *CFTR* in small and large airways; *e–j* expression in airspaces in the more distal regions of the lung. Some variation was found in the proportion of cells transfected in different animals which probably reflects differences in the amounts of DNA delivered. Scale bar, 100 μm. See legend to Fig. 2 for details of methods and hybridization probes.

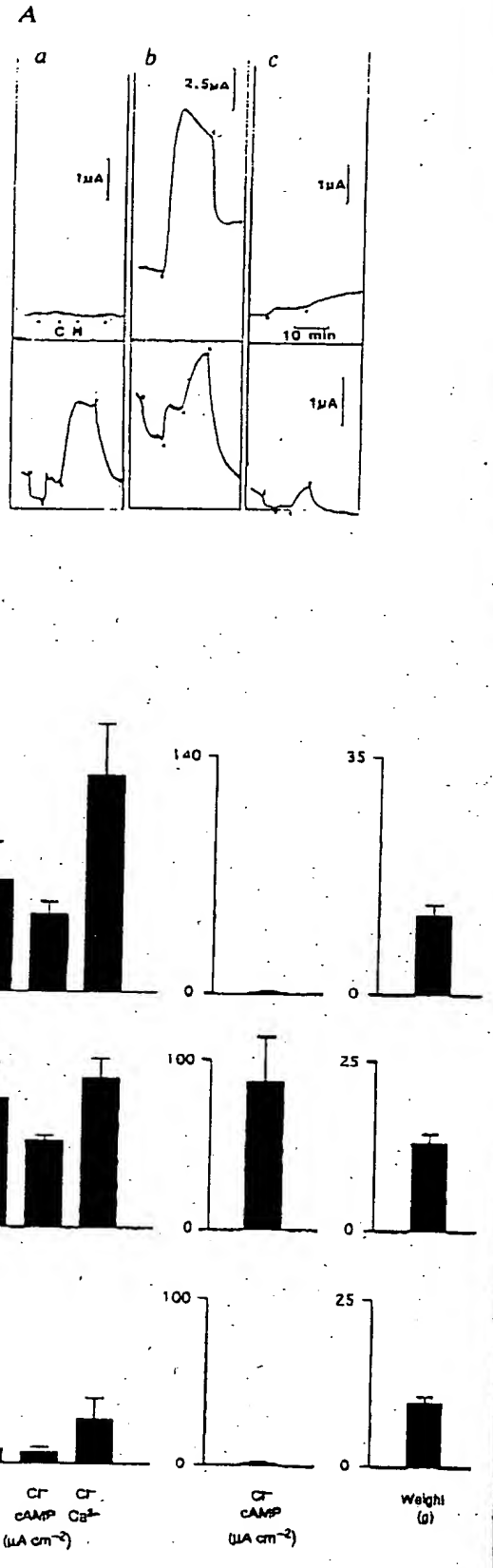

FIG. 4 Correction of the ion channel defects in the trachea of transgenic (*cf/cf*) mice. *A*, Sample traces showing examples of the data from which panel *B* was compiled. Three paired tracheal/caecal preparations are shown. Upper records show measurements for the caecum and lower records for the trachea of the same animal. *a*, *cf/cf* mouse transfected with pREP8-CFTR; *b*, +/+ mouse transfected with pREP8; *c*, *cf/cf* mouse transfected with the vector pREP8. Four additions were made to each of the tracheal preparations at the time points indicated by dots. First, amiloride (100 μM) was added (apically) to block electrogenic sodium absorption and to ensure subsequent current increases were not due to this activity. EC_{50} for amiloride is ~1 μM and 100 μM will give essentially 100% inhibition[31]. Second, forskolin (10 μM) was added to both sides of the membrane to stimulate adenylate cyclase and activate cAMP-sensitive chloride channels, increasing chloride secretion. Third, the Ca^{2+} ionophore A23187 (1 μM) was added to both sides of the membrane to activate Ca^{2+}-dependent chloride secretion. The ionophore-induced responses were much slower than those induced by forskolin. Finally, frusemide (1 mM) was added basolaterally to block chloride secretion, confirming the nature of the electrogenic transporting activity. Frusemide (1 mM) inhibits over 90% of Cl^- secretion[17]. Calibrations for the trachea are the same in each panel. Caecal preparations (upper records) received two additions, forskolin (10 μM, added to both sides of the membrane) and frusemide (1 mM, added basolaterally). Other additions are specifically labelled: C, carbachol (10 μM); H, histamine (10 μM). In both the caecum and the trachea the chloride secretory responses were inhibited by frusemide, indicating that they are due to electrogenic chloride secretion from the basolateral to the luminal side of the epithelium. In 8 out of 10 *cf/cf* caeca, frusemide led to a slight increase in short-circuit current (SSC) (*c*, upper record); this is probably due to a blockage of K^+ secretion and is typical of the caecum of *cf/cf* mice[17]. *B*, Compilation of the data. Mice were subjected to three different treatment protocols: *a*, *cf/cf* mice transfected with pREP8-CFTR; *b*, +/+ mice transfected with the vector pREP8; *c*, *cf/cf* mice transfected with the vector pREP8. Four animals in each group were matched based on a compromise between weight and age. Data were only included when paired airway and caecal measurements could be made for the same animal. The genotypes of the transfected mice, and of the plasmid DNA with which they were transfected, was unknown at the time the measurements were made. For each treatment regime, three sets of data are shown. (1) The left hand columns show SCC measurements for the trachea. Three measurements of SCC changes are presented: Na^+, amiloride-sensitive sodium absorption[31]; Cl^- cAMP, SCC change induced by forskolin, presumed to reflect CFTR function[17,32]; Cl^- Ca^{2+}, SCC change induced by the addition of the calcium ionophore A23187. As about 50% of the basal current in the airways was due to sodium absorption, chloride secretion was measured after the addition of amiloride (100 μM) which abolished electrogenic sodium absorption. (2) The central columns show SCC measurements for the caecum. Only cAMP-sensitive chloride secretion (Cl^- cAMP), induced by the addition of forskolin (10 μM), was measured: Amiloride was not added because the caecum shows no sodium absorptive current[17,33]. (3) The right-hand columns show the weights of the animals used (mean ± s.e.m.). Note: the ion transport characteristics of 4/6 pREP8-CFTR transfected *cf/cf* mice were altered by transfection; the reason for the failure of the other two mice is almost certainly failure in delivery. Nevertheless, the forskolin-sensitive SCC (Cl^- cAMP) in the whole group including the two failures (9.2 ± 2.6 μA cm^{-2}, $n = 6$) was significantly greater ($P < 0.05$, Mann and Witney test) than the value for *cf/cf* mice (1.9 ± 0.5 cm^{-2}, $n = 4$). Finally, data for two other groups of animals were obtained although these are not illustrated in the figure. Untreated, wild-type (+/+) mice ($n = 5$; weight ±s.e.m. = 32.2 ± 2.9 g) had transport parameters as follows (mean ± s.e.m.): for the trachea Na^+ = 10.7 ± 4.8 μA cm^{-2}, Cl^- cAMP = 11.4 ± 4.3 μA cm^{-2}, Cl^- Ca^{2+} = 12.1 ± 4.7 μA cm^{-2}; for the caecum Cl^- cAMP = 35.6 ± 7.0 μA cm^{-2}. Heterozygous (cf/+) mice transfected with pREP8-CFTR ($n = 2$; mean weight, 7.0 g) had the following transport parameters (mean ± s.e.m.): for the trachea: Na^+ = 4.5 μA cm^{-2}, Cl^- cAMP = 6.6 μA cm^{-2}, Cl^- Ca^{2+} = 8.2 μA cm^{-2}; for the caecum Cl^-cAMP = 104.6 μA cm^{-2}. Note that the forskolin-sensitive currents (Cl^- cAMP) in the trachea were smaller than those reported previously for wild-type mice[17]. This is undoubtedly a consequence of edge damage caused by using only 2.27 mm^2 areas of trachea in the present study, necessitated by the small size of the *cf/cf* mice, compared with 4 mm^2 areas of trachea in previous studies.

METHODS. Transgenic mice were genotyped by PCR and/or Southern blot analysis as described[17]. Introduction of plasmid DNA into the mouse airways was as described in the legend to Fig. 2. Trachea and caeca were removed from the transfected animals killed by exposure to 100% CO_2. A single tracheal preparation (2.27 mm^2) and a single caecal preparation (20 mm^2) was prepared from each animal. The reduction in tracheal area, compared with a previous report[17] was due to the necessity of using animals as small as 5 g. The trachea were cleaned and cut longitudinally along the dorsal surface and a piece placed under microscopic control in a specially constructed Ussing chamber designed to preserve the curvature of the tissue. Electrogenic ion transport was measured directly as SCC recorded by voltage clamping the tissue at zero potential, as described previously[17].

compared with the control (+/+) mice, confirming the genotypes of the mice and that the transfection procedure did not affect the gut. Thus, the transfection procedure used can restore CFTR-dependent, cAMP-stimulated chloride secretion by airway epithelia to normal levels.

In the airways of human CF patients there is an increase in amiloride-sensitive sodium absorption, as well as a decrease in chloride secretion, compared with controls[18–20]. It has been suggested that this is crucial to the development of the disease state, as application of amiloride by aerosol alleviates the decline in lung function in CF[21,22]. It is not yet clear how a loss of CFTR function leads to this increase in sodium absorption. In contrast to the human, sodium absorption was reduced in the airways of *cf/cf* mice (Fig. 4*B*). Transfection of the *cf/cf* mice with pREP8-CFTR, but not with the vector pREP8, significantly increased sodium absorption (seven- to eightfold; $P < 0.05$), to essentially wild-type (+/+) levels (Fig. 4*B*). Thus, secondary alterations in sodium transport were also corrected to wild-type levels by the transfection protocol used. Finally, Ca^{2+}-induced chloride secretion reflects an alternative pathway for chloride secretion in the airways distinct from the CFTR pathway[4,23]. Ca^{2+}-stimulated chloride secretory currents were not defective in *cf/cf* trachea, compared with trachea of normal (+/+) mice, but were significantly increased following transfection with *CFTR* ($P < 0.05$; Fig. 4*B*). This latter increase is probably a consequence of hyperpolarization through Ca^{2+}-sensitive K^+ channels, which increases the electrochemical gradient for Cl^- exit through the introduced CFTR channels and the pre-existing second pathway[24].

These data show that the ion transport defects in CF can be corrected *in vivo*. Liposomes, which in clinical trials have been shown to be non-toxic and non-immunogenic, may be safer than viral vectors which have the inherent risks of immunogenicity, replication and transmission. Our results illustrate the invaluable role of transgenic null *cf/cf* mice in assessing the efficiency of various gene therapy approaches. We have shown that functional expression of CFTR not only corrects the primary ion transport defect of the trachea (that is, the cAMP-stimulated chloride secretion), but also corrects secondary alterations in sodium absorption which are a consequence of loss of CFTR function. There seems to be no reason why this approach should not be transferable to humans for the treatment of the pulmonary features of CF. □

Received 4 February; accepted 23 February 1993.

1. Riordan, J. R. *et al. Science* **245**, 1066–1073 (1989).
2. Anderson, M. P. *et al. Science* **253**, 202–205 (1991).
3. Bear, C. E. *et al. Cell* **68**, 809–818 (1992).
4. Anderson, M. P. & Welsh, M. J. *Proc. natn. Acad. Sci. U.S.A.* **88**, 6003–6007 (1991).
5. Wagner, J. A. *et al. Nature* **349**, 793–796 (1991).
6. Chan, H-C., Goldstein, J. & Nelson, D. J. *Am. J. Physiol.* **262**, C1273–C1283 (1992).
7. Snouwaert, J. N. *et al. Science* **257**, 1083–1088 (1992).
8. Dorin, J. R. *et al. Nature* **359**, 211–215 (1992).
9. Colledge, W. H., Ratcliff, R., Foster, D., Williamson, R. & Evans, M. J. *Lancet* **340**, 680 (1992).
10. Yoshimura, K. *et al. Nucleic Acids Res.* **20**, 3233–3240 (1992).
11. Sandling, R., Brunette, E., Light, D., Gaensler, K. & Debs, R. *Proc. natn. Acad. Sci. U.S.A.* **89**, 11277–11281 (1992).
12. Drumm *et al. Cell* **62**, 1227–1233 (1990).
13. Kartner, N. *et al. Cell* **64**, 681–691 (1991).
14. Trezise, A. E. O. & Buchwald, M. *Nature* **353**, 434–437 (1991).
15. Trezise, A. E. O. *et al. EMBO J.* **11**, 4291–4303 (1992).
16. Trezise, A. E. O., Chambers, J. A., Wardle, C. J., Gould, S. & Harris, A. *Hum. molec. Genet.* (in the press).
17. Ratcliff, R. *et al. Nature Genet.* (in the press).
18. Boucher, R. C., Stutts, M. J., Knowles, M. R., Cantley, L. & Gatzy, J. T. *J. clin. Invest.* **78**, 1245–1252 (1986).
19. Cotton, C. U., Stutts, M. J., Knowles, M. R., Gatzy, J. T. & Boucher, R. C. *J. clin. Invest.* **79**, 80–85 (1987).
20. Knowles, M. R. *et al. Science* **221**, 1067–1070 (1983).
21. Knowles, M. R. *et al. N. Engl. J. Med.* **322**, 1189–1194 (1990).
22. App, E. M. *et al. Am. Rev. resp. Dis.* **141**, 605–612 (1990).
23. Williamson, N. J. & Boucher, R. C. *Am. J. Physiol.* **256**, C726–C733 (1989).
24. McCann, J. D., Matsuda, J., Garcia, M., Kaczorowski, G. & Welsh, M. J. *Am. J. Physiol.* **258**, L334–L342 (1990).
25. Crawford, I. *et al. Proc. natn. Acad. Sci. U.S.A.* **88**, 9262–9266 (1991).
26. Zeitlin, P. L. *et al. Proc. natn. Acad. Sci. U.S.A.* **88**, 1344–1347 (1991).
27. Cheng, S. H. *et al. Cell* **63**, 827–834 (1990).
28. Gregory, R. J. *et al. Nature* **347**, 382–386 (1990).
29. Kotin, M. *Cell* **64**, 283–292 (1966).
30. Simmons, D. M., Arriza, J. L. & Swanson, L. W. *J. Histochem.* **12**, 169–181 (1989).
31. Cuthbert, A. W., Drayden, D. J., Dunne, A., Smyth, R. L. & Wallwork, *J. Br. J. clin. Pharm.* **29**, 227–234 (1990).
32. Clarke, L. L. *et al. Science* **257**, 1125–1128 (1992).
33. Smith, S. N., Alton, E. W. F. W. & Geddes, D. M. *Clin. Sci.* **82**, 667–672 (1992).

ACKNOWLEDGEMENTS. We thank S. Tucker for advice on the use of the iodide electrode, C. Wardle for advice on western blotting and A. Harris for helpful discussions. A.E.O.T. is a Bell Memorial Fellow, C.F.H. is a Howard Hughes International Research Scholar. This work was funded by the Wellcome Trust, the Cystic Fibrosis Research Trust and the Imperial Cancer Research Fund.

Germ-line transmission and expression of a human-derived yeast artificial chromosome

Aya Jakobovits, Amy L. Moore, Larry L. Green, German J. Vergara, Catherine E. Maynard-Currie, Harry A. Austin & Sue Klapholz

Cell Genesys Inc., 322 Lakeside Drive, Foster City, California 94404, USA

INTRODUCTION of DNA fragments, hundreds of kilobases in size, into mouse embryonic stem (ES) cells would greatly advance the ability to manipulate the mouse genome. Mice generated from such modified cells would permit investigation of the function and expression of very large or crudely mapped genes. Large DNA molecules cloned into yeast artificial chromosomes (YACs) are stable and genetically manipulable within yeast[1], suggesting yeast-cell fusion as an ideal method for transferring large DNA segments into mammalian cells. Introduction of YACs into different cell types by this technique has been reported[2–4]; however, the incorporation of yeast DNA along with the YAC has raised doubts as to whether ES cells, modified in this way, would be able to recolonize the mouse germ line[5]. Here we provide, to our knowledge, the first demonstration of germ-line transmission and expression of a large human DNA fragment, introduced into ES cells by fusion with yeast spheroplasts. Proper development was not impaired by the cointegration of a large portion of the yeast genome with the YAC.

Yeast spheroplasts, carrying yHPRT, a 670 kilobase (kb) YAC containing the human hypoxanthine phosphoribosyltransferase (HPRT) gene[4], were fused with the HPRT-deficient ES cell line E14TG2a (ref. 9). Clones expressing the HPRT locus were selected in hypoxanthine/aminopterin/thymidine (HAT) medium (Fig. 1 legend) and expanded. The human HPRT gene was detected by hybridization in all ES cell clones analysed (not shown). The integration of additional human sequences was examined by comparing the *Alu* profile of 37 HAT-resistant (ESY) clones to that of yHPRT in yeast. Most, if not all, of the 30 *Alu* fragments characteristic of yHPRT were present and of similar relative intensity in over 90% of the ESY clones (Figs 1*a*, 3*B*). In clones with an incomplete *Alu* profile (such as ESY 8-5, Fig. 1*a*) only a few fragments were missing or altered in size. In most ESY clones, the *Alu* pattern appeared to be intact and without significant deletion, rearrangement or segmental amplification.

Integration of YAC vector sequences was investigated with vector arm-specific probes. A 4.5 kb *Hin*dIII fragment, detected by the right arm probe in yHPRT, was observed in 10 of 20 ESY clones (Fig. 1*b*). This vector arm was lost in eight ESY clones (for example ESY 3-1, 3-6, Fig. 1*b*) and rearranged in two (for example ESY 8-6, Fig. 1*b*). The left arm probe detected the 3 kb and 4.1 kb *Hin*dIII yHPRT fragments in 18 of 20 clones (Fig. 1*c*). In total, 8 of the 20 clones (such as ESY 5-2, 8-7, 7-3, Fig. 1*a–c*) contained complete *Alu* profiles and both intact YAC vector arms.

The structural integrity of yHPRT in ESY clones 5-2 and 8-7 was further evaluated by pulsed-field gel electrophoresis. In yeast carrying yHPRT, five *Sfi*I fragments of the following rough sizes were defined by different probes: 315 kb (*Alu*, left arm),

COMMONWEALTH OF AUSTRALIA

(Patents Act 1990)

IN THE MATTER OF: Australian Patent Application 696764 (73941/94). In the name of: Human Genome Sciences Inc.

- and -

IN THE MATTER OF: Opposition thereto by Ludwig Institute for Cancer Research, under Section 59 of the Patents Act.

Annexure GBC-15

This is **Annexure GBC-15** referred to in my Statutory Declaration made this Thirteenth day of December 2000.

Gary Baxter Cox

WITNESS: _____

Patent Attorney PEYTEE KING

phosphate-buffered saline (overnight). We added 819 empty capsids (100 μl, 5 μg/ml) to each well (in quadruplicate) and detected binding by a mouse anti-B19 monoclonal antibody (Chemicon) followed by ^{125}I-labeled sheep anti-mouse antibody (Amersham). The radioactivity in each well was counted for 2 min with a γ counter. There was no specific binding with CDH or CTH (methanol alone, mean count of 241; CDH, mean count of 262; CTH, mean count of 244), and reduced binding to Forssman antigen (mean count of 2088) compared to globoside (mean count of 7458).

19. B19 capsids and mouse monoclonal antibody to globoside bound to the same band on Western blotting of red cell extract, perhaps to a putative "globoprotein" [Y. Tonegawa and S. Hakomori, *Biochem. Biophys. Res. Commun.* 76, 9 (1977)]. However, this band was removed by digestion with lipase but not by proteases, more consistent with a glycolipid moiety.
20. P. P. Mortimer, R. K. Humphries, J. G. Moore, R. H. Purcell, N. S. Young, *Nature* 302, 426 (1983).
21. A. E. von dem Borne *et al.*, *Br. J. Haematol.* 63, 35 (1986).
22. In addition, our preliminary data indicate that individuals who lack P on their cells (blood-group p phenotype) have no evidence of previous infection with B19, compared with a B19 seroprevalence rate of 60% in the general population.
23. J. M. Liu, S. W. Green, T. Shimada, N. S. Young, *J. Virol.* 66, 4886 (1992).
24. P. Rouger, P. Gane, C. Salmon, *Rev. Fr. Transfus. Immuno. Hematol.* 30, 699 (1987).
25. S. J. Naides and C. P. Weiner, *Prenat. Diagn.* 9, 105 (1989); A. L. Morey, J. W. Keeling, H. J. Porter, K. A. Fleming, *Br. J. Obstet. Gynaecol.* 99, 566 (1992).
26. P. Levine, M. J. Celano, F. Falkowski, *Transfusion* (*Philadelphia*) 3, 278 (1963).
27. C. E. Walsh *et al.*, *Proc. Natl. Acad. Sci. U.S.A.* 89, 7257 (1992).

28. We thank A. von dem Borne and D. Marcus for anti-globoside antibody; M. Collett for the B19 capsids; J. Proctor for red cell typing; J. Storey and M. McCarthy for supply of the rare red cell types; and J. Moss, R. Blumenthal, and D. Roberts for helpful discussions.

2 March 1993; accepted 3 August 1993

In Vivo Gene Therapy of Hemophilia B: Sustained Partial Correction in Factor IX–Deficient Dogs

Mark A. Kay,* Steven Rothenberg, Charles N. Landen, Dwight A. Bellinger, Frances Leland, Carol Toman, Milton Finegold, Arthur R. Thompson, M. S. Read, Kenneth M. Brinkhous, Savio L. C. Woo†

The liver represents a model organ for gene therapy. A method has been developed for hepatic gene transfer in vivo by the direct infusion of recombinant retroviral vectors into the portal vasculature, which results in the persistent expression of exogenous genes. To determine if these technologies are applicable for the treatment of hemophilia B patients, preclinical efficacy studies were done in a hemophilia B dog model. When the canine factor IX complementary DNA was transduced directly into the hepatocytes of affected dogs in vivo, the animals constitutively expressed low levels of canine factor IX for more than 5 months. Persistent expression of the clotting factor resulted in reductions of whole blood clotting and partial thromboplastin times of the treated animals. Thus, long-term treatment of hemophilia B patients may be feasible by direct hepatic gene therapy in vivo.

Hemophilia B is an X-linked blood coagulation disorder resulting from a deficiency of factor IX production in the liver. The disease affects about 1 in 30,000 males and can result in severe bleeding episodes that require infusion of blood products that contain factor IX (*1*). As a result of previous human protein replacement therapy, about half of hemophilia B patients are infected with human immunodeficiency virus or hepatitis viruses. A virus-free and nonthrombogenic factor IX product is now available, but because of high costs the current treatment protocols do not include prophylaxis and therapy is initiated after bleeding begins. A number of tissues are target organs for somatic gene therapy of hemophilia B, including fibroblasts, myoblasts, endothelial cells, keratinocytes, and hepatocytes (*2*–*7*). Because the liver is the organ of factor IX synthesis, it represents a natural target for gene replacement therapy.

We have previously reported that hepatocytes can be transduced in vivo by infusion of recombinant retroviral vectors into the portal vasculature of mice after partial hepatectomy (*8*). To determine if the same can be achieved in larger animals (such as dogs), we infused an amphotropic retroviral vector (LBGpgk) that encodes the *Escherichia coli* β-galactosidase gene (*8*) directly into the portal vasculature of normal dogs three times 1 to 3 days after partial hepatectomy (Fig. 1). Two weeks later, hepatocytes were isolated and stained with 5-bromo-4-chloro-3-imdoyl-6-D-galactopyranoside (x-Gal) (Fig. 1A). Liver sections from these animals were similarly analyzed (Fig. 1B). The proportion of stained (blue) cells in Fig. 1 represents the in vivo transduction frequency of hepatocytes and was about 1 and 0.3% in two animals. Additional tissues, including kidney and spleen, did not stain blue with x-Gal. These transduction efficiencies are similar to that previously observed in mice (*8*). Routine histologic analysis revealed no pathologic conditions in the liver.

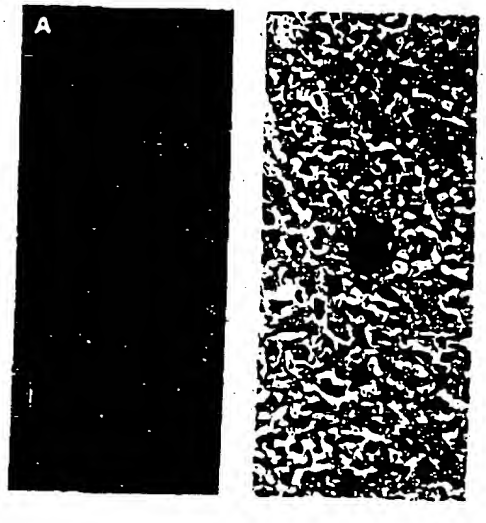

Fig. 1. Retroviral vector–mediated gene transfer of canine hepatocytes in vivo. A two-thirds partial hepatectomy was performed in two, 9-week-old normal dogs (3.5 kg) by resecting the left medial, left lateral, right medial, and caudate lobes. The right lateral lobe and its segmental blood supply and biliary drainage were preserved. The distal tip of a porta-cath catheter (Access Technology, Skokie, IL) was cannulated into a splenic vein. The injection port was placed subcutaneously under the right lateral abdominal wall. The LBGpgk vector was collected from confluent packaging cells cultured in Hg DMEM and 1% Hyclone for 12 hours. About 85 ml of filtered supernatants containing 9 × 10^7 colony-forming units was mixed with Polybrene (20 μg/ml) and infused over 45 to 90 min through the catheter 24, 48, and 72 hours after the hepatectomy. The animals tolerated the procedure well except for occasional vomiting and transient pallor during the beginning of the first infusion. When the dogs were killed, hepatocytes were isolated, cultured (*10*), and stained with x-Gal (*8*) (**A**) (original magnification, ×200), and (**B**) liver sections were stained with x-Gal and counterstained with neutral red (*8*) (original magnification, ×400).

M. A. Kay, Departments of Molecular Genetics and Cell Biology, Baylor College of Medicine, Houston, TX 77030.
S. Rothenberg, Department of Pediatric Surgery, Baylor College of Medicine, Houston, TX 77030.
C. N. Landen, D. A. Bellinger, M. S. Read, K. M. Brinkhous, Department of Pathology, University of North Carolina, Chapel Hill, NC 27599.
F. Leland, C. Toman, S. L. C. Woo, Howard Hughes Medical Institute, Department of Cell Biology, Baylor College of Medicine, Houston, TX 77030.
M. Finegold, Department of Pathology, Baylor College of Medicine, Houston, TX 77030.
A. R. Thompson, Puget Sound Blood Center, 921 Terry Avenue, Seattle, WA 98104.

*Present address: Markey Molecular Medicine Center, Department of Medicine RG-25, University of Washington Seattle, WA 98195.
†To whom correspondence should be addressed.

An amphotropic retroviral vector that encoded the canine factor IX complementary DNA (cDNA) (LX-cFIX) was constructed (9) and transduced into rat embryo 208F cells (8) to assess its ability for in vitro expression of factor IX. The media were changed daily, and canine factor IX was measured by enzyme-linked immunosorbent assay (ELISA) (8, 10) with a species-specific polyclonal antibody that was prepared as described (11). The transduced rodent cells produce 225 ng of canine factor IX antigen per 10^6 cells per day, whereas control cells produce no detectable factor IX (12). This recombinant retroviral vector was used for infusion into the portal vasculature of four hemophilia B dogs (Table 1) from the Chapel Hill inbred strain (13). The molecular defect in these dogs is a missense mutation in the catalytic domain of factor IX that results in a complete lack of antigen in the plasma (14). A partial hepatectomy was performed in these experimental animals, followed by the infusion of the LX-cFIX retrovirus 24, 48, and 72 hours after partial hepatectomy (Table 1). Factor IX concentrations in their plasma were measured by biologic and immunoassays (Figs. 2A and 3A). The hemostatic parameters were monitored by changes in the whole blood clotting time (WBCT) (Figs. 2B and 3B) and partial thromboplastin time (PTT) (Table 1). These tests are indexes of the intrinsic pathway of clotting in which factor IX is the key component.

In dog 1, the plasma factor IX increased from undetectable amounts to a range of 2 to 6 ng/ml; these levels have been maintained constitutively for over 5 months (Fig. 2A), and there is close agreement between the biologic and immunoassay results. Most importantly, this dog had a WBCT of 15 to 20 min during the 5-month period after treatment, whereas the WBCT for untreated factor IX–deficient littermates ranged from 45 to 55 min (Fig. 2B). A long WBCT is characteristic of a dog colony severely deficient in factor IX; normal dogs, on the other hand, have a WBCT of 6 to 8 min (Fig. 2B). In vitro addition of normal dog plasma to whole blood from hemophilia B dogs to a final concentration of 3 ng/ml reduced the WBCT to 20 min. This is in agreement with the WBCT and factor IX concentrations obtained in dog 1 after treatment (Fig. 2). The PTT for dog 1 was also shortened from 322 before treatment to 174 seconds after treatment (Table 1).

Plasma from dog 2 showed factor IX concentrations similar to that of dog 1 (Figs. 2A and 3A), whereas dog 3 had slightly greater concentrations, ranging from 3 to 10 ng/ml (Fig. 3A). Both dogs 2 and 3 had similar reductions in their WBCT, from pretreatment values of 44 to 47 min to 18 to 26 min after treatment (Fig.

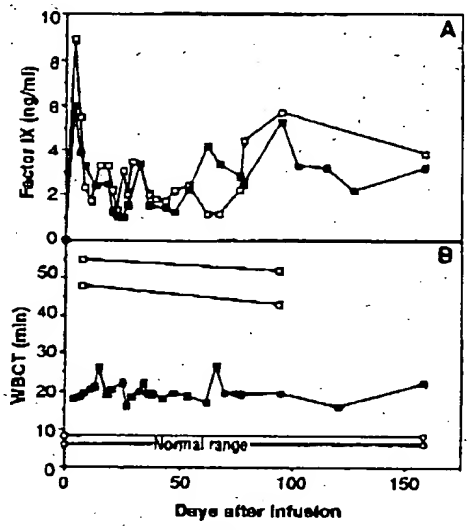

Fig. 2. Plasma factor IX concentrations and WBCTs in hemophilia B dog 1 after hepatic transduction with the LTR-cFIX retroviral vector. The plasma factor IX concentrations were determined immunologically by ELISA and by bioassay. The bioassays were performed by a modified one-stage method (16) in which a kaolin-activated canine hemophilia B plasma was used as a substrate, a limiting dilution of a normal canine plasma pool was used as reference plasma (11.5 μg/ml), and test plasmas were diluted in a 1:10 ratio. The value of 11.5 μg/ml was estimated from the ratio of the concentration of normal human factor IX activity (5.0 μg/ml) to the concentration of normal canine factor IX activity. Hemostatic testing consisted of a determination of the WBCT (with the two-tube method at 28°C with the use of silicone-coated tubes tilted every 30 s until clotted). (**A**) Values for the antigen concentrations of factor IX are shown in solid symbols, and the values from the bioassay are shown in open symbols. (**B**) The WBCTs in dog 1 (solid squares), two affected hemophilia B littermates (open squares), and the range in normal dogs (open circles). The days after infusion represent the number of days after the first retroviral infusion; day 0 represents measurements from samples obtained before any procedural manipulations.

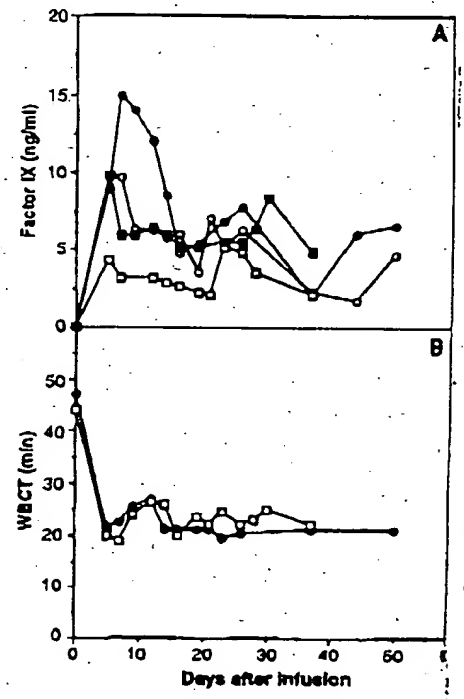

Fig. 3. Plasma factor IX concentrations and WBCTs in hemophilia B dogs 2 and 3 after hepatic transduction with the LTR-cFIX retroviral vector. The hemostatic characterization were as described (Fig. 2). (**A**) The values for the antigen concentrations are in solid symbols: Dog 2, squares; dog 3, circles. Values from the bioassay are in open symbols. (**B**) Whole blood clotting times. Dog 2, open squares; dog 3, solid circles. The study on dog 2 terminated on day 42 as multiple transfusions were given for hemorrhage. Dog 3 developed a minor bleeding episode that required one infusion of normal dog plasma on day 26, which accounts for the hiatus in data for days 27 to 36. Previous studies (22) have shown that by 10 days after infusion exogenous factor IX is undetectable by bioassay.

Table 1. Hemophilia B dogs used in a gene therapy protocol (23). The weight and age were recorded on the day the study was started. The methods for partial hepatectomy were essentially the same as outlined in Fig. 1. Blood samples were obtained from the animals before surgery, and hemostatic coverage was maintained with multiple infusions of normal fresh frozen plasma given immediately before and for 24 hours after the operation (57.4 to 72.7 units of factor IX per kilogram of body weight). Circulating factor IX from plasma infusions in untreated animals is cleared within 8 to 10 days (22). The PTTs (24) were obtained from two to four samples before the start of the experiments (Before) and then were analyzed 6 to 10 times for each animal on different days starting at least 11 days after the viral infusion (After). The times shown indicate nonactivated PTTs, which for normal dogs are 42 to 47 s. The standard deviations are in parentheses.

Dog*	Weight (kg)	Age (weeks)	Infusion volume (ml)	PTT (s)	
				Before	After
1	5.3	11	510	322 (15)	174 (6.5)
2	7.3	14	720	262 (0.8)	180 (7.5)
3	6.7	14	720	195 (13)	154 (8.6)

*One animal died as a result of a surgical complication and was not included.

3B). The PTTs in dogs 2 and 3 were also decreased significantly (Table 1). To further establish the biological activity of plasma factor IX, we treated samples from dogs 1 and 3 with barium sulfate to remove γ-carboxylated proteins, including factor IX (*15*). The barium sulfate–treated plasmas of treated dogs had a prolonged PTT that was similar to the pretreatment PTT values.

Our study demonstrates the feasibility of in vivo retroviral-mediated gene transfer into the liver of a large animal, which results in phenotypic improvement of a deficiency syndrome. The factor IX antigen amounts achieved after gene transfer were only about 0.1% of the endogenous concentration of factor IX in normal animals, which demonstrates that the constitutive expression of a relatively small quantity of the factor IX protein is sufficient to cause a reduction in the WBCT and a shortening of the PTT. Our data indicate that the WBCT is extremely sensitive to changes in factor IX concentration in the hemophilia B dogs. In moderate and mild human hemophilia patients with shortened WBCT and factor levels in the 3 to 8% range, there is still a risk of hemorrhage, although both the frequency and the severity of episodes are considerably less than those of severely affected individuals (*16*). For future human applications, however, increased circulating factor IX levels must first be achieved. This may be accomplished by developing methods that lead to greater efficiencies of hepatocyte transduction in vivo and by creating expression vectors with stronger promoters. These reservations notwithstanding, our results illustrate the efficacy of in vivo gene therapy of hemophilia B and other metabolic disorders secondary to hepatic deficiencies.

Note added in proof: Plasma factor IX concentrations and WBCTs remained at the same values at 9 months after treatment for dog 1 and 6 months after treatment for dog 3.

REFERENCES AND NOTES

1. H. R. Roberts and J. N. Lozier, in *Clinical Aspects and Therapy for Hemophilia B in Hematology: Basic Principles and Practice*, R. Hoffman, E. Benz Jr., S. Shattil, B. Furie, H. Cohen, Eds. (Churchill Livingstone, New York, 1991), pp. 1325–1331.
2. K. M. Brinkhous, *Thromb. Res.* 67, 329 (1992).
3. A. R. Thompson, T. D. Palmer, C. M. Lynch, A. D. Miller, *Curr. Stud. Hematol. Blood Transfus.* 58, 59 (1991).
4. Y. Dai, M. Roman, R. K. Naviaux, I. M. Verma, *Proc. Natl. Acad. Sci. U.S.A.* 89, 10892 (1992).
5. A. Miyanohara *et al.*, *New Biol.* 4, 238 (1992).
6. S. N. Yao and K. Kurachi, *Proc. Natl. Acad. Sci. U.S.A.* 89, 3357 (1992).
7. A. J. Gerrard, D. L. Hudson, G. G. Brownlee, F. M. Watt, *Nature Genet.* 3, 160 (1993).
8. M. A. Kay *et al.*, *Hum. Gene Ther.* 3, 641 (1992).
9. In the construction of the LX-cFIX retroviral vector, the 1.4-kb cFIX cDNA was cloned by reverse transcriptase–polymerase chain reaction (RT-PCR) amplification of canine liver polyadenylate-containing RNA. The 5′ primer was synthesized to contain the 5′-GCCACC-3′ Kozak sequence [M. Kozak, *Nucleic Acids Res.* 15, 8125 (1987)]. The sequence of the cDNA was determined and found to be identical to the published sequence (*14*). The cDNA was cloned into a modified LNCX retroviral vector (*17*), with its *neo* gene and cytomegalovirus promoter removed by Bcl I–Bam HI digestion and religation. The cloned DNA was transfected into GP+E-86 ecotropic packaging cells (*18*), and supernatants were used to infect amphotropic GP+AM12 cells (*19*). The single clone that gave the greatest amount of cFIX production in transduced 208F cells was titered (*20*) by limiting dilution PCR (*21*) and found to have a concentration of 2×10^6 colony-forming units per milliliter.
10. M. A. Kay *et al.*, *Proc. Natl. Acad. Sci. U.S.A.* 89, 89 (1992).
11. A. Thompson, *J. Clin. Invest.* 59, 900 (1977).
12. Viral supernatants contained Polybrene (8 μg/ml) (Sigma) at a multiplicity of infection of 10 (*8*). Control cells were infected with an equal amount of LBGpgk virus. The supernatants from transduced cells were collected at 24-hour intervals and analyzed for cFIX. The LBGpgk-infected cells were stained with x-Gal, and approximately 30 to 40% of these cells stained blue.
13. K. M. Brinkhous, P. D. Davis, J. B. Graham, W. J. Dodds, *Blood* 41, 577 (1973).
14. J. P. Evans *et al.*, *Proc. Natl. Acad. Sci. U.S.A.* 86, 10095 (1989).
15. J. H. Axelrod, M. S. Reed, K. M. Brinkhous, I. M. Verma, *ibid.* 87, 5173 (1990).
16. K. M. Brinkhous *et al.*, *J. Am. Med. Assoc.* 154, 481 (1954).
17. A. D. Miller and G. J. Rosman, *BioTechniques* 7, 980 (1989).
18. D. Markowitz, S. Goff, A. Bank, *J. Virol.* 62, 1120 (1988).
19. ———, *Virology* 167, 400 (1988).
20. C. M. Lynch and A. D. Miller, *J. Virol.* 65, 3887 (1991).
21. Viral supernatants were obtained from clonal packaging cell lines and diluted by 10-fold serial dilutions and infected 208F cells (*20*). Factor IX concentrations in the media were detected by ELISA, and 3 days after infection the cells were isolated and DNA extracted for PCR amplification with primers specific for the canine factor IX cDNA. We compared the PCR signal of the LX-cFIX–infected cells with that of a retroviral vector that contains the cFIX cDNA and a selectable marker that has been titered by standard methods (*20*) and is known to have a titer of 2×10^7 colony-forming units per milliliter. The PCR signal for the LX-cFIX vector is not detectable one dilution before the vector with a known titer. Thus, the titer of the LX-cFIX virus is estimated to be 2×10^6 infectious particles per milliliter.
22. K. M. Brinkhous, C. N. Landen, M. S. Read, unpublished data.
23. All experimental procedures were in accordance with institutional guidelines at the Baylor College of Medicine and the University of North Carolina. Preanesthetic agents included atropine sulfate (0.24 mg per kilogram of body weight) and sodium thiamylal (0.1 to 0.2 g/kg). Maintenance anesthesia was 2% halothane. The postoperative analgesic was butorphanol (0.5 mg) administered intravenously as needed every 4 to 6 hours during the first 24 hours. The animals were treated prophylactically with antibiotics (cefadroxil, 22 mg/kg) for several days before and after the operation. Before retroviral infusion, the animals were given diphenhydramine (10 mg) intramuscularly, and some animals were sedated with acepromazine (5 mg) intravenously.
24. R. D. Langdell, R. H. Wagner, K. M. Brinkhous, *J. Lab. Clin. Med.* 41, 637 (1953).

26. We thank L. Brandon and A. Major (Houston, TX) and S. Olgesbee, A. McCrory, R. Raymer, and P. Mcelveen (Chapel Hill, NC) for their expert technical assistance. Supported in part by NIH grants DK 44080, HL 40162 (Baylor College of Medicine), and HL-01648-46 and HL 26309-12 (University of North Carolina, Chapel Hill). M.A.K. is a recipient of an individual National Research Service Awards fellowship, award GM 13894, and S.L.C.W. is an investigator of the Howard Hughes Medical Institute.

6 May 1993; accepted 6 August 1993

Science

Volume 262(5130) 1 October 1993 pp 117-119

In Vivo Gene Therapy of Hemophilia B: Sustained Partial Correction in Factor IX-Deficient Dogs

[REPORTS]

Kay, Mark A.*; Rothenberg, Steven; Landen, Charles N.; Bellinger, Dwight A.; Leland, Frances; Toman, Carol; Finegold, Milton; Thompson, Arthur R.; Read, M. S.; Brinkhous, Kenneth M.; Woo, Savio L. C.**

M. A. Kay, Departments of Molecular Genetics and Cell Biology, Baylor College of Medicine, Houston, TX 77030.
S. Rothenberg, Department of Pediatric Surgery, Baylor College of Medicine, Houston, TX 77030.
C. N. Landen, D. A. Bellinger, M. S. Read, K. M. Brinkhous, Department of Pathology, University of North Carolina, Chapel Hill, NC 27599.
F. Leland, C. Toman, S. L. C. Woo, Howard Hughes Medical Institute, Department of Cell Biology, Baylor College of Medicine, Houston, TX 77030.
M. Finegold, Department of Pathology, Baylor College of Medicine, Houston, TX 77030.
A. R. Thompson, Puget Sound Blood Center, 921 Terry Avenue, Seattle, WA 98104.
*Present address: Markey Molecular Medicine Center, Department of Medicine RG-25, University of Washington, Seattle, WA 98195.
** To whom correspondence should be addressed.

Outline

Graphics

Abstract

The liver represents a model organ for gene therapy. A method has been developed for hepatic gene transfer in vivo by the direct infusion of recombinant retroviral vectors into the portal vasculature, which results in the persistent expression of exogenous genes. To determine if these technologies are applicable for the treatment of hemophilia B patients, preclinical efficacy studies were done in a hemophilia B dog model. When the canine factor IX complementary DNA was transduced directly into the hepatocytes of affected dogs in vivo, the animals constitutively expressed low levels of canine factor IX for more than 5 months. Persistent expression of the clotting factor resulted in reductions of whole blood clotting and partial thromboplastin times of the treated animals. Thus, long-term treatment of hemophilia B patients may be feasible by direct hepatic gene therapy in vivo.

Hemophilia B is an X-linked blood coagulation disorder resulting from a deficiency of

factor IX production in the liver. The disease affects about 1 in 30,000 males and can result in severe bleeding episodes that require infusion of blood products that contain factor IX [1]. As a result of previous human protein replacement therapy, about half of hemophilia B patients are infected with human immunodeficiency virus or hepatitis viruses. A virus-free and nonthrombogenic factor IX product is now available, but because of high costs the current treatment protocols do not include prophylaxis and therapy is initiated after bleeding begins. A number of tissues are target organs for somatic gene therapy of hemophilia B, including fibroblasts, myoblasts, endothelial cells, keratinocytes, and hepatocytes [2-7]. Because the liver is the organ of factor IX synthesis, it represents a natural target for gene replacement therapy.

We have previously reported that hepatocytes can be transduced in vivo by infusion of recombinant retroviral vectors into the portal vasculature of mice after partial hepatectomy [8]. To determine if the same can be achieved in larger animals (such as dogs), we infused an amphotropic retroviral vector (LBGpgk) that encodes the Escherichia coli beta-galactosidase gene [8] directly into the portal vasculature of normal dogs three times 1 to 3 days after partial hepatectomy Figure 1. Two weeks later, hepatocytes were isolated and stained with 5-bromo-4-chloro-3-imdoyl-6-D-galactopyranoside (x-Gal) Figure 1A. Liver sections from these animals were similarly analyzed Figure 1B. The proportion of stained (blue) cells in Figure 1represents the in vivo transduction frequency of hepatocytes and was about 1 and 0.3% in two animals. Additional tissues, including kidney and spleen, did not stain blue with x-Gal. These transduction efficiencies are similar to that previously observed in mice [8]. Routine histologic analysis revealed no pathologic conditions in the liver.

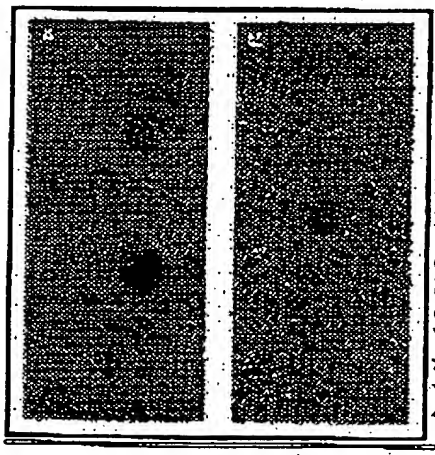

Figure 1. Retroviral vector-mediated gene transfer of canine hepatocytes in vivo. A two-thirds partial hepatectomy was performed in two, 9-week-old normal dogs (3.5 kg) by resecting the left medial, left lateral, right medial, and caudate lobes. The right lateral lobe and its segmental blood supply and biliary drainage were preserved. The distal tip of a porta-cath catheter (Access Technology, Skokie, IL) was cannulated into a splenic vein. The injection port was placed subcutaneously under the right lateral abdominal wall. The LBGpgk vector was collected from confluent packaging cells cultured in Hg DMEM and 1% Hyclone for 12 hours. About 85 ml of filtered supernatants containing 9 times 10^7 colony-forming units was mixed with Polybrene (20 mu g/ml) and infused over 45 to 90 min through the catheter 24, 48, and 72 hours after the hepatectomy. The animals tolerated the procedure well except for occasional vomiting and transient pallor during the beginning of the first infusion. When the dogs were killed, hepatocytes were isolated, cultured [10], and stained with x-Gal [8] (A) (original magnification, times 200), and (B) liver sections were stained with x-Gal and counterstained with neutral red [8] (original magnification, times 400).

An amphotropic retroviral vector that encoded the canine factor IX complementary DNA (cDNA) (LX-cFIX) was constructed [9] and transduced into rat embryo 208F cells [8] to assess its ability for in vitro expression of factor IX. The media were changed daily, and canine factor IX was measured by enzyme-linked immunosorbent assay (ELISA) [8,10] with a species-specific polyclonal antibody that was prepared as described [11]. The transduced rodent cells produce 225 ng of canine factor IX antigen per 10^6 cells per day, whereas control cells produce no detectable factor IX [12]. This recombinant retroviral vector was used for infusion into the portal vasculature of four hemophilia B dogs Table 1 from the Chapel Hill inbred strain [13]. The molecular defect in these dogs is a missense mutation in the catalytic domain of factor IX that results in a complete lack of antigen in the plasma [14]. A partial hepatectomy was performed in these experimental animals, followed by the infusion of the LX-cFIX retrovirus 24, 48, and 72 hours after partial hepatectomy Table 1. Factor IX concentrations in their plasma were measured by biologic and immunoassays Figure s. 2A and 3A). The hemostatic parameters were monitored by changes in the whole blood clotting time (WBCT) (Figs. 2B and 3B) and partial thromboplastin time (PTT) Table 1. These tests are indexes of the

intrinsic pathway of clotting in which factor IX is the key component.

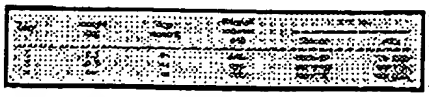

Table 1. Hemophilia B dogs used in a gene therapy protocol [23]. The weight and age were recorded on the day the study was started. The methods for partial hepatectomy were essentially the same as outlined in Figure 1. Blood samples were obtained from the animals before surgery, and hemostatic coverage was maintained with multiple infusions of normal fresh frozen plasm given immediately before and for 24 hours after the operation (57.4 to 72.7 units of factor IX per kilogram of body weight). Circulating factor IX from plasma infusions in untreated animals is cleared within 8 to 10 days [22]. The PTTs [24] were obtained from two to four samples before the start of the experiments (Before) and then were analyzed 6 to 10 times for each animal on different days starting at least 11 days after the viral infusion (After). The times shown indicate nonactivated PTTs, which for normal dogs are 42 to 47 s. The standard deviations are in parentheses.

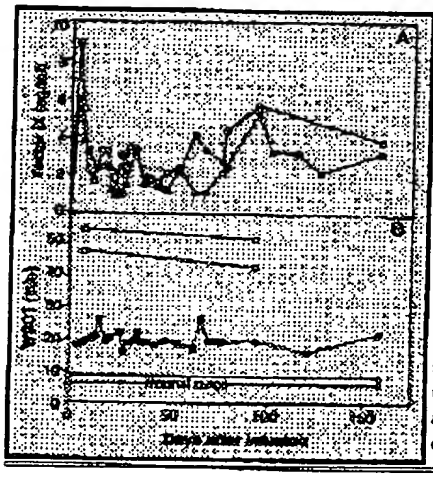

Figure 2. Plasma factor IX concentrations and WBCTs in hemophilia B dog 1 after hepatic transduction with the LTR-cFIX retroviral vector. The plasma factor IX concentrations were determined immunologically by ELISA and by bioassay. The bioassays were performed by a modified one-stage method [16] in which a kaolinactivated canine hemophilia B plasma was used as a substrate, a limiting dilution of a normal canine plasma pool was used as reference plasma (11.5 mu g/ml), and test plasmas were diluted in a 1:10 ratio. The value of 11.5 mu g/ml was estimated from the ratio of the concentration of normal human factor IX activity (5.0 mu g/ml) to the concentration of normal canine factor IX activity. Hemostatic testing consisted of a determination of the WBCT (with the two-tube method at 28 degrees C with the use of silicone-coated tubes tilted every 30 s until clotted). (A) Values for the antigen concentrations of factor IX are shown in solid symbols, and the values from the bioassay are shown in open symbols. (B) The WBCTs in dog 1 (solid squares), two affected hemophilia B littermates (open squares), and the range in normal dogs (open circles). The days after infusion represent the number of days after the first retroviral infusion; day 0 represents measurements from samples obtained before any procedural manipulations.

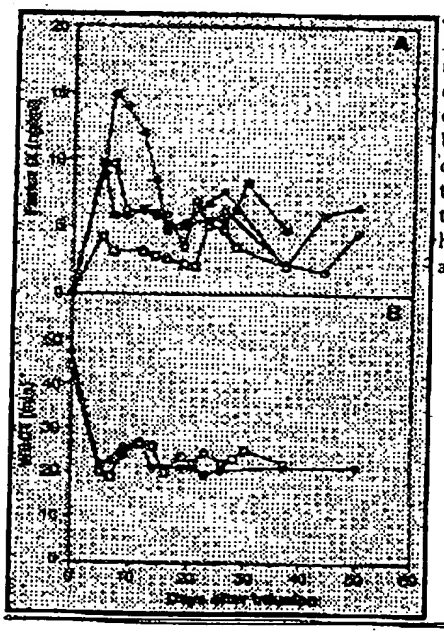

Figure 3. Plasma factor IX concentrations and WBCTs in hemophilia B dogs 2 and 3 after hepatic transduction with the LTR-cFIX retroviral vector. The hemostatic characterizations were as described Figure 2. (A) The values for the antigen concentrations are in solid symbols. Dog 2, squares; dog 3, circles. Values from the bioassay are in open symbols. (B) Whole blood clotting times. Dog 2, open squares; dog 3, solid circles. The study on dog 2 terminated on day 42 as multiple transfusions were given for hemorrhage. Dog 3 developed a minor bleeding episode that required one infusion of normal dog plasma on day 26, which accounts for the hiatus in data for days 27 to 36. Previous studies [22] have shown that by 10 days after infusion exogenous factor IX is undetectable by bioassay.

In dog 1, the plasma factor IX increased from undetectable amounts to a range of 2 to 6 ng/ml; these levels have been maintained constitutively for over 5 months (Figure 2A) and there is close agreement between the biologic and immunoassay results. Most importantly, this dog had a WBCT of 15 to 20 min during the 5-month period after treatment, whereas the WBCT for untreated factor IX-deficient littermates ranged from 45 to 55 min (Figure 2B). A long WBCT is characteristic of a dog colony severely deficient in factor IX; normal dogs, on the other hand, have a WBCT of 6 to 8 min Figure 2B. In vitro addition of normal dog plasma to whole blood from hemophilia B dogs to a final concentration of 3 ng/ml reduced the WBCT to

20 min. This is in agreement with the WBCT and factor IX concentrations obtained in dog 1 after treatment Figure 2. The PTT for dog 1 was also shortened from 322 before treatment to 174 seconds after treatment Table 1.

Plasma from dog 2 showed factor IX concentrations similar to that of dog 1 (Figs. 2A and 3A), whereas dog 3 had slightly greater concentrations, ranging from 3 to 10 ng/ml Figure 3A. Both dogs 2 and 3 had similar reductions in their WBCT, from pretreatment values of 44 to 47 min to 18 to 26 min after treatment Figure 3B. The PTTs in dogs 2 and 3 were also decreased significantly Table 1. To further establish the biological activity of plasma factor IX, we treated samples from dogs 1 and 3 with barium sulfate to remove gamma-carboxylated proteins, including factor IX [15]. The barium sulfate-treated plasmas of treated dogs had a prolonged PTT that was similar to the pretreatment PTT values.

Our study demonstrates the feasibility of in vivo retroviral-mediated gene transfer into the liver of a large animal, which results in phenotypic improvement of a deficiency syndrome. The factor IX antigen amounts achieved after gene transfer were only about 0.1% of the endogenous concentration of factor IX in normal animals, which demonstrates that the constitutive expression of a relatively small quantity of the factor IX protein is sufficient to cause a reduction in the WBCT and a shortening of the PTT. Our data indicate that the WBCT is extremely sensitive to changes in factor IX concentration in the hemophilia B dogs. In moderate and mild human hemophilia patients with shortened WBCT and factor levels in the 3 to 8% range, there is still a risk of hemorrhage, although both the frequency and the severity of episodes are considerably less than those of severely affected individuals [16]. For future human applications, however, increased circulating factor IX levels must first be achieved. This may be accomplished by developing methods that lead to greater efficiencies of hepatocyte transduction in vivo and by creating expression vectors with stronger promoters. These reservations notwith-standing, our results illustrate the efficacy of in vivo gene therapy of hemophilia B and other metabolic disorders secondary to hepatic deficiencies.

Note added in proof: Plasma factor IX concentrations and WBCTs remained at the same values at 9 months after treatment for dog 1 and 6 months after treatment for dog 3.

REFERENCES AND NOTES[2]

1. H. R. Roberts and J. N. Lozier, in Clinical Aspects and Therapy for Hemophilia B in Hematology: Basic Principles and Practice, R. Hoffman, E. Benz Jr., S. Shattil, B. Furie, H. Cohen, Eds. (Churchill Livingstone, New York, 1991), pp. 1325-1331. [Context Link]

2. K. M. Brinkhous, Thromb. Res. 67, 329 (1992). [Context Link]

3. A. R. Thompson, T. D. Palmer, C. M. Lynch, A. D. Miller, Curr. Stud. Hematol. Blood Transfus. 58, 59 (1991). [Context Link]

4. Y. Dai, M. Roman, R. K. Naviaux, I. M. Verma, Proc. Natl. Acad. Sci. U.S.A. 89, 10892 (1992). [Context Link]

5. A. Miyanohara et al., New Biol. 4, 238 (1992). [Context Link]

6. S. N. Yao and K. Kurachi, Proc. Natl. Acad. Sci. U.S.A. 89, 3357 (1992). [Context Link]

7. A. J. Gerrard, D. L. Hudson, G. G. Brownlee, F. M. Watt, Nature Genet. 3, 180 (1993). [Context Link]

8. M. A. Kay et al., Hum. Gene Ther. 3, 641 (1992). [Context Link]

9. In the construction of the LX-cFIX retroviral vector, the 1.4-kb cFIX cDNA was cloned by reverse transcriptase-polymerase chain reaction (RTPCR) amplification of canine liver polyadenylatecontaining RNA. The 5.prime primer

was synthesized to contain the 5 prime-GCCACC-3 prime Kozak sequence [M. Kozak, Nucleic Acids Res. 15, 8125 (1987)]. The sequence of the cDNA was determined and found to be identical to the published sequence *RF 14*. The cDNA was cloned into a modified LNCX retroviral vector *RF 17*, with its neo gene and cytomegalovirus promoter removed by Bcl I-Bam HI digestion and religation. The cloned DNA was transfected into GP plus E-86 ecotropic packaging cells *RF 18*, and supernatants were used to infect amphotropic GP plus AM12 cells *RF 19*. The single clone that gave the greatest amount of cFIX production in transduced 208F cells was titered *RF 20* by limiting dilution PCR *RF 21* and found to have a concentration of 2 times 10 sup 6 colony-forming units per milliliter. [Context Link]

10. M. A. Kay et al., Proc. Natl. Acad. Sci. U.S.A. 89, 89 (1992). [Context Link]

11. A. Thompson, J. Clin. Invest. 59, 900 (1977). [Context Link]

12. Viral supernatants contained Polybrene (8 mu g/ml) (Sigma) at a multiplicity of infection of 10 *RF 8*. Control cells were infected with an equal amount of LBGpgk virus. The supernatants from transduced cells were collected at 24-hour intervals and analyzed for cFIX. The LBGpgk-infected cells were stained with x-Gal, and approximately 30 to 40% of these cells stained blue. [Context Link]

13. K. M. Brinkhous, P. D. Davis, J. B. Graham, W. J. Dodds, Blood 41, 577 (1973). [Context Link]

14. J. P. Evans et al., Proc. Natl. Acad. Sci. U.S.A. 86, 10095 (1989). [Context Link]

15. J. H. Axelrod, M. S. Reed, K. M. Brinkhous, I. M. Verma, ibid. 87, 5173 (1990). [Context Link]

16. K. M. Brinkhous et al., J. Am. Med. Assoc. 154, 481 (1954). [Context Link]

17. A. D. Miller and G. J. Rosman, Bio Techniques 7, 980 (1989).

18. D. Markowitz, S. Goff, A. Bank, J. Virol. 62, 1120 (1988).

19. _____, Virology 167, 400 (1988).

20. C. M. Lynch and A. D. Miller, J. Virol. 65, 3887 (1991).

21. Viral supernatants were obtained from clonal packaging cell lines and diluted by 10-fold serial dilutions and infected 208F cells *RF 20*. Factor IX concentrations in the media were detected by ELISA, and 3 days after infection the cells were isolated and DNA extracted for PCR amplification with primers specific for the canine factor IX cDNA. We compared the PCR signal of the LX-cFIX-infected cells with that of a retroviral vector that contains the cFIX cDNA and a selectable marker that has been titered by standard methods *RF 20* and is known to have a titer of 2 times 10 sup 7 colony-forming units per milliliter. The PCR signal for the LX-cFIX vector is not detectable one dilution before the vector with a known titer. Thus, the titer of the LX-cFIX virus is estimated to be 2 times 10 sup 6 infectious particles per milliliter.

22. K. M. Brinkhous, C. N. Landen, M. S. Read, unpublished data. [Context Link]

23. All experimental procedures were in accordance with institutional guidelines at the Baylor College of Medicine and the University of North Carolina. Preanesthetic agents included atropine sulfate (0.24 mg per kilogram of body weight) and sodium thiamylal (0.1 to 0.2 g/kg). Maintenance anesthesia was 2% halothane. The postoperative analgesic was butorphanol (0. 5 mg) administered intravenously as needed every 4 to 6 hours during the first 24 hours. The animals were treated prophylactically with antibiotics (cefadroxil, 22 mg/kg) for several days before and after the operation. Before retroviral infusion, the animals were given diphenhydramine (10 mg) intramuscularly, and some animals were sedated with acepromazine (5 mg) intravenously. [Context Link]

24. R. D. Langdell, R. H. Wagner, K. M. Brinkhous, J. Lab. Clin. Med. 41, 637 (1953). [Context Link]

25. We thank L. Brandon and A. Major (Houston, TX) and S. Olgesbee, A. McCrory, R. Raymer, and P. McIlveen (Chapel Hill, NC) for their expert technical assistance. Supported in part by NIH grants DK 44080, HL 40162 (Baylor College of Medicine), and HL-01648-46 and HL 26309-12 (University of North Carolina, Chapel Hill). M.A.K. is a recipient of an individual National Research Service Awards fellowship award GM 13894, and S.L.C.W. is an investigator of the Howard Hughes Medical Institute.

COMMONWEALTH OF AUSTRALIA

(Patents Act 1990)

IN THE MATTER OF: Australian Patent Application 696764 (73941/94). In the name of: Human Genome Sciences Inc.

- and -

IN THE MATTER OF: Opposition thereto by Ludwig Institute for Cancer Research, under Section 59 of the Patents Act.

Annexure GBC-16

This is **Annexure GBC-16** referred to in my Statutory Declaration made this Thirteenth day of December 2000.

Gary Baxter Cox

WITNESS: _____

Patent Attorney PEY TEE KHOO

Somatic Cell and Molecular Genetics, Vol. 19, No. 5, 1993, pp. 491–497

Hepatic Gene Therapy: Efficient Retroviral-Mediated Gene Transfer into Rat Hepatocytes In Vivo

Tadeusz M. Kolodka,[1] Milton Finegold,[2] and Savio L.C. Woo[1,3,4]

Departments of [1]Cell Biology, and [3]Molecular Genetics, and [2]Pathology, and [4]Howard Hughes Medical Institute, Baylor College of Medicine, Houston, Texas 77030;

Received August 3, 1993

Abstract—*The rat is an excellent model for gene therapy because there are many rat models for human diseases. We have developed a simple and efficient method to deliver genes to the rat liver using recombinant retroviral vectors. A 70% partial hepatectomy followed by retroviral infusion into the portal vein results in 10–15% hepatocyte transduction in vivo. This is 10 times more efficient than in the mouse due partially to the observation that the rat livers have much more synchronous hepatocyte replication after partial hepatectomy. Using a recombinant retroviral vector containing the human α_1-antitrypsin cDNA, persistent expression of the human protein in recipient rat plasma was observed for at least six months and at a level that is 10 times greater than the mouse. Thus, rats can serve as an excellent model for gene therapy of metabolic disorders secondary to hepatic deficiencies.*

INTRODUCTION

The rat is an extensively investigated animal, and there are many excellent rat models of human genetic and epigenetic diseases (1). In order to investigate the feasibility of treating some of these disease models using the techniques of somatic cell gene transfer, we wanted to develop simple and efficient methods for gene therapy in the rat. An excellent target organ for gene therapy is the liver because it is a large, metabolically active organ, and many genetic diseases result from mutations in genes expressed in the liver (2). Hepatocytes also have a slow turnover rate (3), and thus genetically modified cells will persist long-term.

Presently, the best vector for stable introduction of genes into somatic cells in animals is the recombinant, replication-defective retrovirus. The retrovirus is attractive because it integrates into the host genome and is thus permanent. The problem with using retroviruses to transduce hepatocytes is that retroviruses require host cell division for efficient integration into the genome (5). However, in a normal, healthy liver, very few hepatocytes are replicating (3). To stimulate hepatocyte replication, several laboratories have reported performing a 70% partial hepatectomy on rats. When the remaining hepatocytes divide to regenerate the liver, they are susceptible to retroviral transduction. The retrovirus is delivered by vascular isolation of the liver, followed by perfusion of the liver with retroviral supernatant (6, 7). Although this is an efficient method for gene delivery (5–20% of the hepatocytes were transduced), it is complicated by the need for extensive and elaborate surgery.

0740-7750/93/0900-0491$07.00/0

Recently, Kay et al. (8) performed a 70% partial hepatectomy in mice followed by infusion of retrovirus into the portal vein without vascular isolation. Using a retrovirus encoding the β-galactosidase gene, this technique resulted in 1–2% hepatocyte transduction as determined by X-gal staining. They also introduced the gene for the secreted reporter protein human α_1-antitrypsin (hAAT) and detected constitutive levels of hAAT in mouse serum for more than 200 days. This method, applied in the rat, resulted in 10–15% hepatocyte transduction and constitutive expression of the human protein at a level 10-fold greater than in the mouse.

MATERIALS AND METHODS

Animals and Partial Hepatectomy. Male Lewis rats, 3–4 weeks old were purchased from Harlan, Sprague Dawley Inc. The animals were housed in a vivarium with a 12-h light–dark cycle with water and food (standard laboratory chow) provided ab libitum. The partial hepatectomy was performed under a general combination anesthetic: ketamine (42.8 mg/ml), xylazine (8.6 mg/ml), and acepromazine (1.4 mg/ml), administered at 0.5–0.7 ml/kg. The 70% partial hepatectomy involved removal of the median and left lateral lobes and was performed according to Higgens and Anderson (9). The skin was then closed with autoclip 9-mm wound clips.

Retrovirus Harvest and Preparation. The virus-producing cells were cultured at 37°C with 5.0% CO_2 in 150-mm tissue culture plates with 25 ml of media (high glucose D-modified Eagle's media supplemented with 10% Hyclone bovine calf serum and 1 mM glutamine, 100 units/ml penicillin, 100 μg/ml streptomycine). When the cells were 70–80% confluent, the medium was replaced with 15 ml of fresh medium; 18 h later, the medium was harvested, filtered through a 0.45-μm syringe filter, and polybrene was added to 8.0 μg/ml. The retroviral medium was infused into animals within 1 h of collection.

Infusion of Retrovirus into Remaining Lobes of Liver. At indicated times after the 70% partial hepatectomy, rats were anesthetized as above and opened through the same incision used for the partial hepatectomy. The portal vein was cannulated with a 24-G catheter connected to a 10-cc syringe by a 30-in. extension set. Over the course of 20–30 min, 3.0 ml of retroviral supernatant was infused using a Sage Instruments syringe pump (model 355). After infusion, the catheter was removed and pressure was applied for 10–30 min to control bleeding. The abdominal muscle was sutured with Chromic Gut and the skin closed with autoclips.

Isolation and X-Gal Staining of Hepatocytes. The technique for hepatocyte isolation is adapted from Berry and Friend (10). Briefly, 10 days after retroviral infusion, the rat was anesthetized, the portal vein was cannulated with a 20-G catheter, and the inferior venae cava cut. The liver was then perfused with 150 ml of Earle's balanced salt solution without calcium or magnesium (EBS^-) plus 0.5 mM EGTA, 50 ml of EBS^-, and finally 150 ml of Earle's buffered solution with calcium, with 0.3 mg/ml Boehringer collagenase and 0.05 mg/ml Sigma soybean trypsin inhibitor. All the above solutions were warmed to 37°C and infused at 20 ml/min. Hepatocyte culture conditions and media were described previously (11). The hepatocytes were cultured for 16–20 h before X-gal staining, performed as described previously. Histological X-gal staining of frozen liver sections was performed seven days after retroviral infusion and was described previously (11).

Generation of LX/hAAT Retrovirus. LX/hAAT was constructed by removing the *neo* gene and CMV promoter from LNCX by BclI (blunted), HindIII restriction enzyme digest, and inserting the hAAT coding regio

as a SmaI, HindIII fragment. The LX/hAAT construct was then electroporated into GPAM-12 packaging cells, and individual virus producing colonies were selected and screened for retroviral production (retroviral supernatant from individual colonies were used to transduce rat embryo fibroblast cell line 208F and hAAT production from the fibroblasts was assayed). The apparent titer of LX/hAAT is at least 2×10^6 PFU/ml as determined by comparing the amounts of viral RNA in the supernatant from LX/hAAT producing cells to a retrovirus of known titer (data not shown).

Detection of hAAT in Rat Serum. Rat serum was isolated and the concentration of human α_1-antitrypsin was determined by an ELISA as described in Kay et al. (8).

RESULTS

Recombinant Retroviral Vectors. The amphotropic retrovirus LX/β-Geo (Fig. 1A) has been described previously (8). Briefly, β-Geo is a fusion of the *E. coli* β-galactosidase gene and the neomycin phosphotransferase gene. The fusion protein retains both enzymatic activities. The β-Geo gene is under the transcriptional control of the Moloney murine leukemia virus (MMLV) long terminal repeat (LTR) described by Miller and Rosman (12). The retrovirus is produced from the amphotropic retroviral packaging cell line GPAM-12 and has a titer of 1×10^6 PFU/ml. The LX/hAAT retrovirus (Fig. 1B) encodes the human α_1-antitrypsin gene (8) under the transcriptional control of the MMLV-LTR (12).

In Vivo Retroviral Transduction of Rat Hepatocytes. The MMLV vectors require a cell to be dividing in order to integrate into the host genome. To stimulate hepatocyte replication, a 70% partial hepatectomy can be performed. Since young rats (3–4 weeks old) have a greater rate of DNA synthesis than older rats after partial hepatectomy (13), their hepatocytes will be more susceptible to retroviral transduction. A 70% partial hepatectomy was thus performed on 3 to 4-week-old male Lewis rats and 24 h later, 3 ml of the β-Geo retrovirus was infused into the portal vein over the course of 30 min. Seven days later, the liver was isolated and the frozen section was stained for X-gal. As can be seen in Fig. 2A, there are many cells that have stained in the liver infused with the β-Geo retrovirus, while no blue cells are visible in liver after only a partial hepatectomy and mock infusion (Fig. 2B). It is known that the amphotropic retrovirus can transduce vascular endothelial cells in vivo (4). However, of the sections we inspected, transduction was limited to cells with hepatocyte morphology (Fig. 2A). The blue cells are relatively evenly dispersed in the liver parenchyma, although some appeared in groups and rows, perhaps indicating limited division of hepatocytes following transduction.

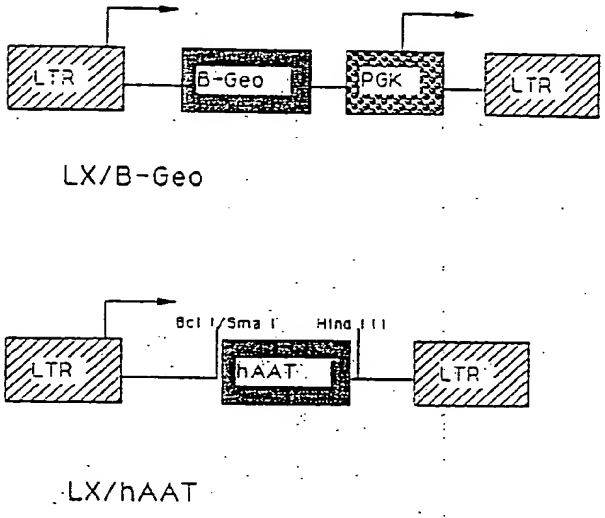

Fig. 1. Diagrams of the retroviruses used in this study. (A) LX/β-Geo, β-Geo is a fusion gene of the neomycin phosphotransferase gene and the β-galactosidase gene. β-Geo is under the transcriptional control of the Moloney murine leukemia virus (MMLV) long terminal repeat (LTR). The retrovirus also encodes for the phosphoglycerol kinase promoter (PGK). (B) LX/hAAT encodes the human α_1-antitrypsin gene under the transcriptional control of MMLV LTR. The arrows indicate transcriptional start sites.

Time Course for Optimal Retroviral Transduction of Rat Hepatocytes In Vivo. To deter-

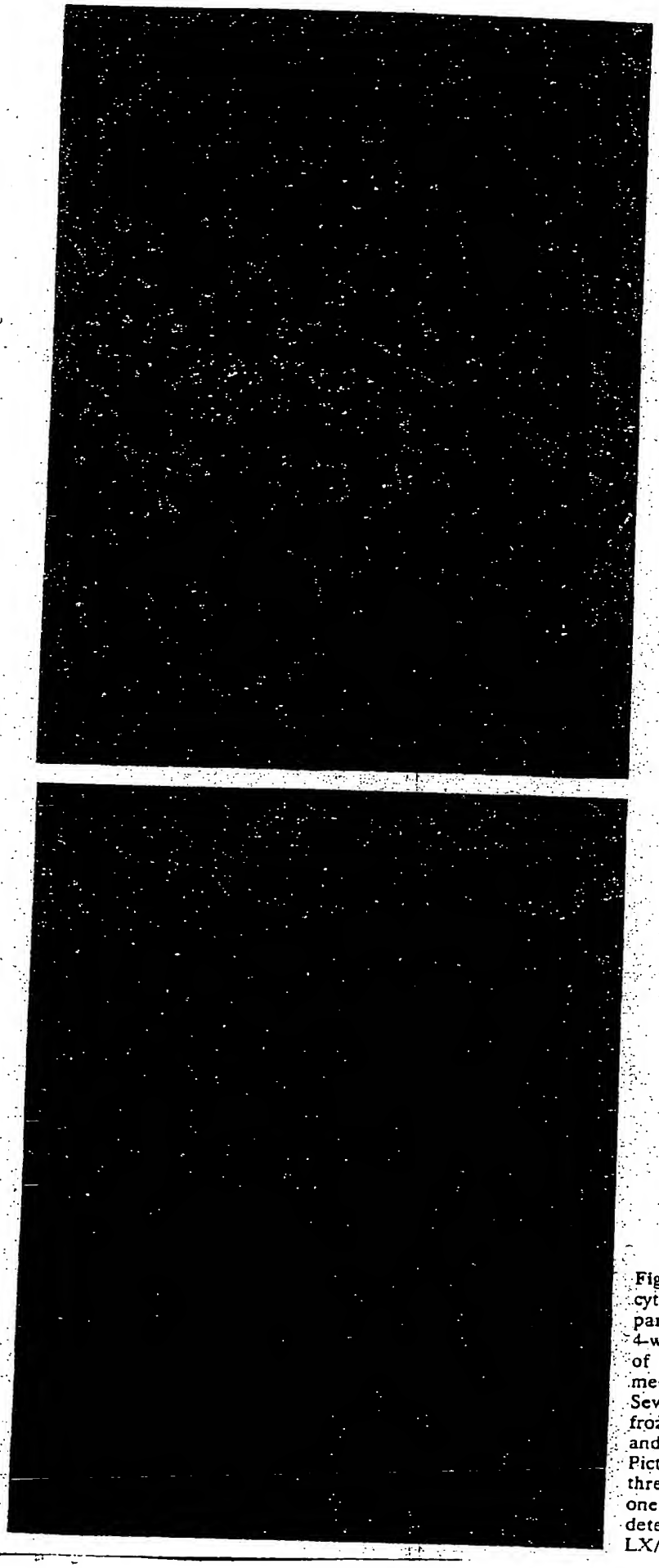

Fig. 2. In vivo transduction of rat hepatocytes with LX/β-Geo retrovirus. A 70% partial hepatectomy was performed on 3 to 4-week-old rats; 24 h later, either (A) 3.0 ml of LX/β-Geo retrovirus or (B) 3.0 ml of medium was infused into the portal vein. Seven days later, the liver was isolated, frozen, sectioned, and stained with X-gal and counterstained with nuclear fast red. Pictures represent sections from one of three rats infused with β-Geo, and one of one mock infused. Blue cells were only detected in the liver sections infused with LX/β-Geo retrovirus.

mine when to infuse retrovirus after partial hepatectomy for optimal transduction of rat hepatocytes, retrovirus was infused into rats at 0, 12, 18, 24, and 36 h after partial hepatectomy. In order to better quantitate the transduction efficiency and to ensure the blue cells were hepatocytes, we isolated and cultured the hepatocytes under conditions that selected for the growth of hepatocytes. Ten days after retroviral infusion, hepatocytes were isolated by collagenase perfusion and cultured overnight as described in Materials and Methods. Even if cell division occurs, the percentage of blue cells should not change, unless transduction affects hepatocyte growth. Twelve hours after X-gal staining, the percent transduction was calculated by scanning random fields at 400× magnification and counting the number of blue cells and the total number of cells (at least 700). The optimal time for retroviral infusion appears to be 24 h after partial hepatectomy, at which time, 10–15% of the hepatocytes were transduced (Fig. 3).

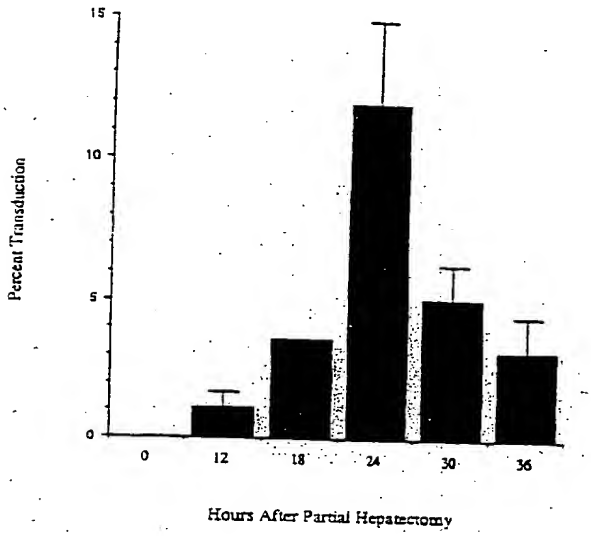

Fig. 3. Time course for in vivo infection of rat hepatocytes. The 70% partial hepatectomies were performed on 3 to 4-week-old male Lewis rats. Then at time 0 h ($N = 2$), 12 h ($N = 5$), 18 h ($N = 1$), 24 h ($N = 5$), 30 h ($N = 4$) or 36 h ($N = 3$) after partial hepatectomy, 3.0 ml of retroviral supernatant was infused into the portal vein. Seven to 10 days after transduction, the hepatocytes were isolated, cultured for 18 h, and stained with X-gal. Plates of hepatocytes were scanned at 400× magnification and random fields were counted for the number of blue cells and the total number of cells. At least 700 cells were counted per time point. Bars represent mean and standard deviation. Range at 24 h is 8.6–16.7%.

Retroviral Transduction Efficiency of Rat and Mouse Hepatocytes In Vitro. Kay et al. (8) reported that using this in vivo retroviral transduction method in the mouse, they achieved a hepatocyte transduction efficiency of 1–2%, while we observed a 10–15% transduction efficiency in the rat. The 10-fold difference in transduction efficiency is not due to inherent differences in susceptibilities to infection by amphotropic retrovirus, since rat and mouse hepatocytes are transduced 20–25% with an amphotropic retrovirus in culture (14, 15, and Dr. M. Kay, personal communication). Thus both the rat and mouse hepatocytes are equally susceptible to amphotropic retroviral transduction.

Histological Study of Regenerating Liver of Rat and Mouse. Since both rat and mouse hepatocytes are equally susceptible to retroviral transduction in vitro, we investigated the regenerating livers of rats and mice. Perhaps, if the rat has a more vigorous hepatocyte replication response after partial hepatectomy than the mouse, it would explain the difference in transduction efficiency. The 70% partial hepatectomies were performed on rats and mice, and the remaining liver lobes were isolated at times when in vivo retroviral transduction is known to be optimal (24 h for the rat and 48 h for the mouse). Random fields were scanned at 400× magnification and the number of mitotic figures and the total number of cells was determined. The mitotic index is the number of mitotic figures per 1000 cells (3). The rat liver had a mitotic index of 84.8, while the mouse liver had a mitotic index of 24.6. In both animals, the mitotic figures did not appear localized in any region of the liver (i.e., periportal).

Expression of Human α_1-Antitrypsin in Transduced Rat Hepatocytes. In order to study the expression of retrovirally transduced

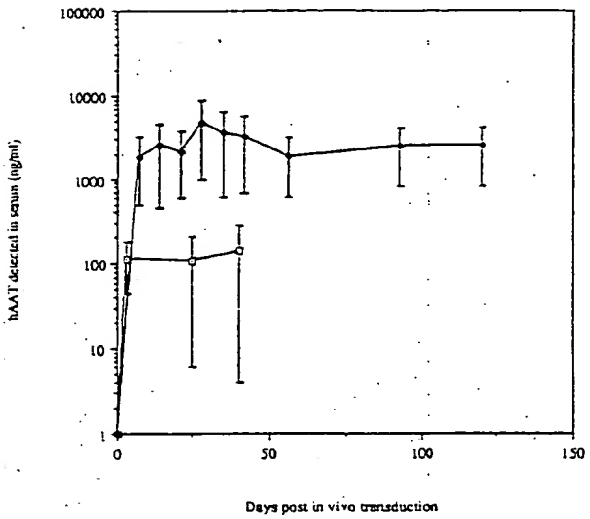

Fig. 4. Detection of human α_1-antitrypsin in the serum of rats (closed squares) and mice (open squares) after in vivo transduction of hepatocytes with LX/hAAT retrovirus. The 70% partial hepatectomies were performed on mice and rats. The rats were infused 24 h later with 3.0 ml of supernatant containing the LX/hAAT retrovirus, while the mice were infused at 48 h with 1.0 ml of supernatant. Serum samples were collected from the animals at the indicated times and assayed for hAAT. The graph represents the mean ± standard deviation for $N = 4$ (mouse) and $N = 7$ (rat).

genes long-term, we transduced rat hepatocytes with a retrovirus encoding the gene for human α_1-antitrypsin (hAAT). hAAT was chosen because, being a secreted protein, its presence can be detected easily in the serum of the animal, and expression can be monitored long-term in each animal. hAAT has also been shown not to elicit an immunological response in dogs and mice when expressed from hepatocytes, but it can be detected and quantitated by an ELISA assay. A 70% partial hepatectomy was performed on rats, followed 24 h later by infusion of 3 ml of supernatant containing the LX/hAAT retrovirus. As can be seen in Fig. 4, hAAT can be detected in the rat serum seven days after retroviral transduction. The average levels reached 2000 ng/ml within a week after viral infusion and remained steady for at least 120 days. No hAAT was ever detected in the serum of rats transduced with a control retroviral vector (data not shown).

Mouse hepatocytes were also transduced in vivo with the same retrovirus under optimal conditions, and the presence of hAAT was monitored in their serum. hAAT levels in the mouse have also remained steady for 40 days of monitoring. As can be seen in Fig. 4, the average level of hAAT in the mouse of about 100–200 ng/ml is 10-fold lower that in the rat. This observation is in agreement with the results from the β-gal staining showing that hepatocyte transduction in the rat is 10-fold higher than in the mouse.

DISCUSSION

A 70% partial hepatectomy followed by infusion of retrovirus into the portal vein results in 1–2% hepatocyte transduction in the mouse (8), while in the rat, the same technique achieves 10–15% hepatocyte transduction. This difference is not due to differences in susceptibilities to retroviral transduction since both rat and mouse hepatocytes are equally transduced by amphotropic retrovirus in vitro. The difference is also not due to a greater number of virus particles being infused into the rat since we infused 3.0 ml into a 50-g rat (or 6×10^4 PFU/g body weight) while Kay et al. (8) infused 8×10^4 PFU/g into the mouse. The difference may be due, in part, to the fact that at the time for optimum transduction by retrovirus, the rat liver has a three to fourfold higher mitotic index than the mouse.

The percentage of transduced cells by our method (10–15%) is comparable to that achieved using the vascular isolation method (5–20%) of Ferry et al. (6) and 16% by Rozga et al. (7). A critical difference is that while the other groups' methods require very intricate surgical procedures to vascularly isolate the liver before infusion of retrovirus into the portal vein, our method only requires infusion of the retrovirus into the portal vein.

To study the expression of transduced

genes long-term, we used the secreted marker protein human α_1-antitrypsin (hAAT). Using hAAT as a marker, one can study both the level of expression and changes in expression levels in one animal. This is superior to transducing several animals and sacrificing them at different times to determine percentage of cells still expressing the gene of interest, since one then introduces variability between animals. The amounts of hAAT being expressed varied from animal to animal. The levels ranged from 200 ng/ml to 4000 ng/ml. The levels of hAAT appear to be steady for at least six months. With respect to hAAT production, the mice produced up to 100–200 ng/ml of hAAT, while the rats averaged 2000 ng/ml. This is the expected result since 10-fold more hepatocytes are shown to be transduced by X-gal staining in the rat than in the mouse.

The focus of this study was to develop a simple and efficient method to deliver genes to the rat liver using recombinant retroviral vectors. We determined that a 70% partial hepatectomy followed 24 h later by infusion of 3 ml of retrovirus into the portal vein results in 10–15% hepatocyte transduction. Genes introduced in this manner are also expressed for at least six months. These results suggest that the rat is an excellent model for hepatic gene therapy of metabolic disorders.

ACKNOWLEDGMENTS

We thank Carol Toman for cloning, producing and titering LX/hAAT, and Frances Leland for assaying the rat serum for hAAT levels. This work was supported in part by NIH grant HL 40162. T.M.K. is the recipient of a March of Dimes Predoctoral Fellowship Award 18-FY92-0992 and S.L.C.W. is an investigator of the Howard Hughes Medical Institute.

LITERATURE CITED

1. Baker, H.J., Lindsey, B.J., and Weisbroth, S.H. (eds.). (1979/1980). *The Laboratory Rat, Vol. I, Biology and Diseases* (1979), *Vol. II, Research Applications* (1980), (Academic Press, New York).
2. Scriver, C.R., Beaudet, A.L., Sly, W.S., and Valle, D. (eds.). (19XX). *The Metabolic Basis of Inherited Disease Vol. 2*, (McGraw-Hill, New York).
3. Reinert, J., and Holtzer, H. (eds.). (1975). *Cell Cycle and Cell Differentiation, Vol. 7*, (Springer-Verlag, New York), pp. 215–223.
4. Nabel, E.G., Plautz, G., and Nabel, G.J. (1990). *Science* 249:1285–1288.
5. Miller, D.G., Adam, M.A., and Miller, A.D. (1990). *Mol. Cell. Biol.* 10:4239–4242.
6. Ferry, N., Duplessis, O., Houssin, D., Danos, O., and Heard, J.-M. (1991). *Proc. Natl. Acad. Sci. U.S.A.* 88:8377–8381.
7. Rozga, J., Moscioni, A.D., Neuzil, D., and Demetriou, A.A. (1992). *J. Surg. Res.* 52:209–213.
8. Kay, M.A., Li, L., Liu, T.J., Leland, F., Toman, C., Finegold, M., and Woo, S.L.C. (1992). *Hum. Gene Ther.* 3:641–647.
9. Higgens, G.M., and Anderson, R.M. (1931). *Arch. Pathol.* 12:186–202.
10. Berry, M.N., and Friend, D.S. (1969). *J. Cell Biol.* 43:506–520.
11. Ponder, K.P., Dunbar, R.D., Wilson, D.R., Darlington, G.J., and Woo, S.L.C. (1991). *Hum. Gene Ther.* 2:41–52.
12. Miller, A.D., and Rosman, G.J. (1989). *BioTechniques* 7:980–990.
13. Bucher, N.L.R., Swaffield, M.N., and DiTroia, J.F. (1964). *Cancer Res.* 24:509–512.
14. Wolff, J.A., Yee, J.-K., Skelly, H.F., Morres, J.C., Respess, J.G., Friedmann, T., and Leffert, H. (1987). *Proc. Natl. Acad. Sci. U.S.A.* 84:3344–3348.
15. Wilson, J.M., Jefferson, D.M., Chowdhury, J.R., Novikoff, P.M., Johnston, D.E., and Mulligan, R.C. (1988). *Proc. Natl. Acad. Sci. U.S.A.* 85:3014–3018.

Somatic Cell and Molecular Genetics, Vol. 20, No. 3, 1994, p. 251

Erratum

The name of one of the authors was inadvertently omitted by the authors from the paper, "Hepatic Gene Therapy: Efficient Retroviral Mediated Gene Transfer into Rat Hepatocytes In Vivo," Vol. 19, No. 5, 1993, pp. 491–497. The listing of authors should read Tadeusz M. Kolodka, Milton Finegold, Mark A. Kay, and Savio L.C. Woo.

0740-7750/94/0500-0251$07.00/0

COMMONWEALTH OF AUSTRALIA

(Patents Act 1990)

IN THE MATTER OF: Australian Patent Application 696764 (73941/94). In the name of: Human Genome Sciences Inc.

- and -

IN THE MATTER OF: Opposition thereto by Ludwig Institute for Cancer Research, under Section 59 of the Patents Act.

Annexure GBC-17

This is **Annexure GBC-17** referred to in my Statutory Declaration made this Thirteenth day of December 2000.

Gary Cox

Gary Baxter Cox

WITNESS: Peyton Kim

Patent Attorney PEYTEE KIM

0023-6837/92/6704-0519$03.00/0
LABORATORY INVESTIGATION

Vol. 67, No. 4, p. 519, 1992
Printed in U.S.A.

Methods in Laboratory Investigation

A Simple, Quantitative Method for Assessing Angiogenesis and Antiangiogenic Agents Using Reconstituted Basement Membrane, Heparin, and Fibroblast Growth Factor

ANTONINO PASSANITI, ROBERT M. TAYLOR, ROBERTO PILI, YUE GUO, PETER V. LONG, JOSEPH A. HANEY, REBECCA R. PAULY, DERRICK S. GRANT, AND GEORGE R. MARTIN

Laboratories of Biological Chemistry and Cardiovascular Science, Gerontology Research Center, National Institute on Aging, National Institutes of Health and Department of Pathology and Dermatology, Johns Hopkins Medical Institutions, Baltimore and Laboratory of Development Biology, National Institute of Dental Research, Bethesda, Maryland

BACKGROUND: Blood vessel growth is necessary for normal tissue homeostasis and contributes to solid tumor growth. Methods to quantitate neovascularization should be useful in testing biological factors and drugs that regulate angiogenesis or to induce a vascular supply to promote wound healing.

EXPERIMENTAL DESIGN: An extract of basement membrane proteins (Matrigel) was found to reconstitute into a gel when injected subcutaneously into C57/BL mice and to support an intense vascular response when supplemented with angiogenic factors.

RESULTS: New vessels and von Willebrand factor antigen staining were apparent in the gel 2–3 days after injection, reaching a maximum after 3–5 days. Hemoglobin content of the gels was found to parallel the increase in vessels in the gel allowing ready quantitation. Angiogenesis was obtained with both acidic and basic fibroblast growth factors and was enhanced by heparin. Several substances were tested for angiostatic activity in this assay by coinjection in Matrigel with fibroblast growth factor and heparin. Platelet-derived growth factor BB, interleukin 1-β, interleukin-6, and transforming growth factor-β were potent inhibitors of neovascularization induced by fibroblast growth factor. Tumor necrosis factor-α did not alter the response but was alone a potent inducer of neovascularization when coinjected with Matrigel and heparin. Consistent with the previously demonstrated importance of collagenase in mediating endothelial cell invasion, a tissue inhibitor of metalloproteinases that also inhibits collagenases was found to be a potent inhibitor of fibroblast growth factor-induced angiogenesis.

CONCLUSIONS: Our assay allows the ready quantitative assessment of angiogenic and antiangiogenic factors and should be useful in the isolation of endothelial cells from the capillaries that penetrate into the gel.

Additional key words: Neovascularization, Matrigel

The development of a vascular supply is essential for the growth, maturation, and maintenance of normal tissues (1). It is also required for wound healing (2) and the rapid growth of solid tumors (3, 4) and is involved in various other pathological conditions (1, 5–7). Current concepts of angiogenesis, based in large part on studies on the vascularization of tumors (1), suggest that cells secrete angiogenic factors that induce endothelial cell migration, proliferation, and capillary formation. Although the factors that induce angiogenesis *in situ* are not well identified, numerous factors have been identified that induce vessel formation *in vitro* or *in vivo* in animal models. These include acidic fibroblast growth factor (aFGF) (1, 8, 9), basic (b) FGF (1, 9, 10), transforming growth factor (TGF)-α (1), TNF-α (11, 12), vascula permeability factor or vascular endothelium growth fac tor (13–15), monobutyrin (16), angiotropin (17), angi ogenin (18), hyaluronic acid degradation products (19) and age-associated glycosylation end-products (20). Alsc many compounds have been described as inhibitors o angiogenesis including a cartilage-derived inhibito identified as tissue inhibitor of metalloproteinase (TIMP) (21, 22), platelet factor-4 (23), thrombospondi (24–26), laminin peptides (27), heparin/cortisone (28 30), minocycline (31), fumagillin (32), difluorometh ornithine (33), and sulfated chitin derivatives (34).

The classic assessment of an angiogenic factor achieved either by embedding the factor in a controlle

release polymer such as ethylene vinyl acetate or cellulose discs (reviewed in Ref. 22) and implanting the substances in the cornea of an animal's eye (35, 36) or by placing these substances on the chorioallantoic membrane of the chick embryo (37) and observing the sprouting of new vessels toward the pellet. Alginate-encapsulated tumor cells (38, 39) and gelatin-impregnated sponges (40) (Gelfoam, Upjohn, Kalamazoo, Michigan) have also been used as angiogenesis inducers. In the alginate tumor cell model, hemoglobin content was used to quantitate angiogenesis. In addition, several *in vitro* models have been used to examine the progression of angiogenesis including the sprouting, attachment, migration, invasion, and morphological differentiation of endothelial cells (8, 12, 41–44).

Here we report on a simple, rapid, and quantitative assay to assess inducers as well as inhibitors of angiogenesis. In brief, we inject a solution a basement membrane proteins supplemented with FGF and heparin subcutaneously in a mouse where it forms a gel. Sprouts from vessels in the adjacent tissue penetrate into the gel within days, connecting it with the external vasculature. Angiogenesis was quantitated by image analysis of vessels and by measuring the hemoglobin present in the vessels within the gel. This assay will facilitate the testing of both angiogenic and angiostatic agents *in vivo* and may allow isolation of the endothelial cells responding to the angiogenic factors for further studies *in vitro*.

EXPERIMENTAL DESIGN

PREPARATION OF ANGIOGENIC FACTORS AND VEHICLE

Liquid Matrigel maintained at 4°C was used as a vehicle to inject angiogenic factors subcutaneously into C57/BL mice. Various components were mixed with liquid Matrigel at 4°C which, when injected into a mouse, formed a single, readily recovered gel. Such gels were removed at various times and processed for histology, total protein, and hemoglobin content.

Matrigel, an extract of murine basement membrane proteins consisting predominantly of laminin, collagen IV, heparan sulfate, proteoglycan, and nidogen/entactin was prepared as a sterile solution as previously described (45). Heparin was dissolved in sterile phosphate-buffered saline (PBS) to 16,000 units/ml. Further dilutions were made with sterile filtered PBS containing 1 mg bovine serum albumin/ml. aFGF (HBGF-1) (R & D, Minneapolis, Minnesota) was diluted to 0.25 μg/ml with PBS/bovine serum albumin. Various amounts of heparin and/or FGF were mixed with 0.5–1.0 ml of Matrigel at 4°C in proportions not exceeding 1% of the volume of Matrigel to be injected. In some cases, other factors were included as noted.

INJECTION AND PROCESSING OF GELS

C57BL mice (five per data point) were each injected subcutaneously with 0.5 ml Matrigel and 0–100 ng aFGF/... and 0–64 units heparin/ml near the abdominal midline using a 25-gauge needle. The injected Matrigel rapidly formed a single, solid gel that persisted for at least 10 days in the mice. Mice were subsequently killed, and gels were recovered and processed for further studies. Typically, the overlying skin was removed, and gels were cut out by retaining the peritoneal lining for support. For most histological sections, the skin and underlying peritoneum were Formalin-fixed immediately after dissection.

QUANTITATION OF NEOVESSELS

Hemoglobin was measured using the Drabkin method (46) and Drabkin reagent kit 525 (Sigma, St Louis, Missouri). Samples for each point were from five different mice. The concentration of hemoglobin was calculated from a known amount of hemoglobin assayed in parallel. Protein content of the supernatant fluid was determined using the BioRad protein assay method (47). The Optomax image analysis system (Optomax, Hollis, New Hampshire) was used for quantitation of histological specimens by light microscopy (see "Methods").

RESULTS AND DISCUSSION

MATRIGEL AS A VEHICLE FOR ANGIOGENIC FACTORS

In developing a more reproducible and quantitative angiogenic model, we utilized FGFs that are proven and potent inducers of neovascularization. When injected alone subcutaneously into mice, neither aFGF nor bFGF induced any visible signs of neovessel formation (data not shown). This is not unexpected since the factors would be expected to be rapidly cleared from the site. We tested Matrigel, a solution of basement membrane proteins isolated from the Engelbreth-Holm-Swarm tumor, as a vehicle for the slow release of angiogenic factors since it is a liquid at 4°C but forms a gel *in vivo*. Indeed, our studies showed that the gels which formed after subcutaneous injection of Matrigel alone were readily distinguished from surrounding tissue, persisted for at least 10 days, and produced little or no local reaction or angiogenic response (Fig. 1*A*).

Matrigel supplemented with FGF alone produced gels that showed a variable angiogenic reaction (data not shown). Magnitude of the angiogenic response was considerably greater in gels supplemented with both FGF and heparin (Fig. 1*B* and *C*). Subcutaneous injection of Matrigel plus aFGF and heparin at the ventral midline achieved optimal and reproducible responses, whereas material injected either anteriorly or posteriorly to the midline resulted in less consistent responses. Auerbach *et al.* (48) found similar regional differences in tumor growth that might also be related to the capacity for vascularization at these sites. Dorsal injections also induced consistent responses, but the abdominal location was used almost exclusively in this study. Gels could be recovered intact by dissection of the underlying peritoneum (Fig. 2). The tissue in contact with the FGF- and heparin-supplemented gels contained abundant and readily visible blood vess ls (Fig. 2). Large neovessels were also present on the surfac (Fig. 3*A*, *B*), whereas small, tortuous vessels were observed within the g l (Fig. 3*C*). The effect of age of the animal on the angiogenic

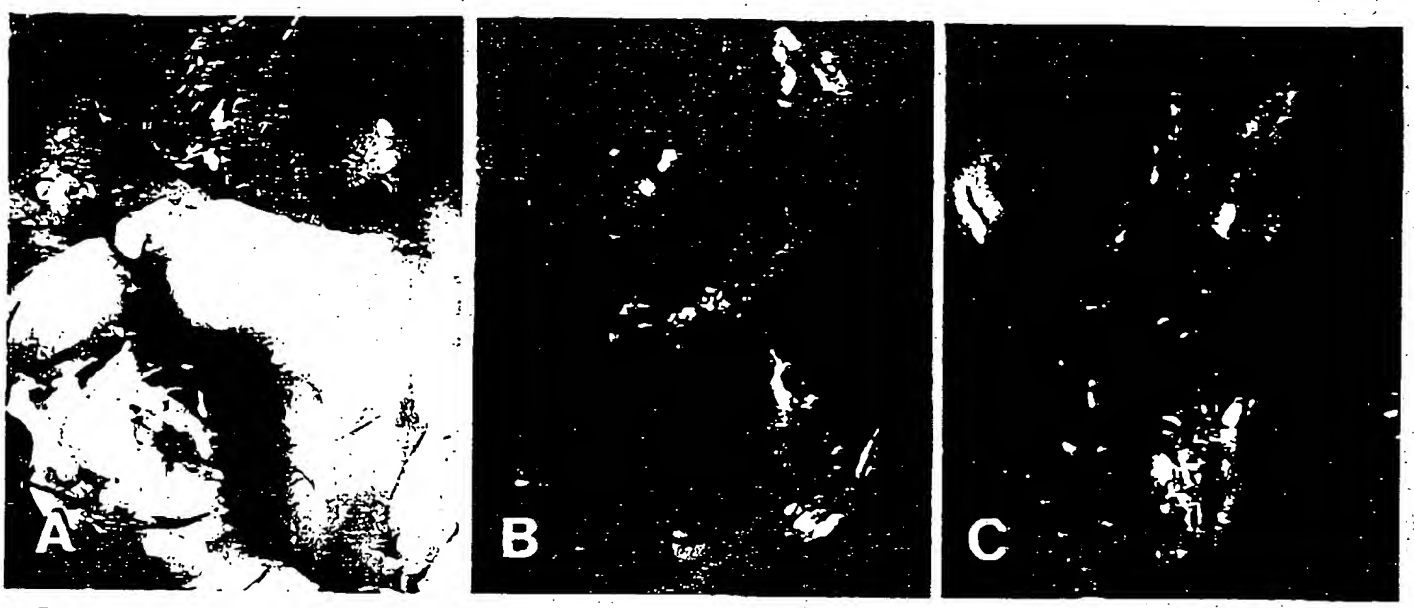

FIG. 1. Appearance of Matrigel gels on day 4 (*A*) or Matrigel supplemented with 1 ng/ml FGF and 40 units/ml heparin on day 1 (*B*) or day 4 (*C*) after subcutaneous injection. Overlying skin was removed to expose gels. Note that surface of gels as well as overlying skin flaps contain many vessels. Bleeding seen here was also seen with some Matrigel/FGF and Matrigel/heparin injections, but these produced little or no vessel infiltration and was <10% of the amount of hemoglobin found in Matrigel/FGF/heparin gels at 4 days (see also Table 1).

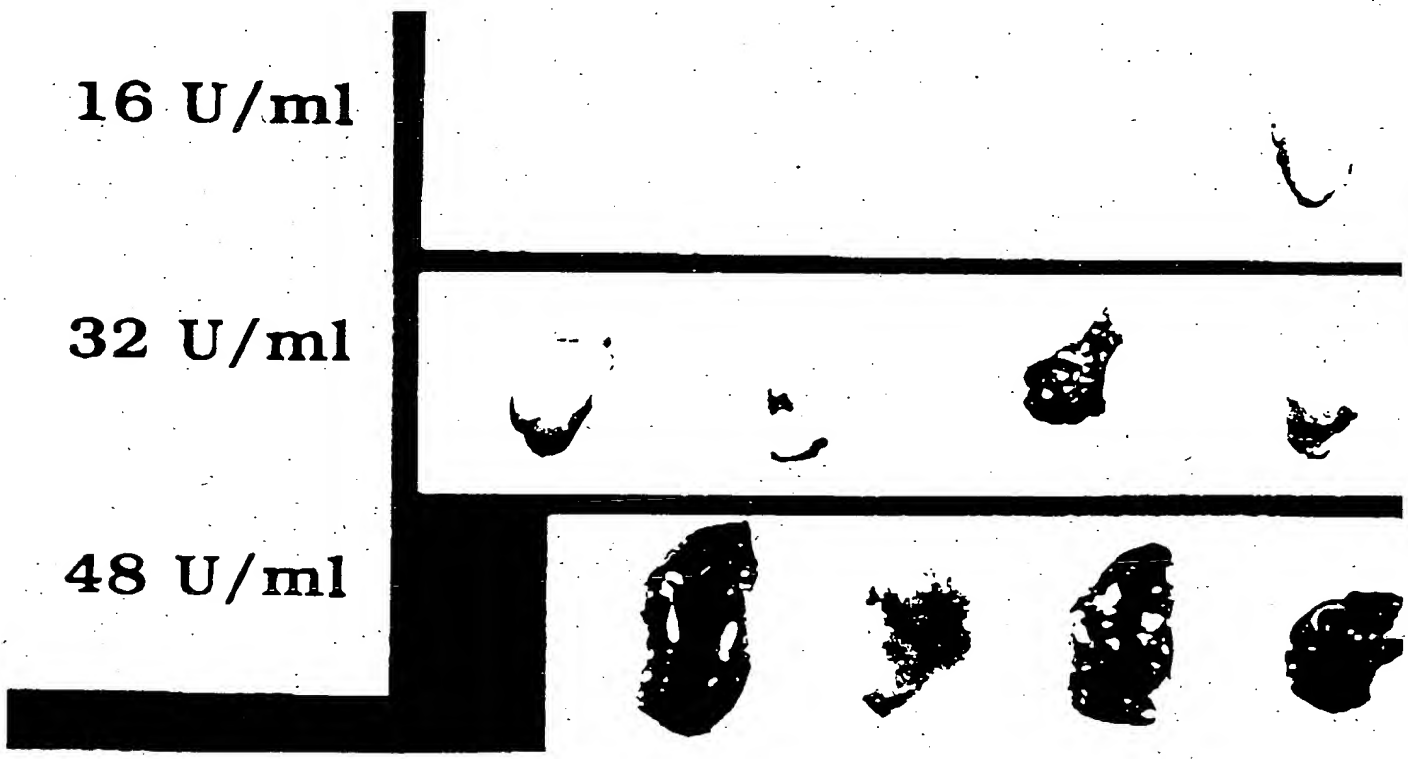

FIG. 2. Appearance of Matrigel gel recovered after 4 days *in vivo*: angiogenic response as a function of heparin concentration. Mice were injected with Matrigel and aFGF as in Figure 1*C* but with various heparin doses. After killing animals, skin was removed, and gels were cut out with intact peritoneal lining for support and placed on tissue culture dishes for photography. Each gel was between 0.8 and 1.4 cm long. Heparin dependence of response is apparent (see also Table 1).

response showed that vessel formation was reduced in young (6 month) animals compared with older mice (12, 18, or 24 months of age) where the response was typically twice as strong.

HISTOLOGY AND ENDOTHELIAL CELL STAINING

Sections examined with the Trichrome-Masson stain (Fig. 4) showed that cells invaded the gel within 24 hours and persisted for up to 8 days with a progressive increase

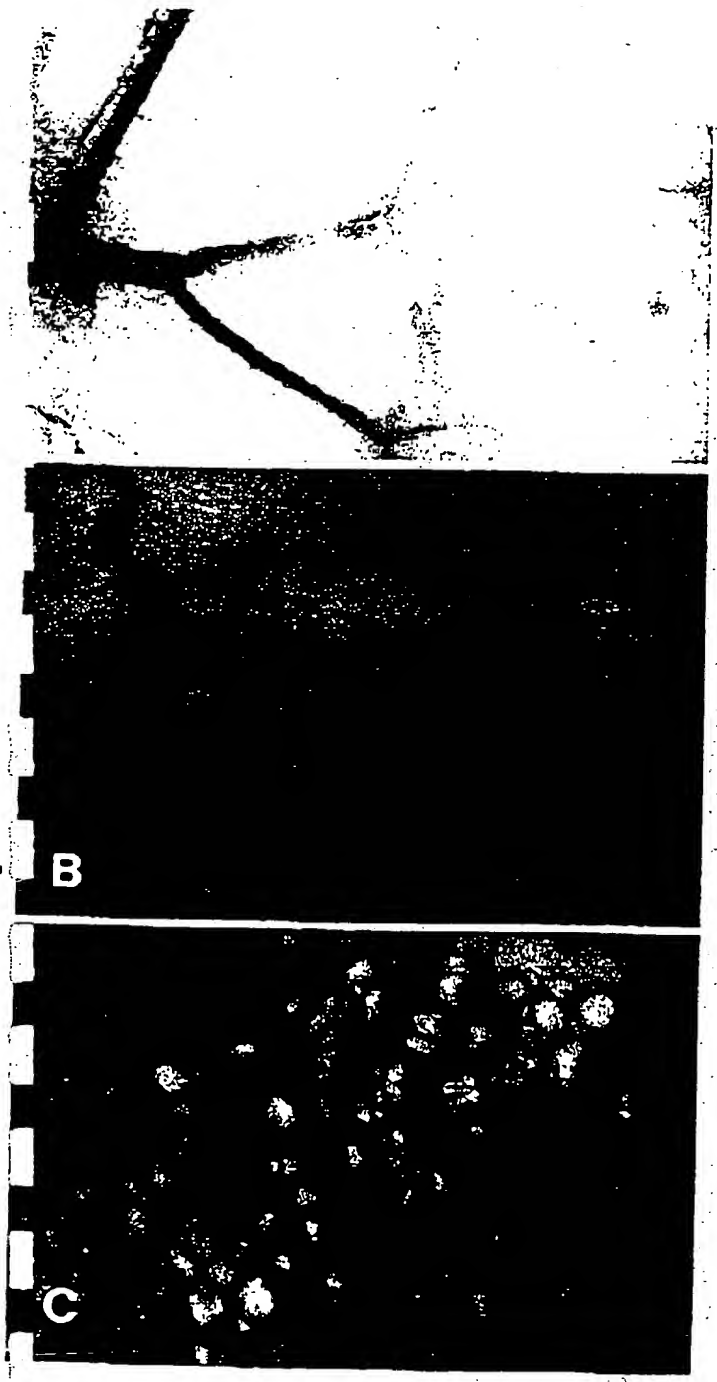

FIG. 3. Appearance of vessels associated with FGF/heparin-supplemented gels. Vessels surrounding gel appear to derive from peritoneal lining (*A*) and skin (*B*). *Arrows*, regions in injected gel that contain tuous neovessels derived from ramified pre-existing vessels. Small tuous tubes are also prevalent inside gel (*C*, *arrows*) that appears atypical.

lin ar structures containing red blood cells which was indicative of functional vessels. Sections of the gel were reacted with antibody to factor VIII antigen (von Willebrand factor) to confirm the presence of endothelial cells association with the vessels. The presence of capillary-sized vessels in the gel was apparent at 72 hours (Fig. 5). These neovessels were also apparent by 48 hours (not shown) and are smaller than other factor VIII positive structures (pre-existing vessels) on the periphery of the Matrigel (Fig. 5, arrowheads). Neovascularization was not observed at 24 hours, although inflammatory cells were observed in the region between the Matrigel and skeletal muscle.

QUANTITATION OF FGF-INDUCED ANGIOGENESIS

The increase in vessels in the gels, based on specific von Willebrand factor stain as quantitated by an image analysis system (Fig. 6), was similar to the increase in cells (hematoxylin/eosin and trichrome stain). Measurement of hemoglobin content indicated formation of a functional vasculature at the site of angiogenesis. As judged by hemoglobin content, the angiogenic response to FGF was time dependent, clearly visible by days 1–2, reached a plateau by days 3–4, and persisted through day 8 (Fig. 6, *lower panel*) occurring with similar kinetics as observed for the accumulation of neovessels (Fig. 6, *upper* and *middle panels*).

In the presence of heparin (64 units/ml), the maximal angiogenic response occurred at 1 ng/ml aFGF (Table 1) followed by a decrease and then a subsequent increase at higher levels of FGF. These data are consistent with the down-regulation of FGF receptors in the presence of higher levels of the growth factor (57). In some experiments, higher doses of FGF were used (125 and 250 ng FGF/ml), and these showed responses similar to those observed at 100 ng/ml. In contrast, heparin induced a linear increase in angiogenesis in the presence of 1 ng/ml FGF (Table 1). The lowest concentration of heparin that resulted in consistent vascularization of the gels was 40 units/ml. At this concentration of heparin, the FGF response was also biphasic with an optimum again at 1 ng/ml (data not shown). The amount of aFGF (0.5 ng) required for an angiogenic response in these assays is similar to the levels of FGF necessary for endothelial cell growth in culture (49, 50) and to the levels required to elicit an angiogenic response in the chick allantoic membrane (10). Our results suggest that the angiogenic response induced by heparin and aFGF occurs at physiologically relevant doses of FGF observed previously using other assays and other angiogenic factors.

INHIBITORS AND ACTIVATORS OF NEOVASCULARIZATION

We tested several cytokines for angiogenic activity in this assay in the presence of heparin to determine whether the assay was comparable to other established angiogenesis assays (Table 2). Of the various factors tested, aFGF, bFGF, and TNF-α induced an angiogenic response (Table 2), consistent with previous reports on these factors (1, 11, 51) whereas TGFβ, PDGF, interleukin (IL)-1, and IL-6 were inactive.

We also assessed the angiostatic activity of certain cytokines when included with aFGF (Table 3). IL-1β, IL-6 (52), and TGFβ inhibited the angiogenic response to aFGF. The TGFβ dose response showed inhibition at concentrations as low as 0.2 ng/ml. PDGF BB was also

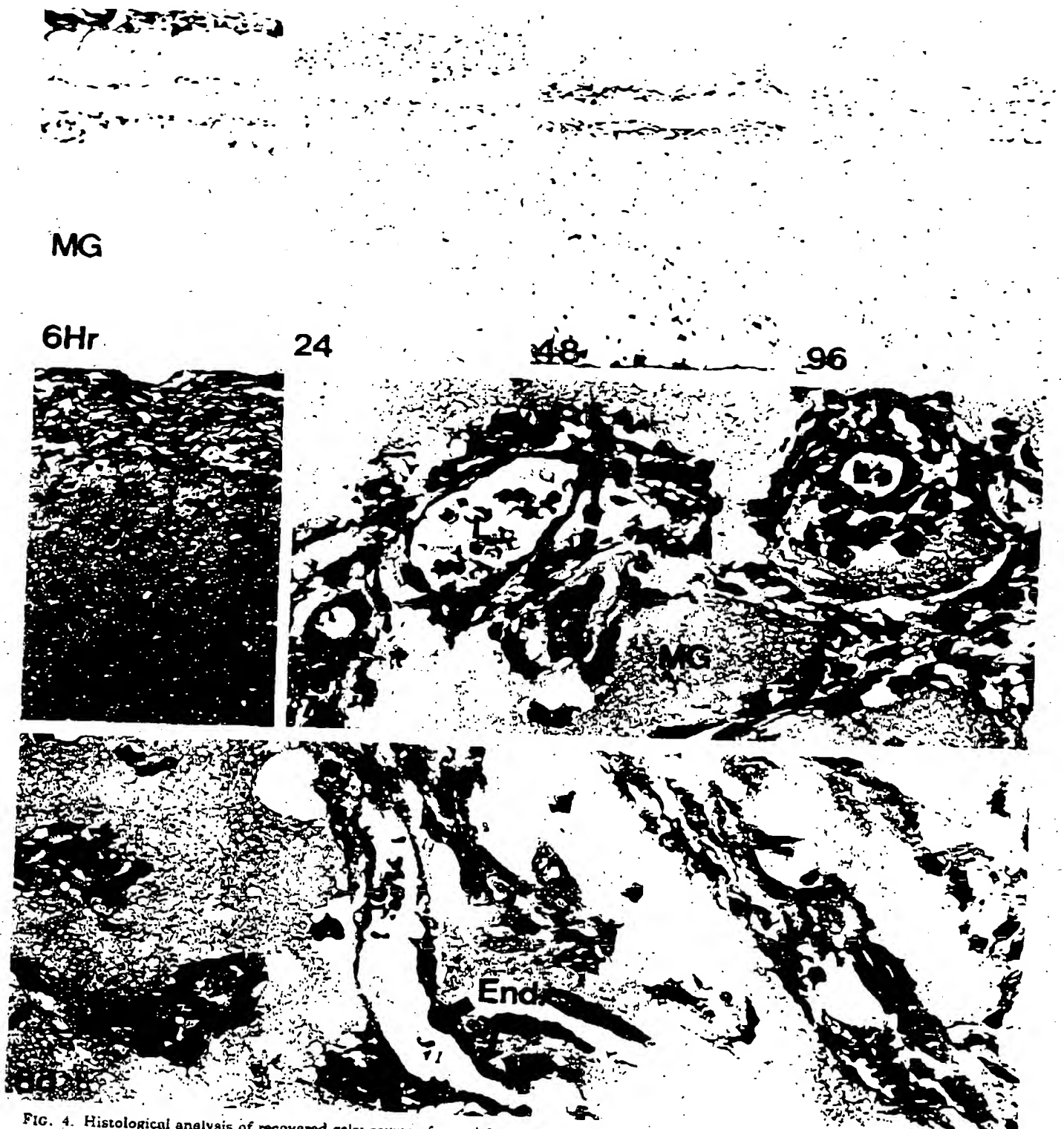

FIG. 4. Histological analysis of recovered gels: course of vessel formation. Samples were prepared for histology as described in "Methods" at different times after injection of Matrigel containing FGF and heparin. Trichrome-Masson stained specimens show the progressive invasion of cells into the Matrigel (MG) over 6, 24, 48, and 96 hours (top four panels; Mag = ×125). By 7 days, there is more organization of the cells into linear structures. At higher magnification (×500; middle panel, 7 day), the connective septa within the Matrigel exhibits large blood vessels from which an extension of a vessel into the Matrigel is evident (*two arrows*). At 8 days, many vessels within the Matrigel are well formed exhibiting a clear endothelium (End).

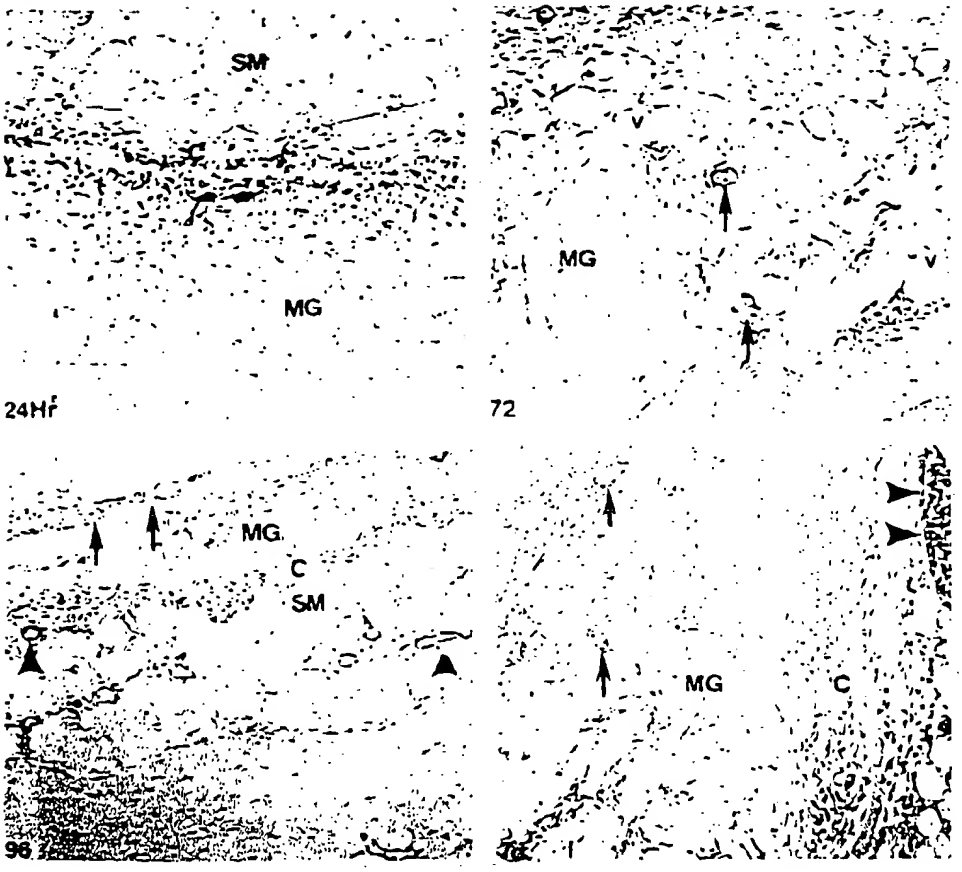

FIG. 5. Factor VIII staining of neovessels. Gels recovered after 1, 3, 4, and 7 days were stained with von Willebrand factor antibody as described in "Methods." Presence of neovessels (*arrows*) in Matrigel (MG) layer can be distinguished from existing vessels (*arrowheads*) near skeletal muscle (SM) and collagen (C) interface. Small vessels (72 hours), horizontally coursing structures (96 hours), and ramifying blood vessels (7 days) are noted. Vacuoles (v); ×40.

a potent inhibitor probably acting indirectly since endothelial cells do not express a receptor for this factor (53).

TIMP, a collagenase inhibitor (21), is also found in cartilage (22) where it may maintain cartilaginous tissue in an avascular state by inhibiting endothelial cell migration (22). Addition of recombinant 0.5 mg/ml TIMP in the Matrigel/heparin/FGF mixtures showed essentially complete inhibition of neovascularization at day 3 as measured both by hemoglobin content (Fig. 7) and by examination of the gel for infiltrating vessels (not shown). These observations are consistent with the known role of metalloproteases in the invasion of endothelial cells through basement membrane (43) and for the role of metalloproteases in angiogenesis (22).

DISCUSSION

We have developed a quantitative angiogenesis assay based on the ability of an extract of basement membrane proteins (Matrigel) to form a solid gel when injected into mice and to support a rapid and intense angiogenic reaction in the presence of FGF and heparin. Matrigel, while stimulating cell attachment and morphogenesis when used as a substratum in tissue culture, does not induce an angiogenic response *in vivo* alone. Matrigel has been found to promote the differentiation of endothelial cells into capillary-like structures in culture (12, 41) and when used as a vehicle *in vivo* may enhance the selectivity of endothelial cells entering the gel since basement membranes are not readily crossed by fibroblasts and certain other cells.

Gels supplemented with FGF and heparin induced intense vascularization. Numerous large vessels were apparent on the surface of the gel, whereas vessels within the gel were smaller and more tortuous. Vessel formation was quantitated by measuring the hemoglobin present in the dissected gels and confirmed by histological staining for von Willebrand factor and with Trichrome-Masson stain. Vessel formation was apparent as early as 2 days, reached a plateau after 4 days, and persisted up to 8 days. Maximal and consistent responses required both FGF and heparin, and distinct concentrations of each factor were required for optimal responses. The site of injection and age of the animal affected magnitude of the response.

The correlation of hemoglobin content with vessel formation was previously described using alginate-entrapped tumor cells to elicit angiogenesis *in vivo*. Factor VIII-stainable vessels were found to correlate with hemoglobin content and pooling of radiolabeled red blood cells at the alginate injection site (38). The requirement for heparin with FGF in angiogenesis assays (54) and fibroblast growth and differentiation (55, 56) appears to be due to both a stabilization of FGF and conformational changes in FGF required for receptor binding (57). Heparin also enhances the angiogenic activity of factors produced by 3T3 adipocytes (58), recently shown to be mediated by monobutyrin (16). In our assays, aFGF was

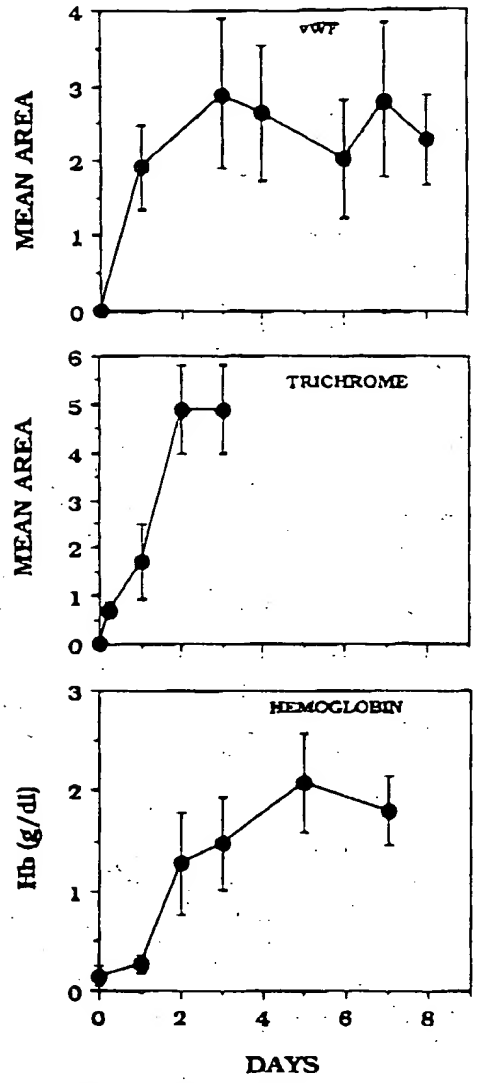

FIG. 6. Quantitation of neovascularization. Histological slides were examined with an Optomax image analysis system, and mean area in a 20× or 40× field was quantitated for slides stained with von Willebrand factor antibody (vWF) or Trichrome-Masson stain (Trichrome). Each point represents mean area per field ($\times 10^3$ μm^2) of 10–20 fields, and error bars are for standard deviation from mean. Hemoglobin measurements at these time points were determined as described in "Methods" and Table 1. Data represent the mean hemoglobin values from at least five mice per point with SEM as indicated.

TABLE 1. ACIDIC FGF DEMONSTRATES A BIPHASIC ANGIOGENIC RESPONSE THAT IS ENHANCED BY HEPARIN

	Hemoglobin[b]
	g/dl
aFGF (ng/ml)[c]	
0	0.28 ± 0.36
0.1	1.00 ± 0.45
1.0	3.20 ± 2.20
10	0.23 ± 0.15
100	0.94 ± 1.18
Heparin (units/ml)[c]	
2.0	ND[d]
6.0	0.04 ± 0.03
20	0.15 ± 0.20
32	0.16 ± 0.49
40[e]	0.69 ± 0.60
64	2.72 ± 1.00

[a] Matrigel gels contained 64 units heparin/ml and were processed 3 days after injection.
[b] Values (±SE) are averages of at least five animals.
[c] Matrigel contained FGF at 1 ng/ml for each experiment.
[d] ND, Not detectable.
[e] Heparin at 40 units/ml was the lowest concentration to yield consistent vessel formation.

TABLE 2. DETECTION OF ANGIOGENIC ACTIVITY USING VARIOUS NEOVASCULARIZATION FACTORS

Factors Added to Matrigel + Heparin	Hemoglobin
	g/dl
None	0.10 ± 0.02
aFGF (1 ng/ml)	1.30 ± 0.07[a]
TGFβ (20 ng/ml)	0.06 ± 0.02
PDGF BB	
2 ng/ml	0.10 ± 0.06
20 ng/ml	0.15 ± 0.08
200 ng/ml	0.07 ± 0.03
PDGF AB (5 units/ml)	0.11 ± 0.04
IL-1β (1 ng/ml)	0.22 ± 0.02
IL-6 (10 ng/ml)	0.18 ± 0.05
bFGF	
1.0 ng/ml	0.14 ± 0.13
10 ng/ml	0.20 ± 0.17[a]
100 ng/ml	0.86 ± 0.70
TNFα (10 ng/ml)	2.30 ± 2.00[a]

Matrigel (0.5 ml) and heparin (40 units/ml) were mixed with various factors and injected subcutaneously. Responses were quantitated 4 days later. TGF-β, PDGF BB, IL-6, IL-1β, or PDGF AB did not induce neovascularization.
[a] Acidic FGF, basic FGF, or TNF-α were potent inducers of angiogenesis.

potent at concentrations reported previously to be effective in both *in vivo* and *in vitro* assays. The course of the response was also comparable to results obtained with FGF in other assays and similar to that reported for other angiogenic agents like angiotropin (17). Heparin was required for angiogenesis in our assay even though heparan sulfate is present in the Matrigel possibly because the amount of heparan sulfate in the Matrigel is relatively low compared with normal basement membrane (59) and since FGF remains bound to heparan sulfate proteoglycan until released by enzymes (60). Not unexpectedly, the angiogenic response to FGF occurred more rapidly than the response observed with alginate-encapsulated tumor cells (38), which presumably require some time to generate their own factor(s). A related angiogenic factor, vascular permeability factor (13), has been shown to induce vascular permeability *in vivo* at 8 ng/animal and is active between 0.1 and 2 ng/ml as a mitogen for endothelial cells *in vitro*. In addition, the vascular permeability factor induces angiogenesis in the rat corneal assay at 20 ng (13). An unrelated chemical inducer of angiogenesis, monobutyrin (16), has been shown to be angiogenic in the chorioallantoic membrane

TABLE 3. INHIBITION OF ANGIOGENESIS BY PDGF, IL-1β, IL-6, AND TGF-β

Factors Added to Matrigel + Heparin + aFGF	Hemoglobin
	g/dl
None	1.30 ± 0.07
TNFα (10 ng/ml)	1.10 ± 1.10
TGFβ	
0.02 (ng/ml)	1.70 ± 1.50
0.2 (ng/ml)	0.08 ± 0.05
2.0 (ng/ml)	0.15 ± 0.13
20 (ng/ml)	0.24 ± 0.25
PDGF BB (200 ng/ml)	0.16 ± 0.07
IL-1β (1 ng/ml)	0.14 ± 0.10
IL-6 (10 ng/ml)	0.17 ± 0.12

Gels contained aFGF (1 ng/ml) + heparin (40 units/ml) and various cytokines. Hemoglobin levels in the gels are shown after 4 days. TNFα and TGF-β had no effect on the angiogenic response. PDGF BB, IL-1β, IL-6, and TGF-β inhibited the response.

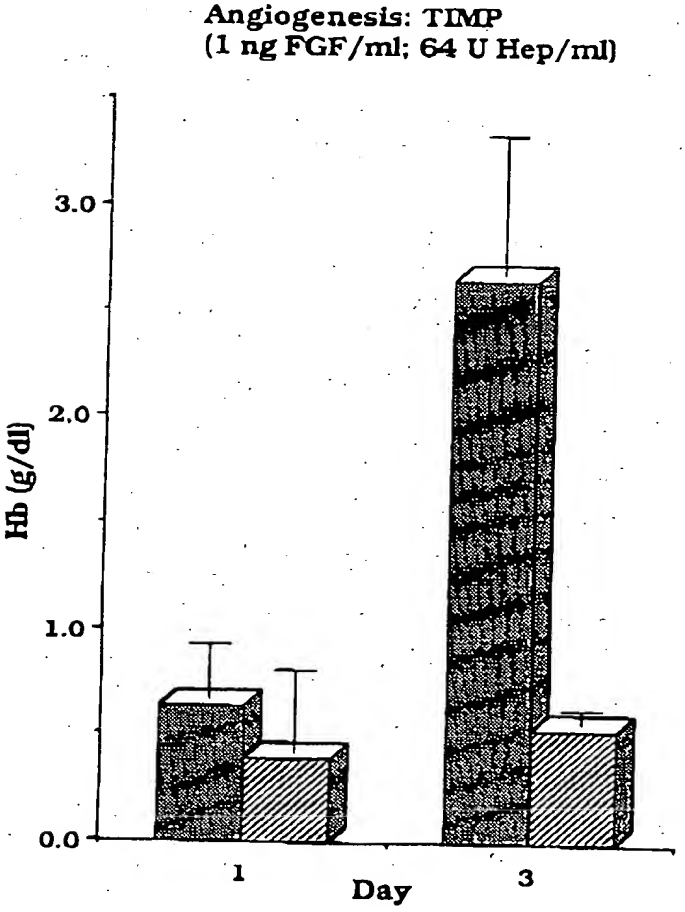

FIG. 7. Inhibition by TIMP: TIMP (collagenase inhibitor) is a potent inhibitor of aFGF-induced angiogenesis. Recombinant TIMP protein (0.5 mg/ml) was included with Matrigel (0.5 ml), FGF (1 ng/ml), and heparin (64 units/ml) at injection (*hatched bars*). Gels from at least five animals per point were analyzed after day 1 or 3. Shown for comparison are hemoglobin levels in gels that contained Matrigel, FGF, and heparin but lacked TIMP (*solid bars*).

assay at 20 pg (0.14 pmol), whereas aFGF in our assays is active at 0.025 pmol.

Other cytokines were tested in this assay including IL-1β, IL-6, and TGF-β and these were found to be potent inhibitors. IL-6 enhances production of TIMP (61), which may inhibit collagenase and endothelial cell migration (62). TGFβ inhibits endothelial cell proliferation and migration (63), although it exhibits angiogenesis *in vivo* in some assays (64). We have measured the content of TGFβ in the Matrigel to be 8–14 ng/ml dependent on batch. However, all TGFβ is in the latent form, and we cannot detect any active TGFβ in the preparations using the CCL64 mink lung epithelial cell bioassay that measures inhibition of proliferation of CCL64 cells by active TGFβ. Therefore the observed results with exogenous TGFβ (active form) reflect activity of the added factor. IL-1 has been shown to regulate endothelial cell growth via autocrine mechanisms (65) that may lead to programmed cell death (apoptosis) as is observed in endothelial cells deprived of FGF (66). TNF-α and bFGF induced neovessel formation. TNFα has been shown to activate macrophages (51) that in turn produce angiogenic factors.

In summary, the advantages of the assay presented here are that it is rapid, reproducible, quantitative, and does not require a surgical procedure for implantation. It allows detection of both angiogenic and anti-angiogenic factors and may allow isolation of those endothelial cells that penetrate into the gel. We have also used this system to assess the capacity of mice of different ages to initiate an angiogenic response, and this type of study would be of interest in both hypertensive and diabetic mice. Such systems may be useful in identifying and isolating biological factors and drugs able to regulate angiogenesis. In addition, the potential exists to induce an additional vascular supply in wounded or ischemic tissue where it is needed to restore normal healing and regeneration.

METHODS

ANIMALS, CELLS, AND GROWTH FACTORS

Female C57Bl/6 mice (Jackson Laboratories, Bar Harbor, Maine) were used at 6–8 weeks of age. Heparin was obtained from Gibco/Bethesda Research Laboratories. Bovine aFGF (HBGF I) bFGF (HBGF II) and TGF-β isolated from human platelets were from R & D Systems. Recombinant TNF-α was a generous gift from Dr. John Isaacs (Johns Hopkins University) and was originally obtained from Cetus Corporati n. PDGF and recombinant IL-6, were from Collaborative Research (Bedford, Massachusetts). IL-1 was a kind gift from Dr. Nigel Waite at Upjohn. TIMP was a gift from Dr. David Carmichael (Synergen, Boulder, Colorado). CCL64 mink lung epithelial cells were obtained from American Type Culture Collection (Rockville, Maryland).

PREPARATION OF BASEMENT MEMBRANE MIXTURES

Reconstituted basement membrane (Matrigel) was prepared from the Engelbreth-Holm-Swarm tumor as described (45), sterilized by dialysis against chloroform, and stored at −20°C. Before use, Matrigel was thawed at 4°C and placed immediately on ice before addition of aFGF, heparin, or other growth factors.

Matrigel prepared by standard methods consists of 5–10 mg protein/ml and yields reproducible results in the angiogenesis assay. The commercial source of heparin (Gibco/Bethesda Research Laboratories) is critical and only batches yielding consistent results were used.

Histology and Factor VIII Related Antigen Staining

All specimens were fixed in 10% buffered Formalin for at least 24 hours, progressively dehydrated in increasing percentages of ethyl alcohol (70, 80, 95, 100, 100, and 100%), cleared in Histoclear, embedded in paraffin under vacuum, sectioned at 5 μm thickness, deparaffinized, and stained with Harris hematoxylin and eosin (67).

Selected specimens were also stained for Factor VIII-related antigen using an immunoperoxidase method (68) or Trichrome-Masson (69). Briefly, 5-μm sections were placed on silanized slides, dried overnight at 64°C, deparaffinized, hydrated, and placed into 3% hydrogen peroxide to quench endogenous peroxide. After rinsing in deionized water, the slides were enzymatically treated with 0.05% Pronase (Calbiochem, San Diego, California) in PBS with 0.114% EDTA at 37°C for 20 minutes. Enzyme activity was then abolished with 95% ethanol for 5 minutes. After PBS rinsing, rabbit anti-human von Willebrand Factor antibody (Dako, Carpinteria, California) diluted 1:1000 in 0.05% nonfat dry milk in PBS was applied to the slides that were placed in a humidity chamber overnight at 4°C. After rinsing in PBS the next morning, test slides were incubated at room temperature for 20 minutes in biotinylated antirabbit IgG (Vector, Burlingame, California) diluted 1:1000 in PBS with 0.5% nonfat dry milk. Nonimmune goat serum (5% v/v) was added to block nonspecific staining. Slides were then rinsed in three changes of PBS, incubated for 20 minutes in horseradish peroxidase conjugated streptavidin (Jackson ImmunoResearch, West Grove, Pennsylvania), diluted 1:1500 in PBS with 0.5% nonfat dry milk, rinsed in tap water, dried, mounted in Crystal Mount, dried at 80°C for 20 minutes, and coverslipped with Permount.

Image Analysis and Neovessel Quantitation

To measure the total area of neovessels, a computerized digitalyzer, the Optomax image analysis system (Optomax), was used. This system consists of a high sensitivity CCTV camera mounted on a Nikon Optiphot-2 microscope. The image is displayed on a color video monitor that is interfaced with a microprocessor. Histological slides stained with von Willebrand factor antibody or Trichrome-Masson stain were examined by adjusting the color contrast to enhance the specifically stained vessels. The mean area per field ($\times 10^6$ μm^2) from 10–20 fields (20× or 40×) was calculated with standard deviation from the mean. The vascularized area to be measured was chosen for its proximity to the skeletal muscle/collagen interface from which the neovessels originated before entering the Matrigel.

Acknowledgments: We thank Dr. Hynda Kleinman for helpful suggestions during these studies and Drs. James Kinsella, Walter Horton, and Hynda Kleinman for critical reading of the manuscript before submission.

Date of acceptance: May 28, 1992.

Address reprint requests to: Antonino Passaniti, Gerontology Research Center, National Institute on Aging, 4940 Eastern Ave., Baltimore, MD 21224.

REFERENCES

1. Folkman J, Klagsbrun M. Angiogenic factors. Science 1987;235: 442–7.
2. Knighton DR, Fiegel VD. Regulation of cutaneous wound healing by growth factors and the microenvironment. Invest Radiol 1991; 26:604–11.
3. Liotta LA, Steeg PS, Stetler-Stevenson WG. Cancer metastasis and angiogenesis: An imbalance of positive and negative regulation. Cell 1991;64:327–36.
4. Weidner N, Semple JP, Welch WR, Folkman J. Tumor angiogenesis and metastasis: Correlation in invasive breast carcinoma. New Engl J Med 1991;324:1–8.
5. Nickoloff B, Karabin G, Barker J, Griffiths C, Sarma V, Mitra R, Elder J, Kunkel S, Dixit V. Cellular localization of interleukin-8 and its inducer, tumor necrosis factor-alpha in psoriasis. Am J Pathol 1991;138:129.
6. Norrby K, Jakobsson A, Simonsen M, Sorbo J. Increased angiogenesis in diabetes. Experientia 1990:46:856–60.
7. Ross, R. The pathogenesis of atherosclerosis and update. N Engl J Med 1986;314:488–500.
8. Folkman, J, Haudenschild C. Angiogenesis in vitro. Nature 1980; 288:551–6.
9. Gospodarowicz D, Ferrara N, Schweigerer L, Neufeld G. Structural characterization and biological functions of fibroblast growth factor. Endocrine Rev 1987;8:95–114.
10. Klagsbrun, M, Vlodavsky I. Biosynthesis and storage of basic fibroblast growth factor (bFGF) by endothelial cells: Implication for the mechanism of action of angiogenesis. In: Growth Factors and Other Aspects of Wound Healing: Biological and Clinical Implications. New York: Alan R. Liss, 1988:55–61.
11. Frater-Schroder M, Risau W, Hallmann R, Gautschi P, Bohlen P. Tumor necrosis factor type α, a potent inhibitor of endothelial cell growth in vitro, is angiogenic in vivo. Proc Natl Acad Sci USA 1987;84:5277–81.
12. Kubota Y, Kleinman HK, Martin GR, Lawley TJ. Role of laminin and basement membrane in the differentiation of human endothelial cells into capillary-like structures. J Cell Biol 1988;107: 1589–97.
13. Connolly DT, Heuvelman DM, Nelson R, Olander JV, Eppley BL, Delfino JJ, Siegel NR, Leingruber RM, Feder J. Tumor vascular permeability factor stimulates endothelial cell growth and angiogenesis. J Clin Invest 1989;84:1470–8.
14. Keck PJ, Hauser SD, Krivi G, Sanzo K, Warren T, Feder J, Connolly DT. Vascular permeability factor, an endothelial cell mitogen related to PDGF. Science 1989;246:1309–12.
15. Leung DW, Cachianes G, Kuang W-J, Goeddel DV, Ferrara N. Vascular endothelial growth factor is a secreted angiogenic mitogen. Science 1989;246:1306–9.
16. Dubson DE, Kambe A, Block E, Dion T, Lu H, Castellot JJ, Spiegelman BM. 1-Butyryl-glycerol: A novel angiogenesis factor secreted by differentiating adipocytes. Cell 1990;61:223–30.
17. Hockel M, Jung W, Vaupel P, Rabes H, Khaledpour C, Wiesler JH. Purified monocyte-derived angiogenic substance (angiotropin) induces controlled angiogenesis associated with regulated tissue proliferation in rabbit skin. J Clin Invest 1988;82:1075–90.
18. Hallahan TW, Shapiro R, Vallee BL. Dual site model for the organogenic activity of angiogenin. Proc Natl Acad Sci U S A 1991; 15:2222–6.
19. West DC, Hampson IN, Arnold F, Kumar S. Angiogenesis induced by degradation products of hyaluronic acid. Science 1986;228: 1324–6.
20. Cozzolino F, Torcia G, Ziche M, Ogawa S, Brett J, Koga S, Vlassara H, Nawroth P, Stern D. Advanced glycosylation endproducts (AGEs) stimulate endothelial cell (EC) growth in vitro and in vivo. Circulation 1990;82:III36.
21. Carmichael DF, Sommer A, Thompson RC, Anderson DC, Smith CC, Welgus HG, Stricklin GP. Primary structure and cDNA cloning of human fibroblast collagenase inhibitor. Proc Natl Acad Sci USA 1986;83:2407–11.
22. Moses MA, Sudhalter J, Langer R. Identification of an inhibitor of neovascularization from cartilage. Science 1990;248:1408–13.
23. Maione TE, Gray GS, Petro J, Hunt AJ, Donner AL, Bauer SI, Carson HF, Sharpe RJ. Inhibition of angiogenesis by recombinant human platelet factor-4 and related peptides. Science 1990;247: 77–9
24. Good DJ, Polverini PJ, Rastinejad F, Le Beau MM, Lemons RS, Frazier WA, Bouck NP. A tumor suppressor-dependent inhibitor of angiogenesis is immunologically and functionally indistinguish-

able from a fragment of thrombospondin. Proc Natl Acad Sci USA 1990;87:6624–8.
25. Iruela-Arispe ML, Bornstein P, Sage H. Thrombospondin exerts an antiangiogenic effect on cord formation by endothelial cells in vitro. Proc Natl Acad Sci USA 1991;88:5026–30.
26. Rastinejad F, Polverini PJ, Bouck NP. Regulation of the activity of a new inhibitor of angiogenesis by a cancer suppressor gene. Cell 1989;56:345–55.
27. Sakamoto N, Iwahana M, Tanaka NG, Osada Y. Inhibition of angiogenesis and tumor growth by a synthetic laminin peptide CDPGYIGSR-NH2. Cancer Res 1991;51:903–6.
28. Crum R, Szabo S, Folkman J. A new class of steroids inhibits angiogenesis in the presence of heparin or a heparin fragment. Science 1985;230:1375–8.
29. Folkman J, Weisz PB, Joullie MM, Li WW, Ewing WR. Control of angiogenesis with synthetic heparin substitutes. Science 1989; 243:1490–3.
30. Lee JK, Choi B, Sobel RA, Chiocca EA, Martuza RL. Inhibition of growth and angiogenesis of human neurofibrosarcoma by heparin and hydrocortisone. J Neurosurg 1990;73:429–35.
31. Tamargo RJ, Bok RA, Brem H. Angiogenesis inhibition by minocycline. Cancer Res 1991;51:672–5.
32. Ingber D, Fujita T, Kishimoto S, Sudo K, Kanamaru, Brem H, Folkman J. Synthetic analogues of fumagillin that inhibit angiogenesis and suppress tumour growth. Nature 1990;348:555–7.
33. Takigawa M, Enomoto M, Nishida Y, Pan H-O, Kinoshita A, Suzuki F. Tumor angiogenesis and polyamines: a-difluoromethylornithine, an irreversible inhibitor of ornithine decarboxylase, inhibits B16 melanoma-induced angiogenesis in ovo and the proliferation of vascular endothelial cells in vitro. Cancer Res 1990; 50:4134–8.
34. Murata, J., Saiki, I., Makabe, T., Tsuta Y, Tokura S, Azuma I. Inhibition of tumor-induced angiogenesis by sulfated chitin derivatives. Cancer Res 1991;51:22–6.
35. Gimbrone MA, Cotran RS, Leapman SB, Folkman J. Tumor growth and neovascularization: An experimental model using the rabbit cornea. J Natl Cancer Inst 1974;52:413.
36. Muthukaruppan VR, Auerbach R. Angiogenesis in the mouse cornea. Science 1979;205:1416.
37. Ausprunk DH, Knighton DR, Folkman J. Vascularization of normal and neoplastic tissues grafted to the chick chorioallantois: Role of host and pre-existing graft blood vessels. Am J Pathol 1975;79: 597.
38. Plunkett, ML, Hailey JA. An in vivo quantitative angiogenesis model using tumor cells entrapped in alginate. Lab Invest 1990; 62:510–7.
39. Robertson NE, Discafani CM, Downs EC, Hailey JA, Sarre O, Runkle RL, Popper TL, Plunkett ML. A quantitative in vivo mouse model used to assay inhibitors of tumor-induced angiogenesis. Cancer Res 1991;51:1339–44.
40. Thompson JA, Anderson KD, DiPietro JM, Zwiebel JA, Zametta M, Anderson WF, Maciag T. Site-directed neovessel formation in vivo. Science 1988;241:1349–52.
41. Grant DS, Tashiro K, Segui-Real B, Yamada Y, Martin GR, Kleinman HK. Two different laminin domains mediate the differentiation of human endothelial cells into capillary-like structures in vitro. Cell 1989;58:933–43.
42. Iruela-Arispe ML, Hasselaar P, Sage H. Differential expression of extracellular proteins is correlated with angiogenesis in vitro. Lab Invest 1991;64:174–86.
43. Mignatti P, Tsuboi R, Robbins E, Rifkin DB. In vitro angiogenesis on the human amniotic membrane: Requirement for basic fibroblast growth factor-induced proteinases. J Cell Biol 1989;108: 671–82.
44. Nicosia RF, Madri JA. The microvascular extracellular matrix: Developmental changes during angiogenesis in the aortic ring-plasma clot model. Am J Pathol 1987;128:78–90.
45. Kleinman HK, McGarvey ML, Hassell JR, Star VL, Cannon FB, Laurie GW, Martin GR. Basement membrane complexes with biological activity. Biochemistry 1986;25:312–8.
46. Drabkin DL, Austin JH. I Spectrophotometric constants for common hemoglobin derivatives in human, dog, and rabbit blood. J Biol Chem 1932;98:719.
47. Bradford MM. A rapid and sensitive method for the quantitation of microgram quantities of protein utilizing the principle of protein dye binding. Anal Biochem 1972;72:248–54.
48. Auerbach R, Morrissey LW, Sidly YA. Regional differences in the incidence and growth of mouse tumors following intradermal or subcutaneous inoculation. Cancer Res 1978;38:1739–44.
49. Gospodarowicz D, Cheng J, Lui G-M, Baird A, Bohlent P. Isolation of brain fibroblast growth factor by heparin-Sepharose affinity chromatography: Identity with pituitary fibroblast growth factor. Proc Natl Acad Sci USA 1984;81:6963–7.
50. Thomas K, Rios-Candelore M, Fitzpatrick S. Purification and characterization of acidic fibroblast growth factor from bovine brain. Proc Natl Acad Sci USA 1984;81:357–61.
51. Leibovich SJ, Polverini PJ, Shepard HM, Wiseman DM, Shively V, Nuseir N. Macrophage-induced angiogenesis is mediated by tumour necrosis factor-α. Nature 1987;329:630–2.
52. Motro B, Itin A, Sachs L, Keshet E. Pattern of interleukin 6 gene expression in vivo suggests a role for this cytokine in angiogenesis. Proc Natl Acad Sci USA 1990;87:3092–6.
53. Heldin CH, Westermark B, Wasteson A. Specific receptors for platelet-derived growth factor on cells derived from connective tissue and glia. Proc Natl Acad Sci USA 1981;78:3664–8.
54. Kessler DA, Langer RS, Pless NA, Folkman J. Mast cells and tumor angiogenesis. Int J Cancer 1976;18:703–9.
55. Rapraeger AC, Krufka A, Olwin BB. Requirement of heparan sulfate for bFGF-mediated fibroblast growth and myoblast differentiation. Science 1991;252:1705–8.
56. Rifkin DB, Moscatelli D. Recent developments in the cell biology of basic fibroblast growth factor. J Cell Biol 1989;109:1–6.
57. Yayon A, Klagsbrun M, Esko JD, Leder P, Ornitz DM. Cell surface, heparin-like molecules are required for binding of basic fibroblast growth factor to its high affinity receptor. Cell 1991;64:841–8.
58. Castellot JJ, Kambe AM, Dobson DE, Spiegelman BM. Heparin potentiation of 3T3-adipocyte stimulated angiogenesis: Mechanism of action on endothelial cells. J Cell Physiol 1986;127:323–9.
59. Grant DS, Leblond CP. Immunogold quantitation of laminin, type IV collagen and heparan sulfate proteoglycan in a variety of basement membrane. J Histochem Cytochem 1988;36:271–83.
60. Bashkin P, Doctrow S, Klagsbrun M, Svahn CM, Folkman J, Vlodasky I. Basic fibroblast growth factor binds to subendothelial extracellular matrix and is released by heparitinase and heparin-like molecules. Biochemistry 1989;28:1737–43.
61. Sato T, Ito A, Mori Y. Interleukin 6 enhances the production of tissue inhibitor of metalloproteinases (TIMP) but not that of matrix metalloproteinases by human fibroblasts. Biochem Biophys Res Commun 1990;170:824–9.
62. Moses MA, Langer R. Inhibitors of angiogenesis. Biotechniques 1991;9:630–4.
63. Pepper MS, Belin D, Montesano R, Orci L, Vassalli J-D. Transforming growth factor-beta 1 modulates basic fibroblast growth factor-induced proteolytic and angiogenic properties of endothelial cells in vitro. J Cell Biol 1990;111:743–56.
64. Roberts AB, Sporn MB, Assoian RK, Smith JM, Roche NS, Wakefield LM, Heine UI, Liotta LA, Falanga V, Kehrl JH, Fauci AS. Transforming growth factor type-β: Rapid induction of fibrosis and angiogenesis in vivo and stimulation of collagen formation in vitro. Proc Natl Acad Sci USA 1986;83:4167–71.
65. Cozzolino F, Torcia M, Aldinucci D, Ziche M, Almerigogna F, Bani D, Stern DM. Interleukin 1 is an autocrine regulator of human endothelial cell growth. Proc Natl Acad Sci USA 1990;87: 6487–91.
66. Araki S, Shimada Y, Kaji K, Hayashi H. Apoptosis of vascular endothelial cells by fibroblast growth factor deprivation. Biochem Biophys Res Commun 1990;168:1194–200.
67. Luna LG. Manual of histologic staining methods of the Armed Forces Institute of Pathology. New York: McGraw-Hill, 1968:32.
68. Cartrun RW, Pederson CA. An immunocytochemical technique offering increased sensitivity and lowered cost with a streptavidin-horseradish peroxidase conjugate. J Histotechnol 1989;12:273–7.
69. Luna LG. Manual of histologic staining methods of the Armed forces Institute of Pathology. New York: McGraw-Hill, 1968:94l.

COMMONWEALTH OF AUSTRALIA

(Patents Act 1990)

IN THE MATTER OF: Australian Patent Application 696764 (73941/94). In the name of: Human Genome Sciences Inc.

- and -

IN THE MATTER OF: Opposition thereto by Ludwig Institute for Cancer Research, under Section 59 of the Patents Act.

Annexure GBC-18

This is **Annexure GBC-18** referred to in my Statutory Declaration made this Thirteenth day of December 2000.

Gary Baxter Cox

WITNESS: _____

Patent Attorney PEYTEE KHOO

Meth and Find Exptl Clin Pharmacol 1988; 10(4): 221-226

Angiogenesis: Quantitative Assessment by the Chick Chorioallantoic Membrane Assay

Jacek Splawinski[1], *Maria Michna*[1], *Ryszard Palczak*[2], *Stanislaw Konturek*[1] *and Barbara Splawinska*[1]

Departments of [1]Pharmacology and [2]Obstetrics and Gynecology, Institute of Medical Sciences, Rzeszow, Poland

SUMMARY

The aim of the present work was to improve quantitative assessment of angiogenesis by chick chorioallantoic membrane (CAM) assay based on measurement of DNA synthesis. Following incubation of [^{3}H]thymidine ([^{3}H]-T) with CAM in vivo, incorporation of ^{3}H-T to DNA fraction was expressed as percent of total ^{3}H-T present in the tissue homogenate of CAM, regardless of CAM weight and full recovery of applied radioactivity. The assay required simple, partial isolation of DNA to remove traces of free or unspecifically bound ^{3}H-T. These modifications gave a reproducible assay with adequate precision (10-20%). DNA content of CAM did not change between 10-15 days of embryo development and growth of CAM was considered on day 11. 10 to 12-day old CAMs were used for evaluation of the assay. Using a qualitative approach (visual scoring), tissues of several tumors were implanted on CAM. Extracts of tumors that produced the highest score stimulated DNA synthesis in CAM. A similar effect was induced by EGF while cytostatics inhibited DNA synthesis in CAM. Since stimulation of angiogenesis is not a cell type-specific phenomenon, the assay in the present modification should aid the studies on angiogenic factors. With the help of this assay the angiogenic activity of adenocarcinoma of human endometrium was described.

Key words: Chorioallantoic membrane - Angiogenesis - DNA - EGF - Carcinoma endometrium

INTRODUCTION

The chorioallantoic membrane (CAM) of the chick embryo has been introduced by Folkman (13) and his colleagues to assay the angiogenic activity of various tumors, normal tissues, and cells (1, 4, 8, 13). Assays on CAM constitute a large-scale screening test for substances that promote or inhibit vascular growth (6, 7, 12, 15). Despite such wide use, the CAM assay has limitations, such as the problems of differentiation of newly formed vessels from the hyperemic response or from the mechanical effect of implant and the problems related to the immune reactions emerging on day 15 of embryo development (4, 5, 6, 18, 22).

Several procedures were introduced to optimize visual assessment of vascular response of CAM, originally relying on the arbitrary scale (13, 21). These include: shell-less culture of chick embryo (2, 10), estimation of vascular density within superimposed circle (6, 11), the calculation of coefficient of angiogenesis (28), and the use of automatic image analyzer (26). However, all these procedures still suffer from subjectivity of evaluation.

Recently, a very simple method, based on the estimation of DNA synthesis, has been used by Thompson *et al.* (27) for quantitative assessment of the angiogenic response on CAM. However, this method is suitable only when pooling (up to five) of CAMs is possible as the low precision of assay for individual eggs exceeds 40% (27). For large-scale screening of angiogenic activity the assay for individual eggs is required. We, therefore, modified accordingly the original method of Thompson *et al.* (27) and the present results show that following modification, this simple assay can be used to monitor quantitatively angiogenic activity on individual CAMs.

MATERIALS AND METHODS

Visual evaluation of CAM response

Fertile hens'eggs (Astra, Sweden), washed in water and 0.5% chlorhexidine in 70% ethanol were placed in a humidified incubator at 37°C. On day 4, following removal of 0.5 ml of albumen, the window was made in the shell over an air space to expose CAM.

0379-0355/88/55.00 | $2.00

On day 10 of embryo growth, in aseptic conditions, slices (2 x 2 x 1 mm) of meningioma, adenocarcinoma of endometrium or normal endometrium (obtained immediately following surgery from the Departments of Neurosurgery or Obstetrics and Gynecology, District Hospital, Rzeszow) were placed directly on CAM or separated from it by a sterile Millipore filter, 0.45 μm (Millipore Corp., Bedford, Mass, USA). During further incubation for 5 days the vessels of CAM were examined each day under a stereomicroscope in a blind fashion and the score according to the arbitrary scale (13) was assigned. Each tissue was implanted on six CAMs and median of CAM maximal scores (occurring usually on day 15) for each clinical specimen was recorded. The frequencies for each scoring interval (see Results) were tabulated and the chi square test was used.

Estimation of DNA synthesis

The entire procedure of Thompson *et al.* (27) was modified. Methyl-[^{3}H]thymidine (specific activity: 87 Ci/mmol, Amersham, UK), usually at a dose of 2.0 μCi in 0.2 ml of phosphate buffered saline (PBS), was incubated with CAM *in vivo* in most experiments for 2 hr. Following incubation the eggs were placed at −20°C for 30 min. The CAM was cut out, rinsed thoroughly in ice cold PBS, weighed and homogenized (Polytron, Ml'W-309) in 2 ml of water for 5 min at 4°C and disintegrated for 30 sec at 4°C in the Ultrasonic Disintegrator (UD-11). During mixing, 0.1 ml of the homogenate was removed for calculation of the total radioactivity in dpm. Homogenate (2 ml) was then mixed with 5 ml of ice-cold 5% perchloric acid. The precipitate obtained after centrifugation (2500 x g, 10 min 4°C) was washed twice with 5 ml of 5% perchloric acid. The precipitate was then shaken and washed twice (each time with centrifugation step, as above) successively with 5 ml of the following solvents: 96% ethanol, 96% ethanol-ethyl ether mixture (4:1 v/v), and ethyl ether. Following evaporation of ether, the precipitate was treated with 5 ml of 5% perchloric acid and heated to 96°C for 15 min. After centrifugation the supernatant was divided. 0.5 ml of supernatant was neutralized (with 0.1 M NaOH) and the radioactivity was estimated in a Beckman LS-7000 scintillation counter using H number for quenching determination. In the second part of the supernatant, DNA was measured colorimetrically (17) following addition of diphenylamine and with the help of Specol colorimeter.

The radioactivity measured (in dpm) in the fraction containing DNA was expressed in percent of total radioactivity of the homogenate. Percent of incorporated thymidine to DNA of CAM, following various treatments, was expressed as mean ± SEM and the results between various groups compared by the Kruskal-Wallis test. Coefficient of variation, CV, (SD x 100):x, was also calculated.

Tissue extracts

Tumors or control tissues were homogenized in PBS (1 g/10 ml) for 3 min at 4°C and centrifuged to remove particulate material. Supernatants were decanted, dialyzed (4000 cut-off) against distilled water for 24 hr at 4°C then lyophilized and stored at −20°C until use. All solutions of extracts in PBS were adjusted to the same (1%) protein concentration, applied onto CAM at a volume of 0.2 ml and incubated at 37°C for 22 hr followed by application of [^{3}H]thymidine for 2 hr.

EGF and drugs

Pure natural mouse epidermal growth factor (EGF) (synthesized by Dr. H. Gregory from I.C.I., Alderley Park, UK) was obtained from Prof. S. Konturek as a lyophilized sample. Doxorubicin and bleomycin were obtained from a local pharmacy. EGF and drugs were dissolved in phosphate buffered saline (PBS) just before use, applied onto CAM at a volume of 0.2 ml and incubated at 37°C for 22 hr followed by 2 hr incubation with thymidine.

RESULTS

Visual assessment of angiogenesis

The angiogenic activities of various tissues are shown in Table 1. The maximal vascular response was attained on day 15 and occasionally on day 14. A typical spoke-wheel response to the implant of meningioma (scores: 4.0+) is shown in Figure 1. When slices of adenocarcinoma of endometrium (3 cases) were heated (100°C for 30 min) they evoked angiogenic responses in CAM scored between 0.1-1.0+.

DNA content in CAM

Table 2 shows that DNA content per mg of CAM was similar in embryos of various ages. When the slices of normal endometrium were implanted on CAM, DNA content —measured on day 15— amounted to 1.36 ± 0.11 μg/mg of CAM (mean ± SEM, n = 6) and was comparable to the DNA content of untreated CAM (Table 2).

TABLE 1. Angiogenic activities of various tissues on CAM

Tissue	Number of explants	Scores of activity					P
		0	0.1-1.0	1.1-2.0	2.1-3.0	3.1-4.0	
Control*	9	5	4	0	0	0	—
Carcinoma of endometrium*	13	0	1	3	7(2)	1(1)	<0.01
Meningioma	1	0	0	0	0	1	

*Normal endometrium.
†Three specimens were separated from CAM by Millipore filter and corresponding scores are given in parentheses.

FIG. 1. CAM of 11 day old chick embryo incubated for 3 days with implanted meningioma. The blood vessels show radial orientation forming a typical sprite-wheels.

TABLE 2. DNA content in CAM of embryos of various ages

Age of embryo	Tissue	DNA, μg/mg of CAM (mean ± SEM)	Number of eggs*
9	—	1.40 ± 0.12	5
10	—	1.24 ± 0.46	4
11	—	1.18 ± 0.08	11
12	—	1.44 ± 0.20	5
13	—	1.20 ± 0.07	16

DNA synthesis

Increasing amounts of [^{125}I]thymidine applied to CAM for 30 min produced linear incorporation into DNA (Fig. 2). Figure 3 illustrates the incorporation of thymidine to DNA when a constant dose (2.0 μCi) was applied onto CAM for various time intervals. Initial linear increase of incorporation of thymidine declined after 2.0 hr to a plateau. Coefficients of variation of most measurements were between 10-20%, and 2.0 hr time of incubation of [^{125}I]thymidine with CAM was chosen for further experiments. Experiments relating age of CAM with the degree of thymidine incorporation into DNA (Fig. 4) indicated that growth of CAM was largely completed by day 11 of embryo development. For subsequent experiments, 11 or 12-day old embryos were used.

Tumor extracts, when incubated with CAM for 24 hr, significantly increased incorporation of thymidine into DNA of CAM (Table 3). CVs of these measurements were between 13.1-17.2%.

Similar to tumor extracts, epidermal growth factor (EGF) stimulated incorporation of thymidine into DNA of CAM (Table 4), while cytostatics, doxorubicin and bleomycin inhibited incorporation of thymidine into DNA of CAM (Table 4). In the case of bleomycin some embryos died following drug treatment.

DISCUSSION

The visual assessment of angiogenic response of CAM of chick embryo precluded large-scale screening of potential angiogenic substances in this assay. A simple quantitative method introduced by Thompson et

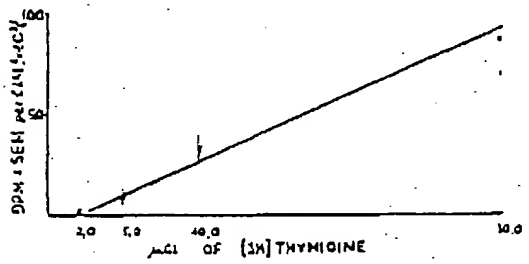

FIG. 2. Effect of increasing concentrations of [^{125}I]thymidine applied to CAM for 30 min; n = 10 for each dose. Means ± SEM are shown.

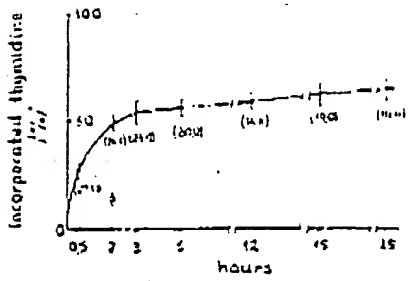

FIG. 3. Effect of constant dose (2.0 μCi) of [³H]thymidine applied to CAM for various incubation times; n = 6 for each time. Means ± SEM are shown, coefficients of variation in parentheses. Open circle: experiments performed on eggs kept for 12 hr at room temperature.

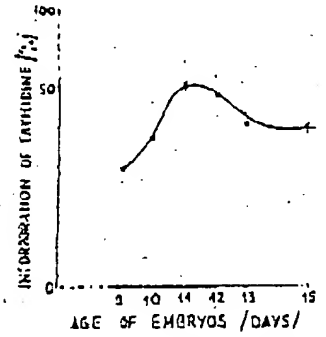

FIG. 4. Thymidine incorporation in CAM of various ages. CAMs were incubated with 2.0 μCi of [³H]thymidine for 2 hr; n = minimum 4 for each day. Means ± SEM are shown.

al. (27) requires, because of low precision, large amounts of CAMs (see Introduction). The aim of the present work was such a modification of the procedure of Thompson *et al.* (27) which would increase the precision and allow for assay of individual eggs.

Our assay measured the ratio of thymidine incorporated into DNA to all forms of thymidine binding in CAM represented by the total radioactivity in the initial homogenate. Accordingly, the results were independent of the CAM's weight, and transfer of total radioactivity added to CAM *in vivo* was not critical. The DNA content per CAM's weight was similar during 10-15 days of embryo development (Table 2), also in the presence of the implant. We think that low precision of the original method (27) resulted from variation in the CAM's weight and uncontrolled losses of radioactivity during isolation of CAM. However, in the present assay, isolation of DNA required lipids removal and separation from tissue proteins. The simple method of isolation of DNA (23) appeared to be sufficient for the present purposes, as evidenced by the linear incorporation of thymidine to DNA (Fig. 2). In this experiment results were expressed as dpm per CAM, being the original data and were in agreement with that of Thompson *et al.* (27). The steady-state conditions for percent of thymidine incorporated to DNA were obtained after 2-3 hr of [³H]thymidine incubation with CAM (Fig. 3) and 2 hr incubation time was chosen for present experiments. Figure 3 also shows that with our approach, precision of the assay was increased, as compared to the work of Thompson *et al.* (27), and coeffi-

TABLE 3. Effect of tumor extracts on [³H]thymidine incorporation to DNA

Type of extract	Number of eggs	% of thymidine incorporated to DNA (mean ± SEM)
Phosphate buffered saline	7	59.8 ± 3.3
Normal endometrium (patient A.P.)	5	50.0 ± 4.0
Normal endometrium (patient U.K.)	9	50.8 ± 3.2
Adenocarcinoma endometrium (patient J.S.)	10	76.0 ± 3.0**
Adenocarcinoma endometrium (patient E.H.)	6	74.1 ± 5.4**
Adenocarcinoma endometrium (patient A.S.)	7	60.0 ± 1.4*
Meningioma (patient S.W.)	7	75.0 ± 3.0*

*$p < 0.05$; **$p < 0.01$ in comparison to parallelly run control.
*$p < 0.01$ in comparison to saline.

TABLE 4. Effects of EGF, doxorubicin, and bleomycin on [^{3}H]thymidine incorporation to DNA of CAM

Treatment	Number of eggs	% of thymidine incorporated to DNA (mean ± SEM)
PBS	9	45.7 ± 3.1
EGF: 0.2 μg/egg	7	51.6 ± 3.3
EGF: 0.8 μg/egg	4	60.4 ± 4.8
Doxorubicin (0.1 mg/egg twice at 0 and 12 hr)	5	12.1 ± 3.6**
Bleomycin (0.2 mg/egg twice at 0 and 12 hr)	3	18.0 ± 1.4*

*$p < 0.05$; **$p \leq 0.01$

cients of variation of the measurements throughout the entire study only exceptionally exceeded 20%. The rate of DNA synthesis was dependent on the age of the embryo. By day 11 of embryo development DNA synthesis was maximal (Fig. 3), in agreement with data of other reports (3, 27). Therefore, 11–12 day-old embryos were used for the present experiments.

The following data may indicate that the simple method of Thompson *et al.* (27) in our modification can quantitatively measure stimulation of angiogenesis on CAM. It has been demonstrated that meningioma, one of the most highly vascularized tumors, induced strong angiogenic response on CAM (20). We have confirmed this finding in the present work (Table 1, Fig. 1). Extract of meningioma was found to increase significantly ($p < 0.01$) incorporation of thymidine to DNA as measured by our method (Table 3). This result is in agreement with autoradiographic studies of Kelly *et al.* (19), who observed the largest increase in thymidine labeling index following incubation of meningioma-conditioned medium with endothelial cultures. The other tumors which induced positive response on CAM assessed qualitatively; *i.e.*, implants of adenocarcinoma of endometrium (Table 1), also significantly increased thymidine incorporation to DNA as assessed by our method (Table 3). The stimulating effects of tumor extracts was shared by EGF (Table 4), similar to its effect on vessels in the hamster chick pouch (24) and on endothelial cultures (9). In addition, doxorubicin and bleomycin, the DNA-synthesis inhibitors, significantly decreased incorporation of thymidine to DNA of CAM as evaluated by our assay (Table 4). This indirect evidence suggests that our method offers the possibility of quantitative assessment of angiogenesis on CAM.

In these studies we have also demonstrated that carcinoma of endometrium of the corpus uteri possesses angiogenic activity. This is, we believe, the first such observation. How angiogenic activity contributes to the spread of carcinoma of endometrium is not known. However, morphological studies are in progress to find out whether vessels of the uterus affected by the adenocarcinoma show signs of activity of angiogenic factor.

In the present method incorporation of thymidine in all cell types in CAM was followed. Therefore, the action directed specifically towards one type of cell would not be differentiated. This is the case of anti-angiogenic agents, protamine or heparin-cortisone mixture, specifically affecting endothelial cells, as opposed to cytostatics, acting on DNA of all cell types (26).

In contrast to anti-angiogenesis, stimulation of angiogenesis appears to involve all embryonic cells of CAM. All cell types in CAM are stimulated by various angiogenic factors, as evidenced by autoradiography (9, 27). Several growth factors such as epidermal and fibroblast growth factors (EGF and FGF) stimulate both angiogenesis *in vivo* and endothelial growth in culture (9, 24). Factors possessing intrinsic mitogenic activity, such as EGF, FGF, transforming growth factor-alpha (TGF-alpha), tumor angiogenesis factor (TAF), and chondrosarcoma-derived endothelial cell growth factor are not cell-type specific (14, 16, 25, 29). It seems, therefore, that the present method is suitable for measurement of angiogenic activity of various tissues. Such a method should be useful for further studies on angiogenic factors.

ACKNOWLEDGEMENTS

We thank Professor M. Chorazy for his comments.

This study was supported by the Central Programme Research and Development, No. 11.5, from the Oncology Center, Warsaw.

REFERENCES

1. Auerbach, G.H., Chalkley, H.H., Lecallum, R.Y. and Park, H.D. *Vascular reactions of normal and malignant tissues in vivo. I. Vascular reactions of mice to wounds and to normal and neoplastic transplants.* J Natl Cancer Inst 1945; 6: 73-85.
2. Auerbach, R., Kubai, L., Knighton, D.R. and Folkman, J. *A simple procedure for the long term cultivation of chicken embryos.* Dev Biol 1974; 41: 391-394.
3. Ausprunk, D.H., Knighton, D.R. and Folkman, J. *Differentiation of vascular endothelium in the chick chorioallantoic membrane: A structural and autoradiographic study.* Dev Biol 1974; 38: 237-248.
4. Barnhill, R.L., Parkinson, E.K. and Ryan, T.J. *Supernatants from cultured human epidermal keratinocytes stimulate angiogenesis.* Br J Pharmacol 1984; 110: 271-281.
5. Barnhill, R.L. and Ryan, T.J. *Mechanical considerations in new vessel growth.* In: Basic Aspects of Microcirculation. M. Cocchiya et al. (Eds.). Excerpta Medica: Amsterdam 1982; 157-163.
6. Barnhill, R.L. and Ryan, T.J. *Biochemical modulation of angiogenesis in the chorioallantoic membrane of the chick embryo.* J Invest Dermatol 1983; 81: 485-488.
7. Brem, H. and Folkman, J. *Inhibition of tumor angiogenesis mediated by cartilage.* J Exp Med 1975; 141: 427-439.
8. Burgos, H. *Angiogenic and growth factors in human uterine mucosa and placenta.* Eur J Invest 1983; 13: 289-296.
9. Cavalla, T., Sala, R., Folkman, J. and Cotran, R.S. *Tumor angiogenesis. Rapid induction of endothelial mitoses demonstrated by autoradiography.* J Cell Biol 1972; 54: 408-420.
10. Dean, R.C., Fishbaugh, C.F. and Burnet, B.D. *Effect of varying chamber constriction and culture perpendicularity upon survival and growth of chick embryos in shell-less culture.* Anat Rec 1981; 199: 31-41.
11. Dusseau, J.W., Hutchins, P.M. and Malbouyt, D.S. *Stimulation of arteriogenesis by adventitia on the chick chorioallantoic membrane.* Circ Res 1986; 59: 163-170.
12. Fett, J.W., Strydom, D.J., Lobb, R.R., Alderman, E.M., Bethune, J.L., Riordan, J.F. and Vallee, B.L. *Isolation and characterization of angiogenin, an angiogenic protein from human carcinoma cells.* Biochemistry 1985; 24: 5480-5486.
13. Folkman, J. *Tumor angiogenesis.* In: Cancer. Vol 3. R.F. Becker (Ed.). Plenum Press: New York 1976, 333-388.
14. Folkman, J. *Toward an understanding of angiogenesis: Search and discovery.* Perspect Biol Med 1985; 29: 10-36.
15. Fenn, D.M. and Auerbach, R. *PGE$_2$ and angiogenesis.* Proc Soc Exp Biol Med 1983; 172: 214-218.
16. Fuselli, J.F. *Cytokines and vascular angiogenesis.* Cell proliferation, cell matrix and growth factors. Lab Invest 1986; 55: 503-509.
17. Gitz, K.W. and Meyers, A. *An improved diphenylamine method for estimation of deoxyribonucleic acid.* Nature 1965; 206: 93-94.
18. Jakob, W., Leutsch, K.D., Mannsberger, G. and Hofer, G. *The chick embryo chorioallantoic membrane as a bioassay for angiogenesis factors: Reactions induced by carrier materials.* Exp Pathol 1978; 15: 241-249.
19. Kelly, P.J., Suddith, R.L., Hutchinson, H.L., Weibach, K.H. and Haber, B. *Endothelial growth factor present in tissue culture of CNS tumors.* J Neurosurg 1980; 53: 342-346.
20. Klagsbrun, K., Knighton, D. and Folkman, J. *Tumor angiogenesis activity in cells grown in tissue culture.* Cancer Res 1976; 36: 110-114.
21. Knighton, D., Ausprunk, D., Tapper, D. and Folkman, J. *Avascular and vascular phases of tumor growth in the chick embryo.* Brit J Cancer 1977; 35: 347-356.
22. Palavalli, S.T. and Saha, B.K. *Fate of tumor cells on the chorioallantoic membrane of chick.* Ind J Exp Biol 1977; 15: 168-173.
23. Schachter, W.C. *Determination of nucleic acids in tissues by pentose analysis.* In: Methods in Enzymology, Vol. III. S.P. Colowick and N.O. Kaplan (Eds.). Academic Press: New York 1957; 680-684.
24. Schreiber, A.B., Winkler, M.E. and Derynck, R. *Transforming growth factor-α: A more potent angiogenic mediator than epidermal growth factor.* Science 1986; 1255-1253.
25. Shing, Y., Folkman, J., Sullivan, R., Butterfield, C., Murray, J. and Klagsbrun, M. *Heparin affinity: Purification of tumor-derived capillary endothelial cell growth factor.* Science 1984; 223: 1296-1299.
26. Tanaka, N.G., Sakamoto, N., Tohgo, A., Nishyama, Y. and Ogawa, H. *Inhibitory effects of anti-angiogenic agents on neovascularization and growth of the chorioallantoic membrane (CAM). The possibility of a new CAM assay for angiogenesis inhibition.* Exp Pathol 1986; 30: 143-150.
27. Thompson, W.D., Campbell, R. and Evans, F. *Fibrin deposition and angiogenesis. Quantitative analysis of the angiogenic response in the chick chorioallantoic membrane.* J Pathol 1985; 145: 27-37.
28. Vu, M.F., Smith, C.D., Burger, P.C. and Kleinworth, C.K. *Methods in laboratory investigation. An evaluation of methods to quantitate the chick chorioallantoic membrane assay in angiogenesis.* Lab Invest 1985; 53: 499-508.
29. Weinstein, R. and Wene, R. *Growth factor requirements of human arterial endothelial cells in vitro.* In Vitro Biol 1986; 22: 549-556.

Address all correspondence to: Dr. J. Splawinski, Department of Pharmacology, Institute of Medical Sciences, 11 Szopena Street, 35-055 Rzeszow, Poland.

COMMONWEALTH OF AUSTRALIA

(Patents Act 1990)

IN THE MATTER OF: Australian Patent Application 696764 (73941/94). In the name of: Human Genome Sciences Inc.

- and -

IN THE MATTER OF: Opposition thereto by Ludwig Institute for Cancer Research, under Section 59 of the Patents Act.

Annexure GBC-19

This is **Annexure GBC-19** referred to in my Statutory Declaration made this Thirteenth day of December 2000.

Gary Baxter Cox

WITNESS: _____

Patent Attorney PEYTEE KHOO

Insulin delivery by somatic cell gene therapy

C Stewart, N A Taylor*, K Docherty* and C J Bailey

Department of Pharmaceutical Sciences, Aston University, Aston Triangle, Birmingham B4 7ET, UK
*Department of Medicine, University of Birmingham, Queen Elizabeth Medical Centre, Birmingham B15 2TH, UK

(Requests for offprints should be addressed to C J Bailey)

ABSTRACT

The feasibility of somatic cell gene therapy as a method of insulin delivery has been studied in mice. Murine pituitary AtT20 cells were transfected with a human preproinsulin DNA in a plasmid containing a metallothionein promoter and a gene conferring resistance to the antibiotic G418. The AtT20MtIns-1·4 clone of cells was selected because of its higher insulin-releasing activity compared with other clones. After culturing for 24 h in Dulbecco's medium containing 10 mM glucose, the AtT20MtIns-1·4 cells released human insulin at about 5 ng/10^6 cells per 24 h. Insulin release was not significantly altered by raised concentrations of glucose, potassium or calcium, but insulin release was increased by 20 mM arginine, 5 mM isomethylbutylxanthine and 90 μM zinc.

AtT20MtIns-1·4 cells (2×10^6) were implanted intraperitoneally into non-diabetic athymic nude (nu/nu) mice, and the mice were made diabetic by injection of streptozotocin after 7 days. Release of human insulin *in vivo* was assessed using a specific plasma human C-peptide assay. Human C-peptide concentrations were maintained at about 0·1 pmol/ml throughout the 29 days of the study. The development of streptozotocin-induced hyperglycaemia was delayed in recipients of the cells releasing human insulin, compared with a control group receiving an implant of non-transfected cells. At autopsy the implanted AtT20MtIns-1·4 cells in each recipient had formed a tumour-like aggregation, with an outer region of insulin-containing cells. The study suggests that somatic cell gene therapy offers a feasible approach to insulin delivery.

Journal of Molecular Endocrinology (1993) 11, 335–341

INTRODUCTION

Somatic cell gene therapy has been considered as a potential method for insulin delivery in insulin-dependent diabetes (Selden *et al.* 1987*b*; Docherty, 1991). The principle of this approach is to introduce and express a new copy of the preproinsulin gene in a somatic cell type which does not express the endogenous gene. This could be achieved by removing cells from a diabetic donor, and transfecting them with the preproinsulin gene linked to a promoter. Cells incorporating and expressing the gene can be identified using a selectable marker such as an antibiotic resistance gene. The engineered cells can be grown in culture and returned to the donor, taking appropriate precautions for containment.

Cultured fibroblasts, COS cells and pituitary AtT20 cells have been transfected with genes encoding rat and human insulins (Lomedico, 1982; Laub & Rutter, 1983; Moore *et al.* 1983; Distloff-Zito *et al.* 1986; Selden *et al.* 1987*b*; Gross *et al.* 1989; Kawakami *et al.* 1992; Taylor & Docherty, 1992). Since proinsulin exerts only weak insulin-like activity *in vivo* (<10% of the potency of insulin) (Revers *et al.* 1984), it is important that proinsulin is processed to insulin. In this respect, the AtT20 cells provide a particularly useful model because they possess the requisite endopeptidases for processing proinsulin to insulin (Moore *et al.* 1983; Taylor & Docherty, 1992).

The present study investigated the feasibility of somatic cell gene therapy using AtT20 cells transfected with the human preproinsulin gene. The insulin-releasing activity of these cells has been assessed *in vitro* and *in vivo* after implantation into immunoincompetent nude mice. The mice were subsequently treated with streptozotocin (STZ) to kill endogenous insulin-secreting islet B-cells and induce a state of insulinopenic diabetes. Insulin

  Printed in Great Britain
0952–5041/93/011–335 $02.00/0

released by the implant was distinguished from endogenous murine insulins using an antiserum specific for the human C-peptide, which is co-secreted with the human insulin.

MATERIALS AND METHODS

Chemicals and animals

Cell culture reagents were from Gibco-BRL (Paisley, Strathclyde, U.K.), STZ was from Sigma Chemical Co. (Poole, Dorset, U.K.), human C-peptide antiserum, tracer and standards were from Novo Nordisk Diagnostics (Cambridge, Cambs, U.K.), insulin antiserum GP6 was a gift from Dr D. F. Steiner (Howard Hughes Medical Institute, University of Chicago, Chicago, IL, U.S.A.), rat C-peptide 1 was a gift from Dr S. Hampton (University of Surrey, Guildford, Surrey, U.K.) and high-performance liquid chromatography (HPLC)-grade ethanol was from Fisons Scientific Equipment (Loughborough, Leics, U.K.).

Adult male athymic nude (nu/nu) mice weighing 20–25 g were obtained from Bantin and Kingman (Hull, Humberside, U.K.). Mice were maintained in an isolated environment with filtered air at 22 °C, with 12 h light per day (08.00–20.00 h) and a standard pellet diet (Mouse Breeding Diet 1; Heygate, Northampton, Northants, U.K.) and tap water available *ad libitum*.

Transfected cells

The ArT20 murine pituitary corticotrophic cell line, transfected with the pMtNeoIns recombinant plasmid, was established and maintained as described previously (Taylor & Docherty, 1992). The plasmid contains a full-length human preproinsulin cDNA (511 bp) driven by the mouse metallothionein-1 promoter and ending in SV40 splice and polyadenylation sequences (Fig. 1). The plasmid also contains genes conferring resistance to ampicillin and G418, to serve as selectable markers. The pMtNeoI plasmid was kindly supplied by Dr K. Peden, NIH, Bethesda, MD, U.S.A. The transfected cells, previously termed ArT20pMtNeohPPI/1 (Stewart *et al.* 1992), have been renamed ArT20MtIns-1 and the clone used in this study was ArT20MtIns-1·4.

Cells were cultured in Dulbecco's modified Eagle's medium (DMEM) supplemented with 10% (v/v) fetal calf serum, 2 mM glutamine, 100 μg streptomycin/ml, 100 units penicillin/ml and a final glucose concentration of 11 mM. In certain experiments, glucose-free medium was supplemented with glucose at different concentrations. Culture conditions were 37 °C in a humidified atmosphere of 95% air and 5% CO_2.

Characterization of ArT20MtIns-1·4 cells *in vitro*

Expression of the human preproinsulin gene was examined after culture of the cells for 48 h in medium supplemented with 90 μM zinc chloride and 5 μM cadmium chloride to enhance expression of the metallothionein promoter (Taylor *et al.* 1991). The medium was replaced with serum-free DMEM and the cells were cultured for a further 4 h. The medium was then removed, concentrated on a SepPak C18 column (Millipore, Watford, Herts, U.K.), and analysed by reverse-phase HPLC using a C18 reverse-phase column. Fractions were neutralized, lyophilized and resuspended in phosphate-buffered saline. The fractions were assayed for insulin-like immunoreactivity using a broad-specificity antiserum (GP6) which reacts similarly with insulin, proinsulin and partially split proinsulin intermediates.

The effects of various agents on insulin release were examined using quadruplicate cultures of $1·5 \times 10^5$ cells for 24 h in 2 ml medium containing 10 mM glucose. The medium was sampled to assay for insulin and replaced with medium containing 10 mM glucose, 16·7 mM glucose or 10 mM glucose plus one of 15 mM potassium chloride, 7·6 mM calcium chloride, 20 mM arginine hydrochloride, 5 mM isomethylbutylxanthine (IBMX) or 90 μM zinc sulphate. Cells were cultured for a further 24 h and the medium was sampled for insulin assay.

Implantation study

Insulin-releasing ArT20MtIns-1·4 cells (2×10^6) were implanted intraperitoneally into non-diabetic nude (nu/nu) mice, and a similar number of non-transfected pituitary cells was administered to a separate group of nude mice to serve as a control. Seven days after implantation, STZ (200 mg/kg i.p. in citrate buffer, pH 4·5) was administered. The study was continued until day 29. Body weight and food and fluid intake were monitored, and plasma glucose and plasma human C-peptide concentrations were determined at intervals using blood collected at 10.00 h from the tail in the freely fed state. Additional blood samples were collected on day 6 at 30 min after an oral glucose challenge (2 g/kg in a 40% (w/v) solution), and on day 7 after a 24-h fast, immediately before STZ administration.

At the end of the study the implants were identified within the abdomen of most recipients.

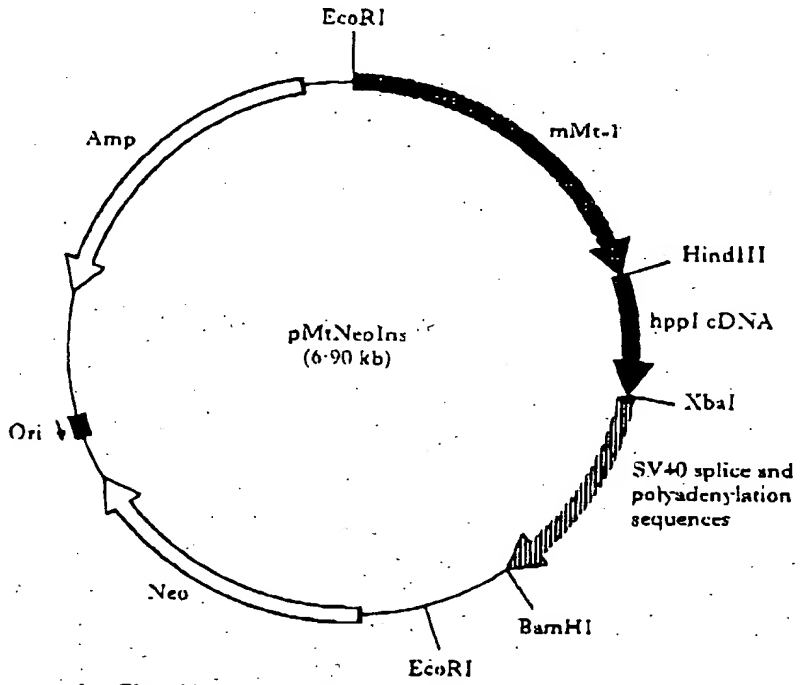

FIGURE 1. Plasmid map of pMtNeoIns. The positions of the ampicillin resistance (Amp) and G418 resistance (Neo) genes, the mouse metallothionein promoter (mMt-1) and the SV40 splice and polyadenylation sequences are indicated. The human preproinsulin cDNA (hppI) was inserted between the metallothionein promoter and the SV40 sequences of pMtNeoIns.

They were removed, weighed and subjected to routine histological examination with haematoxylin–eosin and aldehyde–fuchsin staining. In a separate study, the implants were extracted in 5 ml acid–ethanol/g (750 ml ethanol, 250 ml water, 15 ml concentrated hydrochloric acid) for human C-peptide assay.

Assays

Plasma glucose was determined by an automated glucose oxidase procedure (Stevens, 1971) and immunoreactive insulin-like material in HPLC fractions and cell culture media was measured by radioimmunoassay with polyethylene glycol precipitation (Shakur *et al.* 1989). Human C-peptide in plasma and implant extracts was measured by an ethanol-precipitation radioimmunoassay procedure (Heding & Rasmussen, 1975). The C-peptide antiserum (Novo K6) did not cross-react with rat C-peptide 1 and no reactivity was detected with plasma from normal fed rats and mice (assay sensitivity 0·01 pmol/ml). The inter- and intra-assay coefficients of variation for standards (0·05–0·5 pmol/ml) were 11 and 2·7% respectively.

Statistical analysis

Groups of data are presented as means ± S.E.M. Data were compared using Student's *t*-test. Differences were considered to be significant if $P<0.05$.

RESULTS

Characterization of insulin gene expression

Expression of the human preproinsulin gene by AtT20MtIns-1·4 cells was associated mainly with the release of insulin (80%), together with the release of small amounts of proinsulin and partly split proinsulin intermediates (Fig. 2).

Regulation of insulin gene expression *in vitro*

Under control conditions (10 mM glucose), the release of insulin-like immunoreactive material by

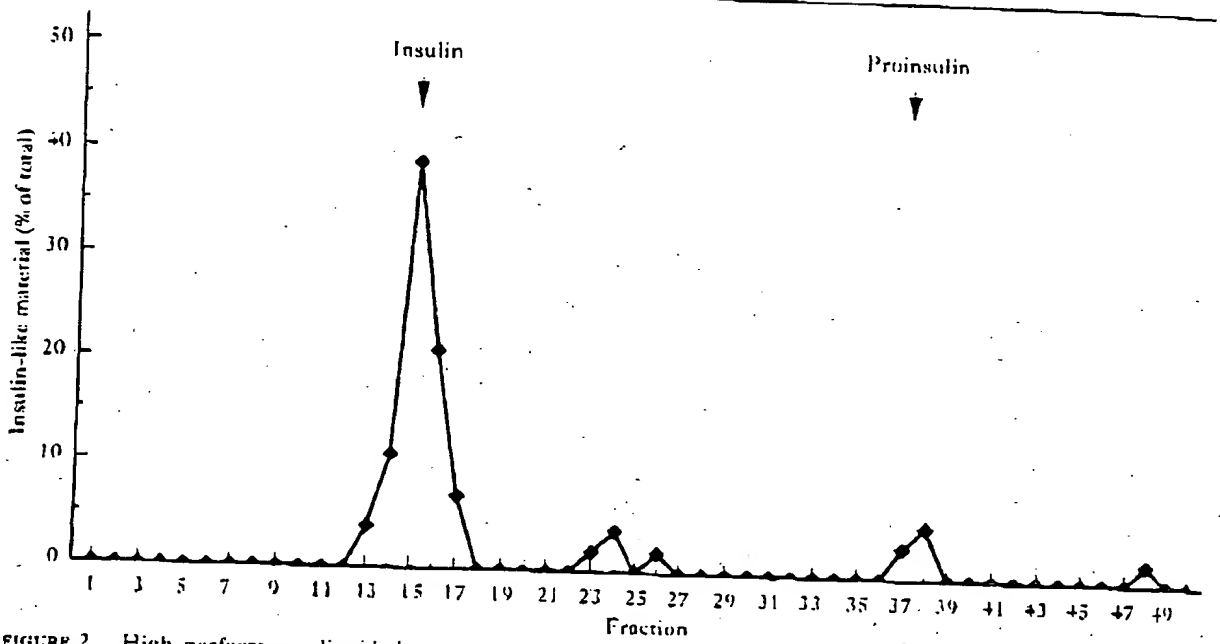

FIGURE 2. High-performance liquid chromatography elution profile of the insulin-like immunoreactivity released by the AtT20MtIns-1·4 cell line. Medium was removed from cultured cells as described in the Materials and Methods, concentrated on a SepPak C18 column, and analysed using a C18 reverse-phase column. Fractions were assayed for insulin-like immunoreactivity using a broad-specificity antiserum.

AtT20MtIns-1·4 cells was 5·06 ± 0·22 ng/10^6 cells per 24 h (n = 24). Insulin release was not significantly altered by incubation for 2 h in medium containing 16·7 mM glucose, 15 mM potassium chloride or 7·6 mM calcium chloride (Fig. 3). However, insulin release was increased by incubation in medium containing 20 mM arginine hydrochloride (275% increase), 5 mM IBMX (137% increase) or 90 μM zinc sulphate (84% increase).

Implantation of AtT20MtIns-1·4 cells

Human C-peptide was not detected in the plasma of nude mice prior to implantation of the cells releasing human insulin, and was not detecredafter implantation of the control (non-transfected pituitary) cells (Fig. 4). However, 6 h after the intraperitoneal implantation of 2 × 10^6 AtT20MtIns-1·4 cells, plasma human C-peptide was detected at 0·1 pmol/ml, and increased to a maximum of 0·16 pmol/ml by day 10 (Fig. 4*a*). Plasma human C-peptide concentrations of about 0·1 pmol/ml were maintained until the end of the study (day 29). The human C-peptide concentration was not significantly altered at 30 min after an oral glucose challenge on day 6 (0·098 ± 0·006 pmol/ml, n = 10) or by a 24-h fast on day 7 (0·108 ± 0·016 pmol/ml, n = 10). Moreover, there was no change in plasma human C-peptide concentrations during the onset of STZ-induced diabetes. The human C-peptide concentrations in the mouse plasma were about one-quarter of the values in normally fed non-diabetic human subjects (mean value 0·4 pmol/ml) measured in the same assay.

In the non-diabetic state, plasma glucose concentrations were slightly reduced by the implantation of the AtT20MtIns-1·4 cells compared with the control pituitary cells (Fig. 4*b*). The hyperglycaemic response 30 min after an oral glucose challenge on day 6 was similar in the two groups (14·0 ± 0·7 mM, n = 10, and 14·8 ± 0·8 mM, n = 11, in test and control mice respectively).

The high dosage of STZ (200 mg/kg i.p.) administered on day 7 produced a rapid and marked hyperglycaemia in controls, resulting in three fatalities by day 14 and subsequent termination of this group. In contrast, mice carrying the human insulin-releasing AtT20MtIns-1·4 cells showed a gradual rise in plasma glucose, with the development of severe hyperglycaemia being delayed by

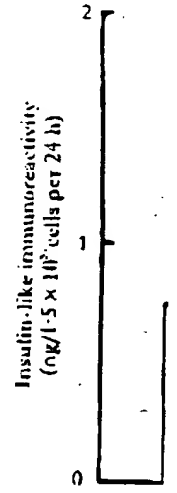

FIGURE 3. Ins
medium after
for 24 h in 2 m
Control mediu
yielded an ILI
24 h, n = 24. T
or 10 mM gluc
$CaCl_2$ (D). 20
isomethylbuty
values from te
versus control

about 14 day
and two fur
appears that
AtT20MtIns
development
endogenous
the AtT20M
for the hype
ficiency of t
noteworthy
became part
by only a sl
cutaneous a
human insul
vations). Th
insulin-relea
development
treated nude

Hyperpha
were observe
in each grou
was consiste
(data not sh

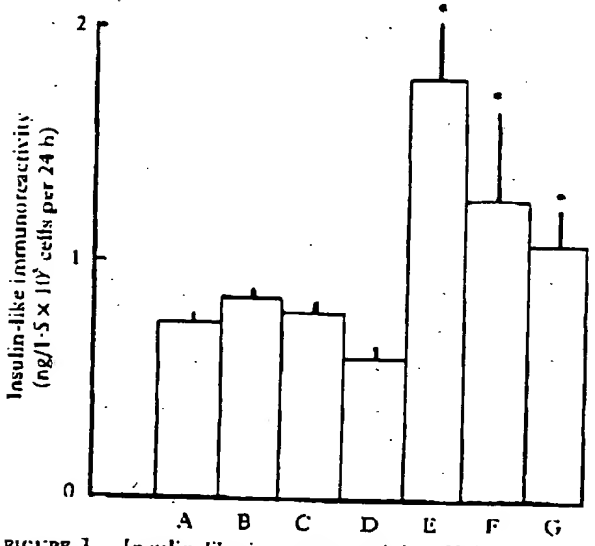

FIGURE 3. Insulin-like immunoreactivity (ILI) in the medium after culturing $1{\cdot}5 \times 10^5$ AtT20MtIns-1·4 cells for 24 h in 2 ml medium containing different agents. Control medium contained 10 mM glucose (A) and yielded an ILI value of $0{\cdot}76 \pm 0{\cdot}03$ ng/$1{\cdot}5 \times 10^5$ cells per 24 h, $n=24$. Test media contained 16·7 mM glucose (B) or 10 mM glucose plus one of 15 mM KCl (C), 7·6 mM $CaCl_2$ (D), 20 mM arginine hydrochloride (E), 5 mM isomethylbutylxanthine (F) or 90 μM $ZnSO_4$ (G). ILI values from test media are means ± S.E.M., $n=4$. $^*P<0{\cdot}05$ versus control (10 mM glucose) (Student's *t*-test).

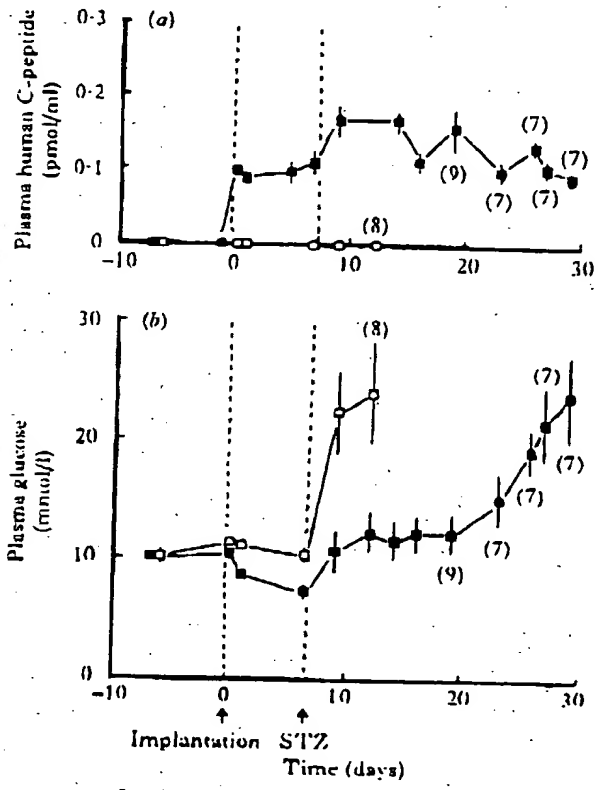

FIGURE 4. Implantation study: (*a*) plasma human C-peptide and (*b*) plasma glucose concentrations of nude (nu/nu) mice implanted intraperitoneally on day 0 with 2×10^6 AtT20MtIns-1·4 cells (■) or non-transfected pituitary cells (□). Streptozotocin (STZ; 200 mg/kg i.p.) was administered on day 7. Values for the group implanted with non-transfected pituitary cells have been terminated at day 14 due to the high incidence of fatalities. Values are means ± S.E.M. of 10 test and 11 control mice, except where shown by values in parentheses.

about 14 days. There was only one fatality by day 19 and two further fatalities up to day 29. Thus it appears that the release of insulin by implanted AtT20MtIns-1·4 cells was sufficient to defer the development of diabetes during the initial period of endogenous B-cell destruction by STZ. However, the AtT20MtIns-1·4 implant could not compensate for the hyperglycaemic effect of prolonged insufficiency of the endogenous B-cell population. It is noteworthy that the STZ diabetic nude mice became particularly insulin resistant, as indicated by only a slight hypoglycaemic response to subcutaneous administration of 10 U short-acting human insulin/kg (C. Stewart, unpublished observations). This is compatible with the failure of the insulin-releasing implant to prevent the eventual development of severe hyperglycaemia in STZ-treated nude mice.

Hyperphagia, polydipsia and body weight loss were observed after the induction of STZ diabetes in each group of mice. The extent of these features was consistent with the extent of hyperglycaemia (data not shown).

At the end of the study autopsies were performed on the mice. The AtT20MtIns-1·4 cells were identified in five out of seven recipients as a tumour-like aggregation (weighing about 50 mg) within the abdomen, adhering to the ventral peritoneum. Gross morphology of the cell aggregates revealed vascularization at the periphery with necrosis towards the centre. Peripheral cells stained positively for aldehyde–fuchsin.

In a separate study 30 days after implantation of 2×10^6 AtT20MtIns-1·4 cells, the abdominal aggregations weighed 56 ± 13 mg, $n=5$. The human C-peptide content of these aggregations was $30{\cdot}5 \pm 1{\cdot}0$ pmol/g, $n=5$, corresponding to $1{\cdot}72 \pm 0{\cdot}46$ pmol/aggregation.

DISCUSSION

The present study has shown that pituitary AtT20 cells can be stably transformed to produce and release human insulin after intraperitoneal implantation into athymic nude mice. Use of a specific assay for plasma human C-peptide has allowed the insulin-releasing activity of the implant to be monitored separately from that of endogenous islet B-cells. The release of human insulin by implanted cells was associated with a delay in the development of STZ diabetes.

Previous studies have inserted and expressed cDNA encoding human preproinsulin in fibroblasts (Moore *et al.* 1983; Diatloff-Zito *et al.* 1986; Selden *et al.* 1987*b*; Kawakami *et al.* 1992) and pituitary AtT20 cells (Moore *et al.* 1983; Taylor & Docherty, 1992). Unlike fibroblasts, which release proinsulin almost exclusively, AtT20 cells can process proinsulin to insulin. In AtT20 cells the insulin is co-localized and co-secreted with adrenocorticotrophic hormone (ACTH) via constitutive and regulated pathways (Moore *et al.* 1983; Orci *et al.* 1987; Powell *et al.* 1988), although the amount of insulin produced is much less than that of ACTH (Moore *et al.* 1983). The release of C-peptide (Moore *et al.* 1983; Powell *et al.* 1988) has been confirmed in the present study.

Regulation of the exogenous preproinsulin gene has been achieved *in vitro* with cyclic AMP (cAMP) analogues (Moore *et al.* 1983; Powell *et al.* 1988; Gross *et al.* 1989), and incubation with IBMX increased insulin release in the present study. It is possible that cAMP activates transcription factors which interact with the metallothionein promoter. Sensitivity of this promotor to zinc is well established (Hammer, 1986; Dickerson *et al.* 1989; Taylor & Docherty, 1992), and the exploitation of this mechanism to regulate cells transfected with the human growth hormone gene has been described (Selden *et al.* 1987*a*). Arginine strongly enhanced the expression of the preproinsulin gene in the present study, but the mechanism of this is unknown.

Attempts to deliver insulin by somatic cell gene therapy have previously been limited to the production of proinsulin from fibroblasts (Selden *et al.* 1987*b*; Kawakami *et al.* 1992). These studies have not distinguished the secretory products of the implanted cells from the endogenous production of insulin-like immunoreactive materials. This has been overcome herein with a specific human C-peptide radioimmunoassay, and with HPLC analysis of the secretory products *in vitro*.

When 2×10^6 insulin-releasing AtT20MtIns-1·4 cells were implanted into non-diabetic mice, which were subsequently made STZ diabetic, the implant continued to release insulin throughout the 29 days of the study. Although the plasma C-peptide concentration achieved by the implant was only about one-quarter of the normal C-peptide concentration (Heding & Rasmussen, 1975), the development of hyperglycaemia was delayed by about 2 weeks. Since STZ diabetic nude mice become very insulin resistant, this could explain why the implants did not prevent the eventual progression to severe hyperglycaemia. Indeed, the release of ACTH and other pro-opiomelanocortin-derived peptides (e.g. opiates) with which insulin is co-processed and co-secreted by the AtT20 cells (Moore *et al.* 1983; Orci *et al.* 1987; Powell *et al.* 1988) could aggravate the hyperglycaemia both directly (Bailey & Flatt, 1987*a*,*b*) and via stimulation of the ACTH-adrenal axis (Lenzen & Bailey, 1984).

The aggregation of implanted cells into a typically tumour-like organization was consistently observed. Even in mice with very low plasma C-peptide concentrations it was possible to detect insulin-containing cells in the outer regions of the cell aggregation. As substantiated by the small amounts of C-peptide extracted from these aggregations, there was only limited intracellular storage of insulin (about 30 pmol/g).

The present study provides evidence for the feasibility of delivering insulin by somatic cell gene therapy. By selecting a cell model (pituitary AtT20 cells) with an active secretory mechanism and appropriate endopeptidase activity, it has been possible to produce and release insulin. AtT20 cells express the high K_m glucose-phosphorylating enzyme glucokinase. Thus it has recently been shown that AtT20 cells transfected with cDNA for preproinsulin and the GLUT-2 glucose transporter exhibit glucose-stimulated insulin biosynthesis and release (Hughes *et al.* 1992). To apply this technology to somatic cell gene therapy will require the use of a convenient source of cells for primary culture, such as fibroblasts. These will require extensive genetic manipulation to achieve regulatable insulin release before implantation back into the donor (Selden *et al.* 1987*b*; Docherty, 1991; Hughes *et al.* 1992). While this approach avoids the need for immunoisolation, it will be necessary to introduce safeguards to contain the growth of implanted cells (Kawakami *et al.* 1992).

ACKNOWLEDGEMENTS

We gratefully acknowledge the support of the British Diabetic Association.

REFERENCI

Bailey, C. J. & I
adrenocortico
(ACTH 1–24
hyperglycaem
11, 175–181.
Bailey, C. J. & I
glucoregulato
mice. *Diabeto*
Diatloff-Zito, C
Moustacchi, I
crosslinking u
corrected by
Proceedings of
83, 703+–703.
Dickerson, I. M
Metallothione
proteins in a
Molecular am
Docherty, K. (I
engineering i
pp. 15+–182.
Publications.
Gross, D. J., V
Halban, P. A
tetrapeptide
(C-peptide) i
Journal of Bi
Hammer, D. H
Biochemistry
Heding, L. G.,
in normal an
Hughes, S. D.,
(1992). Engi
and biosynth
Academy of S
Kawakami, Y.,
Itakura, M. i
for diabetes
complete ren
Laub, O. & Ru
insulin gene
system. *Jour.*
Lenzen, S. & E
and adrenoco
Langerhans.
Lomedico, P. T
to program e

REFERENCES

Bailey, C. J. & Flatt, P. R. (1987*a*). Insulin releasing effects of adrenocorticotropin (ACTH 1–39) and ACTH fragments (ACTH 1–24 and 18–39) in lean and genetically obese hyperglycaemic (ob/ob) mice. *International Journal of Obesity* 11, 173–181.

Bailey, C. J. & Flatt, P. R. (1987*b*). Increased responsiveness to glucoregulatory effect of opiates in obese-diabetic ob/ob mice. *Diabetologia* 30, 33–37.

Diatloff-Zito, C., Papadopoulo, D., Averbeck, D. & Moustacchi, E. (1986). Abnormal response to DNA crosslinking agents of Fanconi anaemia fibroblasts can be corrected by transfection with normal human DNA. *Proceedings of the National Academy of Sciences of the U.S.A.* 83, 7034–7038.

Dickerson, I. M., Peden, K. W. C. & Mains, R. E. (1989). Metallothionein-1 promoter-directed expression of foreign proteins in a mouse pituitary corticotroph tumor cell line. *Molecular and Cellular Endocrinology* 64, 205–212.

Docherty, K. (1991). Prospects for gene therapy and cellular engineering in diabetes. In *Biotechnology of Insulin Therapy*, pp. 154–182. Ed. J. C. Pickup. Oxford: Blackwell Scientific Publications.

Gross, D. J., Villa-Komaroff, L., Kahn, C. R., Weir, G. C. & Halban, P. A. (1989). Deletion of a highly conserved tetrapeptide sequence of the proinsulin connecting peptide (C-peptide) inhibits proinsulin corticotroph (AcT20) cells. *Journal of Biological Chemistry* 264, 21486–21490.

Hammer, D. H. (1986). Metallothionein. *Annual Review of Biochemistry* 55, 913–951.

Heding, L. G. & Rasmussen, S. M. (1975). Human C-peptide in normal and diabetic subjects. *Diabetologia* 11, 201–206.

Hughes, S. D., Johnson, J. H., Quaade, C. & Newgard, C. B. (1992). Engineering of glucose-stimulated insulin secretion and biosynthesis in non-islet cells. *Proceedings of the National Academy of Sciences of the U.S.A.* 89, 688–692.

Kuwakami, Y., Yamaoki, T., Hirochika, R., Yamashita, K., Itakura, M. & Nakauchi, H. (1992). Somatic gene therapy for diabetes with an immunological safety system for complete removal of transplanted cells. *Diabetes* 41, 956–961.

Laub, O. & Rutter, W. J. (1983). Expression of the human insulin gene and cDNA in a heterologous mammalian system. *Journal of Biological Chemistry* 258, 6043–6050.

Lenzen, S. & Bailey, C. J. (1984). Thyroid hormones, gonadal and adrenocortical steroids and the function of the islets of Langerhans. *Endocrine Reviews* 5, 411–434.

Lomedico, P. T. (1982). Use of recombinant DNA technology to program eucaryotic cells to synthesize rat proinsulin – a rapid expression assay for cloned genes. *Proceedings of the National Academy of Sciences of the U.S.A.* 79, 5798–5803.

Moore, H. P.-H., Walker, M. D., Lee, F. & Kelly, R. B. (1983). Expressing a human proinsulin cDNA in a mouse ACTH-secreting cell. Intracellular storage, proteolytic processing, and secretion on stimulation. *Cell* 35, 531–538.

Orci, L., Ravazzola, M., Amherdt, M., Perrelet, A., Powell, S. K., Quinn, D. L. & Moore, H. P.-H. (1987). The trans-most cisternae of the Golgi complex: a compartment for sorting of secretory and plasma membrane proteins. *Cell* 51, 1039–1051.

Powell, S. K., Orci, L., Craik, C. S. & Moore, H. P.-H. (1988). Efficient targeting to storage granules of human proinsulins with altered propeptide domain. *Journal of Cell Biology* 106, 1843–1851.

Revers, R. R., Henry, R., Schmeiser, L., Kolterman, O., Cohen, R., Rubenstein, A., Frank, B., Galloway, J. & Olefsky, J. M. (1984). Biosynthetic human insulin and proinsulin have additive but not synergistic effects on total body glucose disposal. *Journal of Clinical Endocrinology and Metabolism* 58, 1094–1098.

Selden, R. F., Skoskiewicz, M. H., Howie, K. B., Russell, P. S. & Goodman, H. M. (1987*a*). Implantation of genetically engineered fibroblasts into mice: implications for gene therapy. *Science* 236, 714–716.

Selden, R. F., Skoskiewicz, M. J., Russell, P. S. & Goodman, H. M. (1987*b*). Regulation of insulin gene expression. Implications for gene therapy. *New England Journal of Medicine* 317, 1067–1076.

Shakur, Y., Shennan, K. I. J., Taylor, N. A. & Docherty, K. (1989). A major C-peptide deletion prevents secretion of a mutant human proinsulin from transfected monkey kidney cells. *Journal of Molecular Endocrinology* 3, 155–162.

Stevens, J. F. (1971). Determination of glucose by an automatic analyser. *Clinica Chimica Acta* 32, 199–201.

Stewart, C., Taylor, N. A., Docherty, K. & Bailey, C. J. (1992). Insulin replacement by somatic cell gene therapy: pilot study. *Diabetologia* 35, Suppl. 1, A3 (Abstract).

Taylor, N. A. & Docherty, K. (1992). Sequence requirements for processing of proinsulin transfected mouse pituitary AtT20 cells. *Biochemical Journal* 286, 619–622.

Taylor, N. A., Shennan, K. I. J. & Docherty, K. (1991). Inducible expression of mutant human proinsulins in a mouse pituitary cell line controlled by the mouse metallothionein promoter. *Biochemical Society Transactions* 19, 202S.

RECEIVED 28 May 1993

COMMONWEALTH OF AUSTRALIA

(Patents Act 1990)

IN THE MATTER OF: Australian Patent Application 696764 (73941/94). In the name of: Human Genome Sciences Inc.

- and -

IN THE MATTER OF: Opposition thereto by Ludwig Institute for Cancer Research, under Section 59 of the Patents Act.

Annexure GBC-20

This is **Annexure GBC-20** referred to in my Statutory Declaration made this Thirteenth day of December 2000.

Gary Cox

Gary Baxter Cox

WITNESS: _____

Patent Attorney PEYTEE K.HOU

MINIREVIEW

Gene Therapy for Human Hemoglobinopathies (43665)

CHRISTOPHER E. WALSH,* JOHNSON M. LIU,* JEFFERY L. MILLER,* ARTHUR W. NIENHUIS,* AND RICHARD JUDE SAMULSKI†,‡

Clinical Hematology Branch, NHLBI/NIH, Bethesda, Maryland 20892 and Department of Biological Sciences,† University of Pittsburgh, Pittsburgh, Pennsylvania 15260*

The molecular defects in sickle cell disease and β-thalassemia have been well characterized and seem amenable to genetic correction (1). The development of effective genetic therapy could revolutionize treatment of the hemoglobinopathies. Before envisioning treating patients, methodologies will be required to ensure safe, efficient, and stable transfer of globin genes into hematopoietic stem cells and subsequent high-level gene expression in mature erythroid cells. This minireview will focus on the use of viral gene transfer vectors as potential therapeutic agents for the treatment of human hemoglobinopathies.

The thalassemias and clinically significant hemoglobinopathies are among the most common single gene disorders throughout the world. Patients with severe phenotypes rely on regular erythrocyte transfusions that can be associated with life-threatening iron overload despite intensive chelation (2). Long-term transfusion therapy may result in the development of anti-erythrocyte antibodies making subsequent transfusions difficult or, in some instances, impossible (3, 4). Allogeneic bone marrow transplantation has been performed with some success but is feasible in only a small percentage of affected patients (5, 6). Recent work has focused on the pharmacologic manipulation of fetal hemoglobin. Underpinning these efforts is the premise that increased γ-globin gene transcription and fetal hemoglobin synthesis leads to more effective erythropoiesis and/or decreased hemolysis in patients with β-thalassemia and sickle cell disease (7–9). These treatments are, however, potentially toxic with unknown long-term complications.

Globin Gene Organization

Hemoglobin is a tetrameric protein composed of two dimeric polypeptide units encoded by two different gene families on two separate chromosomes. The α-globin gene cluster, located on chromosome 16, includes the duplicated α genes (α_1, α_2) present in the fetal and adult stages of erythropoiesis and the embryonic ζ-gene. Located on chromosome 11 are the cluster of β-like genes including the two adult genes, δ and β, the two fetal genes, γ^A and γ^G, and the embryonic ε-gene (see Fig. 1). During normally developing erythropoiesis, six distinct hemoglobin species are present in the transition from intrauterine to adult life. Coordinated gene expression in the α- and β-gene clusters occurs at each site of erythropoiesis: the yolk sac of the embryo, liver of the fetus, and bone marrow postnatally. This process of coordinated expression, known as "hemoglobin switching," coincides with the change in hemoglobin phenotype. The β-like genes are activated and silenced in the 5′ to 3′ order of their transcriptional positions along chromosome 11.

Current switching models suggest competition between the individual β-like genes for regulatory elements defined within the distant DNase I hypersensitive sites known collectively as the locus control region (described below). A putative switching factor(s) is involved with either the silencing and/or activation of th β-gene cluster. Interaction of switching factors with β-like gene promoters may determine whether active gene transcription occurs. An example is the identification of a stage selector element in the human γ-

‡ To whom requests for reprints should be addressed at Department of Biological Sciences, Room 269, Crawford Hall, University of Pittsburgh, Pittsburgh, PA 15260.

P.S.E.B.M. 1993, Vol 204: 289–300

0037-9727/93/2043-028953.00/0

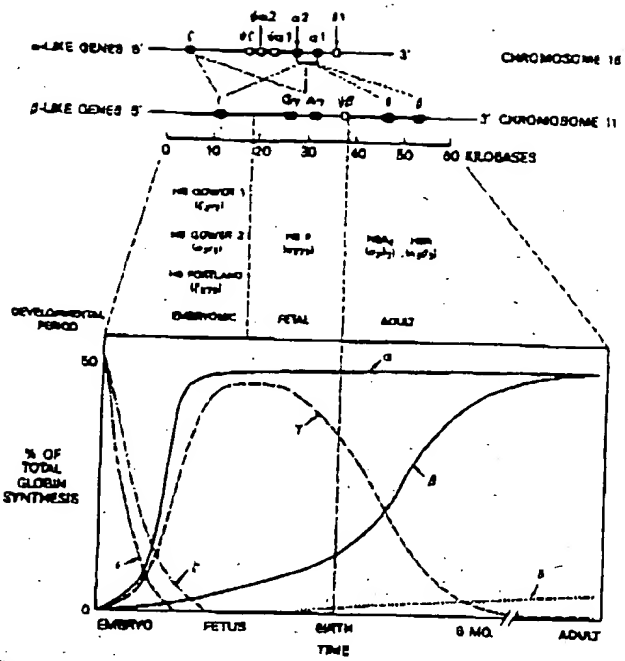

Figure 1. The spatial organization of the α- and β-globin gene clusters (top). Coordinated globin gene expression and hemoglobin switching (center) at each stage of erythrocyte development (bottom) (adapted from Ref. 87).

globin gene promoter and of the nuclear protein which binds to this element and enables the γ-gene to competitively silence the β-globin gene (10). Levels of the specific DNA-binding protein are higher in more developmentally immature cells in which γ-globin expression is elevated. Analysis of the α-like globin gene cluster suggests a similar type of regulation (11).

Regulation of Globin Gene Transcription

The expression of the individual globin genes is regulated at the level of gene transcription, as supported by measurement of globin transcriptional rates and by quantitation of globin mRNA from patients with thalassemia (12). In general, globin transcriptional regulation requires cis-acting DNA sequences located within the globin gene cluster and trans-acting factors which bind sequence-specific motifs within the cis-acting regulatory elements.

Regulation of the human β-globin gene cluster (ε, γ^G, γ^A, δ, β) is mediated via local cis-acting sequences including the globin promoters and enhancers 3′ of the γ- and β-genes. Initial efforts to define cis-acting elements responsible for globin gene expression in transgenic animals revealed that local sequences were not sufficient for normal globin expression. The observation that deletions upstream of the β-globin gene inactivated globin expression suggested that other regulatory elements were necessary. These distant regulatory elements that flank the β-globin cluster are associated with DNase I hypersensitive sites (HS), and inclusion of these sites modulates high level globin expression. These sites are collectively termed the locus control region (LCR). Four sites (5′ HS1–4) are located several kilobases 5′ to the ε-globin gene, and one site (3′ HS1) is mapped 3′ to the β-globin gene. The active elements of the LCR are encompassed within 300–400 base pairs of DNA found at each HS (13, 14). The HS2, 3, and 4, when linked to globin genes singly or in combination, substantially increase globin gene expression in transfected erythroleukemia cells or when introduced into transgenic animals (15).

Recently, several erythroid-specific enhancer sequences and trans-acting factors have been defined that appear to regulate globin gene transcription. One of the most powerful enhancer elements in the β-globin locus lies within the HS2 and is localized to tandem AP-1 binding sites (16). This element is required for high level γ-globin gene expression in stably transfected K562 cells. K562 cells provide a model for the study of globin gene regulation and have been used to define important cis-acting regulatory elements. The HS2 enhances by 150-fold transcriptional activity in hemin-induced K562 cells but is relatively inactive in nonerythroid cells. The trans-acting factor NF-E2 binds to the HS2 enhancer and is required for hemin-inducible activity of the enhancer (17). Transgenic animal experiments using only the HS2 site linked to a β-globin gene enabled the production of 25–50% levels of endogenous globin transcript (18). This factor has been characterized as a 45-kDa basic-leucine zipper DNA binding protein expressed in erythroid and megakaryocytic lineages (19).

The erythroid-specific transcription factor NFE-1 (GATA-1) binds to GATA consensus motifs found in several of the cis-acting elements. Experiments with transgenic mice indicate that GATA-1 may be important in the development and function of red blood cells (20, 21).

Globin Pathophysiology

The thalassemic syndromes are hereditary anemias which occur due to mutations that affect the synthesis of either α- or β-globin chains. The ratio of α- to β-chain synthesis is the major determinant of pathology. Excess of either globin chain can lead to the formation of aggregates or intracellular inclusions causing decreased red blood cell membrane deformity, ineffective erythropoiesis, and accelerated red cell destruction. Discussion of clinically relevant severe thalassemia syndromes is usually directed toward the β-thalassemias.

β-Thalassemia refers to inadequate β-globin chain synthesis encoded by a single β-globin gene on chromosome 11. Heterozygous individuals are characterized by a quantitative deficiency of β-globin production relative to α-globin. In homozygous patients with β-

thalassemia, deficient or absent β-globin gene synthesis causes the production of poorly hemoglobinized, defective erythrocytes resulting in hemolysis and severe anemia (22). Patients with severe disease require frequent red blood cell transfusions with attendant iron accumulation. The severity of this disease is modulated by increased γ-globin synthesis and increased fetal hemoglobin ($\alpha_2\gamma_2$, Hb F) or concomitant α-thalassemia.

In homozygous sickle cell anemia, the mutant hemoglobin (Hb S, $\alpha_2\beta_2^s$) is susceptible to polymerization resulting in altered erythrocyte rheological properties, vaso-occlusion, and multiorgan damage. The severity of sickle cell disease correlates with the degree of hemoglobin polymerization. Hb F has a sparing effect on polymerization and decreases the tendency of Hb S to precipitate within the erythroid cells.

In these disease states, the transfer and expression of either β- or γ-globin genes should be highly effective in correcting these genetic defects. Replacement with a functional β-globin gene could correct the defect in severe β-thalassemia, whereas gene insertion of a γ-globin gene could ameliorate the potential for polymerization in sickle cell disease. Studies of sickle cell and β-thalassemia patients reveal that mild or absent clinical manifestations occur in the presence of hemoglobin F levels of 20–40% (23, 24). Expression of a β-globin transgene at 10–20% of normal endogenous levels is adequate to achieve a dramatic phenotypic improvement in a thalassemic mouse model (25).

Gene Transfer

The following are the major requirements for globin gene transfer to be clinically applicable. (i) Transduced (introduced) globin gene expression must be at sufficient levels. (ii) Expression should be stably regulated and erythroid specific. (iii) The totipotent bone marrow stem cell should be transduced at high frequency and/or maintain a competitive advantage over nontransduced cells for its self-renewal. (iv) The introduction of foreign DNA into the target cell genome should have limited potential for insertional mutagenesis and/or endogenous gene disruption.

Ideally, replacement of a defective gene with the correct genetic sequence by targeting genes to specific sites within the genome would be an optimal method for genetic therapy. Homologous recombination into a β-globin locus has been achieved in cultured embryonic stem cells, albeit at a frequency too low to be of any current therapeutic value (26). However, as a result of recent advances in molecular biology, the introduction of new genetic material by nonhomologous recombination with gene insertion into a target cell genome now appears attainable.

Gene transduction is accomplished by a variety of techniques, including viral vectors, poly-lysine/DNA conjugates, and other physical techniques. Viral gene transfer vectors make use of the inherent efficiency of viruses to transfer and express their genetic information in mammalian cells (for review, see Ref. 27). As now envisioned, hematopoietic stem cells from an affected patient could be infected with an appropriate viral vector containing a correctly functioning globin gene. We will describe current work with retrovirus and the parvovirus, adeno-associated virus, as potential gene transfer vectors.

Retroviral Vectors

Retroviruses contain a single-stranded RNA genome that, upon entry into a cell, is converted into a double-stranded DNA before its integration into the host cell chromosome. Early interest in these viruses stemmed from their ability to induce tumors by insertional mutagenesis. The integrated provirus, containing its own powerful transcriptional elements, is thought to activate nearby proto-oncogenes or inactivate tumor suppressor genes. To avoid the possibility of wild-type retroviral infection, packaging cell lines are used to produce replication-defective recombinant retroviral particles. Vector and packaging cell strategies have been well documented (27).

Globin Retroviral Vectors. Transfer of genomic human β-globin sequences using retroviral vectors has evolved with both the development of improved packaging cell lines and greater understanding of globin gene regulation. Initial experiments utilized a 3.0-kb fragment of genomic β-globin into an ecotropic vector in both orientations (28). A neomycin resistance gene in those constructs was employed to rapidly screen for high titer producer clones subsequently used to generate infectious recombinant retroviral virions. The marker also facilitated isolation of target cells transduced by the retrovirus. Only the reverse orientation construct was functional and sufficient for proviral integration and subsequent viral production. Individual clones contained a single transferred proviral copy. Human β-globin transcripts were detected and the level of expression increased in dimethyl sulfoxide-induced MEL clones. Dimethyl sulfoxide, hemin, and other agents have been used in several human and murine leukemic cell lines to induce β-globin cluster gene expression. Furthermore, negligible globin expression was detected in 3T3 fibroblasts, indicating that the construct carrying a β-globin promoter contributed to erythroid-specific expression. The level of expression (compared with endogenous murine β-globin expression) was approximately 0.01%. Similar experiments using an amphotropic vector containing a neomycin resistance gene with a γ-β globin hybrid were used to infect MEL cells with human β-globin expression at 10% of the endogenous induced expression (29). In both instances, viral titer was low and the provirus rearranged in some of the clones tested. Constructs containing portions of the

5′ untranslated region and intron 2 in the reverse orientation interfered with generation of full-length transcripts and yielded low titer recombinant virus (30). The 5′ region could be removed, but the intron 2 was required for expression. Reverse orientation globin constructs may contain polyA termination signals, possibly accounting for abbreviated transcription and low titer virus generation.

Examination of retrovirally transduced β-globin in human hematopoietic cells demonstrated gene transfer and expression in erythroid colonies (burst-forming unit, erythroid) (31). Expression reached 5% of the endogenous β-globin in several pooled colonies using RNase protection assay. Expression was determined by using a 6-base pair insertion ("marking") at the 5′ untranslated region to allow detection of the transferred gene. Infection frequency was low (0.04%) and attributed to the low viral titer (5×10^4 colony-forming units/ml). A truncated β-globin minigene (lacking introns) was also tested in MEL cells but expressed at undetectable levels regardless of the orientation.

The first *in vivo* experiment described a recombinant retroviral construct encoding a human β-globin gene that was used to infect murine hematopoietic cells and reconstitute transplanted mice (32). Expression was limited primarily to the erythroid lineage and varied from 0.4% to 4.0% of the endogenous mouse β-globin mRNA level. The proviral copy number per cell ranged from 0.02 to 0.40 copies/cell, found in all lineages. Long-term human β-globin gene expression was detected in transplanted animals at 4–9 months. The infection rate was low (18 of 104 animals reconstituted with infected bone marrow), which indicated that the marrow infection conditions needed to be optimized (increased viral titer, enrichment of pluripotent cells, and induction of quiescent stem cell cycling).

Confirmatory experiments in several laboratories demonstrated β-globin retroviral transfer in murine hematopoietic cells (33, 34). Long-term expression in all lineages from secondary recipient animals indicated that pluripotent stem cells rather than committed progenitor cells were infected. Co-culturing conditions for bone marrow target cells with recombinant retrovirus improved, largely through the inclusion of hematopoietic growth factors to shorten G_0 and promote entry into cell cycle required for retroviral replication and integration (35). Despite improved transduction frequency in pluripotent bone marrow cells, globin expression still ranged from 1% to 5% of the endogenous level.

The recently discovered LCR regulatory elements flanking the β-globin gene cluster suggested a new approach to the design of retroviral vectors (36). Individual LCR fragments were included within a marked β-globin/neomycin gene cassette and used to generate recombinant amphotropic virions infectious for MEL cells (37). One construct incorporating an HS2 fragment resulted in high level expression in a few clones (three), but with extreme expression variability (10–310%). The viral titers were 10^4–10^5 colony-forming units/ml. Subsequently, investigators from several laboratories have been unable to generate LCR-globin producer lines of sufficient titer that do not exhibit proviral rearrangement or deletion. A recent report describes the use of a 36-base pair sequence encompassing the NFE-2 binding site within the HS2 region linked to human β-globin (38). The level of β-globin expression increased marginally from 6.0% to 12.0% with the addition of the enhancer element. Viral titers were again low, and introduction of multiple copies of the 36-base pair fragment promoted gross proviral rearrangement.

Generation of an ecotropic retrovirus containing an LCR cassette with truncated HS 4, 3, 2, and 1 sites linked to a human β-globin yielded 60–70% expression in MEL cells compared with endogenous murine globin expression. Transfer into murine hematopoietic progenitors and subsequent transplantation into lethally irradiated recipients resulted in human β-globin expression. These experiments suggest that inclusion of LCR elements may support high level β-globin gene expression in murine hematopoietic stem cells; however, significant rearrangement of the provirus occurred and the vectors employed yield low recombinant viral titers (39).

Many of the alternative viral vectors currently available either do not integrate into host cells at high frequency, are not easily rescuable from the integrated state, are limited in their host range, or include other viral genes, thereby creating a need for the development of a safe and efficient viral vector system. We feel that the human DNA virus, adeno-associated virus, offers a promising alternative to the currently utilized vectors.

Adeno-Associated Virus

Adeno-associated virus (AAV) is a defective member of the parvovirus family. The AAV genome is encapsidated as a single-stranded DNA molecule of plus or minus polarity (40, 41). Strands of both polarities are packaged, but in separate virus particles (42) and both strands are infectious (43). The single-stranded DNA genome of the human virus AAV-2 is 4675 base pairs in length (44) and is flanked by inverted terminal repeated sequences of 145 base pairs each (45). The first 125 nucleotides form a palindromic sequence that can form a T-shaped hairpin structure and can exist in either of two orientations (designated flip or flop). This unique structure has led to the suggestion (46) that AAV may replicate according to a model first proposed by Cavalier-Smith (47) in which the terminal hairpin of AAV is used as a primer for the initiation of DNA replication. The AAV sequences that are required

in cis for packaging, integration/rescue, and replication of viral DNA appear to be located within a 191-base pair (bp) sequence that includes the terminal repeat sequences (48, 49).

The viral DNA sequence displays two major open reading frames, one in the left half and the other in the right half of the conventional AAV map (43). At least three regions which, when mutated, give rise to phenotypically distinct viruses have been identified in the AAV genome (50). The rep region, which occupies the conventional left half of the genome, encodes one or more proteins that are required for DNA replication and for rescue from the recombinant plasmid. The cap and lip regions appear to encode for AAV capsid proteins; mutants within these regions are capable of DNA replication but do not produce virus (50). AAV contains three transcriptional promoters, p5, p19, and p40 (45, 51–53).

AAV-2 can be propagated as a lytic virus or maintained as a provirus, integrated into host cell DNA (54). In a lytic infection, efficient replication requires coinfection with either adenovirus (55, 56) or herpes simplex virus (57)—hence the classification of AAV as a "defective" virus. When no helper virus is available, AAV can persist in the host cell genomic DNA as an integrated provirus (58, 59). Virus integration appears to have no apparent effect on cell growth or morphology (60, 61). Studies of the physical structure of integrated AAV genomes (59, 62) suggest that viral insertion into the host chromosome is usually in a tandem head to tail orientation and occurs within the AAV terminal repeated sequence. Integrated AAV genomes are stable, persisting in tissue culture for greater than 100 passages (59). Although AAV is a human virus, its host range for lytic growth is unusually broad. Virtually every mammalian cell line evaluated (including a variety of human, simian, canine, bovine, and rodent cell lines) can be productively infected with AAV, provided that an appropriate helper virus is used (i.e., canine adenovirus in canine cells) (54). These same cells are also capable of establishing an AAV latent infection in the absence of helper.

Despite the wide range of susceptible cell types, no disease has been associated with AAV in either human or animal populations (63), even though exposure is commonplace. Anti-AAV antibodies have been found frequently in humans and monkeys. Estimates suggest that about 70–80% of infants acquire antibodies to AAV types 1, 2, and 3 within the first decade; more than 50% of adults have been found to maintain detectable anti-AAV antibodies. AAV has been isolated from fecal, ocular, and respiratory specimens during acute adenovirus infections, but not during other illnesses (64).

Infectious AAV Clon . We initially cloned intact duplex AAV DNA into the bacterial plasmid pBR322 (65) and found that the AAV genome could be rescued from the recombinant plasmid by transfection of the plasmid DNA into human cells with adenovirus 5 as helper. The efficiency of rescue from the plasmid was sufficiently high to produce yields of AAV DNA comparable to those observed after transfection with equal amounts of purified virion DNA. The AAV sequences in the recombinant plasmid could be modified, and then "shuttled" into eukaryotic cells by transfection. In the presence of helper adenovirus (Ad), the AAV genome was found to be rescued free of any plasmid DNA sequences and replicated to produce infectious AAV particles (65–68). This developed an approach for mutant construction (67) that enabled us and others to explore viral gene function (43, 69), and to identify the cis-acting sequences needed for AAV rescue, replication, packaging, and integration (49).

AAV has been tested as a viral vector system to express a variety of genes in eukaryotic cells. Hermonat and Muzyczka (69) produced a recombinant AAV (rAAV) viral stock in which the neomycin resistance gene (neo) was substituted for the AAV capsid region and observed rAAV transduction of neomycin resistance into murine and human cell lines. The stable integrated viral vector could be rescued to produce replicating rAAV sequences after superinfection with Ad and wild-type AAV. Tratschin *et al.* (70) created an rAAV that was found to express the chloramphenicol acetyltransferase gene in human cells under the AAV p40 promoter. LaFace *et al.* (71) observed gene transfer into hematopoietic progenitor cells using an AAV vector. Wondisford *et al.* (72) cotransfected cells with two different recombinant AAV vectors, each encoding a subunit of human thyrotropin, and observed expression of biologically active thyrotropin.

The desirable size of inserted non-AAV or foreign DNA is limited to that which permits packaging of the rAAV vector into virions, and this depends on the size of retained AAV sequences. Tratschin *et al.* (70) constructed an AAV/chloramphenicol acetyltransferase genome that was 3% (approximately 150 nucleotides) longer than the wild-type AAV genome, and found that it could be packaged into virions. An AAV genome too large to be packaged resulted from insertion of a 1.1-kbp fragment of bacteriophage-λ into a nonessential region of AAV (R. J. Samulski and T. Shenk, unpublished). Thus, the total size of the rAAV to be packaged into virions should be about 4800–5000 nucleotides in length.

As mentioned above, several AAV vector systems have been designed that contain a recombinant plasmid capable of being packaged into AAV particles. The recombinant virus generated then functions as a vector for stable maintenance or expression of a gene or a DNA sequence in eukaryotic cells when under control of an AAV or SV40 transcriptional promoter. However,

a common problem encountered in all these AAV vector systems has been the inability to produce recombinant virus stocks free of helper AAV virus. Various methods have been used in attempts to decrease the percentage of contaminating helper virus (73). This problem has been a major drawback in the use of AAV as a prevalent viral vector. Our recent work, however, has succeeded in generating high titer viral stocks that are free of helper virus.

AAV Vectors. We have recently developed a method for producing substantially helper-free stocks of rAAV that can be used to efficiently and stably transduce foreign genes into host cells or organisms (49). Our present method for producing recombinant stocks is directed toward producing a viral expression vector system with improved efficiency, applicability, definition, and safety relative to viral vector systems currently utilized. The method utilizes a two-component system comprised of functionally, but not structurally, related rAAV genomes, one of which contains a segment of foreign DNA (the vector) but lacks DNA sequences necessary for viral replication, and the other (the helper AAV) which provides those viral functions not encoded by the vector but which cannot itself be incorporated into virions. Importantly, the vector and the helper DNA are sufficiently nonhomologous so as to preclude homologous recombination events that could generate wild-type AAV. Along with this development of the vector, we have conducted a study characterizing natural AAV integration. In this study, we have encountered the unexpected observation that wild-type AAV utilizes site-specific integration when establishing viral latency (see below).

Production of the AAV Vector System. We have constructed an infectious adeno-associated viral genome that contains two *Xba*I cleavage sites flanking the viral coding domain (43) (Fig. 2); these restriction enzyme cleavage sites were created to allow nonviral sequences to be inserted between the cis-acting terminal repeats of AAV (49). The AAV helper plasmid termed pAAV/Ad contains adenovirus type 5 terminal sequences (107 bp) in place of the normal AAV termini. This helper cannot be packaged into AAV virions, since it lacks the terminal cis-acting domain required for this function. The AAV terminal sequences were originally substituted with adenovirus terminal sequences in pAAV/Ad so as to transcriptionally enhance AAV gene expression (74). This hybrid plasmid did not contain the Ad packaging sequences (75) and therefore could not be packaged into Ad virions either.

The presence of the adenovirus termini substantially enhanced the expression of AAV-specific proteins from pAAV/Ad DNA when compared with pAAV/no TR (DNA which contained neither adenovirus nor AAV terminal sequences). When the helper plasmid pAAV/Ad and a vector pAAV/NEO were co-transfected into human cells in the presence of adenovirus, rescue and replication of the AAV/NEO sequences were detected. The vector viruses generated from this complementation contain only the terminal 191 nucleotides of the viral chromosome, demonstrating that all cis-acting AAV functions required for replication and virion production are located within that region. Recombinant viral DNA carrying a drug resistance marker gene were integrated into the cellular genome. These transduced genes could not be excised and replicated when the cells were subsequently infected with adenovirus, suggesting another level of safety (49). Thus, the AAV termini (145 bp) are sufficient for integration of the AAV chromosome into a host cell genome. No AAV gene expression is required to establish a latent infection using this vector, and up to 70% of the cells can be transduced.

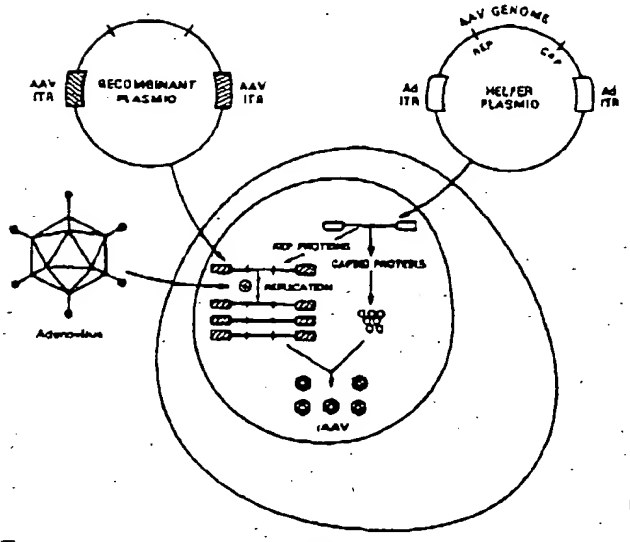

Figure 2. Generation of helper-free recombinant adeno-associated virions. A producer cell line is co-transfected with "helper" and recombinant (rAAV) plasmids. Helper plasmid generates rep and cap protein synthesis required for rAAV replication and encapsidation. Adenovirus infection provides necessary replication and packaging functions (see text for details).

Site-Specific Integration. The proviral integration form of wild-type AAV is a unique feature of this virus. Initial studies characterizing the AAV proviral state using restriction digestion and Southern blotting of genomic DNA demonstrated that the proviral DNA was covalently linked to cellular DNA in tandem concatamers (59, 76). These results have been confirmed and extended by the development of a protein-DNA binding enrichment technique used to isolate AAV proviral DNA from latent human cell lines (77). The strategy for retrieving AAV-cellular junctions involved a protein filter binding procedure that relied upon the interaction between λ repressor and its operator sequences. An infectious recombinant clone was used to

generate an AAV-λ hybrid that contained the λ operator site. The recombinant virus was used to establish latently infected AAV-λ cell lines. Genomic DNA isolated from the latent cell lines digested with restriction enzymes were mixed with purified λ repressor protein and passed over a membrane filter. Southern hybridization analysis of the retained fragments showed a physical linkage between AAV proviral DNA and cellular sequences. Nucleotide comparison of clonal cellular sequences demonstrated viral-cellular junction rearrangements involving deletion of portions of the terminal repeats. An unrearranged preintegration junction cellular sequence used as probe confirmed the sequence location at chromosome 19. Polymerase chain reaction amplification using AAV and junction-specific primers generated viral/junction breakpoints that lay within a 100-bp sequence on chromosome 19. *In situ* analysis of latently infected cell chromosomes using AAV-specific probes further demonstrated that viral DNA integrated into only one locus. Both single and multiple copy number insertion patterns were located within this integration region.

The minimal elements required for AAV integration are currently being delineated. AAV vectors containing only the inverted terminal repeat integrate at high frequency, suggesting the importance of the inverted terminal repeat for integration. This also indicates that AAV integration relies on host cellular enzymes. Furthermore, work in our laboratory demonstrated the lack of site-specific integration with recombinant vectors containing only AAV termini (78). Taken together, this would imply that viral *trans*-acting factors are required for site-specific integration. Since limited amplification of the AAV genome is required for integration, the AAV *rep* proteins described previously are likely candidates for this function.

Since this initial observation, we have documented site-specific integration in a number of cell types (human T cells, colon, lung, and monkey kidney cells). Our preliminary characterization of this chromosomal region has revealed that (i) this sequence is highly conserved in primates, (ii) this chromosomal sequence appears not to be expressed in either latent or nonlatent HeLa cells, and (iii) the integration site maps to the Q arm of chromosome 19. Extensive characterization of this chromosomal region will be essential in understanding regulation of rAAV transduced genes. For this reason, we have recently isolated two overlapping cosmid clones that hybridize to the chromosome 19 integration sequence (N. Epstein and R. J. Samulski, unpublished results). Further analysis of this region should be illuminating regarding both the integration mechanism and the potential of targeted gene delivery.

AAV Vectors Expressing Globin Genes. During our characterization of AAV vectors for targeted integration, we initiated a study to test this minimum AAV vector for the efficient transduction and expression of globin gene sequences in the erythroid cell line K562. We constructed an rAAV vector containing the human γ^A-globin gene, marked with a 6 nt deletion in the 5′ untranslated region to allow its transcript to be distinguished from native γ-globin transcripts (Fig. 3). The globin gene was linked to a 400-nucleotide DNA fragment containing LCR site 2, and a bacterial neomycin resistance gene used for selection. Site 2 alone has been shown to confer high level globin gene expression in erythroleukemic K562 cells (see Regulation of Globin Gene Transcription) and when treated with hemin, these cells can be induced to differentiate and increase expression of ε- and γ-globin genes (79).

We used the packaging strategy describe above (Production of the AAV Vector System) to generate AAV/globin hybrid virus. Recombinant virus was titered using human fibroblast target cells in the presence of geneticin (HeLa and/or Detroit 6) (78). Unconcentrated titers ranged from 10^4 to 10^5 neomycin-resistant colonies/ml. Southern analysis of low molecular weight DNA revealed no detectable wild-type particles using this protocol.

The erythroid cell line K562 was then infected with the recombinant virus and neomycin-resistant colonies were obtained (78). A polyclonal population of 30 isolated clones as well as individual clones were chosen for further study. First we characterized the configura-

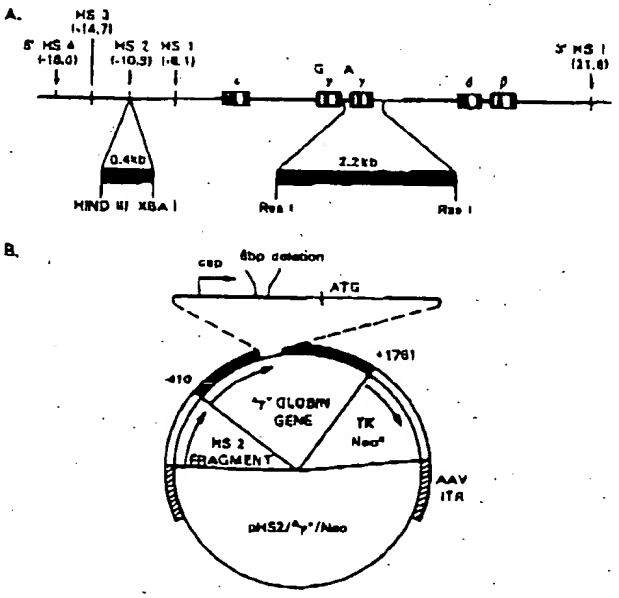

Figure 3. Construction of the rAAV/HS2/γ^A/Neo^R-globin plasmid. (A) Schematic representation of the human β-globin cluster. The five functional genes are indicated. Arrows indicate the locations of the major DNase 1 sites. The HS2 fragment and the γ^A-globin gene used in the vector are shown. (B) HS2 fragment, marked γ^{A*} gene (with the 6 bp deletion) and the Neo^R gene cassette subcloned into the recombinant AAV backbone.

tion of the integrated AAV/globin genome. Digestion of genomic DNA with *Pvu*II demonstrated an expected 1.2-kb globin fragment which corresponded to a single, unrearranged proviral copy per cell. The K562 cell line, which is triploid at chromosome 11 (location of the globin cluster) by karyotype analysis (17), served as a control when estimating the AAV/globin copy number of individual clones. Individual clones digested and characterized as above revealed one to two copies of the transduced gene per cell. No rearrangement of the transduced gene was detected in either individual or pooled clones demonstrating the stability of the transduced gene.

As mentioned above, preliminary data from our laboratory indicates that AAV transducing vectors containing only the viral terminal repeats do not target to chromosome 19 (see Site-Specific Integration). We also probed genomic digests of the globin recombinants with chromosome 19-specific probe to further characterize the provirus integration in K562 cells. As expected, unlike wild-type AAV, which utilizes targeted integration, the AAV/globin viruses appeared to have integrated randomly.

RNase protection assays demonstrated both basal (uninduced) and hemin-induced expression of the marked globin gene. Endogenous and transduced γ^A globin transcripts were identified as predicted bands of 145 nt and 117 nt, respectively. As shown in Figure 4, a strong signal at 145 nt represented transcription from the endogenous γ-globin genes present in K562 cell line. The probe measured both γ^A and γ^G endogenous transcripts. Assuming that all six endogenous copies of globin were expressed, we measured uninduced expression of the marked gene to be 70% that of a single endogenous gene which, with hemin induction, rose to 90%. Several non-erythroid tissue culture lines were examined for evidence of γ-globin transcripts. A small (1–5% of rAAV/K562 signal) but detectable signal was found in Detroit 6 and HeLa cells but not in T lymphoid CEM cells.

To further verify these results, messenger RNA expression was analyzed using the polymerase chain reaction (PCR). We determined previously the transcriptional start site of the marked Ag globin gene in transfected K562 cells by a primer extension; PCR primers were designed accordingly. Cytoplasmic RNA isolated from either single or pooled K562 clones was reverse transcribed and amplified using primers that anneal to both endogenous and marked globin genes. The 6 nt deletion enabled resolution of these transcripts on 8% polyacrylamide-urea gels. Both uninduced and hemin-induced cells were analyzed, with mock-transduced K562 cells serving as a control. The marked transcript was detected in all clones tested.

Quantitation of RNA message by PCR was comparable to that determined by RNase protection and

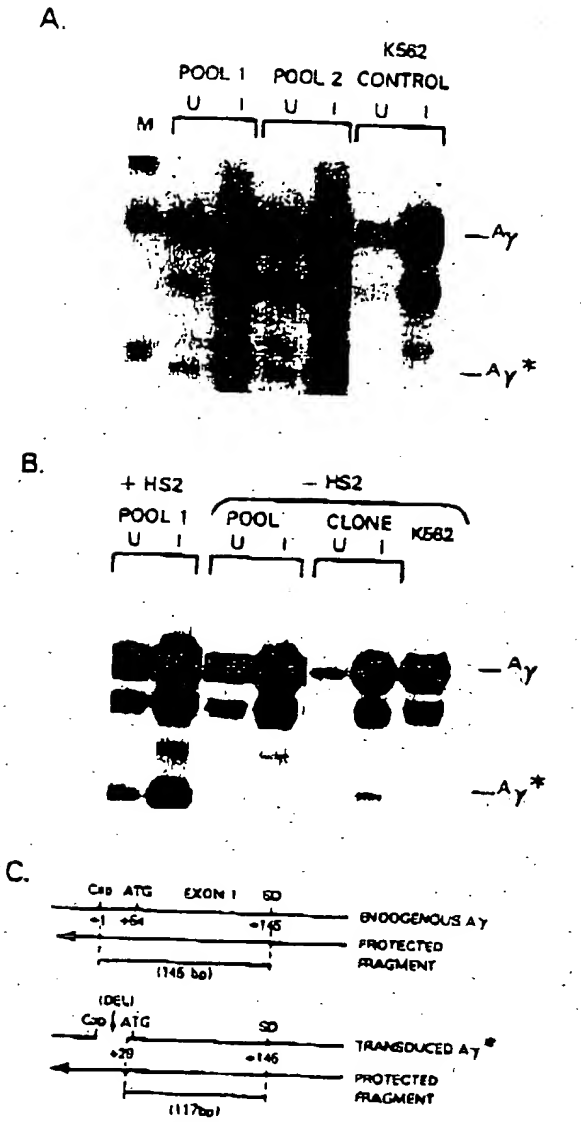

Figure 4. RNase protection assay of RNA extracted from K562 cells infected with (A) rAAV/HS2/γ^{A*}/Neo^R plasmid or (B) rAAV/γ^{A*}/Neo^R. (C) The expected RNA-protected fragments from the endogenous (γ^A) and transduced (γ^{A*}) genes are shown. U, uninduced cells; I, hemin-induced cells. Refer to Ref. 78 for details.

confirmed high level expression of the transduced Ag gene, including induction by hemin. S1 primer extension experiments confirmed that the correct globin start site was used in the proviral state. To rule out the possibility that the regulated globin expression we observed with this construct was due to globin regulatory sequences (LCR2) and not viral sequences or chromosomal positioning, we constructed an AAV/globin hybrid virus identical to the one described above minus the LCR2 site. Similar characterization of these transduced genes indicated a marked reduction in globin expression as expected.

These results represent the first viral-based introduction in which correct levels and regulation of γ-globin gene expression were achieved in an erythroid-derived cell line. High level, regulated globin expression was obtained when using a construct containing the LCR site 2. The LCR/globin construct efficiently integrated into the genome without rearrangement in all clones studied. (Recent extensive data from our laboratory suggests approximately 10–20% rearrangement.) Moreover, the messenger RNA expression of the transduced gene was comparable to endogenous γ-globin levels. The correct globin start site was utilized in the transduced gene, and tissue-specific expression (which was hemin inducible) was maintained.

The rAAV model can also be used to study the effects of specific mutations in the regulatory HS2 element on globin transcription (80). Specific mutations within the HS2 region of the rAAV/γ^/globin vector described in Figure 3B were constructed, and neomycin-resistant clones containing the rAAV genome present in single copy were evaluated. Mutations within the NFE-2 binding motif resulted in a marked reduction of hemin-induced expression of the transduced globin gene when compared with expression from constructs containing the native HS2. In contrast, another set of mutations in the GATA-1 motif, which prevent binding of GATA-1, had no effect on basal and hemin-induced expression from the transduced globin gene. Other analyses of HS function rely on gene transfer methods which result in multiple copy integrants, and cooperative interaction between tandem gene copies are difficult to exclude. In this respect, the rAAV model is superior in that over half of the evaluable clones containing the native and mutant HS2 element had a single unrearranged copy of the rAAV genome. This single copy rAAV transduction model may also useful for evaluating other regulatory elements and their effects on the transcription of genes linked *in cis*.

This suggests that recombinant AAV vectors can be used effectively for the transfer of globin genes into human cells. Previous work has demonstrated that AAV vectors are capable of transducing a selectable marker into murine hematopoietic progenitor cells (71). Moreover, we have generated and tested an AAV vector carrying B19 viral coding sequences for infection in erythroid progenitor cells from human bone marrow (81). B19 is an autonomously replicating parvovirus shown to be the etiologic agent of various clinical disorders in humans (hydrops fetalis, polyarthralgia syndrome, and transient aplastic crises associated with various hemolytic anemias). This parvovirus has so far been shown to replicate only in erythroid progenitor cells in human bone marrow. Using the recombinant AAV vector carrying the B19 coding sequences, rAAV stocks demonstrated that the AAV-based vector was capable of infecting human bone marrow cells (81). Furthermore, the recombinant B19-AAV hybrids inhibited erythroid hematopoietic colony formation, indicating the expression of B19 genes.

We have recently demonstrated transduction of both rAAV and wild-type AAV human pluripotent cells (S. Goodman, unpublished results). rAAV carrying a β-galactosidase gene were capable of infecting CD34⁺ selected bone marrow cells, as assessed by DNA PCR analysis of progenitor colonies derived from CD34⁺ cells grown in methylcellulose. Incubation of wild-type AAV with CD34⁺ selected cells demonstrated site-specific integration on chromosome 19q. rAAV vectors containing LCR-globin cassettes are currently being tested to transduce human and primate CD34⁺ selected bone marrow cells. Gene transfer with rAAV into animal tissue has not yet been demonstrated.

Safety Issues

The safety of retroviral gene transduction has been reevaluated in murine and primate models. Most retroviral vector systems employ components of the Molony murine leukemia virus, known to induce T cell leukemia and lymphomas in mice (82). Initial investigations suggested no apparent pathologic affects of murine amphotropic replication-competent virus in primates (83, 84). However, a bone marrow transplantation/gene therapy experiment in primates using a high titer recombinant retrovirus contaminated with a moderate titer of wild-type retrovirus induced a rapidly progressive T cell lymphoma in three of 10 animals tested (85). Over 50–100 copies of the wild-type replication-competent provirus were detected in the tumor DNA, implicating viral insertional mutagenesis as the pathogenic mechanism. The use of newer retroviral packaging systems to reduce or eliminate wild-type retrovirus is an absolute necessity for human use (86).

One of the salient features of the AAV system is the lack of any demonstrable pathology to the host cell. As mentioned previously, no epidemiologic evidence currently exists linking AAV to human disease. The potential toxicity of rAAV in animals is unknown. Wild-type adenovirus, required for the generation of rAAV, is capable of causing disease in immunocompromised hosts. rAAV packaging systems will need to be modified to eliminate adenoviral contamination.

Summary

Gene transfer of human globin genes into human pluripotent stem cells via viral vectors may soon be realized. The high level of globin gene expression believed to be required for the treatment of severe hemoglobinopathies necessitated the inclusion of cis-acting sequences (LCR). Retroviral vectors containing the LCR elements are prone to rearrangem nt, low titer, and po r expression. Inclusion of a "minilocus" containing four HS sites linked to a globin gene resulted in

higher expression in transplanted mice, but rearrangement of the provirus still occurs, and it is unclear what significance these experiments have with regard to human marrow stem cell transduction.

Recombinant AAV is among the newest of genetic transfer vectors. This once obscure virus possesses unique properties that distinguish it from all other vectors. Its major advantage is the lack of pathogenicity in humans. Wild-type AAV has the unusual ability to selectively integrate into the mammalian genome at a specific region, thus reducing the concern for genomic disruption and insertional mutagenesis. The ability of AAV to carry regulatory elements without interference from the viral template may enable greater control of transferred gene expression. Disadvantages currently include the inferior packaging systems which yield low numbers of recombinant virions which are contaminated with wild-type adenovirus. The small AAV genome that can be packaged (~5 kb) rules out its use for transfer of larger genes. Recombinant AAV viruses do not appear to demonstrate the same site-specific genomic integration as wild-type viruses. Elucidation of the mechanism of site-specific integration should prove useful in the development of safe vectors for gene transfer as well as provide insight into the nature of DNA recombination in humans.

1. McDonagh K, Nienhuis AW. The thalassemias. In: Nathan DG, Oski FA, Eds. Hematology of Infancy and Childhood. Philadelphia: Saunders, pp783–897, 1992.
2. Wolfe L, Olivieri N, Sallan D, Colan S, Rose V, Propper R, Freedman MH, Nathan DG. Prevention of cardiac disease by subcutaneous desferoximine in patients with thalassemia major. N Engl J Med 312:1600–1603, 1985.
3. Rebulla P, Modell B. Transfusion requirements and effects in patients with thalassemia major. Lancet 337:277–280, 1991.
4. Spanos T, Karageorga M, Ladis V, Peristeri J, Hatziiami A, Kattamis C. Red cell alloantibodies in patients with thalassemia. Vox Sang 58:50–55, 1990.
5. Lucarelli G, Galimberti M, Polchi P, Angelucci E, Baroncisani D, Giardini C, Politi P, Durazzi SMT, Muretto P, Albertini MA. Bone marrow transplantation in patients with thalassemia. N Engl J Med 322:417–421, 1990.
6. Ferster A, DeValek C, Azzi N, Fondu P, Toppet M, Sariban E. Bone marrow transplantation in severe sickle cell anemia. Br J Hematol 80:102–105, 1992.
7. Ley TJ, DeSimone J, Anagnou NP, Keller GH, Humphries RK, Turner PH, Young NS, Heller P, Nienhuis AW. 5-Azacytidine selectively increases γ-globin synthesis in a patient with β⁺-thalassemia. N Engl J Med 307:1469–1475, 1982.
8. Dover GJ, Charache S, Boyer SH, Vogelsang G, Moyer M. 5-Azacytidine increases HbF production and reduces anemia in sickle cell anemia disease: Dose response analysis of subcutaneous and oral dosage regimens. Blood 66:527–532, 1985.
9. Perrine SP, Ginder G, Faller GV, Dover GH, Ikuta T, Witkowska HE, Cai S-P, Vichinsky EP, Oliveri NF. A short-term trial of butyrate to stimulate fetal-globin-gene expression in the β-globin disorders. N Engl J Med 328:81–86, 1993.
10. Jane SM, Ney PA, Vanin EF, Gumicio DL, Nienhuis AW. Identification of a stage selector element in the human γ-globin gene promoter that fosters preferential interaction with the 5′ HS 2 enhancer when in competition with the β-globin promoter. EMBO J 11:2961–2969, 1992.
11. Orkin SH. Globin gene regulation and switching: Circa 1990. Cell 63:665–672, 1990.
12. Kantor JA, Kaufman RE, Turner PH, Farquhar M, Stamatoyannopoulos G, Nienhuis AW. Processing of γ, δ, and β-globin mRNA precursors in human, fetal, normal adult, and β+-thalassemia erythroid cells. In: Stamatoyannopoulos G, Nienhuis AW, Eds. Organization and Expression of Globin Genes. New York: Alan Liss, pp219–230, 1981.
13. Talbot D, Philipsen S, Fraser P, Grosveld F. Detailed analysis of the site 3 region of the human β-globin dominant control region. EMBO J 9:2169–2177, 1990.
14. Philipsen S, Talbot D, Fraser P, Grosveld F. The β-globin dominant control region: Hypersensitive site 2. EMBO J 9:2159–2167, 1990.
15. Fraser P, Hurst J, Collis P, Grosveld F. DNase I hypersensitive sites 1, 2, and 3 of the human β-globin dominant control region direct position-independent expression. Nucleic Acids Res 18:3503–1508, 1990.
16. Ney P, Sorrentino BP, Lowrey CH, Nienhuis AW. Tandem AP-1-binding sites within the human β-globin dominant control region function as an inducible enhancer in erythroid cells. Genes Dev 4:993–1006, 1990.
17. Sorrentino BP, Ney P, Bodine D, Nienhuis AW. A46 base pair enhancer sequence with the locus activating region is required for induced expression of the gamma-globin gene during erythroid differentiation. Nucleic Acids Res 18:2721–2731, 1990.
18. Caterina JJ, Ryan TM, Pawlik KM, Palmiter RD, Brinster RL, Behringer RR, Townes TM. Human β-globin locus control region and analysis of the 5′ DNase I hypersensitive site HS2 in transgenic mice. Proc Natl Acad Sci USA 88:1626–1630, 1991.
19. Andrews NC, Erdjument-Bromage H, Davidson MB, Tempst P, Orkin SH. Erythroid transcription factor NF-E2 is a hematopoietic-specific basic leucine zipper protein. Nature 362:722–728, 1993.
20. Yamamoto M, Ko LJ, Leonard MW, Beng H, Orkin SH. Activity and tissue specific expression of the transcription factor NFE-1 multigene family. Genes Dev 4:1650–1652, 1990.
21. Pevny L, Simon MC, Robertson E, Klein WH, Tsai SF. Erythroid differentiation in chimeric mice blocked by a targeted mutation in the gene for transcription factor GATA-1. Nature 349:257–260, 1991.
22. Weatherall DJ, Clegg JB. The thalassemia syndromes. London: Blackwell, 1981.
23. Noguchi CT, Rodgers GP, Serjeant G, Schechter AN. Levels of fetal hemoglobin necessary for treatment of sickle cell disease. N Engl J Med 318:96–99, 1988.
24. Rodgers GP, Dover GJ, Noguchi CT, Schechter AN. Hematologic responses of patients with sickle cell disease to treatment with hydroxyurea. N Engl J Med 322:1037–1045, 1990.
25. Sorensen S, Rubin E, Polster H, Mohandas N, Schrier S. The role of membrane skeletal-associated alpha globin in the pathophysiology of beta-thalassemia. Blood 75:1333–1336, 1990.
26. Sheasly EG, Kim H-S, Shehee WR, Papayannopoulou T, Smithies O, Popovich B. Correction of human β⁰-globin gene targeting. Proc Natl Acad Sci USA 88:4294–4298, 1991.
27. Nienhuis AW, Walsh CE, Liu J. Viruses as therapeutic gene transfer vectors. In: Young NS, Ed. Viruses and Bone Marrow. New York: Marcel Dekker, pp353–414, 1993.
28. Cone RD, Weber-Benarous A, Baorto D, Mulligan CC. Regulated expression of a complete human β-globin gene encoded by a transmissible retrovirus vector. Mol Cell Biol 7:887–897, 1987.
29. Karlsson S, Papayannopoulou T, Schweiger SG, Stamatoyannopoulos G, Nienhuis AW. Retroviral-mediated transfer of genomic

globin genes leads to regulated production of RNA and protein. Proc Natl Acad Sci USA 84:2411–2415, 1987.
30. Miller AD, Bender MA, Harris EAS, Kaleko M, Gelinas RE. Design of retrovirus vector for transfer and expression of the human β-globin gene. J Virol 62:4337–4345, 1988.
31. Bender MA, Miller AD, Gelinas RE. Expression of the human β-globin gene after retroviral transfer into murine erythroleukemia cells and human BFU-E cells. Mol Cell Biol 8:1725–1735, 1988.
32. Dzierzak EA, Papayannopoulou T, Mulligan RC. Lineage-specific expression of a human β-globin gene in murine bone marrow transplant recipients reconstituted with retrovirus-transduced stem cells. Nature 331:35–41, 1988.
33. Bender MA, Gelinas RE, Miller AD. A majority of mice show long-term expression of a human β-globin gene after retrovirus transfer into hematopoietic stem cells. Mol Cell Biol 9:1426–1434, 1989.
34. Karlsson S, Bodine DM, Perry L, Papayannopoulou T, Nienhuis AW. Expression of the human β-globin gene following retroviral-mediated multipotential hematopoietic progenitors of mice. Proc Natl Acad Sci USA 85:6062–6066, 1988.
35. Bodine DM, Karlsson S, Nienhuis AW. Combination of interleukin 3 and 6 preserves stem cell function in culture and enhances retroviral-mediated gene transfer into hematopoietic stem cells. Proc Natl Acad Sci USA 86:8897–8911, 1989.
36. Grosveld F, van Assendelft B, Greaves DR, Kollias G. Position independent, high level expression of the human β-globin gene in transgenic mice. Cell 51:975–985, 1987.
37. Novak U, Harris E, Forrester W, Groudine M, Gelinas R. High-level β-globin expression after retroviral transfer of locus activation region-containing human β-globin gene derivatives into murine erythroleukemia cells. Proc Natl Acad Sci USA 87:3386–3390.
38. Chang JC, Liu D, Kan YW. A 36 base pair core sequence of locus control region enhances retrovirally transferred human β-globin gene expression. Proc Natl Acad Sci USA 89:3107–3110, 1992.
39. Plavec I, Papayannopoulou T, Maury C, Meyer F. A human β-globin gene used to the human β-globin locus control region is exposed at high levels in erythroid cells of mice engrafted with retrovirus transduced hematopoietic stem cells. Blood 81:1384–1392, 1993.
40. Berns KI, Rose JA. Evidence for a single-stranded adenovirus-associated virus genome: Isolation and separation of complementary strands. J Virol 5:693–699, 1970.
41. Blacklow NR, Hoggan MD, Rowe WP. Immunofluorescent studies of the potentiation of an adenovirus-associated virus by adenovirus 7. J Exp Med 125:755–765, 1967.
42. Berns KI, Adler S. Separation of two types of adeno-associated virus particles containing complementary polynucleotide chains. Virology 9:394–396, 1972.
43. Samulski RJ, Chang LS, Shenk T. A recombinant plasmid from which an infectious adeno-associated virus genome can be excised *in vitro* and its use to study viral replication. J Virol 61:3096–3101, 1987.
44. Srivastava A, Lusby EW, Berns KI. Nucleotide sequence and organization of the adeno-associated virus 2 genome. J Virol 45:555–564, 1983.
45. Lusby EW, Berns KI. Mapping of the 5′ termini of two adeno-associated virus 2 RNAs in the left half of the genome. J Virol 41:518–526, 1982.
46. Berns KI, Hauswirth WW. Adeno-associated viruses. Adv Virus Res 25:407–449, 1979.
47. Cavalier-Smith T. Palindromic base sequences and replication of eukaryote chromosome ends. Nature 250:467–470, 1974.
48. McLaughlin SK, Collis P, Hermonat PL, Muzyczka N. Adeno-associated virus general transduction vectors: Analysis of proviral structures. J Virol 62:1963–1973, 1988.
49. Samulski RJ, Chang LS, Shenk T. Helper-free stocks of recombinant adeno-associated viruses: Normal integration does not require viral gene expression. J Virol 63:3822–3828, 1989.
50. Hermonat PL, Labow MA, Wright R, Berns KI, Muzyczka N. Genetics of adeno-associated virus: Isolation and preliminary characterization of adeno-associated virus type 2 mutants. J Virol 51:329–339, 1984.
51. Laughlin CA, Westphal H, Carter BJ. Spliced adenovirus-associated virus RNA. Proc Natl Acad Sci USA 76:5567–5571, 1979.
52. Marcus CJ, Laughlin CA, Carter BJ. Adeno-associated virus RNA transcription in vivo. Eur J Biochem 121:147–154, 1981.
53. Carter BJ, Laughlin CA, Marcus-Sekura CJ. Parvovirus transcription. In: Berns KI, Ed. The Parvoviruses. New York: Plenum Press, pp153–207, 1984.
54. Cukor G, Blacklow NR, Hoggan D, Berns KI. Biology of adeno-associated virus. In: Berns KI, Ed. The Parvoviruses. New York: Plenum Press, pp33–66, 1984.
55. Atchinson RW, Casto BC, Hammon WMcD. Adenovirus-associated defective virus particles. Science 149:754–756, 1965.
56. Hoggan MD. Physical assay and growth cycle studies of a defective adeno-satellite virus. J Virol 1:171–180, 1965.
57. Buller RML, Janik E, Sebring ED, Rose JA. Herpes simplex virus types 1 and 2 completely help adeno-associated virus replication. J Virol 40:241–247, 1981.
58. Berns KI, Pinkerton TC, Thomas GF, Hoggan MD. Detection of adeno-associated virus (AV)-specific nucleotide sequences in DNA isolated from latently infected Detroit 6 cells. Virology 68:556–560, 1975.
59. Cheung A, Hoggan MD, Hauswirth WW, Berns KI. Integration of the adeno-associated virus genome into latently infected Detroit 6 cells. J Virol 33:739–748, 1980.
60. Hoggan MD, Thomas GF, Thomas FB, Johnson FB. Continuous carriage of adenovirus-associated virus genome in cell culture in the absence of helper adenovirus. Proceedings of the Fourth Lepetite Colloquium, Cocoyac Mexico. Amsterdam: North Holland, pp243–249, 1972.
61. Handa H, Shiroki K, Shimojo H. Establishment and characterization of KB cell lines latently infected with adeno-associated virus type 1. Virology 82:84–88, 1977.
62. Berns KI, Cheung A, Ostrove J, Lewis, M. Adeno-associated virus latent infection. In: Mahy BWJ, Minson AC, Darby GK, Eds. Virus Persistence. Cambridge: Cambridge University Press, p249, 1982.
63. Blacklow NR, Hoggan MD, Sereno MS, Brandt CD, Kim HW, Parrott RH, Chanock RM. A seroepidemiologic study of adenovirus-associated virus infection in infants and children. Am J Epidemiol 94:359–366, 1971.
64. Ginsberg HS. Adeno-associated virus. In: Davis BD, Dulbecco R, Eisen HN, Ginsberg HS, Eds. Microbiology. Hagerstown: Harper and Row, p1059, 1980.
65. Samulski RJ, Berns KI, Tan M, Muzyczka N. Cloning of adeno-associated virus into pBR322: Rescue of intact virus from the recombinant plasmid in human cells. Proc Natl Acad Sci USA 79:2077–2081, 1982.
66. Laughlin CA, Tratschin JD, Coon H, Carter BJ. Cloning of infectious adeno-associated virus genomes in bacterial plasmids. Gene 23:65–73, 1983.
67. Samulski RJ, Srivastava A, Berns KI, Muzyczka N. Rescue of adeno-associated virus from recombinant plasmids: Gene correction within the terminal repeats of AAV. Cell 33:135–143, 1983.
68. Senapathy P, Tratschin JD, Carter BJ. Replication of adeno-associated virus DNA. Complementation of naturally occurring rep- mutants by a wild-type genome or an ori- mutant and correction of terminal palindrome deletions. J Mol Biol 171:1–20, 1984.

69. Hermonat PL, Muzyczka N. Use of adeno-associated virus as a mammalian DNA cloning vector: Transduction of neomycin resistance into mammalian tissue culture cells. Proc Natl Acad Sci USA 81:6466–6470, 1984.
70. Tratschin JD, West MH, Sandbank T, Carter BJ. A human parvovirus, adeno-associated virus, as a eucaryotic vector: Transient expression and encapsidation of the procaryotic gene for chloramphenicol acetyltransferase. Mol Cell Biol 4:2072–2081, 1984.
71. LaFace D, Hermonat P, Wakeland E, Peck A. Gene transfer into hematopoietic progenitor cells mediated by an adeno-associated virus vector. Virology 162:483–486, 1988.
72. Wondisford FE, Usala SJ, DeCherney GS, Castren M, Radovick S, Gyves PW, Trempe JP, Kerfoot BP, Nikodem VM, Carter BJ, Weintraub BD. Cloning of the human thyrotropin beta-subunit gene and transient expression of biologically active human thyrotropin after gene transfection. Mol Endocrinol 2:32–39, 1988.
73. Lebkowski JS, McNally MM, Okarma TB, Lerch LB. Adeno-associated virus: A vector system for efficient introduction and integration of DNA into a variety of mammalian cell types. Mol Cell Biol 8:3988–3996, 1988.
74. Hearing P, Shenk T. The adenovirus type 5 E1A transcriptional control region contains a duplicated enhancer element. Cell 33:695–703, 1983.
75. Hearing P, Samulski RJ, Wishart WL, Shenk T. Identification of a repeated sequence element required for efficient encapsidation of the adenovirus type 5 chromosome. J Virol 61:2555–2558, 1987.
76. Kotin RM, Siniscalco M, Samulski RJ, Zhu X, Hunter L, Laughlin CA, McLaughlin S, Muzyczka N, Rocchi M, Berns KI. Site-specific integration by adeno-associated virus. Proc Natl Acad Sci USA 87:2211–2215, 1990.
77. Samulski RJ, Zhu X, Xiao X, Brook JD, Housman DE, Epstein N, Hunter LA. Targeted integration of adeno-associated virus (AAV) into human chromosome 19. EMBO J 10:3941–3950, 1991.
78. Walsh CE, Liu JM, Young N, Xiao X, Nienhuis AW, Samulski RJ. Regulated high level expression of a human γ-globin gene introduced into erythroid cells by an adeno-associated virus vector. Proc Natl Acad Sci USA 89:7257–7261, 1992.
79. Rutherford TR, Clegg JB, Weatherall DJ. K562 human leukaemic cells synthesise embryonic haemoglobin in response to haemin. Nature 280:164–165, 1979.
80. Miller JL, Walsh CE, Ney PA, Samulski RJ, Nienhuis AW. Single copy transduction and expression of human γ-globin in K562 erythroleukemia cells using recombinant adeno-associated virus vectors: The effect of mutations in NF-E2 and GATA-1 binding motifs within the HS2 enhancer. Blood 82:1900–1906, 1993.
81. Srivastava CH, Samulski RJ, Lu L, Larsen SH, Srivastava A. Construction of a recombinant human parvovirus B19: Adeno-associated virus 2 DNA inverted terminal repeats are functional in an AAV-B19 recombinant virus. Proc Natl Acad Sci USA 86:8078–8082, 1989.
82. Tsichlis PN, Lazo PA. Virus-host interactions and the pathogenesis of murine and human oncogene retroviruses. Curr Top Microbiol Immunol 171:75–171, 1991.
83. Cornetta K, Moen RC, Culver K, Morgan RA, McLachlin JR, Sturm S, Selegue J, London W, Blaese RM, Anderson WF. Amphotrophic murine leukemia retrovirus is not an acute pathogen for primates. Hum Gene Ther 1:15–30, 1990.
84. Cornetta K, Morgan RA, Gillio A, Sturm S, Baltrucki L, O'Reilly R, Anderson WF. No retroviremia or pathology in long-term follow-up of monkeys exposed to a murine amphotrophic retrovirus. Hum Gene Ther 2:215–219, 1991.
85. Donahue RE, Kessler SW, Bodine D, McDonagh K, Dunbar C, Goodman S, Agricola B, Byrne E, Raffeld M, Moen R, Bacher J, Zsebo KM, Nienhuis AW. Helper virus induced T cell lymphoma in nonhuman primates after retroviral mediated gene transfer. J Exp Med 176:1125–1135, 1992.
86. Anderson WF. What about those monkeys that got T-cell lymphoma? Hum Gene Ther 4:1–2, 1993.
87. Stamatoyannopoulos G, Nienhuis AW. Hemoglobin switching. In: Stamatoyannopoulos G, Nienhuis AW, Eds. The Molecular Basis of Blood Diseases. Philadelphia: Saunders, pp66–105, 1987.

COMMONWEALTH OF AUSTRALIA

(Patents Act 1990)

IN THE MATTER OF: Australian Patent Application 696764 (73941/94). In the name of: Human Genome Sciences Inc.

- and -

IN THE MATTER OF: Opposition thereto by Ludwig Institute for Cancer Research, under Section 59 of the Patents Act.

Annexure GBC-21

This is **Annexure GBC-21** referred to in my Statutory Declaration made this Thirteenth day of December 2000.

Gary Baxter Cox

WITNESS:

Patent Attorney FEYTEC PTY LTD

Lymphology 20 (1987) 257-266

LYMPHATICS AND BLOOD VESSELS, LYMPHANGIOGENESIS AND HEMANGIOGENESIS: FROM CELL BIOLOGY TO CLINICAL MEDICINE

M.H. Witte, C.L. Witte

Department of Surgery, University of Arizona College of Medicine, Tucson, Arizona, U.S.A.

ABSTRACT

The past 15 years have witnessed an explosion of knowledge about blood vascular endothelium due in large part to in vitro growth of endothelial cells from both large blood vessels and capillaries. In contrast, little comparable information has accumulated on endothelium of lymphatics, which lie in intimate contact with parenchymal cells and drain excess fluid, macromolecules, particles, and immunocompetent cells in a continuous recirculation between tissues and bloodstream. While structural and functional differences between the two vascular systems have been described in vivo, in tissue sections, and in isolated preparations, similarities are notable in ultrastructure, biochemistry, physiology, and pharmacologic responsiveness, and these may predominate under pathologic conditions. In 1984, three separate groups described in vitro culture of lymphatic endothelial cells from collecting ducts and cavernous lymphangiomas. Lymphatic, like blood vascular, endothelium grows in confluent monolayers, "sprouts", synthesizes Factor VIII-associated antigen and fibronectin, and ultrastructurally shows Weibel-Palade bodies; overlapping intercellular junctions and anchoring filaments typical of lymphatic endothelium are also found. Genetic, congenital, and acquired disorders such as strangulating fetal nuchal cystic hygromas (Down and Turner syndromes), vascular tumors and dysmorphogenesis (Maffucci and Klippel-Trenaunay syndromes), Kaposi's sarcoma, lymphogenous and hematogenous spread of cancer, and parasitic infestations such as filariasis, share overlapping abnormalities in formation, growth, and/or neoplasia of lymphatics and blood vessels. In these and similar clinical disorders, confusion often exists as to the nature of the cell or tissue of origin, and insight into the role and control of hemangiogenesis and lymphangiogenesis is still in its infancy. Nonetheless, with the ever widening array of investigative techniques, it is not only timely but imperative to explore the endothelial biology underlying these inborn and acquired disorders.

Blood and lymphatic vasculatures are closely intertwined in embryonic development and respond to many similar stimuli in the microenvironment (e.g. ischemia, inflammation, and neoplasia). The two circulations work together in an integrated fashion in the uptake and transport of interstitial liquid and macromolecules such as extravasated plasma proteins and ingested lipids, which recirculate between lymph, blood, and tissue. Distinct migration streams of immunocompetent cells interchange at various points in the "blood-lymph loop." Anatomic connections exist or open up between the two as lymphatic-venous communications, which function normally (viz. thoracic duct-jugular venous junction) or become operational under physiologic and pathologic conditions (e.g. carcinomatous

venous or lymphatic obstruction or in portal hypertension from alcoholic cirrhosis). While lymphatics closely resemble blood vessels on tissue section, they are more thin-walled attenuated structures containing bloodless fluid, and they ultrastructurally exhibit overlapping intercellular junctional complexes, specialized anchoring filaments, and discontinuous or absent basal lamina (1). Permeability, surface charge distribution, vesicular macromolecular movement, lipid absorption and transport, intrinsic contractility, and vasoresponsiveness of the two vasculatures are distinct in some respects, vary from organ to organ, and also may overlap.

The vascular endothelium is the crucial interface between circulating blood or lymph and the tissues. Two decades ago only surmised by Lord Florey to be more than an inert passive membrane or in "nucleated cellophane", endothelium is now recognized as the biologically active mentor of the microcirculation and of tissue homeostasis--originating, receiving, translating, transducing, and transmitting physical and chemical messages to and from different parts of the body. The ability to culture large and pure endothelial cell populations not only from major blood vessels but since 1979, also from human capillaries has produced an explosion of knowledge (1-3). Despite differences among species and organs, blood vascular endothelium (BVE) exhibits remarkably consistent morphology and function in vitro mimicking its structural, synthetic, and transport properties in vivo and in isolated vascular preparations. In culture, endothelial cells grow as confluent monolayers with characteristic cobblestone appearance, which under appropriate conditions sprout and form tubules, that is, display "angiogenesis in vitro." Distinctive ultrastructural features mirroring those found in tissue section include intricate intercellular junctions, micropinocytotic vesicles, intermediate filaments, and Weibel-Palade bodies, which are thought to manufacture or store Factor VIII-associated antigen (Factor VIIIAA). On immunohistochemical examination, endothelial cells contain Factor VIII-associated antigen, angiotensin-coverting enzyme, and extracellular matrix components such as fibronectin, all of which in addition to prostacyclin and many other vasoactive metabolites can be measured quantitatively after release into the supernatant overlying the monolayer.

Considerable attention has been directed to a search for angiogenic factors controlling blood vessel formation and thereby tumor and organ growth. The genetic code for one such substance, angiogenin, has recently been deciphered. Blood vascular endothelium interacts in a "symbiotic" relationship with immunocompetent cells, directing lymphocyte cell traffic and "homing" and also producing colony-stimulating activity differentiating hemopoietic stem cells into granulocytes and monocytes (4). Immunocompetent cells as well as fibroblasts and adipocytes in turn secrete angiogenic factors and share cell surface receptors with endothelium. Thus, in large part because blood vascular endothelium can now be isolated *in vitro*, its role as a structural barrier as well as active facilitator of small solute and macromolecular transport into and out of tissues, as a director of cellular migration, as a stabilizer of the coagulation cascade, and as a biosynthetic factory is now being unraveled. Blood vascular endothelial damage and/or repair have been implicated in processes as diverse as atherosclerosis, hypertension, inflammation, wound healing, ischemia, diabetes mellitus, and transplant rejection.

Yet, in part because of a lack of analogous *in vitro* models, only rudimentary information is available about the highly permeable vascular interface on the "dark side" of the blood capillary barrier, deep in the tissues, separating circulating "lymph" from extracellular matrix and liquid and parenchymal cells in lymphoid and non-lymphoid tissues. Within this oft forgotten sluggish lymphatic-tissue fluid circulation pass surplus liquid, macromolecules, particles, and migrating cells from the interstitium on their way

through r
before re
(Fig. 1)

*Fig. 1. sh
circulatio
macrom
blood, t
lymphat
In this
organs
return
the blo*

small
phatic
by ov
recurr
from
and
cadav
(7).
theli
micr
blan
blest
4),
mar
Thu
pha
ren
om
um
VII
5)
Pa
les
tir
ju
an
pl
A
st
o

through regional and central lymph nodes before returning to the blood circulation *(Fig. 1)*. In 1984 for the first time,

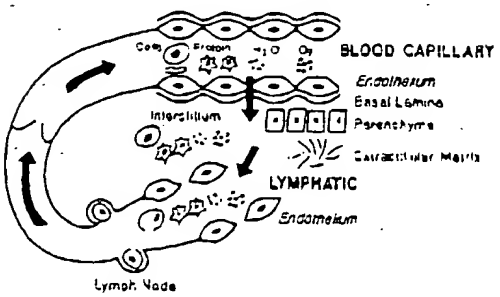

Fig. 1. Blood-lymph loop. There is a continuous circulation and recirculation of cells, particles, macromolecules, small solutes, and gases between blood, tissues, and lymph. Blood vascular and lymphatic endothelium represent crucial interfaces in this circulation. Lymph exiting parenchymal organs filters through lymph nodes on its way to return thru lymphatic-venous communications to the bloodstream.

small relatively pure populations of lymphatic vascular endothelium were isolated by our group from explants of a massive recurrent lymphangioma (5), by Johnston from normal bovine lymphatic ducts (6) and by Gnepp from canine and human cadaveric thoracic ducts *(Figs. 2 and 3)* (7). In culture, lymphatic vascular endothelium (LVE) from large ducts and microvasculature bears a strong resemblance to BVE, forming confluent "cobblestone" monolayers, sprouting *(Fig. 4)*, and staining positively for endothelial markers, Factor VIIIAA and Ulex lectin. Thus, CH3, our second nearly pure lymphatic endothelial cell line from a recurrent chylous retroperitoneal lymphangioma resembles blood vascular endothelium in staining positively for Factor VIIIAA, F-actin, and fibronectin *(Fig. 5)*, and exhibiting numerous Weibel-Palade bodies *(Fig. 6L)* (8). Nonetheless, LVE appears to possess some distinctive features: overlapping intercellular junctions and abundant intermediate anchoring-type filaments typical of lymphatic endothelium *(Fig. 6R)* (8). Although questions may be raised about stromal blood vessels giving rise to some of the endothelial cells found in this lymphangioma cell line, the same question can be but has not been raised about designated blood vascular endothelial cell cultures from microvasculature in such standard sources as omentum and foreskin, tissues rich in lymphatics as well as blood vessels. At this point, there is every reason to believe that lymphatic like blood vascular endothelium is also a vast endocrine organ maintaining a lymph–fluid compatible surface and a changeable selective interface between the lumen and interstitium that is also the target for numerous perturbations affecting not only its intrinsic structure and function but also that of surrounding tissues.

The close interactions between the lymphatic and blood vasculature and lymphangiogenesis and hemangiogenesis on a cellular and organ level are further illustrated in the clinical manifestations of disease. Congenital lymphologic syndromes of genetic or intrauterine origin involving abnormal growth of lymphatics often include widespread blood vascular abnormalities as in Maffucci's and Klippel-Trenaunay syndromes *(Figs. 7 and 8)*. These soft tissue hemangiomas and lymphangiomas are commonly accompanied by lymphedema, venous aplasia or hypoplasia as well as arteriovenous anomalies and striking soft tissue overgrowth such as limb hypertrophy and macrodactyly, likely closely linked to the circulatory disturbances *(Figs. 7 and 8)*. On rare occasions malignant vascular transformation may take place. Blood vascular and lymphatic anomalies also coexist in Turner's XY gonadal dysgenesis syndrome where webbed neck from regressed fetal cystic lymphangiomas, extremity lymphedema associated with lymphatic hypoplasia and aplasia, and coarctation of the aorta are typical manifestations; variants of the syndrome also exhibit severe intracardiac anomalies. Down syndrome (trisomy-21) similarly may present *in utero* with strangulating cystic hygromas, cardiovascular anomalies and lymphedema or survive into adulthood with other variations of these vascular abnormalities. On the other hand, in acquired condi-

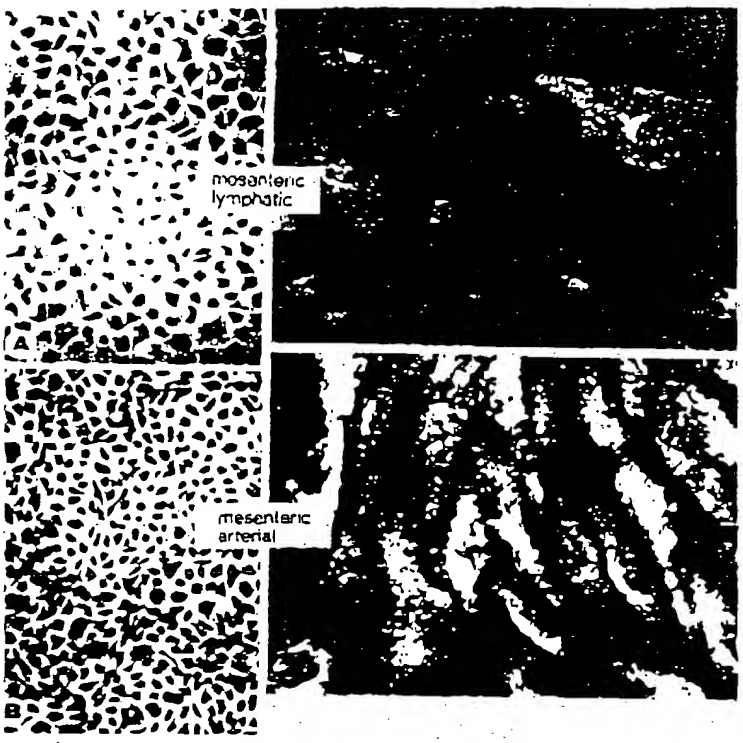

BOVINE MESENTERIC VASCULAR ENDOTHELIUM

(M.G. Johnston and M.A. Walker, In Vitro, 1984)

Fig. 2. Comparison of bovine lymphatic endothelial with bovine superior mesenteric arterial endothelial in tissue culture. The cells in A and B were stained with a Hemacolour stain kit (Harleco) as follows. The cells were washed twice with PBS and fixed for 5 min in methanol. The cells received an eosin solution (30s) followed by a thiazine solution (30s) and were then washed with water. A, Bovine lymphatic endothelial cells, Passage 9; (x141). B, bovine mesenteric artery endothelial cells, Passage 4. (x141); (6; modified by permission). C and D show assay for Factor VIII-related antigen. C, bovine lymphatic endothelium. D, Bovine mesenteric artery endothelium (antibody to human Factor VIII-related antigen diluted 1/10) (6; modified by permission).

tions such as classical or AIDS-associated epidemic Kaposi's sarcoma, abnormal lymphatic-venous communications may comprise or contribute to the multicentric tumor some of its peculiar morphologic and immunohistochemical properties as well as the associated lymphedema and hemorrhage. On rare occasions, malignant vascular tumors appear as Stewart-Treves syndrome after many years of lymphostasis associated with intense hemangiogenesis and lymphangiogenesis, and lymphangiomatoid changes superimposed on exuberant profuse scarring and fat deposition. The latter is well exemplified in filarial infestation, which leads to elephantiasis where thickening and piling up of the lymphatic as well as blood vascular endothelium, intraluminal blood or lymph clots, and exuberant deposition of underlying scar tissue characterize the pathologic process and the

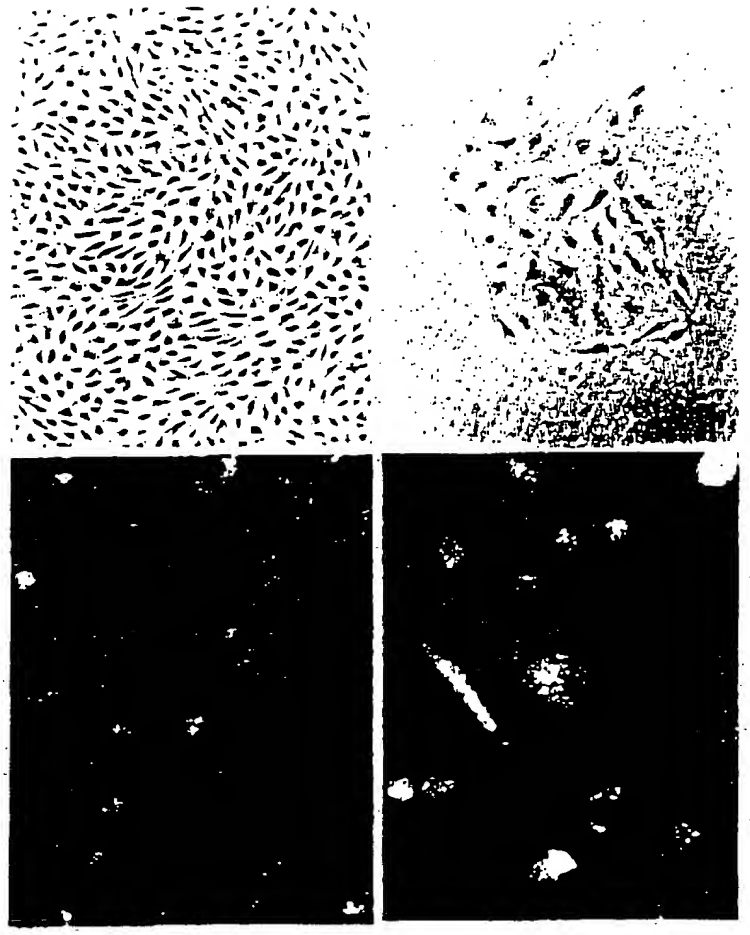

(D. Gnepp and W. Chandler, In Vitro, 1985)

Fig. 3. L, upper, canine thoracic duct culture demonstrating a sheet of uniform contact inhibited non-overlapping endothelial cells with typical cobblestone morphology. (x131). L, lower, indirect immunofluorescence of canine thoracic duct endothelial cells demonstrating marked positivity of Factor VIII antigen (note granular cytoplasmic staining. (x189). R, upper, human thoracic duct culture demonstrating one nest of typical endothelial cells, Day 9. (x129). R, lower, indirect immunofluorescence of human thoracic duct endothelial cells demonstrating granular cytoplasmic and perinuclear fluorescence. (x189). (7; used by permission).

host response to the worm and its products. These interrelationships between lymphangiogenesis and lymphologic syndromes have been summarized by us recently (9), and an analogous interconnected scheme can be postulated for hemangiogenesis and blood vascular syndromes.

Endothelial biologists working in tissue culture have opened up the pheno-

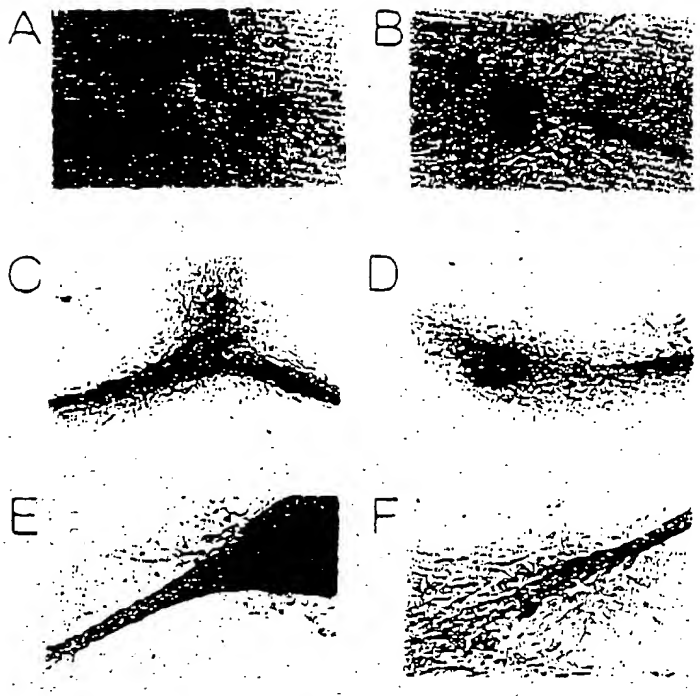

Fig. 4. Photomicrographs (inverted light) depicting in vitro evolution of lymphatic endothelial cell growth derived from a resected lymphangioma of the knee. An "early" phase displays a loose cluster of endothelium with occasional "sprouting" or branching (A; x100). With time, this sprouting pattern becomes more prominent (B; x100) and eventually evolves into a sheet-like cellular aggregate (C,D; x40) with intense "lymphatic-like" tumorous branching (E,F; x100).

menon of tumor angiogenesis to intensive inquiry. In 1972, Folkman (10) first proposed the concept that all tumors are angiogenesis-dependent and once tumor take has occurred, enlargement of the tumor cell population is preceded by growth of new blood capillaries converging on the tumor. Inhibition of angiogenesis, he proposed, might be a therapeutic approach to solid tumors. Interesting questions have arisen about the role of endothelial mitogens in normal tissues and natural mechanisms that restrain and inhibit formation of capillary and thereby tissue and organ growth. Lymphatic vessels have been scarcely mentioned in the context of "angiogenesis", and some workers have even suggested that tumors do not contain lymphatics. Nonetheless, the parallel development and common response of the two vascular systems to varied physiologic and pathologic stimuli suggest, however, that hemangiogenesis and lymphangiogenesis go hand in hand and that the mysterious growth factors stimulating both vasculatures are self-generated as well as arise in or are delivered through the neighboring tissue matrix; that is, the stimuli are autocrine, paracrine, and endocrine.

Despite the mounting interest in tumor angiogenesis, investigation of a related process--what we have termed "angiotumorogenesis," i.e., the growth and development of blood and lymphatic vascular tumors--has been extremely limited despite their frequency as cosmetic imperfections or as disfiguring or even

Fig. 5. Ina... tern of Fa... ized cytosk... fibronectin ...

life-threa...
Genetic, ...
influence ...
by horm...
oral cont...
(e.g., vi...
(e.g., hu...
cytomega...
but thes...
endothel...
mation, ...
tinues at...
tumors, ...
rests (ha...
mere exp...
esis. As ...
areas of ...
strikingly
normal ...
wildly a...
able as ...
Moreov...
tumors ...
multicen...
sionally, ...
tumors. ...
and eve...
sizing l...
hand, b...
tumors ...
Unfortu...

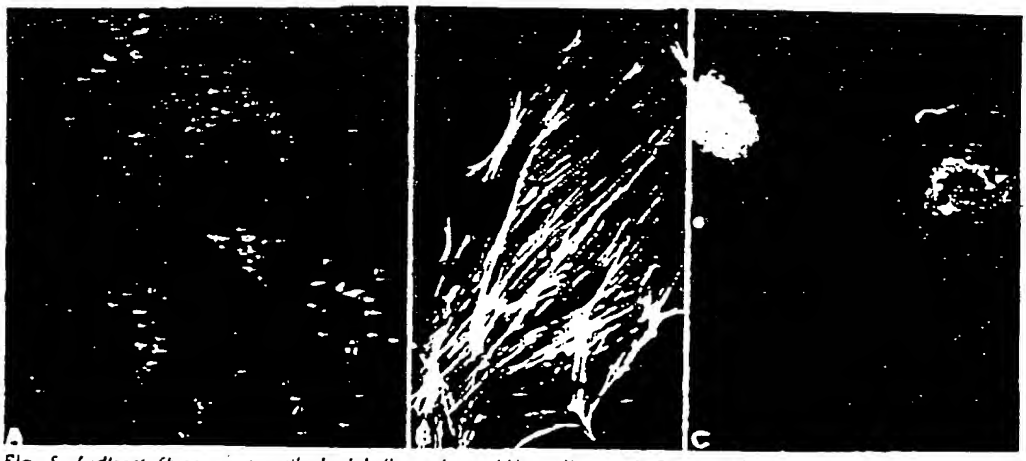

Fig. 5. Indirect fluorescent-antibody labeling using rabbit antihuman IgG shows the characteristic granular pattern of Factor VIII-related antigen (A) (x168). F-actin positive microfilament bundles forming a well-organized cytoskeleton stained with NBD-phalloidin (x591), cell surface-associated fibronectin using rabbit antihuman fibronectin IgG (C) (x168), which is also deposited extracellularly (8; used by permission).

life-threatening tumors of childhood. Genetic, congenital and environmental influences on endothelial growth, such as by hormones and drugs (e.g., estrogens, oral contraceptives), industrial carcinogens (e.g., vinyl chloride) and viral agents (e.g., human immunodeficiency virus and cytomegalovirus) are poorly understood but these agents are known stimulants of endothelial proliferation, DNA transformation, and neoplasia. Controversy continues about the nature of some vascular tumors, i.e., whether they are embryonic rests (hamartomas), true neoplasms or mere expressions of exuberant angiogenesis. As in Kaposi's sarcoma, different areas of the same lesion may appear strikingly heterogenous ranging from normal vessels to highly anaplastic or wildly aberrant structures indistinguishable as lymphatics or blood vessels. Moreover, it is unclear whether multiple tumors in separated or remote sites are multicentric in origin or metastatic. Occasionally, benign-appearing endothelial tumors may exhibit local invasion, recur, and even spread (e.g., "benign metastasizing lymphangioma"). On the other hand, benign and even malignant vascular tumors sometimes spontaneously regress. Unfortunately, immunohistochemical studies to detect the presence of intracytoplasmic or cell surface endothelial markers (e.g., Factor VIIIAA or basement membrane components) have produced more confusion than clarification because of heterogeneity of staining, postulated but disputed differences between the blood and lymphatic vasculature, inconsistent staining techniques, neoplastic or non-neoplastic transformation to more primitive or aberrant cell types or pluripotential nature of the cells, and presence of mixed cell types including mesenchymal and lymphoid elements. Thus, in part because of the paucity of animal models and the lack of *in vitro* systems to study pure populations of tumor cells, classification of endothelial tumors of lymphatic or blood vascular origin remains largely based on morphologic criteria and clinical behavior. Although tumor modulation by hormones, immunoregulatory substances, and growth factors seems almost within our grasp, detection and treatment of these neoplasms has progressed little over the past several decades beyond refinement or extension of surgical resection.

Understanding the structural-functional interrelationships between the blood and lymphatic vasculatures *in vivo*

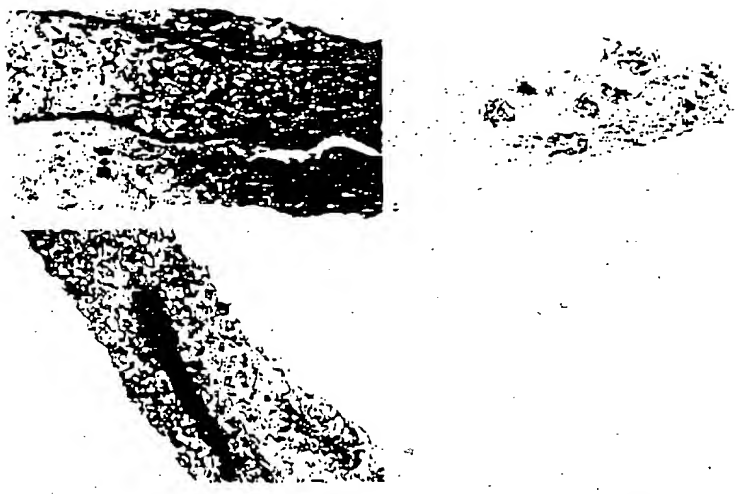

Fig. 6. Transmission electron microscopy (A-D) of cultured tumor cells reveals relatively smooth cell surfaces with few microvillous projections, numerous vesicles, and cytoplasm rich with Golgi and rough endoplasmic reticulum. Abundant Weibel-Palade bodies (A, arrow; B, higher magnification) are seen surrounded by bundles of intermediate filaments characteristic of lymphatic endothelium. Higher power detail of intermediate filaments can be best appreciated in C. Typical macula adherens, overlapping intercellular junctions are also shown (C,D). (A=x8550; B=x41,300; C=x48,450; D=x26,650) (8; used by permission).

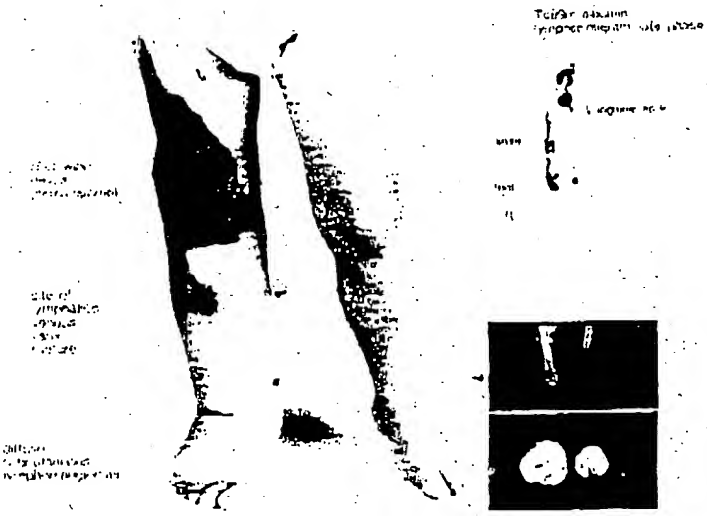

KLIPPEL TRENAUNAY SYNDROME

Fig. 7. 3-year-old girl with Klippel-Trenaunay syndrome involving the right leg. In addition to the characteristic port wine nevus and agenesis of the deep venous system, small pedal arteriovenous fistulae lymphscintigraphy (^{99m}Tc albumin) shows abberrant lateral "pick-up" with a large, dilated truncal "lake" reaching the lateral groin only after many hours. The left leg is unremarkable. Computed tomography with contrast enhancement suggests diffuse lymphangiomatous change with little or no edema fluid in the right leg.

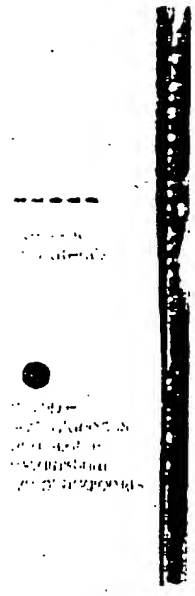

Fig. 8. 13-year-o
present are right

and *in vitro* i
control mecha
tissue growth
life to senesce
variety of *in*
neoplastic en
clues to detec
giogenesis an
enhanced or
tive endotheli
endothelium)
treatment (su
angioinhibitor
occurring ho
dioresistant v
scar formatio
released from
scoped in ti
combined wi
biology can
endothelial c
and distant
shedding lig
transplant re
plastic lympl
mellitus, lym
spread of c

VEGFR-2 were stimulated with tenfold concentrated medium from cultures transfected with mouse VEGF-C expression vector and autophosphorylation was analyzed. For comparison, cells treated with tenfold concentrated medium containing human recombinant VEGF-C (Joukov et al., (1996)), unconcentrated medium from human VEGF-C baculovirus infected insect cells, or pervanadate (a tyrosyl phosphatase inhibitor) were used. In response to human baculoviral VEGF-C as well as pervanadate treatment, VEGFR-2 was prominently phosphorylated, whereas human and mouse recombinant VEGF-C gave a weak and barely detectable enhancement of autophosphorylation, respectively. Media from cell cultures transfected with empty vector or VEGF-C cloned in the antisense orientation did not induce autophosphorylation of VEGFR-2. Therefore, mouse VEGF-C binds to VEGFR-3 and activates this receptor at a much lower concentration than needed for the activation of VEGFR-2. Nevertheless, the invention comprehends methods for using the materials of the invention to take advantage of the interaction of VEGF-C with VEGFR-2, in addition to the interaction between VEGF-C and VEGFR-3.

EXAMPLE 27

VEGF-C E104–E213 Fragment Expressed in Pichia Yeast Stimulates Autophosphorylation of Flt4 (VEGFR-3) and KDR (VEGFR-2)

A truncated form of human VEGF-C cDNA was constructed wherein (1) the sequence encoding residues of a putative mature VEGF-C amino terminus H_2N-E(104)ETIK (SEQ ID NO: 8, residues 104 et seq.) was fused in-frame to the yeast PHO1 signal sequence (Invitrogen Pichia Expression Kit, Catalog #K1710-01), and (2) a stop codon was introduced after amino acid 213 (H_2N- . . . RCMS; i.e., after codon 213 of SEQ ID NO: 7). The resultant truncated cDNA construct was then inserted into the *Pichia pastoris* expression vector pHIL-S1 (Invitrogen). For the cloning, an internal BglII site in the VEGF-C coding sequence was mutated without change of the encoded polypeptide sequence.

This VEGF-C expression vector was then transfected into Pichia cells and positive clones were identified by screening for the expression of VEGF-C protein in the culture medium by Western blotting. One positive clone was grown in a 50 ml culture, and induced with methanol for various periods of time from 0 to 60 hours. About 10 μl of medium was analyzed by gel electrophoresis, followed by Western blotting and detection with anti-VEGF-C antiserum, as described above. An approximately 24 kD polypeptide (band spreading was observed due to glycosylation) accumulated in the culture medium of cells transfected with the recombinant VEGF-C construct, but not in the medium of mock-transfected cells or cells transfected with the vector alone.

The medium containing the recombinant VEGF-C protein was concentrated by Centricon 30 kD cutoff ultrafiltration and used to stimulate NIH 3T3 cells expressing Flt4 (VEGFR-3) and porcine aortic endothelial (PAE) cells expressing KDR (VEGFR-2). The stimulated cells were lysed and immunoprecipitated using VEGFR-specific antisera and the immunoprecipitates were analyzed by Western blotting using anti-phosphotyrosine antibodies, chemiluminescence, and fluorography. As a positive control for maximal autophosphorylation of the VEGFRs, vanadate (VO_4) treatment of the cells for 10 minutes was used. Medium from Pichia cultures secreting the recombinant VEGF-C polypeptide induced autophosphorylation of both Flt41 polypeptides of 195 kD and 125 kD as well as the KDR polypeptide of about 200 kD. Vanadate, on the other hand, induces heavy tyrosyl phosphorylation of the receptor bands in addition to other bands probably coprecipitating with the receptors.

These results demonstrate that a VEGF-homologous domain of VEGF-C consisting of amino acid residues 104L–213S (SEQ ID NO: 8, residues 104–213) can be recombinantly produced in yeast and is capable of stimulating the autophosphorylation of Flt4 (VEGFR-3) and KDR (VEGFR-2). Recombinant VEGF-C fragments such as the fragment described herein, which are capable of stimulating Flt4 or KDR autophosphorylation are intended as aspects of the invention; methods of using these fragments are also within the scope of the invention.

EXAMPLE 28

Properties of the Differentially Processed Forms of VEGF-C

The following oligonucleotides were used to generate a set of VEGF-C variants and analogs:

5'- TCTCTTCTGTGCTTGAGTTGAG-3' (SEQ ID NO: 15), used to generate VEGF-C R102S (arginine mutated to serine at position 102 (SEQ ID NO: 8));

5'-TCTCTTCTGTCCCTGAGTTGAG-3' (SEQ ID NO: 16), used to generate VEGF-C R102G (arginine mutated to glycine at position 102 (SEQ ID NO: 8));

5'-TGTGCTGCAGCAAATTTTATAGTCTCTTCTGTGGCGGCGGC GGCGGCGGGCGCCTCGCGAGGACC-3' (SEQ ID NO: 17), used to generate VEGF-C ΔN (deletion of N-terminal propeptide corresponding to amino acids 32–102 (SEQ ID NO: 8));

5'- CTGGCAGGGAACTGCTAATAATGGAATGAA-3' (SEQ ID NO: 18), used to generate VEGF-C R226,227S (arginine codons mutated to serines at positions 226 and 227 (SEQ ID NO: 8));

5'-GGGCTCCGCGTCCGAGAGGTCGAGTCCGGACTCGTGATGGT GATGGTGATGGGCGGCGGCGGCGGGCGGGCGCCTCGCGAGGACC-3' (SEQ ID NO: 19), used to generate VEGF-C NHis (this construct encodes a polypeptide with a 6xHis tag fused to approximately the N-terminus of the secreted precursor, as described in Example 21 (amino acid 33 of SEQ ID NO: 8)).

Some of the foregoing VEGF-C mutant constructs were further modified to obtain additional constructs. For example, VEGF-C R102G in pALTER (Promega) and oligonucleotide

5'-GTATTATAATGTCCTCCACCAAATTTTATAG-3' (SEQ ID NO: 20) were used to generate VEGF-C 4G, which encodes a polypeptide with four point mutations: R102G, A110G, A111G, and A112G (alanines mutated to glycines at positions 110–112 (SEQ ID NO: 8). These four mutations are adjacent to predicted sites of cleavage of VEGF-C expressed in PC-3 and recombinantly expressed in 293 EBNA cells.

Another construct was created using VEGF-C ΔN and oligonucleotide

5'-GTTCGCTGCCTGACACTGTGGTAGTGTTGCTGGC GGCCGCTAGTGATGGTGATGGTGAT-GAATAATGGAATGAACTTGTCTGTAAACATCC AG-3' (SEQ ID NO: 21) to generate VEGF-C ΔNΔCHis. This construct encodes a polypeptide with a deleted N-terminal propeptide (amino acids 32–102); a deleted C-terminal propeptide.(amino acids 226–419 of SEQ ID NO: 8); and an added 6xHis tag at the C-terminus.

All constructs were further digested with HindIII and NotI, subcloned into HindIII/NotI digested pREP7 vector,

and used to transfect 293 EBNA cells. About 48 hours after transfection, the cells were either metabolically labelled with Pro-mix™ as described above, or starved in serum-free medium for 2 days. Media were then collected and used in subsequent experiments. As can be seen from FIGS. 11A–B, wild type (wt) VEGF-C, VEGF-C NHis and VEGF-C ΔNΔCHis were expressed to similar levels in 293 EBNA cells. At the same time, expression of the VEGF-C 4G polypeptide was considerably lower, possibly due to the changed conformation and decreased stability of the translated product. However, all the above VEGF-C mutants were secreted from the cells (compare FIGS. 11A and 11B).

The conditioned media from the transfected and starved cells were concentrated 5-fold and used to assess their ability to stimulate tyrosine phosphorylation of Flt4 (VEGFR-3) expressed in NIH 3T3 cells and KDR (VEGFR-2) expressed in PAE cells. Wild type (wt) VEGF-C, as well as all three mutant polypeptides, stimulated tyrosine phosphorylation of VEGFR-3. The most prominent stimulation observed was by the short mature VEGF-C ΔNΔCHis. This mutant, as well as VEGF-C NHis, also stimulated tyrosine phosphorylation of VEGFR-2. Thus, despite the fact that a major component of secreted recombinant VEGF-C is a dimer of 32/29 kD, the active part of VEGF-C responsible for its binding to VEGFR-3 and VEGFR-2 is localized between amino acids 102 and 226 (SEQ ID NO: 8) of the VEGF-C precursor. Analysis and comparison of binding properties and biological activities of these VEGF-C proteins and mutants, using assays such as those described herein, will provide data concerning the significance of the observed major 32/29 kD and 21–23 kD VEGF-C processed forms. The data indicate that constructs encoding amino acid residues 103–225 of the VEGF-C precursor (SEQ ID NO: 8) generate a recombinant ligand that is functional for both VEGFR-3 and VEGFR-2.

The data from this and preceding examples demonstrate that numerous fragments of the VEGF-C polypeptide retain biological activity. A naturally occurring VEGF-C polypeptide spanning amino acids 103–226 (or 103–227) of SEQ ID NO: 8, produced by a natural processing cleavage defining the C-terminus, has been shown to be active. Example 27 demonstrates that a fragment with residues 104–213 of SEQ ID NO: 8 retains biological activity.

In addition, data from Example 21 demonstrates that a VEGF-C polypeptide having its amino terminus at position 112 of SEQ ID NO: 8 retains activity. Additional experiments have shown that a fragment lacking residues 1–112 of SEQ ID NO: 8 retains biological activity.

In a related experiment, a stop codon was substituted for the lysine at position 214 of SEQ ID NO: 8 (SEQ ID NO: 7, nucleotides 991–993). The resulting recombinant polypeptide still was capable of inducing Flt4 autophosphorylation, indicating that a polypeptide spanning amino acid residues 113–213 of SEQ ID NO: 8 is biologically active.

Sequence comparisons of members of the VEGF family of polypeptides provides an indication that still smaller fragments of the polypeptide depicted in SEQ ID NO: 8 will retain biological activity. In particular, eight highly conserved cysteine residues of the VEGF family of polypeptides define a region from residues 131–211 of SEQ ID NO: 8 (see FIG. 10) of evolutionary significance; therefore, a polypeptide spanning from about residue 131 to about residue 211 is expected to retain VEGF-C biological activity. In fact, a polypeptide which retains the conserved motif RCXXCC (e.g., a polypeptide comprising from about residue 161 to about residue 211 of SEQ ID NO: 8 is postulated to retain VEGF-C biological activity. To maintain native conformation of these fragments, it may be preferred to retain about 1–2 additional amino acids at the carboxy-terminus and 1–2 or more amino acids at the amino terminus.

Beyond the preceding considerations, evidence exists that smaller fragments and/or fragment analogs which lack the conserved cysteines nonetheless will retain VEGF-C biological activity. Consequently, the materials and methods of the invention include all VEGF-C fragments, variants, and analogs that retain at least one biological activity of VEGF-C, regardless of the presence or absence of members of the conserved set of cysteine residues.

EXAMPLE 29

Expression of Human VEGF-C Under the Human K14 Keratin Promoter in Transgenic Mice Induces Abundant Growth of Lymphatic Vessels in the Skin

The Flt4 receptor tyrosine kinase is relatively specifically expressed in the endothelia of lymphatic vessels. Kaipainen et al., *Proc. Natl. Acad. Sci. (USA)*, 92: 3566–3570 (1995). Furthermore, the VEGF-C growth factor stimulates the Flt4 receptor, showing less activity towards the KDR receptor of blood vessels (Joukov et al., *EMBO J.*, 15: 290–298 (1996); See Example 26).

Experiments were conducted in transgenic mice to analyze the specific effects of VEGF-C overexpression in tissues. The human K14 keratin promoter is active in the basal cells of stratified squamous epithelia (Vassar et al., *Proc. Natl. Acad. Sci. (USA)*, 86:1563–1567 (1989)) and was used as the expression control element in the recombinant VEGF-C transgene. The vector containing the K14 keratin promoter is described in Vassar et al., *Genes Dev.*, 5:714–727 (1991) and Nelson et al., *J. Cell Biol.* 97:244–251 (1983).

The recombinant VEGF-C transgene was constructed using the human full length VEGF-C cDNA (GenBank Acc. No. X94216). This sequence was excised from a pCI-neo vector (Promega) with XhoI/NotI, and the resulting 2027 base pair fragment containing the open reading frame and stop codon (nucleotides 352–1611 of SEQ ID NO: 7) was isolated. The isolated fragment was then subjected to an end-filling reaction using the Klenow fragment of DNA polymerase. The blunt-ended fragment was then ligated to a similarly opened BamHI restriction site in the K14 vector. The resulting construct contained the EcoRI site derived from the polylinker of the pCI-neo vector. This EcoRI site was removed using standard techniques (a Klenow-mediated fill-in reaction following partial digestion of the recombinant intermediate with EcoRI) to facilitate the subsequent excision of the DNA fragment to be injected into fertilized mouse oocytes.

The resulting clone, designated K14-VEGF-C, is illustrated in FIG. 20 of commonly-owned PCT patent application PCT/FI96/00427, filed Aug. 01, 1996.

The EcoRI-HindIII fragment from clone K14 VEGF-C containing the K14 promoter, VEGF-C cDNA, and K14 polyadenylation signal was isolated and injected into fertilized oocytes of the FVB-NIH mouse strain. The injected zygotes were transplanted to oviducts of pseudopregnant C57BL/6×DBA/2J hybrid mice. The resulting founder mice were analyzed for the presence of the transgene by polymerase chain reaction of tail DNA using the primers: 5'-CATGTACGAACCGCCAG-3' (SEQ ID NO: 22) and 5'-AATGACCAGAGAGAGGCGAG-3' (SEQ ID NO: 23).

In addition, the tail DNAs were subjected to EcoRV digestion and subsequent Southern analysis using the EcoRI-HindIII fragment injected into the mice. Out of 8 pups analyzed at 3 weeks of age, 2 were positive, having approximately 40–50 copies and 4–6 copies of the transgene in their respective genomes.

The mouse with the high copy number transgene was small, developed more slowly than its litter mates and had difficulty eating (i.e., suckling). Further examination showed a swollen, red snout and poor fur. Although fed with a special liquid diet, it suffered from edema of the upper respiratory and digestive tracts after feeding and had breathing difficulties. This mouse died eight weeks after birth and was immediately processed for histology, immunohistochemistry, and in situ hybridization.

Histological examination showed that in comparison to the skin of littermates, the dorsal dermis of K14-VEGF-C transgenic mice was atrophic and connective tissue was replaced by large lacunae devoid of red cells, but lined with a thin endothelial layer. These distended vessel-like structures resembled those seen in human lymphangiomas. The number of skin adnexal organs and hair follicles were reduced. In the snout region, an increased number of vessels was also seen. Therefore, VEGF-C overexpression in the basal epidermis is capable of promoting the growth of extensive vessel structure in the underlying skin, including large vessel lacunae. The endothelial cells surrounding these lacunae contained abundant Flt4 MRNA in in situ hybridization (see Examples 23 and 30 for methodology). The vessel morphology indicates that VEGF-C stimulates the growth of vessels having features of lymphatic vessels. The other K14-VEGF-C transgenic mouse had a similar skin histopathology.

Nineteen additional pups were analyzed at 3 weeks of age for the presence of the VEGF-C transgene, bring the number of analyzed pups to twenty-seven. A third transgene-positive pup was identified, having approximately 20 copies of the transgene in its genome. The 20 copy mouse and the 4–6 copy mouse described above transmitted the gene to 6 out of 11 and 2 out of 40 pups, respectively. The physiology of these additional transgenic mice were further analyzed.

The adult transgenic mice were small and had slightly swollen eyelids and poorly developed fur. Histological examination showed that the epidermis was hyperplastic and the number of hair follicles was reduced; these effects were considered unspecific or secondary to other phenotypic changes. The dermis was atrophic (45% of the dermal thickness, compared to 65% in littermate controls) and its connective tissue was replaced by large dilated vessels devoid of red cells, but lined with a thin endothelial cell layer. Such abnormal vessels were confined to the dermis and resembled the dysfunctional, dilated spaces characteristic of hyperplastic lymphatic vessels. See Fossum, et al., *J. Vet. Int. Med.*, 6: 283–293 (1992). Also, the ultrastructural features were reminiscent of lymphatic vessels, which differ from blood vessels by having overlapping endothelial junctions, anchoring filaments in the vessel wall, and a discontinuous or even partially absent basement membrane. See Leak, *Microvasc. Res.*, 2: 361–391 (1970). Furthermore, antibodies against collagen types IV, XVIII [Muragaki et al., *Proc. Natl. Acad. Sci. USA*, 92: 8763–8776 (1995)] and laminin gave very weak or no staining of the vessels, while the basement membrane staining of other vessels was prominent. The endothelium was also characterized by positive staining with monoclonal antibodies against desmoplakins I and II (Progen), expressed in lymphatic, but not in vascular endothelial cells. See Schmelz et al., *Differentiation*, 57: 97–117 (1994). Collectively, these findings strongly suggested that the abnormal vessels were of lymphatic origin.

In Northern hybridization studies, abundant VEGF-C MRNA was detected in the epidermis and hair follicles of the transgenic mice, while mRNAs encoding its receptors VEGFR-3 and VEGFR-2 as well as the Tie-1 endothelial receptor tyrosine kinase [Korhonen et al., *Oncogene*, 9: 395–403 (1994)] were expressed in endothelial cells lining the abnormal vessels. In the skin of littermate control animals, VEGFR-3 could be detected only in the superficial subpapillary layer of lymphatic vessels, while VEGFR-2 was found in all endothelia, in agreement with earlier findings. See Millauer et al., *Cell*, 72: 1–20 (1993); and Kaipainen et al., *Proc. Natl. Acad. Sci. USA*, 92: 3566–3570 (1995).

The lymphatic endothelium has a great capacity to distend in order to adapt to its functional demands. To determine whether vessel dilation was due to endothelial distension or proliferation, in vitro proliferation assays were conducted. Specifically, to measure DNA synthesis, 3mm×3mm skin biopsies from four transgenic and four control mice were incubated in D-MEM with 10 micrograms/ml BrdU for 6 hours at 37° C., fixed in 70% ethanol for 12 hours, and embedded in paraffin. After a 30 minute treatment with 0.1% pepsin in 0.1 M HCl at room temperature to denature DNA, staining was performed using mouse monoclonal anti-BrdU antibodies (Amersham). It appeared that the VEGF-C-receptor interaction in the transgenic mice transduced a mitogenic signal, because, in contrast to littermate controls, the lymphatic endothelium of the skin from young K14-VEGF-C mice showed increased DNA synthesis as demonstrated by BrdU incorporation followed by staining with anti-BrdU antibodies. This data further confirms that VEGF-C acts as a true growth factor in mammalian tissues.

In related experiments, a similar VEGF transgene did not induce lymphatic proliferation, but caused enhanced density of hyperpermeable, tortuous blood microvessels instead.

Angiogenesis is a multistep process which includes endothelial proliferation, sprouting, and migration. See Folkman et al., *J. Biol. Chem.*, 267: 10931–10934 (1992). To estimate the contribution of such processes to the transgenic phenotype, the morphology and function of the lymphatic vessels was analysed using fluorescent microlymphography using techniques known in the art. See Leu et al., *Am. J. Physiol.*, 267: 1507–1513 (1994); and Swartz et al., *Am. J. Physiol.*, 270: 324–329 (1996). Briefly, eight-week old mice were anesthetized and placed on a heating pad to maintain a 37° C. temperature. A 30-gauge needle, connected to a catheter filled with a solution of FITC-dextran 2M (8 mg/ml in PBS), was injected intradermally into the tip of the tail. The solution was infused with a constant pressure of 50 cm water (averaging roughly 0.01 microliters per minute flow rate) until the extent of network filling remained constant (approximately 2 hours). Flow rate and fluorescence intensity were monitorerd continuously throughout the experiment. In these experiments, a typical honeycomb-like network with similar mesh sizes was observed in both control and transgenic mice, but the diameter of lymphatic vessels was about twice as large in the transgenic mice, as summarized in the table below. (The intravital fluorescence microscopy of blood vessels was performed as has been described in the art. See Fukumura et al., *Cancer Res.*, 55: 4824–4829 (1995).)

Structural parameters of lymphatic and blood vessel networks

		transgenic	control	P-value**
lymphatic vessels*	diameter	(n = 4) 142.3 ± 26.2	(n = 5) 58.2 ± 21.7	.0143
	horizontal mesh size***	1303 ± 87.1	950.8 ± 93.1	.2207
	Vertical mesh size	507.3 ± 58.9	488.8 ± 59.9	.5403
blood vessels	median diameter	(n = 3) 8.3 ± 0.6	(n = 6) 7.6 ± 1.1	.1213
	vessel density, cm/cm²	199.2 ± 6.6	216.4 ± 20.0	.3017

n = number of animals
*mean (μm) ± SD
**Mann-Whitney test
***mesh size describes vessel density

Some dysfunction of the abnormal vessels was indicated by the fact that it took longer for the dextran to completely fill the abnormal vessels. Injection of FITC-dextran into the tail vein, followed by fluorescence microscopy of the ear, showed that the blood vascular morphology was unaltered and leukocyte rolling and adherence appeared normal in the transgenic mice. These results suggest that the endothelial proliferation induced by VEGF-C leads to hyperplasia of the superficial lymphatic network but does not induce the sprouting of new vessels.

These effects of VEGF-C overexpression are unexpectedly specific, especially since, as described in other examples, VEGF-C is also capable of binding to and activating VEGFR-2, which is the major mitogenic receptor of blood vessel endothelial cells. In culture, high concentrations of VEGF-C stimulate the growth and migration of bovine capillary endothelial cells which express VEGFR-2, but not significant amounts of VEGFR-3. In addition, VEGF-C induces vascular permeability in the Miles assay. [Miles, A. A., and Miles, E. M., *J. Physiol.*, 118:228–257 (1952); and Udaka, et al., *Proc. Soc. Exp. Biol. Med.*, 133:1384–1387 (1970)], presumably via its effect on VEGFR-2. VEGF-C is less potent than VEGF in the Miles assay, 4- to 5-fold higher concentrations of VEGF-C ΔNΔCHis being required to induce the same degree of permeability. In vivo, the specific effects of VEGF-C on lymphatic endothelial cells may reflect a requirement for the formation of VEGFR-3×VEGFR-2 heterodimers for endothelial cell proliferation at physiological concentrations of the growth factor. Such possible heterodimers may help to explain how three homologous VEGFs exert partially redundant, yet strikingly specific biological effects.

The foregoing in vivo data indicates utilities for both (i) VEGF-C polypeptides and polypeptide variants and analogs having VEGF-C biological activity, and (ii) anti-VEGF-C antibodies and VEGF-C antagonists that inhibit VEGF-C activity (e.g., by binding VEGF-C or interfering with VEGF-C/receptor interactions. For example, the data indicates a therapeutic utility for VEGF-C polypeptides in patients wherein growth of lymphatic tissue may be desirable (e.g., in patients following breast cancer or other surgery where lymphatic tissue has been removed and where lymphatic drainage has therefore been compromised, resulting in swelling; or in patients suffering from elephantiasis). The data indicates a therapeutic utility for anti-VEGF-C antibody substances and VEGF-C antagonists for conditions wherein growth-inhibition of lymphatic tissue may be desirable (e.g., treatment of lymphangiomas). Accordingly, methods of administering VEGF-C and VEGF-C variants, analogs, and antagonists are contemplated as methods and materials of the invention.

EXAMPLE 30

Expression of VEGF-C and Flt4 in the Developing Mouse

Embryos from a 16-day post-coitus pregnant mouse were prepared and fixed in 4% paraformaldehyde (PFA), embedded in paraffin, and sectioned at 6 μm. The sections were placed on silanated microscope slides and treated with xylene, rehydrated, fixed for 20 minutes in 4% PFA, treated with proteinase K (7 mg/ml; Merck, Darmstadt, Germany) for 5 minutes at room temperature, again fixed in 4% PFA and treated with acetic anhydride, dehydrated in solutions with increasing ethanol concentrations, dried and used for in situ hybridization.

In situ hybridization of sections was performed as described (Vastrik et al., *J. Cell Biol.*, 128:1197–1208 (1995)). A mouse VEGF-C antisense RNA probe was generated from linearized pBluescript II SK+plasmid (Stratagene Inc.), containing a fragment corresponding to nucleotides 499–979 of mouse VEGF-C cDNA, where the noncoding region and the BR3P repeat were removed by Exonuclease III treatment. The fragment had been cloned into the EcoRI and HindIII sites of pBluescript II SK+. Radiolabeled RNA was synthesized using T7 RNA Polymerase and [^{35}S]-UTP (Amersham, Little Chalfont, UK). About two million cpm of the VEGF-C probe was applied per slide. After an overnight hybridization, the slides were washed first in 2×SSC and 20–30 mM DDT for 1 hour at 50° C. Treatment continued with a high stringency wash, 4×SSC and 20 mM DTT and 50% deionized formamide for 30 minutes at 65° C. followed by RNase A treatment (20 μg/ml) for 30 minutes at 37° C. The high stringency wash was repeated for 45 minutes. Finally, the slides were dehydrated and dried for 30 minutes at room temperature. The slides were dipped into photography emulsion and exposed for 4 weeks. Slides were developed using Kodak D-16 developer, counterstained with hematoxylin and mounted with Permount (FisherChemical).

For in situ hybridizations of Flt4 sequences, a mouse Flt4 CDNA fragment covering bp 1–192 of the published sequence (Finnerty et al., *Oncogene*, 8:2293–2298 (1993)) was used, and the above-described protocol was followed, with the following exceptions. Approximately one million cpm of the Flt4 probe were applied to each slide. The stringent washes following hybridization were performed in 1×SSC and 30 mM DTT for 105 minutes.

Darkfield and lightfield photomicrographs from these experiments are presented in commonly-owned PCT patent application PCT/FI96/00427, filed Aug. 1, 1996, incorporated by reference herein. Observations from the photomicrographs are summarized below.

The most prominently Flt4-hybridizing structures appeared to correspond to the developing lymphatic and venous endothelium. A plexus-like endothelial vascular structure surrounding the developing nasopharyngeal mucous membrane was observed. The most prominent signal using the VEGF-C probe was obtained from the posterior part of the developing nasal conchae, which in higher magnification showed the epithelium surrounding loose connective tissue/forming cartilage. This structure gave a strong in situ hybridization signal for VEGF-C. With the VEGF-C probe, more weakly hybridizing areas were observed around

the snout, although this signal is much more homogeneous in appearance. Thus, the expression of VEGF-C is strikingly high in the developing nasal conchae.

The conchae are surrounded with a rich vascular plexus, important in nasal physiology as a source for the mucus produced by the epithelial cells and for warming inhaled air. It is suggested that VEGF-C is important in the formation of the concheal venous plexus at the mucous membranes, and that it may also regulate the permeability of the vessels needed for the secretion of nasal mucus. Possibly, VEGF-C and its derivatives, and antagonists, could be used in the regulation of the turgor of the conchal tissue and mucous membranes and therefore the diameter of the upper respiratory tract, as well as the quantity and quality of mucus produced. These factors are of great clinical significance in inflammatory (including allergic) and infectious diseases of the upper respiratory tract. Accordingly, the invention contemplates the use of the materials of the invention, including VEGF-C, Flt4, and their derivatives, in methods of diagnosing and treating inflammatory and infectious conditions affecting the upper respiratory tract, including nasal structures.

EXAMPLE 31

Characterization of the Exon-intron Organization of the Human VEGF-C Gene

Two genomic DNA clones covering exons 1, 2, and 3 of the human VEGF-C gene were isolated from a human genomic DNA library using VEGF-C cDNA fragments as probes. In particular, a human genomic library in bacteriophage EMBL-3 lambda (Clontech) was screened using a PCR-generated fragment corresponding to nucleotides 629–746 of the human VEGF-C cDNA (SEQ ID NO: 7). One positive clone, designated "lambda 3," was identified, and the insert was subcloned as a 14 kb XhoI fragment into the pBluescript II (pBSK II) vector (Stratagene). The genomic library also was screened with a labeled 130 bp NotI-SacI fragment from the 5'-noncoding region of the VEGF-C cDNA (the NotI site is in the polylinker of the cloning vector; the SacI site corresponds to nucleotides 92–97 of SEQ ID NO: 7). Two positive clones, designated "lambda 5" and "lambda 8," were obtained. Restriction mapping analysis showed that clone lambda 3 contains exons 2 and 3, while clone lambda 5 contains exon 1 and the putative promoter region.

Three genomic fragments containing exons 4, 5, 6 and 7 were subcloned from a genomic VEGF-C P1 plasmid clone. In particular, purified DNA from a genomic P1 plasmid clone 7660 (Paavonen et al., *Circulation,* 93: 1079–1082 (1996)) was used. EcoRI fragments of the P1 insert DNA were ligated into pBSK II vector. Subclones of clone 7660 which contained human VEGF-C cDNA homologous sequences were identified by colony hybridization, using the full-length VEGF-C CDNA as a probe. Three different genomic fragments were identified and isolated, which contained the remaining exons 4–7.

To determine the genomic organization, the clones were mapped using restriction endonuclease cleavage. Also, the coding regions and exon-intron junctions were partially sequenced. The result of this analysis is depicted in FIGS. 12 and 13A. The sequences of all intron-exon boundaries (FIG. 13A, SEQ ID NOs: 24–35) conformed to the consensus splicing signals (Mount, *Nucl. Acids Res.*, 10: 459–472 (1982)). The length of the intron between exon 5 and 6 was determined directly by nucleotide sequencing and found to be 301 bp. The length of the intron between exons 2 and 3 was determined by restriction mapping and Southern hybridization and was found to be about 1.6 kb. Each of the other intron is over 10 kb in length.

A similar analysis was performed for the murine genomic VEGF-C gene. The sequences of murine VEGF-C intron-exon boundaries are depicted in FIG. 13B and SEQ ID NOs: 36–47.

The restriction mapping and sequencing data indicated that the VEGF-C signal sequence and the first residues of the N-terminal propeptide are encoded by exon 1. The second exon encodes the carboxy-terminal portion of the N-terminal propeptide and the amino terminus of the VEGF homology domain. The most conserved sequences of the VEGF homology domain are distributed in exons 3 (containing 6 conserved cysteine residues) and 4 (containing 2 cys residues). The remaining exons encode cysteine-rich motifs of the type C-6X-C-10X-CRC (exons 5 and 7) and a fivefold repeated motif of type C-6X-B-3X-C-C-C, which is typical of a silk protein.

To further characterize the human VEGF-C gene promoter, the lambda 5 clone was further analyzed. Restriction mapping of this clone using a combination of single- and double-digestions and Southern hybridizations indicated that it includes: (1) an approximately 6 kb region upstream of the putative initiator ATG codon, (2) exon 1, and (3) at least 5 kb of intron 1 of the VEGF-C gene.

A 3.7 kb Xba I fragment of clone lambda 5, containing exon 1 and 5' and 3' flanking sequences, was subcloned and further analyzed. As reported previously, a major VEGF-C mRNA band migrates at a position of about 2.4 kb. Calculating from the VEGF-C coding sequence of 1257 bp and a 391 bp 3' noncoding sequence plus a polyA sequence of about 50–200 bp, the mRNA start site was estimated to be about 550–700 bp upstream of the translation initiation codon.

RNase protection assays were employed to obtain a more precise localization of the mRNA start site. The results of these experiments indicated that the RNA start site in the human VEGF-C gene is located 539 bp upstream of the ATG translational initiation codon.

To further characterize the promoter of the human VEGF-C gene, a genomic clone encompassing about 2.4 kb upstream of the translation initiation site was isolated, and the 5' noncoding cDNA sequence and putative promoter region were sequenced. The sequence obtained is set forth in SEQ ID NO: 48. (The beginning of the VEGF-C cDNA sequence set forth in SEQ ID NO: 7 corresponds to position 2632 of SEQ ID NO: 48; the translation initiation codon corresponds to positions 2983–2985 of SEQ ID NO: 48.) Similar to what has been observed with the VEGF gene, the VEGF-C promoter is rich in G and C residues and lacks consensus TATA and CCAAT sequences. Instead, it has numerous putative binding sites (5'-GGGCGG-3' or 5'-CCGCCC-3') for Sp1, a ubiquitous nuclear protein that can initiate transcription of TATA-less genes. See Pugh and Tjian, *Genes and Dev.*, 5:105–119 (1991). In addition, sequences upstream of the VEGF-C translation start site were found to contain frequent consensus binding sites for the AP-2 factor (5'-GCCN$_3$GCC-3') and binding sites for the AP-1 factor (5'-TKASTCA-3'). Binding sites for regulators of tissue-specific gene expression, like NFKB and GATA, are located in the distant part of VEGF-C promoter. This suggests that the cAMP-dependent protein kinase and protein kinase C, as activators of AP-2 transcription factor [Curran and Franza, *Cell*, 55:395–397 (1988)], mediate VEGF-C transcriptional regulation.

The VEGF-C gene is abundantly expressed in adult human tissues, such as heart, placenta, ovary and small intestine, and is induced by a variety of factors. Indeed, several potential binding sites for regulators of tissue-specific gene expression, like NFkB (5'-GGGRNTYYC-3') and GATA, are located in the distal part of the VEGF-C promoter. For example, NFkB is known to regulate the expression of tissue factor in endothelial cells. Also, transcription factors of the GATA family are thought to regulate cell-type specific gene expression.

Unlike VEGF, the VEGF-C gene does not contain a binding site for the hypoxia-inducible factor, HIF-1 (Levy et al., *J. Biol. Chem.*, 270: 13333–13340 (1995)). This finding suggests that if the VEGF-C MRNA is regulated by hypoxia, the mechanism would be based mainly on the regulation of MRNA stability. In this regard, numerous studies have shown that the major control point for the hypoxic induction of the VEGF gene is the regulation of the steady-state level of mRNA. See Levy et al., *J. Biol. Chem.*, 271: 2746–2753 (1996). The relative rate of VEGF mRNA stability and decay is considered to be determined by the presence of specific sequence motifs in its 3' untranslated region (UTR), which have been demonstrated to regulate MRNA stability. (Chen and Shyu, *Mol. Cell Biol.*, 14: 8471–8482 (1994)). The 3'-UTR of the VEGF-C gene also contains a putative motif of this type (TTATTT), at positions 1873–1878 of SEQ ID NO: 7.

To identify DNA elements important for basal expression of VEGF-C in transfected cells, a set of luciferase reporter plasmids containing serial 5' deletions through the promoter region was constructed. Restriction fragments of genomic DNA containing 5' portions of the first exon were cloned into the polylinker of the pGL3 reporter vector (Promega) and confirmed by sequencing. About 10 μg of the individual constructs in combination with 2 μg. of pSV2-β-galactosidase plasmid (used as a control of transfection efficiency) were transfected into HeLa cells using the calcium phosphate-mediated transfection method. Two days after transfection, the cells were harvested and subjected to the luciferase assay. The luciferase activity was normalized to that of the pGL3 control vector driven by SV40 promoter/enhancer.

As depicted in FIG. 15, the 5.5 kb XboI-RsrII fragment of clone lambda 5 gave nearly 9-fold elevated activity when compared with a promoterless vector. Deletion of a 5' XhoI-HindIII fragment of 2 kb had no effect on the promoter activity. The activity of the 1.16 kb XbaI-RsrII fragment was about twice that of the pGL3 basic vector, while the activity of the same fragment in the reverse orientation was at background level. Further deletion of the XbaI-SacI fragment caused an increase in the promoter activity, suggesting the presence of silencer elements in the region from −1057 to −199 (i.e., 199 to 1057 bp upstream from the transcription initiation site). The shortest fragment (SacII-RsrII) yielded only background activity, which was consistent with the fact that the mRNA initiation site was not present in this construct.

To determine whether further sequences in the first exon of human VEGF-C are important for basal expression, an RsrII fragment spanning nucleotides 214–495 (i.e., 214–495 bp downstream from the transcription initiation site) was subcloned in between of XbaI-RsrII fragment and the luciferase reporter gene. Indeed, the obtained construct showed an 50 % increase in activity when compared with the XbaI-RsrII construct.

The VEGF gene has been shown to be up-regulated by a number of stimuli including serum derived growth factors. To find out whether the VEGF-C gene also can be stimulated by serum, RNA from serum-starved and serum-stimulated HT1080 cells was subjected to primer extension analysis, which demonstrated that VEGF-C MRNA is up-regulated by serum stimulation.

Additional serum stimulation experiments indicated that the serum stimulation leads to increased VEGF-C promoter activity. Cells were transfected as described above and 24 h after transfection changed into medium containing 0.5% bovine serum albumin. Cells were then stimulated with 10% fetal calf serum for 4 hours and analyzed. The XbaI-RsrII promoter construct derived from lambda 5 yielded a twofold increased activity upon serum stimulation, while the same fragment in the reverse orientation showed no response. All other promoter constructs also showed up-regulation, ranging from 1.4 to 1.6 fold (FIG. 15).

EXAMPLE 32

Identification of a VEGF-C Splice Variant

As reported in Example 16, a major 2.4 kb VEGF-C mRNA and smaller amounts of a 2.0 kb mRNA are observable. To clarify the origin of these RNAS, several additional VEGF-C cDNAs were isolated and characterized. A human fibrosarcoma CDNA library from HT1080 cells in the lambda gt11 vector (Clontech, product #HL1048b) was screened using a 153 bp human VEGF-C cDNA fragment as a probe as described in Example 10. See also Joukov et al., *EMBO J.*, 15:290–298 (1996). Nine positive clones were picked and analyzed by PCR amplification using oligonucleotides 5'-CACGGCTTATGCAAGCAAAG-3' (SEQ ID NO: 49) and 5'-AACACAGTTTTCCATAATAG-3' (SEQ ID NO: 50) These oligonucleotides were selected to amplify the portion of the VEGF-C cDNA corresponding to nucleotides 495–1661 of SEQ ID NO: 7. PCR was performed using an annealing temperature of 55° C. and 25 cycles.

The resultant PCR products were electrophoresed on agarose gels. Five clones out of the nine analyzed generated PCR fragments of the expected length of 1147 base pairs, whereas one was slightly shorter. The shorter fragment and one of the fragments of expected length were cloned into the pCRTMII vector (Invitrogen) and analyzed by sequencing. The sequence revealed that the shorter PCR fragment had a deletion of 153 base pairs, corresponding to nucleotides 904 to 1055 of SEQ ID NO: 7. These deleted bases correspond to exon 4 of the human and mouse VEGF-C genes, schematically depicted in FIGS. 13A and 13B. Deletion of exon 4 results in a frameshift, which in turn results in a C-terminal truncation of the full-length VEGF-C precursor, with fifteen amino acid residues translated from exon 5 in a different frame than the frame used to express the full-length protein. Thus, the C-terminal amino acid sequence of the resulting truncated polypeptide would be —Leu (181)-Ser-Lys-Thr-Val-Ser-Gly-Ser-Glu-Glu-Asp-Leu-Pro-His-Glu-Leu-His-Val-Glu (199) (SEQ ID NO: 51). The polypeptide encoded by this splice variant would not contain the C-terminal cleavage site of the VEGF-C precursor. Thus, a putative alternatively spliced RNA form lacking conserved exon 4 was identified in HT-1080 fibrosarcoma cells and this form is predicted to encode a protein of 199 amino acid residues, which could be an antagonist of VEGF-C.

EXAMPLE 33

VEGF-C is Similarly Processed in Different Cell Cultures in Vitro

To study whether VEGF-C is similarly processed in different cell types, 293 EBNA cells, COS-1 cells and

HT-1080 cells were transfected with wild type human VEGF-C CDNA and labelled with Pro-Mix™ as described in Example 22. The conditioned media from the cultures were collected and subjected to immunoprecipitation using antiserum 882 (described in Example 21, recognizing a peptide corresponding to amino acids 104–120 of SEQ ID NO: 8). The immunoprecipitated polypeptides were separated via SDS-PAGE, and detected via autoradiography. The major form of secreted recombinant VEGF-C observed from all cell lines tested is a 29/32 kD doublet. These two polypeptides are bound to each other by disulfide bonds, as described in Example 22. A less prominent band of approximately 21 kD also was detected in the culture media. Additionally, a non-processed VEGF-C precursor of 63 kDa was observed. This form was more prominent in the COS-1 cells, suggesting that proteolytic processing of VEGF-C in COS cells is less efficient than in 293 EBNA cells. Endogenous VEGF-C (in non-transfected cells) was not detectable under these experimental conditions in the HT-1080 cells, but was readily detected in the conditioned medium of the PC-3 cells. Analysis of the subunit polypeptide sizes and ratios in PC-3 cells and 293 EBNA cells revealed strikingly similar results: the most prominent form was a doublet of 29/32 kDa and a less prominent form the 21 kD polypeptide. The 21 kD form produced by 293 EBNA cells was not recognized by the 882 antibody in the Western blot, although it is recognized when the same antibody is used for immunoprecipitation (see data in previous examples). As reported in Example 21, cleavage of the 32 kD form in 293 EBNA cells occurs between amino acid residues 111 and 112 (SEQ ID NO: 8), downstream of the cleavage site in PC-3 cells (between residues 102 and 103). Therefore, the 21 kD form produced in 293 EBNA cells does not contain the complete N-terminal peptide used to generate antiserum 882. In a related experiment, PC-3 cells were cultured in serum-free medium for varying periods of time (1–8 days) prior to isolation of the conditioned medium. The conditioned medium was concentrated using a Centricon device (Amicon, Beverly, USA) and subjected to Western blotting analysis using antiserum 882. After one day of culturing, a prominent 32 kD band was detected. Increasing amounts of a 21–23 kD form were detected in the conditioned media from 4 day and 8 day cultures. The diffuse nature of this polypeptide band, which is simply called the 23 kD polypeptide in example 5 and several subsequent examples; is most likely due to a heterogeneous and variable amount of glycosylation. These results indicate that, initially, the cells secrete a 32 kD polypeptide, which is further processed or cleaved in the medium to yield the 21–23 kD form. The microheterogeneity of this polypeptide band would then arise from the variable glycosylation degree and, from microheterogeneity of the processing cleavage sites, such as obtained for the amino terminus in PC-3 and 293 EBNA cell cultures. The carboxyl terminal cleavage site could also vary, examples of possible cleavage sites would be between residues 225–226, 226–227 and 227–228 as well as between residues 216–217. Taken together, these data suggest the possibility that secreted cellular protease(s) are responsible for the generation of the 21–23 kD form of VEGF-C from the 32 kD polypeptide. Such proteases could be used in vitro to cleave VEGF-C precursor proteins in solution during the production of VEGF-C, or used in cell culture and in vivo to release biologically active VEGF-C.

EXAMPLE 34

Differential Binding of VEGF-C Forms by the Extracellular Domains of VEGFR-3 and VEGFR-2

In two parallel experiments, 293 EBNA cells were transfected with a construct encoding recombinant wild type VEGF-C or a construct encoding VEGF-C ΔNΔCHis (Example 28) and about 48 hours after transfection, metabolically labelled with Pro-Mix™ as described in previous examples. The media were collected from mock-transfected and transfected cells and used for receptor binding analyses.

Receptor binding was carried out in binding buffer (PBS, 0.5% BSA, 0.02% Tween 20, 1 microgram/ml heparin) containing approximately 0.2 microgram of either (a) a fusion protein comprising a VEGFR-3 extracellular domain fused to an immunoglobulin sequence (VEGFR-3-Ig) or (b) a fusion protein comprising VEGFR-2 extracellular domain fused to an alkaline phosphatase sequence (VEGF-R-2-AP; Cao et al., *J. Biol. Chem.* 271:3154–62 (1996)). As a control, similar aliquots of the 293 EBNA conditioned media were mixed with 2 μl of anti-VEGF-C antiserum (VEGF-C IP).

After incubation for 2 hours at room temperature, anti-VEGF-C antibodies and VEGFR-3-Ig protein were adsorbed to protein A-sepharose (PAS) and VEGFR-2-AP was immunoprecipitated using anti-AP monoclonal antibodies (Medix Biotech, Genzyme Diagnostics, San Carlos, Calif., USA) and protein G-sepharose. Complexes containing VEGF-C bound to VEGFR-3-Ig or VEGFR-2-AP were washed three times in binding buffer, twice in 20 mM Tris-HCl (pH 7.4) and VEGF-C immunoprecipitates were washed three times in RIPA buffer and twice in 20 mM tris-HCl (pH 7.4) and analyzed via SDS-PAGE under reducing and nonreducing conditions. As a control, the same media were precipitated with anti-AP and protein G-sepharose (PGS) or with PAS to control for possible nonspecific adsorption.

These experiments revealed that VEGFR-3 bound to both the 32/29 kD and 21–23 kD forms of recombinant VEGF-C, whereas VEGFR-2 bound preferentially to the 21–23 kD component from the conditioned media. In addition, small amounts of 63 kD and 52 kD VEGF-C forms were observed binding with VEGFR-3. Further analysis under nonreducing conditions indicates that a great proportion of the 21–23 kD VEGF-C bound to either receptor does not contain interchain disulfide bonds. These findings reinforce the results that VEGF-C binds VEGFR-2. This data suggests a utility for recombinant forms of VEGF-C which are active towards VEGFR-3 only or which are active towards both VEGFR-3 and VEGFR-2. On the other hand, these results, together with the results in Example 28, do not eliminate the possibility that the 32/29 kD dimer binds VEGFR-3 but does not activate it. The failure of the 32/29 kD dimer to activate VEGFR-3 could explain the finding that conditioned medium from the N-His VEGF-C transfected cells induced a less prominent tyrosine phosphorylation of VEGFR-3 than medium from VEGF-C ΔNΔCHis transfected cells, even though expression of the former polypeptide was much higher. Stable VEGF-C poly-peptide mutants that bind to a VEGF-C receptor but fail to activate the receptor are useful as VEGF-C antagonists.

EXAMPLE 35

Discovery of VEGF-C Analogs That Selectively Bind to and Activate VEGFR-3, But Not VEGFR-2

To further identify the cysteine residues of VEGF-C that are critical for retaining VEGF-C biological activities, an additional VEGF-C mutant, designated VEGF-CΔNΔCHisC156S, was synthesized, in which the cysteine residue at position 156 of the 419 amino acid VEGF-C precursor (SEQ ID NO: 8; Genbank accession number X94216) was replaced with a serine residue.

The mutagenesis procedure was carried out using the construct of VEGF-CΔNΔCHis (see Example 28), cloned in the pALTER vector, and the Altered sites II in vitro mutagenesis system of Promega. An oligonucleotide, 5'-GACGGACACAGATGGAGGTTTAAAG- 3' (SEQ ID NO: 52) was used to introduce the desired mutation in the CDNA encoding VEGF-CΔNΔCHis. The resulting mutated VEGF-C cDNA fragment was subcloned into the HindIII/NotI sites of the pREP-7 vector (Invitrogen), and the final construct was resequenced to confirm the C156S mutation. The resultant clone has an open reading frame encoding amino acids 103–225 of SEQ ID NO: 8 (with a serine codon at position 156), and further encoding a 6×His tag.

The wildtype VEGF-C cDNA and three VEGF-C mutant constructs (VEGF-C R226,227S, VEGF-C ΔNΔCHis, and VEGF-C ΔNΔCHisC156S) were used to transfect 293 EBNA cells, which were subcultured 16 hours after transfection. About 48 hours after transfection, the media were changed to DMEM/0.1% BSA, and incubation in this medium was continued for an additional 48 hours. The resultant conditioned media were concentrated 30-fold using Centriprep-10 (Amicon), and the amount of VEGF-C in the media was analyzed by Western blotting using the anti-VEGF-C antiserum 882 for immunodetection. Different amounts of the recombinant VEGF-C ΔNΔCHis, purified from a yeast expression system, were analyzed in parallel as reference samples to measure and equalize the VEGF-C concentrations in the conditioned media. The conditioned medium from mock-transfected cells was used to dilute the VEGF-C conditioned media to achieve equal concentrations.

An aliquot of the transfected cells were metabolically labelled for 6 h with 100 microcuries/ml of the PRO-MIX™ L- [^{35}S] in vitro cell labelling mix (Amersham). The conditioned media were collected, and binding of the radioactively labelled VEGF-C proteins to the extracellular domains of VEGFR-3 and VEGFR-2 was analyzed using recombinantly produced VEGFR-3EC-Ig and VEGFR-2EC-Ig constructs (containing seven and three Ig loops of the extracellular domains of the respective receptors, fused to an immunoglobulin heavy chain constant region).

As shown in FIG. 14A, all processed VEGF-C forms secreted to the culture medium bound to VEGFR-3EC domain, with preferential binding of the 21 kDa form (left panel). When present at high concentrations, the VEGF-C forms of 58 kDa and 29/31 kDa bound to some extent non-specifically to protein A Sepharose (PAS, right panel).

The VEGFR-2EC domain preferentially bound the mature 21 kDa form of wildtype VEGF-C and VEGF-CΔNΔCHis. Significantly, VEGF-CΔNΔCHisC156S failed to bind the VEGFR2-EC (FIG. 14A, middle panel).

Next, the ability of the above-described VEGF-C polypeptides to compete with the ^{125}I-VEGF-CΔNΔCHis for binding to VEGFR-2 and VEGFR-3 was analyzed. Scatchard analysis using VEGF-C ΔCΔNHis provided indications of the VEGF-C binding affinity for VEGFR-3 (K_D= 135 pM) and VEGFR-2 (K_D=410 pM). Ten micrograms of the purified yeast VEGF-C ΔNΔCHis was labeled using 3 mCi of Iodine-125, carrier-free (Amersham), and an Iodo-Gen Iodination Reagent (Pierce), according to the standard protocol of Pierce. The resulting specific activity of the labeled VEGF-CΔNΔCHis was 1.25×10^5 cpm/ug.

To study receptor binding, PAE/VEGFR-2 and PAE/VEGFR-3 cells were seeded into 24-well tissue culture plates (Nunclon), which had been coated with 2% gelatin in PBS. The ^{125}-VEGF-C ΔNΔCHis (2×10^5 cpm) and different amounts of media containing equal concentrations of the non-labeled VEGF-C (wildtype and mutants) were added to each plate in Ham's F12 medium, containing 25 mM HEPES (pH 8.0), 0.1% BSA, and 0.1% NaN_3. The binding was allowed to proceed at room temperature for 90 minutes. The plates were then transferred onto ice and washed three times with ice-cold PBS containing 0.1% BSA. The cells were then lysed in 1 M NaOH, the lysates were collected, and the radioactivity was measured using a γ-counter. Binding in the presence of VEGF-C-containing conditioned medium was calculated as a percentage of binding observed in parallel control studies wherein equal volumes of medium from mock-transfected cells were used instead of VEGF-C conditioned media.

As shown in FIG. 14B, left panel, all VEGF-C mutants displaced ^{125}I-VEGF-CΔNΔCHis from VEGFR-3. The efficiency of displacement was as follows: VEGF-CΔNΔCHisC156S>VEGF-CΔNΔCHis>wildtype VEGF-C>VEGF-CR226,227S. These results indicate that enhanced binding to VEGFR-3 was obtained upon "recombinant maturation" of VEGF-C. Recombinant VEGF165 failed to displace VEGF-C from VEGFR-3.

VEGF, VEGF-CΔNΔCHis, and wildtype VEGF-C all efficiently displaced labeled VEGF-CΔNΔCHis from VEGFR-2, with VEGF-CΔNΔCHis being more potent when compared to wildtype VEGF-C (FIG. 1B, right panel). The non-processed VEGF-C R226,227S showed only weak competition of ^{125}I-VEGF-CΔNΔCHis.

Surprisingly, VEGF-CΔNΔCHisR156S failed to displace VEGF-CΔNΔCHis from VEGFR-2, thus confirming the above described results obtained using a soluble extracellular domain of VEGFR-2.

The ability of the above mentioned VEGF-C forms to stimulate tyrosine phosphorylation of VEGFR-3 and VEGFR-2 was also investigated. Importantly, identical dilutions of the conditioned media were used for these experiments and for the competitive binding experiments described above. A Western blot analysis of the conditioned media using anti-VEGF-C antiserum 882 was performed to confirm the approximately equal relative amounts of the factors present.

The stimulation of VEGFR-3 and VEGFR-2 autophosphorylation by the different VEGF-C forms in general correlated with their binding properties, as well as with the degree of "recombinant processing" of VEGF-C. The VEGF-CΔNΔCHisC156S appeared to be at least as potent as VEGF-CΔNΔCHis in stimulating VEGFR-3 autophosphorylation. VEGF-CΔNΔCHis showed a higher potency when compared to wildtype VEGF-C in its ability to stimulate tyrosine autophosphorylation of both VEGFR-2 and VEGFR-3. The VEGF-CR226,227S conditioned medium possessed a considerably weaker effect on autophosphorylation of VEGFR-3, and almost no effect on VEGFR-2 autophosphorylation.

Stimulation of VEGFR-2 tyrosine phosphorylation by VEGF-CΔNΔCHisC156S did not differ from that of conditioned medium from the mock transfected cells, thus confirming the lack of VEGFR-2-binding and VEGFR-2-activating properties of this mutant.

The ability of VEGF-C ΔNΔCHisC156S to alter vascular permeability in vivo was analyzed using the Miles assay (see Example 29). The recombinant VEGF-C forms assayed (ΔNΔCHis, ΔNΔCHisC156S) were produced by 293 cells, purified from conditioned media using Ni-NTA Superflow resin (QIAGEN) as previously described, and pretreated with 15 μg/ml of anti-human VEGF neutralizing antibody

(R&D systems) to neutralize residual amounts of co-purified, endogenously produced VEGF. Eight picomoles of the various VEGF-C forms, as well as 2 pmol of recombinant human VEGF165 (R&D systems) and approximately 2 pmol of VEGF165 from the conditioned medium which were either non-treated or pretreated with the above mentioned VEGF-neutralizing antibody were injected subcutaneously to the back region of a guinea pig. The area of injection was analyzed 20 minutes after injections. Both VEGF and VEGF-C ΔNΔCHis caused increases in vascular permeability, whereas ΔNΔCHisC156S did not affect vascular permeability. The neutralizing antibody completely blocked permeability activity of VEGF but did not affect VEGF-C activity. Residual permeability activity observed for the VEGF-containing conditioned medium even after its treatment with VEGF neutralizing antibody was presumably caused by permeability factors other than VEGF that are produced by 293-cells.

The Miles assay also was used to assay the ability of VEGF-C R226,227S (8 pM, pretreated with anti-VEGF antibody) to induce vascular permeability. The results indicated that the ability of VEGF-C R226,227S to induce vascular permeability was much weaker when compared to wildtype and ΔNΔCHis forms of VEGF-C. Collectively, this Miles assay data is consistent with the VEGFR-2 binding and autophosphorylation data described above, and indicates that VEGF-C effect on vascular permeability is mediated via VEGFR-2.

The foregoing data indicates that proteolytic processing of VEGF-C results in an increase in its ability to bind and to activate VEGFR-3 and VEGFR-2. Non-processed VEGF-C is a ligand and an activator of preferentially VEGFR-3, while the mature 21/23 kDa VEGF-C form is a high affinity ligand and an activator of both VEGFR-3 and VEGFR-2.

Moreover, replacement of the cysteine residue at position 156 (of prepro-VEGF-C, SEQ ID NO: 8) creates a selective ligand and activator of VEGFR-3. This alteration inactivates the ability of processed VEGF-C to bind to VEGFR-2 and to activate VEGFR-2. Importantly, it is believed that the elimination of the cysteine at position 156 is the alteration responsible for this unexpected alteration in VEGF-C selectivity, and not the substitution of a serine per se. It is expected that replacement of the cysteine at position 156 with other amino acids, or the mere deletion of this cysteine, will also result in VEGF-C analogs having selective biological activity with respect to VEGFR-3. All such replacement and deletion analogs (collectively referred to as VEGF-C ΔC_{156} polypeptides) are contemplated as aspects of the present invention.

VEGF-C polypeptides that have the C156S mutation (or functposition equivalent mutations at position 156) and that retain biological activity with respect to VEGFR-3, such as VEGF-C ΔNΔCHisC156S, are useful in all of the same manners described above for wildtype VEGF-C proteins and biologically active fragments thereof where VEGFR-3 stimulation is desired. It is contemplated that most biologically active VEGF-C fragments and processing variants, including but not limited to the biologically active fragments and variants identified in preceding examples, will retain VEGF-C biological activity (as mediated through VEGFR-3) when a ΔC_{156} mutation is introduced. All such biologically active VEGF-C ΔC_{156} polypeptides are intended as an aspect of the present invention.

Moreover, VEGF-C forms containing the C156S mutation or equivalent mutations can be used to distinguish those effects of VEGF-C mediated via VEGFR-3 and VEGFR-2 from those obtained via only VEGFR-3. The ability of such VEGF-C polypeptides to selectively stimulate VEGFR-3 are also expected to be useful in clinical practice, it being understood that selectivity of a pharmaceutical is highly desirable in many clinical contexts. For example, the selectivity of VEGF-C ΔC_{156} polypeptides for VEGFR-3 binding suggests a utility for these peptides to modulate VEGF-C biological activities mediated through VEGFR-3, without significant concomitant modulation of blood vessel permeability or other VEGF-C activities that are modulated through VEGFR-2.

The data presented herein also indicates a utility for ΔC_{156} polypeptides that are capable of binding VEGFR-3, but that do not retain biological activity mediated through VEGFR-3. Specifically, such forms are believed to be capable of competing with wildtype VEGF-C for binding to VEGFR-3, and are therefore contemplated as molecules that inhibit VEGF-C-mediated stimulation of VEGFR-3. Because of the ΔC_{156} alteration, such polypeptides (especially covalent or noncovalent dimers of such polypeptides) are not expected to bind VEGFR-2. Thus, certain ΔC_{156} polypeptides and polypeptide dimers are expected to have utility as selective inhibitors of VEGF-C biological activity mediated through VEGFR-3 (i.e., without substantially altering VEGF-C mediated stimulation of VEGFR-2).

In another embodiment of the invention, heterodimers comprising a biologically active VEGF-C polypeptide in association with a ΔC_{156} polypeptide are contemplated. It is contemplated that such heterodimers can be formed in vitro, as described below in Example 37, or formed in vivo-with endogenous VEGF-C following administration of a ΔC_{156} polypeptide. Such heterodimers are contemplated as modulators of VEGF-C mediated effects in cells where the biological effects of VEGF-C are mediated through VEGFR-2/VEGFR-3 heterodimers. VEGF-C ΔC_{156} polypeptides in homodimers or in heterodimers with wt VEGF-C might selectively inhibit the ability of the latter to induce VEGF-like effects, particularly to increase the vascular permeability.

EXAMPLE 36

Utility for VEGF-C in Promoting Myelopoiesis

The effects of VEGF-C on hematopoiesis were also analyzed. Specifically, leukocytes populations were analyzed in blood samples taken from the F1 transgenic mice described in Example 29, and from their non-transgenic littermates. Leukocyte population data from these mice and from non-transgenic FVB-NIH control mice (i.e., the strain used to generate the transgenic mice) are set forth in the tables below.

	FVB/NIH MICE				
Cell Type	male 5.5 months	male 5.5 months	female 9.5 months	male 9.5 months	mean ± σ
Lymphocytes	72.20%	82.17%	84.25%	74.25%	78.22 ± 5.10
Neutrophils	23.00%	15.17%	14.25%	22.25%	18.67 ± 3.98
Monocytes	0.65%	1.00%	0.25%	0.50%	0.60 ± 0.27
Eosinophils	2.15%	1.70%	1.25%	3.00%	2.03 ± 0.65
Basophils	0.00%	0.00%	0.00%	0.00%	0 ± 0

-continued

VEGF-C TRANSGENIC MICE

Cell Type	male 2 months	male 3.5 months	male 7 months	mean ± σ
Lymphocytes	41.3%	41.50%	18.70%	33.83 ± 10.70
Neutrophils	55.3%	53.80%	80.17%	63.09 ± 12.09
Monocytes	2.16%	1.30%	0.67%	1.38 ± 0.8[illegible]
Eosinophils	1.17%	3.50%	.50%	1.72 ± 1.29
Basophils	0.00%	0.00%	0.00%	0 ± 0

VEGF-C NEGATIVE CONTROL MICE (NON-TRANSGENIC LITTERMATES OF VEGF-C TRANSGENIC MICE)

Cell Type	male 2 months	male 2 months	male 3.5 months	male 7 months	mean ± σ
Lymphocytes	89.00%	67.50%	91.00%	71.50%	79.7 ± 10.41
Neutrophils	7.75%	23.00%	7.00%	23.75%	15.38 ± 8.01
Monocytes	1.50%	0.50%	0.83%	0.75%	0.90 ± 0.37
Eosinophils	1.50%	9.00%	0.67%	4.00%	3.79 ± 3.25
Basophils	0.00%	0.00%	0.50%	0.50%	0.25 ± 0.25

As the foregoing data indicates, the overexpression of VEGF-C in the skin of the transgenic mice correlates with a distinct alteration in leukocyte populations. Notably, the measured populations of neutrophils were markedly increased in the transgenic mice. One explanation for the marked increase in neutrophils is a myelopoietic activity attributable to VEGF-C. A VEGF-C influence on leukocyte trafficking in and out of tissues also may effect observed neutrophil populations. Fluorescence-activated cell sorting analysis, performed on isolated human bone marrow and umbilical cord blood CD34-positive hematopoietic cells, demonstrated that a fraction of these cells are positive for Flt4 (VEGFR-3). Thus, the VEGF-C effect on myelopoiesis may be exerted through this VEGFR-3-positive cell population and its receptors. In any case, the foregoing data indicates a use for VEFG-C polypeptides to increase granulocyte (and, in particular, neutrophil) counts in human or non-human subjects, i.e., in order to assist the subject fight infectious diseases. The exploitation of the myelopoietic activity of VEGF-C polypeptides is contemplated both in vitro (i.e., in cell culture) and in vivo, as a sole myelopoietic agent and in combination with other effective agents (e.g., granulocyte colony stimulating factor (G-CSF)).

Additional studies of the myelopoietic effect of VEGF-C, using VEGF-C mutants (e.g., VEGF-C ΔC_{156} polypeptides, VEGF-C ΔNΔCHis, VEGF-C R226,227S) having altered VEGFR-2 binding affinities, will elucidate whether this effect is mediated through VEGFR-2, VEGFR-3, or both receptors, for example. The results of such analysis will be useful in determining which VEGF-C mutants have utility as myelopoietic agents and which have utility as agents for inhibiting myelopoiesis.

EXAMPLE 37

Generation of Heterodimers Consisting of Members of the VEGF Family of Growth Factors

Both naturally-occurring and recombinantly-produced heterodimers of polypeptides of the PDGF/VEGF family of growth factors have been shown to exist in nature and possess mitogenic activities. See, e.g., Cao et al., *J. Biol. Chem.*, 271:3154–62 (1996); and DiSalvo, et al., *J. Biol. Chem.*, 270:7717–7723 (1995). Heterodimers comprising a VEGF-C polypeptide may be generated essentially as described in Cao et al. (1996), using recombinantly produced VEGF-C polypeptides, such as the VEGF-C polypeptides described in the preceding examples. Briefly, a recombinantly produced VEGF-C polypeptide is mixed at an equimolar ratio with another recombinantly produced polypeptide of interest, such as a VEGF, VEGF-B, PLGF, PDGFα, PDGFβ, or c-fos induced growth factor polypeptide. (See, e.g., Cao et al. (1990); Collins et al., *Nature*, 316:748–750 (1985) (PDGF-β, GenBank Acc. No. X02811); Claesson-Welsh et al., *Proc. Natl. Acad. Sci. USA*, 86(13):4917–4921 (1989) (PDGF-α, GenBank Acc. No. M22734); Claesson-Welsh et al., *Mol. Cell. Biol.* 8:3476–3486 (1988) (PDGF-β, GenBank Acc. No. M21616); Olofsson et al., *Proc. Natl. Acad. Sci.* (*USA*), 93:2576–2581 (1996) (VEGF-B, GenBank Acc. No. U48801); Maglione et al., *Proc. Natl. Acad. Sci.* (*USA*), 88(20):9267–9271 (1996) (PlGF, GenBank Acc. No. X54936); Heldin et al., *Growth Factors*, 8:245–252 (1993); Folkman, *Nature Med.*, 1:27–31 (1995); Frieser et al., *FASEB J.*, 9:919–25 (1995); Mustonen et al., *J. Cell. Biol.*, 129:895–98 (1995); Orlandini, S., *Proc. Natl. Acad. Sci. USA*, 93(21):11675–11680 (1996); and others cited elsewhere herein. The mixed polypeptides are incubated in the presence of guanidine-HCl and DTT. The thiol groups are then protected with S-sulfonation, and the protein is dialyzed overnight, initially against urea/glutathione-SH, glutathione-S-S-glutathione, and subsequently against 20 mM Tris-HCl.

In a preferred embodiment, a variety of differently processed VEGF-C forms and VEGF-C variants and analogs, such as the ones described in the preceding examples, are employed as the VEGF-C polypeptide used to generate such heterodimers. Thereafter, the heterodimers are screened to determine their binding affinity with respect to receptors of the VEGF/PDGF family (especially VEGFR-1, VEGFR-2, and VEGFR-3), and their ability to stimulate the receptors (e.g., assaying for dimer-stimulated receptor phosphorylation in cells expressing the receptor of interest on their surface). The binding assays may be competitive binding assays such as those described herein and in the art. In the initial binding assays, recombinantly produced proteins comprising the extracellular domains of receptors are employable, as described in preceding examples for VEGFR-2 and VEGFR-3. Heterodimers that bind and stimulate receptors are useful as recombinant growth factor polypeptides. Heterodimers that bind but do not stimulate receptors are useful as growth factor antagonists. Heterodimers that display agonistic or antagonistic activities in the screening assays are further screened using, e.g., endothelial cell migration assays, vascular permeability assays, and in vivo assays. It will also be apparent from the preceding examples that dimers comprising two VEGF-C polypeptides (i.e., dimers of identical VEGF-C polypeptides as well as dimers of different VEGF-C polypeptides) are advantageously screened for agonistic and antagonistic activities using the same assays.

In one preferred embodiment, VEGF-C ΔC_{156}, polypeptide is employed to make the dimers. It is anticipated that agonists and antagonists comprising a VEGF-C ΔC_{156} polypeptide will have increased specificity for stimulating and inhibiting VEGFR-3, without concomitant stimulation or inhibition of VEGFR-2.

In another preferred embodiment, VEGF-C polypeptides wherein the C-terminal proteolytic cleavage site has been altered to reduce or eliminate C-terminal processing (e.g. VEGF-C R226,227S) is employed to make dimers for screening for inhibitory activity.

In yet another preferred embodiment, VEGF-C polypeptides comprising amino-terminal fragments (e.g., the VEGF-C 15 kD form described herein) of VEGF-C are employed to make dimers.

It is further contemplated that inactivation of only one polypeptide chain in a dimer could be enough to generate an inhibitory molecule, which is demonstrated e.g., by the generation of PDGF inhibitory mutant as reported in Vassbotn, *Mol. Cell. Biol.*, 13:4066–4076 (1993). Therefore, in one embodiment, inhibition is achieved by expression in vivo of a polynucleotide (e.g., a cDNA construct) encoding the heterodimerization partner which is unable to bind (or binds inefficiently) to the receptor, or by direct administration of that monomer in a pharmaceutical composition.

EXAMPLE 38

Formation and Screening of Useful Recombinant VEGF/VEGF-C Genes and Polypeptides

Amino acid sequence comparison reveals that mature VEGF-C bears structural similarity to VEGF121 [Tischer et al., *J. Biol. Chem.*, 266(18):11947–54 (1991)], with certain noteworthy structural differences. For example, mature VEGF-C contains an unpaired cysteine (position 137 of SEQ ID NO: 8) and is able to form non-covalently bonded polypeptide dimers. In one embodiment of the invention, a VEGF analog is created wherein the unpaired cysteine residue from mature VEGF-C is introduced at an analogous position of VEGF (e.g., introduced at Leu_{58} of the human VEGF165 precursor (FIG. 2, Genbank Acc. No. M32977) to generate a $VEGF^{+cys}$ mutant designated VEGF L58C). Such an alteration is introduced into the VEGF165 coding sequence using site-directed mutagenesis procedures known in the art, such as the procedures described above in preceding examples to generate various VEGF-C mutant forms. This $VEGF^{+cys}$ mutant is recombinantly expressed and is screened (alone and as a heterodimer with other VEGF and VEGF-C forms) for VEGFR-2 and/or VEGFR-3 binding, stimulatory, and inhibitory activities, using in vitro and in vivo activity assays as described elsewhere herein. To form another VEGF analog of the invention, a $VEGF^{+cys}$ mutant is altered to remove a conserved cysteine corresponding to cyst of the VEGF165 precursor. Elimination of this cysteine from the VEGF L58C would result in a VEGF analog resembling VEGF-CΔNΔCHisC156S. This VEGF analog is screened for its VEGF-inhibitory activities with respect to VEGFR-2 and/or VEGFR-1 and for VEGF-C like stimulatory or inhibitory activities.

Another noteworthy structural difference between VEGF and VEGF-C is the absence in VEGF-C of several basic residues found in VEGF (e.g., residues Arg_{108}, Lys_{110} and His_{112} in the VEGF165 precursor shown in FIG. 2) that have been implicated in VEGF receptor binding. See Keyt et al., *J. Biol. Chem.*, 271(10):5638–46 (1996). In another embodiment of the invention, codons for basic residues (lys, arg, his) are substituted into the VEGF-C coding sequence at one or more analogous positions by site-directed mutagenesis. For example, in a preferred embodiment, Glu_{187}, Thr_{189}, and Pro_{191}, in VEGF-C (SEQ ID NO: 8) are replaced with Arg, Lys, and His residues, respectively. The resultant VEGF-C analogs (collectively termed "$VEGF\text{-}C^{basic}$" polypeptides) are recombinantly expressed and screened for VEGFR-1, VEGFR-2, and VEGFR-3 stimulatory and inhibitory activity. The foregoing VEGF and VEGF-C analogs that have VEGF-like activity, VEGF-C-like activity, or that act as inhibitors of VEGF or VEGF-C, are contemplated as additional aspects of the invention. Polynucleotides encoding the analogs also are intended as aspects of the invention.

Deposit of Biological Materials: Plasmid FLT4-L has been deposited with the American Type Culture Collection (ATCC), 12301 Parklawn Dr., Rockville Md. 20952 (USA), pursuant to the provisions of the Budapest Treaty: and has been assigned a deposit date of Jul. 24, 1995 and ATCC accession number 97231.

While the present invention has been described in terms of specific embodiments, it is understood that variations and modifications will occur to those in the art. Accordingly, only such limitations as appear in the appended claims should be placed on the invention.

SEQUENCE LISTING

(1) GENERAL INFORMATION:

(iii) NUMBER OF SEQUENCES: 57

(2) INFORMATION FOR SEQ ID NO:1:

(i) SEQUENCE CHARACTERISTICS:
(A) LENGTH: 4416 base pairs
(B) TYPE: nucleic acid
(C) STRANDEDNESS: single
(D) TOPOLOGY: linear

(ii) MOLECULE TYPE: cDNA

(xi) SEQUENCE DESCRIPTION: SEQ ID NO:1:

CCACGCGCAG CGGCCGGAGA TGCAGCGGGG CGCCGCGCTG TGCCTGCGAC TGTGGCTCTG 60

CCTGGGACTC CTGGACGGCC TGGTGAGTGG CTACTCCATG ACCCCCCCGA CCTTGAACAT 120

CACGGAGGAG TCACACGTCA TCGACACCGG TGACAGCCTG TCCATCTCCT GCAGGGGACA 180

GCACCCCCTC GAGTGGGCTT GGCCAGGAGC TCAGGAGGCG CCAGCCACCG GAGACAAGGA 240

-continued

```
CAGCGAGGAC ACGGGGGTGG TGCGAGACTG CGAGGGCACA GACGCCAGGC CCTACTCCAA   300
GGTGTTCGCG CTGCACGAGG TACATGCCAA CGACACAGGC AGCTACGTCT GCTACTACAA   360
GTACATCAAG GCACGCATCG AGGGCACCAC GGCCGCCAGC TCCTACGTGT TCGTGAGAGA   420
CTTTGAGCAG CCATTCATCA ACAAGCCTGA CACGCTCTTC GTCAACAGGA AGGACGCCAT   480
GTGGGTCGCC TGTCTGGTGT CCATCCCCGG CCTCAATGTC ACGCTGCGCT CGCAAAGCTC   540
GGTGCTGTGG CCAGACGGGC AGGAGGTGGT GTGGGATGAC CGGCGGGCCA TGCTCGTGTC   600
CACGCCACTG CTGCACGATG CCCTGTACCT GCAGTGCGAG ACCACCTGGG GAGACCAGGA   660
CTTCCTTTCC AACCCCTTCC TGGTGCACAT CACAGGCAAC GAGCTCTATG ACATCCAGCT   720
GTTGCCCAGG AAGTCGCTGG AGCTGCTGGT AGGGGAGAAG CTGGTCCTGA ACTGCACCGT   780
GTGGGCTGAG TTCAACTCAG GTGTCACCTT TGACTGGGAC TACCCAGGGA AGCAGGCAGA   840
GCGGGGTAAG TGGGTGCCCG AGCGACGCTC CCAGCAGACC CACACAGAAC TCTCCATCAT   900
CCTGACCATC CACAACGTCA GCCAGCACGA CCTGGGCTCG TATGTGTGCA AGGCCAACAA   960
CGGCATCCAG CGATTTCGGG AGAGCACCGA GGTCATTGTG CATGAAAATC CCTTCATCAG  1020
CGTCGAGTGG CTCAAAGGAC CCATCCTGGA GGCCACGGCA GGAGACGAGC TGGTGAAGCT  1080
GCCCGTGAAG CTGGCAGCGT ACCCCCCGGC CGAGTTCCAG TGGTACAAGG ATGGAAAGGC  1140
ACTGTCCGGG CGCCACAGTC CACATGCCCT GGTGCTCAAG GAGGTGACAG AGGCCAGCAC  1200
AGGCACCTAC ACCCTCGCCC TGTGGAACTC CGCTGCTGGC CTGAGGCGCA ACATCAGCCT  1260
GGAGCTGGTG GTGAATGTGC CCCCCCAGAT ACATGAGAAG GAGGCCTCCT CCCCCAGCAT  1320
CTACTCGCGT CACAGCCGCC AGGCCTTCAC CTGCACGGCC TACGGGGTGC CCCTGCCTCT  1380
CAGCATCCAG TGGCACTGGC GGCCCTGGAC ACCCTGCAAG ATGTTTGCCC AGCGTAGTCT  1440
CCGGCGGCGG CAGCAGCAAG ACCTCATGCC ACAGTGCCGT GACTGGAGGG CGGTGACCAC  1500
GCAGGATGCC GTGAACCCCA TCGAGAGCCT GGACACCTGG ACCGAGTTTG TGGAGGCAAA  1560
GAATAAGACT GTGAGCAAGC TGGTGATCCA GAATGCCAAC GTGTCTGCCA TGTACAAGTG  1620
TGTGGTCTCC AACAAGGTGG GCCAGGATGA GCGGCTCATC TACTTCTACG TGACCACCAT  1680
CCCCGACGGC TTCACCATCG AATCCAAGCC ATCCGAGGAG CTACTAGAGG GCCAGCCGGT  1740
GCTCCTGAGC TGCCAAGCCG ACAGCTACAA GTACGAGCAT CTGCGCTGGT ACCGCCTCAA  1800
CCTGTCCACG CTGCACGATG CGCACGGGAA CCCGCTTCTG CTCGACTGCA AGAACGTGCA  1860
TCTGTTCGCC ACCCCTCTGG CCGCCAGCCT GGAGGAGGTG GCACCTGGGG CGCGCCACGC  1920
CACGCTCAGC CTGAGTATCC CCGCGTCGC GCCCGAGCAC GAGGGCCACT ATGTGTGCGA  1980
AGTGCAAGAC CGGCGCAGCC ATGACAAGCA CTGCCACAAG AAGTACCTGT CGGTGCAGGC  2040
CCTGGAAGCC CCTCGGCTCA CGCAGAACTT GACCGACCTC CTGGTGAACG TGAGCGACTC  2100
GCTGGAGATG CAGTGCTTGG TGGCCGGAGC GCACGCGCCC AGCATCGTGT GGTACAAAGA  2160
CGAGAGGCTG CTGGAGGAAA AGTCTGGAGT CGACTTGGCG GACTCCAACC AGAAGCTGAG  2220
CATCCAGCGC GTGCGCGAGG AGGATGCGGG ACGCTATCTG TGCAGCGTGT GCAACGCCAA  2280
GGGCTGCGTC AACTCCTCCG CCAGCGTGGC CGTGGAAGGC TCCGAGGATA AGGGCAGCAT  2340
GGAGATCGTG ATCCTTGTCG GTACCGGCGT CATCGCTGTC TTCTTCTGGG TCCTCCTCCT  2400
CCTCATCTTC TGTAACATGA GGAGGCCGGC CCACGCAGAC ATCAAGACGG GCTACCTGTC  2460
CATCATCATG GACCCCGGGG AGGTGCCTCT GGAGGAGCAA TGCGAATACC TGTCCTACGA  2520
TGCCAGCCAG TGGGAATTCC CCGAGAGCG GCTGCACCTG GGGAGAGTGC TCGGCTACGG  2580
```

-continued

CGCCTTCGGG AAGGTGGTGG AAGCCTCCGC TTTCGGCATC CACAAGGGCA GCAGCTGTGA 2640

CACCGTGGCC GTGAAAATGC TGAAAGAGGG CGCCACGGCC AGCGAGCACC GCGCGCTGAT 2700

GTCGGAGCTC AAGATCCTCA TTCACATCGG CAACCACCTC AACGTGGTCA ACCTCCTCGG 2760

GGCGTGCACC AAGCCGCAGG GCCCCCTCAT GGTGATCGTG GAGTTCTGCA AGTACGGCAA 2820

CCTCTCCAAC TTCCTGCGCG CCAAGCGGGA CGCCTTCAGC CCCTGCGCGG AGAAGTCTCC 2880

CGAGCAGCGC GGACGCTTCC GCGCCATGGT GGAGCTCGCC AGGCTGGATC GGAGGCGGCC 2940

GGGGAGCAGC GACAGGGTCC TCTTCGCGCG GTTCTCGAAG ACCGAGGGCG GAGCGAGGCG 3000

GGCTTCTCCA GACCAAGAAG CTGAGGACCT GTGGCTGAGC CCGCTGACCA TGGAAGATCT 3060

TGTCTGCTAC AGCTTCCAGG TGGCCAGAGG GATGGAGTTC CTGGCTTCCC GAAAGTGCAT 3120

CCACAGAGAC CTGGCTGCTC GGAACATTCT GCTGTCGGAA AGCGACGTGG TGAAGATCTG 3180

TGACTTTGGC CTTGCCCGGG ACATCTACAA AGACCCTGAC TACGTCCGCA AGGGCAGTGC 3240

CCGGCTGCCC CTGAAGTGGA TGGCCCCTGA AAGCATCTTC GACAAGGTGT ACACCACGCA 3300

GAGTGACGTG TGGTCCTTTG GGGTGCTTCT CTGGGAGATC TTCTCTCTGG GGGCCTCCCC 3360

GTACCCTGGG GTGCAGATCA ATGAGGAGTT CTGCCAGCGG CTGAGAGACG GCACAAGGAT 3420

GAGGGCCCCG GAGCTGGCCA CTCCCGCCAT ACGCCGCATC ATGCTGAACT GCTGGTCCGG 3480

AGACCCCAAG GCGAGACCTG CATTCTCGGA GCTGGTGGAG ATCCTGGGGG ACCTGCTCCA 3540

GGGCAGGGGC CTGCAAGAGG AAGAGGAGGT CTGCATGGCC CCGCGCAGCT CTCAGAGCTC 3600

AGAAGAGGGC AGCTTCTCGC AGGTGTCCAC CATGGCCCTA CACATCGCCC AGGCTGACGC 3660

TGAGGACAGC CCGCCAAGCC TGCAGCGCCA CAGCCTGGCC GCCAGGTATT ACAACTGGGT 3720

GTCCTTTCCC GGGTGCCTGG CCAGAGGGGC TGAGACCCGT GGTTCCTCCA GGATGAAGAC 3780

ATTTGAGGAA TTCCCCATGA CCCCAACGAC CTACAAAGGC TCTGTGGACA ACCAGACAGA 3840

CAGTGGGATG GTGCTGGCCT CGGAGGAGTT TGAGCAGATA GAGAGCAGGC ATAGACAAGA 3900

AAGCGGCTTC AGGTAGCTGA AGCAGAGAGA GACAAGGCAG CATACGTCAG CATTTCGTTC 3960

TCTGCACTTA TAAGAAAGAT CAAAGACTTT AAGACTTTCG CTATTTCTTC TACTGCTATC 4020

TACTACAAAC TTCAAAGAGG AACCAGGAGG ACAAGAGGAG CATGAAAGTG GACAAGGAGT 4080

GTGACCACTG AAGCACCACA GGGAAGGGGT TAGGCCTCCG GATGACTGCG GGCAGGCCTG 4140

GATAATATCC AGCCTCCCAC AAGAAGCTGG TGGAGCAGAG TGTTCCCTGA CTCCTCCAAG 4200

GAAAGGGAGA CGCCCTTTCA TGGTCTGCTG AGTAACAGGT GCNTTCCCAG ACACTGGCGT 4260

TACTGCTTGA CCAAAGAGCC CTCAAGCGGC CCTTATGCCA GCGTGACAGA GGGCTCACCT 4320

CTTGCCTTCT AGGTCACTTC TCACACAATG TCCCTTCAGC ACCTGACCCT GTGCCCGCCA 4380

GTTATTCCTT GGTAATACGA GTAATACATC AAAGAG 4416

(2) INFORMATION FOR SEQ ID NO:2:

(i) SEQUENCE CHARACTERISTICS:
(A) LENGTH: 216 base pairs
(B) TYPE: nucleic acid
(C) STRANDEDNESS: single
(D) TOPOLOGY: linear

(ii) MOLECULE TYPE: cDNA

(xi) SEQUENCE DESCRIPTION: SEQ ID NO:2:

CAAGAAAGCG GCTTCAGCTG TAAAGGACCT GGCCAGAATG TGGCTGTGAC CAGGGCACAC 60

CCTGACTCCC AAGGGAGGCG GCGGCGGCCT GAGCGGGGGG CCCGAGGAGG CCAGGTGTTT 120

-continued

```
TACAACAGCG AGTATGGGGA GCTGTCGGAG CCAAGCGAGG AGGACCACTG CTCCCCGTCT   180

GCCCGCGTGA CTCTCTTCAC AGACAACAGC TACTAA                             216
```

(2) INFORMATION FOR SEQ ID NO:3:

(i) SEQUENCE CHARACTERISTICS:
(A) LENGTH: 4273 base pairs
(B) TYPE: nucleic acid
(C) STRANDEDNESS: single
(D) TOPOLOGY: linear

(ii) MOLECULE TYPE: cDNA

(xi) SEQUENCE DESCRIPTION: SEQ ID NO:3:

```
AAGCTTATCG ATTTCGAACC CGGGGGTACC GAATTCCTCG AGTCTAGAGG AGCATGCCTG    60

CAGGTCGACC GGGCTCGATC CCCTCGCGAG TTGGTTCAGC TGCTGCCTGA GGCTGGACGA   120

CCTCGCGGAG TTCTACCGGC AGTGCAAATC CGTCGGCATC CAGGAAACCA GCAGCGGCTA   180

TCCGCGCATC CATGCCCCCG AACTGCAGGA GTGGGGAGGC ACGATGGCCG CTTTGGTCCC   240

GGATCTTTGT GAAGGAACCT TACTTCTGTG GTGTGACATA ATTGGACAAA CTACCTACAG   300

AGATTTAAAG CTCTAAGGTA AATATAAAAT TTTTAAGTGT ATAATGTGTT AAACTACTGA   360

TTCTAATTGT TTGTGTATTT TAGATTCCAA CCTATGGAAC TGATGAATGG GAGCAGTGGT   420

GGAATGCCTT TAATGAGGAA AACCTGTTTT GCTCAGAAGA AATGCCATCT AGTGATGATG   480

AGGCTACTGC TGACTCTCAA CATTCTACTC CTCCAAAAAA GAAGAGAAAG GTAGAAGACC   540

CCAAGGACTT TCCTTCAGAA TTGCTAAGTT TTTTGAGTCA TGCTGTGTTT AGTAATAGAA   600

CTCTTGCTTG CTTTGCTATT TACACCACAA AGGAAAAAGC TGCACTGCTA TACAAGAAAA   660

TTATGGAAAA ATATTCTGTA ACCTTTATAA GTAGGCATAA CAGTTATAAT CATAACATAC   720

TGTTTTTTCT TACTCCACAC AGGCATAGAG TGTCTGCTAT TAATAACTAT GCTCAAAAAT   780

TGTGTACCTT TAGCTTTTTA ATTTGTAAAG GGGTTAATAA GGAATATTTG ATGTATAGTG   840

CCTTGACTAG AGATCATAAT CAGCCATACC ACATTTGTAG AGGTTTTACT TGCTTTAAAA   900

AACCTCCCAC ACCTCCCCCT GAACCTGAAA CATAAAATGA ATGCAATTGT TGTTGTTAAC   960

TTGTTTATTG CAGCTTATAA TGGTTACAAA TAAAGCAATA GCATCACAAA TTTCACAAAT  1020

AAAGCATTTT TTTCACTGCA TTCTAGTTGT GGTTTGTCCA AACTCATCAA TGTATCTTAT  1080

CATGTCTGGA TCTGCCGGTC TCCCTATAGT GAGTCGTATT AATTTCGATA AGCCAGGTTA  1140

ACCTGCATTA ATGAATCGGC CAACGCGCGG GGAGAGGCGG TTTGCGTATT GGGCGCTCTT  1200

CCGCTTCCTC GCTCACTGAC TCGCTGCGCT CGGTCGTTCG GCTGCGGCGA GCGGTATCAG  1260

CTCACTCAAA GGCGGTAATA CGGTTATCCA CAGAATCAGG GGATAACGCA GGAAAGAACA  1320

TGTGAGCAAA AGGCCAGCAA AAGGCCAGGA ACCGTAAAAA GGACGCGTTG CTGGCGTTTT  1380

TCCATAGGCT CCGCCCCCCT GACGAGCATC ACAAAAATCG ACGCTCAAGT CAGAGGTGGC  1440

GAAACCCGAC AGGACTATAA AGATACCAGG CGTTTCCCCC TGGAAGCTCC CTCGTGCGCT  1500

CTCCTGTTCC GACCCTGCCG CTTACCGGAT ACCTGTCCGC CTTTCTCCCT TCGGGAAGCG  1560

TGGCGCTTTC TCAATGCTCA CGCTGTAGGT ATCTCAGTTC GGTGTAGGTC GTTCGCTCCA  1620

AGCTGGGCTG TGTGCACGAA CCCCCCGTTC AGCCCGACCG CTGCGCCTTA TCCGGTAACT  1680

ATCGTCTTGA GTCCAACCCG GTAAGACACG ACTTATCGCC ACTGGCAGCA GCCACTGGTA  1740

ACAGGATTAG CAGAGCGAGG TATGTAGGCG GTGCTACAGA GTTCTTGAAG TGGTGGCCTA  1800

ACTACGGCTA CACTAGAAGG ACAGTATTTG GTATCTGCGC TCTGCTGAAG CCAGTTACCT  1860
```

-continued

TTGGAAAAAG AGTTGGTAGC TCTTGATCCG GCAAACAAAC CACCGCTGGT AGCGGTGGTT 1920

TTTTTGTTTG CAAGCAGCAG ATTACGCGCA GAAAAAAAGG ATCTCAAGAA GATCCTTTGA 1980

TTTTTTCTAC GGGGTCTGAC GCTCAGTGGA ACGAAAACTC ACGTTAAGGG ATTTTGGTCA 2040

TGAGATTATC AAAAAGGATC TTCACCTAGA TCCTTTTAAA TTAAAAATGA AGTTTTAAAT 2100

CAATCTAAAG TATATATGAG TAAACTTGGT CTGACAGTTA CCAATGCTTA ATCAGTGAGG 2160

CACCTATCTC AGCGATCTGT CTATTTCGTT CATCCATAGT TGCCTGACTC CCCGTCGTGT 2220

AGATAACTAC GATACGGGAG GGCTTACCAT CTGGCCCCAG TGCTGCAATG ATACCGCGAG 2280

ACCCACGCTC ACCGGCTCCA GATTTATCAG CAATAAACCA GCCAGCCGGA AGGGCCGAGC 2340

GCAGAAGTGG TCCTGCAACT TTATCCGCCT CCATCCAGTC TATTAATTGT TGCCGGGAAG 2400

CTAGAGTAAG TAGTTCGCCA GTTAATAGTT TGCGCAACGT TGTTGCCATT GCTACAGGCA 2460

TCGTGGTGTC ACGCTCGTCG TTTGGTATGG CTTCATTCAG CTCCGGTTCC CAACGATCAA 2520

GGCGAGTTAC ATGATCCCCC ATGTTGTGCA AAAAAGCGGT TAGCTCCTTC GGTCCTCCGA 2580

TCGTTGTCAG AAGTAAGTTG GCCGCAGTGT TATCACTCAT GGTTATGGCA GCACTGCATA 2640

ATTCTCTTAC TGTCATGCCA TCCGTAAGAT GCTTTTCTGT GACTGGTGAG TACTCAACCA 2700

AGTCATTCTG AGAATAGTGT ATGCGGCGAC CGAGTTGCTC TTGCCCGGCG TCAATACGGG 2760

ATAATACCGC GCCACATAGC AGAACTTTAA AAGTGCTCAT CATTGGAAAA CGTTCTTCGG 2820

GGCGAAAACT CTCAAGGATC TTACCGCTGT TGAGATCCAG TTCGATGTAA CCCACTCGTG 2880

CACCCAACTG ATCTTCAGCA TCTTTTACTT TCACCAGCGT TTCTGGGTGA GCAAAAACAG 2940

GAAGGCAAAA TGCCGCAAAA AAGGGAATAA GGGCGACACG GAAATGTTGA ATACTCATAC 3000

TCTTCCTTTT TCAATATTAT TGAAGCATTT ATCAGGGTTA TTGTCTCATG AGCGGATACA 3060

TATTTGAATG TATTTAGAAA AATAAACAAA TAGGGGTTCC GCGCACATTT CCCCGAAAAG 3120

TGCCACCTGA CGTCTAAGAA ACCATTATTA TCATGACATT AACCTATAAA AATAGGCGTA 3180

TCACGAGGCC CTTTCGTCTC GCGCGTTTCG GTGATGACGG TGAAAACCTC TGACACATGC 3240

AGCTCCCGGA GACGGTCACA GCTTGTCTGT AAGCGGATGC CGGGAGCAGA CAAGCCCGTC 3300

AGGGCGCGTC AGCGGGTGTT GGCGGGTGTC GGGGCTGGCT TAACTATGCG GCATCAGAGC 3360

AGATTGTACT GAGAGTGCAC CATATGGACA TATTGTCGTT AGAACGCGGC TACAATTAAT 3420

ACATAACCTT ATGTATCATA CACATACGAT TTAGGTGACA CTATAGAACT CGAGCAGAGC 3480

TTCCAAATTG AGAGAGAGGC TTAATCAGAG ACAGAAACTG TTTGAGTCAA CTCAAGGATG 3540

GTTTGAGGGA CTGTTTAACA GATCCGCTTG GTTTACCACC TTGATATCTA CCATTATGGG 3600

ACCCCTCATT GTACTCCTAA TGATTTTGCT CTTCGGACCC TGCATTCTTA ATCGATTAGT 3660

CCAATTTGTT AAAGACAGGA TATCAGTGGT CCAGGCTCTA GTTTTGACTC AACAATATCA 3720

CCAGCTGAAG CCTATAGAGT ACGAGCCATA GATAAAATAA AAGATTTTAT TTAGTCTCCA 3780

GAAAAAGGGG GGAATGAAAG ACCCCACCTG TAGGTTTGGC AAGCTAGCTT AAGTAACGCC 3840

ATTTTGCAAG GCATGGAAAA TACATAACTC GAGAATAGAG AAGTTCAGAT CAAGGTCAGG 3900

AACAGATGGA ACAGCTGAAT ATGGGCCAAA CAGGATATCT GTGGTAAGCA GTTCCTGCCC 3960

CGGCTCAGGG CCAAGAACAG ATGGAACAGC TGAATATGGG CCAAACAGGA TATCTGTGGT 4020

AAGCAGTTCC TGCCCCGGCT CAGGGCCAAG AACAGATGGT CCCCAGATGC GGTCCAGCCC 4080

TCAGCAGTTT CTAGAGAACC ATCAGATGTT TCCAGGGTGC CCCAAGGACC TGAAATGACC 4140

CTGTGCCTTA TTTGAACTAA CCAATCAGTT CGCTTCTCGC TTCTGTTCGC GCGCTTCTGC 4200

TCCCCGAGCT CAATAAAAGA GCCCACAACC CCTCACTCGG GGCGCCAGTC CTCCGATTGA 4260

-continued

CTGAGTTGCC CGG 4273

(2) INFORMATION FOR SEQ ID NO:4:

(i) SEQUENCE CHARACTERISTICS:
(A) LENGTH: 40 amino acids
(B) TYPE: amino acid
(C) STRANDEDNESS: Not Relevant
(D) TOPOLOGY: linear

(ii) MOLECULE TYPE: peptide

(xi) SEQUENCE DESCRIPTION: SEQ ID NO:4:

Pro Met Thr Pro Thr Thr Tyr Lys Gly Ser Val Asp Asn Gln Thr Asp
1 5 10 15

Ser Gly Met Val Leu Ala Ser Glu Glu Phe Glu Gln Ile Glu Ser Arg
20 25 30

His Arg Gln Glu Ser Gly Phe Arg
35 40

(2) INFORMATION FOR SEQ ID NO:5:

(i) SEQUENCE CHARACTERISTICS:
(A) LENGTH: 18 amino acids
(B) TYPE: amino acid
(C) STRANDEDNESS: Not Relevant
(D) TOPOLOGY: linear

(ii) MOLECULE TYPE: peptide

(xi) SEQUENCE DESCRIPTION: SEQ ID NO:5:

Xaa Glu Glu Thr Ile Lys Phe Ala Ala Ala His Tyr Asn Thr Glu Ile
1 5 10 15

Leu Lys

(2) INFORMATION FOR SEQ ID NO:6:

(i) SEQUENCE CHARACTERISTICS:
(A) LENGTH: 219 base pairs
(B) TYPE: nucleic acid
(C) STRANDEDNESS: single
(D) TOPOLOGY: linear

(ii) MOLECULE TYPE: cDNA

(xi) SEQUENCE DESCRIPTION: SEQ ID NO:6:

TCACTATAGG GAGACCCAAG CTTGGTACCG AGCTCGGATC CACTAGTAAC GGCCGCCAGT 60

GTGGTGGAAT TCGACGAACT CATGACTGTA CTCTACCCAG AATATTGGAA AATGTACAAG 120

TGTCAGCTAA GGCAAGGAGG CTGGCAACAT AACAGAGAAC AGGCCAACCT CAACTCAAGG 180

ACAGAAGAGA CTATAAAATT GGCTGCAGCA CACTACAAC 219

(2) INFORMATION FOR SEQ ID NO:7:

(i) SEQUENCE CHARACTERISTICS:
(A) LENGTH: 1997 base pairs
(B) TYPE: nucleic acid
(C) STRANDEDNESS: single
(D) TOPOLOGY: linear

(ii) MOLECULE TYPE: cDNA

(ix) FEATURE:
(A) NAME/KEY: CDS
(B) LOCATION: 352..1608

-continued

(xi) SEQUENCE DESCRIPTION: SEQ ID NO:7:

```
CCCGCCCCGC CTCTCCAAAA AGCTACACCG ACGCGGACCG CGGCGGCGCC CTCCCTCGCC     60

CTCGCTTCAC CTCGCGGGCT CCGAATGCGG GGAGCTCGGA TGTCCGGTTT CCTGTGAGGC    120

TTTTACCTGA CACCCGCCGC CTTTCCCCGG CACTGGCTGG GAGGGCGCCC TGCAAAGTTG    180

GGAACGCGGA GCCCCGGACC CGCTCCCGCC GCCTCCGGCT CGCCCAGGGG GGGTCGCCGG    240

GAGGAGCCCG GGGGAGAGGG ACCAGGAGGG GCCCGCGGCC TCGCAGGGGC GCCCGCCCCC    300

CCACCCCTGC CCCCGCCAGC GGACCGGTCC CCCACCCCCG GTCCTTCCAC C ATG CAC     357
                                                          Met His
                                                           1

TTG CTG GGC TTC TTC TCT GTG GCG TGT TCT CTG CTC GCC GCT GCG CTG      405
Leu Leu Gly Phe Phe Ser Val Ala Cys Ser Leu Leu Ala Ala Ala Leu
          5                  10                  15

CTC CCG GGT CCT CGC GAG GCG CCC GCC GCC GCC GCC GCC TTC GAG TCC      453
Leu Pro Gly Pro Arg Glu Ala Pro Ala Ala Ala Ala Ala Phe Glu Ser
     20                  25                  30

GGA CTC GAC CTC TCG GAC GCG GAG CCC GAC GCG GGC GAG GCC ACG GCT      501
Gly Leu Asp Leu Ser Asp Ala Glu Pro Asp Ala Gly Glu Ala Thr Ala
 35                  40                  45                  50

TAT GCA AGC AAA GAT CTG GAG GAG CAG TTA CGG TCT GTG TCC AGT GTA      549
Tyr Ala Ser Lys Asp Leu Glu Glu Gln Leu Arg Ser Val Ser Ser Val
                 55                  60                  65

GAT GAA CTC ATG ACT GTA CTC TAC CCA GAA TAT TGG AAA ATG TAC AAG      597
Asp Glu Leu Met Thr Val Leu Tyr Pro Glu Tyr Trp Lys Met Tyr Lys
             70                  75                  80

TGT CAG CTA AGG AAA GGA GGC TGG CAA CAT AAC AGA GAA CAG GCC AAC      645
Cys Gln Leu Arg Lys Gly Gly Trp Gln His Asn Arg Glu Gln Ala Asn
         85                  90                  95

CTC AAC TCA AGG ACA GAA GAG ACT ATA AAA TTT GCT GCA GCA CAT TAT      693
Leu Asn Ser Arg Thr Glu Glu Thr Ile Lys Phe Ala Ala Ala His Tyr
    100                 105                 110

AAT ACA GAG ATC TTG AAA AGT ATT GAT AAT GAG TGG AGA AAG ACT CAA      741
Asn Thr Glu Ile Leu Lys Ser Ile Asp Asn Glu Trp Arg Lys Thr Gln
115                 120                 125                 130

TGC ATG CCA CGG GAG GTG TGT ATA GAT GTG GGG AAG GAG TTT GGA GTC      789
Cys Met Pro Arg Glu Val Cys Ile Asp Val Gly Lys Glu Phe Gly Val
                135                 140                 145

GCG ACA AAC ACC TTC TTT AAA CCT GCA TGT GTG TCC GTC TAC AGA TGT      837
Ala Thr Asn Thr Phe Phe Lys Pro Pro Cys Val Ser Val Tyr Arg Cys
            150                 155                 160

GGG GGT TGC TGC AAT AGT GAG GGG CTG CAG TGC ATG AAC ACC AGC ACG      885
Gly Gly Cys Cys Asn Ser Glu Gly Leu Gln Cys Met Asn Thr Ser Thr
        165                 170                 175

AGC TAC CTC AGC AAG ACG TTA TTT GAA ATT ACA GTG CCT CTC TCT CAA      933
Ser Tyr Leu Ser Lys Thr Leu Phe Glu Ile Thr Val Pro Leu Ser Gln
    180                 185                 190

GGC CCC AAA CCA GTA ACA ATC AGT TTT GCC AAT CAC ACT TCC TGC CGA      981
Gly Pro Lys Pro Val Thr Ile Ser Phe Ala Asn His Thr Ser Cys Arg
195                 200                 205                 210

TGC ATG TCT AAA CTG GAT GTT TAC AGA CAA GTT CAT TCC ATT ATT AGA     1029
Cys Met Ser Lys Leu Asp Val Tyr Arg Gln Val His Ser Ile Ile Arg
                215                 220                 225

CGT TCC CTG CCA GCA ACA CTA CCA CAG TGT CAG GCA GCG AAC AAG ACC     1077
Arg Ser Leu Pro Ala Thr Leu Pro Gln Cys Gln Ala Ala Asn Lys Thr
            230                 235                 240

TGC CCC ACC AAT TAC ATG TGG AAT AAT CAC ATC TGC AGA TGC CTG GCT     1125
Cys Pro Thr Asn Tyr Met Trp Asn Asn His Ile Cys Arg Cys Leu Ala
        245                 250                 255
```

-continued

```
CAG GAA GAT TTT ATG TTT TCC TCG GAT GCT GGA GAT GAC TCA ACA GAT     1173
Gln Glu Asp Phe Met Phe Ser Ser Asp Ala Gly Asp Asp Ser Thr Asp
    260                 265                 270

GGA TTC CAT GAC ATC TGT GGA CCA AAC AAG GAG CTG GAT GAA GAG ACC     1221
Gly Phe His Asp Ile Cys Gly Pro Asn Lys Glu Leu Asp Glu Glu Thr
275                 280                 285                 290

TGT CAG TGT GTC TGC AGA GCG GGG CTT CGG CCT GCC AGC TGT GGA CCC     1269
Cys Gln Cys Val Cys Arg Ala Gly Leu Arg Pro Ala Ser Cys Gly Pro
                295                 300                 305

CAC AAA GAA CTA GAC AGA AAC TCA TGC CAG TGT GTC TGT AAA AAC AAA     1317
His Lys Glu Leu Asp Arg Asn Ser Cys Gln Cys Val Cys Lys Asn Lys
            310                 315                 320

CTC TTC CCC AGC CAA TGT GGG GCC AAC CGA GAA TTT GAT GAA AAC ACA     1365
Leu Phe Pro Ser Gln Cys Gly Ala Asn Arg Glu Phe Asp Glu Asn Thr
        325                 330                 335

TGC CAG TGT GTA TGT AAA AGA ACC TGC CCC AGA AAT CAA CCC CTA AAT     1413
Cys Gln Cys Val Cys Lys Arg Thr Cys Pro Arg Asn Gln Pro Leu Asn
    340                 345                 350

CCT GGA AAA TGT GCC TGT GAA TGT ACA GAA AGT CCA CAG AAA TGC CTG     1461
Pro Gly Lys Cys Ala Cys Glu Cys Thr Glu Ser Pro Gln Lys Cys Leu
355                 360                 365                 370

TTA AAA GGA AAG AAG TTC CAC CAC CAA ACA TGC AGC TGT TAC AGA CGG     1509
Leu Lys Gly Lys Lys Phe His His Gln Thr Cys Ser Cys Tyr Arg Arg
                375                 380                 385

CCA TGT ACG AAC CGC CAG AAG GCT TGT GAG CCA GGA TTT TCA TAT AGT     1557
Pro Cys Thr Asn Arg Gln Lys Ala Cys Glu Pro Gly Phe Ser Tyr Ser
            390                 395                 400

GAA GAA GTG TGT CGT TGT GTC CCT TCA TAT TGG AAA AGA CCA CAA ATG     1605
Glu Glu Val Cys Arg Cys Val Pro Ser Tyr Trp Lys Arg Pro Gln Met
        405                 410                 415

AGC TAAGATTGTA CTGTTTTCCA GTTCATCGAT TTTCTATTAT GGAAAACTGT          1658
Ser

GTTGCCACAG TAGAACTGTC TGTGAACAGA GAGACCCTTG TGGGTCCATG CTAACAAAGA  1718

CAAAAGTCTG TCTTTCCTGA ACCATGTGGA TAACTTTACA GAAATGGACT GGAGCTCATC  1778

TGCAAAAGGC CTCTTGTAAA GACTGGTTTT CTGCCAATGA CCAAACAGCC AAGATTTTCC  1838

TCTTGTGATT TCTTTAAAAG AATGACTATA TAATTTATTT CCACTAAAAA TATTGTTTCT  1898

GCATTCATTT TTATAGCAAC AACAATTGGT AAAACTCACT GTGATCAATA TTTTTATATC  1958

ATGCAAAATA TGTTTAAAAT AAAATGAAAA TTGTATTAT                          1997
```

(2) INFORMATION FOR SEQ ID NO:8:

(i) SEQUENCE CHARACTERISTICS:
(A) LENGTH: 419 amino acids
(B) TYPE: amino acid
(D) TOPOLOGY: linear

(ii) MOLECULE TYPE: protein

(xi) SEQUENCE DESCRIPTION: SEQ ID NO:8:

```
Met His Leu Leu Gly Phe Phe Ser Val Ala Cys Ser Leu Leu Ala Ala
 1               5                  10                  15

Ala Leu Leu Pro Gly Pro Arg Glu Ala Pro Ala Ala Ala Ala Ala Phe
            20                  25                  30

Glu Ser Gly Leu Asp Leu Ser Asp Ala Glu Pro Asp Ala Gly Glu Ala
        35                  40                  45

Thr Ala Tyr Ala Ser Lys Asp Leu Glu Glu Gln Leu Arg Ser Val Ser
    50                  55                  60
```

-continued

```
Ser Val Asp Glu Leu Met Thr Val Leu Tyr Pro Glu Tyr Trp Lys Met
 65                  70                  75                  80

Tyr Lys Cys Gln Leu Arg Lys Gly Gly Trp Gln His Asn Arg Glu Gln
                 85                  90                  95

Ala Asn Leu Asn Ser Arg Thr Glu Glu Thr Ile Lys Phe Ala Ala Ala
            100                 105                 110

His Tyr Asn Thr Glu Ile Leu Lys Ser Ile Asp Asn Glu Trp Arg Lys
        115                 120                 125

Thr Gln Cys Met Pro Arg Glu Val Cys Ile Asp Val Gly Lys Glu Phe
    130                 135                 140

Gly Val Ala Thr Asn Thr Phe Phe Lys Pro Pro Cys Val Ser Val Tyr
145                 150                 155                 160

Arg Cys Gly Gly Cys Cys Asn Ser Glu Gly Leu Gln Cys Met Asn Thr
                165                 170                 175

Ser Thr Ser Tyr Leu Ser Lys Thr Leu Phe Glu Ile Thr Val Pro Leu
            180                 185                 190

Ser Gln Gly Pro Lys Pro Val Thr Ile Ser Phe Ala Asn His Thr Ser
        195                 200                 205

Cys Arg Cys Met Ser Lys Leu Asp Val Tyr Arg Gln Val His Ser Ile
    210                 215                 220

Ile Arg Arg Ser Leu Pro Ala Thr Leu Pro Gln Cys Gln Ala Ala Asn
225                 230                 235                 240

Lys Thr Cys Pro Thr Asn Tyr Met Trp Asn Asn His Ile Cys Arg Cys
                245                 250                 255

Leu Ala Gln Glu Asp Phe Met Phe Ser Ser Asp Ala Gly Asp Asp Ser
            260                 265                 270

Thr Asp Gly Phe His Asp Ile Cys Gly Pro Asn Lys Glu Leu Asp Glu
        275                 280                 285

Glu Thr Cys Gln Cys Val Cys Arg Ala Gly Leu Arg Pro Ala Ser Cys
    290                 295                 300

Gly Pro His Lys Glu Leu Asp Arg Asn Ser Cys Gln Cys Val Cys Lys
305                 310                 315                 320

Asn Lys Leu Phe Pro Ser Gln Cys Gly Ala Asn Arg Glu Phe Asp Glu
                325                 330                 335

Asn Thr Cys Gln Cys Val Cys Lys Arg Thr Cys Pro Arg Asn Gln Pro
            340                 345                 350

Leu Asn Pro Gly Lys Cys Ala Cys Glu Cys Thr Glu Ser Pro Gln Lys
        355                 360                 365

Cys Leu Leu Lys Gly Lys Lys Phe His His Gln Thr Cys Ser Cys Tyr
    370                 375                 380

Arg Arg Pro Cys Thr Asn Arg Gln Lys Ala Cys Glu Pro Gly Phe Ser
385                 390                 395                 400

Tyr Ser Glu Glu Val Cys Arg Cys Val Pro Ser Tyr Trp Lys Arg Pro
                405                 410                 415

Gln Met Ser
```

(2) INFORMATION FOR SEQ ID NO:9:

(i) SEQUENCE CHARACTERISTICS:
(A) LENGTH: 17 amino acids
(B) TYPE: amino acid
(C) STRANDEDNESS: Not Relevant
(D) TOPOLOGY: linear

(ii) MOLECULE TYPE: peptide

-continued

(xi) SEQUENCE DESCRIPTION: SEQ ID NO:9:

```
Glu Glu Thr Ile Lys Phe Ala Ala Ala His Tyr Asn Thr Glu Ile Leu
 1               5                  10                  15

Lys
```

(2) INFORMATION FOR SEQ ID NO:10:

(i) SEQUENCE CHARACTERISTICS:
(A) LENGTH: 1835 base pairs
(B) TYPE: nucleic acid
(C) STRANDEDNESS: single
(D) TOPOLOGY: linear

(ii) MOLECULE TYPE: cDNA

(ix) FEATURE:
(A) NAME/KEY: CDS
(B) LOCATION: 158..1412

(xi) SEQUENCE DESCRIPTION: SEQ ID NO:10:

```
GCGGCCGCGT CGACGCAAAA GTTGCGAGCC GCCGAGTCCC GGGAGACGCT CGCCCAGGGG      60

GGTCCCCGGG AGGAAACCAC GGGACAGGGA CCAGGAGAGG ACCTCAGCCT CACGCCCCAG     120

CCTGCGCCAG CCAACGGACC GGCCTCCCTG CTCCCGGTCC ATCCACC ATG CAC TTG       176
                                                    Met His Leu
                                                     1

CTG TGC TTC TTG TCT CTG GCG TGT TCC CTG CTC GCC GCT GCG CTG ATC       224
Leu Cys Phe Leu Ser Leu Ala Cys Ser Leu Leu Ala Ala Ala Leu Ile
  5                  10                  15

CCC AGT CCG CGC GAG GCG CCC GCC ACC GTC GCC GCC TTC GAG TCG GGA      272
Pro Ser Pro Arg Glu Ala Pro Ala Thr Val Ala Ala Phe Glu Ser Gly
 20                  25                  30                  35

CTG GGC TTC TCG GAA GCG GAG CCC GAC GGG GGC GAG GTC AAG GCT TTT      320
Leu Gly Phe Ser Glu Ala Glu Pro Asp Gly Gly Glu Val Lys Ala Phe
                 40                  45                  50

GAA GGC AAA GAC CTG GAG GAG CAG TTG CGG TCT GTG TCC AGC GTA GAT      368
Glu Gly Lys Asp Leu Glu Glu Gln Leu Arg Ser Val Ser Ser Val Asp
             55                  60                  65

GAG CTG ATG TCT GTC CTG TAC CCA GAC TAC TGG AAA ATG TAC AAG TGC      416
Glu Leu Met Ser Val Leu Tyr Pro Asp Tyr Trp Lys Met Tyr Lys Cys
         70                  75                  80

CAG CTG CGG AAA GGC GGC TGG CAG CAG CCC ACC CTC AAT ACC AGG ACA      464
Gln Leu Arg Lys Gly Gly Trp Gln Gln Pro Thr Leu Asn Thr Arg Thr
     85                  90                  95

GGG GAC AGT GTA AAA TTT GCT GCT GCA CAT TAT AAC ACA GAG ATC CTG      512
Gly Asp Ser Val Lys Phe Ala Ala Ala His Tyr Asn Thr Glu Ile Leu
100                 105                 110                 115

AAA AGT ATT GAT AAT GAG TGG AGA AAG ACT CAA TGC ATG CCA CGT GAG      560
Lys Ser Ile Asp Asn Glu Trp Arg Lys Thr Gln Cys Met Pro Arg Glu
                120                 125                 130

GTG TGT ATA GAT GTG GGG AAG GAG TTT GGA GCA GCC ACA AAC ACC TTC      608
Val Cys Ile Asp Val Gly Lys Glu Phe Gly Ala Ala Thr Asn Thr Phe
            135                 140                 145

TTT AAA CCT CCA TGT GTG TCC GTC TAC AGA TGT GGG GGT TGC TGC AAC      656
Phe Lys Pro Pro Cys Val Ser Val Tyr Arg Cys Gly Gly Cys Cys Asn
        150                 155                 160

AGC GAG GGG CTG CAG TGC ATG AAC ACC AGC ACA GGT TAC CTC AGC AAG      704
Ser Glu Gly Leu Gln Cys Met Asn Thr Ser Thr Gly Tyr Leu Ser Lys
    165                 170                 175

ACG TTG TTT GAA ATT ACA GTG CCT CTC TCA CAA GGC CCC AAA CCA GTC      752
Thr Leu Phe Glu Ile Thr Val Pro Leu Ser Gln Gly Pro Lys Pro Val
```

-continued

```
180                 185                 190                 195

ACA ATC AGT TTT GCC AAT CAC ACT TCC TGC CGG TGC ATG TCT AAA CTG      600
Thr Ile Ser Phe Ala Asn His Thr Ser Cys Arg Cys Met Ser Lys Leu
                200                 205                 210

GAT GTT TAC AGA CAA GTT CAT TCA ATT ATT AGA CGT TCT CTG CCA GCA      648
Asp Val Tyr Arg Gln Val His Ser Ile Ile Arg Arg Ser Leu Pro Ala
            215                 220                 225

ACA TTA CCA CAG TGT CAG GCA GCT AAC AAG ACA TGT CCA ACA AAC TAT      696
Thr Leu Pro Gln Cys Gln Ala Ala Asn Lys Thr Cys Pro Thr Asn Tyr
        230                 235                 240

GTG TGG AAT AAC TAC ATG TGC CGA TGC CTG GCT CAG CAG GAT TTT ATC      744
Val Trp Asn Asn Tyr Met Cys Arg Cys Leu Ala Gln Gln Asp Phe Ile
    245                 250                 255

TTT TAT TCA AAT GTT GAA GAT GAC TCA ACC AAT GGA TTC CAT GAT GTC      792
Phe Tyr Ser Asn Val Glu Asp Asp Ser Thr Asn Gly Phe His Asp Val
260                 265                 270                 275

TGT GGA CCC AAC AAG GAG CTG GAT GAA GAC ACC TGT CAG TGT GTC TGC     1040
Cys Gly Pro Asn Lys Glu Leu Asp Glu Asp Thr Cys Gln Cys Val Cys
                280                 285                 290

AAG GGG GGG CTT CGG CCA TCT AGT TGT GGA CCC CAC AAA GAA CTA GAT     1088
Lys Gly Gly Leu Arg Pro Ser Ser Cys Gly Pro His Lys Glu Leu Asp
            295                 300                 305

AGA GAC TCA TGT CAG TGT GTC TGT AAA AAC AAA CTT TTC CCT AAT TCA     1136
Arg Asp Ser Cys Gln Cys Val Cys Lys Asn Lys Leu Phe Pro Asn Ser
        310                 315                 320

TGT GGA GCC AAC AGG GAA TTT GAT GAG AAT ACA TGT CAG TGT GTA TGT     1184
Cys Gly Ala Asn Arg Glu Phe Asp Glu Asn Thr Cys Gln Cys Val Cys
    325                 330                 335

AAA AGA ACG TGT CCA AGA AAT CAG CCC CTG AAT CCT GGG AAA TGT GCC     1232
Lys Arg Thr Cys Pro Arg Asn Gln Pro Leu Asn Pro Gly Lys Cys Ala
340                 345                 350                 355

TGT GAA TGT ACA GAA AAC ACA CAG AAG TGC TTC CTT AAA GGG AAG AAG     1280
Cys Glu Cys Thr Glu Asn Thr Gln Lys Cys Phe Leu Lys Gly Lys Lys
                360                 365                 370

TTC CAC CAT CAA ACA TGC AGT TGT TAC AGA AGA CCG TGT GCG AAT CGA     1328
Phe His His Gln Thr Cys Ser Cys Tyr Arg Arg Pro Cys Ala Asn Arg
            375                 380                 385

CTG AAG CAT TGT GAT CCA GGA CTG TCC TTT AGT GAA GAA GTA TGC CGC     1376
Leu Lys His Cys Asp Pro Gly Leu Ser Phe Ser Glu Glu Val Cys Arg
        390                 395                 400

TGT GTC CCA TCG TAT TGG AAA AGG CCA CAT CTG AAC TAAGATCATA          1422
Cys Val Pro Ser Tyr Trp Lys Arg Pro His Leu Asn
    405                 410                 415

CCAGTCTTCA GTCAGTCACA GTCACTTACT CTCTTGAAGA CTGTTGGAAC AGCACTTAGC   1482

ACTGTCTATG CACAGAAAGA CTCTGTGGGA CCACATGGTA ACAGAGGCCC AAGTCTGTGT   1542

TTATTGAACC ATGTGGATTA CTGCGGGAGA GGACTGGCAC TCATGTGCAA AAAAAACCTC   1602

TTCAAAGACT GGTTTTCTGC CAGGGACCAG ACAGCTGAGG TTTTTCTCCT,GTGATTTAAA   1662

AAAAGAATGA CTATATAATT TATTTCCACT AAAAATATTG TTCCTGCACT CATTTTTATA   1722

GCAATAACAA TTGGTAAAGC TCACTGTGAC CAGTATTTTT ATAACATGCA AAACTATGTT   1782

TAAAATAAAA TGAAAATTGT ATTACAAAAA AAAAAAAAAA AAAAAAAAAA GCTT         1836
```

(2) INFORMATION FOR SEQ ID NO:11:

(i) SEQUENCE CHARACTERISTICS:
(A) LENGTH: 415 amino acids
(B) TYPE: amino acid
(D) TOPOLOGY: linear

-continued

(ii) MOLECULE TYPE: protein

(xi) SEQUENCE DESCRIPTION: SEQ ID NO:11:

```
Met His Leu Leu Cys Phe Leu Ser Leu Ala Cys Ser Leu Leu Ala Ala
 1               5                  10                  15

Ala Leu Ile Pro Ser Pro Arg Glu Ala Pro Ala Thr Val Ala Ala Phe
            20                  25                  30

Glu Ser Gly Leu Gly Phe Ser Glu Ala Glu Pro Asp Gly Gly Glu Val
        35                  40                  45

Lys Ala Phe Glu Gly Lys Asp Leu Glu Glu Gln Leu Arg Ser Val Ser
    50                  55                  60

Ser Val Asp Glu Leu Met Ser Val Leu Tyr Pro Asp Tyr Trp Lys Met
65                  70                  75                  80

Tyr Lys Cys Gln Leu Arg Lys Gly Gly Trp Gln Gln Pro Thr Leu Asn
                85                  90                  95

Thr Arg Thr Gly Asp Ser Val Lys Phe Ala Ala Ala His Tyr Asn Thr
            100                 105                 110

Glu Ile Leu Lys Ser Ile Asp Asn Glu Trp Arg Lys Thr Gln Cys Met
        115                 120                 125

Pro Arg Glu Val Cys Ile Asp Val Gly Lys Glu Phe Gly Ala Ala Thr
    130                 135                 140

Asn Thr Phe Phe Lys Pro Pro Cys Val Ser Val Tyr Arg Cys Gly Gly
145                 150                 155                 160

Cys Cys Asn Ser Glu Gly Leu Gln Cys Met Asn Thr Ser Thr Gly Tyr
                165                 170                 175

Leu Ser Lys Thr Leu Phe Glu Ile Thr Val Pro Leu Ser Gln Gly Pro
            180                 185                 190

Lys Pro Val Thr Ile Ser Phe Ala Asn His Thr Ser Cys Arg Cys Met
        195                 200                 205

Ser Lys Leu Asp Val Tyr Arg Gln Val His Ser Ile Ile Arg Arg Ser
    210                 215                 220

Leu Pro Ala Thr Leu Pro Gln Cys Gln Ala Ala Asn Lys Thr Cys Pro
225                 230                 235                 240

Thr Asn Tyr Val Trp Asn Asn Tyr Met Cys Arg Cys Leu Ala Gln Gln
                245                 250                 255

Asp Phe Ile Phe Tyr Ser Asn Val Glu Asp Asp Ser Thr Asn Gly Phe
            260                 265                 270

His Asp Val Cys Gly Pro Asn Lys Glu Leu Asp Glu Asp Thr Cys Gln
        275                 280                 285

Cys Val Cys Lys Gly Gly Leu Arg Pro Ser Ser Cys Gly Pro His Lys
    290                 295                 300

Glu Leu Asp Arg Asp Ser Cys Gln Cys Val Cys Lys Asn Lys Leu Phe
305                 310                 315                 320

Pro Asn Ser Cys Gly Ala Asn Arg Glu Phe Asp Glu Asn Thr Cys Gln
                325                 330                 335

Cys Val Cys Lys Arg Thr Cys Pro Arg Asn Gln Pro Leu Asn Pro Gly
            340                 345                 350

Lys Cys Ala Cys Glu Cys Thr Glu Asn Thr Gln Lys Cys Phe Leu Lys
        355                 360                 365

Gly Lys Lys Phe His His Gln Thr Cys Ser Cys Tyr Arg Arg Pro Cys
    370                 375                 380

Ala Asn Arg Leu Lys His Cys Asp Pro Gly Leu Ser Phe Ser Glu Glu
385                 390                 395                 400
```

-continued

```
Val Cys Arg Cys Val Pro Ser Tyr Trp Lys Arg Pro His Leu Asn
            405                 410                 415

(2) INFORMATION FOR SEQ ID NO:12:

     (i) SEQUENCE CHARACTERISTICS:
          (A) LENGTH: 1741 base pairs
          (B) TYPE: nucleic acid
          (C) STRANDEDNESS: single
          (D) TOPOLOGY: linear

    (ii) MOLECULE TYPE: cDNA

    (ix) FEATURE:
          (A) NAME/KEY: CDS
          (B) LOCATION: 453..1706

    (xi) SEQUENCE DESCRIPTION: SEQ ID NO:12:

GCCCCCGCCG AGCGCTCCGC GCGCAGCCGC CGGGCCGGGC CGGCCCGCGG AGGGCGCGCT    60

GCGAGCGGCC ACTGGGTCGT GCTTCGCTCC TTCCTCTCCC TCCCGCTCGT CCTCCTTCTC   120

TCTGCGCTTT CCACCGCTCC CGAGCGAGCG CACGCTCGGA TGTCCGGTTT CCTGGTGGGT   180

TTTTTACCTG GCAAAGTCCG GATAACTTCG GTGAGAATTT GCAAAGAGGC TGGGAGCTCC   240

CCTGCAGGCG TCTGGGAGCT GCTGCCGCCG TCGCATCTTC TCCATCCCGC GGATTTTACT   300

GCCTTGGATA TTGCGAGGGG AGGGAGGGGG GTGAGGACAG CAAAAAGAAA GGGGTGGGGG   360

GGGGGAGAGA AAAGGAAAAG AAGGAGCCTC GGAATTGTGC CCGCATTCCT GCGCTGCCCC   420

GCGGCCGCCC TCCGCTCTGC CATCTCCGCA CA ATG CAC TTG CTG GAG ATG CTC      473
                                     Met His Leu Leu Glu Met Leu
                                     1               5

TCC CTG GGC TGC TGC CTC GCT GCT GGC GCC GTG CTC CTG GGA CCC CGG      521
Ser Leu Gly Cys Cys Leu Ala Ala Gly Ala Val Leu Leu Gly Pro Arg
        10                  15                  20

CAG CCG CCC GTC GCC GCC GCC TAC GAG TCC GGG CAC GGC TAC TAC GAG      569
Gln Pro Pro Val Ala Ala Ala Tyr Glu Ser Gly His Gly Tyr Tyr Glu
    25                  30                  35

GAG GAG CCC GGT GCC GGG GAA CCC AAG GCT CAT GCA AGC AAA GAC CTG      617
Glu Glu Pro Gly Ala Gly Glu Pro Lys Ala His Ala Ser Lys Asp Leu
40                  45                  50                  55

GAA GAG CAG TTG CGA TCT GTG TCC AGT GTG GAT GAA CTC ATG ACA GTA      665
Glu Glu Gln Leu Arg Ser Val Ser Ser Val Asp Glu Leu Met Thr Val
                60                  65                  70

CTT TAC CCA GAA TAC TGG AAA ATG TTC AAA TGT CAG TTG AGG AAA GGA      713
Leu Tyr Pro Glu Tyr Trp Lys Met Phe Lys Cys Gln Leu Arg Lys Gly
            75                  80                  85

GGT TGG CAA CAC AAC AGG GAA CAC TCC AGC TCT GAT ACA AGA TCA GAT      761
Gly Trp Gln His Asn Arg Glu His Ser Ser Ser Asp Thr Arg Ser Asp
        90                  95                  100

GAT TCA TTG AAA TTT GCC GCA GCA CAT TAT AAT GCA GAG ATC CTG AAA      809
Asp Ser Leu Lys Phe Ala Ala Ala His Tyr Asn Ala Glu Ile Leu Lys
    105                 110                 115

AGT ACT GAT ACT GAA TGG AGA AAA ACC CAG GGC ATG CCA CGT GAA GTG      857
Ser Ile Asp Thr Glu Trp Arg Lys Thr Gln Gly Met Pro Arg Glu Val
120                 125                 130                 135

TGT GTG GAT TTG GGG AAA GAG TTT GGA GCA ACT ACA AAC ACC TTC TTT      905
Cys Val Asp Leu Gly Lys Glu Phe Gly Ala Thr Thr Asn Thr Phe Phe
                140                 145                 150

AAA CCC CCG TGT GTA TCC ATC TAC AGA TGT GGA GGT TGC TGC AAT AGT      953
Lys Pro Pro Cys Val Ser Ile Tyr Arg Cys Gly Gly Cys Cys Asn Ser
            155                 160                 165
```

-continued

```
GAA GGA CTC CAG TGT ATG AAT ATC AGC ACA AAT TAC ATC AGC AAG ACA     1001
Glu Gly Leu Gln Cys Met Asn Ile Ser Thr Asn Tyr Ile Ser Lys Thr
        170                 175                 180

TTG TTT GAG ATT ACA GTG CCT CTC TCT CAT GGC CCC AAA CGT GTA ACA     1049
Leu Phe Glu Ile Thr Val Pro Leu Ser His Gly Pro Lys Pro Val Thr
    185                 190                 195

GTC AGT TTT GCC AAC CAC ACG TCC TGC CGA TGC ATG TCT AAG TTG GAT     1097
Val Ser Phe Ala Asn His Thr Ser Cys Arg Cys Met Ser Lys Leu Asp
200                 205                 210                 215

GTT TAC AGA CAA GTT CAT TCT ATC ATA AGA CGT TCC TTG CCA GCA ACA     1145
Val Tyr Arg Gln Val His Ser Ile Ile Arg Arg Ser Leu Pro Ala Thr
                220                 225                 230

CAA ACT CAG TGT CAT GTG GCA AAC AAG ACC TGT CCA AAA AAT CAT GTC     1193
Gln Thr Gln Cys His Val Ala Asn Lys Thr Cys Pro Lys Asn His Val
            235                 240                 245

TGG AAT AAT CAG ATT TGC AGA TGC TTA GCA CAG CAC GAT TTT GGT TTC     1241
Trp Asn Asn Gln Ile Cys Arg Cys Leu Ala Gln His Asp Phe Gly Phe
        250                 255                 260

TCT TCT CAC CTT GGA GAT TCT GAC ACA TCT GAA GGA TTC CAT ATT TGT     1289
Ser Ser His Leu Gly Asp Ser Asp Thr Ser Glu Gly Phe His Ile Cys
    265                 270                 275

GGG CCC AAC AAA GAG CTG GAT GAA GAA ACC TGT CAA TGC GTC TGC AAA     1337
Gly Pro Asn Lys Glu Leu Asp Glu Glu Thr Cys Gln Cys Val Cys Lys
280                 285                 290                 295

GGA GGT GTG CGG CCC ATA AGC TGT GGC CCT CAC AAA GAA CTA GAC AGG     1385
Gly Gly Val Arg Pro Ile Ser Cys Gly Pro His Lys Glu Leu Asp Arg
                300                 305                 310

GCA TCA TGT CAG TGC ATG TGC AAA AAC AAA CTG CTC CCC AGT TCC TGT     1433
Ala Ser Cys Gln Cys Met Cys Lys Asn Lys Leu Leu Pro Ser Ser Cys
            315                 320                 325

GGG CCT AAC AAA GAA TTT GAT GAA GAA AAG TGC CAG TGT GTA TGT AAA     1481
Gly Pro Asn Lys Glu Phe Asp Glu Glu Lys Cys Gln Cys Val Cys Lys
        330                 335                 340

AAG ACC TGT CCC AAA CAT CAT CCA CTA AAT CCT GCA AAA TGC ATC TGC     1529
Lys Thr Cys Pro Lys His His Pro Leu Asn Pro Ala Lys Cys Ile Cys
    345                 350                 355

GAA TGT ACA GAA TCT CCC AAT AAA TGT TTC TTA AAA GGA AAA AGA TTT     1577
Glu Cys Thr Glu Ser Pro Asn Lys Cys Phe Leu Lys Gly Lys Arg Phe
360                 365                 370                 375

CAT CAC CAG ACA TGC AGT TGT TAC AGA CCA CCA TGT ACA GTC CGA ACG     1625
His His Gln Thr Cys Ser Cys Tyr Arg Pro Pro Cys Thr Val Arg Thr
                380                 385                 390

AAA CGC TGT GAT GCT GGA TTT CTG TTA GCT GAA GAA GTG TGC CGC TGT     1673
Lys Arg Cys Asp Ala Gly Phe Leu Leu Ala Glu Glu Val Cys Arg Cys
            395                 400                 405

GTA CGC ACA TCT TGG AAA AGA CCA CTT ATG AAT TAAGCGAAGA AAGCACTACT   1726
Val Arg Thr Ser Trp Lys Arg Pro Leu Met Asn
        410                 415

CGCTATATAG TGTCG                                                   1741
```

(2) INFORMATION FOR SEQ ID NO:13:

(i) SEQUENCE CHARACTERISTICS:
(A) LENGTH: 418 amino acids
(B) TYPE: amino acid
(D) TOPOLOGY: linear

(ii) MOLECULE TYPE: protein

(xi) SEQUENCE DESCRIPTION: SEQ ID NO:13:

```
Met His Leu Leu Glu Met Leu Ser Leu Gly Cys Cys Leu Ala Ala Gly
```

-continued

```
 1               5                  10                  15

Ala Val Leu Leu Gly Pro Arg Gln Pro Pro Val Ala Ala Ala Tyr Glu
            20                  25                  30

Ser Gly His Gly Tyr Tyr Glu Glu Glu Pro Gly Ala Gly Glu Pro Lys
        35                  40                  45

Ala His Ala Ser Lys Asp Leu Glu Glu Gln Leu Arg Ser Val Ser Ser
    50                  55                  60

Val Asp Glu Leu Met Thr Val Leu Tyr Pro Glu Cys Trp Lys Met Phe
65                  70                  75                  80

Lys Cys Gln Leu Arg Lys Gly Gly Trp Gln His Asn Arg Glu His Ser
                85                  90                  95

Ser Ser Asp Thr Arg Ser Asp Asp Ser Leu Lys Phe Ala Ala Ala His
            100                 105                 110

Tyr Asn Ala Glu Ile Leu Lys Ser Ile Asp Thr Glu Trp Arg Lys Thr
        115                 120                 125

Gln Gly Met Pro Arg Glu Val Cys Val Asp Leu Gly Lys Glu Phe Gly
    130                 135                 140

Ala Thr Thr Asn Thr Phe Phe Lys Pro Pro Cys Val Ser Ile Tyr Arg
145                 150                 155                 160

Cys Gly Gly Cys Cys Asn Ser Glu Gly Leu Gln Cys Met Asn Ile Ser
                165                 170                 175

Thr Asn Tyr Ile Ser Lys Thr Leu Phe Glu Ile Thr Val Pro Leu Ser
            180                 185                 190

His Gly Pro Lys Pro Val Thr Val Ser Phe Ala Asn His Thr Ser Cys
        195                 200                 205

Arg Cys Met Ser Lys Leu Asp Val Tyr Arg Gln Val His Ser Ile Ile
    210                 215                 220

Arg Arg Ser Leu Pro Ala Thr Gln Thr Gln Cys His Val Ala Asn Lys
225                 230                 235                 240

Thr Cys Pro Lys Asn His Val Trp Asn Asn Gln Ile Cys Arg Cys Leu
                245                 250                 255

Ala Gln His Asp Phe Gly Phe Ser Ser His Leu Gly Asp Ser Asp Thr
            260                 265                 270

Ser Glu Gly Phe His Ile Cys Gly Pro Asn Lys Glu Leu Asp Glu Glu
        275                 280                 285

Thr Cys Gln Cys Val Cys Lys Gly Gly Val Arg Pro Ile Ser Cys Gly
    290                 295                 300

Pro His Lys Glu Leu Asp Arg Ala Ser Cys Gln Cys Met Cys Lys Asn
305                 310                 315                 320

Lys Leu Leu Pro Ser Ser Cys Gly Pro Asn Lys Glu Phe Asp Glu Glu
                325                 330                 335

Lys Cys Gln Cys Val Cys Lys Lys Thr Cys Pro Lys His His Pro Leu
            340                 345                 350

Asn Pro Ala Lys Cys Ile Cys Glu Cys Thr Glu Ser Pro Asn Lys Cys
        355                 360                 365

Phe Leu Lys Gly Lys Arg Phe His His Gln Thr Cys Ser Cys Tyr Arg
    370                 375                 380

Pro Pro Cys Thr Val Arg Thr Lys Arg Cys Asp Ala Gly Phe Leu Leu
385                 390                 395                 400

Ala Glu Glu Val Cys Arg Cys Val Arg Thr Ser Trp Lys Arg Pro Leu
                405                 410                 415

Met Asn
```

-continued

(2) INFORMATION FOR SEQ ID NO:14:

(i) SEQUENCE CHARACTERISTICS:
(A) LENGTH: 10 amino acids
(B) TYPE: amino acid
(C) STRANDEDNESS: Not Relevant
(D) TOPOLOGY: linear

(ii) MOLECULE TYPE: peptide

(xi) SEQUENCE DESCRIPTION: SEQ ID NO:14:

Ala Val Val Met Thr Gln Thr Pro Ala Ser
1 5 10

(2) INFORMATION FOR SEQ ID NO:15:

(i) SEQUENCE CHARACTERISTICS:
(A) LENGTH: 22 base pairs
(B) TYPE: nucleic acid
(C) STRANDEDNESS: single
(D) TOPOLOGY: linear

(ii) MOLECULE TYPE: cDNA

(xi) SEQUENCE DESCRIPTION: SEQ ID NO:15:

TCTCTTCTGT GCTTGAGTTG AG 22

(2) INFORMATION FOR SEQ ID NO:16:

(i) SEQUENCE CHARACTERISTICS:
(A) LENGTH: 22 base pairs
(B) TYPE: nucleic acid
(C) STRANDEDNESS: single
(D) TOPOLOGY: linear

(ii) MOLECULE TYPE: cDNA

(xi) SEQUENCE DESCRIPTION: SEQ ID NO:16:

TCTCTTCTGT CCCTGAGTTG AG 22

(2) INFORMATION FOR SEQ ID NO:17:

(i) SEQUENCE CHARACTERISTICS:
(A) LENGTH: 65 base pairs
(B) TYPE: nucleic acid
(C) STRANDEDNESS: single
(D) TOPOLOGY: linear

(ii) MOLECULE TYPE: cDNA

(xi) SEQUENCE DESCRIPTION: SEQ ID NO:17:

TGTGCTGCAG CAAATTTTAT AGTCTCTTCT GTGGCGGCGG CGGCGGCGGG CGCCTCGCGA 60

GGACC 65

(2) INFORMATION FOR SEQ ID NO:18:

(i) SEQUENCE CHARACTERISTICS:
(A) LENGTH: 30 base pairs
(B) TYPE: nucleic acid
(C) STRANDEDNESS: single
(D) TOPOLOGY: linear

(ii) MOLECULE TYPE: cDNA

(xi) SEQUENCE DESCRIPTION: SEQ ID NO:18:

CTGGCAGGGA ACTGCTAATA ATGGAATGAA 30

-continued

(2) INFORMATION FOR SEQ ID NO:19:

(i) SEQUENCE CHARACTERISTICS:
(A) LENGTH: 84 base pairs
(B) TYPE: nucleic acid
(C) STRANDEDNESS: single
(D) TOPOLOGY: linear

(ii) MOLECULE TYPE: cDNA

(xi) SEQUENCE DESCRIPTION: SEQ ID NO:19:

GGGCTCCGCG TCCGAGAGGT CGAGTCCGGA CTCGTGATGG TGATGGTGAT GGGCGGCGGC 60

GGCGGCGGGC GCCTCGCGAG GACC 84

(2) INFORMATION FOR SEQ ID NO:20:

(i) SEQUENCE CHARACTERISTICS:
(A) LENGTH: 31 base pairs
(B) TYPE: nucleic acid
(C) STRANDEDNESS: single
(D) TOPOLOGY: linear

(ii) MOLECULE TYPE: cDNA

(xi) SEQUENCE DESCRIPTION: SEQ ID NO:20:

GTATTATAAT GTCCTCCACC AAATCTTATA G 31

(2) INFORMATION FOR SEQ ID NO:21:

(i) SEQUENCE CHARACTERISTICS:
(A) LENGTH: 93 base pairs
(B) TYPE: nucleic acid
(C) STRANDEDNESS: single
(D) TOPOLOGY: linear

(ii) MOLECULE TYPE: cDNA

(xi) SEQUENCE DESCRIPTION: SEQ ID NO:21:

GTTCGCTGCC TGACACTGTG GTAGTGTTGC TGGCGGCCGC TAGTGATGGT GATGGTGATG 60

AATAATGGAA TGAACTTGTC TGTAAACATC CAG 93

(2) INFORMATION FOR SEQ ID NO:22:

(i) SEQUENCE CHARACTERISTICS:
(A) LENGTH: 18 base pairs
(B) TYPE: nucleic acid
(C) STRANDEDNESS: single
(D) TOPOLOGY: linear

(ii) MOLECULE TYPE: cDNA

(xi) SEQUENCE DESCRIPTION: SEQ ID NO:22:

CATGTACGAA CCGCCAGG 18

(2) INFORMATION FOR SEQ ID NO:23:

(i) SEQUENCE CHARACTERISTICS:
(A) LENGTH: 20 base pairs
(B) TYPE: nucleic acid
(C) STRANDEDNESS: single
(D) TOPOLOGY: linear

(ii) MOLECULE TYPE: cDNA

(xi) SEQUENCE DESCRIPTION: SEQ ID NO:23:

AATGACCAGA GAGAGGCGAG 20

-continued

(2) INFORMATION FOR SEQ ID NO:24:

(i) SEQUENCE CHARACTERISTICS:
(A) LENGTH: 18 base pairs
(B) TYPE: nucleic acid
(C) STRANDEDNESS: single
(D) TOPOLOGY: linear

(ii) MOLECULE TYPE: DNA (genomic)

(xi) SEQUENCE DESCRIPTION: SEQ ID NO:24:

GCCACGGTAG GTCTGCGT 18

(2) INFORMATION FOR SEQ ID NO:25:

(i) SEQUENCE CHARACTERISTICS:
(A) LENGTH: 18 base pairs
(B) TYPE: nucleic acid
(C) STRANDEDNESS: single
(D) TOPOLOGY: linear

(ii) MOLECULE TYPE: DNA (genomic)

(xi) SEQUENCE DESCRIPTION: SEQ ID NO:25:

CTTCTTTGAC AGGCTTAT 18

(2) INFORMATION FOR SEQ ID NO:26:

(i) SEQUENCE CHARACTERISTICS:
(A) LENGTH: 21 base pairs
(B) TYPE: nucleic acid
(C) STRANDEDNESS: single
(D) TOPOLOGY: linear

(ii) MOLECULE TYPE: DNA (genomic)

(xi) SEQUENCE DESCRIPTION: SEQ ID NO:26:

ATCTTGAAAA GTAAGTATGG G 21

(2) INFORMATION FOR SEQ ID NO:27:

(i) SEQUENCE CHARACTERISTICS:
(A) LENGTH: 20 base pairs
(B) TYPE: nucleic acid
(C) STRANDEDNESS: single
(D) TOPOLOGY: linear

(ii) MOLECULE TYPE: DNA (genomic)

(xi) SEQUENCE DESCRIPTION: SEQ ID NO:27:

ATGACTTGAC AGGTATTGAT 20

(2) INFORMATION FOR SEQ ID NO:28:

(i) SEQUENCE CHARACTERISTICS:
(A) LENGTH: 20 base pairs
(B) TYPE: nucleic acid
(C) STRANDEDNESS: single
(D) TOPOLOGY: linear

(ii) MOLECULE TYPE: DNA (genomic)

(xi) SEQUENCE DESCRIPTION: SEQ ID NO:28:

AGCAAGACGG TGGGTATTGT 20

(2) INFORMATION FOR SEQ ID NO:29:

(i) SEQUENCE CHARACTERISTICS:
(A) LENGTH: 22 base pairs

-continued

(B) TYPE: nucleic acid
(C) STRANDEDNESS: single
(D) TOPOLOGY: linear

(ii) MOLECULE TYPE: DNA (genomic)

(xi) SEQUENCE DESCRIPTION: SEQ ID NO:29:

CCCTTCTTTG TAGTTATTTG AA 22

(2) INFORMATION FOR SEQ ID NO:30:

(i) SEQUENCE CHARACTERISTICS:
(A) LENGTH: 20 base pairs
(B) TYPE: nucleic acid
(C) STRANDEDNESS: single
(D) TOPOLOGY: linear

(ii) MOLECULE TYPE: DNA (genomic)

(xi) SEQUENCE DESCRIPTION: SEQ ID NO:30:

CCACAGTGAG TATGAATTAA 20

(2) INFORMATION FOR SEQ ID NO:31:

(i) SEQUENCE CHARACTERISTICS:
(A) LENGTH: 18 base pairs
(B) TYPE: nucleic acid
(C) STRANDEDNESS: single
(D) TOPOLOGY: linear

(ii) MOLECULE TYPE: DNA (genomic)

(xi) SEQUENCE DESCRIPTION: SEQ ID NO:31:

CTCTTCCAAA GGTGTCAG 18

(2) INFORMATION FOR SEQ ID NO:32:

(i) SEQUENCE CHARACTERISTICS:
(A) LENGTH: 18 base pairs
(B) TYPE: nucleic acid
(C) STRANDEDNESS: single
(D) TOPOLOGY: linear

(ii) MOLECULE TYPE: DNA (genomic)

(xi) SEQUENCE DESCRIPTION: SEQ ID NO:32:

GGAGATGGTA GCAGAATG 18

(2) INFORMATION FOR SEQ ID NO:33:

(i) SEQUENCE CHARACTERISTICS:
(A) LENGTH: 23 base pairs
(B) TYPE: nucleic acid
(C) STRANDEDNESS: single
(D) TOPOLOGY: linear

(ii) MOLECULE TYPE: DNA (genomic)

(xi) SEQUENCE DESCRIPTION: SEQ ID NO:33:

CTATTTGTCT AGACTCAACA GAT 23

(2) INFORMATION FOR SEQ ID NO:34:

(i) SEQUENCE CHARACTERISTICS:
(A) LENGTH: 22 base pairs
(B) TYPE: nucleic acid
(C) STRANDEDNESS: single
(D) TOPOLOGY: linear

-continued

(ii) MOLECULE TYPE: DNA (genomic)

(xi) SEQUENCE DESCRIPTION: SEQ ID NO:34:

CAAACATGCA GGTAAGAGAT CC 22

(2) INFORMATION FOR SEQ ID NO:35:

(i) SEQUENCE CHARACTERISTICS:
(A) LENGTH: 21 base pairs
(B) TYPE: nucleic acid
(C) STRANDEDNESS: single
(D) TOPOLOGY: linear

(ii) MOLECULE TYPE: DNA (genomic)

(xi) SEQUENCE DESCRIPTION: SEQ ID NO:35:

TGTTCTCCTA GCTGTTACAG A 21

(2) INFORMATION FOR SEQ ID NO:36:

(i) SEQUENCE CHARACTERISTICS:
(A) LENGTH: 24 base pairs
(B) TYPE: nucleic acid
(C) STRANDEDNESS: single
(D) TOPOLOGY: linear

(ii) MOLECULE TYPE: DNA (genomic)

(xi) SEQUENCE DESCRIPTION: SEQ ID NO:36:

GGCGAGGTCA AGGTAGGTGC AAGG 24

(2) INFORMATION FOR SEQ ID NO:37:

(i) SEQUENCE CHARACTERISTICS:
(A) LENGTH: 26 base pairs
(B) TYPE: nucleic acid
(C) STRANDEDNESS: single
(D) TOPOLOGY: linear

(ii) MOLECULE TYPE: DNA (genomic)

(xi) SEQUENCE DESCRIPTION: SEQ ID NO:37:

ATTGTCTTTG ACAGGCTTTT TGAAGG 26

(2) INFORMATION FOR SEQ ID NO:38:

(i) SEQUENCE CHARACTERISTICS:
(A) LENGTH: 21 base pairs
(B) TYPE: nucleic acid
(C) STRANDEDNESS: single
(D) TOPOLOGY: linear

(ii) MOLECULE TYPE: DNA (genomic)

(xi) SEQUENCE DESCRIPTION: SEQ ID NO:38:

GAGATCCTGA AAAGTAAGTA G 21

(2) INFORMATION FOR SEQ ID NO:39:

(i) SEQUENCE CHARACTERISTICS:
(A) LENGTH: 24 base pairs
(B) TYPE: nucleic acid
(C) STRANDEDNESS: single
(D) TOPOLOGY: linear

(ii) MOLECULE TYPE: DNA (genomic)

(xi) SEQUENCE DESCRIPTION: SEQ ID NO:39:

-continued

TGTGACTCGA CAGGTATTGA IAAT 24

(2) INFORMATION FOR SEQ ID NO:40:

(i) SEQUENCE CHARACTERISTICS:
(A) LENGTH: 20 base pairs
(B) TYPE: nucleic acid
(C) STRANDEDNESS: single
(D) TOPOLOGY: linear

(ii) MOLECULE TYPE: DNA (genomic)

(xi) SEQUENCE DESCRIPTION: SEQ ID NO:40:

CTCAGCAAGA CGGTAGGTAT 20

(2) INFORMATION FOR SEQ ID NO:41:

(i) SEQUENCE CHARACTERISTICS:
(A) LENGTH: 25 base pairs
(B) TYPE: nucleic acid
(C) STRANDEDNESS: single
(D) TOPOLOGY: linear

(ii) MOLECULE TYPE: DNA (genomic)

(xi) SEQUENCE DESCRIPTION: SEQ ID NO:41:

CTGTCCCTTG TAGTTGTTTG AAATT 25

(2) INFORMATION FOR SEQ ID NO:42:

(i) SEQUENCE CHARACTERISTICS:
(A) LENGTH: 20 base pairs
(B) TYPE: nucleic acid
(C) STRANDEDNESS: single
(D) TOPOLOGY: linear

(ii) MOLECULE TYPE: DNA (genomic)

(xi) SEQUENCE DESCRIPTION: SEQ ID NO:42:

ACATTACCAC AGTGAGTATG 20

(2) INFORMATION FOR SEQ ID NO:43:

(i) SEQUENCE CHARACTERISTICS:
(A) LENGTH: 26 base pairs
(B) TYPE: nucleic acid
(C) STRANDEDNESS: single
(D) TOPOLOGY: linear

(ii) MOLECULE TYPE: DNA (genomic)

(xi) SEQUENCE DESCRIPTION: SEQ ID NO:43:

GTCTCCCCAA AAGGTGTCAG GCAGCT 26

(2) INFORMATION FOR SEQ ID NO:44:

(i) SEQUENCE CHARACTERISTICS:
(A) LENGTH: 23 base pairs
(B) TYPE: nucleic acid
(C) STRANDEDNESS: single
(D) TOPOLOGY: linear

(ii) MOLECULE TYPE: DNA (genomic)

(xi) SEQUENCE DESCRIPTION: SEQ ID NO:44:

AATGTTGAAG ATGGTAAGTA AAA 23

(2) INFORMATION FOR SEQ ID NO:45:

-continued

(i) SEQUENCE CHARACTERISTICS:
(A) LENGTH: 16 base pairs
(B) TYPE: nucleic acid
(C) STRANDEDNESS: single
(D) TOPOLOGY: linear

(ii) MOLECULE TYPE: DNA (genomic)

(xi) SEQUENCE DESCRIPTION: SEQ ID NO:45:

TCTAGACTCA ACCAAT 16

(2) INFORMATION FOR SEQ ID NO:46:

(i) SEQUENCE CHARACTERISTICS:
(A) LENGTH: 22 base pairs
(B) TYPE: nucleic acid
(C) STRANDEDNESS: single
(D) TOPOLOGY: linear

(ii) MOLECULE TYPE: DNA (genomic)

(xi) SEQUENCE DESCRIPTION: SEQ ID NO:46:

CAAACATGCA GGTAAGGAGT GT 22

(2) INFORMATION FOR SEQ ID NO:47:

(i) SEQUENCE CHARACTERISTICS:
(A) LENGTH: 24 base pairs
(B) TYPE: nucleic acid
(C) STRANDEDNESS: single
(D) TOPOLOGY: linear

(ii) MOLECULE TYPE: DNA (genomic)

(xi) SEQUENCE DESCRIPTION: SEQ ID NO:47:

TTTTCCCCTA GTTGTTACAG AAGA 24

(2) INFORMATION FOR SEQ ID NO:48:

(i) SEQUENCE CHARACTERISTICS:
(A) LENGTH: 2991 base pairs
(B) TYPE: nucleic acid
(C) STRANDEDNESS: single
(D) TOPOLOGY: linear

(ii) MOLECULE TYPE: DNA (genomic)

(xi) SEQUENCE DESCRIPTION: SEQ ID NO:48:

GTTTTAAGTA GAGACGGGGT TTCACCAACG GTTGAAAATA TTTATCATGG TCTCCCTAAG 60

ATGGACGGTG TTAGCTAGGA TGGTCTCGAT CTCCTGACCT CATGATCCAC CCGCCTCGGC 120

CTCCCAAAGT GCTGGGATTA CAGGCGTGAG CCACCGTGTC CGACCAACCT TAAGACAAAC 180

AACTACTGCA TGATTGTTTT TGGAGACCTC TTTTTTATTC AAATAAATTT TTGCCAGCAT 240

TTTCTGACTC AAAGTATAGC AGCAGGAAGA TAACACTTTT GTGAGAAAAA AGTTTGAATA 300

CAGCTTACTG CTGTATTTAA ATGAAACAGT AGTTAATATG ATATTAATAT ATTTTGGATA 360

TATTTTGAGT TTGTTGATTT TCCAGTCTTC ACCCGCTGCT AGGCCTGTGG GTGTTGGAAA 420

TGCCTGTGTT TCTCAATTTT GTTTGCCTAC TAGAATCCTG ATGTCCAAGC CTTACTCCAG 480

TTAGACCAGT TAAGCCAGAA AGGCAGAAGG TGTACTCAAG CATCTGTTTT TTCAAAATCT 540

CCTTTTGTGA TGCCAAGTGC AATCAAAGTT TAGAATCATT GTAATAGCAA ATGGTTGAAT 600

GGAAACTCCA CCTTCTATTC AAATCCTACC CCAGTCTGCC CTTAGCTGTT CTCTTTTCAC 660

AGATCTATCA ATGTCTGAAG ATAACTATGG CAGGCTGATC AAATATGCAT AGAGCAGGAA 720

-continued

GACAGCAAGA GAGTGATACA CTGACCATGT TCCAAACCAC AAAACATCTC AACAGGCTAG 780

ATCATGGACC GAGTCTGATG GGATGGAATT TCATAAAGAT ACATAAAAAA GCATCTTGGA 840

CACAGTAAAC TTAACTCCAC AAATACAGGG GAATTTAGAC GTGACTAAGT AGCAGTACAT 900

ATGAAAAATT ATTGAGGAAT TTTGTTGACT TTAAGGGTAG TGTGAGTCAA CACTGTGATT 960

TGGCTGCCAG AAAATAAACT CAATCCAACG CTGTATCAAC AAAGCCATAC TGTCCATTCT 1020

GCATGCTCAT TACAGCACTA AGTACCGAGC CATGTTCTCA ACCGCATACT TCATGAACAT 1080

GGAAAGCTAA CAGTATGGTT AAGGGGGGAA ACTGGAACTG TCATCTTGGG GAATAAAAGG 1140

GATATTTAGC CAGGAGTAAA GTTAGCTTAG GGAGACCATG ATAAATATTT TCAAAATATT 1200

TGAAGGACTC AGTTGTGGAA GTGAGATTAG ATTTATTGTG TAAAACTCCA GGAGTCAAAA 1260

GCAATAGAGA GATAGAAGGA AATGCTTTTC AGCAGTGTTG CTCATCAATA AAGGGAGTGA 1320

ACAGCCACAC AGAATGGAAG GTTCCCTGTC CTTTGAGATA TTTAAGCCTT CAAGTAAATT 1380

ATGGGTGAGG AGTTTCAAAT CTAGAGTTGA ACCAGATAAG AAAGTCTCTT CTTCCGGTAA 1440

GATATTATGG ACCTATAACA TCTGTGTACT TAAAAGTAGA TTGGGAGTGA AAGGCAGACT 1500

TTTGATGTTC TGTACACTGT TGAAACCCCT TAGCGTGGTC CTCTGTAACC TGCTCACCCT 1560

GCCCCAAGGA GGCAGCTAGC CAATGCCACC AGCCCAACGG AAACCCCAGT GCTTTTCCAA 1620

TGGGGAAATG CAGTCACTTT TCTTTGGATG CTACACATCC TTTCTGGAAT ATGTCTCACA 1680

CACATCTCTC TTTATCACCC CCTTCTTCAA GTAAACCAAC TTCTTGCAGA AGCTGACAAT 1740

GTGTCTCTTT ACTCTCCACG AAGATTCTGG CCCTTCTCTT CACCTGTCAG AAGTTTAGGA 1800

TTCCAAAGGG ATCATTAGCA TCCATCCCAA CAGCCTGCAC TGCATCCTGA GAACTGCGGT 1860

TCTTGGATCA TCAGGCAACT TTCAACTACA CAGACCAAGG GAGAGAGGGG ACCCCTCCGA 1920

GGTCCCATAG GGTTCTCTGA CATAGTGATG ACCTTTTTCC AAACTTTGAG CAGGGCGCTG 1980

GGGGCCAGGC GTGCGGGAGG GAGGACAAGA ACTCGGGAGT GGCCGAGGAT AAAGCGGGGG 2040

CTCCCTCCAC CCCACGGTGC CCAGTTCTC CCCGCTGCAC GTGGTCCAGG GTGGTCGCAT 2100

CACCTCTAAA GCCGGTCCCG CCAACCGCCA GCCCCGGGAC TGAACTTGCC CCTCCGGCCG 2160

CCCGCTCCCC GCAGGGGACA GGGGCGGGGA GGGAGAGATC CAGAGGGGGG CTGGGGGAGG 2220

TGGGGCCGCC GGGGAGGAGG CGAGGGAAAC GGGGAGCTCC AGGGAGACGG CTTCCGAGGG 2280

AGAGTGAGAG GGGAGGGCAG CCCGGGCTCG GCACGCTCCC TCCCTCGGCC GCTTTCTCTC 2340

ACATAAGCGC AGGCAGAGGG CGCGTCAGTC ATGCCCTGCC CCTGCGCCCG CCGCCGCCGC 2400

CGCCGCCGCT CAGCCCGGCG CGCTCTGGAG GATCCTGCGC CGCGGCGCTC CCGGGCCCCG 2460

CCGCCGCCAG CCGCCCCGGC GGCCCTCCTC CCGCCCCCGG CACCGCCGCC AGCGCCCCCG 2520

CCGCAGCGCC CGCGGCCCGG CTCCTCTCAC TTCGGGGAAG GGGAGGGAGG AGGGGGACGA 2580

GGGCTCTGGC GGGTTTGGAG GGGCTGAACA TCGCGGGGTG TTCTGGTGTC CCCCGCCCCG 2640

CCTCTCCAAA AAGCTACACC GACGCGGACC GCGGCGGCGT CCTCGCTCGC CCTCGCTTCA 2700

CCTCGCGGGC TCCGAATGCG GGGAGCTCGG ATGTCCGGTT TCCTGTGAGG CTTTTACCTG 2760

ACACCCGCCG CCTTTCCCCG GCACTGGCTG GGAGGGCGCC CTGCAAAGTT GGGAACGCGG 2820

AGCCCCGGAC CCGCTCCCGC CGCCTCCGGC TCGCCCAGGG GGGGTCGCCG GGAGGAGCCC 2880

GGGGGAGAGG GACCAGGAGG GGCCCGCGGC CTCGCAGGGG CGCCCGCGCC CCCACCCCTG 2940

CCCCCGCCAG CGGACCGGTC CCCCACCCCC GGTCCTTCCA CCATGCACTT G 2991

(2) INFORMATION FOR SEQ ID NO:49:

-continued

(i) SEQUENCE CHARACTERISTICS:
(A) LENGTH: 20 base pairs
(B) TYPE: nucleic acid
(C) STRANDEDNESS: single
(D) TOPOLOGY: linear

(ii) MOLECULE TYPE: cDNA

(xi) SEQUENCE DESCRIPTION: SEQ ID NO:49:

CACGGCTTAT GCAAGCAAAG 20

(2) INFORMATION FOR SEQ ID NO:50:

(i) SEQUENCE CHARACTERISTICS:
(A) LENGTH: 20 base pairs
(B) TYPE: nucleic acid
(C) STRANDEDNESS: single
(D) TOPOLOGY: linear

(ii) MOLECULE TYPE: cDNA

(xi) SEQUENCE DESCRIPTION: SEQ ID NO:50:

AACACAGTTT TCCATAACAG 20

(2) INFORMATION FOR SEQ ID NO:51:

(i) SEQUENCE CHARACTERISTICS:
(A) LENGTH: 19 amino acids
(B) TYPE: amino acid
(C) STRANDEDNESS: Not Relevant
(D) TOPOLOGY: linear

(ii) MOLECULE TYPE: peptide

(xi) SEQUENCE DESCRIPTION: SEQ ID NO:51:

Leu Ser Lys Thr Val Ser Gly Ser Glu Gln Asp Leu Pro His Glu Leu
1 5 10 15

His Val Glu

(2) INFORMATION FOR SEQ ID NO:52:

(i) SEQUENCE CHARACTERISTICS:
(A) LENGTH: 25 base pairs
(B) TYPE: nucleic acid
(C) STRANDEDNESS: single
(D) TOPOLOGY: linear

(ii) MOLECULE TYPE: cDNA

(xi) SEQUENCE DESCRIPTION: SEQ ID NO:52:

GACGGACACA GATGGAGGTT TAAAG 25

(2) INFORMATION FOR SEQ ID NO:53:

(i) SEQUENCE CHARACTERISTICS:
(A) LENGTH: 196 amino acids
(B) TYPE: amino acid
(C) STRANDEDNESS: Not Relevant
(D) TOPOLOGY: linear

(ii) MOLECULE TYPE: protein

(xi) SEQUENCE DESCRIPTION: SEQ ID NO:53:

Met Arg Thr Leu Ala Cys Leu Leu Leu Leu Gly Cys Gly Tyr Leu Ala
1 5 10 15

His Val Leu Ala Glu Glu Ala Glu Ile Pro Arg Glu Val Ile Glu Arg
20 25 30

-continued

```
Leu Ala Arg Ser Gln Ile His Ser Ile Arg Asp Leu Gln Arg Leu Leu
        35                  40                  45

Glu Ile Asp Ser Val Gly Ser Glu Asp Ser Leu Asp Thr Ser Leu Arg
    50                  55                  60

Ala His Gly Val His Ala Thr Lys His Val Pro Glu Lys Arg Pro Leu
65                  70                  75                  80

Pro Ile Arg Arg Lys Arg Ser Ile Glu Glu Ala Val Pro Ala Val Cys
                85                  90                  95

Lys Thr Arg Thr Val Ile Tyr Glu Ile Pro Arg Ser Gln Val Asp Pro
            100                 105                 110

Thr Ser Ala Asn Phe Leu Ile Trp Pro Pro Cys Val Glu Val Lys Arg
        115                 120                 125

Cys Thr Gly Cys Cys Asn Thr Ser Ser Val Lys Cys Gln Pro Ser Arg
    130                 135                 140

Val His His Arg Ser Val Lys Val Ala Lys Val Glu Tyr Val Arg Lys
145                 150                 155                 160

Lys Pro Lys Leu Lys Glu Val Gln Val Arg Leu Glu Glu His Leu Glu
                165                 170                 175

Cys Ala Cys Ala Thr Thr Ser Leu Asn Pro Asp Tyr Arg Glu Glu Asp
            180                 185                 190

Thr Asp Val Arg
        195
```

(2) INFORMATION FOR SEQ ID NO:54:

(i) SEQUENCE CHARACTERISTICS:
(A) LENGTH: 241 amino acids
(B) TYPE: amino acid
(C) STRANDEDNESS: Not Relevant
(D) TOPOLOGY: linear

(ii) MOLECULE TYPE: protein

(xi) SEQUENCE DESCRIPTION: SEQ ID NO:54:

```
Met Asn Arg Cys Trp Ala Leu Phe Leu Ser Leu Cys Cys Tyr Leu Arg
1               5                   10                  15

Leu Val Ser Ala Glu Gly Asp Pro Ile Pro Glu Glu Leu Tyr Glu Met
            20                  25                  30

Leu Ser Asp His Ser Ile Arg Ser Phe Asp Asp Leu Gln Arg Leu Leu
        35                  40                  45

His Gly Asp Pro Gly Glu Glu Asp Gly Ala Glu Leu Asp Leu Asn Met
    50                  55                  60

Thr Arg Ser His Ser Gly Gly Glu Leu Glu Ser Leu Ala Arg Gly Arg
65                  70                  75                  80

Arg Ser Leu Gly Ser Leu Thr Ile Ala Glu Pro Ala Met Ile Ala Glu
                85                  90                  95

Cys Lys Thr Arg Thr Glu Val Phe Glu Ile Ser Arg Arg Leu Ile Asp
            100                 105                 110

Arg Thr Asn Ala Asn Phe Leu Val Trp Pro Pro Cys Val Glu Val Gln
        115                 120                 125

Arg Cys Ser Gly Cys Cys Asn Asn Arg Asn Val Gln Cys Arg Pro Thr
    130                 135                 140

Gln Val Gln Leu Arg Pro Val Gln Val Arg Lys Ile Glu Ile Val Arg
145                 150                 155                 160

Lys Lys Pro Ile Phe Lys Lys Ala Thr Val Thr Leu Glu Asp His Leu
                165                 170                 175
```

-continued

```
Ala Cys Lys Cys Glu Thr Val Ala Ala Arg Pro Val Thr Arg Ser
            180                 185                 190

Pro Gly Gly Ser Gln Glu Gln Arg Ala Lys Thr Pro Gln Thr Arg Val
        195                 200                 205

Thr Ile Arg Thr Val Arg Val Arg Arg Pro Pro Lys Gly Lys His Arg
    210                 215                 220

Lys Phe Lys His Thr His Asp Lys Thr Ala Leu Lys Glu Thr Leu Gly
225                 230                 235                 240

Ala
```

(2) INFORMATION FOR SEQ ID NO:55:

(i) SEQUENCE CHARACTERISTICS:
(A) LENGTH: 149 amino acids
(B) TYPE: amino acid
(C) STRANDEDNESS: Not Relevant
(D) TOPOLOGY: linear

(ii) MOLECULE TYPE: protein

(xi) SEQUENCE DESCRIPTION: SEQ ID NO:55:

```
Met Pro Val Met Arg Leu Phe Pro Cys Phe Leu Gln Leu Leu Ala Gly
1               5                   10                  15

Leu Ala Leu Pro Ala Val Pro Pro Gln Gln Trp Ala Leu Ser Ala Gly
            20                  25                  30

Asn Gly Ser Ser Glu Val Glu Val Val Pro Phe Gln Glu Val Trp Gly
        35                  40                  45

Arg Ser Tyr Cys Arg Ala Leu Glu Arg Leu Val Asp Val Val Ser Glu
    50                  55                  60

Tyr Pro Ser Glu Val Glu His Met Phe Ser Pro Ser Cys Val Ser Leu
65                  70                  75                  80

Leu Arg Cys Thr Gly Cys Cys Gly Asp Glu Asn Leu His Cys Val Pro
                85                  90                  95

Val Glu Thr Ala Asn Val Thr Met Gln Leu Leu Lys Ile Arg Ser Gly
            100                 105                 110

Asp Arg Pro Ser Tyr Val Glu Leu Thr Phe Ser Gln His Val Arg Cys
        115                 120                 125

Glu Cys Arg Pro Leu Arg Glu Lys Met Lys Pro Glu Arg Cys Gly Asp
    130                 135                 140

Ala Val Pro Arg Arg
145
```

(2) INFORMATION FOR SEQ ID NO:56:

(i) SEQUENCE CHARACTERISTICS:
(A) LENGTH: 191 amino acids
(B) TYPE: amino acid
(C) STRANDEDNESS: Not Relevant
(D) TOPOLOGY: linear

(ii) MOLECULE TYPE: protein

(xi) SEQUENCE DESCRIPTION: SEQ ID NO:56:

```
Met Asn Phe Leu Leu Ser Trp Val His Trp Ser Leu Ala Leu Leu Leu
1               5                   10                  15

Tyr Leu His His Ala Lys Trp Ser Gln Ala Ala Pro Met Ala Glu Gly
            20                  25                  30

Gly Gly Gln Asn His His Glu Val Val Lys Phe Met Asp Val Tyr Gln
        35                  40                  45
```

-continued

```
Arg Ser Tyr Cys His Pro Ile Glu Thr Leu Val Asp Ile Phe Gln Glu
    50                  55                  60

Tyr Pro Asp Glu Ile Glu Tyr Ile Phe Lys Pro Ser Cys Val Pro Leu
65                  70                  75                  80

Met Arg Cys Gly Gly Cys Cys Asn Asp Glu Gly Leu Glu Cys Val Pro
                85                  90                  95

Thr Glu Glu Ser Asn Ile Thr Met Gln Ile Met Arg Ile Lys Pro His
            100                 105                 110

Gln Gly Gln His Ile Gly Glu Met Ser Phe Leu Gln His Asn Lys Cys
        115                 120                 125

Glu Cys Arg Pro Lys Lys Asp Arg Ala Arg Gln Glu Asn Pro Cys Gly
    130                 135                 140

Pro Cys Ser Glu Arg Arg Lys His Leu Phe Val Gln Asp Pro Gln Thr
145                 150                 155                 160

Cys Lys Cys Ser Cys Lys Asn Thr Asp Ser Arg Cys Lys Ala Arg Gln
                165                 170                 175

Leu Glu Leu Asn Glu Arg Thr Cys Arg Cys Asp Lys Pro Arg Arg
            180                 185                 190
```

(2) INFORMATION FOR SEQ ID NO:57:

(i) SEQUENCE CHARACTERISTICS:
(A) LENGTH: 188 amino acids
(B) TYPE: amino acid
(C) STRANDEDNESS: Not Relevant
(D) TOPOLOGY: linear

(ii) MOLECULE TYPE: protein

(xi) SEQUENCE DESCRIPTION: SEQ ID NO:57:

```
Met Ser Pro Leu Leu Arg Arg Leu Leu Leu Ala Ala Leu Leu Gln Leu
1               5                   10                  15

Ala Pro Ala Gln Ala Pro Val Ser Gln Pro Asp Ala Pro Gly His Gln
            20                  25                  30

Arg Lys Val Val Ser Trp Ile Asp Val Tyr Thr Arg Ala Thr Cys Gln
        35                  40                  45

Pro Arg Glu Val Val Val Pro Leu Thr Val Glu Leu Met Gly Thr Val
    50                  55                  60

Ala Lys Gln Leu Val Pro Ser Cys Val Thr Val Gln Arg Cys Gly Gly
65                  70                  75                  80

Cys Cys Pro Asp Asp Gly Leu Glu Cys Val Pro Thr Gly Gln His Gln
                85                  90                  95

Val Arg Met Gln Ile Leu Met Ile Arg Tyr Pro Ser Ser Gln Leu Gly
            100                 105                 110

Glu Met Ser Leu Glu Glu His Ser Gln Cys Glu Cys Arg Pro Lys Lys
        115                 120                 125

Lys Asp Ser Ala Val Lys Pro Asp Ser Pro Arg Pro Leu Cys Pro Arg
    130                 135                 140

Cys Thr Gln His His Gln Arg Pro Asp Pro Arg Thr Cys Arg Cys Arg
145                 150                 155                 160

Cys Arg Arg Arg Ser Phe Leu Arg Cys Gln Gly Arg Gly Leu Glu Leu
                165                 170                 175

Asn Pro Asp Thr Cys Arg Cys Arg Lys Leu Arg Arg
            180                 185
```

What is claimed is:

1. A purified and isolated VEGF-CΔC_{156} polypeptide that binds to human Flt4 receptor tyrosine kinase (VEGFR-3) and fails to bind to human KDR receptor tyrosine (VEGFR-2), said polypeptide having an amino acid sequence comprising a portion of SEQ ID NO: 8 effective to permit binding to VEGFR-3, wherein the cysteine residue at position 156 of SEQ ID NO: 8 has been deleted or replaced by another amino acid.

2. A polypeptide according to claim 1 wherein said portion of SEQ ID NO: 8 is selected from the group consisting of:

(a) continuous portion having as its amino terminal residue an amino acid between residues 102 and 114 of SEQ ID NO: 8 and having as its carboxy terminal residue an amino acid between residues 212 and 228 of SEQ ID NO: 8, wherein the cysteine residue at position 156 of SEQ ID NO: 8 has been deleted or replaced by another amino acid;

(b) continuous portions that comprise an amino-terminal truncation of (a); and

continuous portions that comprise a carboxy-terminal truncation of (a) or b).

3. A polypeptide according to claim 2, wherein said polypeptide is capable of stimulating tyrosine phosphorylation of VEGFR-3 in a host cell expressing VEGFR-3.

4. A VEGF-C ΔC_{156} polypeptide according to claim 1 comprising amino acids 113 to 213 of SEQ ID NO: 8, wherein the cysteine residue at position 156 of SEQ ID NO: 8 has been deleted or replaced.

5. A VEGF-C ΔC_{156} polypeptide according to claim 1 comprising a continuous portion of SEQ ID NO: 8, said portion having as its amino terminal residue an amino acid between residues 102 and 114 of SEQ ID NO: 8, and having as its carboxy terminal residue an amino acid between residues 212 and 228 of SEQ ID NO: 8, wherein the cysteine residue at position 156 of SEQ ID NO: 8 has been deleted or replaced.

6. A VEGF-C ΔC_{156} polypeptide according to claim 1 wherein the cysteine residue at position 156 of SEQ ID NO: 8 has been replaced by a serine residue.

7. A composition comprising a polypeptide according to claim 1 in a pharmaceutically-acceptable diluent, adjuvant, excipient, or carrier.

8. A purified and isolated polypeptide multimer, wherein at least one monomer thereof is a polypeptide according to claim 1, and wherein said multimer is capable of binding to VEGFR-3.

9. A dimer according to claim 1.

10. A polypeptide according to claim 1 comprising amino acids 1 to 419 of SEQ ID NO: 8, wherein the cysteine residue at position 156 of SEQ ID NO: 8 has been deleted or replaced by another amino acid.

11. A method of imaging Flt4 receptor tyrosine kinase (VEGFR-3) in tissue suspected of containing VEGFR-3, comprising the steps of contacting tissue suspected of containing VEGFR-3 with a polypepude of claim 1 and imaging VEGFR-3 in the tissue by detecting the polypeptide bound to the tissue.

12. A purified and isolated nucleic acid comprising a nucleotide sequence encoding a VEGF-C ΔC_{156} polypeptide that binds to human Flt4 receptor tyrosine kinase (VEGFR-3) and fails to bind to human KDR receptor tyrosine (VEGFR-2), said polypeptide, having an amino acid sequence comprising a portion of SEQ ID NO: 8 effective to permit binding to VEGFR-3, wherein the cysteine residue at position 156 of SEQ ID NO: 8 has been deleted or replaced by another amino acid.

13. A vector comprising a nucleic acid according to claim 13.

14. A host cell transformed or transfected with a nucleic acid according to claim 12.

15. A method of making a polypeptide that binds to VEGFR-3, said method comprising the steps of:

(a) expressing a nucleic acid according to claim 12 in a host cell; and

(b) purifying a polypeptide that binds to VEGFR-3 from said host cell or from a growth medium of said host cell.

16. A polypeptide that binds to the extracellular domain of human Flt4 receptor tyrosine kinase (VEGFR-3),

said polypeptide comprising a fragment of a vertebrate pepro-VEGF-C amino acid sequence that binds to human VEGFR3, with the iproviso that, in said polypeptide a conserved cysteine of the vertebrate prepro-VEGF-C has been deleted or replaced by another amino acid,

wherein the vertebrate prepro-VEGF-C amino acid sequence comprises an amino acid sequence that is encoded by a DNA of vertebrate origin which hybridizes to a non-coding strand complementary to nucleotides 352 to 1611 of SEQ ID NO: 7 under the following hybridization conditions: hybridization at 42° C. in a hybridization solution comprising 50% formamide, 5×SSC, 20 mM Na^*PO_4, pH 6.8; and washing in 0.2×SSC at 55° C.,

wherein nucleotides 352 to 1611 of SEQ ID NO: 7 encode a human prepro-VEGF-C having the amino acid sequence set forth in SEQ ID NO: 8 that is characterized by eight cysteine residues at positions 131, 156, 162, 165, 166, 173, 209, and 211 of SEQ ID NO: 8 that are conserved in human vascular endothelial growth factor (VEGF), human platelet derived growth factors A and B (PDGF-A, PDGF-B), human placenta growth factor (PIGF-1), and human vascular endothelial growth factor B (VEGF-B), and

wherein the conserved cysteine that has been deleted or replaced corresponds to position 156 of SEQ ID NO: 8.

17. A purified polypeptide according to claim 16 wherein the vertebrate is a human.

18. A polypeptide according to claim 16 wherein the vertebrate is a mouse.

19. A polypeptide according to claim 16 that binds VEGFR-3 and has reduced VEGFR-2 binding affinity relative to human VEGF-C having an amino acid sequence consisting of amino acids 103–227 of SEQ ID NO: 8.

20. A composition comprising a polypeptide according to claim 16 in a pharmaceutically-acceptable diluent, adjuvant, excipient, or carrier.

21. A polypeptide according to claim 16, wherein said polypeptide comprises an amino acid sequence selected from the group consisting of:

(a) the amino acid sequence of SEQ ID NO: 11, wherein the cysteine residue at position 152 of SEQ ID NO: 11 has been deleted or replaced by another ammo acid;

(b) amino-terminal trunations of (a); and

(c) carboxyl-terminal truncations of (a) or (b).

22. A polypeptide according to claim 16, wherein said polypeptide comprises an amino acid sequence selected from the group consisting of:

(a) the amino acid sequence of SEQ ID NO: 13, wherein the cysteine residue at position 155 of SEQ ID NO: 13 has been deleted or replaced by another amino acids;

(b) amino-terminal truncations of (a); and

(c) carboxyl-terminal truncations of (a) or (b).

23. A purified and isolated nucleic acid comprising a nucleotide sequence encoding a polypeptide that binds to the extracellular domain of human Flt4 receptor tyrosine kiase (VEGFR-3).

said polypeptide comprising a fragment of a vertebrate prepro-VEGF-C amino acid sequence that binds to human VEGFR-3, with the proviso that, in said polypeptide, a conserved cysteine of the vertebrate prepro-VEGF-C has been deleted or replaced by another amino acid,

wherein the vertebrate prepro-VEGF-C amino acid sequence comprises an amino acid sequence that is encoded by a DNA of vertebrate origin which hybridizes to a non-coding strand complementary to nucleotides at 352 to 1611 of SEQ ID NO: 7 under the following hybridization condition: hybridizatin at 42° C. in a hybridization solution comprising 50% formamide, 5×SSC 20 mM Na.PO. pH 6.8; and washing in 0.2×SSC at 55° C.,

wherein nucleotides 352 to 1611 SEQ ID NO: 7 encoded a human prepro-VEGF-C having the amino acid sequence set forth in SEQ ID NO: 8 that is characterized by eight cysteine residues at position 131, 156, 162, 165, 166, 173, 209, and 211 of SEQ ID NO: 8 that are conserved in human vascular endothelial growth factor (VEGF), human platelet derived growth factors A, and B (PDGF-A, PDGF-B), human placenta growth factor (PlGE-1), and human vascular endothelial growth factor B (VEGR-B), and

wherein the conserved cysteine that has been deleted or replaced corresponds to position 156 of SEQ ID NO: 8.

24. A vector comprising a nucleic acid according to claim 23.

25. A host cell transformed or transfected with a nucleic acid according to claim 23.

26. A method of making a polypeptide that binds to VEGFR-3, said method comprising the steps of:

(a) expressing a nucleic acid according to claim 23 in a host cell; and

(b) purifying a polypeptide that binds to VEGFR-3 from said host cell or from a growth medium of said host cell.

27. A polypeptide that binds to human Flt4 receptor tyrosine kinase (VEGFR-3), said polypeptide comprising an amino acid sequence selected from the group consisting of:

(a) the amino acid sequence of SEQ ID NO: 8, wherein the cysteine residue at position 156 of SEQ ID NO: 8 has been deleted replaced by another amino acid;

(b) the amino acid sequence of SEQ ID NO: 11, wherein the cysteine residue at position 152 of SEQ ID NO: 11 has been deleted or replaced by another amino acid;

(c) the amino acid sequence of SEQ ID NO: 13, wherein the cysteine residue at position 155 of SEQ ID NO: 13 has been deleted or replaced by another amino acid;

(d) amino-terminal truncations of (a), (b), or (c); and

(e) carboxyl-terminal truncations of (a), (b), (c), or (d).

28. A polynucleotide comprising a nucleotide sequence that encodes a polypeptide that binds to human Flt4 receptor tyrosine kinase (VEGFR-3), said polypeptide comprising an amino acid sequence selected from the group consisting of:

(a) the amino acid sequence of SEQ ID NO: 8, wherein the cysteine residue at position 156 of SEQ ID NO: 8 has been deleted or replaced by another amino acid;

(b) the amino acid sequence of SEQ ID NO: 11, wherein the cysteine residue at position 152 of SEQ ID NO: 11 has been deleted or replaced by another amino acid;

(c) the amino acid sequence of SEQ ID NO: 13, wherein the cysteine residue at position 155 of SEQ ID NO: 13 has been deleted or replaced by another amino acid;

(d) amino-terminal truncations of (a), (b), or (c); and

(e) carboxyl-terminal truncations of (a), (b), (c), or (d).

29. A polynucleotide according to claim 28, wherein the nucleotide sequence that encodes the peptide comprises a sequence selected from the group consisting of:

(a) the nucleotide sequence set forth in SEQ ID NO: 7 from nucleotide 352 to 1611, wherein the cysteine codon at positions 817–819 has been deleted or replaced by a codon for an amino acid other than cysteine;

(b) the nucleotide sequence set forth in SEQ ID NO: 10 from nucleotide 168 to 1412, wherein the cysteine codon at positions 621–623 has been deleted or replaced by a codon for an amino acid other than cysteine;

(c) the nucleotide sequence set forth in SEQ ID NO: 12 from nucleotide 453 to 1706, wherein the cysteine codon at positions 915–917 has been deleted or replaced by a codon for an amino aid other than cysteine;

(d) 5'-deletion fragments of (a), (b), or (c); and

(e) 3'-deletion fragments of (a), (b), (c), or (d).

* * * * *

COMMONWEALTH OF AUSTRALIA

(Patents Act 1990)

IN THE MATTER OF: Australian Patent Application 696764 (73941/94). In the name of: Human Genome Sciences Inc.

- and -

IN THE MATTER OF: Opposition thereto by Ludwig Institute for Cancer Research, under Section 59 of the Patents Act.

Annexure GBC-22

This is **Annexure GBC-22** referred to in my Statutory Declaration made this Thirteenth day of December 2000.

Gary Baxter Cox

WITNESS: _____

Patent Attorney FETTES KITCO

Exp. Pathol. 1991; 42: 11–25
Gustav Fischer Verlag Jena

A comparative study of cultured vascular and lymphatic endothelium

By L. C. J. YONG and B. E. JONES

With 11 figures

Received: July 27, 1989; Accepted: October 3, 1989

Address for correspondence: Dr. L. C. J. YONG, Department of Anatomical Pathology, Prince Henry Hospital, Little Bay, New South Wales, Australia 2036

Key words: endothelium, lymphatic; lymphatic endothelium, cultured; factor VIII related antigen; antigen, factor VIII related; Weibel-Palade bodies; aortic endothelial cells

Summary

There is comparatively little knowledge of the structure and function of *cultured* lymphatic endothelium. A study was carried out to compare the intrinsic growth characteristics of cultured lymphatic endothelial cells with cultured endothelia derived from blood vessels. It was found that cultured *lymphatic endothelium* has growth requirements and growth characteristics similar to vascular endothelium. It also possesses FVIIIRA and Weibel-Palade bodies for specific identification. The results of this study have provided important base line data for subsequent studies of the pathobiology of lymphatic endothelium.

Introduction

In vitro studies in the last 10 years have mainly focused on studies of endothelium derived from blood vessels (6). Such studies greatly advanced our understanding of the role that blood vascular endothelia play in blood homeostasis, inflammation, tumour angiogenesis and atherogenesis. *In vitro* studies have established that vascular endothelial cells are site and organ specific, produce a whole range of active substances, and have specific markers for their identification (9). There are no studies of cultured lymphatic endothelium on a comparable scale even though it is generally accepted that lymphatic vessels play important roles in various pathobiological processes such as inflammation, tumour spread and immunologic reactions. Lymphatic vessels are difficult to visualise in ordinary tissue sections and functionally regarded as passive conduits for returning excess fluid from the interstitial tissue to the main circulation, but how they play an active role in the spread of malignant tumours, inflammation, healing and regeneration as well as immunological reactions is not clear. There is little doubt that *in vitro* studies of lymphatic endothelium on a similar scale to vascular endothelium will help to define more specific roles that lymphatic vessels may play in various pathobiological processes.

The techniques for the culture of endothelia from blood vessels are well established (6). Evidence from a few preliminary reports suggests that successful cultures of lymphatic

endothelium could be achieved from the same techniques for the culture of vascular endothelium (9, 10). As a first step towards a subsequent study of the immunological and secretory characteristics of cultured lymphatic endothelium, we set out to establish cultures of lymphatic endothelium, study their growth and structural characteristics and compare them with cultures of endothelium from blood vessels. The results from this study will provide valuable base line data for subsequent studies of the pathobiology of lymphatic endothelium.

Materials and Methods

Isolation of endothelial cells from bovine mesenteric lymphatic vessels

Fresh bovine mesentery was obtained from the local abattoir. The mesenteric vessels were identified by injecting a solution of 0.1 %. Evan's blue dye in phosphate buffered saline (PBS) into a mesenteric lymph node. The dye filled segment was ligated and dissected free from the adipose tissue. The lymphatic vessel was cannulated at both ends and gently flushed with Hank's balanced salt solution (HBSS). The lymphatic was then filled with HBSS containing 1.5 mg/ml of collagenase (Boehringer Mannheim) and 0.2 % foetal calf serum (FCS) and incubated at 37 °C for 10 min. The lymphatic vessel was then drained and the fluid collected. The vessel was flushed with an additional 20 ml of HBSS. The total volume of solution was centrifuged at 3,000 rpm for 15 min. The cell pellet was resuspended in 1 ml of complete culture media and placed in one well of a Linbro multiwell plate (9.62 cm^2). A further 2 ml of culture media was added to the culture well. Usually the cells from 2 lymphatic vessels were pooled and placed in one culture well.

Isolation of bovine aortic endothelial cells

Fresh aorta obtained from the local abattoir was dissected free of all fibrofatty tissue and the branches ligated. The aorta was then filled with HBSS containing 1.5 mg/ml of collagenase and 0.2 % FCS and incubated at 37 °C for 10 min. The perfusate was recovered, centrifuged and the pellet resuspended in 1 ml of HBSS and placed in culture well with an additional 2 ml of complete culture media.

Isolation of human umbilical vein endothelial cells

Human umbilical cords were obtained from the associated obstetrics hospital of the University of New South Wales. The endothelial cells were isolated from the vein using established techniques of collagenase dispersion. Briefly, the umbilical vein was inspected for damage and cannulated at both ends and rinsed with HBBS and then filled with 0.1 % collagenase containing 0.2 % FCS and incubated for 10 min at 37 °C. The solution was then collected and the vein flushed to remove residual endothelial cells. The cells were concentrated into a pellet by centrifugation at 1,000 rpm for 5 min, resuspended in 1 ml of complete culture media and placed in culture well (7).

Culture conditions

All primary and subcultures were grown in modified Medium 199 containing Earl's salts, 20 mMol HEPES buffer and glutamine supplemented with 20 % FCS (Flow), 100 µg/ml endothelial cell growth supplement (ECGS), 100 µg/ml heparin (Sigma), penicillin 50 µ/ml (Flow), streptomycin 50 µg/ml and fugizone 2.5 µg/ml (Flow).

All culture flasks and wells were coated with 1 % gelatin (Sigma) in Ca^{++} and Mg^{++} free PBS. Primary cultures were grown in Linbro multiwell plates and subcultures were grown in Nunclon 25 cm^2 flasks at 37 °C in a humidified incubator with air and 5 % CO_2. Cells were passaged and subcultured by standard techniques of trypsin digestion using 0.25 % trypsin, 0.02 % EDTA in PBS. Cells were passaged at a ratio of 1 : 3 and subcultures reached confluence in 7 days. Half the culture medium was replaced in all cultures at second daily intervals.

Isolation and cult

Human aortic
from head injury.
described in the p
Capillary endo
from circumcision
squeezed with a s
were removed by
during culture. C
Medium 199, 100

Identification of e

It is generally
detection of factc
immunohistochem
immunofluoresce
for 4–5 days and
dried. The cover
incubated with pr
with 3 % pig ser
labelled swine ant
and mounted with

Proliferation Stud

The rate of ce
is the time taken f
were grown in 1
approximately 5
haemocytometer
graph and doubli

Preparation of cu

Cultured cells
ques of HAUDENS
prepared 2.5 % g
standard techniqu
step of processing
sectioned for exa
Cultured cells
Glass coverslips
mately 2–2.5 × 1
Cells were then f

Normal lymphatic

Normal mese
mission and scan
cells.

Isolation and culture of human aortic and capillary endothelial cells

Human aortic endothelium was cultured from thoracic aorta of young adults after death from head injury. Endothelial cells were harvested by the techniques of enzyme dispersion as described in the preceding sections.

Capillary endothelial cells were isolated and cultured from the neonatal foreskin obtained from circumcision. Briefly foreskin was cut into small pieces and after 0.3 % trypsin digestion squeezed with a scalpel blade to extrude endothelial cells from capillaries. Contaminant cells were removed by centrifugation in Percoll and by mechanical weeding with sterile glass probe during culture. Cultures of capillary endothelium were maintained in 20% human serum in Medium 199, 100 µg/ml ECGS and 100 µg/ml heparin.

Identification of endothelial cells

It is generally accepted that the best method of identification of endothelial cells is the detection of factor VIII related antigen (FVIIIRA) which can be readily demonstrated by immunohistochemical techniques (8). All cultured cells in this study were subjected to indirect immunofluorescent microscopy for expression of FVIIIRA. Cells were grown on coverslips for 4–5 days and removed from culture flasks, rinsed in PBS, fixed in cold acetone and air dried. The cover slips were than washed in Triton X 100 (0.3 % in PBS), rinsed in PBS and incubated with primary antibody, rabbit antihuman FVIIIRA at a dilution of 1:100 in PBS with 3 % pig sera for 1 h. The coverslip was then rinsed in PBS and incubated with FITC labelled swine anti-rabbit IgG with 3% pig sera for 30 min. The cover slip was then washed and mounted with glycerol/PBS (1:9), examined and photographed.

Proliferation Studies

The rate of cellular proliferation was determined by estimation of the *doubling time* which is the time taken for cell cultures to double their population in a given culture condition. Cells were grown in Linbro multiwell plates of 2.0 cm each. Each well was inoculated with approximately $5{:}8 \times 10^4$ cells/cm^2. The number of cells in each well was counted in a haemocytometer after 24, 48 and 72 h intervals. The cell counts were plotted on a semilog graph and doubling times determined by analysis of the growth curves (7).

Preparation of cultured cells for electron microscopy

Cultured cells were prepared for transmission electron microscopy by established techniques of HAUDENSCHILD et al. (5). Cells grown in Nuclon flasks were fixed *in situ* with freshly prepared 2.5 % glutaraldehyde in 0.1 M cacodylate buffer at *p*H 7.4 for 1 h and processed by standard techniques. Toluidine blue (0.1 %) was added to identify cell colonies during each step of processing. After processing blocks of flask with attached cell layer were selected and sectioned for examination with a Philips 300 electron microscope.

Cultured cells were prepared for scanning electron microscopy using standard techniques. Glass coverslips were inoculated with 50 µl aliquot of cell suspension containing approximately $2-2.5 \times 10^4$ cells and placed in a petri dish containing culture media for 4–5 days. Cells were then fixed in glutaraldehyde.

Normal lympatic vessels

Normal mesenteric bovine lymphatic vessels were prepared for light microscopy, transmission and scanning electron microscopy by standard methods for comparison with cultured cells.

Results

General growth characteristics of cultured endothelial cells

The techniques used for the isolation and culture of vascular endothelial cells and the growth characteristics of bovine aortic endothelium and human umbilical vein endothelium are well documented (2, 6, 14). The characteristic features of vascular endothelium compared with those of lymphatic endothelium are presented in table 1. It was found that lymphatic

Table 1. Growth and structural characteristics of cultured endothelial cells.

Cell type	Cytology	Growth pattern	Ultrastructural features		Immunohisto-chemistry		Proliferation (doubling time)
			WBP	Tight jns	FVIIIRA	UEA-1	
HUVE	Polygonal	Monolayer	+++	+++	+++	+	14 h
HAE	Polygonal	Monolayer	+++	+++	+++	+	30–40 h
BAE	Polygonal	Monolayer	−	++	+++	+	30–40 h
BLE	Polygonal	Monolayer	++	+	+++	++	16 h

WPB: − = absent; + = present; ++ = frequent; +++ = numerous; FVIIIRA: − = absent; +++ = 100% positive; UEA-1: − = absent; + = faint; ++ = bright staining

endothelial cells were readily detached and dispersed from the vessel wall using a collagenase solution containing 1.5 to 2.0 mg/ml of enzyme. A higher concentration of collagenase appeared to cause detachment and disruption of contaminant cells as well as endothelial cells. A layer of gelatin was also essential for growth of lymphatic endothelial cells. Cells were attached to the gelatin-coated surface of the culture vessels within 3 h of inoculation. By 2–3 d (fig. 1) proliferative activity was well in advance and reached confluence by 5 to 7 days. Associated with endothelial cells were elongated fibroblastic cells. They were eliminated by a process of mechanical weeding using sterile glass probe under phase contrast microscopy. Under these conditions relatively pure cultures of lymphatic endothelial cells were obtained. Cultured vascular and lymphatic endothelial cells at confluence attained cell densities ranged from 2.7×10^4 cells/cm^2 to 7.4×10^4 cells/cm^2. The average cell density for each cell type was highest for Bovine aortic endothelium (BAE) at 4.2×10^4 cells/cm^2. Bovine lymphatic endothelium (BLE) at 3.8×10^4 cells/cm^2 and human umbilical vein endothelium (HUVE) at 3.5×10^4 cells/cm^2. The cell density did not appear to significantly decline with prolonged culture although some large multinucleated cell forms appeared in older cultures. The cells did not increase in size with repeated sub-cultures.

Cultured cells were examined by indirect immunofluorescent microscopy and for FVIIIRA. Cryostat sections of *normal* lymphatic vessels were also examined for FVIIIRA expression by indirect immunofluorescence.

Ultrastructural features of cultured lymphatic endothelial cells

To our knowledge, there are no detailed reports of the ultrastructure of *cultured lymphatic endothelium*. The method of preparation of monolayers of cultured cells for ultrastructural studies ensured that the integrity and intercellular as well as the cell/substrate relationship of

Fig. 1. Cultured hur elongated morpholo

Fig. 2. Cultured bovine lymphatic endothelial cell. Note Weibel-Palade body (WPB) in close proximity to cisterna (arrow) of Golgi apparatus (G). × 71,000.

endothelial cells and the
ilical vein endothelium are
ar endothelium compared
was found that lymphatic

ial cells.

histo-ry		Proliferation (doubling time)
A	UEA-1	
	∓	14 h
	+	30–40 h
	+	30–40 h
	++	16 h

us; FVIIIRA: − = absent;
right staining

sel wall using a collagenase
ncentration of collagenase
as well as endothelial cells.
ndothelial cells. Cells were
h of inoculation. By 2–3 d
onfluence by 5 to 7 days.
They were eliminated by a
hase contrast microscopy.
helial cells were obtained.
tained cell densities ranged
l density for each cell type
lls/cm^2. Bovine lymphatic
ein endothelium (HUVE) at
dy decline with prolonged
lder cultures. The cells did

scent microscopy and for
so examined for FVIIIRA

cture of *cultured lymphatic*
ed cells for ultrastructural
cell/substrate relationship of

Palade body (WPB) in close

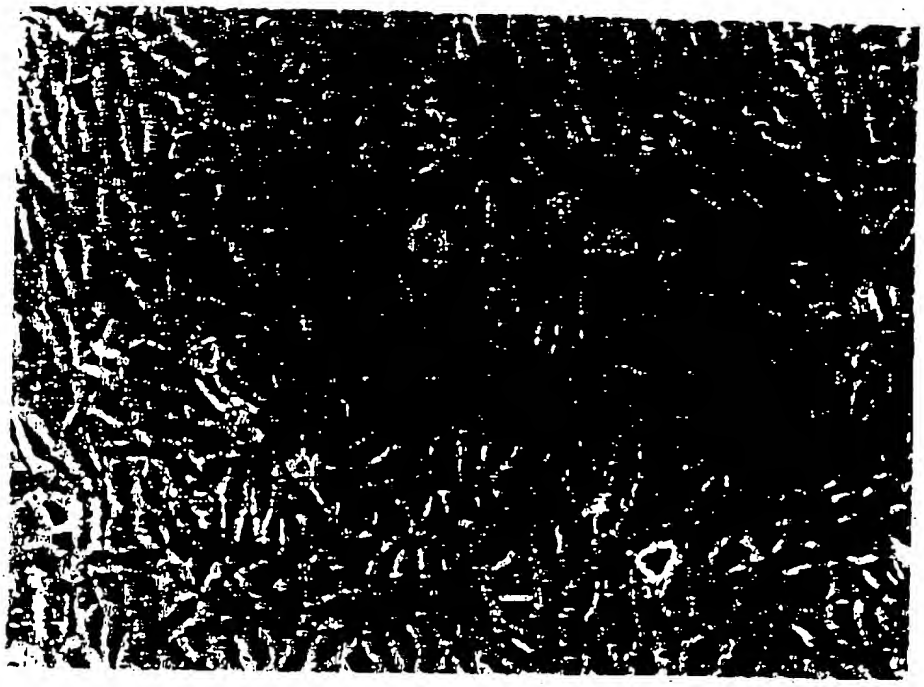

Fig. 1. Cultured human umbilical vein endothelial cells after 3 days showing polygonal and elongated morphology. Phase contrast ×350.

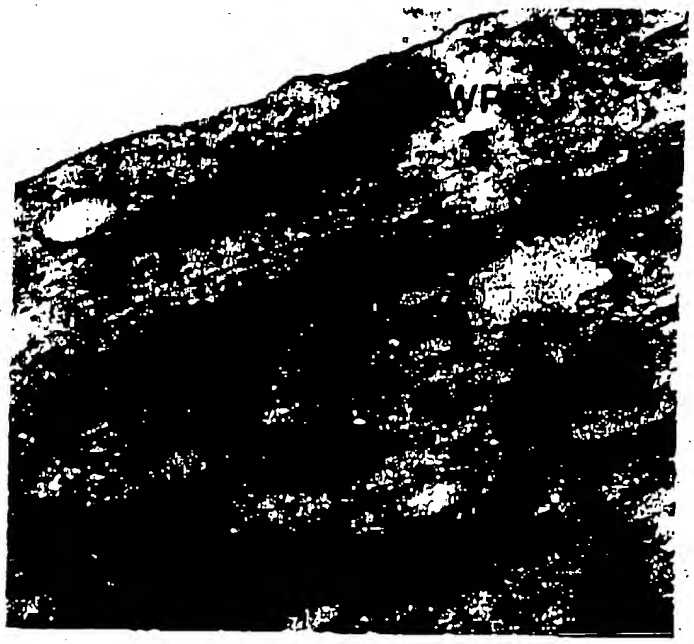

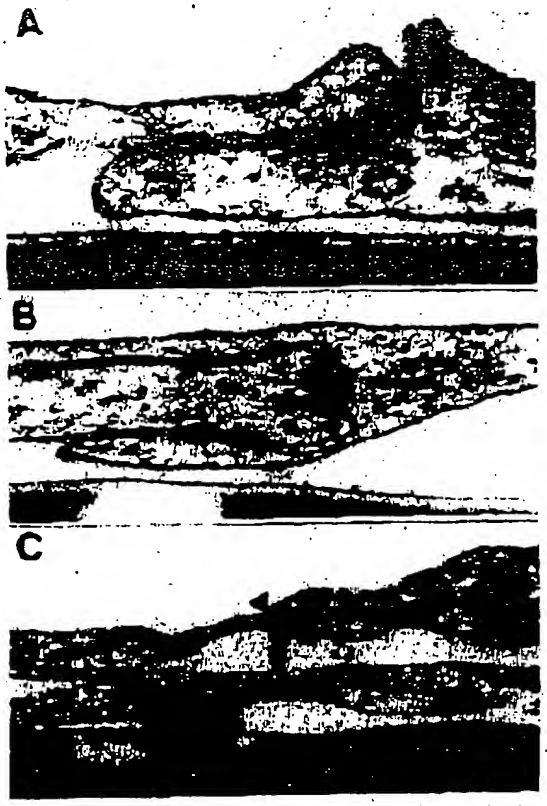

Fig. 3. Different types of intercellular junctions of cultured endothelial cells. A = simple overlapping of adjacent cells. × 94,000. B = Mortice-like junction. × 74,000. C = tight junction, rarely seen in cultured lymphatic endothelium. × 28,000.

the monolayer was maintained. Cultured endothelial cells covered the gelatin surface as a distinct monolayer at confluence. The cells have central nuclei with cell borders extending over considerable distances in all directions. Cells were bound by a distinct cytoplasmic membrane with invaginations and often narrow openings forming caveolae. There were also numerous randomly placed surface projections most of which have club-shaped ends similar to those seen in vascular endothelium. The cytoplasm contained the usual cytoplasmic organelles including mitochondria, ribosomes, rough endoplasmic reticulum, Golgi apparatus, filaments and vesicular bodies. The Weibel-Palade (WPB) or specific endothelial granule was frequently seen in the cytoplasm, sometimes situated in a position close to the Golgi apparatus (fig. 2). The WPB had a specific internal substructure characterised by a series of longitudinal fine tubular structures arranged in a parallel fashion to the longitudinal axis. The appearance of the WPB varied considerably depending on whether it was cut in cross or oblique sections or whether the section transected the broad or narrow end of the club-shaped structure. Consequently the WPB could be easily mistaken for mitochondria. Cultured lymphatic endothelial cells maintained a close intercellular relationship. There were 3 types of intercellular junctions in vascular and lymphatic endothelial cultures (fig. 3). The most common type was a simple overlapping of one cell on another. The less commonly encountered type was the

Fig. 4. Surface re
mitochondria (Mc
and (allow heads)

interdigitating jun
which were locke
membranes. The
junctions". Such j
classical and distii

Ultrastructural
of cultured lymph
of cytoplasmic fin
well as WPB wer
also observed.

The ultrastructure
and human capill

There was ger
lial cells from d
summarised in tab
nucleoli. The cyt
rough and smooth
Golgi apparatus, i
the cell surface th
exocytic vesicles.

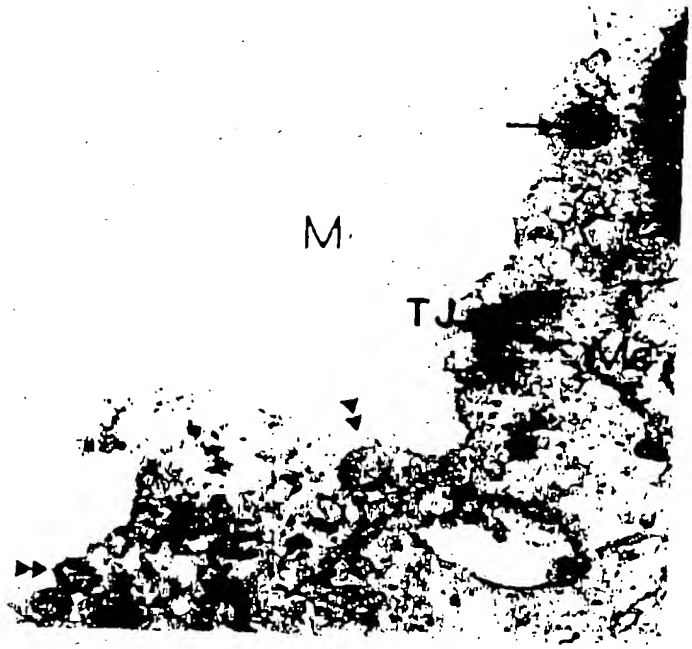

Fig. 4. Surface region of normal *(in vitro)* lymphatic endothelium showing tight junction (TJ), mitochondria (Mc), micro-projection (M) and Weibel-Palade bodies (arrow) in oblique section and (allow heads) in cross section. × 45,000.

xhelial cells. A = simple
tion. × 74,000. C = tight
).

d the gelatin surface as a
with cell borders extending
by a distinct cytoplasmic
caveolae. There were also
club-shaped ends similar to
sual cytoplasmic organelles
Golgi apparatus, filaments
lial granule was frequently
e Golgi apparatus (fig. 2).
series of longitudinal fine
xis. The appearance of the
oss or oblique sections or
he club-shaped structure.
ondria. Cultured lymphatic
were 3 types of intercellu-
). The most common type
y encountered type was the

interdigitating junction whereby 2 adjacent cells are joined by several finger like processes which were locked together but are still distinctly separated by their respective cellular membranes. The rarest type of cellular junction was the type of junction resembling "tight junctions". Such junctions consisted of closely opposed electron dense areas but it lacks the classical and distinctive features seen in true tight junctions in the epidermis.

Ultrastructural studies of *normal (in vivo)* lymphatic endothelium showed all the features of cultured lymphatic endothelial cells (fig. 4) On the luminal surface were varying numbers of cytoplasmic finger-like projections and also caveolae. The usual cytoplasmic organelles as well as WPB were present. Indistinct and poorly formed "tight" intercellular junctions were also observed.

The ultrastructure of bovine aortic endothelial cells, human umbilical vein endothelial cells and human capillary endothelial cells

There was generally little difference in the ultrastructural characteristics of these endothelial cells from different sources. Only minor differences exist. The main features are summarised in table 2. Cultured endothelial cells have a centrally located nucleus with one or 2 nucleoli. The cytoplasm contains the usual cytoplasmic organelles including mitochondria, rough and smooth endoplasmic reticulum, pinocytic vesicles, free and attached ribosomes, Golgi apparatus, filaments, multivesicular bodies and varying numbers of myelin bodies. On the cell surface there are blunt protrusions with varying numbers of caveolae and occasional exocytic vesicles. Weibel-Palade bodies, the unique ultrastructure of endothelial cells were

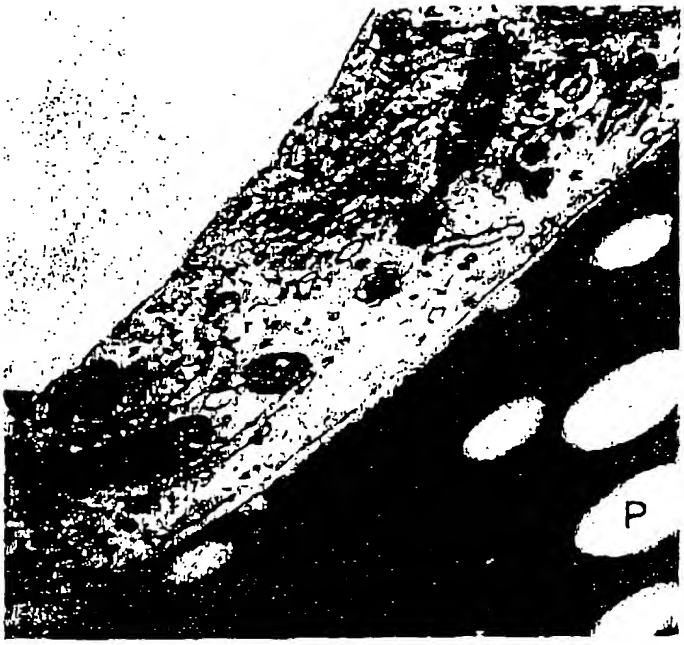

Fig. 5. Cultured human endothelial cell showing caveola (arrow head) and several Weibel-Palade bodies (arrows). P = gelatin substrate. × 45,000.

Fig. 6. Cultured hu
× 75,000.

present in all cultured endothelial cells examined (fig. 5). However, the number varied depending on the source of cultured cells. It was surprising to note that, contrary to popular belief, human capillary endothelial cells contained many Weibel-Palade bodies (fig. 6).

Cultured endothelial cells from the various sources maintain a close intercellular relationship. Most of the different types of cell junctions are encountered. These include simple overlapping, end to end abutment, complex interdigitating and mortice-like junjctions (fig. 3). Tight junctions are frequently encountered. There are also micro-channels were pinocytic vesicles often open into (fig. 7).

Immunofluorescent studies on cultured endothelial cells

All cultured endothelial cells in this study were examined by indirect immunofluorescent microscopy for the presence of FVIIIRA. The expression of FVIIIRA has been recognised as a specific feature of endothelial cells. In this study all cultured cells were found to express FVIIIRA. All primary and subcultures of endothelial cells exhibit brilliant granular green fluorescence (fig. 8a). By using phase contrast microscopy it was possible to determine the exact proportion of cells containing FVIIIRA (fig. 8b). There was slight variation in the staining intensity but cultured cells still exhibited strong fluorescence after 8 passages. In an effort to ensure specific staining for FVIIIRA steps were taken to block non-specific staining by incubating cultured cells in diluted pit antisera or incubating cells with dilute 3% pig serum in the staining procedure. Negative controls were also included. Cultured endothelial cells were also stained with Ulex europaeus I lectin (UEA-1). It was found that endothelial cells showed variable staining intensity.

Fig. 7. Cultured bo
nel (arrow) and sur

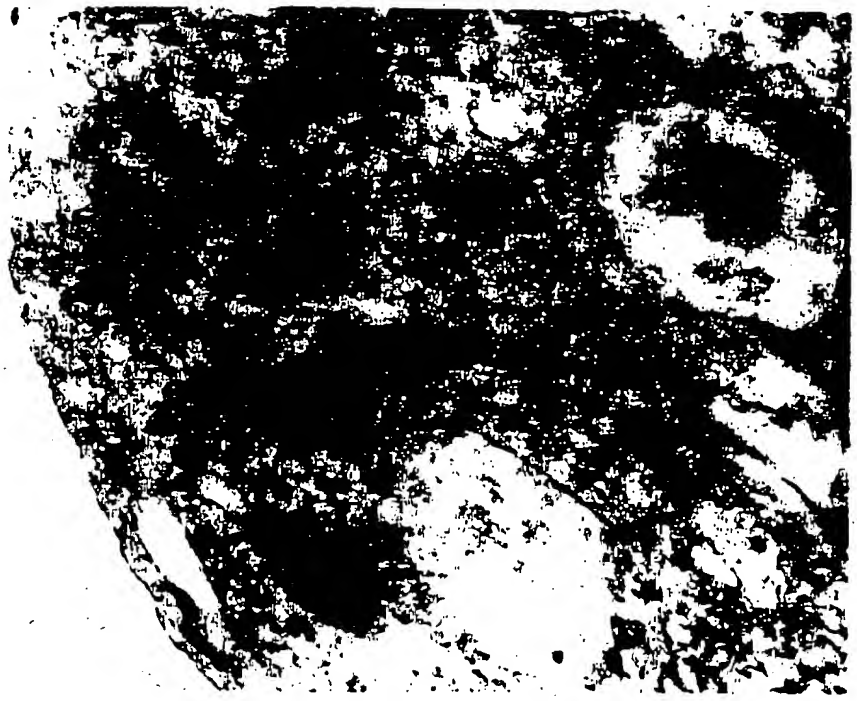

Fig. 6. Cultured human *capillary* endothelial cell showing several Weibel-Palade bodies. × 75,000.

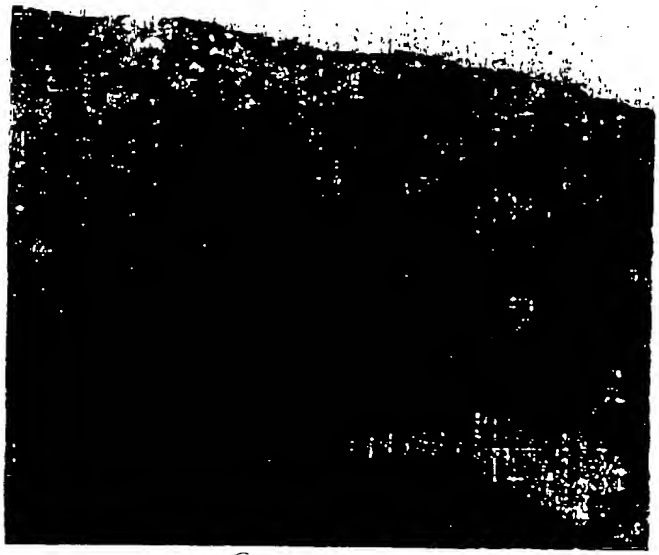

Fig. 7. Cultured bovine endothelium showing tight junction (TJ), an intercellular microchannel (arrow) and surface vesicle (V). × 74,000.

Fig. 8. a) Cultured lymphatic endothelial cells exhibiting bright granular immunofluorescence for FVIIIRA. × 430. b) Phase contrast view of the same field verifying that all cells show FVIIIRA. × 370.

Proliferation studies and doubling times

The growth rate of various types of cultured endothelial cells were studied in different culture conditions during their logarithmic growth phase. It was established that the optimal period of determining the doubling time of cell growth was between 24 to 48 h of passage. By

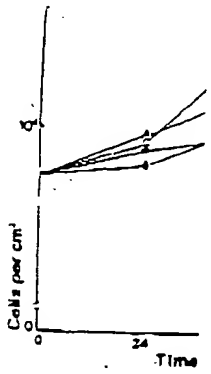

Fig. 9. Growth cur
passage inoculated
A = ECGF (100 µ;
ml), 20% FCS, ar
plastic; D = ECGF

Fig. 10. Growth c
inoculated at 8 × 1
A = ECFG (100 µ
ml), 20% FCS an
20% FCS and gel
human AB negativ

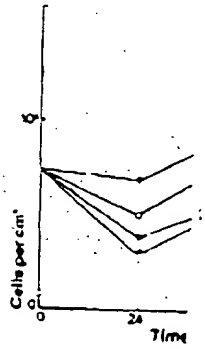

this time the cell
confluence. The
conditions are sh
culture conditions
heparin, FCS an
previous works it

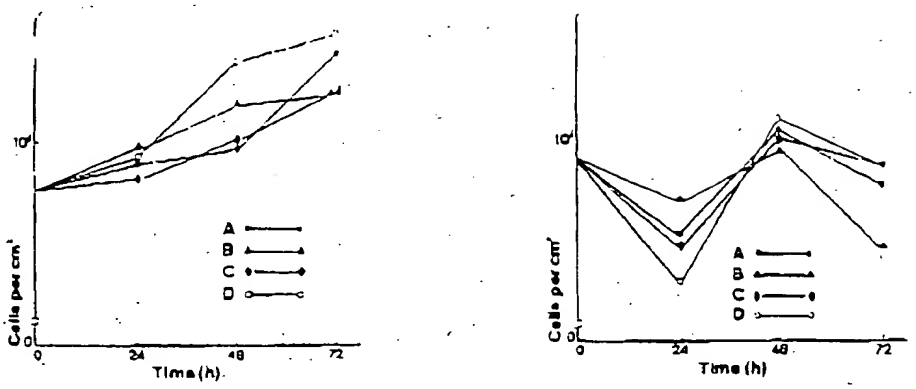

Fig. 9. Growth curve for cultured lymphatic endothelium after the 4th (D) and 7th (A, B, C) passage inoculated at 5.8×10^4 cells/cm^2 in the following culture conditions:

A = ECGF (100 µg/ml), heparin (100 µg/ml), 20% FCS, and gelatin; B = ECGF (100 µg/ml), 20% FCS, and gelatin; C = ECGF (100 µg/ml), heparin (100 µg/ml), 20% FCS and plastic; D = ECGF (100 µg/ml), heparin (100 µg/ml), 20% FCS and gelatin.

Fig. 10. Growth curves for cultured human umbilical vein endothelium after 2 passages inoculated at 8×10^4 cells/cm^2 in the following conditions:

A = ECFG (100 µg/ml), heparin (100 µg/ml), 20% FCS and gelatin; B = heparin (100 µg/ml), 20% FCS and gelatin; C = ECGF (crude preparation, 50 µl/ml), heparin (100 µg/ml), 20% FCS and gelatin, D = ECGF (crude preparation, 50 µl/ml), heparin (100 µg/ml), 20% human AB negative serum and gelatin.

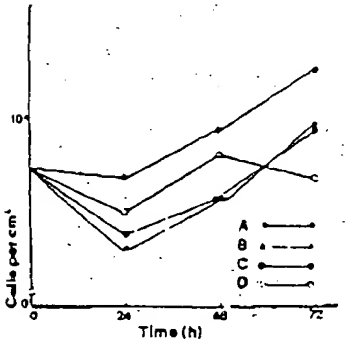

Fig. 11. Growth curves for cultured human aortic endothelium after 7 passages and inoculated at 5.4×10^4 cells/cm^2 in the following culture conditions:

A = ECGF (100 µg/ml), heparin (100 µg/ml), 20% human AB negative serum and gelatin; B = ECGF (100 µg/ml), 20% human AB negative serum and gelatin; C = ECGF (crude preparation, 50 µl/ml), heparin (100 µg/ml), 20% human AB negative serum and gelatin; D = heparin (100 µg/ml), 20% human AB negative serum and gelatin.

ght granular immunofluorescence
field verifying that all cells show

al cells were studied in different
was established that the optimal
between 24 to 48 h of passage. By

this time the cells would have recovered from the shock of passage and by 48 h reached confluence. The relative growth curves of various endothelial cells under various growth conditions are shown in figs. 9, 10 and 11. It is evident that the doubling times varied with culture conditions. Lymphatic endothelial cells grow best in culture media containing ECGF, heparin, FCS and on a substrate of gelatin. The results are compared with results from previous works in table 2.

Table 2. Growth characteristics of endothelial cells from various sources.

Type of endothelium	Culture conditions					Doubling time	C.P.D.L.	Reference
	Culture medium	FCS	ECFG*	Heparin	Surface substrate			
Human umbilical vein	199	20%	–	–	plastic	92 h	ND	JAFFE et al. 1973 (5)
	199	20%	–	–	plastic	42–48 h	ND	GIMBONE 1976 (3)
	199	20%	100 µl/ml	–	fibronectin	42–72 h	27–34	MAUAG et al. 1981 (13)
	199	20%	100 µl/ml	–	gelatin	64 h	ND	THORNTON et al. 1983 (19)
	199	20%	150 µl/ml	–	fibronectin	25 h	ND	MAUAG et al. 1984 (13)
	199	20%	20 µl/ml	90 µl/ml	gelatin	18–21 h	42–79	THORNTON et al. 1983 (19)
Human aorta	199	20%	20 µl/ml	90 µl/ml	gelatin	18–21 h	42–79	THORNTON et al. 1983 (19)
Bovine aorta	RPMI-164	35%	–	–	plastic	29–34 h	ND	BOOYSE et al. 1975 (2)
	Waymouth	30%	–	–	plastic	24–48 h	35–40	SAGE 1984 (15)
Bovine lymphatic	199	20%	–	–	plastic	ND	ND	JOHNSTONE and WALKER 1984 (9)
Canine lymphatic	199	20%	–	–	plastic	36–68 h	ND	GNEPP and CHANDLER 1985 (4)
	199	20%	150 µl/ml	–	plastic	36–68 h	ND	GNEPP and CHANDLER 1985 (4)

C.P.D.L. = Cumulative population doubling level is the number of population doublings that fail to proliferate further. ND = no data available. FCS = Foetal calf serum. ECGF = Endothelial cell growth factor.

Endothelium of normal

It is unnecessary to
sufficient to say that th
main purpose of includi
in vitro features of endo
vessels and lymphatics

Discussion

There is considerab
secretes substances wit
states (6). Cultured hu
possess intrinsic abilit
fibronectin, thrombosp
endothelia have a simil
function as passive co
system. This notion is l
or modulating activity
information on the sec
characterise and establi
vascular endothelia anc

This study has sho
endothelium are also su
the growth characterist
growth pattern, formin
stone pattern at conflu
have similar ultrastru
Weibel-Palade bodies
and caveolae. Some
capillary endothelium
that Weibel-Palade bod
Weibel-Palade body h
composition and serves
as a specific marker fo
that cultured endotheli
subcultures, but we ha

The types of inter
However, it was noted
whereas they are frec
consistent with the re
associated with a relati

We have found th
results reported by o
necessary for the optim
of gelatine is the most
rate and doubling time
cultured endothelia. C
more without significa

JOHNSTONE and W
cells contain FVIIIRA.
combination of immur
lymphatic endothelial

C.P.D.L. = Cumulative population doubling level is the number of population doublings that fail to proliferate further. ND = no data available. FCS = Foetal calf serum. ECGF = Endothelial cell growth factor.

Endothelium of normal in vivo blood vessels and lymphatic

It is unnecessary to describe in detail the structure of normal endothelium. However, it is sufficient to say that the findings in this study are not at variance with published data. The main purpose of including normal tissues in this study is to enable a comparison of *in vivo* and *in vitro* features of endothelial cells. Results have shown that all endothelia from normal blood vessels and lymphatics contain FVIIIRA and Weibel-Palade bodies.

Discussion

There is considerable experimental evidence to show that cultured vascular endothelium secretes substances with biochemical activity important for normal function and in disease states (6). Cultured human vascular endothelia have been shown to express ABO antigens, possess intrinsic ability to form 3-dimensional networks in culture, produce prostacyclin, fibronectin, thrombospondin, and type III procollagen (6). It is not known whether lymphatic endothelia have a similar intrinsic secretory ability. It is generally assumed that lymphatics function as passive conduits returning excessive interstitial fluid to the main circulatory system. This notion is based on the current assumption that lymphatics do not have secretory or modulating activity. Past studies of the composition of lymph do not provide reliable information on the secretory activity of lymphatic endothelium. This study was designed to characterise and establish long-term cultures of lymphatic endothelia, to compare them with vascular endothelia and to subsequently investigate their pathobiological activities.

This study has shown that the current techniques for the isolation and culture of vascular endothelium are also suitable for culturing lymphatic endothelium. The culture conditions and the growth characteristics are similar for all types of endothelium. They all have a common growth pattern, forming a monolayer during the early growth period and develop a cobble stone pattern at confluence. Cultured endothelia derived from blood vessels and lymphatics have similar ultrastructural features. All cultured endothelia express FVIIIRA, possess Weibel-Palade bodies and the usual cytoplasmic organelles including cell surface projections and caveolae. Some workers have questioned the existence of Weibel-Palade bodies in capillary endothelium and expecially lymphatic endothelium. This study has clearly shown that Weibel-Palade bodies are present in both normal and cultured lymphatic endothelium. The Weibel-Palade body has been shown in this study to be an integral part of the cytoplasmic composition and serves as a specific ultrastructural marker for its identification just as it serves as a specific marker for the identification of vascular endothelium. This study has also shown that cultured endothelial cells have retained all the structural characteristics even after several subcultures, but we have not studied whether lymphatic endothelia are site or organ specific.

The types of intercellular cell junctions did not differ in different types of endothelia. However, it was noted that tight junctions are rarely found in cultures of lymphatic endothelia whereas they are frequently seen in cultures of endothelia from blood vessels. This is consistent with the respective functions of lymphatic and bood vessels, lymphatics being associated with a relatively low pressure system.

We have found that the growth requirements of cultured endothelia are comparable to results reported by other researchers (table 2). Growth supplements and a substrate are necessary for the optimal growth of lymphatic endothelial cells. It was found that a thin layer of gelatine is the most suitable substrate for the culture of lymphatic endothelium. The growth rate and doubling time of lymphatic endothelium were comparable with that of other types of cultured endothelia. Cultures of lymphatic endothelium can be maintained for 3 months or more without significant alteration in growth and structural characteristics.

JOHNSTONE and WALKER (9) studied cultured lymphatics and reported that not all of their cells contain FVIIIRA. This is at variance with our findings. We were able to demonstrate by a combination of immunological staining and phase contrast microscopy that all our cultured lymphatic endothelial cells possess FVIIIRA. The difference is probably due to a difference in

the purity of cultures or that some of JOHNSTONE and WALKER's cultured cells may have lost their expression for FVIIIRA. We were also able to show that cultured lymphatic endothelial cells have Weibel-Palade bodies. JOHNSTONE and WALKER (9) did not publish any data on ultrastructural studies of their cells. Other workers have also shown variation in FVIIIRA expression of lymphatic endothelia (1, 17).

Our findings that blood vascular and lymphatic endothelia have similar growth requirements, growth characteristics and have FVIIIRA further support the notion of a common origin of blood and lymphatic vessels. There are 2 opposing views on the origin of lymphatic endothelium. One view is that lymphatic vessels differentiate *de novo* from local mesenchyme as a series of channels which subsequently connect centrally to form the lymphatic system. The opposing view is that the lymphatic system develops as a series of venous outpouchings during early embryonic life, the channels ramify and extend peripherally to eventually form the definitive lymphatic system (11, 20). If we accept the latter theory, it is therefore not surprising to find that endothelium from blood and lymphatic vessels share common characteristics. This does not imply that there are subtle biochemical or immunological differences between blood and lymphatic endothelium or that lymphatic endothelia may also be site and organ specific. More work, with particular emphasis on cultures of lymphatic endothelium from capillaries and a study of their antigenic expression as well as biochemical features may help to elucidate some of the issues

The Weibel-Palade body is a unique endothelial cell structure. It has an internal substructure of parallel micro-tubules bound by a membrane. Its exact function is not fully known, but recent work has shown that it may be the site of production and/or storage of von Willebrand factor. This notion is supported by the fact that the Weibel-Palade body has been seen to be closely associated with the Golgi apparatus. Some researchers have doubted the existence of Weibel-Palade bodies in lymphatic endothelium. TABUCHI and YAMAMOTO (18) have shown Weibel-Palade bodies in canine lymphatic endothelium. There is also evidence that Weibel-Palade bodies may occur in clusters in certain types of large vessel endothelia and scarcely in endothelia of small capillaries. Our work has shown the presence of Weibel-Palade bodies in cultured and normal lymphatic endothelium. However, we have not examined the distribution or the density of Weibel-Palade bodies in lymphatic endothelium. Nevertheless, the fact that Weibel-Palade bodies are found in lymphatic endothelium and the suggestion of Weibel-Palade bodies being a source of von Willebrand factor raises the possibility that lymphatics may be an important source of von Willebrand factor in health and disease states. It is also reasonable to postulate that the structure and biochemical activity of von Willebrand factor derived from lymphatics may differ from that derived from blood vessels.

Acknowledgement

We gratefully acknowledge the help of Dr. R. MARKS with cultures of capillary endothelia from human foreskin.

References

1. BECKSTEAD, J. H., WOOD, G. S., FLECHER, V.: Evidence for the origin of Kaposi's sarcoma from lymphatic endothelium. Am. J. Pathol. 1985; 119: 294–300.
2. BOOYSE, F. M., SEDLAK, B. J., RAPELSON, M. E.: Culture of arterial endothelial cells: characterisation and growth of bovine aortic cells. Thromb. Diath. Haemorrh. 1975; 34: 825–839.
3. GIMBONE, M. A. JR.: Culture of vascular endothelium. Prog. Hemost. Thromb. 1976; 3: 1–28.
4. GNEPP, D. R., CHANDLER, W.: Tissue culture of human and canine thoracic duct endothelium. In Vitro 1985; 21: 200–206.
5. HAUDENSCHILD, C. C., COTRAN, R. S., GIMBONE, M. A., JR., FULKMAN, J.: Fine structure of vascular endothelium in culture. J. Ultrastruct. Res. 1975; 50: 22–32.
6. JAFFE, E. A.: Biolo
7. – HOYER, L. W., J cells. J. Clin. Invest
8. – NACHMAN, R. L. Identification by mo
9. JOHNSTONE, M. O., Vitro 1984; 20. 566
10. JONES, B. E., YONO, Vitro 1987; 23: 698
11. LEWIS, F. T.: The d
12. MAUAO, T., HOOVEI human umbilical vei Martinus Nyhoff Pul
13. – – – – Serial pa
14. ROSEN, E. M., MCI endothelial cell strai
15. SAGE, H.: Collagen JAFFE, E. A.). Mart
16. SMITH, G. J., MES characterization of t 401–405.
17. SVANHOLM, H., NIE Virchows Arch. 198
18. TABUCHI, H., YAM cardiac valves of do
19. THORNTON, S. C., I and long term serial
20. YOFFEY, J. M., COU 1956.

6. JAFFE, E. A.: Biology of endothelial cells. Martinus Nyhoff Publ., Boston 1984.
7. – HOYER, L. W., NACHMAN, R. L.: Synthesis of antihemophilic factor antigen by cultured endothelial cells. J. Clin. Invest. 1973; 52: 2757–2764.
8. – NACHMAN, R. L., BECKER, C. G.: Culture of human endothelial cells derived from umbilical veins. Identification by morphological criteria. J. Clin. Invest. 1973; 52: 2745–2756.
9. JOHNSTONE, M. G., WALKER, M. A.: Lymphatic endothelial and smooth muscle cells in tissue culture. In Vitro 1984; 20: 566–572.
10. JONES, B. P., YONG, L. C. J.: Culture and characterization of bovine mesenteric lymphatic endothelium. In Vitro 1987; 23: 698–706.
11. LEWIS, F. T.: The development of the lymphatic system in rabbits. Am. J. Anat. 1906; 5: 95–111.
12. MAUAG, T., HOOVER, G. A., STEMERMAN, M. B., WEINSTEIN, R.: Factors which stimulate the growth of human umbilical vein endothelial cells *in vitro*. Chap. 9. Biology of endothelial cells (ed. JAFFE, E. A.). Martinus Nyhoff Publ., Boston 1984.
13. – – – – Serial propagation of human endothelial cells *in vitro*. J. Cell Biol. 1981; 91: 420–426.
14. ROSEN, E. M., MUELLER, S. N., NOVERAL, J. P., LEVINE, E. M.: Proliferative characteristics of clonal endothelial cell strains. J. Cell. Physiol. 1981; 107: 123–137.
15. SAGE, H.: Collagen synthesis by endothelial cells in culture. Chap. 16. Biology of endothelial cells (ed. JAFFE, E. A.). Martinus Nyhoff Publ., Boston 1984.
16. SMITH, G. J., MESURIER, S. M. DE, MONTFORD, M. L. DE. LYKKE, A. W. J.: Development and characterization of type 2 pneumocyte related cell line from normal adult mouse lung. Pathology 1984; 16: 401–405.
17. SVANHOLM, H., NIELSEN, K., HAUGE, P.: Factor VIII-related antigen and lymphatic collecting vessels. Virchows Arch. 1984; 404: 224–228.
18. TABUCHI, H., YAMAMOTO, T.: Specific granules in the endothelia of blood and lymphatic vessels in the cardiac valves of dogs. Arch. Histol. Jpn. 1974; 37: 217–225.
19. THORNTON, S. C., MUELLER, S. N., LEVINE, E. M.: Human endothelial cells: use of heparin in cloning and long term serial cultivation. Science 1983; 222: 623–625.
20. YOFFEY, J. M., COURTICE, F. C.: Lymphatics, lymph and lymphoid tissue. Edward Arnold Publ., London 1956.

Lymphology 20 (1987) 257-266

LYMPHATICS AND BLOOD VESSELS, LYMPHANGIOGENESIS AND HEMANGIOGENESIS: FROM CELL BIOLOGY TO CLINICAL MEDICINE

M.H. Witte, C.L. Witte

Department of Surgery, University of Arizona College of Medicine, Tucson, Arizona, U.S.A.

ABSTRACT

The past 15 years have witnessed an explosion of knowledge about blood vascular endothelium due in large part to in vitro *growth of endothelial cells from both large blood vessels and capillaries. In contrast, little comparable information has accumulated on endothelium of lymphatics, which lie in intimate contact with parenchymal cells and drain excess fluid, macromolecules, particles, and immunocompetent cells in a continuous recirculation between tissues and bloodstream. While structural and functional differences between the two vascular systems have been described* in vivo, *in tissue sections, and in isolated preparations, similarities are notable in ultrastructure, biochemistry, physiology, and pharmacologic responsiveness, and these may predominate under pathologic conditions. In 1984, three separate groups described* in vitro *culture of lymphatic endothelial cells from collecting ducts and cavernous lymphangiomas. Lymphatic, like blood vascular, endothelium grows in confluent monolayers, "sprouts", synthesizes Factor VIII-associated antigen and fibronectin, and ultrastructurally shows Weibel-Palade bodies; overlapping intercellular junctions and anchoring filaments typical of lymphatic endothelium are also found. Genetic, congenital, and acquired disorders such as strangulating fetal nuchal cystic hygromas (Down and Turner syndromes), vascular tumors and dysmorphogenesis (Maffucci and Klippel-Trenaunay syndromes), Kaposi's sarcoma, lymphogenous and hematogenous spread of cancer, and parasitic infestations such as filariasis, share overlapping abnormalities in formation, growth, and/or neoplasia of lymphatics and blood vessels. In these and similar clinical disorders, confusion often exists as to the nature of the cell or tissue of origin, and insight into the role and control of hemangiogenesis and lymphangiogenesis is still in its infancy. Nonetheless, with the ever widening array of investigative techniques, it is not only timely but imperative to explore the endothelial biology underlying these inborn and acquired disorders.*

Blood and lymphatic vasculatures are closely intertwined in embryonic development and respond to many similar stimuli in the microenvironment (e.g. ischemia, inflammation, and neoplasia). The two circulations work together in an integrated fashion in the uptake and transport of interstitial liquid and macromolecules such as extravasated plasma proteins and ingested lipids, which recirculate between lymph, blood, and tissue. Distinct migration streams of immunocompetent cells interchange at various points in the "blood-lymph loop." Anatomic connections exist or open up between the two as lymphatic-venous communications, which function normally (viz. thoracic duct-jugular venous junction) or become operational under physiologic and pathologic conditions (e.g. carcinomatous

venous or lymphatic obstruction or in portal hypertension from alcoholic cirrhosis). While lymphatics closely resemble blood vessels on tissue section, they are more thin-walled attenuated structures containing bloodless fluid, and they ultrastructurally exhibit overlapping intercellular junctional complexes, specialized anchoring filaments, and discontinuous or absent basal lamina (1). Permeability, surface charge distribution, vesicular macromolecular movement, lipid absorption and transport, intrinsic contractility, and vasoresponsiveness of the two vasculatures are distinct in some respects, vary from organ to organ, and also may overlap.

The vascular endothelium is the crucial interface between circulating blood or lymph and the tissues. Two decades ago only surmised by Lord Florey to be more than an inert passive membrane or in "nucleated cellophane", endothelium is now recognized as the biologically active mentor of the microcirculation and of tissue homeostasis--originating, receiving, translating, transducing, and transmitting physical and chemical messages to and from different parts of the body. The ability to culture large and pure endothelial cell populations not only from major blood vessels but since 1979, also from human capillaries has produced an explosion of knowledge (1-3). Despite differences among species and organs, blood vascular endothelium (BVE) exhibits remarkably consistent morphology and function in vitro mimicking its structural, synthetic, and transport properties in vivo and in isolated vascular preparations. In culture, endothelial cells grow as confluent monolayers with characteristic cobblestone appearance, which under appropriate conditions sprout and form tubules, that is, display "angiogenesis in vitro." Distinctive ultrastructural features mirroring those found in tissue section include intricate intercellular junctions, micropinocytotic vesicles, intermediate filaments, and Weibel-Palade bodies, which are thought to manufacture or store Factor VIII-associated antigen (Factor VIIIAA). On immunohistochemical examination, endothelial cells contain Factor VIII-associated antigen, angiotensin-coverting enzyme, and extracellular matrix components such as fibronectin, all of which in addition to prostacyclin and many other vasoactive metabolites can be measured quantitatively after release into the supernatant overlying the monolayer.

Considerable attention has been directed to a search for angiogenic factors controlling blood vessel formation and thereby tumor and organ growth. The genetic code for one such substance, angiogenin, has recently been deciphered. Blood vascular endothelium interacts in a "symbiotic" relationship with immunocompetent cells, directing lymphocyte cell traffic and "homing" and also producing colony-stimulating activity differentiating hemopoietic stem cells into granulocytes and monocytes (4). Immunocompetent cells as well as fibroblasts and adipocytes in turn secrete angiogenic factors and share cell surface receptors with endothelium. Thus, in large part because blood vascular endothelium can now be isolated *in vitro*, its role as a structural barrier as well as active facilitator of small solute and macromolecular transport into and out of tissues, as a director of cellular migration, as a stabilizer of the coagulation cascade, and as a biosynthetic factory is now being unraveled. Blood vascular endothelial damage and/or repair have been implicated in processes as diverse as atherosclerosis, hypertension, inflammation, wound healing, ischemia, diabetes mellitus, and transplant rejection.

Yet, in part because of a lack of analogous *in vitro* models, only rudimentary information is available about the highly permeable vascular interface on the "dark side" of the blood capillary barrier, deep in the tissues, separating circulating "lymph" from extracellular matrix and liquid and parenchymal cells in lymphoid and non-lymphoid tissues. Within this oft forgotten sluggish lymphatic-tissue fluid circulation pass surplus liquid, macromolecules, particles, and migrating cells from the interstitium on their way

through r
before re
(Fig. 1)

Fig. 1.
circulatio
macrom
blood, t
lymphat
In this
organs,
return
the bloo

small
phatic
by ov
recurr
from
and
cadav
(7).
theli
micr
blan
blest
4),
mar
The
pha
ren
om
um
VII
5)
Pa
les
tir
ju
an
pl
A
st
o

through regional and central lymph nodes before returning to the blood circulation *(Fig. 1)*. In 1984 for the first time,

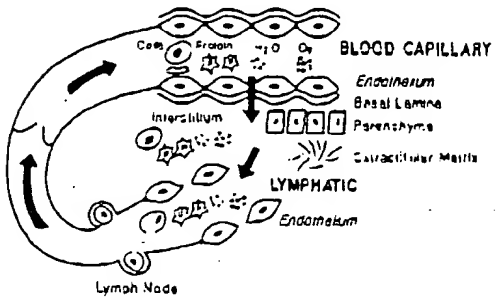

Fig. 1. Blood-lymph loop. There is a continuous circulation and recirculation of cells, particles, macromolecules, small solutes, and gases between blood, tissues, and lymph. Blood vascular and lymphatic endothelium represent crucial interfaces in this circulation. Lymph exiting parenchymal organs filters through lymph nodes on its way to return thru lymphatic-venous communications to the bloodstream.

small relatively pure populations of lymphatic vascular endothelium were isolated by our group from explants of a massive recurrent lymphangioma (5), by Johnston from normal bovine lymphatic ducts (6) and by Gnepp from canine and human cadaveric thoracic ducts *(Figs. 2 and 3)* (7). In culture, lymphatic vascular endothelium (LVE) from large ducts and microvasculature bears a strong resemblance to BVE, forming confluent "cobblestone" monolayers, sprouting *(Fig. 4)*, and staining positively for endothelial markers, Factor VIIIAA and Ulex lectin. Thus, CIII, our second nearly pure lymphatic endothelial cell line from a recurrent chylous retroperitoneal lymphangioma resembles blood vascular endothelium in staining positively for Factor VIIIAA, F-actin, and fibronectin *(Fig. 5)*, and exhibiting numerous Weibel-Palade bodies *(Fig. 6L)* (8). Nonetheless, LVE appears to possess some distinctive features: overlapping intercellular junctions and abundant intermediate anchoring-type filaments typical of lymphatic endothelium *(Fig. 6R)* (8). Although questions may be raised about stromal blood vessels giving rise to some of the endothelial cells found in this lymphangioma cell line, the same question can be but has not been raised about designated blood vascular endothelial cell cultures from microvasculature in such standard sources as omentum and foreskin, tissues rich in lymphatics as well as blood vessels. At this point, there is every reason to believe that lymphatic like blood vascular endothelium is also a vast endocrine organ maintaining a lymph-fluid compatible surface and a changeable selective interface between the lumen and interstitium that is also the target for numerous perturbations affecting not only its intrinsic structure and function but also that of surrounding tissues.

The close interactions between the lymphatic and blood vasculature and lymphangiogenesis and hemangiogenesis on a cellular and organ level are further illustrated in the clinical manifestations of disease. Congenital lymphologic syndromes of genetic or intrauterine origin involving abnormal growth of lymphatics often include widespread blood vascular abnormalities as in Maffucci's and Klippel-Trenaunay syndromes *(Figs. 7 and 8)*. These soft tissue hemangiomas and lymphangiomas are commonly accompanied by lymphedema, venous aplasia or hypoplasia as well as arteriovenous anomalies and striking soft tissue overgrowth such as limb hypertrophy and macrodactyly, likely closely linked to the circulatory disturbances *(Figs. 7 and 8)*. On rare occasions malignant vascular transformation may take place. Blood vascular and lymphatic anomalies also coexist in Turner's XY gonadal dysgenesis syndrome where webbed neck from regressed fetal cystic lymphangiomas, extremity lymphedema associated with lymphatic hypoplasia and aplasia, and coarctation of the aorta are typical manifestations; variants of the syndrome also exhibit severe intracardiac anomalies. Down syndrome (trisomy-21) similarly may present *in utero* with strangulating cystic hygromas, cardiovascular anomalies and lymphedema or survive into adulthood with other variations of these vascular abnormalities. On the other hand, in acquired condi-

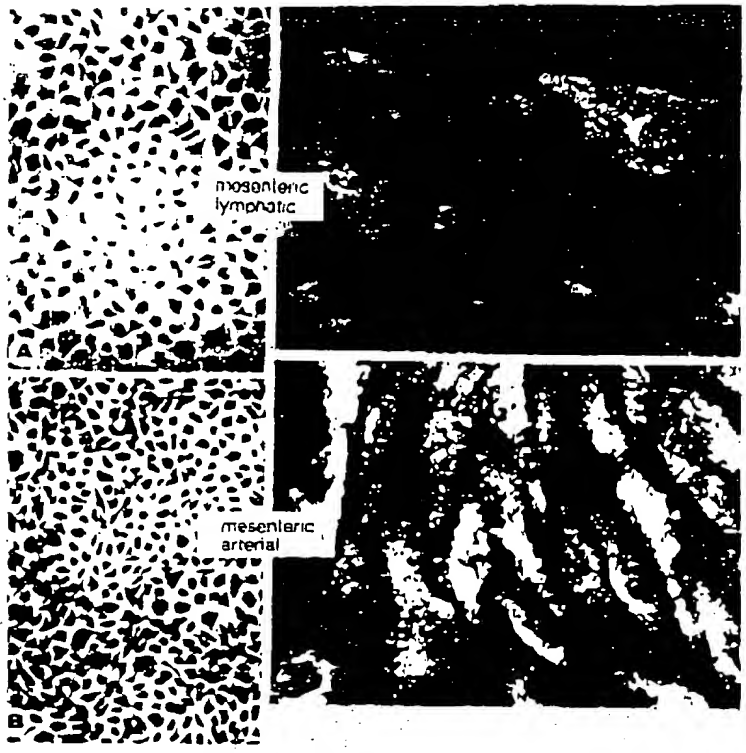

BOVINE MESENTERIC VASCULAR ENDOTHELIUM

(M.G. Johnston and M.A. Walker, In Vitro, 1984)

Fig. 2. Comparison of bovine lymphatic endothelial with bovine superior mesenteric arterial endothelial in tissue culture. The cells in A and B were stained with a Hemacolour stain kit (Harleco) as follows. The cells were washed twice with PBS and fixed for 5 min in methanol. The cells received an eosin solution (30s) followed by a thiazine solution (30s) and were then washed with water. A, Bovine lymphatic endothelial cells, Passage 9; (x141). B, bovine mesenteric artery endothelial cells, Passage 4. (x141); (6; modified by permission). C and D show assay for Factor VIII-related antigen. C, bovine lymphatic endothelium. D, Bovine mesenteric artery endothelium (antibody to human Factor VIII-related antigen diluted 1/10) (6; modified by permission).

tions such as classical or AIDS-associated epidemic Kaposi's sarcoma, abnormal lymphatic-venous communications may comprise or contribute to the multicentric tumor some of its peculiar morphologic and immunohistochemical properties as well as the associated lymphedema and hemorrhage. On rare occasions, malignant vascular tumors appear as Stewart-Treves syndrome after many years of lymphostasis associated with intense hemangiogenesis and lymphangiogenesis, and lymphangiomatoid changes superimposed on exuberant profuse scarring and fat deposition. The latter is well exemplified in filarial infestation, which leads to elephantiasis where thickening and piling up of the lymphatic as well as blood vascular endothelium, intraluminal blood or lymph clots, and exuberant deposition of underlying scar tissue characterize the pathologic process and the

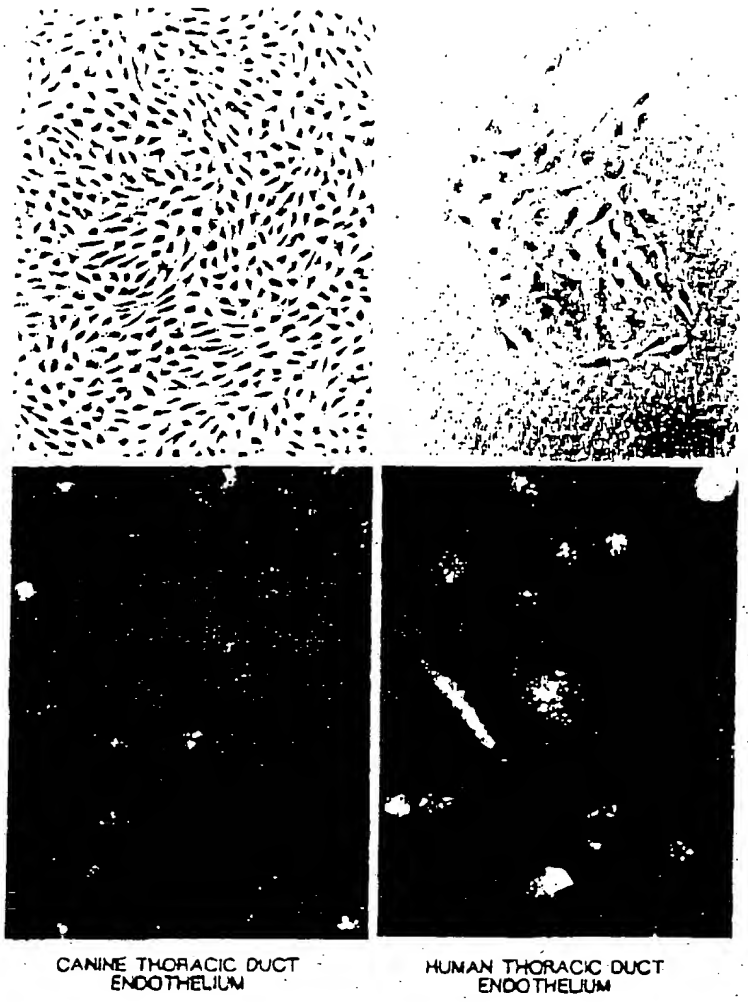

(D. Gnepp and W. Chandler, In Vitro, 1986)

Fig. 3. L, upper, canine thoracic duct culture demonstrating a sheet of uniform contact inhibited non-overlapping endothelial cells with typical cobblestone morphology. (x131). L, lower, indirect immunofluorescence of canine thoracic duct endothelial cells demonstrating marked positivity of Factor VIII antigen (note granular cytoplasmic staining. (x189). R, upper, human thoracic duct culture demonstrating one nest of typical endothelial cells, Day 9. (x179). R, lower, indirect immunofluorescence of human thoracic duct endothelial cells demonstrating granular cytoplasmic and perinuclear fluorescence. (x189). (7; used by permission).

host response to the worm and its products. These interrelationships between lymphangiogenesis and lymphologic syndromes have been summarized by us recently (9), and an analogous interconnected scheme can be postulated for hemangiogenesis and blood vascular syndromes.

Endothelial biologists working in tissue culture have opened up the pheno-

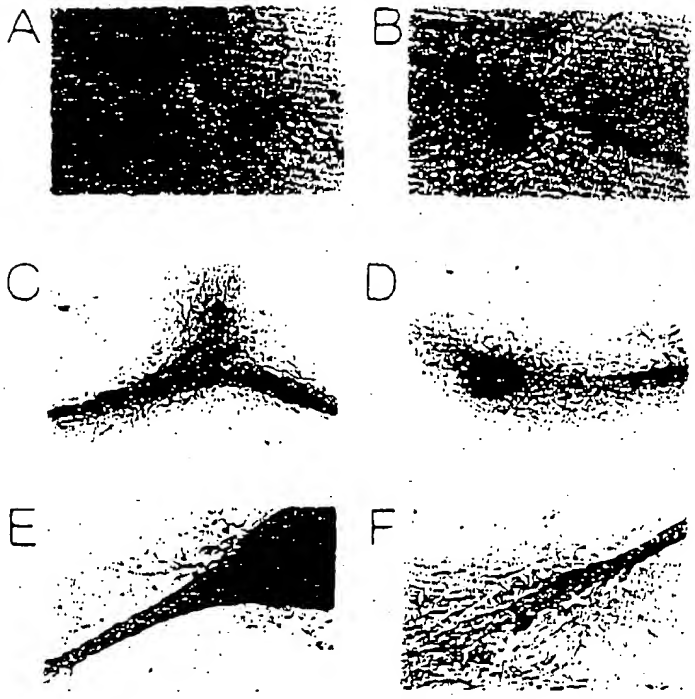

Fig. 4. Photomicrographs (inverted light) depicting in vitro evolution of lymphatic endothelial cell growth derived from a resected lymphangioma of the knee. An "early" phase displays a loose cluster of endothelium with occasional "sprouting" or branching (A: x100). With time, this sprouting pattern becomes more prominent (B; x100) and eventually evolves into a sheet-like cellular aggregate (C,D: x40) with intense "lymphatic-like" tumorous branching (E,F: x100).

menon of tumor angiogenesis to intensive inquiry. In 1972, Folkman (10) first proposed the concept that all tumors are angiogenesis-dependent and once tumor take has occurred, enlargement of the tumor cell population is preceded by growth of new blood capillaries converging on the tumor. Inhibition of angiogenesis, he proposed, might be a therapeutic approach to solid tumors. Interesting questions have arisen about the role of endothelial mitogens in normal tissues and natural mechanisms that restrain and inhibit formation of capillary and thereby tissue and organ growth. Lymphatic vessels have been scarcely mentioned in the context of "angiogenesis", and some workers have even suggested that tumors do not contain lymphatics. Nonetheless, the parallel development and common response of the two vascular systems to varied physiologic and pathologic stimuli suggest, however, that hemangiogenesis and lymphangiogenesis go hand in hand and that the mysterious growth factors stimulating both vasculatures are self-generated as well as arise in or are delivered through the neighboring tissue matrix; that is, the stimuli are autocrine, paracrine, and endocrine.

Despite the mounting interest in tumor angiogenesis, investigation of a related process--what we have termed "angiotumorogenesis," i.e., the growth and development of blood and lymphatic vascular tumors--has been extremely limited despite their frequency as cosmetic imperfections or as disfiguring or even

Fig. 5. Inc... tern of Fa... ized cytosk... fibronectin ...

life-threa...
Genetic, ...
influence ...
by horm...
oral cont...
(e.g., vi...
(e.g., ht...
cytomega...
but thes...
endothel...
mation, ...
tinues at...
tumors, ...
rests (ha...
mere exp...
esis. As ...
areas of ...
strikingly ...
normal ...
wildly a ...
able as ...
Moreov...
tumors ...
multicen...
sionally, ...
tumors ...
and eve...
sizing l...
hand, b...
tumors ...
Unfortu...

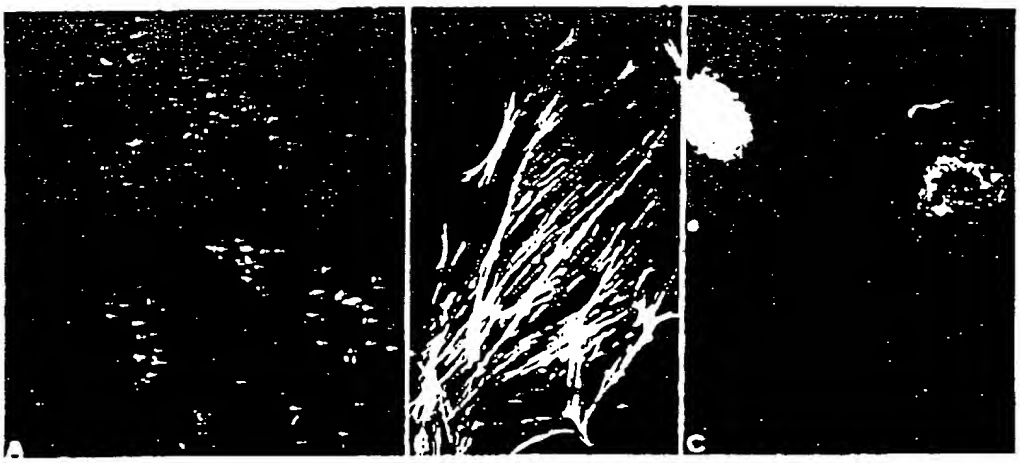

Fig. 5. Indirect fluorescent-antibody labelling using rabbit antihuman IgG shows the characteristic granular pattern of Factor VIII-related antigen (A) (x168). F-actin positive microfilament bundles forming a well-organized cytoskeleton stained with NBD-phalloidin (x591), cell surface-associated fibronectin using rabbit antihuman fibronectin IgG (C) (x168), which is also deposited extracellularly (8; used by permission).

life-threatening tumors of childhood. Genetic, congenital and environmental influences on endothelial growth, such as by hormones and drugs (e.g., estrogens, oral contraceptives), industrial carcinogens (e.g., vinyl chloride) and viral agents (e.g., human immunodeficiency virus and cytomegalovirus) are poorly understood but these agents are known stimulants of endothelial proliferation, DNA transformation, and neoplasia. Controversy continues about the nature of some vascular tumors, i.e., whether they are embryonic rests (hamartomas), true neoplasms or mere expressions of exuberant angiogenesis. As in Kaposi's sarcoma, different areas of the same lesion may appear strikingly heterogenous ranging from normal vessels to highly anaplastic or wildly aberrant structures indistinguishable as lymphatics or blood vessels. Moreover, it is unclear whether multiple tumors in separated or remote sites are multicentric in origin or metastatic. Occasionally, benign-appearing endothelial tumors may exhibit local invasion, recur, and even spread (e.g., "benign metastasizing lymphangioma"). On the other hand, benign and even malignant vascular tumors sometimes spontaneously regress. Unfortunately, immunohistochemical studies to detect the presence of intracytoplasmic or cell surface endothelial markers (e.g., Factor VIIIAA or basement membrane components) have produced more confusion than clarification because of heterogeneity of staining, postulated but disputed differences between the blood and lymphatic vasculature, inconsistent staining techniques, neoplastic or non-neoplastic transformation to more primitive or aberrant cell types or pluripotential nature of the cells, and presence of mixed cell types including mesenchymal and lymphoid elements. Thus, in part because of the paucity of animal models and the lack of *in vitro* systems to study pure populations of tumor cells, classification of endothelial tumors of lymphatic or blood vascular origin remains largely based on morphologic criteria and clinical behavior. Although tumor modulation by hormones, immunoregulatory substances, and growth factors seems almost within our grasp, detection and treatment of these neoplasms has progressed little over the past several decades beyond refinement or extension of surgical resection.

Understanding the structural-functional interrelationships between the blood and lymphatic vasculatures *in vivo*

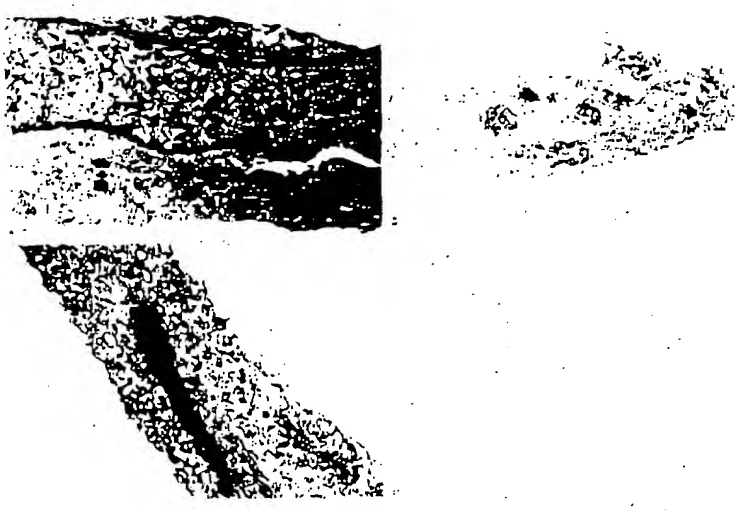

Fig. 6. Transmission electron microscopy (A-D) of cultured tumor cells reveals relatively smooth cell surfaces with few microvillous projections, numerous vesicles, and cytoplasm rich with Golgi and rough endoplasmic reticulum. Abundant Weibel-Palade bodies (A, arrow; B, higher magnification) are seen surrounded by bundles of intermediate filaments characteristic of lymphatic endothelium. Higher power detail of intermediate filaments can be best appreciated in C. Typical macula adherens, overlapping intercellular junctions are also shown (C,D). (A=x8550; B=x41,800; C=x48,450; D=x26,650) (8; used by permission).

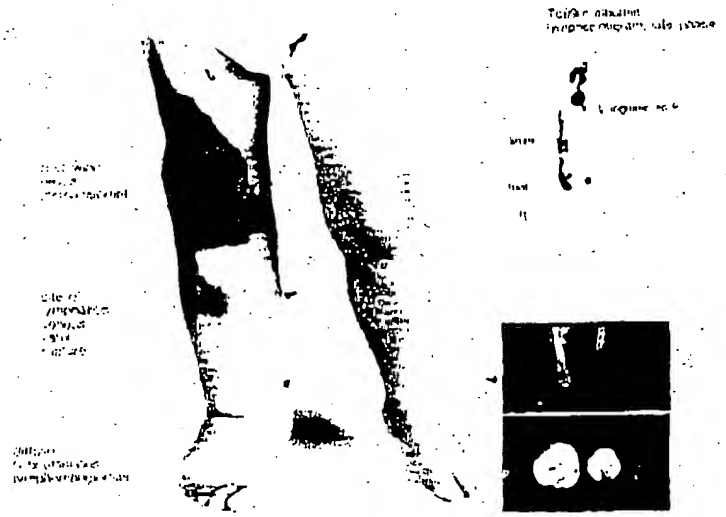

KLIPPEL TRENAUNAY SYNDROME

Fig. 7. 3-year-old girl with Klippel-Trenaunay syndrome involving the right leg. In addition to the characteristic port wine nevus and agenesis of the deep venous system, small pedal arteriovenous fistulae lymphscintigraphy (^{99m}Tc albumin) shows abberrant lateral "pick-up" with a large, dilated truncal "lake" reaching the lateral groin only after many hours. The left leg is unremarkable. Computed tomography with contrast enhancement suggests diffuse lymphangiomatous change with little or no edema fluid in the right leg.

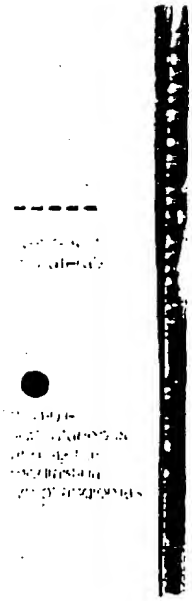

Fig. 8. 13-year-o
present are right

and *in vitro* i
control mecha
tissue growth
life to senesce
variety of *in*
neoplastic en
clues to detec
giogenesis an
enhanced or
tive endotheli
endothelium)
treatment (su
angioinhibitor
occurring hor
dioresistant v
scar formatio
released from
scoped in ti
combined wi
biology can
endothelial c
and distant
shedding ligl
transplant re
plastic lympl
mellitus, lym
spread of c

Fig. 8. 13-year-old girl with multiple lymphangiomas including of the back, mediastinum and left axilla. Also present are right arm hypertrophy, macrodactyly, digital hyperemia.

and *in vitro* is key to unraveling the control mechanisms and detailed steps of tissue growth and repair from embryonic life to senescence. Greater availability and variety of *in vitro* models of normal and neoplastic endothelium should provide clues to detection of abnormal lymphangiogenesis and hemangiogenesis (e.g., enhanced or inhibited release of distinctive endothelial products from neoplastic endothelium) as well as more effective treatment (such as by angiostatic and angioinhibitory agents including naturally occurring hormones for chemo- and radioresistant vascular tumors or excessive scar formation. Isolated in pure culture, released from central control and telescoped in time, such *in vitro* models combined with the tools of molecular biology can also be used to explore endothelial cell interactions with related and distant cell types thereby potentially shedding light on disorders as varied as transplant rejection, inflammation, hypoplastic lymphedema, scleroderma, diabetes mellitus, lymphogenous vs. hematogenous spread of cancer, and limb ischemia.

What these test tube models teach us about fundamental biology must then be returned to the body, validated, and applied to this bewildering array of human disorders characterized by defective, exuberant, or uncontrolled hemangiogenesis and/or lymphangiogenesis and a wide variety of interrelated and dependent phenomena.

ACKNOWLEDGEMENTS

Supported in part by Arizona Disease Control Research Commission Contracts #8277-000000-1-1-AT-6625, ZB-7492, and ZM-8036.

REFERENCES

1. Shepro, D, PA D'Amore: Physiology and biochemistry of the vascular wall endothelium. In *Handbook of Physiology--The Cardiovascular System IV*, Chapter 4. Am. Physiol. Soc., Washington, DC (1984), 103-164.
2. Gospodarowicz, D: Control of vascular endothelial cell proliferation and respiration. Cryer, A (Editor): *Biochemical Interactions at the Endothelium*. New York, Elsevier (1983), 363-403.

3. Mohammed, SF, RO Mason, E Eidwald, J Shively: Healthy and impaired vascular endothelium. Lasslo, A (Editor): *Blood Platelet Function and Medicinal Chemistry*. Elsevier Biomedica (1984), 129-174.
4. Baldwin, WM,III: The symbiosis of immunocompetent and endothelial cells. Immunol. Today 3 (1982), 267.
5. Bowman, C, MH Witte, CL Witte, et al: Cystic hygroma reconsidered: Hamartoma or neoplasm? Primary culture of an endothelial cell line from a massive cervicomediastinal cystic hygroma with bony lymphangiomatosis. Lymphology 17 (1984), 15-22.
6. Johnston, MG, MA Walker: Lymphatic endothelial and smooth-muscle cells in tissue culture. In Vitro 20 (1984), 566-572.
7. Gnepp, DR, W Chandler: Tissue culture of human and canine thoracic duct endothelium. In Vitro 21 (1985), 200-206.
8. Way, D, M Hendrix, M Witte, et al: Lymphatic endothelial cell line (CH3) from a recurrent retroperitoneal lymphangioma. In Vitro 23 (1987), 647-652.
9. Witte, MH, CL Witte: Lymphangiogenesis and lymphologic syndromes. Lymphology 19 (1986), 21-28.
10. Folkman, J: Toward an understanding of angiogenesis: Search and discovery. Perspect. Biol. Med. 29 (1985), 10-32.

Marlys H. Witte, M.D.
Department of Surgery
University of Arizona
College of Medicine
1501 North Campbell Avenue
Tucson, AZ 85724

DR. M. talk abou between t DR. RY. he thinks th having to found a f DR. MOR quite obv cused on h But, I've a because t ting out f being fac station w the entr can't get in case of t cell migr associate can get sheep n node thr occurs i athymic have be that the located and hig rodents, that yo where taking It's not lial str has bee DR. R endothe with ar any qu studies vessels and th way? DR. MO has do permea patche that u sels th tention sented mize

COMMONWEALTH OF AUSTRALIA

(Patents Act 1990)

IN THE MATTER OF: Australian Patent Application 696764 (73941/94). In the name of: Human Genome Sciences Inc.

- and -

IN THE MATTER OF: Opposition thereto by Ludwig Institute for Cancer Research, under Section 59 of the Patents Act.

Annexure GBC-23

This is **Annexure GBC-23** referred to in my Statutory Declaration made this Thirteenth day of December 2000.

Gary Baxter Cox

WITNESS: _____

Patent Attorney PEYTEE KIM.